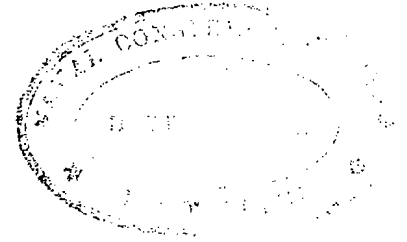


Lat NO - 657

BASIC SHIP PROPULSION



J.P. Ghose

R.P. Gokarn

Formerly with

Department of Ocean Engineering and Naval Architecture
Indian Institute of Technology
Kharagpur



ALLIED PUBLISHERS Pvt. LIMITED

New Delhi • Mumbai • Kolkata • Lucknow • Chennai
Nagpur • Bangalore • Hyderabad • Ahmedabad

722 - 04/10

Allied Publishers Pvt. Limited

Regd. Off.: 15 J. N. Heredia Marg, Ballard Estate, Mumbai - 400 038

Prarthna Flats (2nd Floor), Navrangpura, Ahmedabad - 380 009

3-5-1114/1 Kachiguda Cross Road, Hyderabad - 500 027

16A Ashok Marg, Patiala House, Lucknow - 226001

5th Main Road, Gandhinagar, Bangalore - 560 009

17 Chittaranjan Avenue, Kolkata - 700 072

81 Hill Road, Ramnagar, Nagpur - 400 010

13/14 Asaf Ali Road, New Delhi - 110 002

751 Anna Salai, Chennai - 600 002

© 2004, Allied Publishers Pvt. Limited

No part of the material protected by this copyright notice may be reproduced or utilised in any form or by any means, electronic or mechanical including photocopying, recording or by any information storage and retrieval system, without written permission from the copyright owners.

ISBN 81-7764-606-0

Published by Sunil Sachdev for Allied Publishers Limited, 1-13/14 Asaf Ali Road, New Delhi 110 002 and printed by Ravi Sachdev at Allied Publishers Limited (Printing Division), A-104 Mayapuri II, New Delhi 110 092.

Laser typeset by FineLine dtp, 304 Forest Lane, Neb Sarai, New Delhi 110 068.

*Dedicated
to our Teachers:*

Professor S.C. Mitra (b. 1914)

Professor S.D. Nigam (b. 1924)

Professor T.S. Raghuram (b. 1928)

Acknowledgements

The authors acknowledge their debt to the students of the Department of Naval Architecture and Ocean Engineering, Indian Institute of Technology, Kharagpur, who provided the motivation for writing this book. The authors would also like to acknowledge the support and encouragement they received from their colleagues in the Department. Professor O.P. Sha gave valuable guidance in matters relating to the use of computers. Mr. R.K. Banik typed the manuscript. The authors are deeply grateful to them.

The manuscript of this book was initially written by Professor Ghose, who wishes to acknowledge the financial support received from the University Grants Commission. Professor Chengi Kuo of Strathclyde University reviewed Professor Ghose's manuscript and made some suggestions, for which the authors are very grateful. The book was then completely revised and rewritten by Professor Gokarn taking into account Professor Kuo's comments as well as the comments of an expert who reviewed Professor Ghose's manuscript. The authors are greatly indebted to Allied Publishers Limited and particularly to Mr. Suresh Gopal, Publishing Consultant, for their patience, support, encouragement and guidance during the period that the book was being rewritten.

Copyright Acknowledgements

A book such as this leans heavily on the work of others, and the authors gratefully acknowledge their debt to the writers of the publications listed in the Bibliography.

Specific thanks are due to the following for permission to reproduce copyright material:

1. Dover Publications Inc., New York, for Tables A2.1, A5.1, A5.2 and A5.3.
2. The Indian Register of Shipping, Mumbai, for Equation 7.41 and Table 7.6.
3. *The International Organisation for Standardisation (ISO), Geneva, Switzerland, for Table 11.3.
4. International Shipbuilding Progress, Delft, The Netherlands, for Equations 9.1, 9.37, A3.1, A3.2, A3.3, A3.4, A3.7, A3.8, A3.9, A3.10, A4.13, A4.14, A4.25, A4.26, A4.27, A4.33, A4.34 and A4.35, Figures 4.5, 4.6 and 4.7, and Tables 4.2, 9.6, A3.1, A3.2, A3.3, A3.4, A3.5, A3.6, A3.8, A3.9, A3.10, A3.11, A3.12 and A4.3.
5. *The International Towing Tank Conference for Equations 8.8, 8.9, 8.10, 8.11, 8.25, 8.30 and 8.31.
6. *Lloyd's Register of Shipping, London, for Equation 7.39, Figure 9.1 and Tables 7.2, 7.3 and 7.4.
7. The Royal Institution of Naval Architects, London, for Equations A4.12, A4.24 and A4.32, Figure 4.4 and Table 4.1.
8. *The Society of Naval Architects and Marine Engineers, New Jersey, for Equations 9.31, 9.38, 11.13, 11.20, 11.21, 11.22, 11.23, A4.3, A4.4, A4.5, A4.6, A4.17, A4.18, A4.19, A4.28 and A4.29, Figures 9.2 and 12.11, and Table 9.5.

*Some of the organisations which have given permission to reproduce copyright material require the following to be explicitly stated:

1. International Organisation for Standardisation:

Table 11.3 - Summary of manufacturing tolerances for ship propellers taken from ISO 484/2:1981 has been reproduced with the permission of the International Organisation for Standardisation, ISO. This standard can be obtained from any member body or directly from the Central Secretariat, ISO, Case postal 56, 1211 Geneva 20, Switzerland. Copyright remains with ISO.

2. International Towing Tank Conference:

The ITTC cannot take any responsibility that the authors have quoted the latest version and/or quoted correctly.

3. Lloyd's Register of Shipping:

Equation 7.39, Figure 9.1 and Tables 7.2, 7.3 and 7.4 of this publication reproduce matter contained in the Lloyd's Register of Shipping Rules and Regulations for the Classification of Ships/Rules for the Maintenance, Testing and Certification of Materials produced under licence from Lloyd's Register of Shipping, 71 Fenchurch Street, London, England EC3M 4BS.

4. Society of Naval Architects and Marine Engineers:

Equations 9.31, 9.38, 11.13, 11.20, 11.21, 11.22, 11.23, A4.3, A4.4, A4.5, A4.6, A4.17, A4.18, A4.19, A4.28, and A4.29, Figures 9.2 and 12.11, Table 9.5 and parts of Section 12.14 are reproduced with the permission of the Society of Naval Architects and Marine Engineers (SNAME). Material originally appearing in SNAME publications cannot be reproduced without the written permission from the Society, 601 Pavonia Avenue, Jersey City, NJ 7306, USA.

The authors are grateful to the following individuals for their help in getting copyright permissions:

1. Ms. Pam Cote and Mr. John Grafton, Dover Publications Inc.
2. Mr. D.G. Sarangdhar, Chief Surveyor, Indian Register of Shipping.
3. Mr. Jacques-Olivier Chabot, Director (General Services and Marketing, International Organisation for Standardisation).
4. Ir. J.H. Vink, Chief Editor, International Shipbuilding Progress.
5. Admiral U. Grazioli, Chairman, and Dr. E. De Bernardis, Secretary, 23rd Executive Committee, International Towing Tank Conference.

6. Mr. K. Neelakantan, Administrative Manager for India and Sri Lanka, Lloyd's Register of Shipping.
7. Mr. Trevor Blakeley, Chief Executive, The Royal Institution of Naval Architects.
8. Ms. Susan Grove Evans, Publications Manager, The Society of Naval Architects and Marine Engineers.

The authors would further like to add that the equations, figures and tables taken from previously published books and papers have been modified, where necessary to conform to the format of this book. Any errors resulting from these modifications are the sole responsibility of the authors.

Preface

In our long experience of teaching the subject of Ship Propulsion to undergraduate and postgraduate students of Naval Architecture at the Indian Institute of Technology, Kharagpur, we have often felt the need for a basic text which would describe adequately the essential elements of ship propulsion. This book attempts to fulfil this need. "Basic Ship Propulsion", as implied in its title, deals with the fundamentals of ship propulsion. However, an attempt has also been made to cover the subject comprehensively. A bibliography is provided for those readers who wish to pursue particular topics in greater detail and to an advanced level. A special feature of this book is the large number of examples and problems. These examples and problems have been specially designed to illustrate the principles described in the text and to aid the reader in understanding the subject.

Chapter 1 introduces the subject of ship propulsion beginning with a short description of ships and ship propulsion machinery. The various propulsion devices used in ships are briefly reviewed. Chapter 2 considers the terminology and geometry of screw propellers, which are the dominant form of propulsion device used in ships today. The theory of propellers is discussed next in Chapter 3. Chapter 4 describes the behaviour of a propeller in undisturbed ("open") water and the methods of representing propeller open water characteristics, including those of methodical propeller series. The behaviour of a propeller when fitted in its customary position at the stern of a ship, and the resulting hull propeller interaction are discussed next in Chapter 5. Chapter 6 deals with the phenomenon of propeller cavitation. The topic of propeller blade strength is considered in Chapter 7. Propulsion experiments using models are described in Chapter 8. Chapter 9 deals with the important topic of propeller design, in which methods using experimen-

tal model data and methods based on propeller theory are both considered. Speed trials and service performance of ships are discussed in Chapter 10. Chapter 11 deals with some miscellaneous topics concerning screw propellers. The last chapter of the book describes ship propulsion devices other than conventional propellers

Each chapter, except the first, includes examples and problems based on the material covered in that chapter. The SI system of units has been used throughout the book, although for historical reasons there are occasional references to the British system. A notable exception to the use of SI units in this book is the unit of speed which, in conformity with accepted marine practice, is the *knot* (1 metric knot = 1852 m per hour, 1 British knot = 6080 ft per hour = 1853.1 m per hour; the metric knot has been used as the unit of speed along with m per sec).

In applying the principles of ship propulsion discussed in this book, it is now usual to make extensive use of computers. Although we make full use of computers in our work, we feel that the fundamentals are best learnt without undue reliance on computers. Therefore, there are only occasional references to computers in this book. Almost all the problems may be solved without using computers. However, the reader may save considerable time and effort by using a "spreadsheet" for those problems involving tabular calculations. We have solved many of the problems and examples using Microsoft "Excel". We have also preferred to give much of the data required for designing propellers and similar tasks in the form of equations or tables rather than as design charts. This should facilitate the use of computers for these tasks.

Some useful data are given in the appendices at the end of the book, and there is a glossary of technical terms to help a reader unfamiliar with terms commonly used by naval architects and marine engineers.

Glossary

Added inertia	The difference between the "virtual inertia" and the actual inertia of a body undergoing angular acceleration in a fluid. The virtual inertia is the ratio of a moment applied to the body and the resulting angular acceleration.
Added mass	The difference between the "virtual mass" and the actual mass of a body undergoing linear acceleration in a fluid. The virtual mass is the ratio of a force applied to the body and the resulting acceleration.
Amidships	The mid-length of the ship.
Anchor windlass	A device to raise the anchor of a ship.
Appendages	Small attachments to the hull of a ship, e.g. bilge keels and rudders.
Auxiliaries	Equipment necessary to allow the main equipment, e.g. the main engine in a ship, to function effectively.
Ballast	A load placed in a ship to bring it to a desired condition of draught, trim and stability.
Bilge keels	Small projections fitted to the bottom corners (bilges) of a ship to reduce its rolling (oscillation about a longitudinal axis).

Block coefficient	The ratio of the volume of water displaced by the ship (displacement volume) and the volume of a rectangular block having the same length and breadth as the ship and a height equal to the draught of the ship.
Bollard	A fitting on a ship, pier or quayside to which mooring ropes may be attached.
Bossings	Longitudinal streamlined attachments to the hull of a ship to support the propeller shafts in a twin screw ship.
Boundary layer	A thin layer adjacent to the surface of a body moving in a viscous fluid to which the viscous effects are almost entirely confined.
Bow	The forward (front) part of the ship.
Crash stop	A manoeuvre in which a ship moving at full speed is stopped and its direction of motion reversed as quickly as possible, normally by stopping the propeller revolution in one direction and starting it in the opposite direction.
Damping	The phenomenon by which the amplitude of an oscillation decreases with time and dies out.
Displacement volume	The volume of water displaced by a floating ship.
Displacement	The mass of water displaced by a floating ship, equal to the mass of the ship.
Draught	The vertical distance between the bottom (keel) of the ship and the surface of water in which the ship is floating.
Hovercraft	The popular name for an air cushion vehicle in which a cushion of air beneath the vehicle supports its weight.

Hull	The main body of a ship to which are attached superstructures and appendages.
Hydrofoil craft	A high speed marine craft in which the weight of the craft at high speed is entirely supported by the lift of hydrofoils (attachments like aircraft wings) fitted to the craft below the hull.
Laminar flow	A flow in which the fluid appears to move in a series of thin sheets (laminae).
Longitudinal centre of buoyancy	The longitudinal coordinate of the centre of buoyancy (centroid of the underwater volume) of the ship, often measured from amidships as a percentage of the length of the ship.
Midship coefficient	The ratio of the area of the immersed midship section of the ship to the product of its breadth and draught.
Pitching	An angular oscillation of the ship about a transverse axis.
Prismatic coefficient	The ratio of the displacement volume of the ship and the volume of a "prism" having a cross sectional area equal to the area of the maximum immersed cross section (maximum section) of the ship and a length equal to the length of the ship.
Rolling	An angular oscillation of the ship about a longitudinal axis.
Rudder	A device for steering and manoeuvring a ship, consisting usually of a wing-like shape in a vertical plane capable of being turned from side to side about a vertical axis.
Stern	The after (rear) part of the ship.
Torsionmeter	A device to measure the torque being transmitted by the propeller shafting in a ship.

Towboat	A ship designed to tow other ships.
Trawler	A fishing vessel which drags fishing gear.
Trim	The difference between the draughts forward and aft of a ship.
Tug	A small ship meant for pushing or pulling a large ship that is not capable of moving safely on its own.
Turbulent flow	A flow in which, in addition to the average motion of the fluid, there are small random movements of the fluid particles in all directions.
Waterline	The line of intersection of the surface of water and the hull of the ship.
Waterplane	The intersection of the surface of water in which a ship is floating and the hull of the ship.
Waterplane coefficient	The ratio of the area of the waterplane to the product of the length and breadth of the ship.
Wetted surface	The area of the outer surface of the ship hull in contact with the water.

Nomenclature

Coordinates

Cylindrical polar coordinates (r, θ, z) have been used for defining propeller geometry, with r along the radius, θ being measured from the upwardly directed vertical and the z -axis coinciding with the propeller axis. The reference axis of a propeller blade is taken to coincide with the $\theta = 0$ line, i.e. the blade is pointing vertically up. The x -axis is thus vertical and positive upward, the y -axis horizontal and positive to the right (for a right hand propeller) and the z -axis positive forward, the axes forming a right hand system. The origin of coordinates is at the intersection of the propeller axis and the blade reference line.

For a blade section, the origin is taken at the leading edge, the x -axis being along the chord positive towards the trailing edge and the y -axis positive from the face to the back of the section. The principal axes of the section are denoted as the x_0 - and y_0 -axes.

Subscripts

The subscripts M and S refer to the model and the ship respectively. Other subscripts have been defined in the text.

Symbols

a	Area of blade section Axial inflow factor
a'	Tangential inflow factor
A	Area
A_D	Developed blade area
A_E	Expanded blade area
A_J	Area of jet cross section
A_O	Propeller disc area
A'_O	Immersed disc area of surface propeller
A_P	Projected blade area
A_T	Transverse projected area of ship above water
BP	Bollard pull
B_P	Taylor delivered power coefficient
c	Added mass coefficient Blade section chord
c_{max}	Maximum chord (width) of a blade
C_A	Correlation allowance
C_{AA}	Air and wind resistance coefficient
C_B	Block coefficient
C_D	Drag coefficient
C_{DR}	Drag coefficient of a rough propeller surface

C_{DS}	Drag coefficient of a smooth propeller surface
C_F	Frictional resistance coefficient
C_L	Lift coefficient
C_N	Correlation factor for propeller revolution rate
C_P	Pressure coefficient
C_{pmin}	Minimum pressure coefficient
$C_{\bar{p}}$	Mean pressure coefficient
C_P	Correlation factor for delivered power Power coefficient
C_R	Residuary resistance coefficient
C_T	Total resistance coefficient
C_{TL}	Thrust loading coefficient
C_{TLi}	Ideal thrust loading coefficient
C_V	Viscous resistance coefficient
d	Boss diameter
D	Drag Propeller diameter
D_D	Duct drag
D_I	Pump inlet diameter
D_M	Momentum drag
e	Clearance between duct and propeller Eccentricity ratio
E	Modulus of elasticity

E_n	Euler number
f	Blade section camber Frequency
f_f	Fundamental frequency of flexural vibration
f_t	Fundamental frequency of torsional vibration
F	Force Tangential force on the propeller Tow force in self-propulsion test
F_C	Centrifugal force
F_H	Horizontal component of the tangential force
F_i	Tangential force on the i^{th} blade
F_n	Froude number
F_V	Vertical component of the tangential force
g	Acceleration due to gravity
G	Non-dimensional circulation Modulus of rigidity
h	Depth of immersion of propeller shaft axis Depth of water Height of jet above waterline Maximum tip immersion of surface propeller
h'	Musker's roughness parameter
H	Head of pump
I_{boss}	Mass polar moment of inertia of boss
I_P	Mass polar moment of inertia of propeller

I_{x0}	Second moment of area about the x_0 -axis of a blade section
I_{y0}	Second moment of area about the y_0 -axis of a blade section
J	Advance coefficient
k_w	Wind direction coefficient
k_α	Lifting surface correction factor for angle of attack
k_c	Lifting surface correction factor for camber
k_D	Drag correction factor
k_i	Inertia coefficient
k_m	Mass coefficient
k_p	Average propeller surface roughness
k_s	Average roughness of ship surface
k_t	Correction factor for blade thickness
K_Q	Torque coefficient
K_{QB}	Torque coefficient in the behind condition
K_T	Thrust coefficient
K_{TB}	Thrust coefficient in the behind condition
K_{TD}	Duct thrust coefficient
K'_Q	Modified torque coefficient of surface propeller
K'_T	Modified thrust coefficient of surface propeller
l	Duct length
L	Length of the ship Lift

\underline{L}	Length dimension
L_p	Noise level based on pressure
L_P	Noise level based on power
m	Mass of fluid per unit time
m_b	Mass of a blade
M	Mass of propeller
\underline{M}	Mass dimension
M_{boss}	Mass of boss
M_Q	Bending moment due to torque
M_R	Bending moment due to rake
M_S	Bending moment due to skew
M_T	Bending moment due to thrust
M_{x0}	Bending moment about the x_0 -axis of a blade section
M_{y0}	Bending moment about the y_0 -axis of a blade section
n	Propeller revolution rate (revolutions per unit time)
N_Q	Torsion in a blade section due to torque
N_S	Specific speed of pump
N_T	Torsion in a blade section due to thrust
p	Pressure
\bar{p}	Mean pressure
p_A	Atmospheric pressure

p_c	Roughness peak count per mm Pressure due to cavitation
p_v	Vapour pressure
p_0	Pressure without cavitation
P	Pitch of the propeller
\bar{P}	Mean pitch of propeller
P_B	Brake power
P_D	Delivered power
P_{DO}	Delivered power in open water
P_e	Effective pitch
P_E	Effective power
P_{En}	Effective power of naked hull
P_I	Indicated power
P_J	Power of waterjet
P_S	Shaft power
P_T	Thrust power
P_{Tow}	Towrope power
P_{TO}	Thrust power in open water
q	Stagnation pressure
Q	Propeller torque Pump discharge
Q_i	Ideal torque Torque of the i^{th} blade

Q_o	Torque in open water
Q_V^i	Vane wheel torque at inner radius
Q_V^o	Vane wheel torque at outer radius
r	Radius of a blade section
\bar{r}	Radius of blade centroid
r_b	Boss radius
r_V^i	Inner radius of vane wheel
r_V^o	Outer radius of vane wheel
R	Propeller radius
$R_{a2.5}$	Root mean square roughness height in microns over a 2.5 mm length
R_{AA}	Air and wind resistance
R_n	Reynolds number
R_T	Total resistance
s	Distance Slip ratio Span of a wing
s_e	Effective slip ratio
S	Stress Wetted surface of the ship
S_{BK}	Wetted surface of bilge keels
S_C	Compressive stress due to thrust and torque
S'_C	Additional compressive stress due to centrifugal force

S_T	Tensile stress due to thrust and torque
S'_T	Additional tensile stress due to centrifugal force
$S_\zeta(\omega_E)$	Encounter spectrum of seaway
t	Blade section thickness Thrust deduction fraction
\hat{t}	Time
\bar{t}	Mean thickness of blade
t_0	Blade thickness extrapolated to propeller axis
t_1	Blade thickness at tip
T	Draught of the ship Propeller thrust
\underline{T}	Time dimension
T_D	Thrust of duct
T_G	Gross thrust of waterjet propulsion unit
T_i	Ideal thrust Thrust of the i^{th} blade
T_O	Thrust in open water
TP	Towrope pull
T_P	Propeller thrust in a ducted propeller
T_V^i	Vane wheel thrust at inner radius
T_V^o	Vane wheel thrust at outer radius
u	Induced velocity
u_a	Axial induced velocity

u_{AV}^i	Axial induced velocity of vane wheel at inner radius
u_{AV}^o	Axial induced velocity of vane wheel at outer radius
u_t	Tangential induced velocity
u_{TV}^i	Tangential induced velocity of vane wheel at inner radius
u_{TV}^o	Tangential induced velocity of vane wheel at outer radius
v	Velocity of flow
v	Cavity volume
v_D	Velocity induced due to duct
\bar{v}	Mean wake velocity
$v'(r)$	Average wake velocity at radius r
$v(r, \theta)$	Velocity at the point (r, θ)
V	Characteristic velocity Ship speed
V_a	Axial component of velocity
V_A	Speed of advance
$\overline{V_A}$	Average speed of advance
V_C	Speed of current
V_G	Speed of ship over ground
V_J	Waterjet exit velocity
V_K	Ship speed in knots
V_O	Observed ship speed
V_{rt}	Tangential velocity of propeller blade relative to water
V_{rw}	Relative wind velocity

V_R	Resultant velocity
V_t	Tangential component of velocity
V_W	Speed of ship through water
$V_{0.7R}$	Resultant velocity at $0.7R$
w	Wake fraction
\bar{w}	Average wake fraction
$w'(r)$	Wake fraction at radius r
$w(r, \theta)$	Wake fraction at the point (r, θ)
w_{eff}	Effective wake fraction
w_{nom}	Nominal wake fraction
w_{max}	Local maximum wake fraction
w_Q	Wake fraction (torque identity)
w_T	Wake fraction (thrust identity)
W	Weather intensity factor
W_n	Weber number
x	Non-dimensional radius (r/R) Overload fraction Distance from the leading edge of a blade section
x_b	Non-dimensional boss radius
\bar{x}	Non dimensional radius of the blade centroid
y_c	Distance normal to the axis between the centroids of the blade and the root section

$y_c(x)$	Camber distribution of blade section
$y_t(x)$	Thickness distribution of blade section
z_c	Distance parallel to the axis between the centroids of the blade and the root section
Z	Number of blades in propeller
Z_V	Number of blades in vane wheel
$1 + k$	Form factor
$1 + x$	Load factor
α	Angle of attack Duct dihedral angle
α_i	Ideal angle of attack
α_t	Angle of attack correction for blade thickness
α_0	No-lift angle
β	Duct exit angle Hydrodynamic pitch angle excluding induced velocities
β_I	Hydrodynamic pitch angle including induced velocities
γ	Angle related to lift-drag ratio
Γ	Circulation
δ	Taylor advance coefficient
δP	Increase in average power in waves

δR	Resistance augment
δT	Thrust deduction
Δ	Displacement of the ship
ΔC_D	Change in drag coefficient due to roughness
ΔC_F	Roughness allowance
ΔC_{FC}	Correlation allowance for frictional resistance coefficient
ΔC_L	Change in lift coefficient due to roughness
ΔK_Q	Change in torque coefficient due to roughness
ΔK_T	Change in thrust coefficient due to roughness
Δp	Pressure difference
ΔP_E	Increase in effective power due to wind
ΔV	Speed correction for effect of wind
Δw_c	Correlation allowance for wake fraction
ε	Rake angle
ε_E	Effective rake angle
$\bar{\zeta}$	Average wave amplitude
η	Efficiency
η_B	Propeller efficiency in the behind condition
η_D	Propulsive efficiency
η_H	Hull efficiency
η_i	Ideal efficiency

η_{iJ}	Ideal jet efficiency
η_I	Inlet efficiency
η_J	Jet efficiency
η_N	Nozzle efficiency
$\eta_{overall}$	Overall propulsive efficiency
η_O	Propeller open water efficiency
η_P	Pump efficiency
η_{PO}	Pump efficiency in open water (uniform inflow)
η_R	Relative rotative efficiency
η_S	Shafting efficiency
θ	Angular position of the blade Relative wind direction off the bow
θ_S	Skew angle
κ	Coefficient of kinematic capillarity Goldstein factor
λ	Advance ratio Scale ratio (ship dimension : model dimension)
λ_I	Advance ratio including induced velocities
μ	Coefficient of dynamic viscosity Viscous correction factor Propeller coefficient in the set (μ, σ, φ)

Nomenclature

xxxi

ν	Coefficient of kinematic viscosity
ρ	Mass density of water
ρ_a	Density of air
ρ_m	Density of propeller material
σ	Cavitation numbers Propeller coefficient in the set (μ, σ, φ)
$\sigma_{0.7R}$	Cavitation number at $0.7R$
τ	Ratio of propeller thrust to total thrust in a ducted propeller
τ_c	Burrill's thrust loading coefficient
φ	Pitch angle Propeller coefficient in the set (μ, σ, φ)
ψ_E	Effective skew angle
ω	Angular velocity
ω_E	Wave encounter frequency
∇	Volume of displacement

Physical Constants

The following standard values have been used in the examples and problems:

Density of sea water	= 1025 kg per m ³
Density of fresh water	= 1000 kg per m ³
Kinematic viscosity of sea water	= 1.188×10^{-6} m ² per sec
Kinematic viscosity of fresh water	= 1.139×10^{-6} m ² per sec
Acceleration due to gravity	= 9.81 m per sec ²
Atmospheric pressure	= 101.325 kN per m ²
Vapour pressure of water	= 1.704 kN per m ²
1 knot	= 0.5144 m per sec
1 hp	= 0.7457 kW

Contents

	DEDICATION	v
	ACKNOWLEDGEMENTS	vii
	PREFACE	xi
	GLOSSARY	xiii
	NOMENCLATURE	xvii
	PHYSICAL CONSTANTS	xxxiii
CHAPTER 1	GENERAL INTRODUCTION	1
1.1	Ships	1
1.2	Propulsion Machinery	2
1.3	Propulsion Devices	3
CHAPTER 2	SCREW PROPELLERS	6
2.1	Description	6
2.2	Propeller Geometry	10
2.3	Propeller Blade Sections	15
2.4	Alternative Definition of Propeller Geometry	17
2.5	Pitch	19
2.6	Non-dimensional Geometrical Parameters	21
2.7	Mass and Inertia	24

CHAPTER 3	PROPELLER THEORY	28
3.1	Introduction	28
3.2	Axial Momentum Theory	29
3.3	Momentum Theory Including Rotation	34
3.4	Blade Element Theory	39
3.5	Circulation Theory	45
3.6	Further Development of the Circulation Theory	56
CHAPTER 4	THE PROPELLER IN "OPEN" WATER	60
4.1	Introduction	60
4.2	Laws of Similarity	61
4.3	Dimensional Analysis	64
4.4	Laws of Similarity in Practice	66
4.5	Open Water Characteristics	74
4.6	Methodical Propeller Series	78
4.7	Alternative Forms of Propeller Coefficients	82
CHAPTER 5	THE PROPELLER "BEHIND" THE SHIP	94
5.1	Introduction	94
5.2	Wake	95
5.3	Thrust Deduction	99
5.4	Relative Rotative Efficiency	100
5.5	Power Transmission	103
5.6	Propulsive Efficiency and its Components	106
5.7	Estimation of Propulsion Factors	111
CHAPTER 6	PROPELLER CAVITATION	115
6.1	The Phenomenon of Cavitation	115
6.2	Cavitation Number	119
6.3	Types of Propeller Cavitation	121

6.4	Effects of Cavitation	124
6.5	Prevention of Cavitation	126
6.6	Cavitation Criteria	128
6.7	Pressure Distribution on a Blade Section	135
CHAPTER 7	STRENGTH OF PROPELLERS	140
7.1	Introduction	140
7.2	Bending Moments due to Thrust and Torque	142
7.3	Bending Moments due to Centrifugal Force	148
7.4	Stresses in a Blade Section	151
7.5	Approximate Methods	155
7.6	Classification Society Requirements	163
7.7	Propeller Materials	166
7.8	Some Additional Considerations	167
CHAPTER 8	PROPULSION MODEL EXPERIMENTS	179
8.1	Introduction	179
8.2	Resistance Experiments	180
8.3	Open Water Experiments	185
8.4	Self-propulsion Experiments	190
8.5	Wake Measurements	201
8.6	Cavitation Experiments	207
CHAPTER 9	PROPELLER DESIGN	216
9.1	Propeller Design Approaches	216
9.2	General Considerations in Propeller Design	217
9.3	Propeller Design using Methodical Series Data	222
9.4	Design of Towing Duty Propellers	236
9.5	Propeller Design using Circulation Theory	250

CHAPTER 10	SHIP TRIALS AND SERVICE PERFORMANCE	277
10.1	Introduction	277
10.2	Dock Trials	278
10.3	Speed Trials	279
10.4	Bollard Pull Trials	294
10.5	Service Performance Analysis	294
CHAPTER 11	SOME MISCELLANEOUS TOPICS	308
11.1	Unsteady Propeller Loading	308
11.2	Vibration and Noise	319
11.3	Propulsion in a Seaway	327
11.4	Propeller Roughness	331
11.5	Propeller Manufacture	338
11.6	Acceleration and Deceleration	343
11.7	Engine-Propeller Matching	347
CHAPTER 12	UNCONVENTIONAL PROPULSION DEVICES	359
12.1	Introduction	359
12.2	Paddle Wheels	360
12.3	Controllable Pitch Propellers	365
12.4	Ducted Propellers	369
12.5	Supercavitating Propellers	386
12.6	Surface Propellers	391
12.7	Contra-rotating Propellers	401
12.8	Tandem Propellers	402
12.9	Overlapping Propellers	404
12.10	Other Multiple Propeller Arrangements	406
12.11	Vane Wheel Propellers	408
12.12	Other Unconventional Screw Propellers	410

Contents

xxxix

12.13	Cycloidal Propellers	412
12.14	Waterjet Propulsion	420
12.15	Flow Improvement Devices	431
12.16	Design Approach	436

APPENDICES

1	Some Properties of Air and Water	440
2	Aerofoil Sections used in Marine Propellers	442
3	Propeller Methodical Series Data	444
4	Propulsion Factors	465
5	Propeller Blade Section Pressure Distribution	477
6	Goldstein Factors	482
7	Cavitation Buckets	484
8	Lifting Surface Correction Factors	485

REVIEW QUESTIONS	489
------------------	-----

MISCELLANEOUS PROBLEMS	496
------------------------	-----

ANSWERS TO PROBLEMS	514
---------------------	-----

BIBLIOGRAPHY	540
--------------	-----

INDEX	553
-------	-----

CHAPTER 1

General Introduction

1.1 Ships

The Earth may be regarded as a “water planet”, since 71 percent of its surface is covered by water having an average depth of 3.7 km. Transportation across the oceans must therefore have engaged the attention of humankind since the dawn of history. Ships started thousands of years ago as simple logs or bundles of reeds and have developed into the huge complicated vessels of today. Wooden sailing ships are known to have appeared by about 1500 BC and had developed into vessels sailing around the world by about 1500 AD. Mechanical propulsion began to be used in ships by the beginning of the 19th Century, and iron followed by steel gradually took the place of wood for building large oceangoing ships, with the first iron-hulled ship, the “Great Britain”, being launched in 1840.

Ships today can be characterised in several ways. From the point of view of propulsion, ships may be either self-propelled or non-propelled requiring external assistance to move from one point to another. Ships may be ocean-going or operating in coastal waters or inland waterways. Merchant ships which engage in trade are of many different kinds such as tankers, bulk carriers, dry cargo ships, container vessels and passenger ships. Warships may be divided into ships that operate on the surface of water such as frigates and aircraft carriers, and ships that are capable of operating under water, viz. submarines. There are also vessels that provide auxiliary services such as tugs and dredgers. Fishing vessels constitute another important ship type.

Most of these types of ships have very similar propulsion arrangements. However, there are some types of very high speed vessels such as hovercraft and hydrofoil craft that make use of unconventional propulsion systems.

1.2 Propulsion Machinery

For centuries, ships were propelled either by human power (e.g. by oars) or by wind power (sails). The development of the steam engine in the 18th Century led to attempts at using this new source of power for ship propulsion, and the first steam driven ship began operation in Scotland in 1801. The early steam engines were of the reciprocating type. Steam was produced in a boiler from raw sea water using wood or coal as fuel. Gradual advances in steam propulsion plants took place during the 19th Century, including the use of fresh water instead of sea water and oil instead of coal, improvements in boilers, the use of condensers and the development of compound steam engines. Reciprocating steam engines were widely used for ship propulsion till the early years of the 20th Century, but have since then been gradually superseded by steam turbines and diesel engines.

The first marine steam turbine was fitted in the vessel "Turbinia" in 1894 by Sir Charles Parsons. Since then, steam turbines have completely replaced reciprocating steam engines in steam ships. Steam turbines produce less vibration than reciprocating engines, make more efficient use of the high steam inlet pressures and very low exhaust pressures available with modern steam generating and condensing equipment, and can be designed to produce very high powers. On the other hand, turbines run at very high speeds and cannot be directly connected to ship propellers; nor can turbines be reversed. This makes it necessary to adopt special arrangements for speed reduction and reversing, the usual arrangements being mechanical speed reduction gearing and a special astern turbine stage, or a turbo-electric drive. These arrangements add to the cost and complexity of the propulsion plant and also reduce its efficiency.

Since its invention in 1892, the diesel engine has continued to grow in popularity for use in ship propulsion and is today the most common type of engine used in ships. Diesel engines come in a wide range of powers and speeds, are capable of using low grade fuels, and are comparatively efficient.

Low speed diesel engines can be directly connected to ship propellers and can be reversed to allow the ship to move astern.

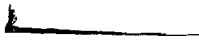
Another type of engine used for ship propulsion is the gas turbine. Like the steam turbine, the gas turbine runs at a very high speed and cannot be reversed. Gas turbines are mostly used in high speed ships where their low weight and volume for a given power give them a great advantage over other types of engines.

Nuclear energy has been tried for ship propulsion. The heat generated by a nuclear reaction is used to produce steam to drive propulsion turbines. However, the dangers of nuclear radiation in case of an accident have prevented nuclear ship propulsion from being used in non-combatant vessels except for a few experimental ships such as the American ship "Savannah", the German freighter "Otto Hahn" and the Russian icebreaker "V.I. Lenin". Nuclear propulsion has been used in large submarines with great success because nuclear fuel contains a large amount of energy in a very small mass, and because no oxygen is required for generating heat. This enables a nuclear submarine to travel long distances under water, unlike a conventional submarine which has to come to the surface frequently to replenish fuel and air for combustion.

In addition to the conventional types of ship propulsion plant discussed in the foregoing, attempts are being made to harness renewable and non-polluting energy sources such as solar energy, wind energy and wave energy for ship propulsion and to develop advanced technologies such as superconductivity and magneto-hydrodynamics. However, these attempts are still in a preliminary experimental stage.

1.3 Propulsion Devices

Until the advent of the steam engine, ships were largely propelled by oars imparting momentum to the surrounding water or by sails capturing the energy of the wind. The first mechanical propulsion device to be widely used in ships was the paddle wheel, consisting of a wheel rotating about a transverse axis with radial plates or paddles to impart an astern momentum to the water around the ship giving it a forward thrust. The early steamers of the 19th Century were all propelled by paddle wheels. Paddle wheels



are quite efficient when compared with other propulsion devices but have several drawbacks including difficulties caused by the variable immersion of the paddle wheel in the different loading conditions of the ship, the increase in the overall breadth of the ship fitted with side paddle wheels, the inability of the ship to maintain a steady course when rolling and the need for slow running heavy machinery for driving the paddle wheels. Paddle wheels were therefore gradually superseded by screw propellers for the propulsion of oceangoing ships during the latter half of the 19th Century.

The Archimedean screw had been used to pump water for centuries, and proposals had been made to adapt it for ship propulsion by using it to impart momentum to the water at the stern of a ship. The first actual use of a screw to propel a ship appears to have been made in 1804 by the American, Colonel Stevens. In 1828, Josef Ressel of Trieste successfully used a screw propeller in an 18 m long experimental steamship. The first practical applications of screw propellers were made in 1836 by Ericsson in America and Petit Smith in England. Petit Smith's propeller consisted of a wooden screw of one thread and two complete turns. During trials, an accident caused a part of the propeller to break off and this surprisingly led to an increase in the speed of the ship. Petit Smith then improved the design of his propeller by decreasing the width of the blades and increasing the number of threads, producing a screw very similar to modern marine propellers. The screw propeller has since then become the predominant propulsion device used in ships.

Certain variants of the screw propeller are used for special applications. One such variant is to enclose the propeller in a shroud or nozzle. This improves the performance of heavily loaded propellers, such as those used in tugs. A controllable pitch propeller allows the propeller loading to be varied over a wide range without changing the speed of revolution of the propeller. It is also possible to reverse the direction of propeller thrust without changing the direction of revolution. This allows one to use non-reversing engines such as gas turbines. When propeller diameters are restricted and the propellers are required to produce large thrusts, as is the case in certain very high speed vessels, the propellers are likely to experience a phenomenon called "cavitation", which is discussed in Chapter 6. In circumstances where extensive cavitation is unavoidable, the propellers are specially designed to

operate in conditions of full cavitation. Such propellers are popularly known as "supercavitating propellers".

Problems due to conditions of high propeller thrust and restricted diameter, which might lead to harmful cavitation and reduced efficiency, may be avoided by dividing the load between two propellers on the same shaft. Multiple propellers mounted on a single shaft and turning in the same direction are called "tandem propellers". Some improvement in efficiency can be obtained by having the two propellers rotate in opposite directions on coaxial shafts. Such "contra-rotating propellers" are widely used in torpedoes.

Two other ship propulsion devices may be mentioned here. One is the vertical axis cycloidal propeller, which consists of a horizontal disc carrying a number of vertical blades projecting below it. As the disc rotates about a vertical axis, each blade is constrained to turn about its own axis such that all the blades produce thrusts in the same direction. This direction can be controlled by a mechanism for setting the positions of the vertical blades. The vertical axis propeller can thus produce a thrust in any direction, ahead, astern or sideways, thereby greatly improving the manoeuvrability of the vessel. The second propulsion device that may be mentioned is the waterjet. Historically, this is said to be the oldest mechanical ship propulsion device, an English patent for it having been granted to Toogood and Hayes in 1661. In waterjet propulsion, as used today in high speed vessels, an impeller draws water from below the ship and discharges it astern in a high velocity jet just above the surface of water. A device is provided by which the direction of the waterjet can be controlled and even reversed to give good manoeuvrability. Waterjet propulsion gives good efficiencies in high speed craft and is becoming increasingly popular for such craft.

Because of their overwhelming importance in ship propulsion today, this book deals mainly with screw propellers. Other propulsion devices, including variants of the screw propeller, are discussed in Chapter 12.

CHAPTER 2

Screw Propellers

2.1 Description

A screw propeller consists of a number of blades attached to a hub or boss, as shown in Fig. 2.1. The boss is fitted to the propeller shaft through which the power of the propulsion machinery of the ship is transmitted to the propeller. When this power is delivered to the propeller, a turning moment or torque Q is applied making the propeller revolve about its axis with a speed ("revolution rate") n , thereby producing an axial force or thrust T causing the propeller to move forward with respect to the surrounding medium (water) at a speed of advance V_A . The units of these quantities in the SI system are:

- Q : Newton-metres
- n : revolutions per second
- T : Newtons
- V_A : metres per second

The revolution rate of the propeller is often given in terms of revolutions per minute (rpm), and the speed of advance in knots (1 knot = 0.5144 metres per second).

The point on the propeller blade farthest from the axis of revolution is called the blade tip. The blade is attached to the propeller boss at the root. The surface of the blade that one would see when standing behind

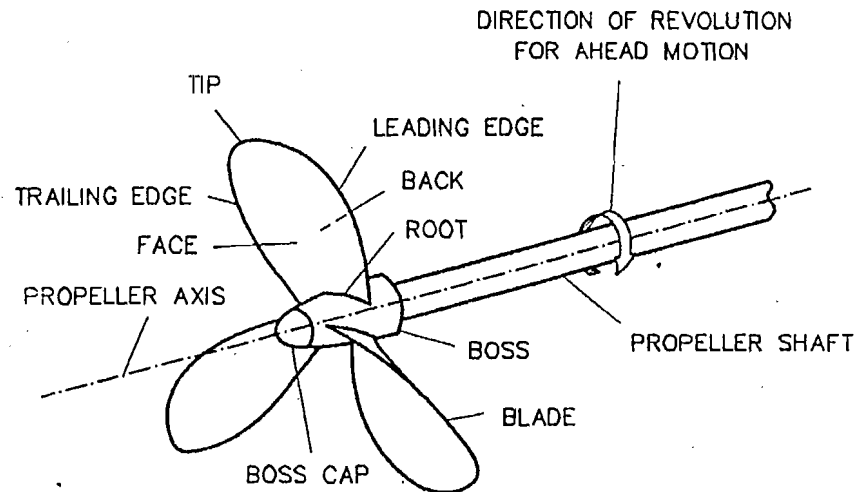


Figure 2.1 : A Three-Bladed Right Hand Propeller.

the ship and looking at the propeller fitted at the stern is called the face of the propeller blade. The opposite surface of the blade is called its back. A propeller that revolves in the clockwise direction (viewed from aft) when propelling the ship forward is called a right hand propeller. If the propeller turns anticlockwise when driving the ship ahead, the propeller is left handed. The edge of the propeller blade which leads the blade in its revolution when the ship is being driven forward is called the leading edge. The other edge is the trailing edge.

When a propeller revolves about its axis, its blade tips trace out a circle. The diameter of this circle is the propeller diameter D . The number of propeller blades is denoted by Z . The face of the propeller blade either forms a part of a helicoidal or screw surface, or is defined with respect to it; hence the name "screw propeller". A helicoidal surface is generated when a line revolves about an axis while simultaneously advancing along it. A point on the line generates a three-dimensional curve called a helix. The distance that the line (or a point on it) advances along the axis in one revolution is called the pitch of the helicoidal surface (or the helix). The pitch of the

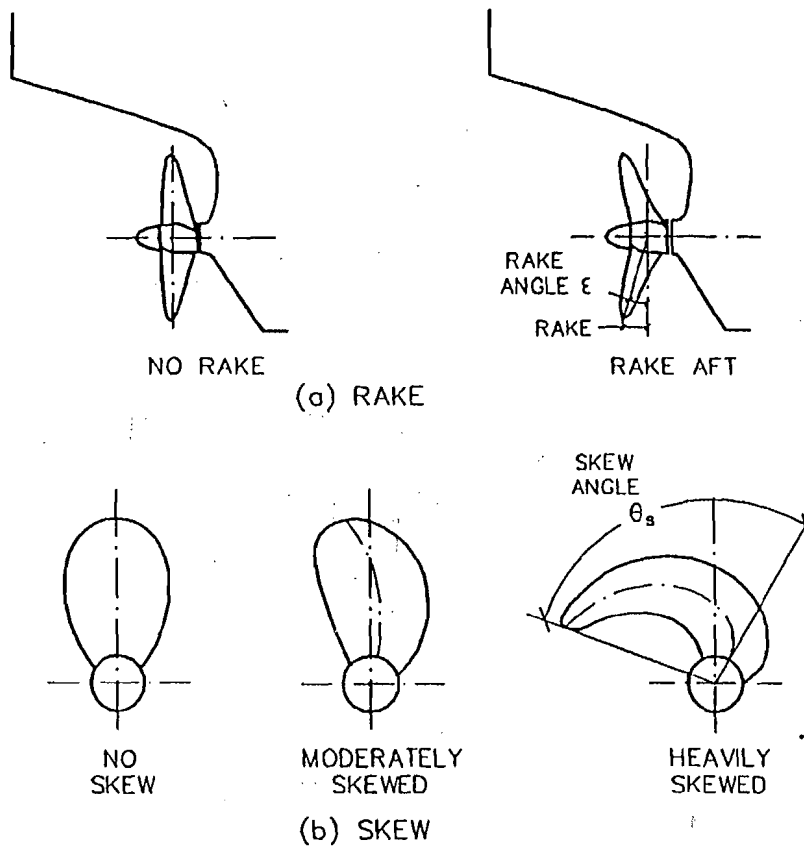


Figure 2.2 : Rake and Skew.

helicoidal surface which defines the face of a propeller blade is called the (face) pitch P of the propeller.

If the line generating the helicoidal surface is perpendicular to the axis about which it rotates when advancing along it, the helicoidal surface and the propeller blade defined by it are said to have no rake. If, however, the generating line is inclined by an angle ϵ to the normal, then the propeller has a rake angle ϵ . The axial distance between points on the generating line at the blade tip and at the propeller axis is the rake. Propeller blades are sometimes raked aft at angles up to 15 degrees to increase the clearance (space) between the propeller blades and the hull of the ship, Fig. 2.2(a).

Consider the line obtained by joining the midpoints between the leading and trailing edges of a blade at different radii from the axis. If this line is straight and passes through the axis of the propeller, the propeller blades have no skew. Usually however, the line joining the midpoints curves towards the trailing edge, resulting in a propeller whose blades are skewed back. Skew is adopted to reduce vibration. Some modern propeller designs have heavily skewed blades. The angle θ_s between a straight line joining the centre of the propeller to the midpoint at the root and a line joining the centre and the midpoint at the blade tip is a measure of skew, Fig. 2.2(b).

Example 1

In a propeller of 4.0 m diameter and 3.0 m constant pitch, each blade face coincides with its defining helicoidal surface. The distance of the blade tip face from a plane normal to the axis is 263.3 mm, while the distance of a point on the face at the root section (radius 400 mm) from the same plane is 52.7 mm, both distances being measured in a plane through the propeller axis. The midpoint of the root section is 69.5 mm towards the leading edge from a plane through the propeller axis, while the blade tip is 1285.6 mm towards the trailing edge from the same plane. Determine the rake and skew angles of the propeller.

The tangent of the rake angle is given by:

$$\begin{aligned}\tan \epsilon &= \frac{\text{difference in rake of the two sections}}{\text{difference in their radii}} = \frac{263.3 - 52.7}{2000 - 400} \\ &= 0.131625\end{aligned}$$

$$\text{Rake angle } \epsilon = 7.5^\circ$$

The angles which the midpoints of the root section and the tip make with the reference plane are given by:

$$\begin{aligned}\sin \theta_0 &= \frac{69.5}{400} = 0.17375 & \theta_0 &= 10.00^\circ \\ \sin \theta_1 &= \frac{-1285.6}{2000} = -0.64280 & \theta_1 &= -40.00^\circ\end{aligned}$$

The skew angle is therefore $(\theta_0 - \theta_1) = 50^\circ$

2.2 Propeller Geometry

The shape of the blades of a propeller is usually defined by specifying the shapes of sections obtained by the intersection of a blade by coaxial right circular cylinders of different radii. These sections are called radial sections or cylindrical sections. Since all the Z propeller blades are identical, only one blade needs to be defined. It is convenient to use cylindrical polar coordinates (r, θ, z) to define any point on the propeller, r being the radius measured from the propeller axis, θ an angle measured from a reference plane passing through the axis, and z the distance from another reference plane normal to the axis. The $z = 0$ reference plane is usually taken to pass through the intersection of the propeller axis and the generating line of the helicoidal surface in the $\theta = 0$ plane.

Consider the section of a propeller blade by a coaxial circular cylinder of radius r , as shown in Fig. 2.3(a). The blade is pointing vertically up. The figure also shows the helix over one revolution defining the blade face at radius r , and the reference planes $\theta = 0$ and $z = 0$. The projections of this figure on a plane perpendicular to the propeller axis and on a horizontal plane are shown in Fig. 2.3(b) and (c). If the surface of the cylinder is now cut along the line AA_1 , joining the two ends of the helix, and the surface unwrapped into a plane, a rectangle of length $2\pi r$ and breadth P (the pitch of the helix) is obtained, the helix being transformed into the diagonal as shown in Fig. 2.3(d). The radial section takes the shape shown in the figure, and this shape is the expanded section at the radius r . The angle $\varphi = \tan^{-1}(P/2\pi r)$ is the pitch angle, and L and T are the leading and trailing edges at the radius r .

The expanded blade section is fundamental to the hydrodynamics of the propeller because its behaviour when advancing at a speed V_A and revolving at a speed n is analogous to the behaviour of an aerofoil of the same shape moving at a velocity obtained by compounding the axial velocity V_A and the tangential velocity $2\pi nr$. The detailed design of a propeller therefore essentially consists in designing the expanded sections. The geometry of the propeller is thus defined through its expanded sections at a number of radii, usually at $r/R = 0.2, 0.3, \dots 1.0$, where $R = 0.5D$ is the propeller radius. The expanded sections at these radii are obtained as shown in Fig. 2.3 and drawn as shown in Fig. 2.4(a). A line joining the projections, L' and T' ,

of the leading and trailing edges on the base line of each section gives the expanded blade outline. The area within the expanded outlines of all the blades is the expanded blade area, A_E .

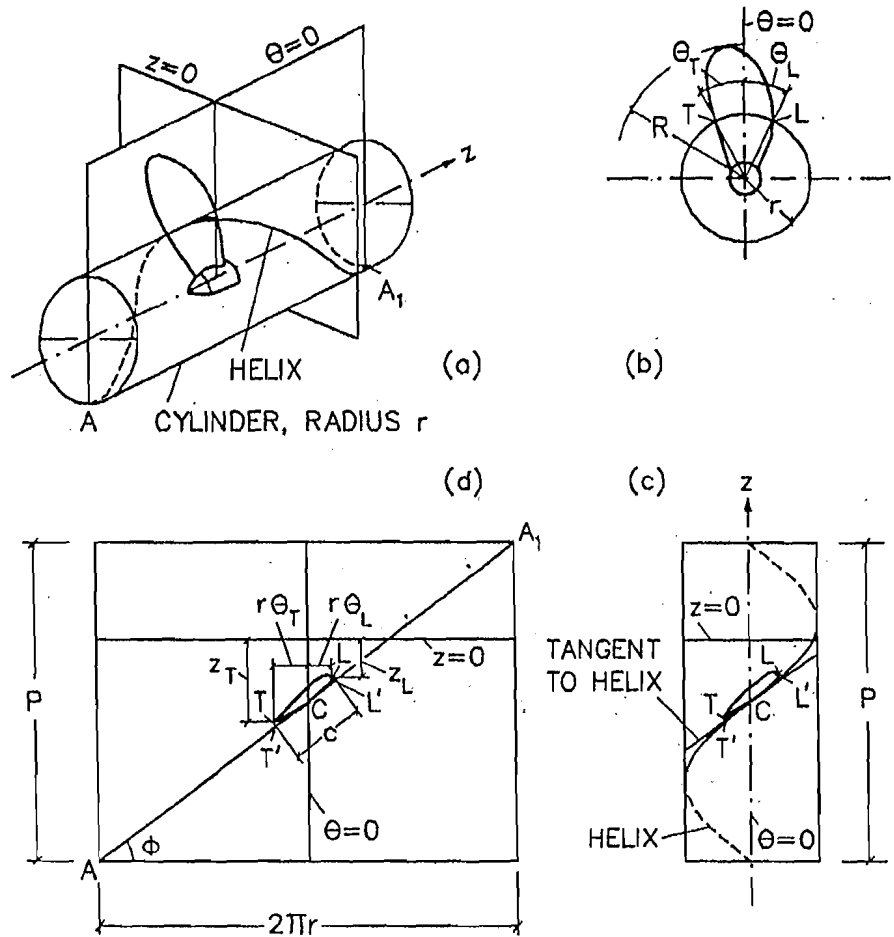


Figure 2.3 : Propeller Blade Cylindrical Section.

Given the expanded blade outline and sections, it is quite simple to obtain the actual shape of the propeller blade as represented by its projections on three orthogonal planes. This is so because from the expanded outline and sections one readily obtains the cylindrical polar coordinates (r, θ, z) of the leading and trailing edges, or indeed of any other point on the propeller blade

surface. It is usually convenient to transform these coordinates to Cartesian coordinates using the axes shown in Fig. 2.4: $x = r \cos \theta$, $y = r \sin \theta$, $z = z$. The blade outline projected on a plane normal to the z -axis is called the projected blade outline, and the area contained within the projected outlines of all the blades is called the projected blade area, A_p .

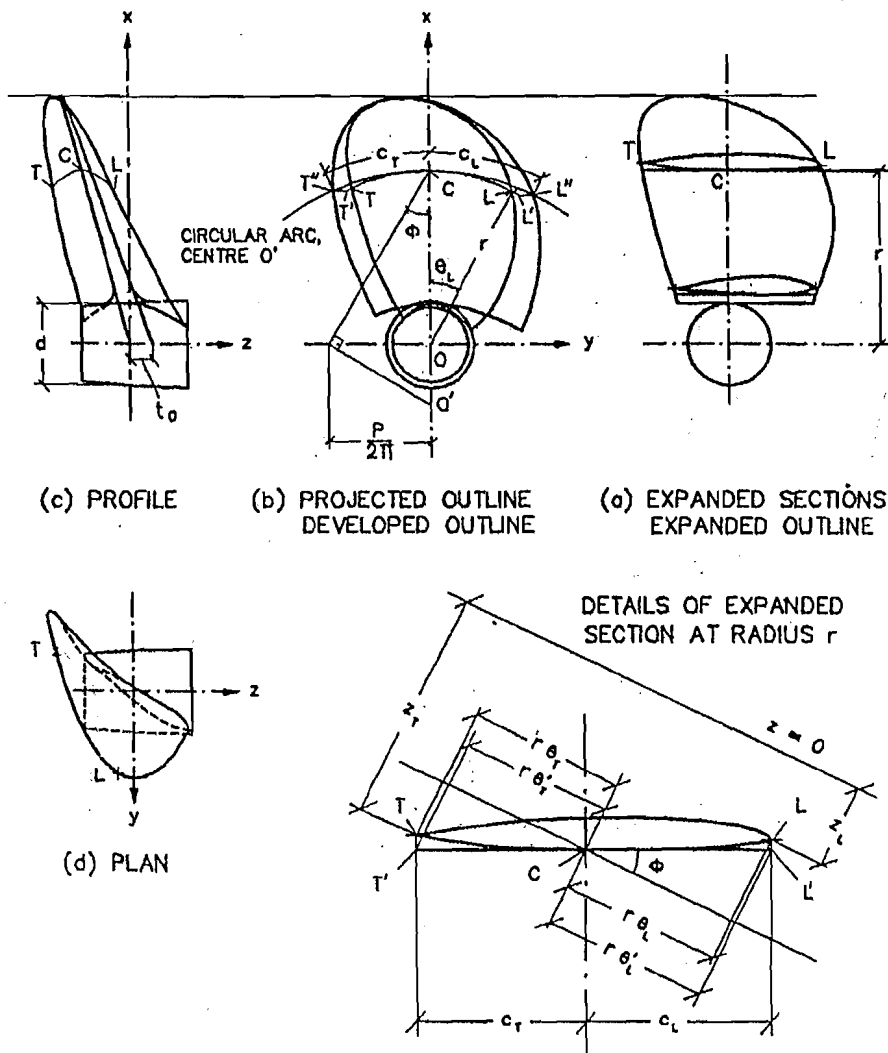


Figure 2.4 : Propeller Drawing.

The projections of the leading and trailing edges of a blade section on a plane tangential to the helix at the point C in Fig. 2.3(d), i.e. L' and T' , are also associated with what is called the developed blade outline. If these tangent planes for the different radial sections are rotated through the pitch angles φ about the point C, the line joining the projections of the leading and trailing edges at the different radii gives the developed blade outline. The intersection of the tangent plane to the helix with the circular cylinder of radius r is an ellipse of semi-major axis $r \sec \varphi$ and semi-minor axis r . Therefore, in order to obtain the points on the developed outline corresponding to L' and T' , it is necessary to draw this ellipse and to move the points L' and T' horizontally to L'' and T'' on the ellipse, Fig. 2.4(b). Alternatively, L'' and T'' may be obtained by measuring off distances equal to CL' and CT' in Fig. 2.4(a) on the circumference of the ellipse as CL'' and CT'' respectively in Fig. 2.4(b). Since drawing an ellipse manually is somewhat tedious, it is usual to approximate the ellipse by a circle having the same radius of curvature as the ellipse at the point C, i.e. $r \sec^2 \varphi$. The centre O'' of this circle may be obtained by the construction shown in Fig. 2.4(b). Paradoxically, the approximation of the ellipse by this circle gives more accurate results because the radius of the circle is exactly equal to the radius of curvature of the helix, which is constant. The developed outline represents what would be obtained if the curved surface of a propeller blade could be developed into a plane. The developed blade outline is sometimes of use during the manufacture of a propeller. The area contained within the developed outlines of all the blades is called the developed blade area, A_D .

A typical propeller drawing consists of the expanded outline and blade sections, the developed outline and the projections of the blade outline on the three orthogonal planes, $x = 0$, $y = 0$ and $z = 0$, as shown in Fig. 2.4. Instead of the projection of the propeller blade on the $x - z$ plane shown in Fig. 2.4(c), the values of z for the leading and trailing edges are sometimes plotted as a function of r to obtain the blade sweep, i.e. the space swept by the blade during its revolution. This is important for determining the clearances of the propeller blade from the hull and the rudder, particularly for heavily skewed blades. The construction lines are naturally not given in the drawing. There are instead a number of additional details. Detailed offsets of the expanded sections are provided. A line showing the variation of the position of maximum thickness with radius is drawn on the expanded outline, and sometimes the loci of the points at which the face of the propeller

blade departs from its base line at the different radii. The offset of the face above its base line is variously called wash-back, wash-up, wash-away or setback, a negative offset (below the base line) being called wash-down. The offsets of the leading and trailing edges are called nose tilt and tail tilt. The distribution of pitch over the radius, if not constant, is shown separately. The variation of maximum blade thickness with radius r and the fillet radii where the blade joins the boss are also indicated. The internal details of the boss showing how it is fitted to the propeller shaft may also be given.

Example 2

In a propeller of 5.0 m diameter and 4.0 m pitch, radial lines from the leading and trailing edges of the section at $0.6R$ make angles of 42.2 and 28.1 degrees with the reference plane through the propeller axis. Determine the width of the expanded blade outline at $0.6R$.

The radius of the section at $0.6R$, $r = 0.6 \times \frac{5}{2} = 1.5 \text{ m} = 1500 \text{ mm}$

The pitch angle at this section is given by:

$$\tan \varphi = \frac{P}{2\pi r} = \frac{4}{2\pi \times 1.5} = 0.4244 \quad \cos \varphi = 0.9205$$

$$\varphi = 22.997^\circ$$

Referring to Fig. 2.3,

$$\theta_L = 42.2^\circ \quad \theta_T = 28.1^\circ \text{ (given)}$$

The width of the expanded outline at $0.6R$ is:

$$c = \frac{r(\theta_L + \theta_T)}{\cos \varphi} \quad \theta_L \text{ and } \theta_T \text{ being in radians}$$

so that,

$$c = \frac{1500 \left[\frac{42.2^\circ + 28.1^\circ}{57.3} \right]}{0.9205} = 1999.2 \text{ mm}$$

This assumes that the section is flat faced, i.e. L and T in Fig. 2.3(c) coincide with L' and T' respectively.

Example 3

The cylindrical polar coordinates (r, θ, z) of the trailing edge of a flat faced propeller blade radial section are (1500 mm, -30° , -400 mm). If the pitch of the propeller is 3.0 m, and the expanded blade width is 2000 mm, determine the coordinates of the leading edge.

The leading and trailing edges of a radial section have the same radius, i.e. $r = 1500$ mm.

The pitch angle is given by:

$$\tan \varphi = \frac{P}{2\pi r} = \frac{3000}{2\pi \times 1500} = 0.3183$$

$$\varphi = 17.657^\circ \quad \cos \varphi = 0.9529 \quad \sin \varphi = 0.3033$$

If the θ coordinates of the leading and trailing edges are θ_L and θ_T , then the expanded blade width c is given by:

$$c = \frac{r(\theta_L - \theta_T)}{\cos \varphi}, \text{ see Fig. 2.3(c)}$$

$$\text{i.e.} \quad 2000 = \frac{1500 [\theta_L^\circ - (-30^\circ)] / 57.3}{0.9529}$$

$$\text{or} \quad \theta_L = 42.80^\circ$$

$$\text{Also,} \quad z_L = z_T + c \sin \varphi$$

$$= -400 + 2000 \times 0.3033 = 206.6 \text{ mm}$$

i.e. the coordinates of the leading edge are (1500 mm, 42.80° , 206.6 mm).

2.3 Propeller Blade Sections

The expanded blade sections used in propeller blades may generally be divided into two types: segmental sections and aerofoil sections. Segmental sections are characterised by a flat face and a circular or parabolic back, the maximum thickness being at the midpoint between the leading and trailing edges, the edges being quite sharp, Fig. 2.5(a). In aerofoil sections, the face

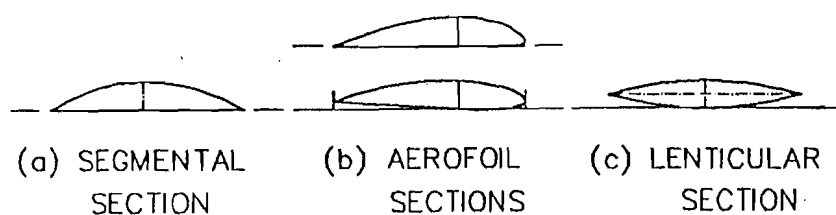
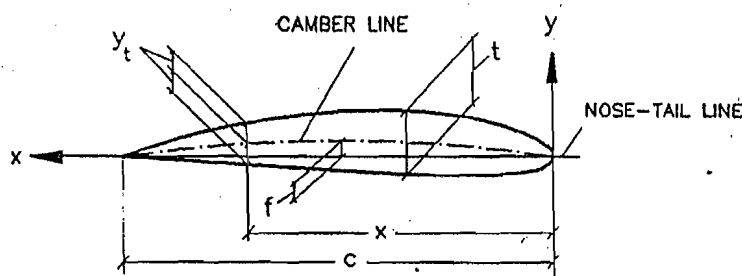


Figure 2.5 : Propeller Blade Sections.

may or may not be flat, the maximum thickness is usually nearer the leading edge, which is often more rounded than the trailing edge, Fig. 2.5(b). More rarely, a propeller may have lens-shaped or lenticular blade sections, Fig. 2.5(c); such sections are used in propellers that are required to work equally efficiently for both directions of revolution.



c = chord t = maximum thickness f = camber
 $y_t(x)$ = thickness distribution

Figure 2.6 : Definition of an Aerofoil Section.

An aerofoil section is usually defined in terms of the mean line or centre line between its lower and upper surfaces, i.e. the face and the back, and a thickness distribution along its length, as shown in Fig. 2.6. The length of the section, or its chord c , is measured between the leading edge or nose and the trailing edge or tail, and the centre line is defined by its offsets $y_c(x)$ from the nose-tail line at different distances x from the leading edge. The offsets of the face and back, $y_t(x)$, are measured from the mean line perpendicular to it. The maximum offset of the mean line is the section camber f and the maximum thickness of the section is its thickness t . Mean lines and thickness

distributions of some aerofoil sections used in marine propellers are given in Appendix 2.

Instead of measuring the section chord on the nose-tail line, it is usual in an expanded propeller blade section to define the chord as the projection of the nose-tail line on the base line, which corresponds to the helix at the given radius, i.e. the chord c is taken as $L'T'$ rather than LT in Fig. 2.3(c) or Fig. 2.4(a). If the resultant velocity of flow to a blade section is V_R as shown in Fig. 2.7, the angle between the base chord and the resultant velocity is

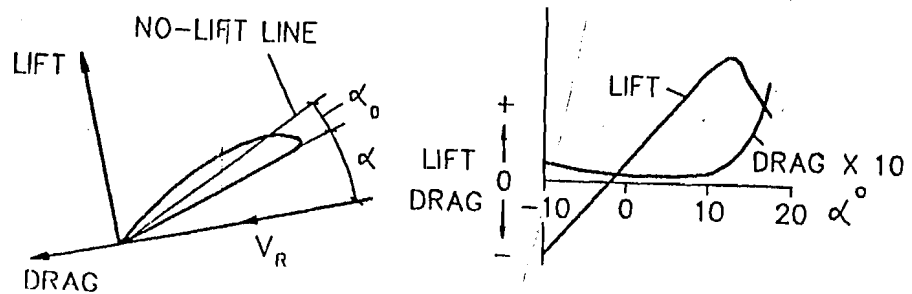


Figure 2.7 : Angle of Attack.

called the angle of attack, α . The blade section then produces a force whose components normal and parallel to V_R are the lift and the drag respectively. For a given section shape, the lift and drag are functions of the angle of attack, and for a certain (negative) angle of attack the lift of the section is zero. This angle of attack is known as the no-lift angle, α_0 .

2.4 Alternative Definition of Propeller Geometry

When a propeller is designed in detail beginning with the design of the expanded sections, the geometry of the propeller is sometimes defined in a slightly different way. The relative positions of the expanded sections are indicated in terms of a blade reference line, which is a curved line in space that passes through the midpoints of the nose-tail lines (chords) of the sections at the different radii. A cylindrical polar coordinate system (r, θ, z) is chosen as shown in Fig. 2.8. The $z = 0$ reference plane is normal to the propeller axis, the $\theta = 0$ plane passes through the propeller axis (z -axis),

and both pass through the blade reference line at the boss. The pitch helix at any radius r passes through the $\theta = 0$ plane at that radius. The angle between the plane passing through the z -axis and containing the point on blade reference line at any radius and the $\theta = 0$ plane is the skew angle θ_S at that radius. The distance of the blade reference line at any radius from the $z = 0$ reference line is the total rake i_T at that radius, and consists of the generator line rake i_G and skew induced rake i_S as shown in Fig. 2.8. Rake aft and skew back (i.e. towards the trailing edge) are regarded as positive. This requires the positive z -axis to be directed aft.

Rake and skew may be combined in such a way as to produce a blade reference line that lies in a single plane normal to the propeller axis. Warp is that particular combination of rake and skew that produces a zero value for the total axial displacement of the reference point of a propeller blade section.

2.5 Pitch

As mentioned earlier, the face of a propeller blade is defined with respect to a helicoidal surface, the pitch of this surface being the face pitch P of the propeller. The helicoidal surface is composed of helices of different radii r from the root to the tip of the propeller blade. If all the helices have the same pitch, the propeller is said to have a constant pitch. If, however, the pitch of the helicoidal surface varies with the radius the propeller has a radially varying or variable pitch. (In theory, it is also possible to have circumferentially varying pitch when the ratio of the velocity of advance to the tangential velocity of the generating line of the helicoidal surface is not constant.) If $P(r)$ is the pitch at the radius r , the mean pitch \bar{P} of the propeller is usually determined by taking the "moment mean":

$$\bar{P} = \frac{\int_{r_b}^R P(r) r \, dr}{\int_{r_b}^R r \, dr} \quad (2.1)$$

r_b being the radius at the root section where the blade joins the boss and R the propeller radius.

- Consider a propeller of diameter D and pitch P operating at a revolution rate n and advancing at a speed V_A . If the propeller were operating in an unyielding medium, like a screw in a nut, it would be forced to move an axial distance nP in unit time. Because the propeller operates in water, the advance per unit time is only V_A , i.e. the propeller slips in the water, the slip being $nP - V_A$. The slip ratio is defined as:

$$s = \frac{nP - V_A}{nP} \quad (2.2)$$

If $V_A = 0$, $s = 1$ and the propeller operates in the 100 percent slip condition. If $V_A = nP$, $s = 0$, and the propeller operates at zero slip. If the value of P used in Eqn. (2.2) is the face (nominal) pitch, s is the nominal slip ratio. However, at zero slip the thrust T of a propeller should be zero, and the effective pitch P_e may be determined in this way, i.e. by putting $P_e = V_A/n$ for $T = 0$. If the effective pitch is used in Eqn. (2.2), one obtains the effective slip ratio, s_e . If in defining slip the speed of the ship V is used instead of the speed of advance V_A , one obtains the apparent slip. (V and V_A are usually not the same).

Example 4

A propeller running at a revolution rate of 120 rpm is found to produce no thrust when its velocity of advance is 11.7 knots and to work most efficiently when its velocity of advance is 10.0 knots. What is the effective pitch of the propeller and the effective slip ratio at which the propeller is most efficient?

$$\text{Effective slip ratio } s_e = \frac{nP_e - V_A}{nP_e}$$

When the propeller produces zero thrust, $s_e = 0$, and:

$$P_e = \frac{V_A}{n} = \frac{11.7 \times 0.5144}{\frac{120}{60}} = 3.0092 \text{ m}$$

When the propeller works most efficiently:

$$s_e = 1 - \frac{V_A}{nP_e} = 1 - \frac{10.0 \times 0.5144}{\frac{120}{60} \times 3.0092} = 0.1453$$

2.6 Non-dimensional Geometrical Parameters

As will be seen in subsequent chapters, the study of propellers is greatly dependent upon the use of scale models. It is therefore convenient to define the geometrical and hydrodynamic characteristics of a propeller by non-dimensional parameters that are independent of the size or scale of the propeller. The major non-dimensional geometrical parameters used to describe a propeller are:

- Pitch ratio P/D : the ratio of the pitch to the diameter of the propeller.
- Expanded blade area ratio A_E/A_O : the ratio of the expanded area of all the blades to the disc area A_O of the propeller, $A_O = \pi D^2/4$. (The developed blade area ratio A_D/A_O and the projected blade area ratio A_P/A_O are similarly defined.)
- Blade thickness fraction t_0/D : the ratio of the maximum blade thickness extrapolated to zero radius, t_0 , divided by the propeller diameter; see Fig. 2.4(c).
- Boss diameter ratio d/D : the ratio of the boss diameter d to the propeller diameter; the boss diameter is measured as indicated in Fig. 2.4(c).

Aerofoil sections are also described in terms of non-dimensional parameters: the camber ratio f/c and the thickness-chord ratio t/c , where c , f and t are defined in Fig. 2.6. The centre line camber distribution and the thickness distribution are also given in a non-dimensional form: $y_c(x)/t$ and $y_t(x)/t$ as functions of x/c .

Example 5

In a four-bladed propeller of 5.0 m diameter, the expanded blade widths at the different radii are as follows:

r/R	:	0.2	0.3	0.4	0.5	0.6	0.7	0.8	0.9	1.0
c mm	:	1454	1647	1794	1883	1914	1876	1724	1384	0

The thickness of the blade at the tip is 15 mm and at $r/R = 0.25$, it is 191.25 mm. The propeller boss is shaped like the frustum of a cone with a length of 900 mm, and has forward and aft diameters of 890 mm and 800 mm. The propeller has a rake of 15 degrees aft and the reference line intersects the axis at the mid-length of the boss. Determine the expanded blade area ratio, the blade thickness fraction and the boss diameter ratio of the propeller.

By drawing the profile (elevation) of the boss, and a line at 15 degrees from its mid-length, the boss diameter is obtained as $d = 834$ mm, giving a boss diameter ratio:

$$\frac{d}{D} = \frac{834}{5000} = 0.1668$$

By drawing the expanded outline (i.e. c as a function of r), the blade width at the root section ($r/R = 0.1668$ or $r = 417$ mm) is obtained as 1390 mm. The area within the blade outline from the root section to $r/R = 0.2$ or $r = 500$ mm is thus:

$$A_1 = \frac{1390 + 1454}{2} (500 - 417) = 118026 \text{ mm}^2$$

The area of the rest of the blade may be obtained by Simpson's First Rule, according to which:

$$\int f(x) dx = \frac{1}{3} \times s \times \sum_{i=1}^n SM_i \times f(x_i)$$

where $1/3$ is the common multiplier, s is the spacing between the n equidistant values of x_i , and SM_i are the Simpson Multipliers 1, 4, 2, 4, ..., 4, 2, 4, 1; n must be an odd integer. Here, c is to be integrated over the radius from $0.2R$ to $1.0R$, the spacing between the radii being $0.1R = 250$ mm. The integration is usually carried out in a table as shown in the following:

$\frac{r}{R}$	c mm	SM	$f(A)$	
0.2	1454	1	1454	
0.3	1647	4	6588	$A_2 = \frac{1}{3} \times 250 \times 39478$ $= 3289833 \text{ mm}^2$
0.4	1794	2	3588	
0.5	1883	4	7532	
0.6	1914	2	3828	
0.7	1876	4	7504	
0.8	1724	2	3448	
0.9	1384	4	5536	
1.0	0	1	0	
			39478	

The expanded blade area of all the four blades is thus:

$$A_E = 4(118026 + 3289833) \text{ mm}^2 = 13.6314 \text{ m}^2$$

The disc area of the propeller is:

$$A_O = \frac{\pi}{4} D^2 = \frac{\pi}{4} \times 5.000^2 = 19.6350 \text{ m}^2$$

The expanded blade area is therefore:

$$\frac{A_E}{A_O} = \frac{13.6314}{19.6350} = 0.6942$$

The blade thickness extrapolated linearly to the shaft axis is:

$$t_0 = t_1 - \frac{t_1 - t_{0.25}}{1 - 0.25} = 15 - \frac{15 - 191.25}{1 - 0.25} = 250 \text{ mm}$$

where t_0 , t_1 and $t_{0.25}$ are the blade thicknesses at $r/R = 0$, 1.0 and 0.25 respectively.
The blade thickness fraction is therefore:

$$\frac{t_0}{D} = \frac{250}{5000} = 0.050.$$

2.7 Mass and Inertia

The mass of a propeller needs to be calculated to estimate its cost, and both the mass and the polar moment of inertia are required for determining the vibration characteristics of the propeller shafting system. The mass and polar moment of inertia of the propeller blades can be easily determined by integrating the areas of the blade sections over the radius. The mass and inertia of the boss must be added. Thus, one may write:

$$M = \rho_m Z \int_{r_b}^R a \, dr + M_{\text{boss}} \quad (2.3)$$

$$I_P = \rho_m Z \int_{r_b}^R a r^2 \, dr + I_{\text{boss}} \quad (2.4)$$

where M and I_P are the mass and polar moment of inertia of the propeller, ρ_m is the density of the propeller material, a the area of the blade section at radius r , and M_{boss} and I_{boss} the mass and polar moment of inertia of the propeller boss, the other symbols having been defined earlier.

The area of a blade section depends upon its chord c and thickness t so that for a blade section of a given type, one may write:

$$a = \text{constant} \times c \times t \quad (2.5)$$

The chords or blade widths at the different propeller radii are proportional to the expanded blade area ratio per blade, while the section thicknesses depend upon the blade thickness fraction. One may therefore write:

$$M = k_m \rho_m \frac{A_E t_0}{A_O D} D^3 + M_{\text{boss}} \quad (2.6)$$

$$I_P = k_i \rho_m \frac{A_E t_0}{A_O D} D^5 + I_{\text{boss}} \quad (2.7)$$

where k_m and k_i are constants which depend upon the shape of the propeller blade sections.

Problems

1. A propeller of 6.0 m diameter and constant pitch ratio 0.8 has a flat faced expanded section of chord length 480 mm at a radius of 1200 mm. Calculate the arc lengths at this radius of the projected and developed outlines.
2. The distances of points on the face of a propeller blade from a plane normal to the axis measured at the trailing edge and at 10 degree intervals up to the leading edge at a radius of 1.75 m are found to be as follows:

	TE							LE
Angle, deg :	-37.5	-30	-20	-10	0	10	20	32.5
Distance, mm:	750	770	828	939	1050	1161	1272	1430

The propeller has a diameter of 5.0 m. The blade section has a flat face except near the trailing edge (TE) and the leading edge (LE). Determine the pitch at this radius. If the propeller has a constant pitch, what is its pitch ratio?

3. The cylindrical polar coordinates (r, θ, z) of a propeller, r being measured in mm from the propeller axis, θ in degrees from a reference plane through the axis and z in mm from a plane normal to the axis, are found to be (1500, 10, 120) at the leading edge and (1500, -15, -180) at the trailing edge at the blade section at $0.6R$. The blade section at this radius has a flat face. Determine the width of the expanded outline at this radius and the position of the reference line, $\theta = 0$, with respect to the leading edge. What is the pitch ratio of the propeller at $0.6R$? The propeller has no rake.
4. The expanded blade widths of a three-bladed propeller of diameter 4.0 m and pitch ratio 0.9 are as follows:

$r/R :$	0.2	0.3	0.4	0.5	0.6	0.7	0.8	0.9	1.0
c mm:	1477	1658	1808	1917	1976	1959	1834	1497	0

Find the expanded, developed and projected blade area ratios of the propeller. Assume that the root section is at $0.2R$, the blade outline is symmetrical and the blade sections are flat faced.

5. The face and back offsets of a propeller blade section with respect to a straight line joining the leading and trailing edges ("nose-tail line") are as follows:

Distance from leading edge	Face offset	Back offset
mm	mm	mm
0	0	0
50	-24.2	37.8

Distance from leading edge	Face offset	Back offset
mm	mm	mm
100	-32.4	54.8
200	-42.5	77.5
300	-48.0	91.1
400	-50.2	98.3
500	-49.4	99.4
600	-45.3	94.3
700	-38.3	82.8
800	-29.1	64.2
900	-19.2	37.1
1000	-5.0	5.0

Determine the thickness-chord ratio and the camber ratio of the section.

6. A propeller of a single screw ship has a diameter of 6.0 m and a radially varying pitch as follows:

r/R :	0.2	0.3	0.4	0.5	0.6	0.7	0.8	0.9	1.0
P/D :	0.872	0.902	0.928	0.950	0.968	0.982	0.992	0.998	1.000

Calculate the mean pitch ratio of the propeller. What is the pitch at $0.7R$?

7. A propeller of 5.0 m diameter and 1.1 effective pitch ratio has a speed of advance of 7.2 m per sec when running at 120 rpm. Determine its slip ratio. If the propeller rpm remains unchanged, what should be the speed of advance for the propeller to have (a) zero slip and (b) 100 percent slip?
8. In a four-bladed propeller of 5.0 m diameter, each blade has an expanded area of 2.16 m^2 . The thickness of the blade at the tip is 15 mm, while at a radius of 625 mm the thickness is 75 mm with a linear variation from root to tip. The boss diameter is 835 mm. The propeller has a pitch of 4.5 m. Determine the pitch ratio, the blade area ratio, the blade thickness fraction and the boss diameter ratio of the propeller.
9. A crudely made propeller consists of a cylindrical boss of 200 mm diameter to which are welded three flat plates set at an angle of 45 degrees to a plane normal to the propeller axis. Each flat plate is 280 mm wide with its inner edge shaped to fit the cylindrical boss and the outer edge cut square so that the distance of its midpoint from the boss is 700 mm. Determine the diameter, the mean pitch ratio and the expanded and projected blade area ratios of this propeller.

10. A three-bladed propeller of diameter 4.0 m has blades whose expanded blade widths and thicknesses at the different radii are as follows:

r/R	:	0.2	0.3	0.4	0.5	0.6	0.7	0.8	0.9	1.0
Width, mm	:	1000	1400	1700	1920	2000	1980	1800	1320	0
Thickness, mm	:	163.0	144.5	126.0	107.5	89.0	70.5	52.0	33.5	15.0

The blade sections are all segmental with parabolic backs, and the boss may be regarded as a cylinder of length 900 mm and inner and outer diameters of 400 mm and 650 mm respectively. The propeller is made of Aluminium Nickel Bronze of density 7600 kg per m^3 . Determine the mass and polar moment of inertia of the propeller.

CHAPTER 3

Propeller Theory

3.1 Introduction

A study of the theory of propellers is important not only for understanding the fundamentals of propeller action but also because the theory provides results that are useful in the design of propellers. Thus, for example, propeller theory shows that even in ideal conditions there is an upper limit to the efficiency of a propeller, and that this efficiency decreases as the thrust loading on the propeller increases. The theory also shows that a propeller is most efficient if all its radial sections work at the same efficiency. Finally, propeller theory can be used to determine the detailed geometry of a propeller for optimum performance in given operating conditions.

Although the screw propeller was used for ship propulsion from the beginning of the 19th Century, the first propeller theories began to be developed only some fifty years later. These early theories followed two schools of thought. In the momentum theories as developed by Rankine, Greenhill and R.E. Froude for example, the origin of the propeller thrust is explained entirely by the change in the momentum of the fluid due to the propeller. The blade element theories, associated with Weissbach, Redtenbacher, W. Froude, Drzewiecki and others, rest on observed facts rather than on mathematical principles, and explain the action of the propeller in terms of the hydrodynamic forces experienced by the radial sections (blade elements) of which the propeller blades are composed. The momentum theories are based on correct fundamental principles but give no indication of

the shape of the propeller. The blade element theories, on the other hand, explain the effect of propeller geometry on its performance but give the erroneous result that the ideal efficiency of a propeller is 100 percent. The divergence between the two groups of theories is explained by the circulation theory (vortex theory) of propellers initially formulated by Prandtl and Betz (1927) and then developed by a number of others to a stage where it is not only in agreement with experimental results but may also be used for the practical design of propellers.

3.2 Axial Momentum Theory

In the axial momentum theory, the propeller is regarded as an "actuator disc" which imparts a sudden increase in pressure to the fluid passing through it. The mechanism by which this pressure increase is obtained is ignored. Further, it is assumed that the resulting acceleration of the fluid and hence the thrust generated by the propeller are uniformly distributed over the disc, the flow is frictionless, there is no rotation of the fluid, and there is an unlimited inflow of fluid to the propeller. The acceleration of the fluid involves a contraction of the fluid column passing through the propeller disc and, since this cannot take place suddenly, the acceleration takes place over some distance forward and some distance aft of the propeller disc. The pressure in the fluid decreases gradually as it approaches the disc, it is suddenly increased at the disc, and it then gradually decreases as the fluid leaves the disc. Consider a propeller (actuator disc) of area A_0 advancing into undisturbed fluid with a velocity V_A . A uniform velocity equal and opposite to V_A is imposed on this whole system, so that there is no change in the hydrodynamic forces but one considers a stationary disc in a uniform flow of velocity V_A . Let the pressures and velocities in the fluid column passing through the propeller disc be p_0 and V_A far ahead, p_1 and $V_A + v_1$ just ahead of the disc, p'_1 and $V_A + v_1$ just behind the disc, and p_2 and $V_A + v_2$ far behind the disc, as shown in Fig. 3.1. From considerations of continuity, the velocity just ahead and just behind the disc must be equal, and since there is no rotation of the fluid, the pressure far behind the propeller must be equal to the pressure far ahead, i.e. $p_2 = p_0$.

The mass of fluid flowing through the propeller disc per unit time is given by:

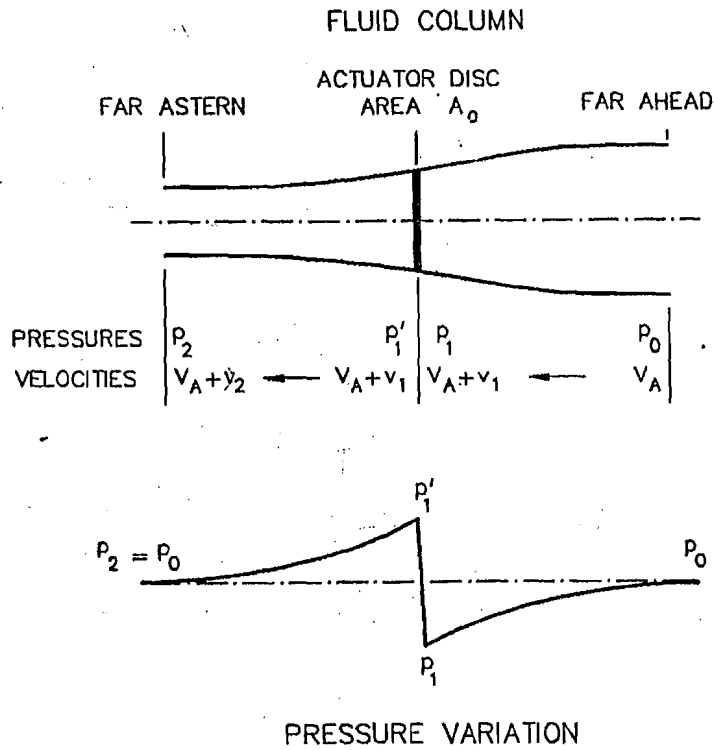


Figure 3.1 : Action of an Actuator Disc in the Axial Momentum Theory.

$$m = \rho A_0 (V_A + v_1) \quad (3.1)$$

where ρ is the density of the fluid. This mass of fluid is accelerated from a velocity V_A to a velocity $V_A + v_2$ by the propeller, and since the propeller thrust T is equal to the change of axial momentum per unit time :

$$T = m (V_A + v_2 - V_A) = \rho A_0 (V_A + v_1) v_2 \quad (3.2)$$

The total power delivered to the propeller P_D is equal to the increase in the kinetic energy of the fluid per unit time, i.e. :

$$\begin{aligned} P_D &= \frac{1}{2} m [(V_A + v_2)^2 - V_A^2] = \rho A_0 (V_A + v_1) v_2 \left(V_A + \frac{1}{2} v_2 \right) \\ &= T \left(V_A + \frac{1}{2} v_2 \right) \end{aligned} \quad (3.3)$$

This delivered power is also equal to the work done by the thrust on the fluid per unit time, i.e.:

$$P_D = T(V_A + v_1) \quad (3.4)$$

It therefore follows that:

$$v_1 = \frac{1}{2} v_2 \quad (3.5)$$

i.e. half the increase in axial velocity due to the propeller takes place ahead of it and half behind it.

The same result may be obtained in a different way. By applying the Bernoulli theorem successively to the sections far ahead and just ahead of the propeller, and to the sections far behind and just behind the propeller, one obtains:

$$p_0 + \frac{1}{2} \rho V_A^2 = p_1 + \frac{1}{2} \rho (V_A + v_1)^2 \quad (3.6)$$

$$p_2 + \frac{1}{2} \rho (V_A + v_2)^2 = p'_1 + \frac{1}{2} \rho (V_A + v_1)^2 \quad (3.7)$$

so that, noting that $p_2 = p_0$:

$$\begin{aligned} p'_1 - p_1 &= \frac{1}{2} \rho [(V_A + v_2)^2 - V_A^2] \\ &= \rho (V_A + \frac{1}{2} v_2) v_2 \end{aligned} \quad (3.8)$$

The propeller thrust is given by:

$$T = (p'_1 - p_1) A_O = \rho A_O (V_A + \frac{1}{2} v_2) v_2 \quad (3.9)$$

so that by comparing Eqns. (3.2) and (3.9), one again obtains Eqn. (3.5).

The useful work done by the propeller per unit time is TV_A . The efficiency of the propeller is therefore:

$$\eta_i = \frac{TV_A}{P_D} = \frac{TV_A}{T(V_A + \frac{1}{2} v_2)} = \frac{1}{1 + \frac{v_1}{V_A}} = \frac{1}{1 + a} \quad (3.10)$$

where $a = v_1/V_A$ is the axial inflow factor, and v_1 and v_2 are the axial induced velocities at the propeller and far behind it. The efficiency η_i is called the "ideal efficiency" because the only energy loss considered is the kinetic energy lost in the fluid column behind the propeller, i.e. in the propeller slipstream, and the other losses such as those due to viscosity, the rotation of the fluid and the creation of eddies are neglected.

The thrust loading coefficient of a propeller is defined as:

$$C_{TL} = \frac{T}{\frac{1}{2} \rho A_O V_A^2} \quad (3.11)$$

Substituting the value of T from Eqn. (3.2) and noting that $v_1 = aV_A$, $v_2 = 2aV_A$, and $a = (1/\eta_i) - 1$, one obtains:

$$\eta_i = \frac{2}{1 + \sqrt{1 + C_{TL}}} \quad (3.12)$$

This is an important result, for it shows that the maximum efficiency of a propeller even under ideal conditions is limited to a value less than 1, and that this efficiency decreases as the thrust loading increases. It therefore follows that for a given thrust, the larger the propeller the greater its efficiency, other things being equal.

Example 1

A propeller of 2.0 m diameter produces a thrust of 30.0 kN when advancing at a speed of 4.0 m per sec in sea water. Determine the power delivered to the propeller, the velocities in the slipstream at the propeller disc and at a section far astern, the thrust loading coefficient and the ideal efficiency.

$$D = 2.0 \text{ m} \quad A_O = \frac{\pi}{4} D^2 = 3.1416 \text{ m}^2 \quad V_A = 4.0 \text{ ms}^{-1}$$

$$T = 30.0 \text{ kN} \quad \rho = 1025 \text{ kg m}^{-3}$$

$$T = \rho A_O (V_A + v_1) 2 v_1$$

so that:

$$1025 \times 3.1416 (4.0 + v_1) 2 v_1 = 30.0 \times 1000$$

which gives:

$$v_1 = 0.9425 \text{ ms}^{-1}$$

$$a = 0.2356$$

$$v_2 = 1.8850 \text{ ms}^{-1}$$

$$\eta_i = \frac{1}{1+a} = 0.8093$$

$$P_D = \frac{T V_A}{\eta_i} = \frac{30.0 \times 4.0}{0.8093} = 148.27 \text{ kW}$$

$$C_{TL} = \frac{T}{\frac{1}{2} \rho A_O V_A^2} = \frac{30.0 \times 1000}{\frac{1}{2} \times 1025 \times 3.1416 \times 4.0^2} = 1.1645$$

⇒ If C_{TL} reduces to zero, i.e. $T = 0$, the ideal efficiency η_i becomes equal to 1. If, on the other hand, V_A tends to zero, η_i also tends to zero, although the propeller still produces thrust. The relation between thrust and delivered power at zero speed of advance is of interest since this condition represents the practical situations of a tug applying a static pull at a bollard or of a ship at a dock trial. For an actuator disc propeller, the delivered power is given by:

$$P_D = \frac{T V_A}{\eta_i} = \frac{1}{2} T V_A (1 + \sqrt{1 + C_{TL}}) \quad (3.13)$$

As V_A tends to zero, $1 + \sqrt{1 + C_{TL}}$ tends to $\sqrt{C_{TL}}$, so that in the limit:

$$\begin{aligned} P_D &= \frac{1}{2} T V_A \sqrt{C_{TL}} = \left[\frac{1}{4} T^2 V_A^2 \frac{T}{\frac{1}{2} \rho A_O V_A^2} \right]^{\frac{1}{2}} \\ &= \left[\frac{T^3}{2 \rho A_O} \right]^{\frac{1}{2}} \end{aligned}$$

that is,

$$\frac{T}{P_D} \sqrt{\frac{T}{\rho A_O}} = \sqrt{2}, \quad V_A = 0 \quad (3.14)$$

This relation between thrust and delivered power at zero velocity of advance for a propeller in ideal conditions thus has a value of $\sqrt{2}$. In actual practice, the value of this relation is considerably less.

Example 2

A propeller of 3.0 m diameter absorbs 700 kW in the static condition in sea water. What is its thrust?

$$D = 3.0 \text{ m} \quad A_O = \frac{\pi}{4} D^2 = 7.0686 \text{ m}^2 \quad P_D = 700 \text{ kW}$$

$$\rho = 1025 \text{ kg m}^{-3}$$

$$T^3 = 2 \rho A_O P_D^2 = 2 \times 1025 \times 7.0686 \times (700 \times 1000)^2 \text{ kg m}^{-3} \text{ m}^2 (\text{N ms}^{-1})^2$$

$$= 7100.39 \times 10^{12} \text{ N}^3$$

$$T = 192.20 \text{ kN}$$

3.3 Momentum Theory Including Rotation

In this theory, also sometimes called the impulse theory, the propeller is regarded as imparting both axial and angular acceleration to the fluid flowing through the propeller disc. Consider a propeller of disc area A_O advancing into undisturbed water with an axial velocity V_A while revolving with an angular velocity ω . Impose a uniform velocity equal and opposite to V_A on the whole system so that the propeller is revolving with an angular velocity ω at a fixed position. Let the axial and angular velocities of the fluid then be $V_A + v_1$ and ω_1 at the propeller disc and $V_A + v_2$ and ω_2 far downstream, as shown in Fig. 3.2. The mass of fluid flowing per unit time through an annular element between the radii r and $r + dr$ is given by:

$$dm = \rho dA_O (V_A + v_1) \quad (3.15)$$

where dA_O is the area of the annular element.

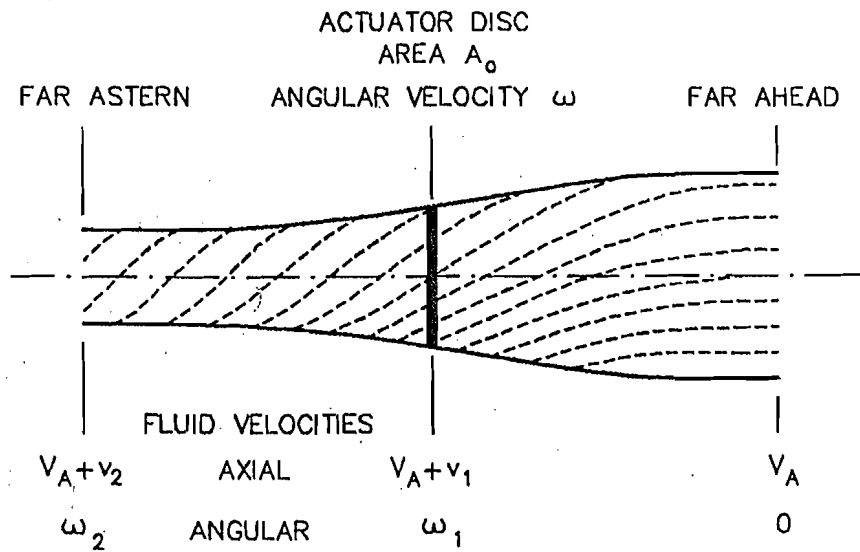


Figure 3.2 : Action of a Propeller in the Impulse Theory.

The thrust developed by the element is determined from the change in the axial momentum of the fluid per unit time:

$$dT = dm [(V_A + v_2) - V_A] = \rho dA_O (V_A + v_1) v_2 \quad (3.16)$$

The torque of the element is similarly obtained from the change in angular momentum per unit time:

$$dQ = dm r^2 (\omega_2 - 0) = \rho dA_O (V_A + v_1) \omega_2 r^2 \quad (3.17)$$

The work done by the element thrust is equal to the increase in the axial kinetic energy of the fluid flowing through the annular element. Per unit time, this is given by:

$$dT(V_A + v_1) = \frac{1}{2} dm [(V_A + v_2)^2 - V_A^2]$$

that is,

$$\rho dA_O (V_A + v_2) v_2 (V_A + v_1) = \frac{1}{2} \rho dA_O (V_A + v_1) v_2 (2 V_A + v_2)$$

so that:

$$v_1 = \frac{1}{2} v_2 \quad (3.18)$$

This is the same result as obtained in the axial momentum theory, Eqn. (3.5). The work done per unit time by the element torque is similarly equal to the increase in the rotational kinetic energy of the fluid per unit time, i.e.:

$$\begin{aligned} dQ \omega_1 &= \frac{1}{2} dm r^2 [\omega_2^2 - 0] \\ &= \frac{1}{2} \rho dA_O (V_A + v_1) \omega_2 r^2 \omega_2 \\ &= \frac{1}{2} dQ \omega_2 \end{aligned}$$

so that,

$$\omega_1 = \frac{1}{2} \omega_2 \quad (3.19)$$

Thus, half the angular velocity of the fluid is acquired before it reaches the propeller and half after the fluid leaves the propeller.

The total power expended by the element must be equal to the increase in the total kinetic energy (axial and rotational) per unit time, or the work done by the element thrust and torque on the fluid passing through the element per unit time:

$$dQ \omega = dT (V_A + v_1) + dQ \omega_1$$

that is,

$$dT (V_A + v_1) = dQ (\omega - \omega_1)$$

and the efficiency of the element is then:

$$\eta = \frac{dT V_A}{dQ \omega} = \frac{(\omega - \omega_1) V_A}{(V_A + v_1) \omega} = \frac{1 - \frac{\omega_1}{\omega}}{1 + \frac{v_1}{V_A}} = \frac{1 - a'}{1 + a} \quad (3.20)$$

where $a' = \omega_1/\omega$ and $a = v_1/V_A$ are the rotational and axial inflow factors, v_1 and v_2 are the axial induced velocities at the propeller and far downstream, ω_1 and ω_2 being the corresponding angular induced velocities. It may be seen by comparing this expression for efficiency, Eqn. (3.20), with the expression obtained in the axial momentum theory, Eqn. (3.10), that the effect of slipstream rotation is to reduce the efficiency by the factor $(1 - a')$.

By making the substitutions:

$$\begin{aligned} dA_O &= 2\pi r dr, & v_1 &= a V_A, & v_2 &= 2a V_A \\ \omega_1 &= a' \omega & \omega_2 &= 2a' \omega \end{aligned}$$

in Eqns. (3.16) and (3.17), one obtains:

$$dT = 4\pi \rho r dr V_A^2 a(1+a) \quad (3.21)$$

$$dQ = 4\pi \rho r^3 dr V_A \omega a'(1+a) \quad (3.22)$$

The efficiency of the annular element is then given by:

$$\eta = \frac{dT V_A}{dQ \omega} = \frac{4\pi \rho r dr V_A^2 a(1+a)V_A}{4\pi \rho r^3 dr V_A \omega a'(1+a)\omega} = \frac{a}{a'} \frac{V_A^2}{\omega^2 r^2} \quad (3.23)$$

Comparing this with Eqn. (3.20), one then obtains:

$$\eta = \frac{a}{a'} \frac{V_A^2}{\omega^2 r^2} = \frac{1-a'}{1+a}$$

or,

$$a'(1-a')\omega^2 r^2 = a(1+a)V_A^2 \quad (3.24)$$

This gives the relation between the axial and rotational induced velocities in a propeller when friction is neglected.

Example 3

A propeller of diameter 4.0 m has an rpm of 180 when advancing into sea water at a speed of 6.0 m per sec. The element of the propeller at $0.7R$ produces a thrust of 200 kN per m. Determine the torque, the axial and rotational inflow factors, and the efficiency of the element.

$$D = 4.0 \text{ m} \quad n = 180 \text{ rpm} = 3.0 \text{ s}^{-1} \quad V_A = 6.0 \text{ m s}^{-1}$$

$$r = 0.7 R = 0.7 \times 2.0 = 1.4 \text{ m} \quad \frac{dT}{dr} = 200 \text{ kN m}^{-1}$$

$$\omega = 2\pi n = 6\pi \text{ radians per sec}$$

$$\frac{dT}{dr} = 4\pi \rho r V_A^2 a(1+a)$$

so that,

$$4\pi \times 1025 \times 1.4 \times 6.0^2 a(1+a) = 200 \times 1000$$

which gives,

$$a = 0.2470$$

$$a'(1-a')\omega^2 r^2 = a(1+a)V_A^2$$

that is,

$$a'(1-a')(6\pi)^2 \times 1.4^2 = 0.2470(1+0.2470) \times 6.0^2$$

or,

$$a' = 0.01619$$

$$\frac{dQ}{dr} = 4\pi \rho r^3 V_A \omega a'(1+a)$$

$$= 4\pi \times 1025 \times 1.4^3 \times 6.0 \times 6\pi \times 0.01619 \times 1.2470$$

$$= 80.696 \text{ kN m m}^{-1}$$

$$\eta = \frac{1-a'}{1+a} = \frac{1-0.01619}{1+0.2470} = 0.7889$$

$$= \frac{\frac{dT}{dr} V_A}{\frac{dQ}{dr} \omega} = \frac{200 \times 6.0}{80.696 \times 6\pi} = 0.7889$$

3.4 Blade Element Theory

The blade element theory, in contrast to the momentum theory, is concerned with how the propeller generates its thrust and how this thrust depends upon the shape of the propeller blades. A propeller blade is regarded as being composed of a series of blade elements, each of which produces a hydrodynamic force due to its motion through the fluid. The axial component of this hydrodynamic force is the element thrust while the moment about the propeller axis of the tangential component is the element torque. The integration of the element thrust and torque over the radius for all the blades gives the total thrust and torque of the propeller.

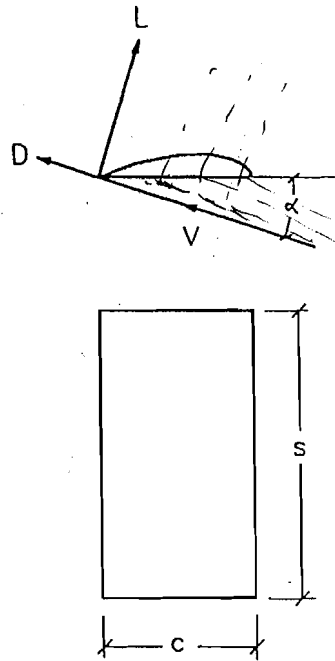


Figure 3.3: Lift and Drag of a Wing.

Consider a wing of chord (width) c and span (length) s at an angle of attack α to an incident flow of velocity V in a fluid of density ρ , as shown in Fig.3.3. The wing develops a hydrodynamic force whose components normal and parallel to V are the lift L and the drag D . One defines non-dimensional lift and drag coefficients as follows:

$$C_L = \frac{L}{\frac{1}{2}\rho A V^2} \quad (3.25)$$

$$C_D = \frac{D}{\frac{1}{2}\rho A V^2}$$

where $A = sc$ is the area of the wing plan form. These coefficients depend upon the shape of the wing section, the aspect ratio s/c and the angle of attack, and are often determined experimentally in a wind tunnel. These experimental values may then be used in the blade element theory, which may thus be said to rest on observed fact.

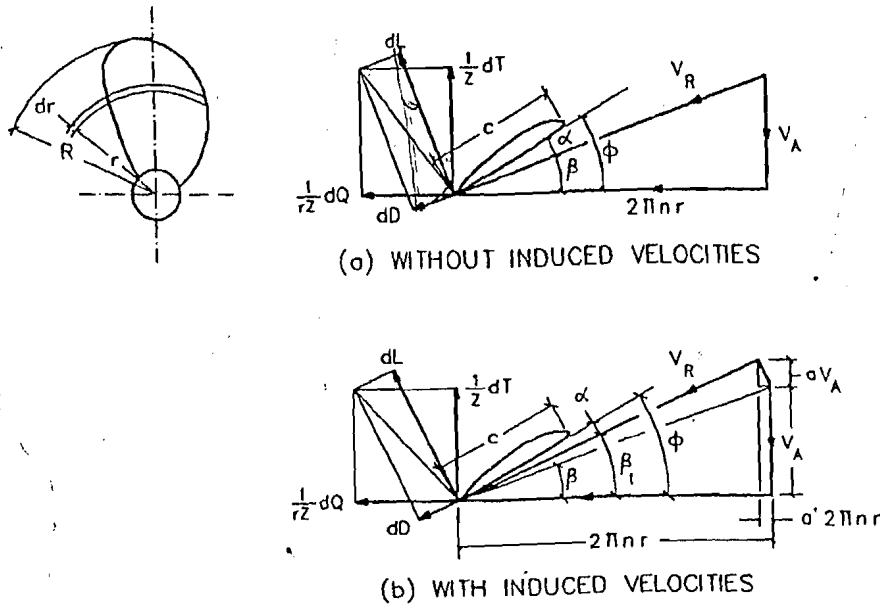
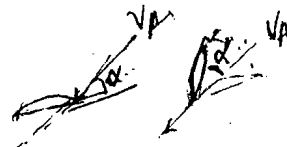


Figure 3.4: Blade Element Velocities and Forces.

Now consider a propeller with Z blades, diameter D and pitch ratio P/D advancing into undisturbed water with a velocity V_A while turning at a revolution rate n . The blade element between the radii r and $r + dr$ when expanded will have an incident flow whose axial and tangential velocity components are V_A and $2\pi nr$ respectively, giving a resultant velocity V_R



at an angle of attack α , as shown in Fig. 3.4(a). The blade element will then produce a lift dL and a drag dD , where:

$$\begin{aligned} dL &= C_L \frac{1}{2} \rho c dr V_R^2 \\ dD &= C_D \frac{1}{2} \rho c dr V_R^2 \end{aligned} \quad (3.26)$$

If the thrust and torque produced by the elements between r and $r + dr$ for all the Z blades are dT and dQ , then from Fig. 3.4(a):

$$\begin{aligned} \frac{1}{Z} dT &= dL \cos \beta - dD \sin \beta = dL \cos \beta \left(1 - \frac{dD}{dL} \tan \beta \right) \\ \frac{1}{rZ} dQ &= dL \sin \beta + dD \cos \beta = dL \cos \beta \left(\tan \beta + \frac{dD}{dL} \right) \end{aligned} \quad (3.27)$$

where

$$\tan \beta = \frac{V_A}{2\pi n r}$$

Putting $\tan \gamma = dD/dL$, and writing dL and dD in terms of C_L and C_D , one obtains:

$$\begin{aligned} dT &= Z C_L \cdot \frac{1}{2} \rho c dr V_R^2 \cos \beta (1 - \tan \beta \tan \gamma) \\ dQ &= r Z C_L \cdot \frac{1}{2} \rho c dr V_R^2 \cos \beta (\tan \beta + \tan \gamma) \end{aligned} \quad (3.28)$$

The efficiency of the blade element is then:

$$\eta = \frac{dT V_A}{dQ 2\pi n r} = \frac{V_A}{2\pi n r} \frac{1 - \tan \beta \tan \gamma}{\tan \beta + \tan \gamma} = \frac{\tan \beta}{\tan (\beta + \gamma)} \quad (3.29)$$

It will be shown later that for a propeller to have the maximum efficiency in given conditions, all its blade elements must have the same efficiency. Eqn. (3.29) thus also gives the efficiency of the most efficient propeller for the specified operating conditions.

✓ If the propeller works in ideal conditions, there is no drag and hence $\tan \gamma = 0$, resulting in the blade element efficiency and hence the efficiency

of the most efficient propeller being $\eta = 1$. This is at variance with the results of the momentum theory which indicates that if a propeller produces a thrust greater than zero, its efficiency even in ideal conditions must be less than 1.

The primary reason for this discrepancy lies in the neglect of the induced velocities, i.e. the inflow factors a, a' . If the induced velocities are taken into account, as shown in Fig. 3.4(b), one obtains:

$$\begin{aligned} dT &= Z C_L \cdot \frac{1}{2} \rho c dr V_R^2 \cos \beta_I (1 - \tan \beta_I \tan \gamma) \\ dQ &= r Z C_L \cdot \frac{1}{2} \rho c dr V_R^2 \cos \beta_I (\tan \beta_I + \tan \gamma) \end{aligned} \quad (3.30)$$

and:

$$\begin{aligned} \eta &= \frac{dT V_A}{dQ 2\pi n} = \frac{V_A}{2\pi n r} \frac{1 - \tan \beta_I \tan \gamma}{\tan \beta_I + \tan \gamma} = \frac{\tan \beta}{\tan(\beta_I + \gamma)} \\ &= \frac{\tan \beta}{\tan \beta_I} \cdot \frac{\tan \beta_I}{\tan(\beta_I + \gamma)} = \frac{1 - a'}{1 + a} \frac{\tan \beta_I}{\tan(\beta_I + \gamma)} \end{aligned} \quad (3.31)$$

since,

$$\tan \beta = \frac{V_A}{2\pi n r} \quad \text{and} \quad \tan \beta_I = \frac{V_A (1 + a)}{2\pi n r (1 - a')} = \tan \beta \frac{1 + a}{1 - a'}$$

In Eqn. (3.31), the expression for efficiency consists of three factors: (i) $1/(1 + a)$, which is associated with the axial induced velocity, Eqn. (3.10), (ii) $(1 - a')$, which reflects the loss due to the rotation of the slipstream, and (iii) $\tan \beta_I / \tan(\beta_I + \gamma)$, which indicates the effect of blade element drag. If there is no drag and $\tan \gamma = 0$, the expression for efficiency, Eqn. (3.31), becomes identical to the expression obtained from the impulse theory, Eqn. (3.20).

In order to make practical use of the blade element theory, it is necessary to know C_L, C_D, a and a' for blade elements at different radii so that dT/dr and dQ/dr can be determined and integrated with respect to the radius r . C_L and C_D may be obtained from experimental data, and a and a' with the help of the momentum theory. Unfortunately, this procedure does not yield realistic results because it neglects a number of factors.

Example 4

A four bladed propeller of 3.0 m diameter and 1.0 constant pitch ratio has a speed of advance of 4.0 m per sec when running at 120 rpm. The blade section at $0.7R$ has a chord of 0.5 m, a no-lift angle of 2 degrees, a lift-drag ratio of 30 and a lift coefficient that increases at the rate of 6.0 per radian for small angles of attack. Determine the thrust, torque and efficiency of the blade element at $0.7R$ (a) neglecting the induced velocities and (b) given that the axial and rotational inflow factors are 0.2000 and 0.0225 respectively.

$$Z = 4 \quad D = 3.0 \text{ m} \quad \frac{P}{D} = 1.0 \quad V_A = 4.0 \text{ m s}^{-1}$$

$$n = 120 \text{ rpm} = 2.0 \text{ s}^{-1}$$

$$x = \frac{r}{R} = 0.7 \quad c = 0.5 \text{ m} \quad \alpha_0 = 2^\circ \quad \frac{C_L}{C_D} = 30$$

$$\frac{\partial C_L}{\partial \alpha} = 6.0 \text{ per radian} \quad \rho = 1025 \text{ kg m}^{-3}$$

(a) Neglecting induced velocities:

$$\tan \varphi = \frac{P/D}{\pi x} = \frac{1.0}{\pi \times 0.7} = 0.4547 \quad \varphi = 24.4526^\circ$$

$$\tan \beta = \frac{V_A}{2\pi n r} = \frac{4.0}{2\pi \times 2.0 \times (0.7 \times 1.5)} = 0.3032 \quad \beta = 16.8648^\circ$$

$$\tan \gamma = \frac{C_D}{C_L} = \frac{1}{30} = 0.03333 \quad \gamma = 1.9091^\circ$$

$$\alpha = \varphi - \beta = 7.5878^\circ$$

$$C_L = \frac{\partial C_L}{\partial \alpha} (\alpha_0 + \alpha) = 6.0 \frac{2 + 7.5878}{180/\pi} = 1.0040$$

$$V_R^2 = V_A^2 + (2\pi n r)^2 = 4.0^2 + (2\pi \times 2.0 \times 1.05)^2 \\ = 190.0998 \text{ m}^2 \text{ s}^{-2}$$

$$\frac{dT}{dr} = Z C_L \frac{1}{2} \rho c V_R^2 \cos \beta (1 - \tan \beta \tan \gamma)$$

$$\frac{dQ}{dr} = r Z C_L \frac{1}{2} \rho c V_R^2 \cos \beta (\tan \beta + \tan \gamma)$$

Substituting the numerical values calculated:

$$\frac{dT}{dr} = 185.333 \text{ kN m}^{-1} \quad \frac{dQ}{dr} = 66.148 \text{ kN m m}^{-1}$$

$$\eta = \frac{\tan \beta}{\tan(\beta + \gamma)} = 0.8918$$

(b) Given: $a = 0.2000$ $a' = 0.0225$

$$\begin{aligned} V_R^2 &= [(1+a) V_A]^2 + [(1-a') 2\pi n r]^2 \\ &= [(1+0.2000) 4.0]^2 + [(1-0.0225) 2\pi \times 2.0 \times 1.05]^2 \\ &= 23.0400 + 166.3535 = 189.3935 \text{ m}^2 \text{ s}^{-2} \end{aligned}$$

$$\tan \beta_I = \frac{V_A (1+a)}{2\pi n r (1-a')} = \frac{4.0 (1+0.2000)}{2\pi \times 2.0 \times 1.05 (1-0.0225)} = 0.3722$$

$$\beta_I = 20.4131^\circ$$

$$\alpha = \varphi - \beta_I = 24.4526 - 20.4131 = 4.0395^\circ$$

$$C_L = \frac{\partial C_L}{\partial \alpha} (\alpha_0 + \alpha) = 6.0 \frac{2 + 4.0395}{\frac{180}{\pi}} = 0.6325$$

Substituting these values in:

$$\frac{dT}{dr} = Z C_L \frac{1}{2} \rho c V_R^2 \cos \beta_I (1 - \tan \beta_I \tan \gamma)$$

$$\frac{dQ}{dr} = r Z C_L \frac{1}{2} \rho c V_R^2 \cos \beta_I (\tan \beta_I + \tan \gamma)$$

one obtains:

$$\frac{dT}{dr} = 113.640 \text{ kN m}^{-1}$$

$$\frac{dQ}{dr} = 48.991 \text{ kN m m}^{-1}$$

$$\eta = \frac{1 - a'}{1 + a} \frac{\tan \beta_I}{\tan(\beta_I + \gamma)} = \frac{1 - 0.0225}{1 + 0.2000} \times \frac{0.3722}{0.4104} = 0.7383$$

3.5 Circulation Theory

The circulation theory or vortex theory provides a more satisfactory explanation of the hydrodynamics of propeller action than the momentum and blade element theories. The lift produced by each propeller blade is explained in terms of the circulation around it in a manner analogous to the lift produced by an aircraft wing, as described in the following.

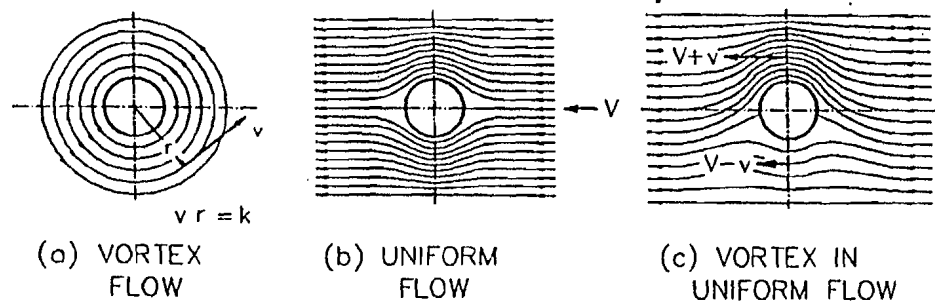


Figure 3.5 : Flow of an Ideal Fluid around a Circular Cylinder.

Consider a flow in which the fluid particles move in circular paths such that the velocity is inversely proportional to the radius of the circle, Fig. 3.5(a). Such a flow is called a vortex flow, and the axis about which the fluid particles move in a three dimensional flow is called a vortex line. In an ideal fluid, a vortex line cannot end abruptly inside the fluid but must either form a closed curve or end on the boundary of the fluid (Helmholz theorem). A circular cylinder placed in a uniform flow of an ideal fluid, Fig. 3.5(b), will experience

no force because of the symmetry of the velocity and pressure distributions around the cylinder (D'Alembert's paradox). If, however, a vortex flow is superposed on the uniform flow, there will be an asymmetry in the flow, the resultant velocity will increase and the pressure decrease on one side of the cylinder as compared to the other, resulting in a force (lift) normal to the direction of the uniform flow, Fig. 3.5(c).

The line integral of the velocity along a closed curve around the cylinder is called circulation. If the cylinder is placed in a uniform flow of velocity V on which is superposed a vortex flow such that the velocity tangential to a circle of radius r is given by $v = k/r$, then the circulation Γ obtained by taking the line integral around the circle of radius r is:

$$\Gamma = \oint v ds = \int_0^{2\pi} \frac{k}{r} r d\theta = 2\pi k \quad (3.32)$$

The contribution due to the uniform velocity V is zero, the contribution on one side of the cylinder cancelling that on the other. The circulation is independent of r , and it can be shown that the same value is obtained for any closed curve around the cylinder by transforming the curve into radial and tangential segments.

The flow past an aerofoil can be regarded as composed of a uniform flow of velocity V and a vortex flow of circulation Γ , the resulting asymmetry in the flow causing the aerofoil to develop a lift. This lift per unit length (span) of the aerofoil is given by the Kutta-Joukowski theorem:

$$L = \rho \Gamma V \quad (3.33)$$

where the circulation Γ depends upon the shape of the aerofoil and its angle of attack. A simple but non-rigorous proof of this result can be obtained as follows.

Referring to Fig. 3.6, let the tangential velocity due to the circulation be v . If the pressure on the upper and lower surfaces of the aerofoil at a section a distance x from the leading edge are p_u and p_l , then by the Bernoulli theorem:

$$p_u + \frac{1}{2} \rho (V + v)^2 = p_l + \frac{1}{2} \rho (V - v)^2$$

so that the difference between the pressures on the lower and upper surfaces of the aerofoil at the section is:

$$\Delta p = p_l - p_u = 2 \rho V v$$

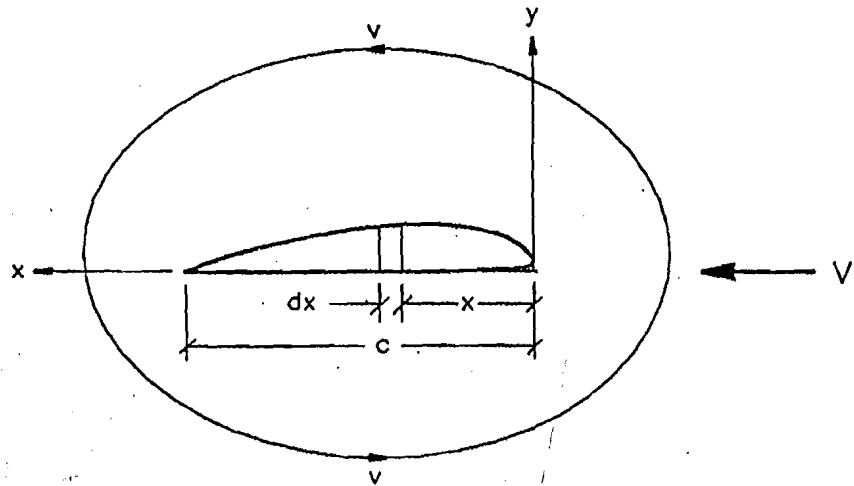


Figure 3.6 : Circulation around an Aerofoil.

If the x-coordinate of the trailing edge is x_1 , the lift produced by the aerofoil per unit length (span) is:

$$L = 1 \cdot \int_0^{x_1} \Delta p dx = \rho V \int_0^{x_1} 2v dx = \rho \left[\int_0^{x_1} v dx + \int_{x_1}^0 -v dx \right] V$$

$$= \rho \Gamma V$$

as given in Eqn. (3.33).

If a wing of infinite aspect ratio with an aerofoil cross-section is given a velocity V , the flow around it is initially as shown in Fig. 3.7(a), with a stagnation point S_1 near the leading edge and a stagnation point S_2 upstream of the trailing edge on the upper surface with flow taking place around the trailing edge towards S_2 in an adverse pressure gradient. Such a flow is unstable and as a result a vortex is shed from the trailing edge causing the stagnation point S_2 to move to the trailing edge and a circulation to develop around the wing, Fig. 3.7(b). The vortex, which is shed from the aerofoil at the start of the flow is called the starting vortex while the vortex associated with the circulation around the wing is called the bound vortex.

In a wing of finite span, the starting vortex and the bound vortex cannot end abruptly in the fluid and there must exist vortex lines which connect the

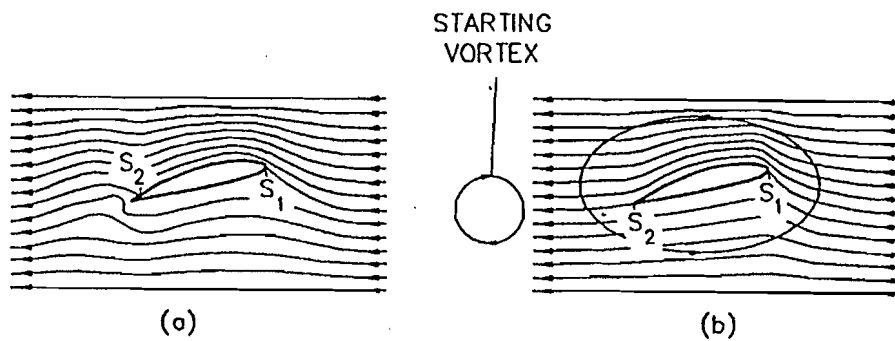


Figure 3.7 : Start of Flow past an Aerofoil.

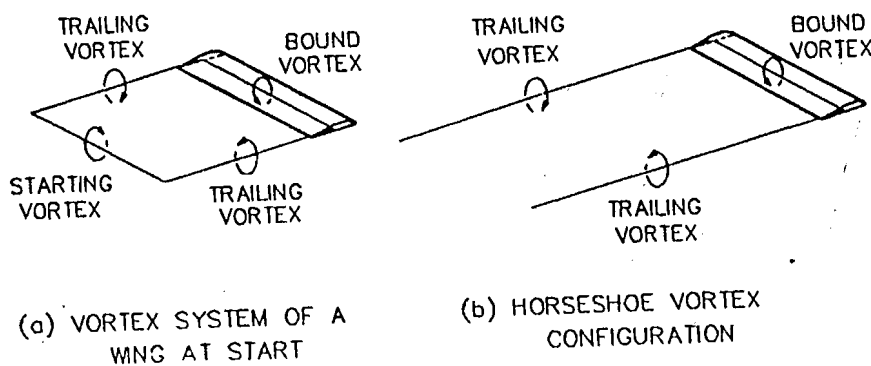


Figure 3.8 : Vortex System of a Wing of Finite Span.

ends of the starting vortex and the bound vortex, as shown in Fig. 3.8(a). These vortex lines which are shed downstream from the wing tips are called trailing vortices. These trailing vortices, which are aligned parallel to the velocity V in contrast to the bound vortex which is at right angles to V , belong to the class of free vortices which do not produce lifting forces. In the course of time, the starting vortex is left far downstream of the wing, and the vortex system has a horseshoe shape, Fig. 3.8(b). The trailing vortices induce a downward velocity in the flow behind the wing. The magnitude of this velocity far behind the wing is twice that at the wing because the trailing vortices extend infinitely in both directions far behind the wing while at the wing the trailing vortices extend infinitely only in one direction.

In the vortex system shown in Fig. 3.8, the circulation along the span of the wing has been taken to be constant. Actually, however, the circulation in a wing of finite span decreases from a maximum at mid-span to zero at the ends, and this is represented by the vortex system shown in Fig. 3.9. The trailing vortices are shed not only from the wing tips but from all along

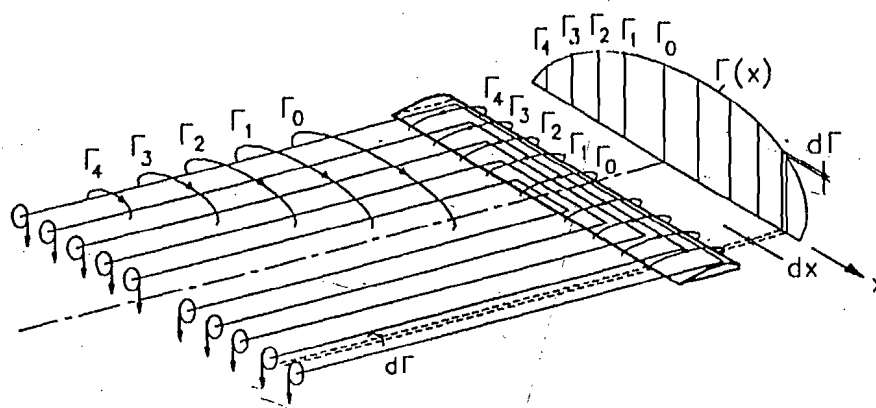


Figure 3.9 : Vortex System of a Wing with Circulation Varying along the Span.

the trailing edge, forming a vortex sheet. The strength of a free vortex shed from any element along the trailing edge is equal to the change in circulation across that element.

The vortex system of a propeller is similar to that of a wing as described in the foregoing. Each blade of the propeller is represented by a bound vortex or lifting line of strength varying along the length of the blade, and a vortex sheet is shed from the trailing edge. Since the propeller revolves about its axis while simultaneously advancing along it, this trailing vortex sheet is helicoidal in shape, and there are as many such vortex sheets as there are blades in the propeller. These trailing vortex sheets produce induced velocities that are perpendicular to the vortex sheets, the induced velocity at the blade being half the induced velocity far downstream.

Consider a propeller with Z blades and diameter D advancing in an inviscid fluid with a velocity V_A while turning at a revolution rate n . Let the circulation at a radius r of the blade be Γ , and let the induced velocity far downstream be u with axial and tangential components u_a and u_t . A

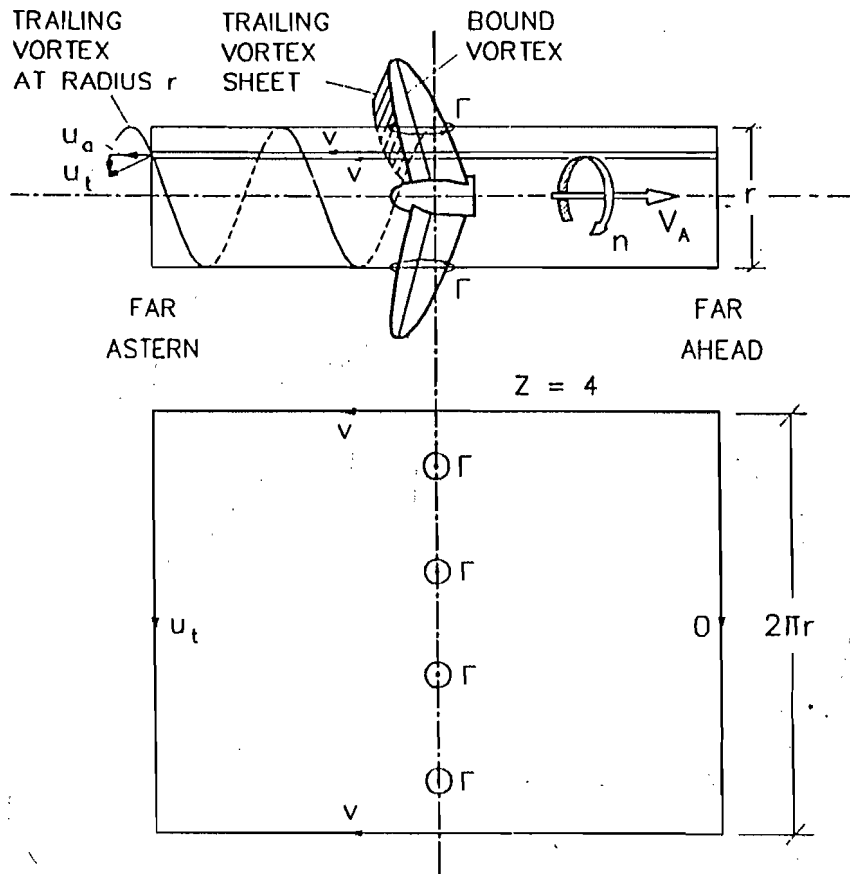


Figure 3.10 : Vortex System of a Propeller.

relationship between the circulation Γ and the induced velocity u_t is found by taking the line integral of the velocity along the closed curve defined by the ends of a cylinder of radius r extending from far ahead of the propeller to far behind it, the end circles being connected by two parallel straight lines very close to each other, as shown in Fig. 3.10. The velocity along the circle far ahead is zero and along the circle far astern is u_t . The line integrals along the two parallel straight lines cancel each other, so that the circulation is obtained as:

$$Z\Gamma = 2\pi r u_t \quad (3.34)$$

provided that there are so many blades Z that u_t is constant along the circle far astern. The effect of a finite number of blades is considered later.

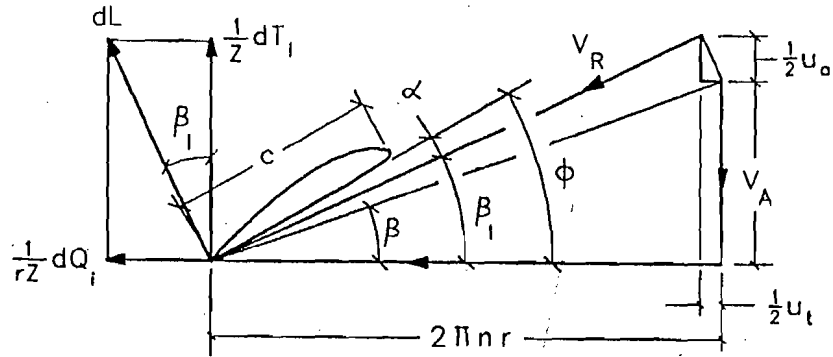


Figure 3.11: Velocities and Forces on a Blade Element in Inviscid Flow.

Fig. 3.11 shows the velocities and forces acting on a blade element of length dr at the radius r . The velocities are taken relative to the blade element. The induced velocities at the blade element are half those far behind the propeller, and since the fluid is assumed to be without viscosity there is no drag. The lift on the blade element is dL . The ideal thrust and torque due to the elements at radius r for all the blades are denoted by dT_i and dQ_i so that the axial and tangential force components on each blade element are dT_i/Z and dQ_i/rZ as shown in the figure. V_R is the resultant velocity, α the angle of attack, and β and β_I are the hydrodynamic pitch angles excluding and including the induced velocities respectively.

The lift on a blade element of length dr at the radius r is now obtained by the Kutta-Joukowski theorem:

$$dL = \rho \Gamma V_R dr = \rho \frac{2\pi r u_t}{Z} V_R dr \quad (3.35)$$

substituting for Γ from Eqn. (3.34). From Fig. 3.11, one obtains:

$$\begin{aligned} \frac{1}{Z} dT_i &= dL \cos \beta_I \\ \frac{1}{rZ} dQ_i &= dL \sin \beta_I \end{aligned}$$

so that, using Eqn. (3.35):

$$\begin{aligned}dT_i &= 2\pi \rho u_t V_R \cos \beta_I r dr \\dQ_i &= 2\pi \rho u_t V_R \sin \beta_I r^2 dr\end{aligned}\tag{3.36}$$

and:

$$\eta'_i = \frac{dT_i V_A}{dQ_i 2\pi n r} = \frac{V_A \cos \beta_I}{2\pi n r \sin \beta_I} = \frac{\tan \beta}{\tan \beta_I} \tag{3.37}$$

where η'_i is the ideal efficiency of the blade section at radius r .

One may now derive the condition for a propeller of maximum efficiency, or the "minimum energy loss condition" derived by Betz (1927). Suppose that there are two radii r_1 and r_2 where the blade element efficiencies are η'_{i1} and η'_{i2} , with η'_{i1} being greater than η'_{i2} . It is now possible to modify the design of the propeller (by changing the radial distribution of pitch, for example) in such a way that the torque is increased by a small amount at the radius r_1 and decreased by an equal amount at the radius r_2 . However, because η'_{i1} is greater than η'_{i2} , the increase in thrust at r_1 will be greater in magnitude than the decrease in thrust at r_2 . There will thus be a net increase in the total thrust T_i without any increase in the total torque Q_i of the propeller, and hence an increase in its efficiency. This process of increasing the efficiency of the propeller can be continued so long as there exist two radii in the propeller where the blade element efficiencies are not equal. If the efficiencies of the blade elements at all the radii from root to tip are equal, then the efficiency of the propeller cannot be increased further, and one has a propeller of the highest efficiency or minimum energy loss. The condition for minimum energy loss is therefore that η'_{i1} be independent of r , i.e. for all radii:

$$\tan \beta_I = \frac{\tan \beta}{\eta_i} = \frac{1}{\eta_i} \frac{V_A}{2\pi n r} \tag{3.38}$$

where $\eta_i = \eta'_i$ and is the ideal efficiency of the propeller. Eqn. (3.38) implies that the vortex sheets shed by the propeller blades have the form of helicoidal surfaces of constant pitch $V_A/(\eta_i n)$.

From the blade section velocity diagram in Fig. 3.11, it can be shown that:

$$\begin{aligned}\frac{V_R}{V_A} &= \frac{\cos(\beta_I - \beta)}{\sin \beta} \\ \frac{\frac{1}{2} u_a}{V_A} &= \frac{\tan \beta_I - \tan \beta}{\tan \beta (1 + \tan^2 \beta_I)} \\ \frac{\frac{1}{2} u_t}{V_A} &= \frac{\tan \beta_I (\tan \beta_I - \tan \beta)}{\tan \beta (1 + \tan^2 \beta_I)}\end{aligned}\quad (3.39)$$

The ideal thrust loading coefficient is defined as:

$$C_{TLi} = \frac{T_i}{\frac{1}{2} \rho A_O V_A^2}$$

where $A_O = \pi D^2/4$ is the disc area of the propeller. The ideal thrust loading coefficient for a blade element at radius r is then:

$$\begin{aligned}dC_{TLi} &= \frac{dT_i}{\frac{1}{2} \rho \frac{\pi}{4} D^2 V_A^2} = \frac{2\pi \rho u_t V_R \cos \beta_I r dr}{\frac{\pi}{8} \rho D^2 V_A^2} \\ &= \frac{16 u_t V_R \cos \beta_I r dr}{D^2 V_A^2}\end{aligned}\quad (3.40)$$

Using Eqns. (3.38), (3.39) and (3.40), one can write:

$$\frac{dC_{TLi}}{dr} = f(\lambda, \eta_i, r) \quad (3.41)$$

so that:

$$C_{TLi} = \int f(\lambda, \eta_i, r) dr = F(\lambda, \eta_i)$$

where $\lambda = V_A/\pi n D = r \tan \beta/R$. The function $F(\lambda, \eta_i)$ was calculated by Kramer (1939) for different values of Z , the number of blades. His results are usually given in the form of a diagram. The Kramer diagram, which often forms the starting point for designing a propeller using the circulation theory, is given later.

In determining the circulation Γ around a propeller blade at radius r , Eqn. (3.34), it has been assumed that the tangential induced velocity u_t is

constant along the circular path in the slipstream far behind the propeller. This implies that the propeller has an infinite number of blades. The effect of a finite number of blades was calculated by Goldstein (1929) for a propeller having an optimum distribution of circulation. The effect of a finite number of blades is taken into account by incorporating a correction factor, the Goldstein factor κ , in Eqn. (3.34) and the subsequent equations based on it. Goldstein factors have been calculated and are given in the form of diagrams with κ as a function of $\tan \beta_I$ and $x = r/R$ for different values of Z . The use of Goldstein factors to account for the finite number of blades in a propeller is valid only for a lightly loaded propeller operating in a uniform velocity field and having an optimum distribution of circulation. When these conditions are not fulfilled, it is more correct to use the induction factors calculated by Lerbs (1952). However, the Goldstein factors are much simpler to use than the Lerbs induction factors. Many propeller design methods based on the circulation theory therefore use the Goldstein factors.

In order to use the circulation theory for propeller design, it is necessary to be able to calculate the lift coefficient required at each blade section of the propeller. By definition, the lift coefficient for the blade section at radius r is given by:

$$C_L = \frac{dL}{\frac{1}{2} \rho c dr V_R^2} \quad (3.42)$$

Substituting for dL from Eqn. (3.34) after incorporating the Goldstein factor, one obtains:

$$C_L = \frac{\rho \frac{2\pi r \kappa u_t}{Z} V_R dr}{\frac{1}{2} \rho c dr V_R^2} = \frac{8\pi r \kappa \frac{1}{2} u_t}{c Z V_R}$$

so that:

$$C_L \frac{c}{D} = \frac{4\pi}{Z} x \kappa \sin \beta_I \tan(\beta_I - \beta) \quad (3.43)$$

where c is the chord length of the blade section at radius r , $x = r/R$, and use has been made of the Eqns. (3.39). Eqn. (3.43) is used to determine the detailed geometry of the blade sections when designing a propeller. The use of the circulation theory in propeller design is considered in Chapter 9.

Example 5

A propeller of 5.0 m diameter has an rpm of 120 and a speed of advance of 6.0 m per sec when operating with minimum energy loss at an ideal efficiency of 0.750. The root section is at 0.2 R . Determine the thrust and torque of the propeller in an inviscid fluid neglecting the effect of a finite number of blades.

$$D = 5.0 \text{ m} \quad n = 120 \text{ rpm} = 2.0 \text{ s}^{-1} \quad V_A = 6.0 \text{ m s}^{-1}$$

$$\rho = 1025 \text{ kg m}^{-3} \quad \text{Root section } x = \frac{r}{R} = 0.2$$

$$\eta'_i = \eta_i = 0.750 = \frac{\tan \beta}{\tan \beta_I}$$

$$\tan \beta = \frac{V_A}{2\pi n r} = \frac{V_A}{\pi n x D} = \frac{6.0}{\pi \times 2.0 \times x \times 5.0} = \frac{0.190986}{x}$$

$$\tan \beta_I = \frac{\tan \beta}{\eta'_i} = \frac{\tan \beta}{0.750}$$

$$\frac{\frac{1}{2} u_t}{V_A} = \frac{\tan \beta_I (\tan \beta_I - \tan \beta)}{\tan \beta (1 + \tan^2 \beta_I)} \quad V_R = V_A \frac{\cos(\beta_I - \beta)}{\sin \beta}$$

$$\frac{dT_i}{dr} = 2\pi \rho u_t V_R \cos \beta_I r$$

$$\frac{dQ_i}{dr} = 2\pi \rho u_t V_R \sin \beta_I r^2$$

The subsequent calculation is carried out in a tabular form, using Simpson's rule for the integration.

x	r m	$\tan \beta$	$\tan \beta_I$	$\frac{1}{2} u_t / V_A$	u_t m s^{-1}	β_I°	β°
0.2	0.500	0.9549	1.2732	0.1619	1.9430	51.8540	43.6793
0.3	0.750	0.6366	0.8488	0.1645	1.9734	40.3255	32.4816
0.4	1.000	0.4775	0.6366	0.1510	1.8121	32.4816	25.5228
0.5	1.250	0.3820	0.5093	0.1348	1.6176	26.9896	20.9055
0.6	1.500	0.3183	0.4244	0.1199	1.4385	22.9970	17.6568
0.7	1.750	0.2728	0.3638	0.1071	1.2851	19.9905	15.2610
0.8	2.000	0.2387	0.3183	0.0963	1.1561	17.6568	13.4270

x	r m	$\tan \beta$	$\tan \beta_I$	$\frac{1}{2}u_t/V_A$	u_t ms^{-1}	β_I°	β°
0.9	2.250	0.2122	0.2829	0.0873	1.0479	15.7984	11.9808
1.0	2.500	0.1910	0.2546	0.0797	0.9566	14.2866	10.8125

x	V_R ms^{-1}	dT_i/dr kNm^{-1}	dQ_i/dr kNm m^{-1}	SM	$f(T_i)$ kNm^{-1}	$f(Q_i)$ kNm m^{-1}
0.2	8.5996	33.2342	21.1576	1	33.2342	21.1576
0.3	11.0680	80.4315	51.2044	4	321.7260	204.8176
0.4	13.8228	136.0798	86.6308	2	272.1596	173.2616
0.5	16.7200	194.0184	123.5160	4	776.0736	494.0640
0.6	19.6956	251.9514	160.3973	2	503.9028	320.7946
0.7	22.7172	309.1963	196.8405	4	1236.7852	787.3620
0.8	25.7687	365.6541	232.7829	2	731.3082	465.5658
0.9	28.8399	421.3677	268.2506	4	1685.4708	1073.0024
1.0	31.9248	476.4799	303.3362	1	476.4799	303.3362
					6037.1403	3843.3618

$$T_i = \frac{1}{3} \times (0.1 \times 2.5) \times 6037.1403 = 503.095 \text{ kN}$$

$$Q_i = \frac{1}{3} \times (0.1 \times 2.5) \times 3843.3618 = 320.280 \text{ kNm}$$

$$\eta_i = \frac{T_i V_A}{2\pi n Q_i} = \frac{503.095 \times 6.0}{2\pi \times 2.0 \times 320.280} = 0.7500 = \eta'_i$$

3.6 Further Development of the Circulation Theory

The circulation theory as discussed in the previous section has been used for designing propellers for over sixty years, although it has been necessary to use empirical or semi-theoretical corrections to bring the results of the theory in line with experiment, and to account for some of the simplifications in the theory. One of the major defects of the circulation theory

discussed in Sec. 3.5 is that the propeller blade is represented by a vortex line or lifting line. This neglects the effect of the finite width of the blade on the flow around it due to which the induced velocity varies across the width of the blade. The variation of the induced velocity along the chord of a blade section causes a curvature of the flow over the blade resulting in changes to the effective camber of the blade sections and the ideal angle of attack. Corrections to account for the width of propeller blades were first calculated by Ludwig and Ginzler (1944) and used extensively thereafter. The Ludwig-Ginzler curvature correction factors have now been superseded by more accurate lifting surface corrections such as those due to Morgan, Silovic and Denny (1968).

The modern development of the circulation theory is based on considering the propeller blades as lifting surfaces rather than lifting lines. Sparenberg derived the three-dimensional integral lifting surface equation for a screw propeller in steady flow and this has been used to calculate the induced velocity at a number of points over the chord of each blade section. Two different approaches have been adopted. In the first approach, used by Pien (1961) and Cheng (1964) for example, the singular integral is evaluated by direct numerical integration and a three-dimensional camber line is obtained by using a large number of control points over the section chord. In the second approach, which has been used by Kerwin and Leopold (1964) among others, the lifting surface is represented by a discrete lattice of vortices and the induced velocities are calculated over an interval from about the quarter-chord to the three-quarter chord to determine an average camber correction factor. The lifting surface theory is used today basically to determine the camber and pitch angle at the different radii of the propeller.

A major shortcoming of the lifting surface theory is that it neglects the effect of blade thickness, so that complicated approximations become necessary to treat thickness effects properly. This problem is overcome in surface panel methods in which the propeller blades are represented by a distribution of singularities on their surfaces, thereby automatically taking blade thickness into account. The effect of viscosity is taken into account by empirical corrections, by boundary layer calculations or by suitable reductions in the circulation.

The effect of viscosity on the flow around the propeller can be handled using numerical solutions of the Navier Stokes equations governing viscous

fluid flows, i.e. by RANS (Reynolds Averaged Navier Stokes) solvers. The propeller parameters are calculated for inviscid flow and then used with the viscous flow equations in an iterative procedure to account for the interaction between the inflow velocity and the velocities induced by the propeller. However, RANS solver approaches do not model the actual geometry of the propeller and the mutual interference between the propeller blades. It is believed that RANS solvers that include wake calculations and model turbulence properly will eventually prove better than surface panel methods because RANS solvers would also model the trailing vortex field of the propeller more accurately.

Problems

1. A propeller of diameter 4.0 m operates at a depth of 4.5 m below the surface of water with a speed of advance of 5.0 m per sec and produces a thrust of 200 kN. Determine the pressures and velocities (with respect to the propeller) in the water far ahead, just ahead, just behind and far behind the propeller on the basis of the axial momentum theory.
2. A propeller of diameter 3.0 m has a speed of advance of 4.5 m per sec. The velocity of water relative to the propeller in the slipstream far astern is 7.5 m per sec. Determine the thrust and the efficiency of the propeller using the axial momentum theory.
3. A propeller is required to produce a thrust of 150 kN at a speed of advance of 6.0 m per sec with an ideal efficiency of 0.7. What should be the diameter of the propeller on the basis of the axial momentum theory?
4. A propeller of diameter 3.0 m is required to produce a thrust of 100 kN at zero speed of advance. Determine the power input required, using the axial momentum theory.
5. A propeller of diameter 4.0 m has a speed of advance of 8.0 m per sec and an rpm of 150. The axial velocity of water with respect to the propeller is constant over the cross-section in the ultimate wake (i.e. far downstream) and has a value of 10.0 m per sec. Using the momentum theory considering both axial and angular momentum, determine the thrust and torque distribution over the propeller radius, and hence the total thrust and torque of the propeller and its efficiency. Consider only the radii from $0.2R$ to $1.0R$ at intervals of $0.1R$.
6. A propeller of 5.0 m diameter has a speed of advance of 6.0 m per sec and a revolution rate of 120 rpm. The root section is at $0.2R$. The propeller operates

in an inviscid fluid of density 1025 kg per m³ and has an efficiency of 0.750. Determine the axial and rotational inflow factors a and a' at the different radii, and calculate the propeller thrust and torque if the propeller operates at the highest efficiency.

7. A four-bladed propeller of diameter 5.0 m and constant face pitch ratio 0.800 is advancing through undisturbed water at a speed of 6.0 m per sec and 120 rpm. The blades are composed of radial sections all of which have a chord of 1.0 m, a lift coefficient of 0.1097 per degree angle of attack (measured from the no-lift line), a no-lift angle of 2.0 degrees and a lift-drag ratio of 40. The root section is at $0.2R$. Calculate the thrust, torque and efficiency of the propeller neglecting the induced velocities.
8. The lift coefficients and hydrodynamic pitch angles of the blade sections of a screw propeller are as follows:

$x = r/R$:	0.2	0.4	0.6	0.8	0.9
C_L	:	0.345	0.292	0.224	0.183	0.165
β_I deg	:	52.0	32.6	23.1	17.7	15.9

Assuming that the lift contributions of the angle of attack and of the camber are equal, compute the angles of attack, camber ratios and pitch ratios at the given radii. Lift coefficient due to angle of attack is 0.1097 per degree, and the section camber ratio is 0.055 per unit lift coefficient.

9. A four-bladed propeller of 6.0 m diameter produces an ideal thrust of 500 kN at a speed of advance of 8.0 m per sec and 90 rpm. Determine the ideal thrust loading coefficient C_{TLi} and the advance ratio λ . If for these values of C_{TLi} and λ the ideal efficiency η_i is 0.815 and the Goldstein factors κ are as follows:

$x = r/R$:	0.2	0.3	0.4	0.5	0.6	0.7	0.8	0.9	1.0
κ	:	1.141	1.022	0.976	0.943	0.926	0.861	0.765	0.595	-

determine the distribution of thrust and torque over the propeller radius and the ideal delivered power.

10. A three-bladed propeller of diameter 6.2 m has a speed of advance of 18.707 knots at 132 rpm and produces an ideal thrust of 1024.6 kN. The ideal efficiency is 0.795 and the Goldstein factors are:

$x = r/R$:	0.2	0.3	0.4	0.5	0.6	0.7	0.8	0.9	1.0
κ	:	1.104	0.980	0.941	0.917	0.890	0.834	0.739	0.569	-

Determine the values of $C_L \frac{c}{D}$ at these radii.

CHAPTER 4

The Propeller in "Open" Water

4.1 Introduction

A propeller is normally fitted to the stern of a ship where it operates in water that has been disturbed by the ship as it moves ahead. The performance of the propeller is thus affected by the ship to which it is fitted, so that the same propeller will perform slightly differently "behind" different ships. If therefore one wishes to determine the intrinsic performance characteristics of a propeller, unaffected by the ship to which it is fitted, it is necessary to make the propeller operate in undisturbed or "open" water. The performance characteristics of a propeller usually refer to the variation of its thrust, torque and efficiency with its speed of advance and revolution rate in open water.

It is difficult to determine the characteristics of a full-size propeller either in "open" water or "behind" the ship by varying the speed of advance and the revolution rate over a range and measuring the thrust and torque of the propeller. Therefore, recourse is had to experiments with models of the propeller and the ship in which the thrust and torque of the model propeller can be conveniently measured over a range of speed of advance and revolution rate. However, before one embarks upon model experiments, it is essential to know the conditions under which the quantities measured on the model can be applied to the full-size ship. These conditions are obtained from the "laws of similarity" between a model and its prototype.

4.2 Laws of Similarity

The laws of similarity provide the conditions under which a model must be made to operate so that its performance will faithfully reflect the performance of the prototype. For studying the performance of a propeller, or indeed studying hydrodynamic phenomena in general through the use of models, the conditions that need to be fulfilled are:

- (i) condition of geometrical similarity
- (ii) condition of kinematic similarity
- (iii) condition of kinetic (dynamic) similarity

The first condition requires that the model be geometrically similar to the full-size body. For this, it is necessary that the ratio of every linear dimension of the body bear a constant ratio to the corresponding dimension of the model. Thus, if the diameter of a ship propeller is $D_S = 5$ m and the diameter of the model propeller is $D_M = 20$ cm, the scale ratio $\lambda = D_S/D_M = 25$, and this should be held constant for all linear dimensions such as the boss diameter or the blade section chord lengths and thicknesses at corresponding radii.

Kinematic similarity requires that the ratio of any velocity in the flow field of the full-size body to the corresponding velocity in the model be constant. This, in effect, means that the flow fields around the full-size body and the model are geometrically similar since the ratio of the velocity components at corresponding points are equal and hence the directions of the resultant velocities at these points are identical. For propellers, the condition for kinematic similarity can be conveniently expressed by considering the speed of advance and the tangential velocity at the blade tip:

$$\frac{V_{AS}}{V_{AM}} = \frac{\pi n_S D_S}{\pi n_M D_M}, \quad \text{or} \quad \frac{V_{AS}}{n_S D_S} = \frac{V_{AM}}{n_M D_M}$$

that is,

$$J_S = J_M \tag{4.1}$$

the suffixes S and M referring to the ship and the model respectively. $J = V_A/nD$ is called the advance coefficient.

The condition for kinetic or dynamic similarity is somewhat more complicated, and requires that the ratios of the various forces acting on the full-size body be equal to the corresponding ratios in the model. Consider a body in a flow in which the dimensions of length and time are denoted by \underline{L} and \underline{T} . Then, some of the forces acting on the body can be expressed in terms of \underline{L} and \underline{T} as follows:

Inertia Force = mass \times acceleration

$$\propto \rho \underline{L}^3 \times \underline{L} \underline{T}^{-2} = \rho \underline{L}^4 \underline{T}^{-2}$$

Gravity Force = mass \times gravitational acceleration

$$\propto \rho \underline{L}^3 \times g = \rho g \underline{L}^3$$

Viscous Force = coefficient of viscosity \times velocity gradient \times area

$$\propto \mu \times \frac{\underline{L}}{\underline{T}} \times \underline{L}^2 = \mu \underline{L}^2 \underline{T}^{-1}$$

Pressure Force = pressure \times area

$$\propto p \times \underline{L}^2 = p \underline{L}^2$$

In this, ρ and μ are the density and coefficient of dynamic viscosity of the fluid, g is the acceleration due to gravity, and p the pressure.

Dynamic similarity then involves the following ratios:

$$\frac{\text{Inertia Force}}{\text{Gravity Force}} = \frac{\rho \underline{L}^4 \underline{T}^{-2}}{\rho g \underline{L}^3} = \frac{\underline{L}^2 \underline{T}^{-2}}{g \underline{L}} = \frac{V^2}{gL}$$

$$\frac{\text{Inertia Force}}{\text{Viscous Force}} = \frac{\rho \underline{L}^4 \underline{T}^{-2}}{\mu \underline{L}^2 \underline{T}^{-1}} = \frac{\rho (\underline{L}^2 \underline{T}^{-1})}{\mu} = \frac{VL}{\frac{\mu}{\rho}} = \frac{VL}{\nu}$$

$$\frac{\text{Pressure Force}}{\text{Inertia Force}} = \frac{p \underline{L}^2}{\rho \underline{L}^4 \underline{T}^{-2}} = \frac{p}{\rho (\underline{L} \underline{T}^{-1})^2} = \frac{p}{\rho V^2}$$

In the foregoing, the various constants of proportionality have been taken as 1, and L , V and p are a characteristic length, a characteristic velocity and a characteristic pressure associated with the body and the flow around it, while $\nu = \mu/\rho$ is the kinematic viscosity of the fluid. The ratio of inertia force to gravity force, or rather its square root, is called the Froude number F_n after William Froude, who was among the first to show the connection between the gravity waves generated by a ship and its speed. The ratio of inertia force to viscous force is called the Reynolds number R_n after Osborne Reynolds who studied the flow of viscous fluids. The ratio of pressure force to inertia force, expressed in the form $p/\frac{1}{2}\rho V^2$, is called the pressure coefficient or sometimes the Euler number E_n , after Leonhard Euler, the famous 18th century mathematician; a special form of the pressure coefficient is called the cavitation number. The Froude number, the Reynolds number and the Euler number (or pressure coefficient) being ratios of forces are dimensionless numbers and have the same values in any consistent system of units.

The condition for dynamic similarity requires that these force ratios for the full-size body be equal to the corresponding ratios for the model, i.e.:

$$F_n = \frac{V}{\sqrt{gL}}, \quad R_n = \frac{VL}{\nu}, \quad E_n = \frac{p}{\frac{1}{2}\rho V^2} \quad (4.2)$$

should be the same for both the full-size body and the model. If forces other than those considered here are involved, then other force ratios must be considered. Thus, if surface tension is important the Weber number $W_n = V^2 L/\kappa$, where κ is the kinematic capillarity (surface tension per unit length / density) of the fluid, must be the same for the body and its model.

In considering the dynamic similarity of propellers, one may take the characteristic linear dimension as the propeller diameter D , the characteristic velocity as the speed of advance V_A and the characteristic pressure as the static pressure at the centre of the propeller p_0 . The condition for dynamic similarity then becomes:

$$\begin{aligned}
 F_{nS} &= F_{nM}, \text{ i.e. } \frac{V_{AS}}{\sqrt{gD_S}} = \frac{V_{AM}}{\sqrt{gD_M}} \\
 R_{nS} &= R_{nM}, \text{ i.e. } \frac{V_{AS} D_S}{\nu_S} = \frac{V_{AM} D_M}{\nu_M} \\
 E_{nS} &= E_{nM}, \text{ i.e. } \frac{p_{0S}}{\frac{1}{2}\rho_S V_{AS}^2} = \frac{p_{0M}}{\frac{1}{2}\rho_M V_{AM}^2}
 \end{aligned} \tag{4.3}$$

Sometimes, other parameters instead of D , V_A and p_0 are chosen for defining F_n , R_n and E_n , the choice depending upon the purpose for which these dimensionless numbers are required. Thus, for example, when considering the nature of the viscous flow around a propeller, the characteristic length may be the length (chord) of the blade section at $0.7R$ and the characteristic velocity the resultant of the axial and tangential velocities at the section (neglecting induced velocities), so that the Reynolds number of the propeller may be defined as:

$$R_{n_{0.7R}} = \frac{V_{0.7R} c_{0.7R}}{\nu} \tag{4.4}$$

where:

$c_{0.7R}$ = the chord length of the blade section at $0.7R$

$$V_{0.7R} = \sqrt{V_A^2 + (0.7\pi n D)^2}$$

4.3 Dimensional Analysis

The laws of similarity for propellers may be obtained directly by dimensional analysis, though without the insight provided by the analysis of the preceding section. If the thrust T of a propeller depends upon its size as characterised by its diameter D , its speed of advance V_A and revolution rate n , the density ρ and viscosity μ of the fluid, the acceleration due to gravity g and a suitably defined pressure p , one may write:

$$\begin{aligned}
 T &= f(D, V_A, n, \rho, \mu, g, p) \\
 &= \Sigma K D^{i_1} V_A^{i_2} n^{i_3} \rho^{i_4} \mu^{i_5} g^{i_6} p^{i_7}
 \end{aligned} \tag{4.5}$$

or, in terms of the dimensions mass \underline{M} , length \underline{L} and time \underline{T} :

$$\begin{aligned} [\underline{M} \underline{L} \underline{T}^{-2}] &= [\underline{L}]^{i_1} [\underline{L} \underline{T}^{-1}]^{i_2} [\underline{T}^{-1}]^{i_3} [\underline{M} \underline{L}^{-3}]^{i_4} [\underline{M} \underline{L}^{-1} \underline{T}^{-1}]^{i_5} \\ &\quad [\underline{L} \underline{T}^{-2}]^{i_6} [\underline{M} \underline{L}^{-1} \underline{T}^{-2}]^{i_7} \\ &= [\underline{M}]^{i_4+i_5+i_7} [\underline{L}]^{i_1+i_2-3i_4-i_5+i_6-i_7} [\underline{T}]^{-i_2-i_3-i_5-2i_6-2i_7} \end{aligned}$$

so that:

$$i_4 + i_5 + i_7 = 1$$

$$i_1 + i_2 - 3i_4 - i_5 + i_6 - i_7 = 1$$

$$-i_2 - i_3 - i_5 - 2i_6 - 2i_7 = -2$$

and:

$$i_1 = 2 + i_3 - i_5 + i_6 - 2i_7$$

$$i_2 = 2 - i_3 - i_5 - 2i_6 - 2i_7$$

$$i_4 = 1 - i_5 - i_7$$

Therefore:

$$\begin{aligned} T &= \sum K D^{2+i_3-i_5+i_6-2i_7} V_A^{2-i_3-i_5-2i_6-2i_7} n^{i_3} \rho^{1-i_5-i_7} \mu^{i_5} g^{i_6} p^{i_7} \\ &= \rho D^2 V_A^2 \sum K \left(\frac{nD}{V_A} \right)^{i_3} \left(\frac{\mu}{\rho V_A D} \right)^{i_5} \left(\frac{gD}{V_A^2} \right)^{i_6} \left(\frac{p}{\rho V_A^2} \right)^{i_7} \end{aligned}$$

or:

$$\begin{aligned} \frac{T}{\rho D^2 V_A^2} &= f \left[\left(\frac{V_A}{nD} \right) \left(\frac{V_A D}{\nu} \right) \left(\frac{V_A}{\sqrt{gD}} \right) \left(\frac{p}{\frac{1}{2}\rho V_A^2} \right) \right] \\ &= f(J, R_n, F_n, E_n) \end{aligned} \quad (4.6)$$

Multiplying both sides by J^2 does not alter the nature of the functional relationship, so that one may write:

$$\frac{T}{\rho D^2 V_A^2} \frac{V_A^2}{n^2 D^2} = \frac{T}{\rho n^2 D^4} = f(J, R_n, F_n, E_n) \quad (4.7)$$

One may similarly show that:

$$\checkmark \quad \frac{Q}{\rho n^2 D^5} = f(J, R_n, F_n, E_n) \quad (4.8)$$

All the parameters on the right hand side in Eqns. (4.7) and (4.8) are dimensionless numbers, and the thrust and torque coefficients of a propeller are thus defined as:

$$\parallel \quad \checkmark \quad K_T = \frac{T}{\rho n^2 D^4} \quad K_Q = \frac{Q}{\rho n^2 D^5} \quad (4.9)$$

The thrust and torque coefficients along with the advance coefficient J and the 'open water' efficiency:

$$\parallel \quad \checkmark \quad \eta_o = \frac{TV_A}{2\pi n Q} = \frac{K_T}{K_Q} \frac{J}{2\pi} \quad (4.10)$$

are generally used to describe the open water characteristics of a propeller.

Since Eqns. (4.7) and (4.8) involve only dimensionless quantities, these equations are independent of the units of the different quantities involved provided that a consistent system of units is used. In addition, the equations are independent of the size of the propeller provided that the geometry is fixed, i.e. for given values of J , R_n , F_n and E_n , the values of K_T and K_Q and hence η_o , are the same for a full size propeller and its geometrically similar model.

4.4 Laws of Similarity in Practice

Consider a full size ship propeller of diameter D_S operating at a speed of advance V_{AS} and revolution rate n_S , the pressure at the centre of the propeller being p_S . The question that arises is at what speed of advance, revolution rate and pressure should a model propeller of diameter D_M operate so that the laws of similarity are satisfied. The model scale is given by:

$$\lambda = \frac{D_S}{D_M} \quad (4.11)$$

The laws of similarity require that the advance coefficient J , the Reynolds number R_n , the Froude number F_n and the Euler number E_n for the ship propeller and the model propeller be the same.

If the Reynolds number of the model propeller is to be equal to the Reynolds number of the ship propeller:

$$\frac{V_{AM} D_M}{\nu_M} = \frac{V_{AS} D_S}{\nu_S} \quad (4.12)$$

Neglecting any differences between the fluids in which the ship and the model propellers operate, this leads to the requirement:

$$V_{AM} = V_{AS} \frac{D_S}{D_M} = V_{AS} \lambda \quad (4.13)$$

i.e. the smaller the model propeller the greater must be its speed of advance compared to the ship propeller.

The equality of the advance coefficients requires:

$$\frac{V_{AM}}{n_M D_M} = \frac{V_{AS}}{n_S D_S} \quad (4.14)$$

that is,

$$n_M = n_S \frac{V_{AM}}{V_{AS}} \frac{D_S}{D_M}$$

and this in association with the equality of Reynolds numbers, i.e. Eqn. (4.13), leads to the result:

$$n_M = n_S \lambda^2 \quad (4.15)$$

Now, suppose that with the advance coefficients and Reynolds numbers of the model propeller and the ship propeller being equal, the thrust coefficients are also equal,

that is:

$$K_{TM} = K_{TS} \quad (4.16)$$

or,

$$\frac{T_M}{\rho_M n_M^2 D_M^4} = \frac{T_S}{\rho_S n_S^2 D_S^4}$$

so that

$$T_M = T_S \left(\frac{n_M}{n_S} \right)^2 \left(\frac{D_M}{D_S} \right)^4$$

neglecting any difference between ρ_M and ρ_S .

This in association with Eqn. (4.15), gives:

$$T_M = T_S \lambda^4 \lambda^{-4} = T_S \quad (4.17)$$

The practical implications of Eqns. (4.13), (4.15) and (4.17) become clear if one considers an example. Let a ship propeller of 5 m diameter have a thrust of 500 kN at a speed of advance of 10 m per sec and an rpm of 100, and let the model propeller have a diameter of 20 cm. Then:

$$\lambda = \frac{D_S}{D_M} = \frac{5 \text{ m}}{20 \text{ cm}} = 25$$

$$V_{AM} = V_{AS} \lambda = 10 \text{ ms}^{-1} \times 25 = 250 \text{ ms}^{-1}$$

$$n_M = n_S \lambda^2 = 100 \text{ rpm} \times 25^2 = 62500 \text{ rpm} \quad (4.18)$$

$$T_M = T_S = 500 \text{ kN}$$

An experimental facility capable of achieving these values is practically impossible.

On the other hand, if the Froude number of the model propeller is to be equal to the Froude number of the ship propeller,

$$\frac{V_{AM}}{\sqrt{g D_M}} = \frac{V_{AS}}{\sqrt{g D_S}}$$

so that:

$$V_{AM} = V_{AS} \sqrt{\frac{D_M}{D_S}} = V_{AS} \lambda^{-0.5} \quad (4.19)$$

Comparing this with Eqn. (4.13), it is clear that the condition for equal Reynolds numbers and the condition for equal Froude numbers cannot be satisfied simultaneously unless $\lambda = 1$, i.e. the model propeller is of the same size as the ship propeller. If with equal Froude numbers the advance coefficients of the model propeller and the ship propeller are also made equal, then:

$$n_M = n_S \frac{V_{AM}}{V_{AS}} \frac{D_S}{D_M} = n_S \lambda^{-0.5} \lambda = n_S \lambda^{0.5} \quad (4.20)$$

If with equal Froude numbers and advance coefficients, the thrust coefficient of the model propeller is equal to the thrust coefficient of the ship propeller:

$$T_M = T_S \left(\frac{n_M}{n_S} \right)^2 \left(\frac{D_M}{D_S} \right)^4 = T_S \lambda \lambda^{-4} = T_S \lambda^{-3} \quad (4.21)$$

This means that a 20 cm diameter model of a ship propeller of 5 m diameter producing 500 kN thrust at 10 m per sec and 100 rpm must have the following values:

$$\lambda = \frac{D_S}{D_M} = 25$$

$$V_{AM} = V_{AS} \lambda^{-0.5} = 10 \text{ m s}^{-1} \times \frac{1}{5} = 2.0 \text{ m s}^{-1}$$

$$n_M = n_S \lambda^{0.5} = 100 \text{ rpm} \times 5 = 500 \text{ rpm} \quad (4.22)$$

$$T_M = T_S \lambda^{-3} = 500 \text{ kN} \times \frac{1}{25^3} = 0.032 \text{ kN}$$

These values can be achieved in practice with comparative ease. Since Reynolds similarity and Froude similarity cannot simultaneously be achieved and Reynolds similarity is almost impossible, it is usual in model experiments with propellers to satisfy only Froude similarity and to make such corrections as are necessary to account for the difference between the Reynolds numbers of the ship propeller and the model propeller. A similar situation exists for model experiments regarding ship resistance.

The laws of similarity also require that the Euler number of the model propeller be equal to the Euler number of the ship propeller:

$$\frac{p_{0M}}{\frac{1}{2} \rho_M V_{AM}^2} = \frac{p_{0S}}{\frac{1}{2} \rho_S V_{AS}^2}$$

or

$$p_{0M} = p_{0S} \left(\frac{V_{AM}}{V_{AS}} \right)^2 = p_{0S} \lambda^{-1} \quad (4.23)$$

If p_{0M} and p_{0S} are the hydrostatic pressures, then this condition is automatically satisfied because of the geometrical similarity between the model propeller and the ship propeller, since the hydrostatic pressure is proportional to the depth of immersion and hence to the propeller diameter. It is permissible to take the characteristic pressure used in defining the Euler number as the hydrostatic pressure provided that "cavitation" does not occur. Cavitation is discussed in Chapter 6. If there is a possibility of cavitation occurring in the ship propeller, it is necessary to take the total pressure minus the vapour pressure as the characteristic pressure in the Euler number, which is then called the cavitation number σ . For the ship propeller:

$$\sigma = \frac{p_A + \rho_S g h_S - p_V}{\frac{1}{2} \rho_S V_{AS}^2} \quad (4.24)$$

where p_A is the atmospheric pressure, h_S the depth of immersion of the ship propeller and p_V the vapour pressure. The total pressure for the model propeller should then be:

$$p_{0M} = (p_A + \rho_S g h_S - p_V) \lambda^{-1} \quad (4.25)$$

neglecting the small difference between ρ_M and ρ_S . Special measures are necessary to achieve the value of p_{0M} required by Eqn. (4.25).

Example 1

A ship propeller of 5.76 m diameter, 0.8 pitch ratio, 0.55 blade area ratio, 0.05 blade thickness fraction and 0.18 boss diameter ratio produces a thrust of 1200 kN with a delivered power of 15000 kW at 150 rpm and 7.5 m per sec speed of advance in sea water. The depth of immersion of the propeller is 6.0 m. A 0.16 m diameter model of this propeller is to be tested in fresh water. Determine for the model propeller (a) pitch, (b) blade area, (c) blade thickness at shaft axis, (d) boss diameter, (e) speed of advance, (f) revolution rate, (g) thrust, (h) delivered power and (i) total

pressure if the Froude numbers of the model and the ship propellers are to be made equal. What is the ratio of the Reynolds number of the ship propeller to the Reynolds number of the model propeller?

$$D_S = 5.76 \text{ m} \quad \frac{P}{D} = 0.8 \quad \frac{A_E}{A_O} = 0.55 \quad \frac{t_0}{D} = 0.05 \quad \frac{d}{D} = 0.18$$

$$T_S = 1200 \text{ kN} \quad P_{DS} = 15000 \text{ kW} \quad V_{AS} = 7.5 \text{ ms}^{-1} \quad n_S = 150 \text{ rpm} = 2.5 \text{ s}^{-1}$$

$$h_S = 6.0 \text{ m} \quad \rho_S = 1025 \text{ kg m}^{-3} \quad \rho_M = 1000 \text{ kg m}^{-3} \quad p_A = 101.325 \text{ kN m}^{-2}$$

$$D_M = 0.16 \text{ m} \quad \nu_S = 1.188 \times 10^{-6} \text{ m}^2 \text{ s}^{-1} \quad \nu_M = 1.139 \times 10^{-6} \text{ m}^2 \text{ s}^{-1}$$

$$p_V = 1.704 \text{ kN m}^{-2} \quad \lambda = \frac{D_S}{D_M} = \frac{5.76}{0.16} = 36$$

From geometrical similarity, one obtains for the model:

Pitch,

$$P_M = \frac{P}{D} \times D_M = 0.8 \times 0.16 = 0.128 \text{ m}$$

Expanded blade area,

$$A_{EM} = \frac{A_E}{A_O} \times \frac{\pi}{4} D_M^2 = 0.55 \times \frac{\pi}{4} \times 0.16^2 = 0.01106 \text{ m}^2$$

Blade thickness at shaft axis,

$$t_{0M} = \left(\frac{t_0}{D} \right) D_M = 0.050 \times 0.16 = 0.008 \text{ m}$$

Boss diameter,

$$d_M = \left(\frac{d}{D} \right) D_M = 0.180 \times 0.16 = 0.0288 \text{ m}$$

For equal Froude numbers:

$$\frac{V_{AM}}{\sqrt{g D_M}} = \frac{V_{AS}}{\sqrt{g D_S}}, \quad V_{AM} = V_{AS} \lambda^{-0.5} = 7.5 \times \frac{1}{6} = 1.25 \text{ ms}^{-1}$$

For equal advance coefficients:

$$\frac{V_{AM}}{n_M D_M} = \frac{V_{AS}}{n_S D_S}, \quad n_M = n_S \lambda^{0.5} = 2.5 \times 6 = 15 \text{ s}^{-1} = 900 \text{ rpm}$$

For equal thrust coefficients:

$$\frac{T_M}{\rho_M n_M^2 D_M^4} = \frac{T_S}{\rho_S n_S^2 D_S^4}, \quad T_M = T_S \frac{\rho_M}{\rho_S} \lambda^{-3} = 1200 \times \frac{1000}{1025} \times \left(\frac{1}{36}\right)^3 \text{ kN}$$

$$= 0.02509 \text{ kN}$$

For equal torque coefficients, and noting that $P_D = 2\pi n Q$,

$$\frac{P_{DM}}{2\pi \rho_M n_M^3 D_M^5} = \frac{P_{DS}}{2\pi \rho_S n_S^3 D_S^5},$$

That is,

$$P_{DM} = P_{DS} \frac{\rho_M}{\rho_S} \lambda^{1.5} \lambda^{-5} = 15000 \times \frac{1000}{1025} \times 36^{-3.5} \text{ kW} = 0.05228 \text{ kW}$$

For equal cavitation numbers,

$$\frac{p_{0M} - p_V}{\frac{1}{2} \rho_M V_{AM}^2} = \frac{p_A + \rho_S g h_S - p_V}{\frac{1}{2} \rho_S V_{AS}^2}$$

that is,

$$p_{0M} = (p_A + \rho_S g h_S - p_V) \frac{\rho_M}{\rho_S} \lambda^{-1} + p_V$$

$$= (101.325 + 1.025 \times 9.81 \times 6.0 - 1.704) \frac{1.000}{1.025} \times \frac{1}{36} + 1.704 \text{ kN m}^{-2}$$

$$= 6.0388 \text{ kN m}^{-2}$$

The ratio of the Reynolds numbers is:

$$\frac{R_{nS}}{R_{nM}} = \frac{V_{AS} \frac{D_S}{\nu_S}}{V_{AM} \frac{D_M}{\nu_M}} = \lambda^{0.5} \lambda \frac{\nu_M}{\nu_S} = 6 \times 36 \times \frac{1.139 \times 10^{-6}}{1.188 \times 10^{-6}} = 207.091$$

✓ Because of this large difference between the Reynolds number of the ship propeller and the Reynolds number of the model propeller, there will be

differences between the thrust and torque coefficients of the ship and model propellers.

When considering the performance characteristics of a propeller in open water, some simplifications are usually made in Eqns. (4.7) and (4.8). It is known that the Froude number governs the gravity waves generated at the free surface due to the motion of a body in a fluid. If the body is submerged sufficiently deep in the fluid no waves are generated at the free surface and the Froude number ceases to influence the flow. It has been observed that if the immersion of the propeller centre line below the surface of water is at least equal to the propeller diameter, the Froude number can be omitted from Eqns. (4.7) and (4.8) without significant error. Further, since the model and ship propeller Reynolds numbers cannot be made equal in any case, the Reynolds number is also omitted from these equations, and a correction made for this separately.

If the phenomenon of cavitation is present, the Euler number must be put in the form of the cavitation number, Eqn. (4.24). Based on these considerations one may write:

$$\begin{Bmatrix} K_T \\ K_Q \end{Bmatrix} = f(J, \sigma) \quad (4.26)$$

Frequently, the possibility of cavitation can be eliminated, and then:

$$\begin{Bmatrix} K_T \\ K_Q \end{Bmatrix} = f(J) \quad (4.27)$$

the exact nature of the function depending upon the geometry of the propeller.

Eqns. (4.26) and (4.27) being relations between dimensionless quantities should be independent of the size of the propeller. Unfortunately, this is not strictly correct because the Reynolds number, which has been neglected in these equations, depends upon the size of the propeller. The correction that must be made for the difference between the Reynolds number of the ship propeller and the Reynolds number of the model propeller is usually small provided that the flow around the model propeller is turbulent in nature just as the flow around the ship propeller. This requirement is met by not making the model propeller too small, giving it a dull matt surface

finish and ensuring that the Reynolds number is above a certain critical value. In order to further reduce the Reynolds number correction, the model propeller in open water is run at as high an axial speed and revolution rate as possible for the required range of advance coefficient, so that the difference between the Reynolds numbers of the model propeller and the ship propeller is minimised. A method to determine the Reynolds number correction for propeller open water characteristics is given in Chapter 8.

4.5 Open Water Characteristics

The open water characteristics of a propeller are usually given in terms of the advance coefficient J , the thrust coefficient K_T , the torque coefficient K_Q and the open water efficiency η_O . These values are given in the form of a table, or K_T , K_Q and η_O are plotted as functions of J . A typical K_T - K_Q diagram is shown in Fig. 4.1. The values of K_Q are usually a little more than one-tenth the values of K_T at the same values of J , so that it is convenient

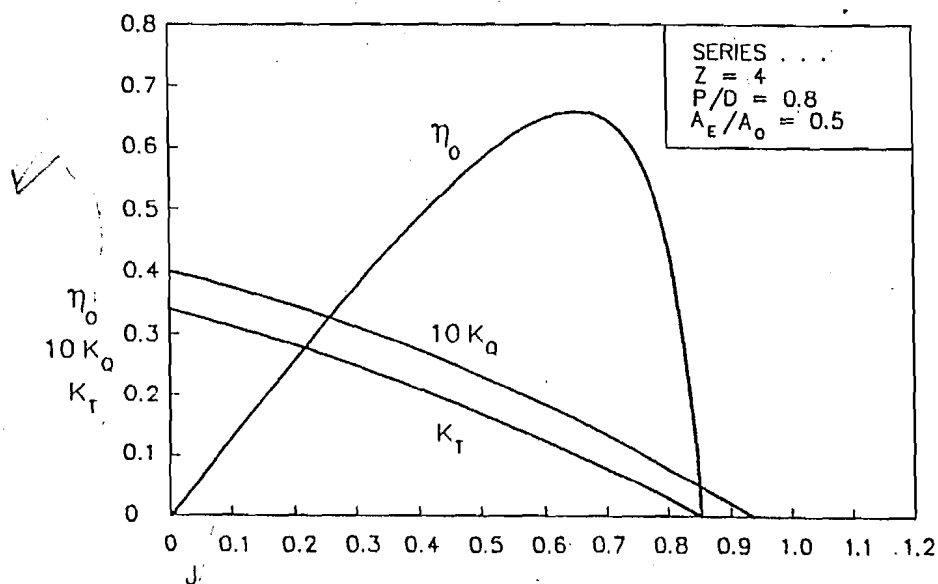


Figure 4.1 : K_T - K_Q Diagram.

to plot $10 K_Q$ rather than K_Q in the diagram. The K_T - K_Q diagram has some interesting features.

K_T and K_Q have their largest values at $J = 0$, i.e. when the propeller is revolving about its own axis without advancing through the water ($V_A = 0$). This condition of propeller operation occurs, for example, when a tug just begins to tow a stationary ship or during the dock trial of a new ship, and is known as the static condition. It is also known as the bollard pull condition from the trial in which a tug is attached to a bollard by a tow rope and the maximum pull of which the tug is capable is determined. This static condition also corresponds to the 100 percent slip condition discussed in Sec. 2.4. In this condition, with $V_A = 0$, a typical propeller blade section has the highest angle of attack equal to the pitch angle as shown in Fig. 4.2(a), and this results in K_T and K_Q having their largest values. (Only values of J greater than or equal to zero are considered here).

The value of J at which $K_T = 0$ is also of interest. In this condition, the resultant velocity V_R may be regarded as being directed along the no-lift line of the representative blade section, Fig. 4.2(b), and since no lift is developed there is no thrust. (Strictly, this is true only if the negative contribution of drag to the thrust is neglected). This condition of propeller operation is

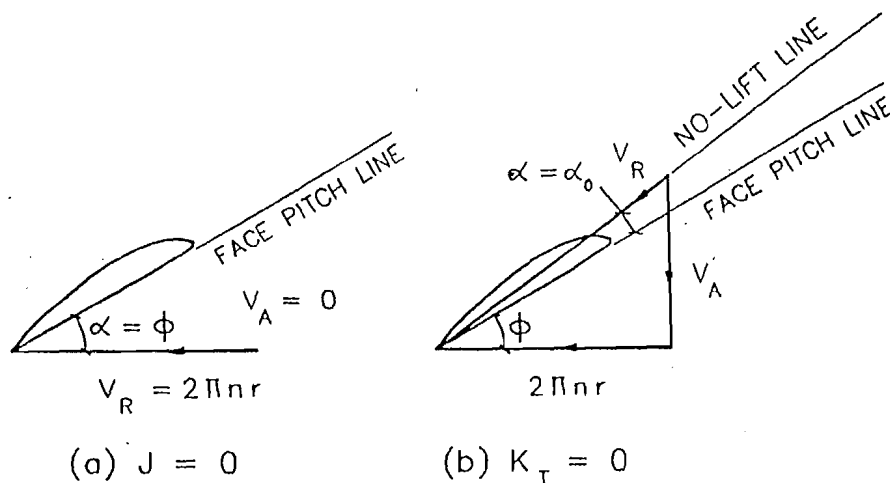


Figure 4.2 : Blade Section Velocity Diagrams at 100 percent Slip and Zero Slip.

known as the feathering condition. It also corresponds to the condition of zero slip, Sec. 2.4, and since the effective slip ratio is given by:

$$s_e = \frac{n P_e - V_A}{n P_e} = \frac{\frac{P_e}{D} - \frac{V_A}{n D}}{\frac{P_e}{D}} = \frac{\frac{P_e}{D} - J}{\frac{P_e}{D}} \quad (4.28)$$

by putting $s_e = 0$ it is seen that the value of J at $K_T = 0$ is numerically equal to the effective pitch ratio.

A propeller normally operates between the zero and the 100 percent slip conditions. In both these conditions the open water efficiency η_O is zero. The maximum value of η_O occurs at an effective slip ratio of between 10 and 20 percent, and for values of J greater than that corresponding to the maximum η_O , the value of η_O falls sharply to zero.

✓ Example 2

The open water characteristics of a propeller of 0.8 pitch ratio are as follows:

J	:	0	0.2000	0.4000	0.6000	0.8000
K_T	:	0.3400	0.2870	0.2182	0.1336	0.0332
$10K_Q$:	0.4000	0.3568	0.2905	0.2010	0.0883

If these results are obtained by running a model propeller of 0.2 m diameter at 3000 rpm over a range of speeds in fresh water, determine (a) the power of the motor required to drive the propeller (neglecting losses), (b) the maximum thrust, (c) the maximum open water efficiency, (d) the speed at which maximum efficiency occurs, (e) the speed at which the propeller has zero thrust, and (f) the effective pitch factor, i.e. the ratio of the effective pitch to the face pitch of the propeller.

$$D_M = 0.200 \text{ m} \quad n_M = 3000 \text{ rpm} = 50 \text{ s}^{-1} \quad \rho = 1000 \text{ kg m}^{-3}$$

The maximum power and thrust occur at $J = 0$, for which $K_T = 0.3400$ and $K_Q = 0.04000$. The power required and the maximum thrust are then:

$$P_{DM} = 2\pi \rho n_M^3 D_M^5 K_Q = 2\pi \times 1000 \times 50^3 \times 0.2^5 \times 0.0400 \text{ N ms}^{-1}$$

$$= 10.0531 \text{ kW}$$

$$T_M = K_T \rho n_M^2 D_M^4 = 0.340 \times 1000 \times 50^2 \times 0.2^4 \text{ N}$$

$$= 1.3600 \text{ kN}$$

By calculating $\eta_O = \frac{K_T}{K_Q} \frac{J}{2\pi}$ for different values of J , one obtains:

Maximum $\eta_O = 0.6153$ at $J = 0.6650$.

$$\text{Corresponding speed } V_A = J n D = 0.6650 \times 50 \times 0.2 \text{ ms}^{-1}$$

$$= 6.650 \text{ ms}^{-1}$$

$K_T = 0$ at $J = 0.860$, and the corresponding speed.

$$V_A = J n D = 0.860 \times 50 \times 0.2 = 8.6 \text{ ms}^{-1}$$

$$\text{Effective pitch ratio } \frac{P_e}{D} = 0.860$$

$$\text{Face pitch ratio } \frac{P}{D} = 0.800$$

$$\text{Effective pitch factor } \frac{P_e/D}{P/D} = \frac{0.860}{0.800} = 1.075$$

A propeller is normally used to propel the ship ahead, i.e. the speed of advance V_A and the revolution rate n of the propeller are positive. However, the propeller may be run in the reverse direction to propel the ship astern (V_A and n both negative). The propeller may also be reversed to decelerate the ship when it is going forward (V_A positive, n negative). When a ship going astern is to be stopped the propeller is run in the forward direction, i.e. V_A negative and n positive. The open water characteristics of a propeller for both directions of advance and revolution, "four quadrant characteristics", are illustrated in Fig. 4.3.

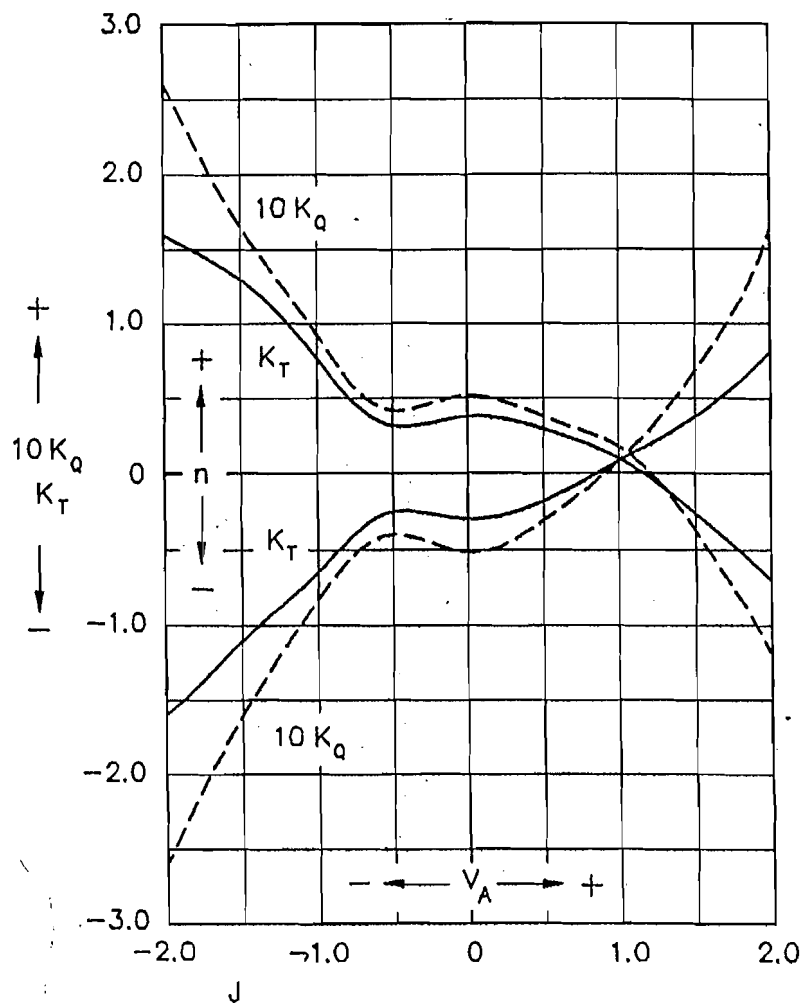


Figure 4.3 : Four Quadrant Open Water Characteristics.

4.6 Methodical Propeller Series

In a systematic or methodical series of propellers, all the propellers belonging to the series are related to one another according to a defined "system" or "method". Then, by determining the open water characteristics of a small number of propellers of the series, the characteristics of any propeller of the

series may be easily calculated. Generally, only the gross parameters of the propeller such as pitch ratio and blade area ratio are systematically varied. Details such as blade section shapes (camber ratio and thickness distribution) are kept unchanged. Methodical propeller series data are widely used in propeller design. Several methodical propeller series have been developed over the years. Two such series that have been widely used in propeller design are described in the following.

The Gawn or the AEW (Admiralty Experimental Works) 20-inch methodical series (Gawn, 1953) consists of propellers that have elliptical developed blade outlines and segmental blade sections. The parameters that are systematically varied in the Gawn series are the pitch ratio and the developed blade area ratio. The major particulars of the Gawn series propellers are given in Table 4.1 and Fig. 4.4. The open water characteristics of the propellers are given in the form of K_T - K_Q diagrams. Each diagram contains K_T , K_Q and η_O curves for $P/D = 0.6, 0.8, 1.0, \dots, 2.0$, and there are different diagrams for $A_D/A_O = 0.20, 0.35, 0.50, \dots, 1.10$. Expressions for K_T and K_Q as polynomial functions of J , P/D and A_D/A_O are given in Appendix 3.

Table 4.1

Particulars of Gawn Series Propellers

No. of blades	$Z = 3$
Pitch ratio	$P/D = 0.60-2.00$
Blade area ratio (developed)	$A_D/A_O = 0.20-1.10$
Blade thickness fraction	$t_0/D = 0.06$
Boss diameter ratio	$d/D = 0.20$

Another noteworthy methodical series of propellers is the B-series of MARIN, also known as the Troost, Wageningen or NSMB B-series, Oosterveld and Oossanen (1975). The B-series has been developed over several years, beginning with the results presented by Troost (1938). Propellers of the B-series are described by a number indicating the number of blades followed by one indicating the expanded blade area ratio, e.g. a B 4.40 propeller

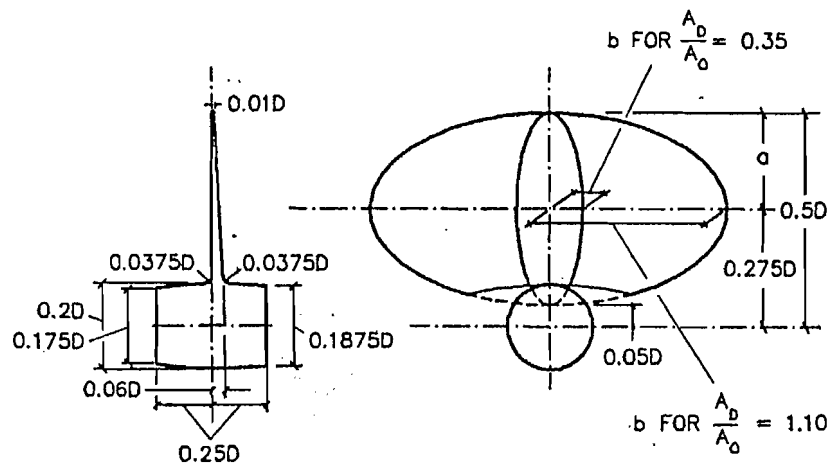


Figure 4.4 : Gawn Propeller Series Geometry.

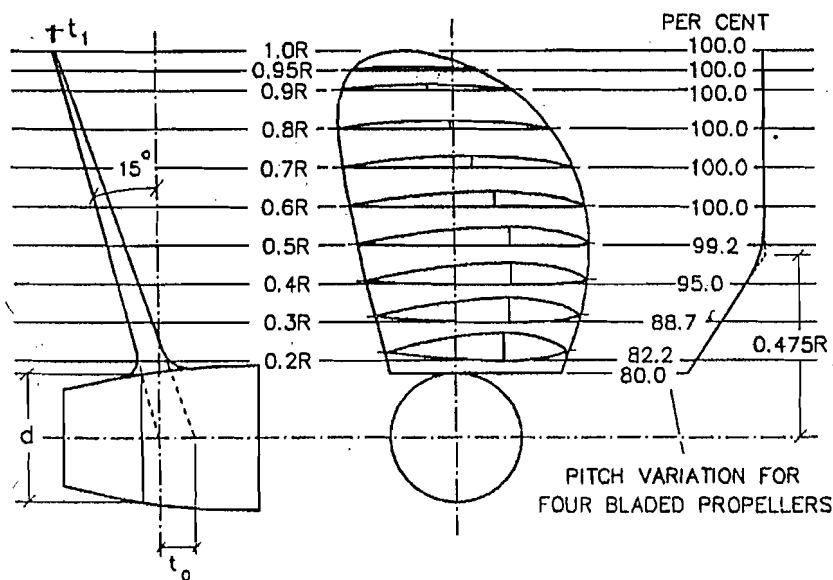


Figure 4.5 : B-Series Propeller Geometry.

is a B-series propeller with $Z = 4$ and $A_E/A_O = 0.40$. Fig. 4.5 shows some of the features of the B-series propellers: an asymmetric wide-tipped blade

outline, and aerofoil sections at the inner radii changing gradually to segmental sections at the blade tip. In the B-series, the parameters that have been varied include the number of blades, the expanded blade area ratio and the pitch ratio. The range of the variation of the blade area ratio depends upon the number of blades, and is given in Table 4.2 along with the other main particulars. All the propellers have a constant pitch, except for the four-bladed propellers, which have the pitch reduced by 20 percent at the blade root. Further geometrical details of the B-series are given in Appendix 3. The open water characteristics of the B-series propellers are available in a variety of forms including diagrams giving K_T and K_Q as functions of J for $P/D = 0.5, 0.6, 0.8, 1.0, 1.2$ and 1.4 , with different diagrams for the different values of Z and A_E/A_O . The values of K_T and K_Q have also been put into the form of polynomials:

$$K_T = \sum_{i,j,k,l} C_T(i,j,k,l) J^i \left(\frac{P}{D}\right)^j \left(\frac{A_E}{A_O}\right)^k Z^l$$

$$K_Q = \sum_{i,j,k,l} C_Q(i,j,k,l) J^i \left(\frac{P}{D}\right)^j \left(\frac{A_E}{A_O}\right)^k Z^l.$$
(4.29)

The values of C_T and C_Q are also given in Appendix 3.

Table 4.2

Particulars of B-Series Propellers

Z	P/D	A_E/A_O	t_0/D	d/D
2	0.5-1.4	0.30	0.055	0.180
3	0.5-1.4	0.35-0.80	0.050	0.180
4	0.5-1.4	0.40-1.00	0.045	0.167
5	0.5-1.4	0.45-1.05	0.040	0.167
6	0.5-1.4	0.45-1.05	0.035	0.167
7	0.5-1.4	0.55-0.85	0.030	0.167

4.7 Alternative Forms of Propeller Coefficients

Although the K_T - K_Q - J coefficients are the normal mode of presenting the open water characteristics of propellers, other coefficients have been developed which are more convenient to use, especially for propeller design and performance analysis using methodical series data. The major difficulty of using the K_T - K_Q - J coefficients is that all of them contain both the propeller revolution rate n and the diameter D , and in propeller design at least one of these variables is initially unknown and is to be determined during the design process. This makes propeller design using the K_T - K_Q diagrams of a methodical propeller series a process of trial and error to determine the optimum design parameters. Table 4.3 gives the values of K_T and K_Q for a hypothetical methodical series in an abbreviated form.

Example 3

A propeller running at 126 rpm is required to produce a thrust of 800 kN at a speed of advance of 12.61 knots. Determine the optimum diameter and pitch ratio of the propeller and the delivered power in open water. The propeller belongs to the methodical series for which the open water characteristics are given in Table 4.3.

$$n = 126 \text{ rpm} = 2.1 \text{ s}^{-1} \quad T = 800 \text{ kN} \quad V_A = 12.61 \text{ k} = 6.4866 \text{ m s}^{-1}$$

The straightforward way to solve this problem is to assume different propeller diameters D , calculate the corresponding values of K_T and J , and determine by interpolation between the K_T - J and K_Q - J curves for the different pitch ratios, the values of P/D , K_Q and hence η_O for each assumed value of D . Plotting η_O and P/D as functions of D then enables the optimum diameter and the corresponding pitch ratio to be determined. A slightly different approach, which avoids the need for interpolation between the K_T - J and K_Q - J curves, is used here.

$$\frac{K_T}{J^4} = \frac{T}{\rho n^2 D^4} \frac{n^4 D^4}{V_A^4} = \frac{n^2 T}{\rho V_A^4} = \frac{2.1^2 \times 800}{1.025 \times 6.4866^4} = 1.9442$$

The values of K_T and J corresponding to this value of K_T/J^4 are:

J	:	0.40	0.45	0.50	0.55	0.60	0.65	0.70
K_T	:	0.0497	0.0797	0.1215	0.1779	0.2520	0.3470	0.4668

Table 4.3
Open Water Characteristics of a Methodical Series

$$Z = 4 \quad A_E/A_O = 0.500$$

$P/D:$	0.5		0.6		0.7		0.8		0.9	
J	K_T	$10K_Q$	K_T	$10K_Q$	K_T	$10K_Q$	K_T	$10K_Q$	K_T	$10K_Q$
0	0.2044	0.1826	0.2517	0.2455	0.2974	0.3187	0.3415	0.4021	0.3840	0.4956
0.1	0.1795	0.1642	0.2254	0.2247	0.2702	0.2956	0.3114	0.3767	0.3567	0.4681
0.2	0.1499	0.1423	0.1949	0.2001	0.2393	0.2684	0.2831	0.3471	0.3263	0.4362
0.3	0.1156	0.1168	0.1603	0.1718	0.2047	0.2373	0.2489	0.3133	0.2929	0.3999
0.4	0.0765	0.0879	0.1215	0.1369	0.1665	0.2021	0.2115	0.2753	0.2564	0.3593
0.5	0.0327	0.0553	0.0786	0.1036	0.1246	0.1629	0.1707	0.2331	0.2169	0.3143
0.6	-	-	0.0315	0.0639	0.0790	0.1197	0.1266	0.1867	0.1743	0.2649
0.7	-	-	-	-	0.0297	0.0725	0.0792	0.1361	0.1287	0.2112
0.8	-	-	-	-	-	-	0.0284	0.0813	0.0800	0.1530
0.9	-	-	-	-	-	-	-	-	0.0283	0.0906
1.0	-	-	-	-	-	-	-	-	-	-

Table 4.3 (Contd.)

P/D	1.0		1.1		1.2		1.3		1.4	
J	K_T	$10K_Q$	K_T	$10K_Q$	K_T	$10K_Q$	K_T	$10K_Q$	K_T	$10K_Q$
0	0.4250	0.5994	0.4644	0.7133	0.5022	0.8374	0.5384	0.9717	0.5730	1.1161
0.1	0.3984	0.5698	0.4391	0.6818	0.4787	0.8040	0.5173	0.9366	0.5548	1.0794
0.2	0.3689	0.5357	0.4109	0.6456	0.4523	0.7659	0.4931	0.8967	0.5333	1.0378
0.3	0.3365	0.4971	0.3799	0.6048	0.4231	0.7231	0.4959	0.8520	0.5086	0.9915
0.4	0.3013	0.4540	0.3461	0.5594	0.3910	0.6757	0.4358	0.8026	0.4805	0.9403
0.5	0.2631	0.4064	0.3095	0.5094	0.3560	0.6234	0.4026	0.7484	0.4492	0.8843
0.6	0.2221	0.3543	0.2701	0.4548	0.3181	0.5665	0.3663	0.6894	0.4146	0.8235
0.7	0.1782	0.2976	0.2278	0.3955	0.2774	0.5049	0.3271	0.6257	0.3768	0.7579
0.8	0.1314	0.2365	0.1827	0.3317	0.2338	0.4385	0.2848	0.5571	0.3357	0.6875
0.9	0.0818	0.1708	0.1348	0.2632	0.1874	0.3675	0.2396	0.4839	0.2913	0.6122
1.0	0.0292	0.1007	0.0841	0.1900	0.1381	0.2917	0.1913	0.4058	0.2437	0.5322
1.1	-	-	0.0305	0.1123	0.0859	0.2113	0.1400	0.3229	0.1928	0.4474
1.2	-	-	-	-	0.0308	0.1261	0.0857	0.2353	0.1386	0.3577
1.3	-	-	-	-	-	-	0.0284	0.1429	0.0812	0.2632
1.4	-	-	-	-	-	-	-	-	0.0205	0.1640

Plotting this on the K_T - K_Q - J diagram obtained from the data in Table 4.3, one obtains at the points of intersection with the K_T - J lines for the different pitch ratios the values of J and K_T given in the following table. The corresponding value of K_Q is obtained from the K_Q - J lines, and the value of η_O calculated.

$\frac{P}{D}$:	0.6	0.8	1.0	1.2
J	:	0.4676	0.5327	0.5854	0.6299
K_T	:	0.0930	0.1566	0.2283	0.3063
$10K_Q$:	0.1156	0.2184	0.3622	0.5486
η_O	:	0.5987	0.6079	0.5872	0.5597

Finally, plotting η_O as a function of P/D , the maximum efficiency is found to be 0.608, corresponding to the optimum values: $J = 0.521$, $10K_Q = 0.196$, $P/D = 0.762$. Then, the optimum diameter and the corresponding delivered power are obtained:

$$D = \frac{V_A}{nJ} = \frac{6.4866}{2.1 \times 0.521} = 5.929 \text{ m} \quad \frac{P}{D} = 0.762$$

$$P_D = 2\pi \rho n^3 D^5 K_Q = 2\pi \times 1.025 \times 2.1^3 \times 5.929^5 \times 0.0196 \\ = 8565 \text{ kW}$$

Several other forms of propeller coefficients have been developed of which two sets of coefficients that have been widely used are considered here. The B_P - δ coefficients were introduced by Admiral D. W. Taylor and are defined as follows:

$$B_P = \frac{n P_D^{0.5}}{V_A^{2.5}} \quad \delta = \frac{n D}{V_A} \quad (4.30)$$

where:

D = propeller diameter in feet;

n = propeller rpm;

P_D = delivered power in British horsepower (1 hp = 0.7457 kW) for the open water condition in fresh water;

V_A = speed of advance in knots.

A typical B_P - δ chart, as shown in Fig. 4.6, consists of contours of δ and η_O on a grid of B_P and P/D . The values of B_P are usually plotted on a square root scale, i.e. the horizontal scale of the B_P - δ diagram is linear in $\sqrt{B_P}$. The "optimum efficiency" line shown in the B_P - δ diagram indicates the point at which η_O is maximum for a given B_P . The B_P - δ diagram is convenient to use when the speed of advance V_A , the propeller rpm n and the delivered power P_D are known and the propeller diameter D and pitch ratio P/D for optimum efficiency are to be determined. If, however, instead of the delivered power it is the thrust power $P_T = T V_A$ that is known, it is more convenient to use the coefficient B_U defined as:

$$B_U = \frac{n P_T^{0.5}}{V_A^{2.5}} \quad (4.31)$$

where P_T is the thrust power in hp for the open water condition in fresh water. The system of propeller coefficients introduced by Admiral Taylor includes a number of other coefficients, but methodical series data are usually available only in the form of B_P - δ diagrams.

Since the B_P - δ coefficients involve the use of specific units (feet, rpm, hp and knots), the values of parameters expressed in different units have to be first converted into these units, and since the coefficients are given for fresh water, parameters such as delivered power have also to be corrected to fresh water. These difficulties are avoided if, instead of the B_P - δ coefficients, truly dimensionless parameters are used. It can be shown that:

$$B_P = 33.053 \left(\frac{K_Q}{J^5} \right)^{0.5} \quad \text{and} \quad \delta = \frac{101.26}{J} \quad (4.32)$$

and, therefore, the dimensionless equivalent of the B_P - δ diagram consists of contours of η_O and $1/J$ on a grid of $(K_Q/J^5)^{0.25}$ and P/D .

Example 4

A propeller absorbs a delivered power of 7500 kW in open water at 120 rpm the speed of advance being 12.0 knots. Using the B_P - δ diagram in Fig. 4.6, determine the optimum diameter of the propeller, the corresponding pitch ratio and the propeller thrust.

$$P_D = 7500 \text{ kW} \quad n = 120 \text{ rpm} \quad V_A = 12.0 \text{ k} = 6.1728 \text{ m s}^{-1}$$

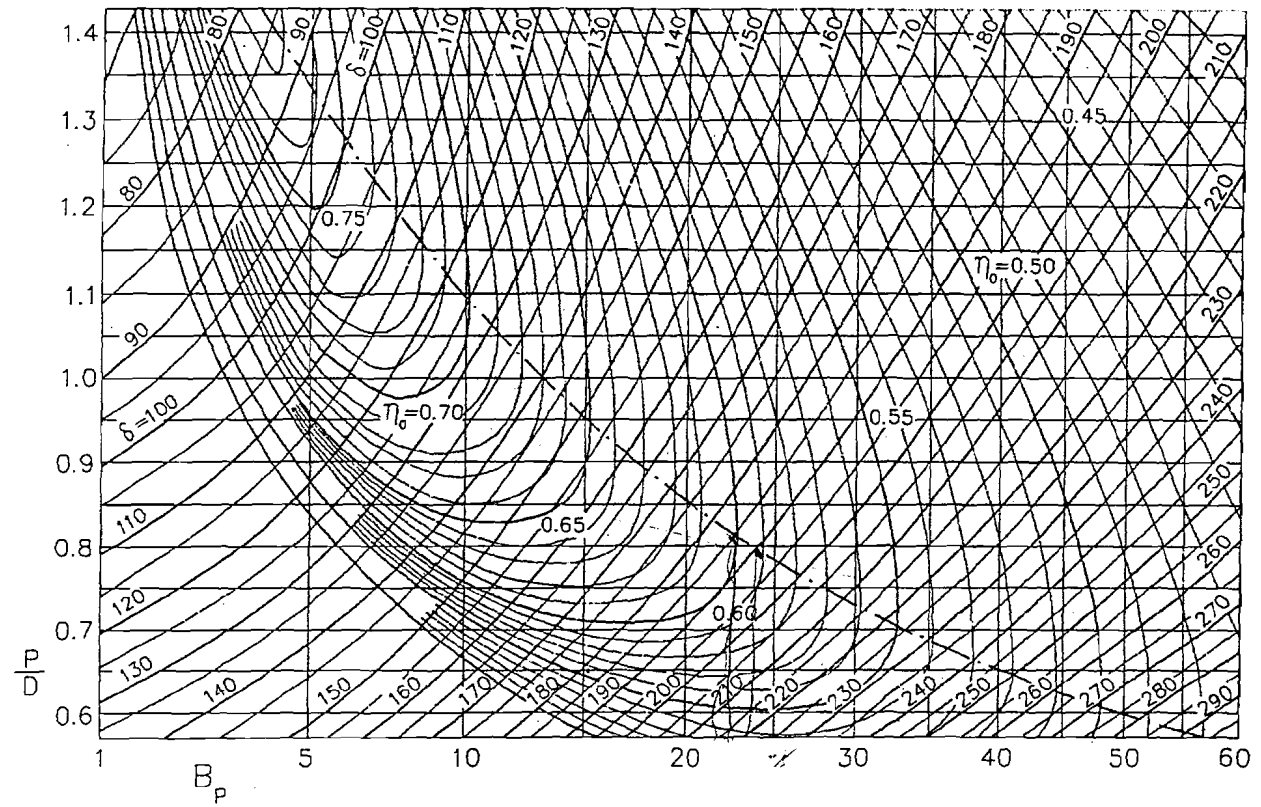


Figure 4.6 : B_p - δ Diagram.

For using the B_P - δ diagram, the delivered power must be converted to fresh water, and British units used.

$$P_D = \frac{7500 \text{ kW}}{0.7457 \frac{\text{kW}}{\text{hp}}} \times \frac{1}{1.025} = 9812.35 \text{ hp (Fresh water)}$$

$$B_P = \frac{n P_D^{0.5}}{V_A^{2.5}} = \frac{120 \times 9812.35^{0.5}}{12.0^{2.5}} = 23.83$$

From the optimum efficiency line in the B_P - δ diagram (Fig. 4.6), one obtains:

$$\frac{P}{D} = 0.798 \quad \delta = 190.5 \quad \eta_O = 0.593$$

Hence:

$$D = \frac{V_A \delta}{n} = \frac{12.0 \times 190.5}{120} = 19.05 \text{ ft} = 5.806 \text{ m}$$

$$T = \frac{P_D \eta_O}{V_A} = \frac{7500 \times 0.593}{6.1728} = 720.5 \text{ kN}$$

For propellers which operate at very high slip ratios (small values of J or high values of δ), such as tug and trawler propellers, the B_P - δ diagram often cannot be used since the values of B_P and δ fall outside the normal range. In such cases, one may use the μ - σ system of coefficients due to F. Gutsche (1934):

$$\mu = \left(\frac{\rho n^2 D^5}{Q} \right)^{0.5} = K_Q^{-0.5}$$

$$\varphi = V_A \left(\frac{\rho D^3}{Q} \right)^{0.5} = J K_Q^{-0.5} \quad (4.33)$$

$$\sigma = \frac{DT}{2\pi Q} = K_T (2\pi K_Q)^{-0.5}$$

A μ - σ diagram consists of contours of η_O , φ and P/D on a grid of μ and σ . A typical μ - σ diagram is shown in Fig. 4.7.

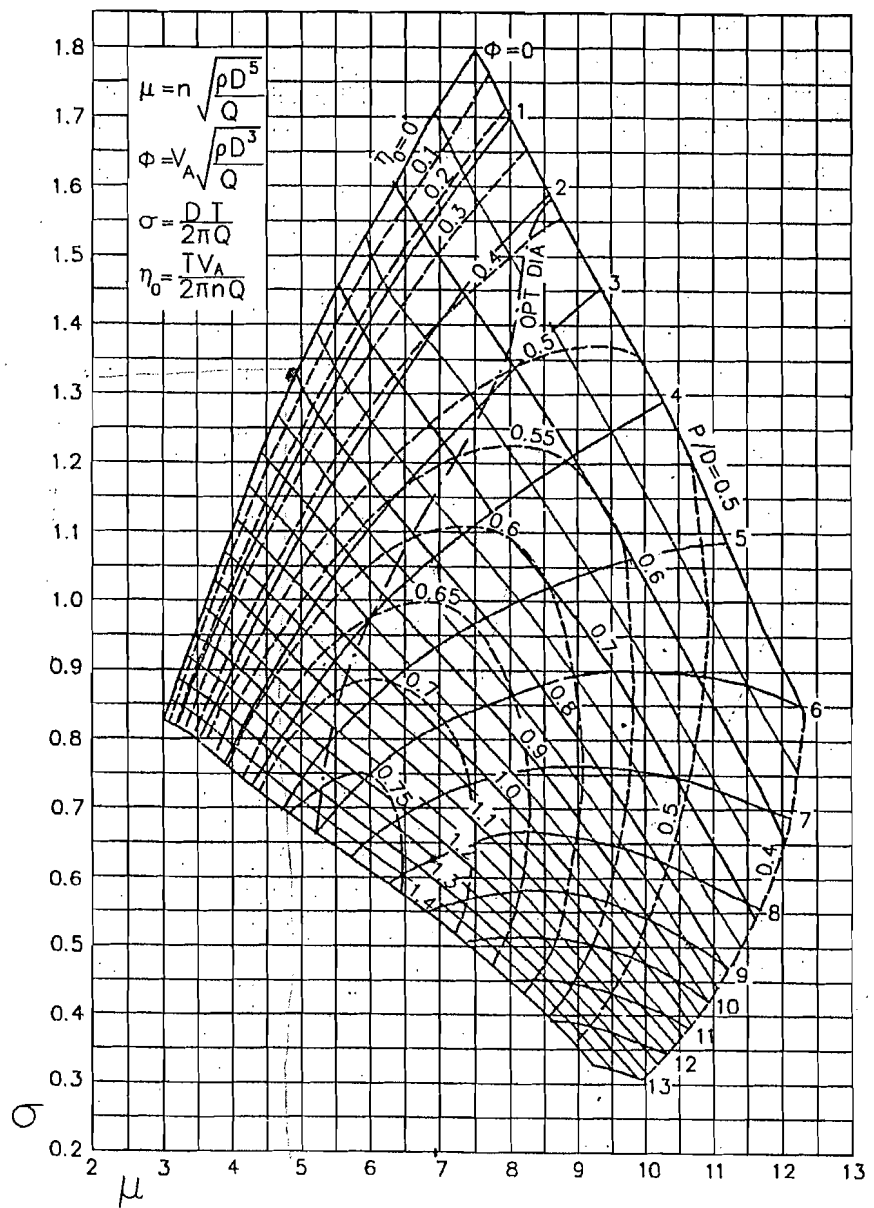


Figure 4.7: μ - σ Diagram.

The use of computers for propeller design and analysis has greatly reduced the need for special propeller coefficients aimed at reducing the amount of calculation involved. Computer programs for propeller design usually make direct use of the K_T - K_Q - J coefficients.

Example 5

A propeller of 3.0 m diameter and 0.8 pitch ratio runs at 150 rpm at zero speed of advance. If the engine driving the propeller produces a constant torque, find the propeller rpm, delivered power and thrust at the following speeds of advance: 0, 3, 6, 9 and 12 knots. Use the μ - σ diagram of Fig. 4.7.

$$D = 3.0 \text{ m} \quad \frac{P}{D} = 0.8 \quad \text{At } V_A = 0, \quad n = 150 \text{ rpm} = 2.5 \text{ s}^{-1}$$

$$\mu = \left(\frac{\rho n^2 D^5}{Q} \right)^{0.5} = \left(\frac{1.025 \times n^2 \times 3.0^5}{Q} \right)^{0.5} = 15.7821 n Q^{-0.5}$$

$$\varphi = V_A \left(\frac{\rho D^3}{Q} \right)^{0.5} = V_A \left(\frac{1.025 \times 3.0^3}{Q} \right)^{0.5} = 5.2607 V_A Q^{-0.5}$$

$$\sigma = \frac{DT}{2\pi Q} = \frac{3.0 \times T}{2\pi \times Q} = 0.4775 T Q^{-1}$$

At $V_A = 0$, $n = 2.5 \text{ s}^{-1}$, and $\varphi = 0$. For $\varphi = 0$, $\frac{P}{D} = 0.8$, from the μ - σ diagram:

$$\mu = 4.945$$

so that:

$$15.7821 \times 2.5 \times Q^{-0.5} = 4.945$$

and:

$$Q = 63.6615 \text{ kNm}$$

Hence:

$$\mu = 1.9780 n \quad n = 0.5056 \mu$$

$$\varphi = 0.6593 V_A \quad P_D = 2\pi n Q$$

$$\sigma = 0.0075 T \quad T = 133.33 \sigma$$

V_A k	:	0	3	6	9	12
ms ⁻¹	:	0	1.5432	3.0864	4.6296	6.1728
φ	:	0	1.0174	2.0349	3.0523	4.0697
μ	:	4.943	5.264	5.713	6.292	6.929
ρ	:	1.329	1.270	1.206	1.136	1.057
ns ⁻¹	:	2.499	2.661	2.888	3.184	3.503
rpm	:	150	160	173	191	210
P_D kW	:	1000	1064	1155	1274	1401
T kN	:	177.2	179.3	160.8	151.5	140.9

Problems

1. A ship propeller of 5.0 m diameter has a thrust of 500 kN and a torque of 375 kNm at a revolution rate of 120 rpm and a speed of advance of 6.0 m per sec. Determine the speed of advance, rpm, thrust and torque of a model propeller of diameter 0.25 m if the Froude numbers of the ship propeller and the model propeller are equal. If the depths of immersion of the ship and model propellers are 6.0 m and 0.3 m respectively, what is the ratio of their cavitation numbers? What is the ratio of the Reynolds number of the ship propeller to that of the model propeller?
2. A ship propeller of 4.0 m diameter has a thrust of 160 kN and a torque of 120 kNm when running at 150 rpm and 8.0 m per sec speed of advance in open water. In order to make the Reynolds number and the Froude number of the ship propeller respectively equal to the Reynolds number and the Froude number of the model propeller, it is proposed to test the model propeller in a liquid whose density is 800 kg per m³ and kinematic viscosity 1.328×10^{-8} m² per sec. Determine the diameter of the model propeller and its speed of advance, rpm, thrust and torque. (Note : Unfortunately, no liquid anything like this exists.)
3. A model propeller of 0.15 m diameter is run at 3600 rpm over a range of speeds of advance and the following values of thrust and torque are recorded:

Speed of Advance m per sec	Thrust N	Torque Nm
0	770.71	16.930
1.000	715.94	15.850

Speed of Advance m per sec	Thrust N	Torque Nm
2.000	654.83	14.654
3.000	587.55	13.338
4.000	513.93	11.904
5.000	433.95	10.352
6.000	347.64	8.684
7.000	254.97	6.897
8.000	155.96	4.993
9.000	50.78	2.970

Obtain the open water diagram for the ship propeller given that the values of K_T for the ship propeller are 0.5 percent higher and the values of K_Q 1.5 percent lower than the corresponding values of the model propeller because of the differences between the ship and model propeller Reynolds numbers. Show that the ship propeller has a maximum efficiency of 0.7016 at an advance coefficient of 0.797. What is the effective pitch ratio of the ship propeller?

4. A propeller is required to absorb a delivered power of 10000 kW at 150 rpm when advancing into open water at a speed of 10.0 m per sec. Determine the optimum diameter and pitch ratio of the propeller using the methodical series data given in Table 4.3. What is the thrust of the propeller?
5. A propeller of 4.0 m diameter is required to produce an open water thrust of 300 kN at a speed of advance of 6.0 m per sec. Determine the rpm of the propeller for it to work at the optimum efficiency and the corresponding pitch ratio and delivered power. Use the data of Table 4.3.
6. A propeller of 3.0 m diameter and 0.8 pitch ratio absorbs its maximum delivered power when running at 180 rpm at a speed of advance of 13.5 knots. If the propeller torque remains constant, determine the propeller rpm, thrust and delivered power at speeds of advance of 0, 2.5, 5.0, 7.5 and 10.0 knots, using the data of Table 4.3.
7. A propeller is required to produce a thrust of 500 kN when running at 150 rpm and a speed of advance of 15.5 knots in open water. Using the B_P - δ diagram given in Fig. 4.6, determine the optimum diameter and pitch ratio of the propeller and the corresponding delivered power.
8. A propeller of diameter 5.0 m is to have a delivered power of 7500 kW at a speed of advance of 15.0 knots in open water. Using the B_P - δ diagram of Fig. 4.6, determine the rpm of the propeller for optimum efficiency as well as its pitch ratio and thrust.
9. A propeller of 3.0 m diameter absorbs a delivered power of 1400 kW at 210 rpm and 12.0 knots speed of advance in open water. The propeller torque is

constant. Using the μ - σ diagram of Fig. 4.7, determine the pitch ratio of the propeller, and calculate the rpm, delivered power and thrust at speeds of advance of 0, 3, 6, 9 and 12 knots.

10. A propeller with a delivered power of 1000kW at 120rpm is required to produce the maximum thrust at zero speed of advance in open water. Using the μ - σ diagram of Fig. 4.7, determine the diameter and pitch ratio of the propeller (within the limits of the diagram). If the propeller diameter is not to exceed 3.5 m, what will be the pitch ratio and the corresponding thrust?

CHAPTER 5

The Propeller "Behind" the Ship

5.1 Introduction

When a propeller is fitted at the stern of a ship, it operates in water that has been disturbed by the ship during its forward motion. The behaviour of the propeller is therefore affected by the ship. In a similar manner, the operation of the propeller "behind" the ship hull affects the behaviour of the ship. There is thus a mutual interaction between the hull and the propeller, each affecting the other. This "hull-propeller interaction" has three major effects on the performance of the propeller and the ship taken together as compared to their behaviour considered individually:

- (i) The propeller advances into water disturbed by the ship so that the flow is not uniform over the propeller disc, and in general the speed of advance of the propeller V_A (averaged over the propeller disc) is different from the speed of the ship V with respect to undisturbed water. The disturbance behind the ship due to its motion ahead is called "wake".
- (ii) The action of the propeller alters the pressure and velocity distributions around the hull, and there is therefore an increase in the total resistance R_T of the ship at a given speed V with the propeller working compared to the resistance when there is no propeller. (The resistance of a ship at a given speed is the force opposing the steady ahead motion of the ship in calm water.) The

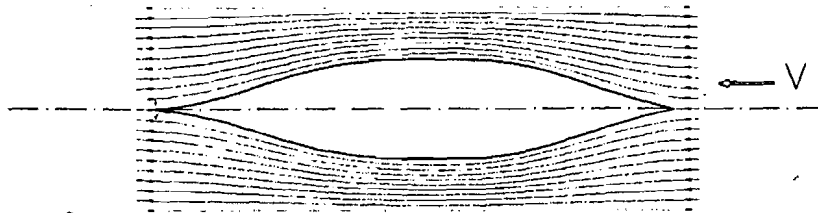
increase in the resistance of the ship due to the action of the propeller, or "resistance augment" is for convenience replaced by an equivalent decrease in the propeller thrust and called "thrust deduction".

- (iii) The efficiency of the propeller in the "behind" condition when working in non-uniform flow is different from its efficiency η_0 in open water (uniform flow). The ratio of the propeller efficiency in the behind condition to the open water efficiency is called "relative rotative efficiency".

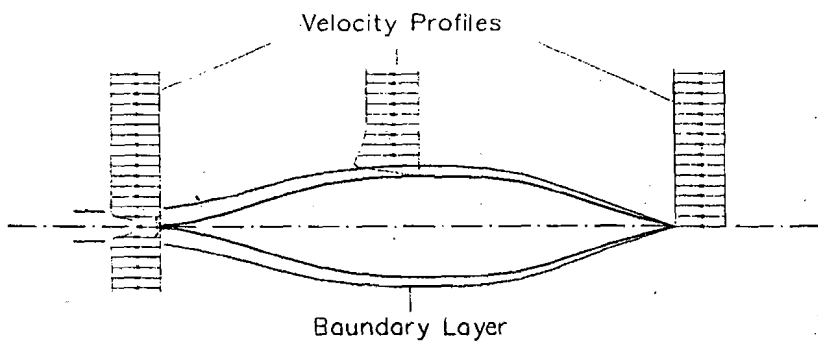
5.2 Wake

The effect of the disturbance created behind the ship by its forward motion is to impart a velocity to the particles of water in the wake. This wake velocity arises basically from three causes.

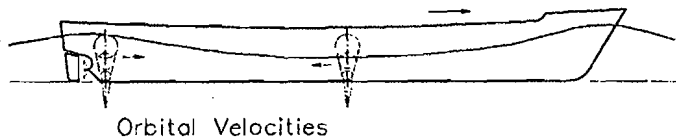
The first cause may be explained by regarding the ship to be moving in an inviscid fluid so that the flow around the ship can be regarded as potential flow and the streamlines around the hull determined accordingly, Fig. 5.1(a). The nature of the streamlines indicates that at the bow and the stern there are stagnation points (zero fluid velocity relative to the hull), so that the forward and after ends of the ship are regions of low relative velocity. Considering the fluid to be at rest far from the ship, a low relative velocity at the stern means a high wake velocity directed forward in addition to the velocity components normal to the direction of motion of the ship. The disturbance in the flow due to this cause is called potential or streamline wake. If now one considers the ship to be moving in water, then due to the viscosity of water a "boundary layer" forms over the hull surface in which the velocity increases from zero at the surface to nearly the value determined by the potential flow around the hull. This boundary layer increases in thickness from the forward end of the ship to the after end, where its thickness may be considerable, Fig. 5.1(b). The relative velocity of the water within the boundary layer with respect to the ship at the stern is therefore lower than that of the undisturbed water far from the ship, which means that the water in the boundary layer has a velocity component directed forward. The disturbance in the flow due to this cause is called viscous, frictional or boundary layer wake.



(a) STREAMLINES IN POTENTIAL FLOW



(b) VELOCITY PROFILES IN THE BOUNDARY LAYER



(c) ORBITAL VELOCITIES IN A WAVE

Figure 5.1 : Origin of Wake.

The third cause for the existence of wake velocity arises from the waves generated by a ship moving at the surface of water. Waves in deep water cause the particles of water to move in circular orbits, the radius of the orbit decreasing exponentially with depth below the surface. The orbital velocities of the water particles constitute the third component of wake velocity, and

this is called wave wake} The orbital velocities are directed forward below a wave crest and aft below a wave trough, Fig. 5.1(c), so that at the location of the propeller the wave wake velocity in the direction of motion of the ship is positive or negative depending upon whether a wave crest or a wave trough accompanies the stern of the ship. In a high speed twin screw ship such as a destroyer, in which the propellers largely lie outside the boundary layer of the ship and there is a large wave trough at the stern, the wave wake is often predominant at the propeller and the overall wake velocity is small and may even be negative (i.e. directed aft).

The wake velocity at the location of the propeller is not uniformly distributed and can be resolved into three components – a component along the axis of the propeller, and tangential and radial components in the plane of the propeller disc. The tangential velocity components on the port and starboard sides of the ship's centre plane are equal due to the symmetry of the hull, while the radial components are generally small. Therefore, in considering the average steady thrust and torque of a propeller behind a ship only the axial wake velocity is taken into account. The tangential velocity component of the wake velocity is important when considering unsteady propeller forces.

The axial wake velocity varies from point to point over the propeller disc. If $v(r, \theta)$ is the axial wake velocity at a point (r, θ) in the propeller disc, then one may determine the average wake velocity at a radius r :

$$\bar{v}'(r) = \frac{\int_0^{2\pi} v(r, \theta) d\theta}{\int_0^{2\pi} d\theta} = \frac{1}{2\pi} \int_0^{2\pi} v(r, \theta) d\theta \quad (5.1)$$

The average wake velocity over the propeller disc is given by:

$$\begin{aligned} \bar{v} &= \frac{1}{\pi(R^2 - r_b^2)} \int_{r_b}^R \int_0^{2\pi} v(r, \theta) r d\theta dr \\ &= \frac{2}{(R^2 - r_b^2)} \int_{r_b}^R \bar{v}'(r) r dr \end{aligned} \quad (5.2)$$

where R is the radius of the propeller and r_b the radius of the boss. \bar{v} is called the volumetric mean wake velocity since the volume of water flowing through the propeller disc per unit time is equal to $\pi(R^2 - r_b^2)\bar{v}$.

The ratio of the average axial wake velocity \bar{v} to the ship speed V is called the "wake fraction". w :

$$w = \frac{\bar{v}}{V} \quad (5.3)$$

The speed of advance of the propeller is then given by:

$$V_A = V - \bar{v} = (1 - w) V \quad (5.4)$$

This definition of wake fraction is due to D. W. Taylor. Another definition, due to R. E. Froude, in which the wake fraction is taken as the ratio of the wake velocity to the speed of advance is no longer used.

The wake velocity at the location of the propeller in a ship can be measured by instruments in the absence of the propeller. The wake fraction determined by such measurements is called the "nominal" wake fraction. The propeller when fitted at the stern and producing thrust alters the wake velocity, and the wake fraction determined from the wake velocity with the propeller operating is called the "effective" wake fraction. Since the wake velocity at the propeller location cannot normally be measured by instruments in the wake when the propeller is fitted, the effective wake is determined in an indirect manner by putting the speed of advance in the behind condition equal to that speed of advance in open water at which the propeller has the same thrust (or, alternatively, the same torque) at the same revolution rate. When the thrusts in the behind and open water conditions are made equal, the wake fraction is denoted by w_T and is said to be based on "thrust identity". If the torques are made equal, the wake fraction w_Q is said to be based on "torque identity".

Example 1

A ship has a propeller which produces a thrust of 500 kN with a torque of 450 kN m when the ship speed is 16.0 knots, and the propeller rpm is 120. The same propeller running at 120 rpm produces a thrust of 500 kN when advancing into open water at a speed of 12.8 k, and a torque of 450 kN m at a speed of 13.0 k. Determine the wake fraction on the basis of (a) thrust identity, and (b) torque identity.

- (a) For thrust identity, $V = 16.0\text{ k}$ $V_A = 12.8\text{ k}$

$$w_T = \frac{V - V_A}{V} = \frac{16.0 - 12.8}{16.0} = 0.2000$$

- (b) For torque identity, $V = 16.0\text{ k}$ $V_A = 13.0\text{ k}$

$$w_Q = \frac{V - V_A}{V} = \frac{16.0 - 13.0}{16.0} = 0.1875$$

In actual practice, the open water data are obtained with the help of a model propeller which may not be run at the same axial and rotational speeds in open water as in the behind condition, and in that case the wake fraction is determined by making the thrust coefficients in the open water and behind conditions equal, or by making the torque coefficients equal, i.e. by " K_T identity" or " K_Q identity". Experiments with models of ships and propellers are considered in Chapter 8.

5.3 Thrust Deduction

When a propeller produces thrust it accelerates the water flowing through the propeller disc and reduces the pressure in the flow field ahead of it. The increased velocity of water at the stern of the ship and the reduced pressure cause an increase in the resistance of the ship. If R_T is the total resistance of the ship at a given speed in the absence of the propeller and R'_T the total resistance at the same speed when the propeller is producing a thrust T , then the increase in resistance due to the action of the propeller is:

$$\delta R = R'_T - R_T$$

and if the ship speed is constant:

$$T = R'_T = R_T + \delta R$$

Since this increase in resistance is an effect due to the propeller, it is convenient to put $\delta T = \delta R$ and to write:

$$T - \delta T = R_T$$

where δT is the "thrust deduction". The ratio of the thrust deduction to the thrust is called the thrust deduction fraction t :

$$t = \frac{\delta T}{T}$$

so that:

$$(1 - t)T = R_T \quad (5.5)$$

The thrust deduction fraction is related to the wake fraction, a high wake fraction usually being associated with a high thrust deduction fraction. The thrust deduction fraction also depends to some extent on the rudder if placed in the slipstream of the propeller.

5.4 Relative Rotative Efficiency

Since the propeller in the open water condition works in undisturbed water whereas the propeller behind the ship works in water that has been disturbed by the ship, the efficiencies of the propeller in the two conditions are not equal. If T_O and Q_O are the thrust and torque of a propeller at a speed of advance V_A and revolution rate n in open water, and T and Q are the thrust and torque at the same values of V_A and n with the propeller operating behind the ship, the propeller efficiencies in open water and behind the ship are respectively:

$$\eta_O = \frac{T_O V_A}{2\pi n Q_O} \quad \eta_B = \frac{T V_A}{2\pi n Q}$$

and the relative rotative efficiency, which is the ratio of η_B to η_O , is then given by:

$$\eta_R = \frac{T}{T_O} \frac{Q_O}{Q} \quad (5.6)$$

As discussed in Sec. 5.2, the speed of advance is determined indirectly through thrust identity (K_T identity) or torque identity (K_Q identity), so that:

$$\eta_R = \frac{Q_O}{Q} \quad \text{Thrust Identity}$$

$$\eta_R = \frac{T}{T_O} \quad \text{Torque Identity}$$

(5.7)

The relative rotative efficiency is usually quite close to 1, lying between 1.00 and 1.10 for most single screw ships and between 0.95 and 1.00 for twin screw ships.

✓ Example 2

A ship has a speed of 20.0 knots when its propeller of 5.0 m diameter has an rpm of 150 and produces a thrust of 500 kN at a delivered power of 5650 kW. The resistance of the ship at 20.0 knots is 390 kN, and the open water characteristics of the propeller are as follows:

J	:	0.500	0.550	0.600	0.650	0.700
K_T	:	0.174	0.154	0.133	0.110	0.085
$10K_Q$:	0.247	0.225	0.198	0.173	0.147

Using (a) thrust identity and (b) torque identity, determine the wake fraction, the thrust deduction fraction, the relative rotative efficiency and the open water efficiency.

$$V = 20.0 \text{ k} = 10.288 \text{ ms}^{-1} \quad D = 5.0 \text{ m} \quad n = 150 \text{ rpm} = 2.5 \text{ s}^{-1}$$

$$T = 500 \text{ kN} \quad P_D = 5650 \text{ kW} \quad R_T = 390 \text{ kN}$$

$$Q = \frac{P_D}{2\pi n} = \frac{5650}{2\pi \times 2.5} = 359.690 \text{ kNm}$$

(a) Thrust Identity:

$$K_T = \frac{T}{\rho n^2 D^4} = \frac{500}{1.025 \times 2.5^2 \times 5.0^4} = 0.1249$$

From the open water characteristics for this value of K_T :

$$J = 0.617 \quad K_Q = 0.0191$$

$$Q_O = K_Q \rho n^2 D^5 = 0.0191 \times 1.025 \times 2.5^2 \times 5.0^5 = 382.373 \text{ kN m}$$

$$1 - w = \frac{J n D}{V} = \frac{0.617 \times 2.5 \times 5.0}{10.288} = 0.7497 \quad w = 0.2503$$

$$1 - t = \frac{R_T}{T} = \frac{390}{500} = 0.7800 \quad t = 0.2200$$

$$\eta_R = \frac{Q_O}{Q} = \frac{382.373}{359.690} = 1.0631$$

$$\eta_O = \frac{K_T}{K_Q} \frac{J}{2\pi} = \frac{0.1249}{0.0191} \times \frac{0.617}{2\pi} = 0.6421$$

(b) Torque Identity:

$$K_Q = \frac{Q}{\rho n^2 D^5} = \frac{359.690}{1.025 \times 2.5^2 \times 5.0^5} = 0.01797$$

From the open water characteristics for this value of K_Q :

$$J = 0.637 \quad K_T = 0.116$$

$$T_O = K_T \rho n^2 D^4 = 0.116 \times 1.025 \times 2.5^2 \times 5.0^4 = 464.453 \text{ kN}$$

$$1 - w = \frac{J n D}{V} = \frac{0.637 \times 2.5 \times 5.0}{10.288} = 0.7740 \quad w = 0.2260$$

$$1 - t = \frac{R_T}{T} = \frac{390}{500} = 0.7800 \quad t = 0.2200$$

$$\eta_R = \frac{T}{T_O} = \frac{500}{464.453} = 1.0765$$

$$\eta_O = \frac{K_T}{K_Q} \frac{J}{2\pi} = \frac{0.116}{0.01797} \times \frac{0.637}{2\pi} = 0.6544$$

5.5 Power Transmission

The power delivered to the propeller is produced by the propulsion plant of the ship and is transmitted to the propeller usually by a mechanical system, or sometimes by an electrical system. The propulsion plant or main engine may be a steam turbine, a gas turbine or a reciprocating internal combustion (diesel) engine. A turbine runs at a very high speed and it is necessary to reduce the speed by using a speed reducing device such as mechanical gearing. High speed and medium speed diesel engines also require speed reducing devices, whereas low speed diesel engines do not. The power produced by the main engine is transmitted to the propeller, after speed reduction if necessary, through a shafting system consisting of one or more shafts supported on bearings. The shaft on which the propeller is mounted is called the tail shaft, propeller shaft or screw shaft and is supported by bearings in a stern tube. There is also a thrust bearing to transmit the propeller thrust to the ship hull. In an electrical propulsion drive, the main engine drives an electric generator and the electrical power is transmitted by cables to an electric motor which drives the propeller through the propeller shaft.

The power produced by a diesel engine may be determined by measuring the variation of pressure in the engine cylinders by an instrument called an indicator. The power so determined is called the indicated power P_I . It is also possible to measure the power of the engine by operating it against a load applied through a brake dynamometer. The power determined in this manner is called the brake power P_B . The brake power is slightly less than the indicated power due to the mechanical losses that take place within the engine. The brake power is thus the power output of the engine and is carefully measured at the engine manufacturer's works along with the other operating parameters of the engine.

The power produced by a steam turbine or a gas turbine is usually determined by a torsionmeter fitted to the shafting connecting the turbine to the propeller through the gearbox. The power determined by measuring the torsion of the shaft is called the shaft power P_S . A torsionmeter may also be used to determine the shaft power when the ship has a diesel engine. The shaft power varies with the location of the torsionmeter on the propeller

shafting, being slightly higher when the torsionmeter is fitted close to the engine than when it is fitted close to the propeller.

The power that finally reaches the propeller is the delivered power P_D , and this is related to the propeller torque Q :

$$P_D = 2\pi n Q \quad (5.8)$$

n being the propeller revolution rate. The delivered power is somewhat less than the brake power or the shaft power because of the transmission losses that take place between the engine and the propeller, i.e. in the gearing and the bearings in mechanical transmission, and in the generator, cables, motor and bearings in an electrical propulsion drive.

The propeller produces a thrust T and this multiplied by the speed of advance V_A gives the thrust power P_T :

$$P_T = T V_A \quad (5.9)$$

The propeller thrust causes the ship to move at a speed V overcoming its resistance R_T , and the product of the resistance and the ship speed is the effective power P_E :

$$P_E = R_T V \quad (5.10)$$

It may be noted that Eqns. (5.8), (5.9) and (5.10) being dimensionally homogeneous are correct as they stand for any consistent system of units. Thus, if forces are measured in kN, speeds in m per sec, torque in kN m and revolutions are per sec, the powers will be in kW.

Fig. 5.2 shows a schematic arrangement of the propulsion system of a ship, and the powers available at different points of the system. The brake power P_B or the shaft power P_S , depending upon whether the main engine is a diesel engine or a steam or gas turbine, may be regarded as the input to the propulsion system and the effective power P_E as its output. If one wishes to focus only on the hydrodynamics of the system then the delivered power P_D is taken as the input.

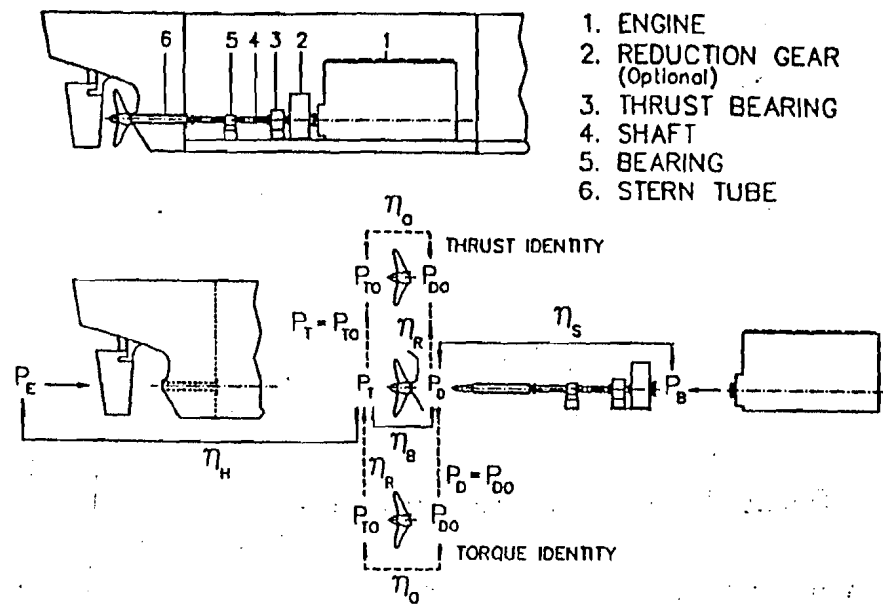


Figure 5.2: Propulsion System of a Ship.

Example 3

A ship moving at a speed of 18.0 knots is propelled by a gas turbine of shaft power 10000 kW at 5400 rpm. The turbine is connected to the propeller through 45:1 reduction gearing. The losses in the gearing and shafting are 5 percent. The propeller has a thrust of 900 kN, and the wake fraction and thrust deduction fraction are 0.250 and 0.200 respectively. Determine the delivered power, the thrust power and the effective power, as well as the propeller torque.

$$V = 18.0 \text{ k} = 9.2592 \text{ ms}^{-1} \quad P_S = 10000 \text{ kW} \quad n_{eng} = 5400 \text{ rpm}$$

$$\text{Gear ratio} = 45 : 1 \quad \text{Transmission losses} = 5 \text{ percent}$$

$$T = 900 \text{ kN} \quad w = 0.250 \quad t = 0.200$$

$$\text{Propeller revolution rate } n = \frac{\text{engine rpm}}{\text{gear ratio}} = \frac{5400}{45} = 120 \text{ rpm} = 2.0 \text{ s}^{-1}$$

$$P_D = P_S - \text{losses} = 10000(1 - 0.05) = 9500 \text{ kW}$$

$$V_A = (1 - w)V = (1 - 0.250) 9.2592 = 6.9444 \text{ m s}^{-1}$$

$$P_T = TV_A = 900 \times 6.9444 = 6250 \text{ kW}$$

$$R_T = (1 - t)T = (1 - 0.200) 900 = 720 \text{ kN}$$

$$P_E = R_T V = 720 \times 9.2592 = 6667 \text{ kW}$$

$$Q = \frac{P_D}{2\pi n} = \frac{9500}{2\pi \times 2} = 756 \text{ kNm}$$

5.6 Propulsive Efficiency and its Components

As indicated in the previous section, the brake power P_B (for diesel engines) or the shaft power P_S (for turbines) may be regarded as the input to the propulsion system, and the effective power P_E as its output. The efficiency of the system as a whole or the overall propulsive efficiency is then:

$$\begin{aligned} \eta_{\text{overall}} &= \frac{P_E}{P_B} \quad (\text{for diesel engine}) \\ &= \frac{P_E}{P_S} \quad (\text{for turbines}) \end{aligned} \quad (5.11)$$

If one considers only the hydrodynamic phenomena occurring outside the hull, the input to the propulsion system is the delivered power P_D , and the propulsive efficiency is given by:

$$\eta_D = \frac{P_E}{P_D} \quad (5.12)$$

This is sometimes called the quasi-propulsive coefficient qpc.

As indicated earlier, the delivered power P_D is slightly less than the brake power P_B or the shaft power P_S due to the losses which take place in the transmission of power from the main engine to the propeller. The efficiency

of power transmission from the engine to the propeller is called the shafting efficiency η_S :

$$\eta_S = \frac{P_D}{P_B} \text{ or } \frac{P_D}{P_S} \quad (5.13)$$

The losses that take place in the transmission of power are usually expressed as a percentage of the brake power or shaft power. In installations in which the engine is directly connected to the propeller by shafting, the transmission losses are usually taken as 3 percent when the engine is amidships and 2 percent when the engine is aft. With mechanical reduction gearing or electric propulsion drives, the transmission losses are higher, 4 to 8 percent.

The propeller receives the power P_D delivered to it and converts it to the thrust power P_T when it operates behind the ship, and hence the propeller efficiency in the behind condition is given by:

$$\eta_B = \frac{P_T}{P_D} \quad (5.14)$$

If the propeller were operating in open water at the same speed of advance and revolution rate with a delivered power P_{DO} and a thrust power P_{TO} , then its efficiency in open water would be:

$$\eta_O = \frac{P_{TO}}{P_{DO}} \quad (5.15)$$

The propeller efficiency in the behind condition may be written as:

$$\eta_B = \frac{P_{TO}}{P_{DO}} \cdot \left[\frac{P_T}{P_{TO}} \cdot \frac{P_{DO}}{P_D} \right] = \eta_O \cdot \eta_R \quad (5.16)$$

where:

$$\eta_R = \frac{P_T}{P_{TO}} \cdot \frac{P_{DO}}{P_D} \quad (5.17)$$

is the relative rotative efficiency discussed in Sec. 5.4. For thrust identity $P_T = P_{TO}$, while for torque identity $P_D = P_{DO}$, so that:

$$\begin{aligned}
 \eta_R &= \frac{P_{DO}}{P_D} && \text{for thrust identity} \\
 &= \frac{P_T}{P_{TO}} && \text{for torque identity}
 \end{aligned}
 \tag{5.18}$$

Eqns. (5.6) and (5.17) are equivalent, and so are Eqns. (5.7) and (5.18).

The thrust power P_T "input" to the hull enables the ship to obtain the effective power P_E required to propel it at a steady speed V . The ratio of the effective power to the thrust power is known as the hull efficiency:

$$\eta_H = \frac{P_E}{P_T} = \frac{R_T V}{T V_A} = \frac{1-t}{1-w} \tag{5.19}$$

The hull efficiency is usually slightly more than 1 for single screw ships and slightly less than 1 for twin screw ships. The fact that the hull efficiency and the relative rotative efficiency can have values more than 1 may seem somewhat curious, but is explained by regarding these "efficiencies" merely as ratios and not real efficiencies.

From Eqn. (5.19), one may note that for a high hull efficiency, the wake fraction w should be high and the thrust deduction fraction t should be low. If the propeller were placed at the bow of the ship instead of the stern, it would be advancing into almost undisturbed water so that the wake fraction would be much lower than if the propeller were at the stern. On the other hand, the ship would be advancing into water disturbed by the propeller, and since the propeller accelerates the water flowing through it and increases its pressure, there would be a greater increase in the resistance of the ship, and hence a higher thrust deduction fraction, due to propeller action when the propeller is fitted at the bow than when it is fitted at the stern. Therefore, a propeller at the stern results in a higher hull efficiency than a propeller at the bow.

The open water propeller efficiency, the relative rotative efficiency and the hull efficiency are the components of the propulsive efficiency η_D , as is easily shown:

$$\begin{aligned}
 \eta_D &= \frac{P_E}{P_D} = \frac{P_E}{P_T} \frac{P_T}{P_{TO}} \frac{P_{TO}}{P_{DO}} \frac{P_{DO}}{P_D} \\
 &= \frac{P_E}{P_T} \frac{P_{TO}}{P_{DO}} \left(\frac{P_T}{P_{TO}} \frac{P_{DO}}{P_D} \right) \\
 &= \eta_H \eta_O \eta_R
 \end{aligned} \tag{5.20}$$

Example 4

A ship has a speed of 18.0 knots when its engine has a brake power of 10000 kW at 150 rpm. The engine is directly connected to the propeller which has a diameter of 6.0 m. The effective power of the ship is 6700 kW and the propeller produces a thrust of 900 kN. The open water characteristics of the propeller are given by:

$$K_T = 0.319 - 0.527 J + 0.169 J^2$$

$$10K_Q = 0.354 - 0.578 J + 0.203 J^2$$

Determine the propulsive efficiency and its components based on thrust identity. The shafting efficiency is 0.970.

$$\begin{aligned}
 V &= 18.0 \text{ k} = 9.2592 \text{ ms}^{-1} & P_B &= 10000 \text{ kW} & n &= 150 \text{ rpm} = 2.5 \text{ s}^{-1} \\
 D &= 6.0 \text{ m} & P_E &= 6700 \text{ kW} & T &= 900 \text{ kN} & \eta_S &= 0.970
 \end{aligned}$$

$$R_T = \frac{P_E}{V} = \frac{6700}{9.2592} = 723.605 \text{ kN}$$

$$P_D = P_B \eta_S = 10000 \times 0.970 = 9700 \text{ kW}$$

$$K_{TB} = \frac{T}{\rho n^2 D^4} = \frac{900}{1.025 \times 2.5^2 \times 6.0^4} = 0.1084$$

$$Q = \frac{P_D}{2\pi n} = \frac{9700}{2\pi \times 2.5} = 617.521 \text{ kNm}$$

$$K_{QB} = \frac{Q}{\rho n^2 D^5} = \frac{617.521}{1.025 \times 2.5^2 \times 6.0^5} = 0.01240$$

Thrust identity: $K_T = K_{TB}$

that is:

$$0.319 - 0.527 J + 0.169 J^2 = 0.1084$$

$$J^2 - 3.1183 J + 1.2462 = 0 \quad \text{or } J = 0.4707$$

$$10 K_Q = 0.354 - 0.578 J + 0.203 J^2 = 0.1269$$

$$V_A = J n D = 0.4707 \times 2.5 \times 6.0 = 7.0599 \text{ ms}^{-1}$$

$$1 - w = \frac{V_A}{V} = \frac{7.0599}{9.2592} = 0.7625 \quad w = 0.2375$$

$$1 - t = \frac{R_T}{T} = \frac{723.605}{900} = 0.8040 \quad t = 0.1960$$

$$\eta_H = \frac{1 - t}{1 - w} = \frac{0.8040}{0.7625} = 1.0544$$

$$\eta_R = \frac{K_Q}{K_{QB}} = \frac{0.01269}{0.01240} = 1.0234$$

$$\eta_O = \frac{K_T}{K_Q} \frac{J}{2\pi} = \frac{0.1084}{0.01269} \times \frac{0.4707}{2\pi} = 0.6399$$

$$\eta_D = \eta_H \eta_O \eta_R = 1.0544 \times 0.6399 \times 1.0234 = 0.6905$$

$$= \frac{P_E}{P_D} = \frac{6700}{9700} = 0.6907$$

Example 5

This is the same as Example 4 except that the propulsive efficiency and its components are to be determined by torque identity.

From the previous example:

$$K_{TB} = 0.1084 \quad K_{QB} = 0.01240$$

Torque identity: $10 K_Q = 10 K_{QB} = 0.1240$

that is:

$$0.354 - 0.578 J + 0.203 J^2 = 0.1240$$

$$J^2 - 2.8473 J + 1.1330 = 0 \quad \text{or } J = 0.4783$$

$$K_T = 0.319 - 0.527 J + 0.169 J^2 = 0.1056$$

$$V_A = J n D = 0.4783 \times 2.5 \times 6.0 = 7.1738 \text{ ms}^{-1}$$

$$1 - w = \frac{V_A}{V} = \frac{7.1738}{9.2592} = 0.7748 \quad w = 0.2252$$

$$1 - t = \frac{R_T}{T} = \frac{723.605}{900} = 0.8040 \quad t = 0.1960$$

$$\eta_H = \frac{1 - t}{1 - w} = \frac{0.8040}{0.7748} = 1.0377$$

$$\eta_R = \frac{K_{TB}}{K_T} = \frac{0.1084}{0.1056} = 1.0265$$

$$\eta_O = \frac{K_T}{K_Q} \frac{J}{2\pi} = \frac{0.1056}{0.01240} \times \frac{0.4783}{2\pi} = 0.6483$$

$$\eta_D = \eta_H \eta_O \eta_R = 1.0377 \times 0.6483 \times 1.0265 = 0.6906$$

$$= \frac{P_E}{P_D} = \frac{6700}{9700} = 0.6907$$

From these examples, it may be seen that there are small differences between the individual components of propulsive efficiency based on thrust identity and those based on torque identity. However, the thrust deduction fraction is the same, and so is the propulsive efficiency, the small differences being due to round-off errors.

5.7 Estimation of Propulsion Factors

The propulsion factors – wake fraction, thrust deduction fraction, relative rotative efficiency and open water efficiency – are often determined with the help of model experiments as described in Chapter 8. However, it is usually necessary to have an estimate of the wake fraction, the thrust deduction fraction and the relative rotative efficiency for designing a propeller, and for this a number of empirical formulas and diagrams, based on statistical analyses of model data and ship trials data, are available. Some of these formulas are given in Appendix 4.

Problems

1. A ship has a resistance of 550 kN at a speed of 16.0 knots with its propelling machinery developing 6000 kW brake power at 120 rpm. The transmission losses are 2 percent. The wake fraction is 0.250, the thrust deduction fraction 0.200 and the relative rotative efficiency 1.030 based on thrust identity. Calculate the effective power, the thrust power and the delivered power, and the thrust, torque and open water efficiency of the propeller. What is the overall propulsive efficiency?
2. A ship has a resistance of 500 kN at a speed of 16.0 knots with the engine producing a brake power of 6000 kW at 120 rpm. The propeller thrust is 600 kN and the loss of power in transmission from the engine to the propeller is 180 kW. In order to produce the same thrust at the same rpm in open water, the propeller would have to advance at a speed of 12.0 knots and require a torque of 500 kNm. Calculate the effective power, the thrust power and the delivered power, as well as the hull efficiency, the relative rotative efficiency, the open water efficiency and the propulsive efficiency (quasi-propulsive coefficient).
3. A ship has a speed of 20.0 knots when the propeller rpm is 180 and the brake power of the engine is 15000 kW. The effective power of the ship at 20.0 knots is 10000 kW, and the wake fraction is 0.200, the thrust deduction fraction 0.120 and the relative rotative efficiency 1.050, based on thrust identity. The shafting efficiency is 0.970. Calculate the delivered power and thrust power, the hull efficiency, propeller open water efficiency and propulsive efficiency, and the propeller thrust and torque.
4. A ship moving at a speed of 19.5 knots has a propeller directly connected to a diesel engine developing 7500 kW brake power at 180 rpm. The shafting efficiency is 0.970, the open water efficiency of the propeller is 0.650, the wake fraction is 0.250, the thrust deduction fraction 0.200 and the relative rotative efficiency 1.050. Calculate the effective power of the ship and the propeller thrust and torque.
5. A ship with a propeller of diameter 5.0 m has a speed of 11.66 knots with the propeller running at 90 rpm. The propulsion factors based on torque identity are : wake fraction 0.250, thrust deduction fraction 0.190, relative rotative efficiency 1.060 and shafting efficiency 0.970. The open water characteristics of the propeller are as follows:

J	:	0	0.200	0.400	0.600	0.800
K_T	:	0.342	0.288	0.215	0.124	0.028
$10 K_Q$:	0.402	0.350	0.276	0.195	0.108

Determine the brake power of the engine and the effective power of the ship at this speed.

6. A twin screw ship has a design speed of 18.0 knots. Its propellers have a diameter of 3.0 m and are designed to operate at an advance coefficient $J = 0.7$, the corresponding open water thrust and torque coefficients being: $K_T = 0.350$, $10 K_Q = 0.560$. The propulsion factors are: $w = 0.050$, $t = 0.060$, $\eta_R = 0.980$, $\eta_S = 0.960$. Determine the design propeller rpm and the brake power of each of the two engines. What is the effective power of the ship at the design speed?
7. A ship has a speed of 17.0 knots when its propeller of 4.0 m diameter has an rpm of 150 and the engine has a brake power of 4850 kW, the shafting efficiency being 0.970. The effective power of the ship at 17.0 knots is 3660 kW. If the propeller operates at the following open water characteristics $J = 0.650$, $K_T = 0.300$, $10 K_Q = 0.475$, determine the wake fraction, the thrust deduction fraction, the relative rotative efficiency and the open water efficiency for thrust identity.
8. A ship with a resistance of 500 kN at a speed of 15.0 knots has a propeller of 5.0 m diameter whose thrust is 585 kN and torque 425 kN m. The propeller rpm is 120 and the shaft losses are 3 percent. It is estimated that a model propeller of 20 cm diameter when run in open water would produce a thrust of 312.381 N with a torque of 955.317 N cm in fresh water at 1800 rpm and 3.704 m per sec speed of advance. Use these data to determine (a) the effective power, the thrust power, the delivered power and the brake power of the ship, (b) the wake fraction and the thrust deduction fraction, and (c) the hull efficiency, the propeller open water efficiency and the relative rotative efficiency. What is the overall propulsive efficiency?
9. A ship has a propeller of diameter 5.0 m whose open water characteristics are as follows:

J	:	0	0.100	0.200	0.300	0.400	0.500	0.600	0.700
K_T	:	0.300	0.275	0.243	0.207	0.167	0.125	0.081	0.031
$10 K_Q$:	0.315	0.295	0.270	0.240	0.206	0.170	0.128	0.082

The effective power of the ship is 3840 kW at the design speed of 16.0 knots, and the propulsion factors based on thrust identity are: wake fraction 0.200, thrust deduction fraction 0.160, relative rotative efficiency 1.050 and shafting efficiency 0.970. Determine the brake power and the propeller rpm at the design speed.

10. A ship has an effective power of 9000 kW at a design speed of 18.0 knots. It has twin screws each of 4.0 m diameter connected through reduction gearing

to two medium speed diesel engines of brake power 7500 kW each running at 600 rpm. The propellers are designed to operate at $J = 0.600$, $K_T = 0.150$ and $10K_Q = 0.230$. Determine the gear ratio, the wake fraction and the thrust deduction fraction. The shafting efficiency is 0.950 and the relative rotative efficiency 1.000.

CHAPTER 6

Propeller Cavitation

6.1 The Phenomenon of Cavitation

A liquid such as water begins to vaporise when its pressure becomes equal to the saturation vapour pressure. The vapour pressure of water is 1.704 kN per m² at 15 °C and 101.325 kN per m² (i.e. atmospheric pressure) at 100 °C, the boiling point of water or the temperature at which water evaporates to form steam. If at a point the pressure in water drops to a value equal to the vapour pressure, the water at that point begins to vaporise forming cavities filled with water vapour. The formation of such low pressure vapour filled cavities is called cavitation.

A propeller produces its thrust by creating a difference between the pressures acting on the face and the back of the propeller blades, the pressure on the back of a blade section falling below the ambient pressure and the pressure on the face rising above it, as shown in Fig. 6.1. If the pressure at any point A on the back of the blade falls to the vapour pressure, the water at that point begins to cavitate. In actual practice, sea water contains minute solid particles in suspension and dissolved gases, and these impurities cause cavitation to start at pressures somewhat higher than the vapour pressure as the solid particles act as nuclei for the formation of cavities and the dissolved gases come out of solution before the water itself starts vaporising. Thus, cavitation in sea water may start when the pressure reaches a value of 17 kN per m² (absolute) instead of the actual vapour pressure, which has

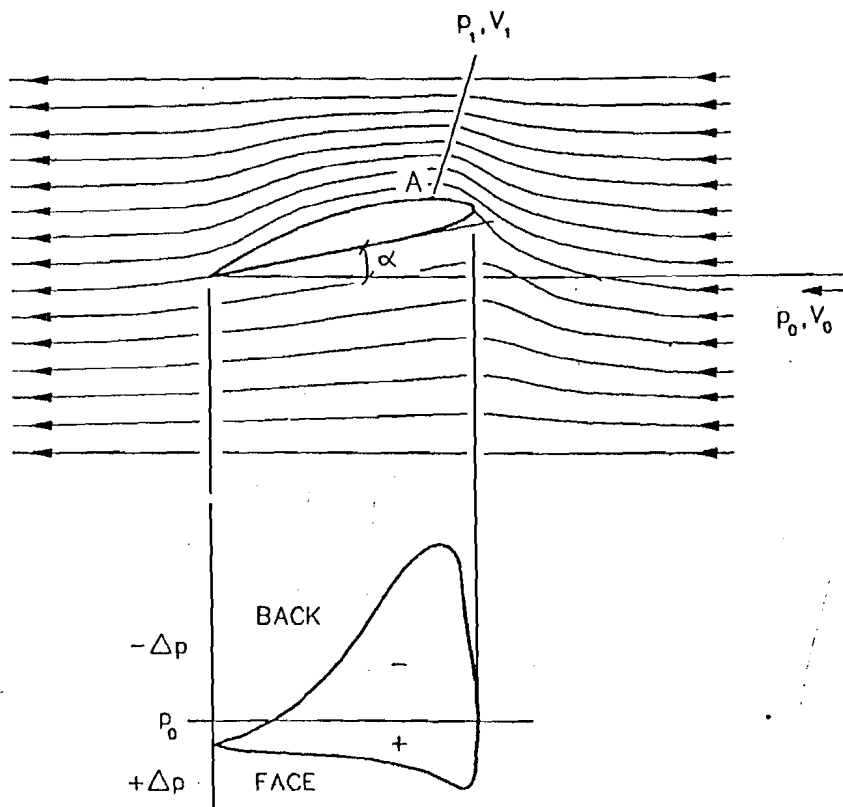


Figure 6.1 : Streamlines and Pressure Distribution around a Propeller Blade Section.

a value of 1.704 kN per m² at 15 °C for fresh water, the value for sea water being slightly lower.

Cavitation in marine propellers usually first manifests itself by an increase in the propeller rpm without a commensurate increase in the speed of the ship. This "racing" of propellers was first noted by Osborne Reynolds in 1873 and was later recorded during the trials of the British torpedo boat "Daring" in 1894. This vessel failed to attain its specified speed with the propellers fitted initially, but when these were replaced by propellers of a greater blade area the speed attained was considerably in excess of that specified. Propeller cavitation also played a part in the trials of the vessel "Turbinia" used by

Sir Charles Parsons to demonstrate the steam turbine. The initial trials of the "Turbinia" with a single propeller proved to be disappointing but when three shafts each carrying three tandem propellers were fitted to the ship, speeds in excess of 34 knots were achieved. In the cases of both the "Daring" and the "Turbinia", the improved performance was shown to be due to the elimination of cavitation by decreasing the loading on the propellers.

The condition for cavitation to occur at a point A on a propeller blade, Fig. 6.1. may be obtained as follows. Let the pressure and velocity at A be p_1 and V_1 and the pressure and velocity at a point at the same depth far ahead of the propeller be p_0 and V_0 , the velocities being measured with respect to the propeller. Then, by the Bernoulli theorem:

$$p_1 + \frac{1}{2} \rho V_1^2 = p_0 + \frac{1}{2} \rho V_0^2$$

so that the difference between the pressures at the point A and at the point far ahead is:

$$\Delta p = p_1 - p_0 = \frac{1}{2} \rho V_0^2 - \frac{1}{2} \rho V_1^2$$

or dividing by the "stagnation pressure" $q = \frac{1}{2} \rho V_0^2$ to make the equation non-dimensional:

$$\frac{\Delta p}{q} = \frac{p_1 - p_0}{\frac{1}{2} \rho V_0^2} = 1 - \left(\frac{V_1}{V_0} \right)^2$$

If cavitation starts at the point A, then $p_1 = p_V$ so that the condition for cavitation to occur is:

$$-\frac{\Delta p}{q} = \frac{p_0 - p_V}{\frac{1}{2} \rho V_0^2} = \left(\frac{V_1}{V_0} \right)^2 - 1 \quad (6.1)$$

If the pressure p_0 is taken as the total static pressure (atmospheric plus hydrostatic pressure) at the point A and V_0 as the relative velocity of water then the condition for cavitation to occur may be written as:

$$-\frac{\Delta p}{q} = \frac{p_0 - p_V}{\frac{1}{2} \rho V_0^2} = \sigma_A \quad (6.2)$$

where σ_A is the "local" cavitation number at A. The quantity $\Delta p/q$ is sometimes written as the pressure coefficient C_p , so that the condition for cavitation to occur on a propeller blade section is that the minimum value of C_p be equal to the local cavitation number. This is normally written as follows:

$$-C_{p_{\min}} = \sigma_A \quad (6.3)$$

For a blade section at a non-dimensional radius $x = r/R$ and angle θ to the upwardly directed vertical line ("12 o'clock position"),

$$-C_{p_{\min}} = \frac{p_A + \rho g(h - x R \cos \theta) - p_V}{\frac{1}{2}\rho [V_A^2 + \{2\pi n x R - V_t\}^2]} \quad (6.4)$$

where V_a is the axial component of the velocity and V_t the tangential component (taken positive in the direction of motion of the blade) at the point (x, θ) , h being the depth of immersion of the propeller shaft axis.

Example 1

A propeller blade section begins to cavitate when its relative velocity with respect to undisturbed water is 32 m per sec and its depth below the surface of water is 4.0 m. Determine the velocity of water with respect to the blade at the point where cavitation occurs, assuming that cavitation occurs when the local pressure falls to the vapour pressure.

$$V_0 = 32.0 \text{ m s}^{-1} \quad h = 4.0 \text{ m} \quad p_A = 101.325 \text{ kN m}^{-2} \quad p_V = 1.704 \text{ kN m}^{-2}$$

$$p_0 = p_A + \rho g h = 101.325 + 1.025 \times 9.81 \times 4.0 = 141.546 \text{ kN m}^{-2}$$

$$q = \frac{1}{2}\rho V_0^2 = \frac{1}{2} \times 1.025 \times 32.0^2 = 524.8 \text{ kN m}^{-2}$$

$$-\frac{\Delta p}{q} = \frac{p_0 - p_V}{\frac{1}{2}\rho V_0^2} = \frac{141.546 - 1.704}{524.8} = 0.2665 = \left(\frac{V_1}{V_0}\right)^2 - 1$$

$$V_1 = 1.2665^{0.5} \times V_0 = 1.1254 \times 32.0 = 36.012 \text{ m s}^{-1}$$

6.2 Cavitation Number

As indicated in Section 4.4, the cavitation number σ of a propeller is often defined by taking p_0 as the total static pressure at the propeller axis and V_0 as the speed of advance V_A :

$$\sigma = \frac{p_A + \rho g h - p_V}{\frac{1}{2} \rho V_A^2} \quad (6.5)$$

where p_A is the atmospheric pressure and h the depth of immersion of the propeller axis.

Instead of the speed of advance, one may take the propeller blade tip speed $\pi n D$ as V_0 :

$$\sigma_n = \frac{p_A + \rho g h - p_V}{\frac{1}{2} \rho (\pi n D)^2} \quad (6.6)$$

or even the resultant of the speed of advance and the tip speed:

$$\sigma_R = \frac{p_A + \rho g h - p_V}{\frac{1}{2} \rho [V_A^2 + (\pi n D)^2]} \quad (6.7)$$

The propeller blade section at $0.7R$ is often taken as representing the whole propeller, and the cavitation number is then defined in terms of the pressure at the shaft axis and the relative velocity of the blade section at $0.7R$ with respect to undisturbed water (induced velocities being neglected):

$$\sigma_{0.7R} = \frac{p_A + \rho g h - p_V}{\frac{1}{2} \rho [V_A^2 + (0.7 \pi n D)^2]} \quad (6.8)$$

On the other hand, it has been observed that in many propellers it is the blade section at $0.8R$ that is most susceptible to cavitation, and since cavitation is most likely to occur when the blade section is at its minimum depth of immersion, the cavitation number should be defined in terms of the pressure and relative velocity in this condition:

$$\sigma_{0.8R} = \frac{p_A + \rho g (h - 0.8R) - p_V}{\frac{1}{2} \rho [V_A^2 + (0.8 \pi n D)^2]} \quad (6.9)$$

With so many different definitions of the cavitation number of a propeller, it is essential to state clearly the definition being used in a particular application. The widely different values obtained for the cavitation numbers defined in different ways are shown by the following example.

Example 2

A propeller of 6.0 m diameter has a speed of advance of 8.0 m per sec and an rpm of 108, its axis being 5.0 m below the surface of water. Calculate the different cavitation numbers.

$$D = 6.0 \text{ m} \quad V_A = 8.0 \text{ ms}^{-1} \quad n = 108 \text{ rpm} = 1.8 \text{ s}^{-1} \quad h = 5.0 \text{ m}$$

Cavitation number based on pressure at the shaft axis and the speed of advance:

$$\sigma = \frac{p_A + \rho gh - p_v}{\frac{1}{2} \rho V_A^2} = \frac{101.325 + 1.025 \times 9.81 \times 5.0 - 1.704}{\frac{1}{2} \times 1.025 \times 8.0^2} = 4.5700$$

Cavitation number based on blade tip speed:

$$\sigma_n = \frac{p_A + \rho gh - p_v}{\frac{1}{2} \rho (\pi n D)^2} = \frac{101.325 + 1.025 \times 9.81 \times 5.0 - 1.704}{\frac{1}{2} \times 1.025 \times (\pi \times 1.8 \times 6.0)^2} = 0.2541$$

Cavitation number based on the resultant velocity at blade tip:

$$\sigma_R = \frac{p_A + \rho gh - p_v}{\frac{1}{2} \rho [V_A^2 + (\pi n D)^2]} = \frac{101.325 + 1.025 \times 9.81 \times 5.0 - 1.704}{\frac{1}{2} \times 1.025 [8.0^2 + (\pi \times 1.8 \times 6.0)^2]} = 0.2407$$

Cavitation number based on the resultant velocity at 0.7R:

$$\begin{aligned} \sigma_{0.7R} &= \frac{p_A + \rho gh - p_v}{\frac{1}{2} \rho [V_A^2 + (0.7 \pi n D)^2]} = \frac{101.325 + 1.025 \times 9.81 \times 5.0 - 1.704}{\frac{1}{2} \times 1.025 [8.0^2 + (0.7 \pi \times 1.8 \times 6.0)^2]} \\ &= 0.4657 \end{aligned}$$

Cavitation number based on the pressure and relative velocity at $0.8R$:

$$\begin{aligned}\sigma_{0.8R} &= \frac{p_A + \rho g(h - 0.8R) - p_v}{\frac{1}{2} \rho [V_A^2 + (0.8 \pi n D)^2]} \\ &= \frac{101.325 + 1.025 \times 9.81 (5.0 - 0.8 \times 3.0) - 1.704}{\frac{1}{2} \times 1.025 [8.0^2 + (0.8 \times \pi \times 1.8 \times 6.0)^2]} \\ &= 0.3065\end{aligned}$$

6.3 Types of Propeller Cavitation

Cavitation in a propeller may be classified according to the region on the propeller where it occurs, viz. tip cavitation, root cavitation, boss or hub cavitation, leading edge cavitation, trailing edge cavitation, face cavitation and back cavitation. Cavitation at a particular location of the propeller indicates a region of low pressures and high velocities. It is often possible to reduce or eliminate such local cavitation by making suitable changes in the propeller geometry, e.g. reducing the pitch and increasing the blade width locally.

Cavitation may also be classified according to the nature of the cavities or their appearance: sheet cavitation, spot cavitation, streak cavitation, cloud cavitation, bubble cavitation and vortex cavitation. In sheet cavitation, the cavity is in the form of a thin sheet covering a large part of the propeller blade surface. Spot cavitation occurs at isolated spots on an uneven blade surface where rough spots cause localised pressure drops. A large number of cavitation spots close together may result in a cavity in the form of a streak. Cloud cavitation usually occurs at the end of a sheet cavity when it disintegrates to form a large number of very small cavities having the appearance of a cloud. In bubble cavitation, spherical cavities are formed at points where the local pressure approaches the vapour pressure. These bubbles grow in size as they move downstream into a region where the pressure would theoretically fall had there been no cavitation. When these vapour filled bubbles then move into a region of pressure which is higher than the vapour pressure the vapour condenses and the bubbles collapse, often suddenly and with tremendous force in a process called implosion (the opposite of explosion). A

propeller blade producing thrust sheds vortices from its trailing edge, these vortices being particularly strong at the tip and the root. The pressure at the core of a vortex is lower than that in the outer layers, and if the pressure at the vortex core falls to the vapour pressure vortex cavitation results.

Sheet cavitation usually begins at the leading edge of a propeller blade when blade sections work at large angles of attack causing a sharp negative pressure peak to occur close to the leading edge. If the angle of attack is positive sheet cavitation occurs on the back of the blade, whereas if the angle of attack has a large negative value sheet cavitation occurs on the propeller blade face. Blade sections that work at zero ("shock free entry") or small angles of attack usually do not suffer from sheet cavitation unless the sections are specially designed to promote sheet cavitation as in "supercavitating" propellers. (Such propellers are discussed in Chapter 12.)

Bubble cavitation occurs in propellers which have aerofoil sections not specially designed for a uniform pressure distribution over the back. Bubbles are formed just upstream of the position of maximum thickness where the pressure falls close to the vapour pressure, grow larger as they move downstream, and collapse violently shortly after they reach the point where the pressure rises above the vapour pressure. The impact of the collapsing bubble is extremely high, and stresses which may be as high as 2800 N per mm² are said to be generated. The repeated collapse of these bubble cavities on the propeller blade surface causes rapid erosion of the blade eventually causing it to break. Cavitation erosion due to bubble cavitation is a serious problem in heavily loaded propellers. Cloud cavitation is also similarly harmful.

Vortex cavitation occurs in the vortices that are shed from the propeller blade tips and roots. The strength of the vortex shed from the blade tip increases downstream as the induced velocities increase, and cavitation in the tip vortex begins some distance downstream of the propeller. This type of cavitation is called unattached tip vortex cavitation. An increase in the loading of the propeller causes the vortex cavity to move upstream gradually until it begins at the blade tip, resulting in attached tip vortex cavitation. A further increase in propeller loading causes the cavity to enlarge at the blade and spread progressively in the form of a sheet from the tip to lower radii on the back of the blade. Cavitation in the vortices shed by the roots of the propeller blades has the appearance of a thick rope consisting of a number

of strands, one for each blade of the propeller. Sometimes, a vortex cavity extends from the propeller to the hull of the ship; this is called propeller hull vortex cavitation.

Fig. 6.2 depicts the various types of propeller cavitation. The occurrence of the different types of cavitation on a propeller depends upon the cavitation

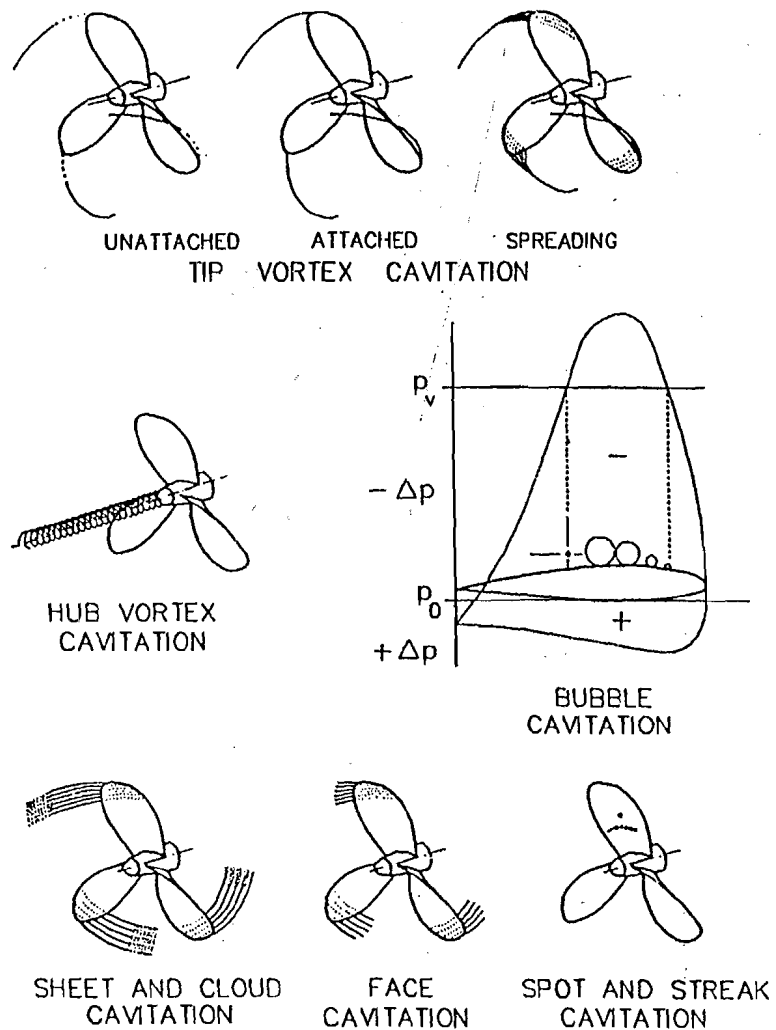


Figure 6.2 : Types of Propeller Cavitation.

number σ and the advance coefficient J , and this is illustrated in Fig. 6.3 by a type of diagram due to R. N. Newton (1961).

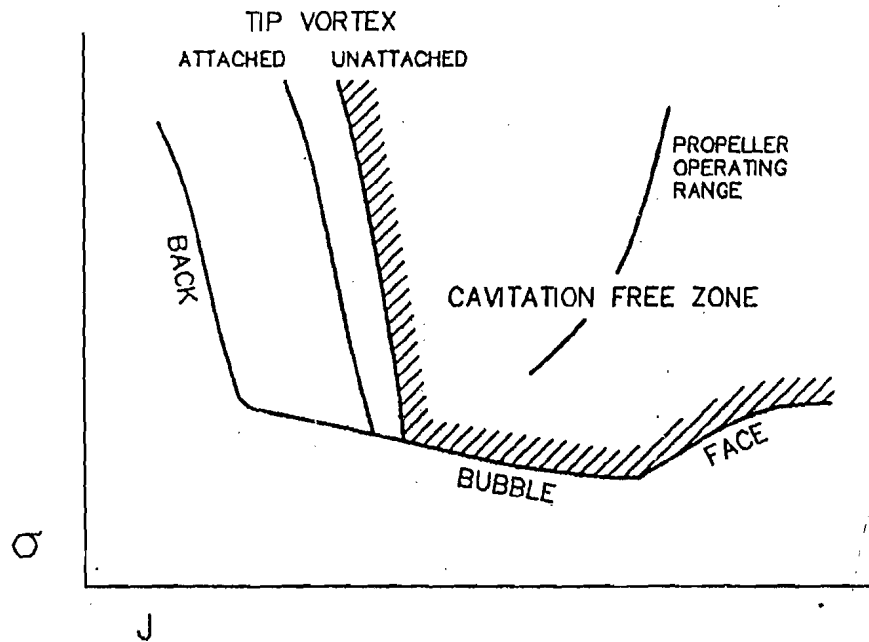


Figure 6.3 : Occurrence of Different Types of Propeller Cavitation.

6.4 Effects of Cavitation

Cavitation affects the nature of the flow around a propeller since the flow is no longer homogeneous. The formation of cavities has the effect of virtually altering the shape of the propeller blade sections, and as a result the thrust and, to a lesser extent, the torque of the propeller are reduced, and so also the propeller efficiency. The effect of cavitation on the open water characteristics of a propeller is shown in Fig. 6.4. The result is that increased power is required to attain a given speed, and in cases of severe cavitation the ship may not achieve the specified speed.

Cavitation can also cause serious damage to a propeller, and sometimes to a rudder placed in the propeller slipstream. As indicated earlier, the collapse

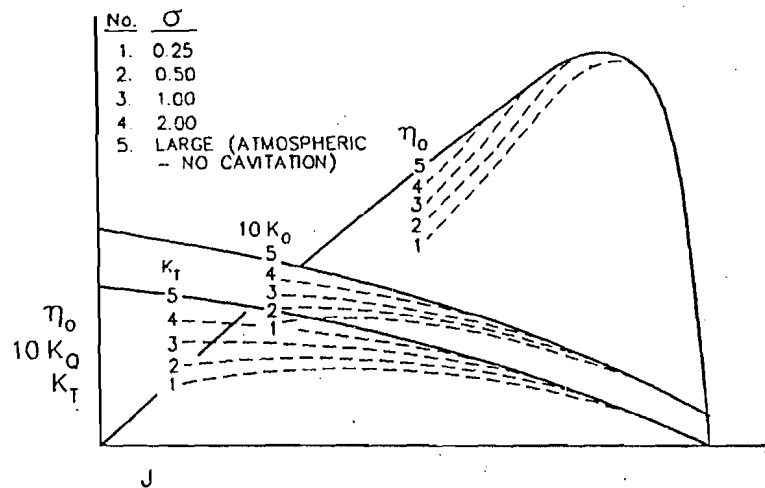


Figure 6.4 : Effect of Cavitation on Propeller Performance.

of bubble cavities results in very high impact pressures and the repeated collapse of such bubbles at a particular location of the propeller blade can cause rapid erosion of the blade leading to its breaking off. If these bubbles collapse near the blade tip or the trailing edge where the blade section is thin, the resulting impact pressures may cause the blades to bend. Sheet cavities and vortex cavities usually disintegrate into clouds of very small bubbles and the collapse of these bubbles on the propeller blades may also damage the propeller. The bubbles in cloud cavitation may be carried to the rudder placed behind the propeller, and adversely affect its performance due to the disruption of flow around it. If these bubbles collapse on the rudder, the rudder surface may be damaged due to cavitation erosion. Corrosion and erosion tend to reinforce each other since the roughened spots created by corrosion promote cavitation, and the pitting produced by cavitation erosion provides a site for corrosion attack.

Another important effect of propeller cavitation is vibration and noise. The propeller induces ship hull vibration through the pressure fluctuations it produces when operating in a non-uniform wake. These pressure impulses are greatly magnified by the occurrence of cavitation. In addition to this low frequency excitation, propeller cavitation also causes high frequency vibration of the propeller blades and the surrounding structure. The resulting

underwater noise is particularly unacceptable in warships, whose propellers have therefore to be designed to be free of cavitation over their complete operating range.

6.5 Prevention of Cavitation

Owing to the detrimental effects of cavitation, propellers are normally designed so that they do not cavitate in their operating conditions, or at least so that cavitation is restricted to a level at which its effects are negligible. In the case of small high speed craft, however, the propeller operating conditions – very high speeds and powers, high rpm, restricted diameter – are sometimes such that avoiding cavitation is virtually impossible, and the propellers are then designed to operate in the fully cavitating regime.

Propeller cavitation can be reduced or eliminated basically by three methods:

- (i) Increasing the cavitation number,
- (ii) Decreasing the loading on the propeller,
- (iii) Designing the propeller for uniform loading.

As may be observed from Fig. 6.4, a lower cavitation number is associated with increasing cavitation. It follows, therefore, that a higher cavitation number will reduce cavitation. The cavitation number may be increased by increasing the depth of immersion of the propeller, and also by decreasing the relative velocities of the propeller blade sections, i.e. decreasing the speed of advance and rpm of the propeller. Generally, however, these variables are determined by other considerations, and increasing the cavitation number to reduce cavitation is an option that is rarely available.

The loading on a propeller is usually taken to mean the thrust per unit projected blade area, T/A_p . Therefore, if it is anticipated that a propeller is likely to cavitate, a possible solution to the problem is to increase the blade area – the solution adopted in the case of the “Daring”. The loading may, of course, also be reduced by distributing the load among a larger number of propellers, which is what was done for the “Turbinia”. Decreasing the

speed of the ship and hence the thrust of the propeller would also reduce cavitation, but this may not be an acceptable design solution.

Designing a propeller to have uniform loading requires that the propeller blade sections be so selected that the pressure distribution on the back of a blade section is as constant as possible over the chord. It has been observed that uniform suction (i.e. uniform negative pressure with respect to the ambient pressure) on a propeller blade section is more likely to be achieved if the blade section has a "shock free entry", i.e. the incident velocity is tangential to the camber centre line of the section or the angle of attack is zero, the centre line has a uniform curvature, and the face and back of the section also have a uniform curvature. Thus, segmental sections (as used in the Gawn Series for example) are less prone to cavitation than aerofoil sections (as used at the inner radii in the B-Series). A popular section shape for propeller blades in which uniform suction is required is the Karman-Trefftz section consisting of two circular arcs. Fig. 6.5 shows the streamlines around

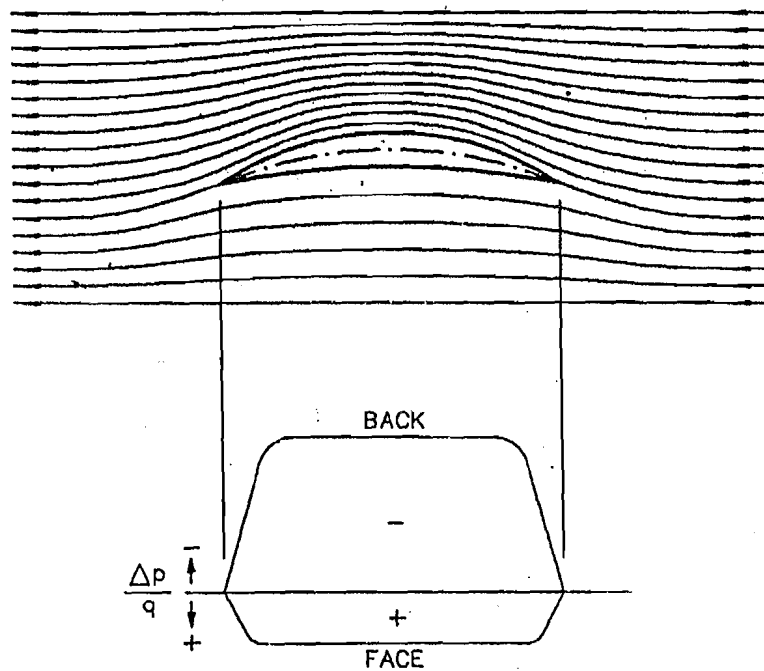


Figure 6.5 : Uniform Suction Section.

such a section and the pressure distribution on it. One may compare this figure with Fig. 6.1. Other blade sections widely used in heavily loaded propellers are the NACA-16 and NACA-66 sections with $a = 0.8$ and $a = 1.0$ mean lines, in which the pressures at the back of the section are uniform over 80 percent and 100 percent of the chord respectively. Details of these section shapes are given in Appendix 2.

It is difficult to avoid cavitation when a heavily loaded propeller works in a non-uniform wake since the incident velocity and the angle of attack for any radial section fluctuate over a wide range depending upon how much the wake velocity varies at that radius. Reducing cavitation therefore also requires the hull form to be designed and the propeller located so that it works in as uniform an inflow as possible.

6.6 Cavitation Criteria

Following the trials of the "Daring" and the "Turbinia", it was suggested that cavitation in a propeller could be avoided if its thrust loading was limited to a figure such as 11.25 lbs per square inch of projected area (77.57 kN per m²). Later on, it was felt that the propeller blade tip speed was a better criterion for preventing propeller cavitation, a recommended value being 12000 ft per min (about 61 m per sec). More modern concepts about the mechanism of cavitation and data based on the performance of propellers in ships as well model tests have led to cavitation criteria based on a non-dimensional form of the thrust loading and the cavitation number.

One of the most widely used cavitation criteria for marine propellers is a diagram introduced by Burrill (1943), Fig. 6.6. The diagram gives the limiting value of a thrust loading coefficient τ_C as a function of the cavitation number $\sigma_{0.7R}$, Eqn. (6.8), for:

- (i) Warship propellers with special sections,
- (ii) Merchant ship propellers (aerofoil sections),
- (iii) Tug and trawler propellers,

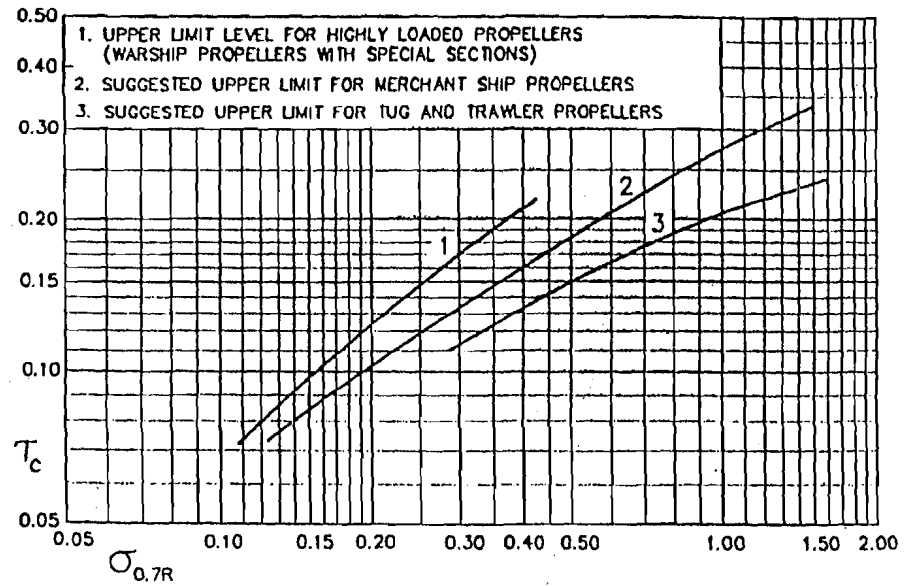


Figure 6.6: Burrill Cavitation Diagram.

where:

$$\tau_c = \frac{\frac{T}{A_P}}{\frac{1}{2} \rho [V_A^2 + (0.7\pi n D)^2]} \quad (6.10)$$

The projected blade area A_P is given approximately by:

$$A_P = \left(1.067 - 0.229 \frac{P}{D}\right) A_D \quad (6.11)$$

where A_D is the developed blade area, which for practical purposes may be taken to be equal to the expanded blade area. It has been suggested that for propellers having elliptical blade outlines, this formula should be modified to:

$$A_P = \left(1.082 - 0.229 \frac{P}{D}\right) A_D \quad (6.12)$$

Experimental data subsequently published by Burrill and Emerson (1962) showed that the limiting line for warship propellers lies close to a line

representing 10 percent back cavitation, while the limiting line for merchant ship propellers lies close to a line representing 5 percent back cavitation. The three lines in the Burrill diagram can be represented quite accurately by the following equations:

(i) Warship propellers with special sections:

$$\tau_C = 0.0130 + 0.5284 \sigma_{0.7R} + 0.3285 \sigma_{0.7R}^2 - 1.0204 \sigma_{0.7R}^3 \quad (6.13)$$

$$(0.11 \leq \sigma_{0.7R} \leq 0.43)$$

(ii) Merchant ship propellers with aerofoil sections:

$$\tau_C = 0.0321 + 0.3886 \sigma_{0.7R} - 0.1984 \sigma_{0.7R}^2 + 0.0501 \sigma_{0.7R}^3 \quad (6.14)$$

$$(0.12 \leq \sigma_{0.7R} \leq 1.50)$$

(iii) Tug and trawler propellers:

$$\tau_C = 0.0416 + 0.2893 \sigma_{0.7R} - 0.1756 \sigma_{0.7R}^2 + 0.0466 \sigma_{0.7R}^3 \quad (6.15)$$

$$(0.28 \leq \sigma_{0.7R} \leq 1.60)$$

These equations should not be used outside the ranges specified.

Another criterion which may be used to determine the expanded blade area required to avoid cavitation is due to Keller (1966):

$$\frac{A_E}{A_O} = \frac{(1.3 + 0.3 Z) T}{(p_0 - p_V) D^2} + k \quad (6.16)$$

where k is a constant, equal to 0 for high speed twin screw ships such as naval vessels with transom sterns, 0.1 for twin screw ships of moderate speed with cruiser sterns and 0.2 for single screw ships.

Although cavitation-free propellers have been successfully designed for decades using simple cavitation criteria such as those due to Burrill and to Keller, it must be realised that cavitation depends not merely on the thrust loading and the cavitation number, but also on the non-uniformity of

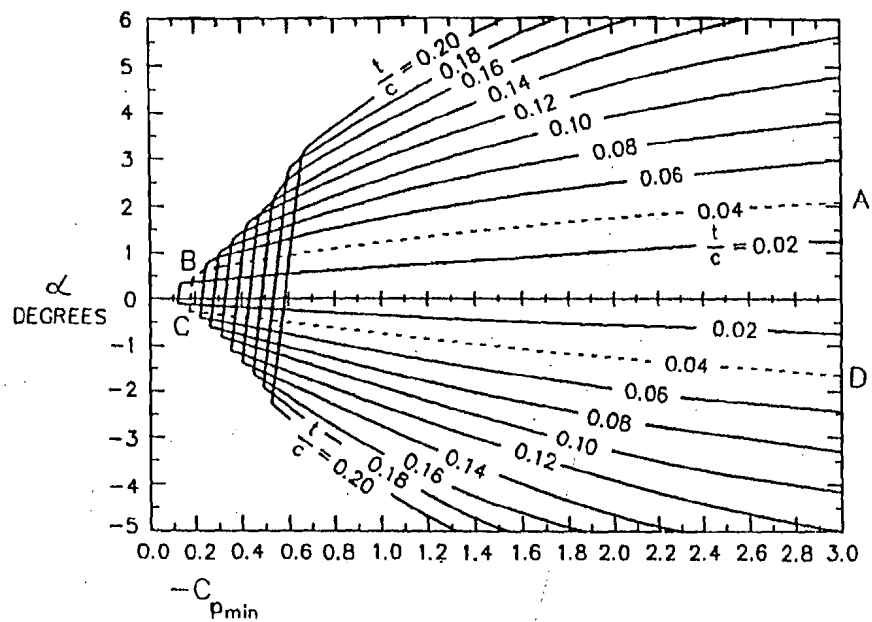


Figure 6.7: Minimum Pressure Envelopes.

wake and the detailed geometry of the propeller blade sections. Cavitation characteristics of aerofoil sections have therefore been determined as a function of the thickness-chord ratio and the angle of attack for different camber ratios and thickness distributions. A typical diagram of this type, as shown in Fig. 6.7, may be obtained for a section shape having a specified thickness distribution (e.g. NACA-66), camber line (e.g. $a = 0.8$) and camber ratio (e.g. 0.02). The region within the "bucket" ABCD for a particular thickness chord ratio (say $t/c = 0.04$) is the region for cavitation-free operation, the regions above AB and below CD are regions for sheet cavitation on the back and face respectively, while the region to the left of BC (low values of $-C_{pmin}$) is the region for bubble cavitation on the back of the section.

The following examples illustrate the use of these cavitation criteria.

Example 3

A propeller of diameter 5.5 m and pitch ratio 1.0 has its axis 4.0 m below the water-line. The propeller has a speed of advance of 7.0 m per sec when running at 120 rpm

and produces a thrust of 520 kN. Determine the expanded blade area ratio of the propeller using the Burrill criterion for merchant ship propellers.

$$D = 5.50 \text{ m} \quad \frac{P}{D} = 1.0 \quad h = 4.0 \text{ m} \quad V_A = 7.0 \text{ ms}^{-1}$$

$$n = 120 \text{ rpm} = 2.0 \text{ s}^{-1} \quad T = 520 \text{ kN}$$

$$V_{0.7R}^2 = V_A^2 + (0.7\pi n D)^2 = 7.0^2 + (0.7\pi \times 2.0 \times 5.50)^2 = 634.169 \text{ m}^2 \text{ s}^{-2}$$

$$\sigma_{0.7R} = \frac{p_A + \rho g h - p_V}{\frac{1}{2} \rho V_{0.7R}^2} = \frac{101.325 + (1.025 \times 9.81 \times 4.0) - 1.704}{\frac{1}{2} \times 1.025 \times 634.169} = 0.4303$$

$$\tau_C = 0.0321 + 0.3886 \sigma_{0.7R} - 0.1984 \sigma_{0.7R}^2 + 0.0501 \sigma_{0.7R}^3 = 0.1666$$

$$\tau_C = \frac{\frac{T}{A_P}}{\frac{1}{2} \rho V_{0.7R}^2} = \frac{\frac{520}{A_P}}{\frac{1}{2} \times 1.025 \times 634.169} = \frac{1.5999}{A_P} = 0.1666$$

$$A_P = \frac{1.5999}{0.1666} = 9.6032 \text{ m}^2$$

$$A_E = \frac{A_P}{1.067 - 0.229 P/D} = \frac{9.6032}{1.067 - 0.229 \times 1.0} = 11.460 \text{ m}^2$$

$$\frac{A_E}{A_O} = \frac{A_E}{\pi D^2/4} = \frac{11.460}{\pi \times 5.50^2/4} = 0.4824$$

Example 4

A twin screw high speed ship with a transom stern has three-bladed propellers of 3.0 m diameter, the propeller axis being 3.5 m below the water surface. The ship has a speed of 30 knots at which its effective power is 10000 kW and the thrust deduction fraction is 0.06. Determine the expanded blade area ratio using the Keller criterion.

$$\text{No. of propellers} = 2 \quad D = 3.0 \text{ m} \quad Z = 3 \quad h = 3.5 \text{ m} \quad P_E = 10000 \text{ kW}$$

$$V = 30 \text{ k} = 15.432 \text{ ms}^{-1} \quad t = 0.06$$

$$\begin{aligned}
 p_0 - p_V &= p_A + \rho gh - p_V = 101.325 + 1.025 \times 9.81 \times 3.5 - 1.704 \\
 &= 134.814 \text{ kN m}^{-2}
 \end{aligned}$$

$$R = \frac{P_E}{V} = \frac{10000}{15.432} = 648.004 \text{ kN}$$

$$T = \frac{1}{2} \frac{R}{1-t} = \frac{648.004}{2(1-0.06)} = 344.683 \text{ kN}$$

$$\begin{aligned}
 \frac{A_E}{A_O} &= \frac{(1.3 + 0.3 Z) T}{(p_0 - p_V) D^2} + k = \frac{(1.3 + 0.3 \times 3) \times 344.683}{134.814 \times 3.0^2} + 0 \\
 &= 0.6250
 \end{aligned}$$

Example 5

In a twin screw ship, the propellers have a diameter of 3.0 m. The pitch ratio is 0.670 at $0.7R$. The propeller centre line is 2.0 m below the waterline. The blade section at $0.7R$ is of an aerofoil shape for which the limiting angles of attack to avoid sheet cavitation on the face and the back are given respectively by $\alpha_{\min} = -0.40 - 0.60 (-C_{p_{\min}})$ and $\alpha_{\max} = 1.35 + 0.65 (-C_{p_{\min}})$, α in degrees. The propellers run at 120 rpm. The axial and tangential velocity components at $0.7R$ when a propeller blade is in the vertically upward position are 3.50 m per sec and 0 respectively. When the blade makes an angle of 120 degrees with its vertically upward position, the axial velocity component is 5.05 m per sec and the tangential velocity component directed opposite to the revolution of the blade is 2.50 m per sec. If these blade positions result in the maximum and minimum angles of attack of the blade section at $0.7R$, show that it operates without cavitation.

$$D = 3.00 \text{ m} \quad \frac{P}{D} = 0.670 \quad h = 2.00 \text{ m} \quad x = \frac{r}{R} = 0.7$$

$$n = 120 \text{ rpm} = 2.0 \text{ s}^{-1}$$

$$\text{Limiting values of } \alpha : \quad \alpha_{\min} = -0.40 - 0.60 (-C_{p_{\min}})$$

$$\alpha_{\max} = 1.35 + 0.65 (-C_{p_{\min}})$$

$$\begin{array}{lll} \theta = 0 & V_a = 3.5 \text{ ms}^{-1} & V_t = 0 \\ \theta = 120^\circ & V_a = 5.05 \text{ ms}^{-1} & V_t = -2.5 \text{ ms}^{-1} \end{array}$$

$$\tan \varphi = \frac{P/D}{\pi x} = \frac{0.670}{\pi \times 0.7} = 0.3047 \quad \varphi = 16.944^\circ$$

$\theta = 0$:

$$\begin{aligned} -C_{p_{\min}} &= \frac{p_A + \rho g(h - x R \cos \theta) - p_V}{\frac{1}{2} \rho [V_a^2 + (2\pi n x R - V_t)^2]} \\ &= \frac{101.325 + 1.025 \times 9.81 (2.0 - 0.7 \times 1.5 \times \cos 0) - 1.704}{\frac{1}{2} \times 1.025 [3.5^2 + (2 \times \pi \times 2.0 \times 0.7 \times 1.5 - 0)^2]} \\ &= 1.1431 \end{aligned}$$

$$\begin{aligned} \text{Limiting values of } \alpha: \quad \alpha_{\min} &= -0.40 - 0.60 (1.1431) = -1.086^\circ \\ \alpha_{\max} &= 1.35 + 0.65 (1.1431) = 2.093^\circ \end{aligned}$$

$$\tan \beta = \frac{V_a}{2\pi n x R - V_t} = \frac{3.5}{2 \times \pi \times 2.0 \times 0.7 \times 1.5 - 0} = 0.2653 \quad \beta = 14.856^\circ$$

$$\alpha = \varphi - \beta = 16.944 - 14.856 = 2.088^\circ : \text{ within the limit for back cavitation.}$$

$\theta = 120^\circ$:

$$\begin{aligned} -C_{p_{\min}} &= \frac{101.325 + 1.025 \times 9.81 (2.0 - 0.7 \times 1.5 \times \cos 120^\circ) - 1.704}{\frac{1}{2} \times 1.025 [5.05^2 + \{2 \times \pi \times 2.0 \times 0.7 \times 1.5 - (-2.5)\}^2]} \\ &= 0.8974 \end{aligned}$$

$$\begin{aligned} \text{Limiting values of } \alpha: \quad \alpha_{\min} &= -0.40 - 0.60 (0.8974) = -0.938^\circ \\ \alpha_{\max} &= 1.35 + 0.65 (0.8974) = 1.933^\circ \end{aligned}$$

$$\tan \beta = \frac{5.05}{2 \times \pi \times 2.0 \times 0.7 \times 1.5 + 2.5} = 0.3218 \quad \beta = 17.836^\circ$$

$$\alpha = \varphi - \beta = 16.944 - 17.836 = -0.892^\circ : \text{within the limit for face cavitation.}$$

The minimum and maximum angles are within the limiting values of angle of attack, and hence there is no cavitation.

6.7 Pressure Distribution on a Blade Section

The pressure distribution on the face and back of a propeller blade may be determined through the lifting surface theory. The pressure distribution on an individual blade section may also be obtained by conformal mapping techniques. However, a simple approximate method has been found to give sufficiently accurate results and is therefore widely used to determine the pressure distribution over aerofoil sections and propeller blade sections. In this method, which is due to Allen (1939) and is described in Abbott and Doenhoff (1959), the increase in velocity $\Delta V = V_1 - V_0$ at any point on the surface of a blade section (see Fig. 6.1) compared to the undisturbed velocity V_0 is taken to be due to three causes: (i) the blade section camber, (ii) the thickness distribution and (iii) the angle of attack.

The increase in velocity ΔV_f due to camber is given for the "ideal" angle of attack α_i (the angle of attack for which the most favourable pressure distribution on the back of the blade section is obtained), the camber ratio f/c being such that the lift coefficient C_{Li} at the ideal angle of attack is 1.0. ΔV_f is proportional to the camber ratio, so that :

$$\Delta V_f = \Delta V_{f1} \frac{f/c}{(f/c)_1} \quad (6.17)$$

where ΔV_{f1} is the increase in velocity due to camber for $C_{Li} = 1.0$ and $(f/c)_1$ is the corresponding camber ratio. Values of ΔV_{f1} , for some blade sections used in marine propellers are given in Appendix 5.

The increase in velocity ΔV_t due to the thickness distribution ("fairing shape") depends on the thickness-chord ratio t/c for a given section shape.

Values of ΔV_t for some blade sections used in marine propellers are given in Appendix 5.

The increase in velocity ΔV_α due to the angle of attack α depends on the thickness-chord ratio of the blade section and the angle of attack measured with respect to the ideal angle of attack α_i . The values of ΔV_{α_i} corresponding to the ideal angle of attack and some standard thickness-chord ratios are given for different mean lines. These values must be first corrected to the desired thickness-chord ratio by interpolation. The values of ΔV_α for a given angle of attack α are then obtained from:

$$\Delta V_\alpha = 2\pi(\alpha - \alpha_i) \Delta V_{\alpha_i} \quad (6.18)$$

α and α_i being in radians.

The increases in velocity due to camber, thickness distribution and angle of attack are added together and the velocity at a point on the blade section obtained:

$$V_1 = V_0 \pm \Delta V_f + \Delta V_t \pm \Delta V_\alpha \quad (6.19)$$

the positive signs corresponding to the back (suction surface) of the blade section and the negative signs to the face (pressure surface). The change in pressure compared to the undisturbed pressure is then obtained as:

$$\frac{\Delta p}{q} = 1 - \left(\frac{V_1}{V_0} \right)^2 \quad (6.20)$$

This can be calculated for different positions along the face and back of the section to obtain its pressure distribution.

Problems

1. A propeller of diameter 4.0 m, pitch ratio 0.8 and blade area ratio 0.50 has its axis 3.0 m below the surface of water. The operating conditions of the propeller correspond to $J = 0.500$, $K_T = 0.140$. The propeller cavitates when its rpm exceeds 150. Calculate the limiting value of thrust per unit projected blade area and the corresponding cavitation number based on the speed of advance.

2. A propeller of 6.0 m diameter has an rpm of 150, its axis being 4.5 m below the surface of water. What is the maximum speed of advance that the propeller can have before the blade sections at $0.8R$ begin to cavitate, given that the maximum relative velocity of water at a point on the section is 7.5 percent greater than the velocity of that point with respect to undisturbed water? Assume that the propeller operates in a uniform wake and that cavitation occurs at the vapour pressure.
3. A ship has a propeller of diameter 5.0 m, pitch ratio 0.8 and expanded blade area ratio 0.750. The ship has a speed of 20 knots with the propeller running at 180 rpm. The effective power of the ship at this speed is 8000 kW, the wake fraction being 0.200 and the thrust deduction fraction 0.120. The upper permissible limit of propeller thrust loading is given by:

$$\tau_c = 0.27 \sigma_{0.7R}^{0.6}$$

What should be the minimum depth of the propeller shaft axis below the waterline?

4. A ship has a resistance of 677 kN at its design speed of 15 knots. The wake fraction is 0.250 and the thrust deduction fraction 0.200. The propeller of diameter 5.0 m and pitch ratio 0.8 has its axis 6.5 m below the load water line and has a design rpm of 150. Determine its expanded blade area ratio based on the Burrill criterion for merchant ship propellers.
5. A propeller of diameter 4.0 m and pitch ratio 0.9 has an expanded blade area ratio of 0.500. The propeller axis is 2.5 m below the surface of water. As the propeller rpm is changed, the speed of the ship changes in such a way that the advance coefficient remains constant:

$$J = 0.500 \quad K_T = 0.150 \quad 10K_Q = 0.170$$

The wake fraction based on thrust identity is 0.250, the thrust deduction 0.200 and the relative rotative efficiency 1.050. Find the speed at which the propeller will begin to cavitate, and the corresponding effective power and delivered power. Use the Burrill criterion for merchant ships.

6. A four bladed propeller of 5.0 m diameter and 0.55 expanded blade area ratio in a single screw ship is required to produce a thrust of 500 kN. Determine the minimum depth of immersion of the shaft axis if the propeller is not to cavitate. Use the Keller criterion.
7. A single screw ship has a five-bladed propeller of 6.0 m diameter and 0.75 expanded blade area ratio with the propeller axis 5.0 m below the waterline. The effective power of the ship can be approximated by $P_E = 0.463 V_K^{3.5}$ with P_E in kW and the ship speed V_K in knots. The thrust deduction fraction is

0.260. Estimate the ship speed at which the propeller will begin to cavitate. Use the Keller criterion.

8. A single screw ship has a propeller of 6.0 m diameter running at 108 rpm. The blade section at $0.7R$ has a pitch ratio of 0.8 and a thickness chord ratio of 0.08, for which the cavitation bucket data to avoid face and back cavitation are as follows:

$-C_{pmin}$:	0.40	0.50	0.60	0.70
α_{min}°	:	-0.69	-0.80	-0.91	-1.12
α_{max}°	:	1.55	1.70	1.85	2.05

The axial and tangential components of the relative velocity of water at $0.7R$ are 7.80 m per sec and 0 when the propeller blade is in the vertically up position (0 degrees), and 8.25 m per sec and 2.00 m per sec when the blade is horizontal (90 degrees). Determine the minimum depths of immersion of the propeller shaft axis to avoid back cavitation and face cavitation completely for these two blade positions.

9. A twin screw ship has propellers of 4.0 m diameter running at 150 rpm, the immersion of the shaft axes being 3.6 m. For the starboard propeller at $0.75R$, the maximum and minimum axial velocity components of water are 10.20 m per sec when the blade is at an angle of 105 degrees to the upward vertical, and 9.40 m per sec at 270 degrees. The tangential velocity components are negligible. The propeller blade section at $0.75R$ is an aerofoil of thickness chord ratio 0.06 for which the following cavitation data are given:

$$C_L = 0.1097 \left(1 - 0.83 \frac{t}{c} \right) (\alpha^\circ + 2.35)$$

$-C_{pmin}$:	0.40	0.50	0.60	0.70
α_{min}°	:	-0.44	-0.59	-0.71	-0.80
α_{max}°	:	1.26	1.41	1.55	1.68

Find the pitch ratio at $0.75R$ such that there is equal margin against both face and back cavitation and the range of values of C_L .

10. A single screw ship has a propeller of 5.0 m diameter running at 120 rpm. The propeller shaft axis has an immersion of 4.8 m. The blade section at $0.7R$ has a pitch ratio of 0.75 and a thickness chord ratio of 0.07. The cavitation data for the section are as follows:

$-C_{p_{min}}$:	0.40	0.50	0.60	0.70	0.80	0.90	1.00
α_{min}°	:	-0.75	-0.90	-1.04	-1.17	-1.29	-1.39	-1.48
α_{max}°	:	1.16	1.29	1.42	1.54	1.66	1.75	1.86

The longitudinal, transverse and vertical components of the relative velocity of water at $0.7R$ for the different angular positions of the propeller blades are as follows:

θ°	:	0	30	60	90	120	150	180
$V_x \text{ m s}^{-1}$:	6.17	6.42	6.91	7.24	7.41	7.16	7.65
$V_y \text{ m s}^{-1}$:	0	-1.86	-1.60	-1.94	-1.72	-0.96	0
$V_z \text{ m s}^{-1}$:	0.54	0.79	1.09	1.41	1.17	0.88	0.59

(x -axis is positive aft, y -axis positive starboard, z -axis positive upward, and the propeller is right-handed.)

Plot α as a function of $-C_{p_{min}}$ and indicate the region in which cavitation occurs in the blade section at $0.7R$.

CHAPTER 7

Strength of Propellers

7.1 Introduction

The propeller is a vital component essential to the safe operation of a ship at sea. It is therefore important to ensure that ship propellers have adequate strength to withstand the forces that act upon them. On the other hand, providing excessive strength would result in heavier propellers with thicker blades than necessary, leading to a reduction in propeller efficiency. A method is therefore needed to calculate the forces acting on a propeller and the resulting stresses, so that the propeller has just the necessary strength for safe operation in service.

The forces that act on a propeller blade arise from the thrust and torque of the propeller and the centrifugal force on each blade caused by its revolution around the axis. Owing to the somewhat complex shape of propeller blades, the accurate calculation of the stresses resulting from these forces is extremely difficult. Moreover, while one may be able to estimate the thrust and torque of a propeller with reasonable accuracy for a ship moving ahead at a steady speed in calm water, it is difficult to determine the loading on a propeller when a ship oscillates violently in a seaway and the propeller emerges out of water and then plunges sharply into it at irregular intervals. The effects of the manoeuvring of a ship on the forces acting on the propeller are also difficult to estimate, particularly for extreme manoeuvres such as "crash stops". One must also take into account the fact that even in calm water the forces acting on the propeller blades are not constant but vary dur-

ing each revolution due to the non-uniform wake in which a propeller works. Finally, a propeller must also withstand the effects of the stresses that may be locked into it during its manufacture, of propeller blade vibration and of corrosion and erosion during its service life.

It is thus evident that the accurate determination of propeller strength is an extremely complex problem. In practice, therefore, it is usual to adopt fairly simple procedures based on a number of assumptions to make the problem less intractable, and to allow for the simplifications by ensuring that the nominal stresses determined by these procedures have values which experience has shown to be satisfactory. The ratio of the ultimate tensile strength of a propeller material and the allowable stress (factor of safety or load factor) used in the simplified procedures for determining propeller blade strength is high, often lying between 10 to 20.

Among the simplifications made in the procedures for determining propeller blade strength are:

- (i) Each propeller blade is assumed to be a beam cantilevered to the boss.
- (ii) The bending moments due to the forces acting on the blade are assumed to act on a cylindrical section, i.e. a section at a constant radius.
- (iii) The stresses in the cylindrical section are calculated on the basis of the simple theory of the bending of beams, the neutral axes of the cylindrical section being assumed to be parallel and perpendicular to the chord of the expanded section.
- (iv) Only the radial distribution of the loading is considered, its distribution along the chord at each radius being ignored.
- (v) Calculations are carried out only for the ship moving at constant velocity in calm water, the effects of manoeuvring, ship motions in a seaway and variable wake not being taken into account.

Further simplifications are made in some methods for estimating propeller blade strength.

7.2 Bending Moments due to Thrust and Torque

Consider a propeller with Z blades and diameter D operating at a speed of advance V_A and revolution rate n with a thrust T and a torque Q . The bending moments due to thrust and torque at the propeller blade section at a radius r_0 may then be determined.

Let dT be the thrust produced by the Z blade elements between the radii r and $r + dr$, Fig. 7.1. The bending moment due to the thrust on each element at the section r_0 is then:

$$dM_T = \frac{1}{Z} dT (r - r_0) \quad (7.1)$$

so that the bending moment at the section due to the thrust on the blade is:

$$M_T = \int_{r_0}^R \frac{1}{Z} \frac{dT}{dr} (r - r_0) dr \quad (7.2)$$

The thrust T and the bending moment due to thrust M_T act in a plane parallel to the propeller axis.

If dQ is the torque of the Z blade elements between r and $r + dr$, the force causing this torque on each of these elements in a plane normal to the propeller axis is dQ/rZ , the resulting bending moment at the section at radius r_0 being:

$$dM_Q = \frac{1}{rZ} dQ (r - r_0) \quad (7.3)$$

The bending moment due to torque is then:

$$M_Q = \int_{r_0}^R \frac{1}{rZ} \frac{dQ}{dr} (r - r_0) dr \quad (7.4)$$

and this acts in a plane normal to the propeller axis.

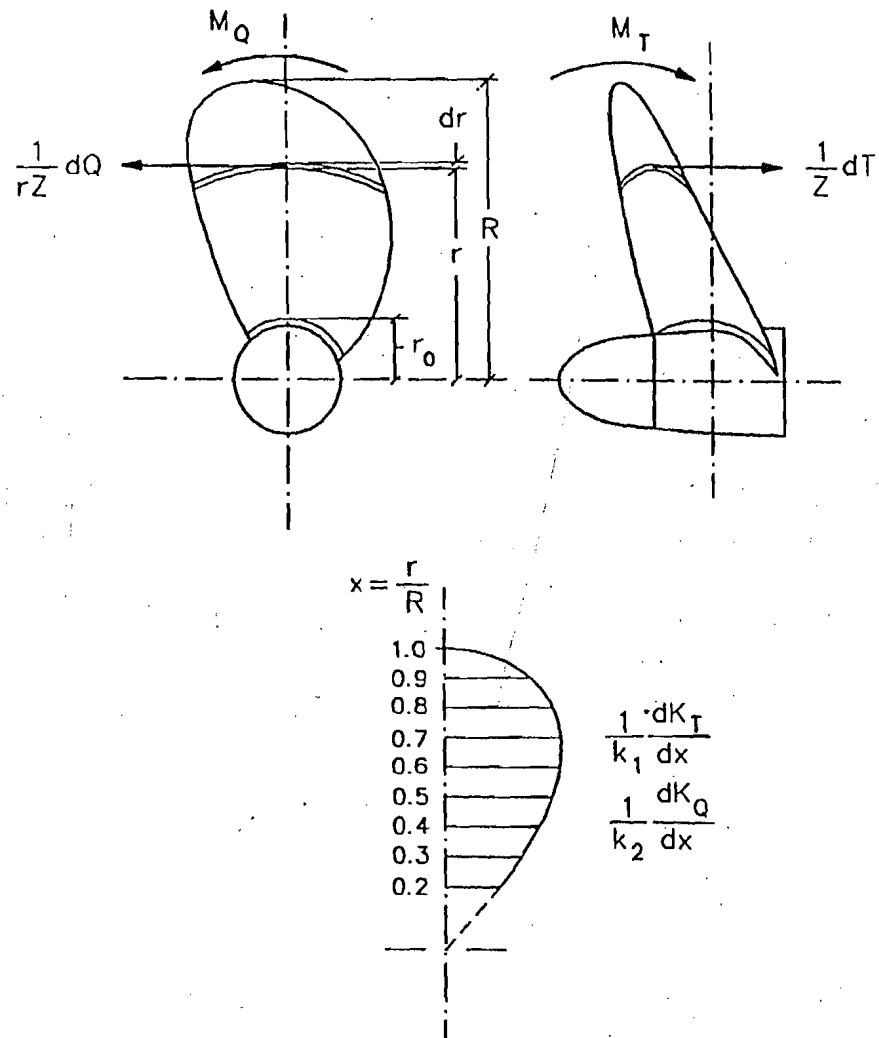


Figure 7.1 : Bending Moments due to Thrust and Torque.

Example 1

A three-bladed propeller of 3.0 m diameter has a thrust of 360 kN and a torque of 300 kN m. Determine the bending moments due to thrust and torque in the root section at 0.3 m radius, assuming that the thrust and torque are uniformly distributed between this radius and the propeller blade tip.

$$Z = 3 \quad D = 3.0 \text{ m} \quad T = 360 \text{ kN} \quad Q = 300 \text{ kNm}$$

$$r_0 = 0.3 \text{ m} \quad \frac{dT}{dr} \text{ and } \frac{dQ}{dr} \text{ constant.}$$

Hence:

$$T = \int_{r_0}^R \frac{dT}{dr} dr = \frac{dT}{dr} (R - r_0)$$

$$\frac{dT}{dr} = \frac{T}{R - r_0} = \frac{360}{1.50 - 0.30} = 300 \text{ kNm}^{-1}$$

Similarly,

$$\frac{dQ}{dr} = \frac{Q}{R - r_0} = \frac{300}{1.50 - 0.30} = 250 \text{ kN}$$

$$\begin{aligned} M_T &= \int_{r_0}^R \frac{1}{Z} \frac{dT}{dr} (r - r_0) dr = \int_{0.30}^{1.50} \frac{1}{3} 300 (r - 0.30) dr \\ &= 100 (0.5 r^2 - 0.3 r) \Big|_{0.30}^{1.50} = 72.000 \text{ kNm} \end{aligned}$$

$$\begin{aligned} M_Q &= \int_{r_0}^R \frac{1}{rZ} \frac{dQ}{dr} (r - r_0) dr = \int_{0.30}^{1.50} \frac{1}{3} \times 250 \left(1 - \frac{0.30}{r}\right) dr \\ &= \frac{250}{3} (r - 0.3 \ln r) \Big|_{0.30}^{1.50} = 59.764 \text{ kNm} \end{aligned}$$

It is often convenient to express the bending moments due to thrust and torque in terms of non-dimensional coefficients. Putting:

$$T = K_T \rho n^2 D^4, \quad Q = K_Q \rho n^2 D^5, \quad x = \frac{r}{R} \quad (7.5)$$

in Eqns. (7.2) and (7.4), one obtains:

$$M_T = \frac{\rho n^2 D^5}{2Z} \int_{x_0}^{1.0} \frac{dK_T}{dx} (x - x_0) dx \quad (7.6)$$

and

$$M_Q = \frac{\rho n^2 D^5}{Z} \int_{x_0}^{1.0} \frac{dK_Q}{dx} \frac{x - x_0}{x} dx \quad (7.7)$$

If $r_0 = x_0 R$ is the radius of the root section, then:

$$K_T = \int_{x_0}^1 \frac{dK_T}{dx} dx \quad K_Q = \int_{x_0}^1 \frac{dK_Q}{dx} dx \quad (7.8)$$

so that:

$$M_T = \frac{K_T \rho n^2 D^5}{2Z} \frac{\int_{x_0}^1 \frac{dK_T}{dx} (x - x_0) dx}{\int_{x_0}^1 \frac{dK_T}{dx} dx} \quad (7.9)$$

and

$$M_Q = \frac{K_Q \rho n^2 D^5}{Z} \frac{\int_{x_0}^1 \frac{dK_Q}{dx} \frac{x - x_0}{x} dx}{\int_{x_0}^1 \frac{dK_Q}{dx} dx} \quad (7.10)$$

The evaluation of M_T and M_Q thus depends upon the distribution of thrust and torque over the radius. A linear distribution is sometimes assumed. However, circulation theory calculations indicate that in most propellers the thrust and torque distributions may be approximately represented by:

$$\frac{dK_T}{dx} = k_1 x^2 (1 - x)^{0.5} \quad (7.11)$$

$$\frac{dK_Q}{dx} = k_2 x^2 (1 - x)^{0.5} \quad (7.12)$$

where k_1 and k_2 are constants. Substituting these expressions into Eqns. (7.9) and (7.10), the bending moments due to thrust and torque become:

$$M_T = \frac{K_T \rho n^2 D^5}{6Z} \frac{16 - 6x_0^2 - 10x_0^3}{8 + 12x_0 + 15x_0^2} \quad (7.13)$$

and

$$M_Q = \frac{K_Q \rho n^2 D^5}{Z} \frac{8 - 2x_0 - 6x_0^2}{8 + 12x_0 + 15x_0^2} \quad (7.14)$$

In many propellers, the root section may be assumed to be at $0.2R$, so that for such propellers $x_0 = 0.2$ and:

$$M_T = 0.2376 \frac{K_T \rho n^2 D^5}{Z} = 0.2376 \frac{T D}{Z} \quad (7.15)$$

$$M_Q = 0.6691 \frac{K_Q \rho n^2 D^5}{Z} = 0.6691 \frac{Q}{Z} \quad (7.16)$$

Example 2

A three-bladed propeller of diameter 3.0 m has a thrust of 360 kN and a torque of 300 kNm at 180 rpm. The thrust and the torque may be assumed to be linearly distributed:

$$\frac{dK_T}{dx} = k_1 x \quad \frac{dK_Q}{dx} = k_2 x$$

between the root section at $x = 0.2$ and $x = 1.0$. Determine the bending moments due to thrust and torque at the root section. How do these values compare with the values obtained by using the distributions of Eqns. (7.11) and (7.12)?

$$Z = 3 \quad D = 3.0 \text{ m} \quad T = 360 \text{ kNm} \quad n = 180 \text{ rpm} = 3.0 \text{ s}^{-1}$$

$$Q = 300 \text{ kN}$$

$$\frac{dK_T}{dx} = k_1 x \quad \frac{dK_Q}{dx} = k_2 x \quad x_0 = 0.2$$

$$\therefore K_T = \frac{T}{\rho n^2 D^4} = \frac{360}{1.025 \times 3.0^2 \times 3.0^4} = 0.4818$$

$$K_Q = \frac{Q}{\rho n^2 D^5} = \frac{300}{1.025 \times 3.0^2 \times 3.0^5} = 0.1338$$

$$K_T = \int_{x_0}^{1.0} \frac{dK_T}{dx} dx = \int_{0.2}^{1.0} k_1 x dx = 0.4818$$

that is:

$$k_1 \frac{x^2}{2} \Big|_{0.2}^{1.0} = \frac{1}{2} k_1 (1.0 - 0.04) = 0.48 k_1 = 0.4818$$

$$k_1 = 1.00375$$

$$K_Q = \int_{x_0}^{1.0} \frac{dK_Q}{dx} dx = \int_{0.2}^{1.0} k_2 x dx = 0.48 k_2 = 0.1338$$

$$k_2 = 0.27875$$

$$\begin{aligned} M_T &= \frac{\rho n^2 D^5}{2 Z} \int_{x_0}^{1.0} \frac{dK_T}{dx} (x - x_0) dx \\ &= \frac{1.025 \times 3.0^2 \times 3.0^5}{2 \times 3} \int_{0.2}^{1.0} 1.00375 x (x - 0.2) dx \\ &= 375.0135 \left(\frac{1}{3} x^3 - 0.1 x^2 \right) \Big|_{0.2}^{1.0} = 88.003 \text{ kNm} \end{aligned}$$

$$\begin{aligned} M_Q &= \frac{\rho n^2 D^5}{Z} \int_{x_0}^{1.0} \frac{dK_Q}{dx} \frac{x - x_0}{x} dx \\ &= \frac{1.025 \times 3.0^2 \times 3.0^5}{3} \int_{0.2}^{1.0} 0.27875 x \frac{x - 0.2}{x} dx \\ &= 208.2890 \left(\frac{x^2}{2} - 0.2 x \right) \Big|_{0.2}^{1.0} = 66.652 \text{ kNm} \end{aligned}$$

Using the thrust and torque distributions of Eqns. (7.11) and (7.12) with $x_0 = 0.2$,

$$M_T = 0.2376 \frac{T D}{Z} = 0.2376 \frac{360 \times 3}{3} = 85.536 \text{ kN m}$$

$$M_Q = 0.6691 \frac{Q}{Z} = 0.6691 \frac{300}{3} = 66.910 \text{ kN m}$$

(Compare these results with those of Example 1 in which uniform thrust and torque distributions have been used.)

7.3 Bending Moments due to Centrifugal Force

In addition to the bending moments due to thrust and torque, bending moments in planes parallel to the propeller axis and normal to it also arise due to the centrifugal force on each blade. If a is the area of the blade section at radius r , the mass of the propeller blade between a radius r_0 and the blade tip is given by:

$$m_b = \int_{r_0}^R \rho_m a \, dr \quad (7.17)$$

where ρ_m is the density of the propeller material. The centroid of the propeller blade will be at a radius :

$$\bar{r} = \frac{\int_{r_0}^R a r \, dr}{\int_{r_0}^R a \, dr} \quad (7.18)$$

so that the centrifugal force on the blade will be:

$$F_C = m_b \bar{r} (2\pi n)^2 = (2\pi n)^2 \rho_m \int_{r_0}^R a r \, dr \quad (7.19)$$

If the distances between the centroid C of the blade and the centroid C_0 of the blade section at radius r_0 are measured as shown in Fig. 7.2, the bending

x	a	SM	$f(m_b)$	$f(m_b) \bar{r}$
0.7	0.0538	4	0.2152	0.15064
0.8	0.0358	2	0.0716	0.05728
0.9	0.0168	4	0.0672	0.06048
1.0	0	1	0	0
			1.3695	0.68942

$$\int_{r_0}^R a \, dr = \frac{1}{3} \times \frac{1.50}{10} \times 1.3695 = 0.068475 \, \text{m}^3$$

$$\int_{r_0}^R a r \, dr = \frac{1}{3} \times \frac{1.50}{10} \times 0.68942 \times 1.50 = 0.0517065 \, \text{m}^4$$

$$\bar{r} = \frac{\int_{r_0}^R a r \, dr}{\int_{r_0}^R a \, dr} = \frac{0.0517065}{0.068475} = 0.755 \, \text{m}$$

$$m_b = \rho_m \int_{r_0}^R a \, dr = 8300 \times 0.068475 = 568.34 \, \text{kg}$$

$$\begin{aligned} F_C &= m_b \bar{r} (2\pi n)^2 = 568.34 \times 0.755 \times (2\pi \times 3)^2 \, \text{kg m s}^{-2} \\ &= 152.461 \, \text{kN} \end{aligned}$$

$$M_R = F_C z_c = 152.461 \times 0.150 = 22.869 \, \text{kN m}$$

$$M_S = F_C y_c = 152.461 \times 0.035 = 5.336 \, \text{kN m}$$

7.4 Stresses in a Blade Section

The bending moments on the blade section at radius r_0 due to thrust and torque and those due to centrifugal force, illustrated in Figs. 7.1 and 7.2, are shown in Fig. 7.3 with reference to the blade section and its principal axes (x_0 - and y_0 - axes). The components of the resultant bending moment along the principal axes are then:

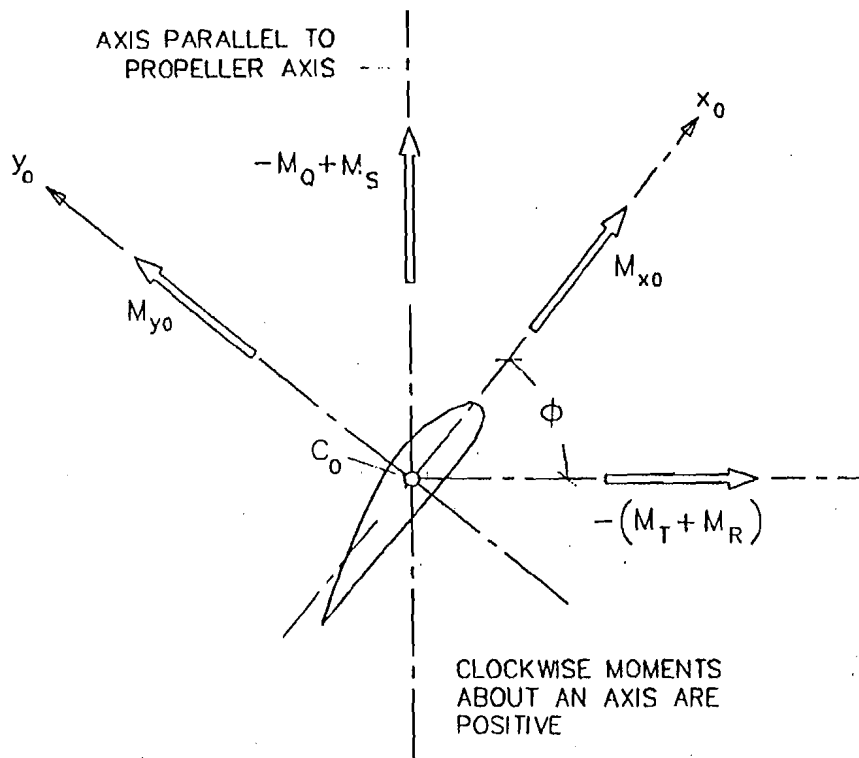


Figure 7.3 : Bending Moments at a Blade Section.

$$M_{x0} = -(M_T + M_R) \cos \varphi - M_Q \sin \varphi \quad (7.22)$$

$$M_{y0} = (M_T + M_R) \sin \varphi - M_Q \cos \varphi \quad (7.23)$$

in which φ is the pitch angle of the blade section, and the bending moment due to skew has been neglected.

If I_{x0} and I_{y0} are the moments of inertia (second moments of area) of the blade section about the x_0 - and y_0 - axes, and a_0 the area of the section, one may determine the stress due to the bending moment and the direct tensile stress due to the centrifugal force at any point of the section whose coordinates are (x_0, y_0) :

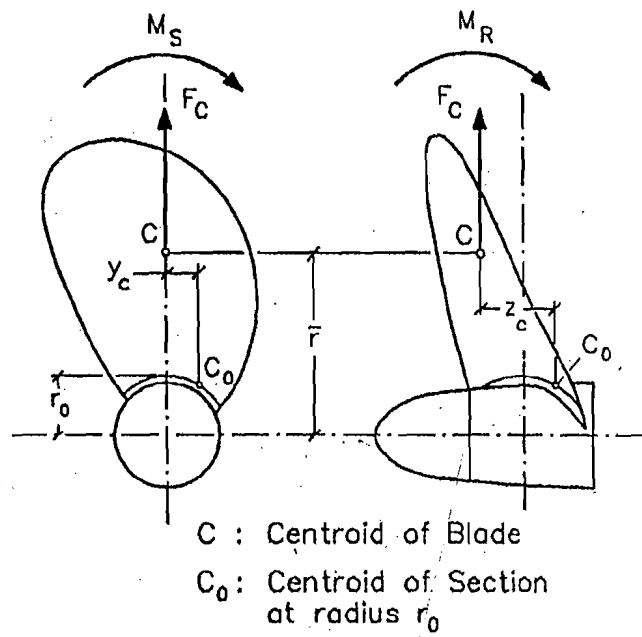


Figure 7.2 : Bending Moments due to Centrifugal Force.

moments due to the centrifugal force in planes through the propeller axis and normal to it are respectively:

$$M_R = F_C \cdot z_c \quad (7.20)$$

$$M_S = F_C \cdot y_c \quad (7.21)$$

The bending moment M_R arises due to the rake of the propeller blades and acts in the same direction as the bending moment due to the propeller thrust M_T in propellers with blades raked aft. If the blades were raked forward so that the line of action of the centrifugal force passed through the centroid of the section at radius r_0 , i.e. if $z_c = 0$, the bending moment due to centrifugal force in a plane through the propeller axis would be zero. The bending moment M_S arises from the skew of the propeller blades and acts in a direction opposite to the bending moment due to the torque M_Q in propellers with skewed back blades. In propellers with moderate skew, the bending

moment due to skew is small and may be neglected, particularly since the error due to this overestimates the resulting bending moments and yields conservative stress values. Moreover, the existence of a bending moment due to skew contradicts the assumption made earlier that the distribution of loading across the blade is ignored. In propellers with heavily skewed blades such an assumption is obviously untenable.

Example 3

The areas of blade sections at various radii of a propeller of 3.0 m diameter are as follows:

r/R	:	0.2	0.3	0.4	0.5	0.6	0.7	0.8	0.9	1.0
Area, m^2	:	0.0651	0.0802	0.0843	0.0807	0.0691	0.0538	0.0358	0.0168	0

The propeller runs at 180 rpm. The propeller is made of Manganese Bronze with a density of 8300 kg per m^3 . Determine the centrifugal force on the blade if the root section is at $0.2R$. If the centroid of the section is at distances of 0.150 m and 0.035 m from the line of action of the centrifugal force measured parallel and perpendicular to the propeller axis, determine the bending moments due to rake and skew.

$$D = 3.0 \text{ m} \quad n = 180 \text{ rpm} = 3.0 \text{ s}^{-1} \quad \rho_m = 8300 \text{ kg m}^{-3}$$

$$x_0 = 0.2 \quad z_c = 0.150 \text{ m} \quad y_c = 0.035 \text{ m}$$

$$m_b = \int_{r_0}^R \rho_m a \, dr \quad \bar{r} = \frac{\int_{r_0}^R a r \, dr}{\int_{r_0}^R a \, dr}$$

m_b and \bar{r} are calculated using Simpson's Rule as follows:

x	a	SM	$f(m_b)$	$f(m_b) \bar{r}$
0.2	0.0651	1	0.0651	0.01302
0.3	0.0802	4	0.3208	0.09624
0.4	0.0843	2	0.1686	0.06744
0.5	0.0807	4	0.3228	0.16140
0.6	0.0691	2	0.1382	0.08292

$$S = \frac{M_{x0}}{I_{x0}/y_0} - \frac{M_{y0}}{I_{y0}/x_0} + \frac{F_C}{a_0} \quad (7.24)$$

a positive stress indicating tension and a negative stress indicating compression. It is usual to calculate the stresses at the leading and trailing edges and at the face and back at the position of maximum thickness of the blade section. For sections of normal aerofoil shape the maximum tensile and compressive stresses occur at the face and the back respectively, close to the position of maximum thickness of the section. The maximum tensile stress in the root section due to bending is then equal to the bending moment M_{x0} divided by the section modulus I_{x0}/y_0 where y_0 is the distance of the centroid from the face chord.

Example 4

A propeller of 3.0 m diameter and constant face pitch ratio 1.0 runs at 180 rpm. The bending moments due to thrust and torque are respectively 65.700 kN m and 59.800 kN m. The mass of each blade is 570 kg, the centroid being at a radius of 0.755 m. The centroid of the root section at $0.2R$ is 0.150 m forward of the centroid of the blade and 0.035 m towards the leading edge from it. The root section has a chord of 0.800 m, a thickness of 0.160 m and an area of 0.0900 m². The position of maximum thickness is 0.270 m from the leading edge. The centroid of the section is 0.065 m from the face and 0.290 m from the leading edge. The leading and trailing edges at the root section have offsets of 0.020 m and 0.010 m from the face chord. The moments of inertia of the section about axes through its centroid and parallel and perpendicular to the face chord are respectively 1.5×10^{-4} m⁴ and 3.2×10^{-3} m⁴. Determine the stresses at the leading and trailing edges, and at the face and the back.

$$D = 3.0 \text{ m} \quad \frac{P}{D} = 1.0 \quad n = 180 \text{ rpm} = 3.0 \text{ s}^{-1}$$

$$M_T = 65.700 \text{ kN m} \quad M_Q = 59.800 \text{ kN m} \quad m_b = 570 \text{ kg} \quad \bar{r} = 0.755 \text{ m}$$

$$z_c = 0.150 \text{ m} \quad y_c = 0.035 \text{ m} \quad a_0 = 0.0900 \text{ m}^2$$

$$I_{x0} = 1.5 \times 10^{-4} \text{ m}^4 \quad I_{y0} = 3.2 \times 10^{-3} \text{ m}^4$$

Coordinates with respect to the given axes:

$$\text{Face:} \quad x_0 = 0.290 - 0.270 = 0.020 \text{ m} \quad y_0 = -0.065 \text{ m}$$

$$\text{Back:} \quad x_0 = 0.020 \text{ m} \quad y_0 = 0.160 - 0.065 = 0.095 \text{ m}$$

$$\text{Leading Edge:} \quad x_0 = 0.290 \text{ m} \quad y_0 = 0.020 - 0.065 = -0.045 \text{ m}$$

$$\text{Trailing Edge:} \quad x_0 = -0.800 + 0.290 = -0.510 \text{ m} \\ y_0 = 0.010 - 0.065 = -0.055 \text{ m}$$

$$F_C = m_b \bar{r} (2\pi n)^2 = 570 \times 0.755 \times (2\pi \times 3.0)^2 \text{ kg m s}^{-2} \\ = 152.906 \text{ kN}$$

$$M_R = F_C z_c = 152.906 \times 0.150 = 22.936 \text{ kN m}$$

$$M_S = F_C y_c = 152.906 \times 0.035 = 5.352 \text{ kN m}$$

$$\tan \varphi = \frac{P/D}{\pi x} = \frac{1.000}{\pi \times 0.2} = 1.5915 \quad \varphi = 57.858 \text{ deg}$$

$$M_{x0} = -(M_T + M_R) \cos \varphi - (M_Q - M_S) \sin \varphi \\ = -(65.700 + 22.936) 0.5320 - (59.800 - 5.352) 0.8467 \\ = -93.255 \text{ kN m}$$

$$M_{y0} = (M_T + M_R) \sin \varphi - (M_Q - M_S) \cos \varphi \\ = (65.700 + 22.936) 0.8467 - (59.800 - 5.352) 0.5320 \\ = 46.082 \text{ kN m}$$

Stress:

$$S = \frac{M_{x0}}{I_{x0}/y_0} - \frac{M_{y0}}{I_{y0}/x_0} + \frac{F_C}{a_0}$$

At the leading edge:

$$S = \frac{-93.255}{1.5 \times 10^{-4}/(-0.045)} - \frac{46.082}{3.2 \times 10^{-3}/0.290} + \frac{152.906}{0.0900} \text{ kNm}^{-2}$$
$$= 2.5499 \times 10^4 \text{ kNm}^{-2} = 25.499 \text{ Nmm}^{-2}$$

Similarly, stresses at the other points are obtained as:

$$\text{Trailing edge } S = 43.236 \text{ Nmm}^{-2}$$

$$\text{Face } S = 41.821 \text{ Nmm}^{-2}$$

$$\text{Back } S = -57.651 \text{ Nmm}^{-2}$$

7.5 Approximate Methods

Owing to the comparative complexity of the method to determine propeller blade stresses discussed in the preceding sections, various approximate methods have been proposed. Such methods have been found to give satisfactory results and are sometimes used in the preliminary stages of propeller design when all the design details are not known. Two such methods are considered here.

A widely used approximate method is due to Admiral D. W. Taylor (1933), who considered the problem of propeller blade strength in great detail but by making various assumptions succeeded in reducing the problem to a few formulas for estimating the maximum compressive and tensile stresses in the root section of the propeller blade. The major assumptions in Taylor's method in addition to those given in Sec. 7.1 are:

- (i) The thrust distribution along the propeller radius is linear.
- (ii) The maximum thickness of the blade also varies linearly with radius.
- (iii) The root section is at $0.2R$.
- (iv) The propeller efficiency is a linear function of the apparent slip in the normal operating condition.

Based on these assumptions, the maximum compressive and tensile stresses in the root section due to thrust and torque are given by formulas, which can be put into the following form:

$$S_C = \frac{C_0 P_D}{Z n D^3 \frac{c}{D} \left(\frac{t_0}{D}\right)^2} \quad (7.25)$$

$$S_T = S_C \left(0.666 + C_1 \frac{t}{c}\right) \quad (7.26)$$

The additional compressive and tensile stresses due to centrifugal force are given by:

$$S'_C = C_2 \rho_m n^2 D^2 \left[\frac{C_3 \tan \epsilon}{2 \frac{t_0}{D}} - 1 \right] \quad (7.27)$$

$$S'_T = C_2 \rho_m n^2 D^2 \left[\frac{C_3 \tan \epsilon}{3 \frac{t_0}{D}} + \frac{C_4 \tan \epsilon}{\frac{c_{\max}}{D}} + 1 \right] \quad (7.28)$$

where:

C_0, C_1, C_2, C_3, C_4 = coefficients dependent on the pitch ratio P/D

P_D = delivered power

n = revolution rate

Z = number of blades

D = diameter

$\frac{c}{D}$ = chord-diameter ratio of the root section

$\frac{t_0}{D}$ = blade thickness fraction

$\frac{t}{c}$ = thickness-chord ratio of the root section

ρ_m = density of propeller material

ϵ = rake angle

$\frac{c_{\max}}{D}$ = maximum chord-diameter ratio of the propeller.

Equations (7.25)–(7.28) are dimensionally homogeneous. However, the values of the coefficients in Table 7.1 give the stresses in kN per m² if P_D is in kW, n in revolutions per sec, D in m and ρ_m in kg per m³.

Table 7.1
Coefficients for Taylor's Method

$\frac{P}{D}$	C_0	C_1	C_2	C_3	C_4
0.600	7.499	0.650	0.002568	2.750	1.590
0.700	6.471	0.710	0.002568	2.600	1.690
0.800	5.659	0.754	0.002568	2.400	1.790
0.900	5.073	0.784	0.002568	2.200	1.870
1.000	4.583	0.804	0.002568	2.070	1.925
1.100	4.190	0.817	0.002568	1.920	1.980
1.200	3.895	0.823	0.002568	1.800	2.020
1.300	3.674	0.820	0.002568	1.690	2.050

Taylor's method has been found to give satisfactory results for propellers with normal blade outlines and moderate blade area ratios. For very large blade area ratios the method gives stress values which are 10–15 percent lower than values obtained by more accurate methods.

Another approximate method for estimating propeller blade stress is due to Burrill (1959). In this method it is assumed that the thrust distribution

is such that the thrust on each blade can be taken to act at a point whose distance from the root section is 0.6 times the length of the blade from root to tip. The transverse force on each blade which gives rise to the torque is similarly taken to act at a distance from the root section of 0.55 times the length of the blade. The thrust and torque bending moments can therefore be written as:

$$M_T = \frac{T}{Z} \times 0.60 (R - r_0) = \frac{T D}{Z} \times 0.30 (1 - x_0) \quad (7.29)$$

$$M_Q = \frac{Q \times 0.55 (R - r_0)}{Z[0.55 (R - r_0) + r_0]} = \frac{Q \times 0.55 (1 - x_0)}{Z (0.55 + 0.45 x_0)} \quad (7.30)$$

where $r_0 = x_0 R$ is the radius of the root section.

The mass of each blade is approximated by:

$$m_b = \rho_m \bar{t} \frac{A_D}{Z} k \quad (7.31)$$

where \bar{t} is the mean thickness of the blade from root to tip, A_D the developed blade area and k a coefficient. For a linear distribution of thickness,

$$\bar{t} = 0.50 \left[(1 - x_0) \frac{t_0}{D} + (1 + x_0) \frac{t_1}{D} \right] D \quad (7.32)$$

where t_0/D is the blade thickness fraction of the propeller and t_1 is the blade thickness at the tip. A value of $k = 0.75$ is often used.

The distance of the centroid of the blade from the root section is taken as 0.32 times the length of the blade from root to tip for blades with normal outlines and 0.38 times the blade length for blades with wide tips, i.e.

$$\bar{x} R = x_0 R + k_1 (1 - x_0) R \quad (7.33)$$

where $\bar{r} = \bar{x} R$ is the radius of the blade centroid, $k_1 = 0.32$ for normal blade outlines and $k_1 = 0.38$ for wide tipped outlines.

The centrifugal force is then given by:

$$F_C = m_b (2\pi n)^2 \bar{x} R \quad (7.34)$$

The bending moment due to rake is:

$$M_R = F_C (\bar{x} - x_0) R \tan \varepsilon_E \quad (7.35)$$

where ε_E is the effective rake angle, about 6 degrees greater than the geometric rake angle. The effect of skew is neglected.

The cross-sectional area of the root section and its section modulus are estimated as follows:

$$a = k_2 c t \quad (7.36)$$

$$\frac{I}{y} = k_3 c t^2 \quad (7.37)$$

where c and t are the chord and thickness of the root section, and k_2 and k_3 are coefficients whose values are as follows:

Section Shape	k_2	k_3
Segmental	0.667	0.112
Aerofoil	0.725	0.100
Lenticular	0.667	0.083

The stress in the root section is then given by:

$$S = \frac{(M_T + M_R) \cos \varphi + M_Q \sin \varphi}{\frac{I}{y}} + \frac{F_C}{a} \quad (7.38)$$

where φ is the pitch angle of the root section. Burrill's method gives the stress on the face of the root section at the position of maximum thickness. The maximum tensile stress normally occurs at this point.

Example 5

- (a) A four-bladed propeller of 5.0 m diameter has a constant pitch ratio of 0.950, an expanded blade area ratio of 0.550 and a blade thickness fraction of 0.045. The root section is at $0.2R$ and has a chord-diameter ratio of 0.229 and a thickness-chord ratio of 0.160. The maximum chord-diameter ratio of the blade is 0.301. The propeller blades have a rake of 10 degrees aft. The propeller is made of Nickel Aluminium Bronze, which has a density of 7600 kg per m^3 . The propeller has a delivered power of 5000 kW at 120 rpm. Determine the propeller blade stresses by Taylor's method.
- (b) Determine the propeller blade stress by Burrill's method given the following additional data: speed of advance 7.0 m per sec, propeller efficiency 0.690 and blade thickness at tip 17.5 mm. The propeller blades have a normal outline and aerofoil sections.

(a) Taylor's method:

$$Z = 4 \quad D = 5.0 \text{ m} \quad \frac{P}{D} = 0.950 \quad \frac{A_E}{A_O} = 0.550 \quad \frac{t_0}{D} = 0.045$$

$$x_0 = 0.2 \quad \frac{c}{D} = 0.229 \quad \frac{t}{c} = 0.160 \quad \frac{c_{\max}}{D} = 0.301$$

$$\epsilon = 10^\circ \quad \rho_m = 7600 \text{ kg m}^{-3} \quad P_D = 5000 \text{ kW}$$

$$n = 120 \text{ rpm} = 2.0 \text{ s}^{-1}$$

From Table 7.1 for $\frac{P}{D} = 0.950$,

$$C_0 = 4.828 \quad C_1 = 0.794 \quad C_2 = 0.002568$$

$$C_3 = 2.135 \quad C_4 = 1.898$$

$$S_C = \frac{C_0 P_D}{Z n D^3 \frac{c}{D} \left(\frac{t_0}{D} \right)^2} = \frac{4.828 \times 5000}{4 \times 2.0 \times 5.0^3 \times 0.229 \times (0.045)^2}$$

$$= 52057 \text{ kN m}^{-2} = 52.057 \text{ N mm}^{-2}$$

$$S_T = S_C \left(0.666 + C_1 \frac{t}{C} \right) = 52057 (0.666 + 0.794 \times 0.160)$$

$$= 41283 \text{ kNm}^{-2} = 41.283 \text{ Nmm}^{-2}$$

$$S'_C = C_2 \rho_m n^2 D^2 \left[\frac{C_3 \tan \epsilon}{2t_0/D} - 1 \right]$$

$$= 0.002568 \times 7600 \times 2.0^2 \times 5.0^2 \left[\frac{2.135 \tan 10^\circ}{2 \times 0.045} - 1 \right]$$

$$= 6212 \text{ kNm}^{-2} = 6.212 \text{ Nmm}^{-2}$$

$$S'_T = C_2 \rho_m n^2 D^2 \left[\frac{C_3 \tan \epsilon}{3t_0/D} + \frac{C_4 \tan \epsilon}{c_{\max}/D} + 1 \right]$$

$$= 1951.68 \left[\frac{2.135 \tan 10^\circ}{3 \times 0.045} + \frac{1.898 \tan 10^\circ}{0.301} + 1 \right]$$

$$= 9564 \text{ kNm}^{-2} = 9.564 \text{ Nmm}^{-2}$$

Compressive stress, $S_C + S'_C = 58.269 \text{ Nmm}^{-2}$

Tensile stress, $S_T + S'_T = 50.847 \text{ Nmm}^{-2}$

(b) Burrill's method:

$$V_A = 7.0 \text{ ms}^{-1} \quad \eta = 0.690 \quad t_1 = 17.5 \text{ mm}$$

Normal blade outline, aerofoil sections

$$k = 0.75 \quad k_1 = 0.32 \quad k_2 = 0.725 \quad k_3 = 0.100$$

$$P_T = P_D \eta = 5000 \times 0.690 = 3450 \text{ kW}$$

$$T = \frac{P_T}{V_A} = \frac{3450}{7.0} = 492.857 \text{ kN}$$

$$Q = \frac{P_D}{2\pi n} = \frac{5000}{2\pi \times 2.0} = 397.887 \text{ kNm}$$

$$M_T = \frac{T D}{Z} \times 0.30 (1 - x_0) = \frac{492.857 \times 5.0}{4} \times 0.30 (1 - 0.20)$$

$$= 147.857 \text{ kNm}$$

$$M_Q = \frac{Q}{Z} \times \frac{0.55 (1 - x_0)}{0.55 + 0.45 x_0} = \frac{397.887}{4} \times \frac{0.55 (1 - 0.20)}{0.55 + 0.45 \times 0.20}$$

$$= 68.387 \text{ kNm}$$

$$\frac{t_1}{D} = \frac{17.5}{5000} = 0.0035$$

$$\bar{t} = 0.50 \left[(1 - x_0) \frac{t_0}{D} + (1 + x_0) \frac{t_1}{D} \right] D$$

$$= 0.50 [(1 - 0.20) 0.45 + (1 + 0.20) 0.0035] 5.000 \text{ m}$$

$$= 0.1005 \text{ m}$$

$$A_E = \frac{A_E}{A_O} \frac{\pi D^2}{4} = 0.55 \times \frac{\pi \times 5.0^2}{4} = 10.799 \text{ m}^2 \approx A_D$$

$$m_b = \rho_m \bar{t} \frac{A_D}{Z} k$$

$$= 7600 \times 0.1005 \times \frac{10.799}{4} \times 0.75 = 1546.584 \text{ kg}$$

$$\bar{x} R = [x_0 + k_1 (1 - x_0)] R = [0.20 + 0.32 (1 - 0.20)] 2.500$$

$$= 1.140 \text{ m}$$

$$F_C = m_b (2\pi n)^2 \bar{x} R = 1546.584 \times (2\pi \times 2.0)^2 \times 1.140 \text{ N}$$

$$= 278418.5 \text{ N} = 278.419 \text{ kN}$$

$$\begin{aligned}
 M_R &= F_C (\bar{x} - x_0) R \tan \varepsilon_E \\
 &= 278.419 (0.456 - 0.20) \times 2.500 \tan (10 + 6)^\circ \text{ kNm} \\
 &= 51.095 \text{ kNm}
 \end{aligned}$$

$$\begin{aligned}
 a &= k_2 c t = k_2 \left(\frac{c}{D} \right)^2 \frac{t}{c} D^2 = 0.725 \times 0.229^2 \times 0.160 \times 5.0^2 \\
 &= 0.1521 \text{ m}^2
 \end{aligned}$$

$$\begin{aligned}
 \frac{I}{y} &= k_3 c t^2 = k_3 \left(\frac{c}{D} \right)^3 \left(\frac{t}{c} \right)^2 D^3 = 0.100 \times 0.229^3 \times 0.160^2 \times 5.0^3 \\
 &= 3.8429 \times 10^{-3} \text{ m}^3
 \end{aligned}$$

$$\begin{aligned}
 \tan \varphi &= \frac{P/D}{\pi x_0} = \frac{0.950}{\pi \times 0.20} = 1.5120 \\
 \varphi &= 56.520^\circ \quad \cos \varphi = 0.5516 \quad \sin \varphi = 0.8341
 \end{aligned}$$

$$\begin{aligned}
 \text{Stress } S &= \frac{(M_T + M_R) \cos \varphi + M_Q \sin \varphi}{I/y} + \frac{F_C}{a} \\
 &= \frac{(147.857 + 51.095) 0.5516 + 68.387 \times 0.8341}{3.8429 \times 10^{-3}} + \frac{278.419}{0.1521} \\
 &= 45230 \text{ kNm}^{-2} = 45.230 \text{ Nmm}^{-2}
 \end{aligned}$$

7.6 Classification Society Requirements

Classification Societies such as the American Bureau of Shipping and the Lloyd's Register of Shipping prescribe the strength requirements that propellers must fulfil. These include requirements for the minimum blade thickness, the fitting of the propeller to the shaft, and the mechanical properties of the propeller material.

Lloyd's Register (LR), for example, specifies the minimum propeller blade thickness at $0.25R$ and $0.60R$ for solid propellers (i.e. propellers in which the

blades are cast integral with the boss, unlike controllable pitch propellers). For a propeller having a skew angle less than 25 degrees, the blade thickness neglecting any increase due to fillets is given by a formula which, in LR's notation, is:

$$T = \frac{KCA}{EFULN} + 100 \sqrt{\frac{3150MP}{EFRULN}} \quad (7.39)$$

where:

$$K = \frac{GBD^3R^2}{675}$$

G = density of the propeller material in g/cm³

B = developed blade area ratio

D = propeller diameter in m

R = propeller rpm at maximum power

C = 1.0 for 0.25 R and 1.6 for 0.60 R

A = rake at blade tip in mm (positive aft)

E = actual face modulus/0.09 T^2L , but may be taken as 1.0 and 1.25 respectively for aerofoil sections with and without trailing edge washback

T = blade thickness in mm at the radius considered, i.e. 0.25 R or 0.60 R

L = length in mm of the expanded cylindrical section at the radius considered

U = allowable stress in N per mm²

$$F = \frac{P_{0.25}}{D} + 0.8 \text{ for } 0.25R$$

$$= \frac{P_{0.6}}{D} + 4.5 \text{ for } 0.6R$$

N = number of blades

$$\begin{aligned} M &= 1.0 + \frac{3.75}{P_{0.7}/D} + 2.8 \frac{P_{0.25}}{D} \text{ for } 0.25R \\ &= 1.35 + \frac{5}{P_{0.7}/D} + 1.35 \frac{P_{0.6}}{D} \text{ for } 0.60R \end{aligned}$$

P = maximum shaft power in kW

(Note the units of the different quantities.)

The fillet radius between the root section and the propeller boss is not to be less than the thickness of the root section. Composite radiused fillets or elliptical fillets which provide a greater effective radius to the blade are preferred. Where fillet radii of the required size cannot be provided, the allowable stress must be appropriately reduced.

The allowable stress for propellers of cast iron, carbon steels or low alloy steels may be increased if an approved method of cathodic protection is provided. The allowable stress given in Table 7.4 may be increased by 10 percent for twin screws.

For propellers with skew angles exceeding 25 degrees, a detailed blade stress computation based on calculated hydrodynamic pressure distributions along the length and width of the blades must be carried out. For propellers operating in more than one operating regime, e.g. tug and trawler propellers, detailed stress computations for each condition must be carried out.

There are special requirements for propellers in ships operating in ice-covered waters.

Detailed requirements for the fitting of the propeller to the shaft are also given. These requirements are important because the propeller shaft and the boss are regions of high stress, which can lead to the loss of the propeller at sea. Special care is required to see that the keys and keyways do not lead to high stress concentrations. Round ended or sled runner keys are to be used, and the corners of the keyways must be provided with smooth fillets of radii at least equal to 0.0125 times the shaft diameter. Effective means must be provided to prevent sea water coming into contact with the steel propeller shaft inside the propeller boss, since this reduces the fatigue strength of the shaft significantly.

7.7 Propeller Materials

The material of which a propeller is made should have certain desirable properties. The processes involved in the manufacture of a propeller are casting and machining, and the propeller material must be amenable to these processes. It may be necessary to consult the propeller manufacturer when deciding on a propeller material. The material should be easy to cast into large castings, which should have uniform shrinkage and low internal stresses. The propeller casting should be capable of being machined to a high degree of accuracy and given a smooth surface with a high degree of polish. The propeller material should have a high strength and toughness so that the propeller blade thickness is not so large as to impair efficiency. Fatigue strength is also important. Resistance to corrosion in sea water and to erosion are desirable qualities in a propeller material. It is also advantageous if the material is such that a damaged propeller can be easily repaired. A low density allows a propeller to be made lighter. The cost of the propeller material is also a consideration.

The first material to be widely used for ship propellers was cast iron, which is easy to cast and has a low cost. However, it has a low strength and ductility, a low resistance to corrosion and erosion, cannot be finished to a smooth surface and cannot be easily repaired. Cast iron propellers have thicker blades and are less efficient. Spheroidal graphite cast iron, which is stronger and more ductile, is preferred. However, for propellers in oceangoing ships, copper alloys have largely superseded cast iron as a propeller material, except in some tugs, ice breakers and similar vessels in which cast iron is used for propellers because the blades break off cleanly when they strike an obstacle without damaging the rest of the propulsion system. Cast steel is also used sometimes for making propellers. However, cast steel propellers have a fairly rough surface finish and run the risk of corrosion and have reduced fatigue strength in sea water. Copper alloys ranging from Manganese Bronze to Nickel Aluminium Bronze are now widely used as propeller materials since they have the desired qualities. There is some risk of dezincification with Manganese Bronze. Nickel Aluminium Bronze has a high fatigue strength. Stainless steels are somewhat difficult to cast but are highly resistant to corrosion and erosion and have high strength and toughness.

Classification Societies generally specify the chemical composition and mechanical properties of the materials which may be used for propeller manufacture. Lloyd's Register, for instance, specifies the chemical composition for carbon-manganese steels for cast steel propellers given in Table 7.2.

Table 7.2

**Chemical Composition of Carbon-Manganese Steels
for Cast Steel Propellers
(Lloyd's Register of Shipping)**

Carbon	0.25% max	Residual elements:	
Silicon	0.60% max	Copper	0.30% max
Manganese	0.50-1.60%	Chromium	0.30% max
Sulphur	0.040% max	Nickel	0.40% max
Phosphorus	0.040% max	Molybdenum	0.15% max
		Total	0.80% max

For alloy and stainless steels, the chemical composition, heat treatment, mechanical properties, microstructure and repair procedures must be submitted for approval. The chemical composition of copper alloys used for propellers is given in Table 7.3, while the mechanical properties of materials normally used for propeller manufacture are given in Table 7.4.

7.8 Some Additional Considerations

Although the propeller blade thickness is determined primarily from considerations of allowable stress, propeller designers often adopt higher blade thicknesses than those determined by strength calculations. Apart from providing a greater margin against structural failure, a higher blade thickness also provides a greater margin against cavitation. This is evident from Fig. 6.7.

In heavily loaded propellers operating in a non-uniform wake, it is also necessary to consider fatigue strength. The minimum and maximum values

Table 7.3

Chemical Composition of Copper Alloys for Propellers
(Lloyd's Register of Shipping)

Alloy Designation	Chemical Composition (percent)							
	Cu	Sn	Zn	Pb	Ni	Fe	Al	Mn
Grade Cu 1 Manganese Bronze (High Tensile Brass)	52-62	0.1-1.5	35-40	0.5 max	1.0 max	0.5-2.5	0.5-3.0	0.5-4.0
Grade Cu 2 Nickel Manganese Bronze (High Tensile Brass)	50-57	0.1-1.5	33-38	0.5 max	2.5-8.0	0.5-2.5	0.5-2.0	1.0-4.0
Grade Cu 3 Nickel Aluminium Bronze	77-82	0.1 max	1.0 max	0.03 max	3.0-6.0	2.0-6.0	7.0-11.0	0.5-4.0
Grade Cu 4 Manganese Aluminium Bronze	70-80	1.0 max	6.0 max	0.05 max	1.5-3.0	2.0-5.0	6.5-9.0	8.0-20.0

Table 7.4
Mechanical Properties of Propeller Materials
 (Lloyd's Register of Shipping)

Material	Minimum Tensile Strength	Density	Allowable Stress
	N/mm ²	g/cm ³	N/mm ²
Grey Cast Iron	250	7.2	17.2
Spheroidal or Nodular Graphite Cast Iron	400	7.3	20.6
Carbon Steels	400	7.9	20.6
Low Alloy Steels	440	7.9	20.6
13% Chromium Stainless Steels	540	7.7	41.0
Chromium-Nickel Austenitic Stainless Steel	450	7.9	41.0
Duplex Stainless Steels	590	7.8	41.0
Grade Cu 1 Manganese Bronze (High Tensile Brass)	440	8.3	39.0
Grade Cu 2 Nickel Manganese Bronze (High Tensile Brass)	440	8.3	39.0
Grade Cu 3 Nickel Aluminium Bronze	590	7.6	56.0
Grade Cu 4 Manganese Aluminium Bronze	630	7.5	46.0

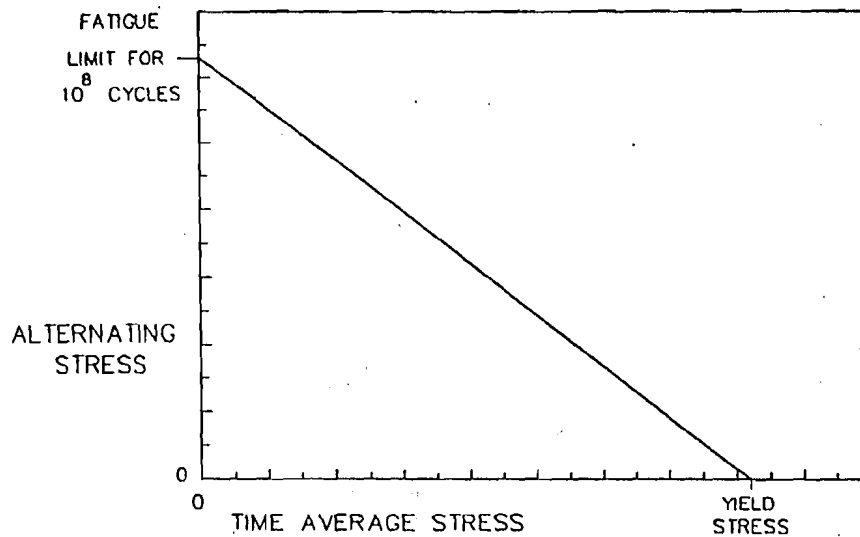


Figure 7.4 : Allowable Alternative Stress.

of the bending moments due to the thrust and torque of a propeller working in a non-uniform wake field can be determined using lifting line or lifting surface theory, and the minimum and maximum stresses at the blade root calculated. The allowable alternating stress for a given number of cycles depends upon the temporal mean stress, and can be determined by a Goodman diagram, Fig. 7.4. The fatigue strength of some propeller materials in sea water is given in Table 7.5 along with their yield stress or 0.2 percent proof stress.

For heavily skewed propellers, the stresses calculated by the methods discussed earlier, i.e. using the beam theory and neglecting the distribution of loading in a chordwise direction, do not correlate well with experimental data. The beam theory calculations predict neither the magnitude nor the location of the maximum stress at the blade root correctly. This is partly due to the fact that in addition to the bending moments due to thrust and torque there are also twisting moments because the centre of action of the hydrodynamic forces does not lie close to the radial line through the centroid of the root section. It is thus necessary to consider both bending and torsion in heavily skewed propeller blades. Lifting surface calculations, or lifting line calculations in conjunction with two-dimensional pressure distri-

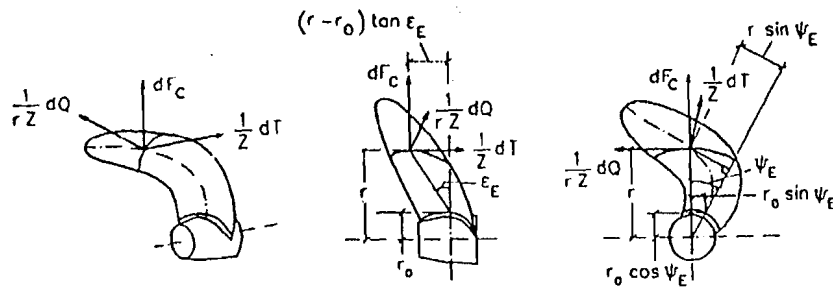
Table 7.5

**Fatigue and Yield Strengths of
some Propeller Materials**

Material	Fatigue Strength for 10^8 cycles in Sea Water	Yield Stress or 0.2% Proof Stress
	N/mm ²	N/mm ²
Manganese Bronze	41	175
Nickel Manganese Bronze	41	175
Nickel Aluminium Bronze	86	245
Manganese Aluminium Bronze	62	275

bution calculations, are used to determine the hydrodynamic loading on the blades of highly skewed propellers, and then finite element procedures are used to determine the blade stresses. A modified form of the beam theory has also been used for estimating the stresses in highly skewed propeller blades, Boswell and Cox (1974). The axis of the beam is assumed to be a radial line through the centroid of the cylindrical blade section at which the stress is being calculated. The blade section shape is modified to a thickness distribution at zero camber since it has been seen that this gives better correlation with experiments. The hydrodynamic loading at each radius then produces a force normal to the axis of the beam and a moment (torsion) about the axis. The centrifugal loading, on the other hand, produces a force parallel to the axis and a bending moment perpendicular to the axis. The forces and moments on the root section of a propeller blade with rake and skew are shown in Fig. 7.5.

Heavily skewed propeller blades may also suffer from a form of structural instability in which the loading causes the blades to deflect in such a way that the effective pitch is increased resulting in a further increase in loading and so on. A large skew also reduces the natural frequency of the propeller blades and may lead to stresses due to blade vibration.



Moments at Root Section (radius r_0)
due to Forces on Section at radius r

$$\begin{aligned} \text{Bending Moment due to Thrust} &: dM_T = \frac{1}{2} dT (r - r_0) \\ \text{Bending Moment due to Torque} &: dM_Q = \frac{1}{2} dQ (r - r_0 \cos \psi_E) \\ \text{Bending Moment due to Centrifugal Force and Rake} &: dM_R = dF_c (r - r_0) \tan \epsilon_E \\ \text{Bending Moment due to Centrifugal Force and Skew} &: dM_S = dF_c r_0 \sin \psi_E \\ \text{Twisting Moment due to Thrust} &: dN_T = \frac{1}{2} dT r_0 \sin \psi_E \\ \text{Twisting Moment due to Torque} &: dN_Q = \frac{1}{2} dQ (r - r_0) \tan \epsilon_E \end{aligned}$$

ϵ_E and ψ_E are the effective rake and skew angles. The centre of hydrodynamic pressure and the centroid of the blade section are assumed to be coincident.

Figure 7.5: Forces and Moments in a Blade with Large Rake and Skew.

The thickness of a propeller blade at the tip and at the edges should be sufficient to prevent the blade from bending due to the hydrodynamic loading since the resulting change in section shape may cause an increase in the effective pitch of the propeller and lead to cavitation erosion. Experience has shown that the blade thickness at the tip before rounding should be between $0.003D$ and $0.004D$. The blade edge is normally rounded and has a radius which reduces from between $0.00175D$ and $0.002D$ at $0.2R$ to about $0.0006D$ at $0.95R$. The blade thicknesses at the leading and trailing edges before rounding are given approximately by:

$$\begin{aligned}\frac{t_{LE}}{D} &= 0.0058 - 0.0043 \frac{r}{R} \\ \frac{t_{TE}}{D} &= 0.0030 - 0.0015 \frac{r}{R}\end{aligned}\tag{7.40}$$

The dimensions of the propeller boss are determined by the geometry of the propeller blades and the diameter of the propeller shaft. The boss diameter is usually between $0.15D$ and $0.20D$, and the length is just sufficient to accommodate the blade at the root. The diameter of the boss at the forward end is 10-15 percent more than in the middle, and the diameter at the after end less than that in the middle by about the same amount. An internal recess may be provided in the boss, in which case the length of this recess should not exceed one-third the length of the boss, and the minimum wall thickness should not be less than the thickness of the blade root section. The blades should join the boss through fillets of adequate radii, usually 0.03 - $0.04D$ but not less than the thickness of the root section. A streamlined boss cap or "cone" is usually fitted at the after end of the boss.

Problems

1. A four-bladed propeller of 6.0 m diameter and 0.9 constant pitch ratio has a thrust of 1100 kN and a torque of 1250 kN m at 150 rpm. Each blade of the propeller has a mass of 1800 kg with its centroid at a radius of 1.4 m. The thrust and torque distributions in a non-dimensional form can be assumed to be given by:

$$\frac{dK_T}{dx} = k_1 x \quad \frac{dK_Q}{dx} = k_2 x$$

The root section at $0.2R$ has a section modulus of $7.5 \times 10^6 \text{ mm}^3$ and an area of $2.5 \times 10^5 \text{ mm}^2$. Determine the stress in the root section, neglecting the bending moments due to centrifugal force.

2. In a three-bladed propeller of 4.0 m diameter and 0.7 pitch ratio, the thrust and torque distributions are linear between $x = 0.2$ and $x = 0.5$, and constant from $x = 0.5$ to $x = 1.0$ as follows:

$$x = 0.2: \quad \frac{dK_T}{dx} = 0.080 \quad \frac{dK_Q}{dx} = 0.012$$

$$x = 0.5: \quad \frac{dK_T}{dx} = 0.200 \quad \frac{dK_Q}{dx} = 0.030$$

The propeller runs at 180 rpm. The root section at $0.2R$ has a thickness chord ratio $t/c = 0.250$ and a section modulus of $0.105 ct^2$. The thickness of the propeller blades at the tip is 15 mm. Determine the thickness and chord of the root section and the blade thickness fraction of the propeller if the thickness distribution from root to tip is linear and the stress due to thrust and torque is not to exceed 40 N per mm².

3. A ship has a four-bladed propeller of 5.0 m diameter and 0.8 constant pitch ratio. The propeller develops a thrust of 800 kN and a torque of 700 kN m at 150 rpm. The radial distributions of thrust and torque are as follows:

$$\frac{dT}{dr} = k_1 r^2 (R - r) \quad \frac{dQ}{dr} = k_2 r^2 (R - r)$$

Each blade has a mass of 1500 kg. The blades are raked aft and skewed back in such a way that the centroid of each blade is at a radius of 1.2 m and at distances of 0.40 m and 0.25 m respectively from two reference planes, the first passing through the propeller axis and the other being normal to it. The root section at $0.2R$ has an area of 2×10^5 mm² and a minimum section modulus of 6.5×10^6 mm³, its centroid being at distances of 0.15 m and 0.05 m respectively from the two reference planes. Determine the maximum blade stress.

4. A ship is to have a four-bladed propeller of 5.5 m diameter and 0.75 pitch ratio with an expanded blade area ratio of 0.500 and a rake of 15 degrees aft. The propeller is required to absorb a delivered power of 7500 kW at 138 rpm and 8.0 m per sec speed of advance, its efficiency being 0.650. The propeller belongs to a methodical series for which:

$$\text{Mass of each blade} = 0.0625 \rho_m \frac{t_0}{D} \frac{A_E}{A_O} D^3$$

$$\text{Centroid of blade from the propeller axis} = 0.48R$$

The root section at $0.2R$ has a thickness chord ratio $t/c = 0.250$ and the following properties:

$$\text{Area of section} = 0.700 ct$$

$$\text{Ordinate of leading edge from face chord} = 0.40 t$$

$$\text{Ordinate of trailing edge from face chord} = 0.35 t$$

A, B, C, C_n and C_s are coefficients as follows:

$$A = 1.0 + 6.0 \frac{D}{P_{0.7}} + 4.3 \frac{P_{0.25}}{D}$$

$$B = \frac{4300 w a}{N} \left(\frac{R}{100} \right)^2 \left(\frac{D}{20} \right)^3$$

$$C = \left(1 + 1.5 \frac{P_{0.25}}{D} \right) (L_{0.25} f - B)$$

$$C_n = \frac{I_0}{U_f L_{0.25} t_{0.25}^2} \text{ but not greater than } 0.10$$

$$C_s = \frac{a_s}{L_{0.25} t_{0.25}}$$

$P_{0.7}$ = Pitch at 0.7 radius in m

$P_{0.25}$ = Pitch at 0.25 radius in m

w = material constant given in Table 7.6

a = expanded blade area ratio

D = propeller diameter in m

$L_{0.25}$ = width of the blade at 0.25 radius in m

f = material constant given in Table 7.6

I_0 = moment of inertia of the section at 0.25 radius about an axis through the centre of area and parallel to the pitch line of the section in mm^4

U_f = maximum distance of the section axis from the face of the section in mm

a_s = area of cross-section at 0.25 radius in mm^2

Table 7.6
Material Constants

Material		Minimum Ultimate	f	w
		Tensile Strength N/mm^2		
Manganese Bronze	Grade Cu 1	440	20.6	8.3
Nickel Manganese Bronze	Grade Cu 2	440	20.9	8.0
Nickel Aluminium Bronze	Grade Cu 3	590	25.7	7.5
Manganese Aluminium Bronze	Grade Cu 4	630	23.25	7.5
Cast Iron		250	11.77	7.2
Carbon and Low Alloy Steels		400	14.0	7.9

Determine the blade thickness fraction of the propeller whose particulars are given in Problem 8. Take $C_n = 0.090$ and $C_s = 0.700$.

10. A large single-screw oceangoing ship has a speed of 25 knots with a delivered power of 22500 kW at 108 rpm, the wake fraction being 0.220, the thrust deduction fraction 0.160 and the propeller efficiency in the behind condition 0.680. The propeller has six blades and a diameter of 7.0 m. The pitch ratio P/D , the chord diameter ratio c/D , the thickness chord ratio t/c , the effective skew angle ψ_E (i.e. the angle between radial lines passing through the mid-chords of the root section at $0.2R$ and a section at any other radius r , and the effective rake angle ϵ_E (the angle which a line joining the centroid of the root section and the centroid of the section at radius r makes with a plane normal to the propeller axis) are given in the following table:

r/R :	0.2	0.3	0.4	0.5	0.6	0.7	0.8	0.9	1.0
P/D :	0.675	0.767	0.836	0.900	0.902	0.900	0.874	0.824	0.750
c/D :	0.201	0.238	0.265	0.282	0.288	0.281	0.256	0.203	-
t/c :	0.199	0.159	0.128	0.102	0.080	0.061	0.047	0.039	-
ψ_E^0 :	0	-1.25	0	3.75	10.00	18.75	30.00	43.75	60.00
ϵ_E^0 :	0	3.67	7.00	10.00	12.67	15.00	17.00	18.67	20.00

The sectional area at each radius is given by $0.7ct$. The propeller is made of Nickel Aluminium Bronze of density 7500 kg per m^3 . The thrust and torque distributions are given by:

$$\frac{dK_T}{dx} = k_1 x^2 (1-x)^{0.5} \quad \frac{dK_Q}{dx} = k_2 x^2 (1-x)^{0.5}$$

while the loading along the chord at each radius may be taken as uniformly distributed over the face. Determine the bending moments about the principal axes and the torsion about a radial axis through the centroid of the root section. The centroids of all the blade sections may be assumed to be at mid-chord. Calculate also the tensile force on the root section.

CHAPTER 8

Propulsion Model Experiments

8.1 Introduction

The performance of a propeller in a ship and the resulting hull-propeller interaction are usually determined through model experiments. Experiments with full-size ships and propellers are difficult to carry out and purely theoretical approaches are as yet inadequate for predicting the behaviour of ships and propellers fully. The conditions under which model experiments can be used to determine ship performance have been considered in Chapter 4. It is not practicable to fulfil all these conditions exactly, and therefore some empirical corrections are necessary in determining ship performance from experiments with models.

The experiments that are normally carried out with ship models and model propellers are:

- (i) resistance experiments,
- (ii) open water experiments,
- (iii) self-propulsion experiments,
- (iv) wake measurements, and
- (v) cavitation experiments.

Model experiments in waves are not considered here. Resistance experiments are also not really within the scope of the present work but are discussed briefly because they are essential for analysing self-propulsion experiments. The resistance, open water and self-propulsion experiments are normally carried out in towing tanks. Cavitation experiments require a cavitation tunnel or a depressurised towing tank. Wake measurements may be carried out in a towing tank or in a circulating water channel.

A towing tank is a long narrow tank in which a ship model is towed through water at a steady speed usually by a towing carriage running on rails along the sides of the tank. Instruments are provided to measure the speed and the resistance of the ship model, and the thrust, torque and revolution rate of a model propeller if fitted. In a circulating water channel, the ship model is stationary and the water is made to move past it at a steady speed. A cavitation tunnel, which is discussed in more detail in Sec. 8.6, is similar except that the pressure in the tunnel water can be varied over a wide range.

8.2 Resistance Experiments

Resistance experiments are carried out with ship models to determine the resistance of the model and thereby of the ship in a given condition. Such experiments are useful in optimising the hull form and for predicting the power required for propelling a ship at a specified speed. Before discussing resistance experiments, it is necessary to consider the relationship between the resistance of a ship and the resistance of a geometrically similar model.

It can be shown in a manner similar to that described in Sec. 4.3 that the total resistance R_T of a ship can be expressed in the form:

$$\frac{R_T}{\rho L^2 V^2} = f \left(\frac{VL}{\nu}, \frac{V}{\sqrt{gL}} \right) \quad (8.1)$$

where L is the length of the ship, V its speed, g the acceleration due to gravity, and ρ and ν the density and kinematic viscosity of water respectively. This may be written in terms of non-dimensional parameters as follows:

$$C_T = f(R_n, F_n) \quad (8.2)$$

where:

$$C_T = \frac{R_T}{\frac{1}{2}\rho S V^2} \quad \text{is the total resistance coefficient,}$$

$$R_n = \frac{V L}{\nu} \quad \text{is the Reynolds number,}$$

$$F_n = \frac{V}{\sqrt{g L}} \quad \text{is the Froude number, and}$$

S is the wetted surface of the ship, proportional to L^2 .

Following W. Froude, it is usual to divide the total resistance into a viscous resistance component which is a function of the Reynolds number and a residuary resistance component which is a function of the Froude number. This is expressed in terms of a viscous resistance coefficient C_V and a residuary resistance coefficient C_R :

$$C_T = C_V(R_n) + C_R(F_n) \quad (8.3)$$

The viscous resistance coefficient is determined with the help of a "friction line", i.e. an equation giving the resistance of a plane surface in terms of the Reynolds number. Several friction lines have been proposed, based on theoretical considerations and experimental measurements, but the standard formulation in use at present is the ITTC (International Towing Tank Conference) 1957 friction line:

$$C_F = 0.075 (\log_{10} R_n - 2)^{-2} \quad (8.4)$$

where C_F is the frictional resistance coefficient. (The ITTC friction line is not strictly a "two-dimensional" friction line.) The viscous resistance coefficient and the frictional resistance coefficient are related by a "form factor" $(1 + k)$, which accounts for the increase in viscous resistance due to the three-dimensional hull form of a ship:

$$C_V = (1 + k) C_F \quad (8.5)$$

One therefore has the following expression for the resistance of a ship:

$$C_T = (1 + k) C_F + C_R \quad (8.6)$$

It is then assumed that the residuary resistance, which for most ships is mainly wave making resistance, obeys the Froude law: the residuary resistances of geometrically similar ships are proportional to their displacements if their speeds are proportional to the square roots of their lengths. This implies that:

$$C_{RS} = C_{RM} \quad \text{if} \quad F_{nS} = F_{nM} \quad (8.7)$$

where the suffix S refers to the ship and M to the geometrically similar model, and F_n is the Froude number.

This allows the total resistance of a ship at a given speed to be estimated from the total resistance of a model at the "corresponding" speed (the speed for which the Froude numbers of the model and the ship are equal), as illustrated by the following example.

Example 1

A ship of length 100 m and wetted surface of 2700 m² has a speed of 15 knots. A 4.0 m long geometrically similar model of the ship has a total resistance of 25.0 N at the corresponding speed. Determine the total resistance of the ship assuming a form factor of 1.05.

$$L_S = 100 \text{ m} \quad S_S = 2700 \text{ m}^2 \quad V_S = 15 \text{ k} = 7.716 \text{ ms}^{-1}$$

$$L_M = 4.0 \text{ m} \quad S_M = S_S \left(\frac{L_M}{L_S} \right)^2 = 2700 \times \left(\frac{4.0}{100} \right)^2 = 4.32 \text{ m}^2$$

$$V_M = V_S \sqrt{\frac{L_M}{L_S}} = 7.716 \sqrt{\frac{4}{100}} = 1.5432 \text{ ms}^{-1}$$

$$R_{TM} = 25.0 \text{ N} \quad 1 + k = 1.05$$

$$C_{TM} = \frac{R_{TM}}{\frac{1}{2} \rho_m S_M V_M^2} = \frac{25.0}{\frac{1}{2} \times 1000 \times 4.32 \times 1.5432^2} = 4.860 \times 10^{-3}$$

$$R_{nM} = \frac{V_M L_M}{\nu_M} = \frac{1.5432 \times 4}{1.139 \times 10^{-6}} = 5.419 \times 10^6$$

$$C_{FM} = 0.075 (\log_{10} R_{nM} - 2)^{-2} = 3.347 \times 10^{-3}$$

$$\begin{aligned} C_{RM} &= C_{TM} - (1 + k) C_{FM} = [4.860 - 1.05 \times 3.347] 10^{-3} \\ &= 1.346 \times 10^{-3} \end{aligned}$$

$$C_{RS} = C_{RM} \quad \text{since} \quad F_{nS} = F_{nM}$$

$$R_{nS} = \frac{V_S L_S}{\nu_S} = \frac{7.716 \times 100}{1.188 \times 10^{-6}} = 6.495 \times 10^8$$

$$C_{FS} = 0.075 (\log_{10} R_{nS} - 2)^{-2} = 1.616 \times 10^{-3}$$

$$C_{TS} = (1 + k) C_{FS} + C_{RS} = [1.05 \times 1.616 + 1.346] \times 10^{-3} = 3.043 \times 10^{-3}$$

$$\begin{aligned} R_{TS} &= C_{TS} \frac{1}{2} \rho_S S_S V_S^2 = 3.043 \times 10^{-3} \times \frac{1}{2} \times 1.025 \times 2700 \times 7.716^2 \\ &= 250.7 \text{ kN} \end{aligned}$$

The total resistance R_T or the total resistance coefficient C_T determined in this manner must be corrected for the differences between the conditions of the model experiment and the operating conditions of a ship. A simple way to carry out this correction is to add a "correlation allowance" C_A to the total resistance coefficient of the ship. The correlation allowance, which primarily accounts for the roughness of the ship surface, is determined by correlating the performance of ships on speed trials and the results of the corresponding model experiments. Other differences between the operating conditions of the ship and the controlled conditions of the model experiments are taken into account by adding a "service allowance" or a "trial allowance" to the resistance of a ship determined through model experiments.

More detailed methods may also be used to correct the resistance for differences between the model and the ship. Three such corrections are used in the standard ITTC ship performance prediction method (ITTC 1978):

- (i) The wetted surface of the ship hull is normally rough whereas the model surface is smooth. It is therefore necessary to add to the viscous resistance coefficient of the ship a "roughness allowance" given by:

$$\Delta C_F = \left[105 \left(\frac{k_S}{L} \right)^{\frac{1}{3}} - 0.64 \right] \times 10^{-3} \quad (8.8)$$

where k_S is the average amplitude of roughness of the wetted surface of the ship. A standard value of $k_S = 150 \times 10^{-6}$ m is used in the ITTC method.

- (ii) It is usually impracticable to reproduce bilge keels on a ship model, and therefore a correction is required. This correction is made by increasing the wetted surface S_S of the ship hull by the surface area S_{BK} of the bilge keels in calculating the viscous resistance of the ship.
- (iii) It is also necessary to account for the resistance of the above-water part of the ship. This "air resistance" can be determined by model tests in a wind tunnel. For a ship moving in still air, the ITTC performance prediction method uses an air resistance coefficient as follows:

$$C_{AA} = \frac{R_{AA}}{\frac{1}{2} \rho_S S_S V_S^2} = 0.001 \frac{A_T}{S_S} \quad (8.9)$$

where R_{AA} is the air resistance, C_{AA} the air resistance coefficient and A_T the transverse projected area of the above water part of the ship.

After making these three corrections, the total resistance coefficient of the ship is given by:

$$C_{TS} = \frac{S_S + S_{BK}}{S_S} [(1 + k) C_{FS} + \Delta C_F] + C_R + C_{AA} \quad (8.10)$$

Eqn. (8.10) gives the total resistance coefficient of a ship in ideal conditions. To allow for the actual conditions during ship trials or in service one may multiply the total resistance coefficient by a "load factor" $(1 + x)$, the "overload fraction" x corresponding to a "trial allowance" or a "service allowance", ranging from 10 to 40 percent depending upon the type of ship and its service route.

For resistance experiments, it is first necessary to make an accurate geometrically similar model to an appropriate scale, which should be large enough for making the ship model and model propellers of sufficient accuracy and yet be within the limits imposed by the size of the towing tank and the speed of its towing system. Large models are also necessary to ensure turbulent flow around the model, and even then it is necessary to fit artificial turbulence stimulators at the bow of the model. The model is then accurately ballasted to the required waterline and towed at a number of steady speeds in still water, the speeds covering slightly more than the normal operating speed range of the ship. The tow force or resistance is measured by a resistance dynamometer at each speed, and the results analysed in a manner similar to that given in Example 1. In addition to speed and resistance, it is also necessary to measure the temperature of the towing tank water, since the density and viscosity of water depend on its temperature. Resistance experiments may be carried out on a model without appendages such as rudders and shaft brackets, in which case one obtains the "naked hull" resistance. The model may also be tested when fitted with appendages made to the same scale. If only a naked hull resistance test is carried out, it is necessary to add an empirical appendage resistance to the naked hull resistance.

8.3 Open Water Experiments

The object of an open water experiment is to determine the open water characteristics of a propeller. A geometrically similar model is made of the propeller, the size of the model propeller being governed by the size of the ship model if it is intended to use the model propeller for self-propulsion tests also. If only open water tests are to be carried out, when generating propeller methodical series data for example, the model propeller is made somewhat larger, its size depending upon the capacity of the propeller dynamometer available. In any case, model propellers should be large enough to be made accurately and to have a sufficiently high Reynolds number so that the flow is turbulent. A further measure to promote turbulent flow is not to give the model propeller a highly polished surface. It is recommended that the model propeller Reynolds number based on the resultant of the axial and tangential velocities and the section chord at $0.7R$ be at least 3.2×10^5 ;

otherwise turbulence should be artificially stimulated, e.g. by roughening the leading edges of the blades.

For the open water experiment, the model propeller is attached to a propeller dynamometer fitted in an "open water boat" as shown in Fig. 8.1. The propeller dynamometer measures the thrust and torque of the propeller. The propeller shaft extends a sufficient length forward from the boat to ensure that the flow around the propeller is not disturbed by the boat. A fairing cap is provided at the forward end of the propeller boss. The open water boat is ballasted so that the propeller shaft is horizontal and its depth below the water surface is at least equal to the model propeller diameter.

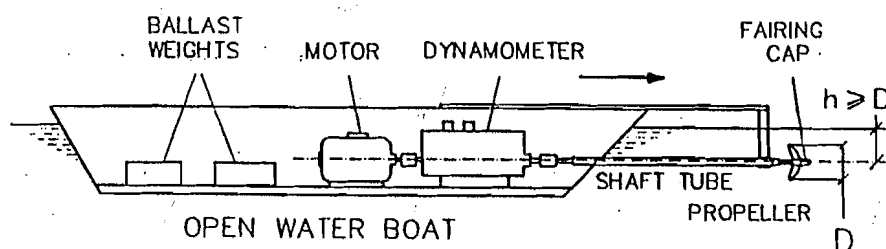


Figure 8.1 : Open Water Experiment.

The open water experiment is conducted by towing the open water boat at a steady speed while running the propeller at a constant revolution rate. The speed of the boat (i.e. speed of advance V_A), and the revolution rate n , thrust T and torque Q of the propeller are measured in each run. It is usual to run the model propeller for all the speeds of advance at a constant revolution rate, this preferably being the highest that can be attained at zero speed of advance at which the torque is maximum and which must be within the capacity of the driving motor and dynamometer. The speed of advance is varied in steps from zero to the value at which the propeller thrust just becomes negative. (Four quadrant measurements involving negative speeds and revolution rates are not considered here.) The measured thrust and torque are corrected for the "idle" thrust and torque, i.e. the thrust and torque measured by the dynamometer when the experiment is carried out with a dummy boss of equal weight replacing the propeller.

The open water characteristics of the model propeller can be easily calculated from the measured values of V_A and n , and the corrected values of T and Q . The open water characteristics of the ship propeller will be

slightly different because of the difference between the Reynolds numbers of the model propeller and the ship propeller.

The surface of the ship propeller may also be rough. A procedure for correcting the open water characteristics for Reynolds number and roughness effects has been given in the ITTC 1978 performance prediction method. This procedure, which is based on the assumption that the blade section at $0.75R$ can be assumed to represent the propeller as a whole, is summarized by the following equations:

$$\begin{aligned}
 V_{RM}^2 &= V_{AM}^2 + (0.75 \pi n_M D_M)^2 \\
 R_{ncM} &= \frac{V_{RM} c_M}{\nu_M} \\
 C_{DM} &= 2 \left[1 + 2 \left(\frac{t}{c} \right) \right] \left[\frac{0.044}{R_{ncM}^{\frac{1}{6}}} - \frac{5}{R_{ncM}^{\frac{2}{3}}} \right] \\
 C_{DS} &= 2 \left[1 + 2 \left(\frac{t}{c} \right) \right] \left[1.89 + 1.62 \log_{10} \frac{c_S}{k_p} \right]^{-2.5} \quad (8.11)
 \end{aligned}$$

$$\Delta C_D = C_{DM} - C_{DS}$$

$$\Delta K_T = -0.3 \Delta C_D \frac{P}{D} \frac{c}{D} Z$$

$$\Delta K_Q = 0.25 \Delta C_D \frac{c}{D} Z$$

$$K_{TS} = K_{TM} - \Delta K_T$$

$$K_{QS} = K_{QM} - \Delta K_Q$$

where:

V_{RM} = resultant velocity of blade section at $0.75R$

V_{AM} = speed of advance of the model propeller

- n_M = revolution rate of the model propeller
 D_M = model propeller diameter
 c_M, c_S = expanded blade widths (chords) of the section at $0.75R$ of the model propeller and the ship propeller respectively
 ν_M = kinematic viscosity of water for the model experiment
 R_{nCM} = Reynolds number of the model propeller
 C_{DM}, C_{DS} = drag coefficients of the blade section at $0.75R$ for the model propeller and the ship propeller respectively
 $\frac{t}{c}$ = thickness chord ratio of the blade section at $0.75R$
 $\frac{c}{D}$ = chord diameter ratio at $0.75R$
 Z = number of blades
 k_p = propeller surface roughness (standard value 30×10^{-6} m)
 K_{TM}, K_{TS} = thrust coefficients of the model propeller and the ship propeller respectively
 K_{QM}, K_{QS} = torque coefficients of the model propeller and the ship propeller respectively.

Example 2

In an open water experiment with a model propeller of 200 mm diameter, a thrust of 252 N and a torque of 9.250 N m are measured with the propeller running at 2400 rpm at a speed of advance of 5.6 m per sec. The idle thrust and torque (to be subtracted from the measured values) are -4.0 N and 0.034 N m respectively. Determine the thrust, torque and advance coefficients of the model propeller and its open water efficiency. The ship propeller has four blades, a diameter of 5.0 m and a constant pitch ratio of 0.8. The blade section at $0.75R$ has a thickness of 0.0675 m and a chord of 1.375 m. If the roughness of the propeller blade surface is 30 microns, determine the thrust and torque coefficients of the ship propeller and its open water efficiency.

$$D_M = 200 \text{ mm} = 0.200 \text{ m}$$

$$T_M = 252 - (-4.0) = 256 \text{ N}$$

$$n_M = 2400 \text{ rpm} = 40.0 \text{ s}^{-1}$$

$$Q_M = 9.250 - 0.034 = 9.216 \text{ N m}$$

$$V_{AM} = 5.6 \text{ m s}^{-1} \quad \rho_M = 1000 \text{ kg m}^{-3} \quad \nu_M = 1.139 \times 10^{-6} \text{ m}^2 \text{ s}^{-1}$$

$$D_S = 5.0 \text{ m} \quad \frac{P}{D} = 0.8 \quad c_S = 1.375 \text{ m at } 0.75R \quad t_S = 0.0675 \text{ m}$$

$$k_p = 30 \mu\text{m} = 30 \times 10^{-6} \text{ m}$$

$$J = \frac{V_{AM}}{n_M D_M} = \frac{5.6}{40.0 \times 0.200} = 0.7000$$

$$K_{TM} = \frac{T_M}{\rho_M n_M^2 D_M^4} = \frac{256}{1000 \times 40.0^2 \times 0.200^4} = 0.1000$$

$$K_{QM} = \frac{Q_M}{\rho_M n_M^2 D_M^5} = \frac{9.216}{1000 \times 40.0^2 \times 0.200^5} = 0.01800$$

$$\eta_{OM} = \frac{K_{TM} J}{K_{QM} 2\pi} = \frac{0.1000}{0.01800} \times \frac{0.7000}{2\pi} = 0.6189$$

$$c_M = c_S \frac{D_M}{D_S} = 1.375 \times \frac{0.200}{5.0} = 0.0550 \text{ m}$$

$$\begin{aligned} V_{RM}^2 &= V_{AM}^2 + (0.75\pi n_M D_M)^2 = 5.6^2 + (0.75\pi \times 40.0 \times 0.2)^2 \\ &= 386.6658 \text{ m}^2 \text{ s}^{-2} \end{aligned}$$

$$V_{RM} = 19.6638 \text{ m s}^{-1}$$

$$R_{ncM} = \frac{V_{RM} c_M}{\nu_M} = \frac{19.6638 \times 0.0550}{1.139 \times 10^{-6}} = 0.9495 \times 10^6$$

$$\frac{t}{c} = \frac{0.0675}{1.375} = 0.04909$$

$$C_{DM} = 2 \left[1 + 2 \left(\frac{t}{c} \right) \right] \left[\frac{0.044}{R_{ncM}^{\frac{1}{3}}} - \frac{5}{R_{ncM}^{\frac{2}{3}}} \right]$$

$$= 2 [1 + 2 \times 0.04909] \left[\frac{0.044}{(0.9495 \times 10^6)^{\frac{1}{3}}} - \frac{5}{(0.9495 \times 10^6)^{\frac{2}{3}}} \right]$$

$$= 2 \times 1.09818 (4.4381 \times 10^{-3} - 0.5176 \times 10^{-3}) = 8.6110 \times 10^{-3}$$

$$\begin{aligned} C_{DS} &= 2 \left[1 + 2 \left(\frac{t}{c} \right) \right] \left[1.89 + 1.62 \log \frac{c_S}{k_p} \right]^{-2.5} \\ &= 2 [1 + 2 \times 0.04909] \left[1.89 + 1.62 \log \frac{1.375}{30 \times 10^{-6}} \right]^{-2.5} \\ &= 2 \times 1.09818 [1.89 + 7.5511]^{-2.5} = 8.0195 \times 10^{-3} \end{aligned}$$

$$\Delta C_D = C_{DM} - C_{DS} = 8.6110 \times 10^{-3} - 8.0195 \times 10^{-3} = 0.5915 \times 10^{-3}$$

$$\begin{aligned} \Delta K_T &= -0.3 \Delta C_D \frac{P}{D} \frac{c}{D} Z = -0.3 \times 0.5915 \times 10^{-3} \times 0.8 \times \frac{1.375}{5.0} \times 4 \\ &= -0.1562 \times 10^{-3} \end{aligned}$$

$$\begin{aligned} \Delta K_Q &= 0.25 \Delta C_D \frac{c}{D} Z = 0.25 \times 0.5915 \times 10^{-3} \times \frac{1.375}{5.0} \times 4 \\ &= 0.1627 \times 10^{-3} \end{aligned}$$

$$K_{TS} = K_{TM} - \Delta K_T = 0.1000 - (-0.1562 \times 10^{-3}) = 0.1002$$

$$K_{QS} = K_{QM} - \Delta K_Q = 0.01800 - (0.1627 \times 10^{-3}) = 0.01784$$

$$\eta_{OS} = \frac{K_{TS}}{K_{QS}} \frac{J}{2\pi} = \frac{0.1002}{0.01784} \times \frac{0.7000}{2\pi} = 0.6256$$

8.4 Self-propulsion Experiments

Self-propulsion experiments are used to determine the performance of the ship hull and propeller taken together. An analysis of the results of a self-propulsion experiment allows one to predict the delivered power and the revolution rate of the ship propeller at a given speed of the ship, and to determine the wake fraction, thrust deduction fraction and relative rotative efficiency. The data of the resistance and open water experiments are, however, required for analysing the data of the self-propulsion experiment.

For a self-propulsion experiment, the model propeller is fitted in its correct position at the stern of the ship model and connected to a propeller dynamometer for measuring the thrust and torque of the propeller at various revolution rates. The ship model should be fitted with all appendages as far as possible, particularly those lying in the propeller slipstream, e.g. a rudder. The ship model is attached to a resistance dynamometer, which in this test measures the force required to make the ship model move at a constant speed with the propeller running. The ship model is accurately ballasted so that it floats at the correct waterline. The model is then towed at a steady speed with the propeller running at a constant revolution rate, and the thrust and torque of the propeller and the force applied to the ship model through the resistance dynamometer are measured. Fig. 8.2 illustrates the experimental set up.

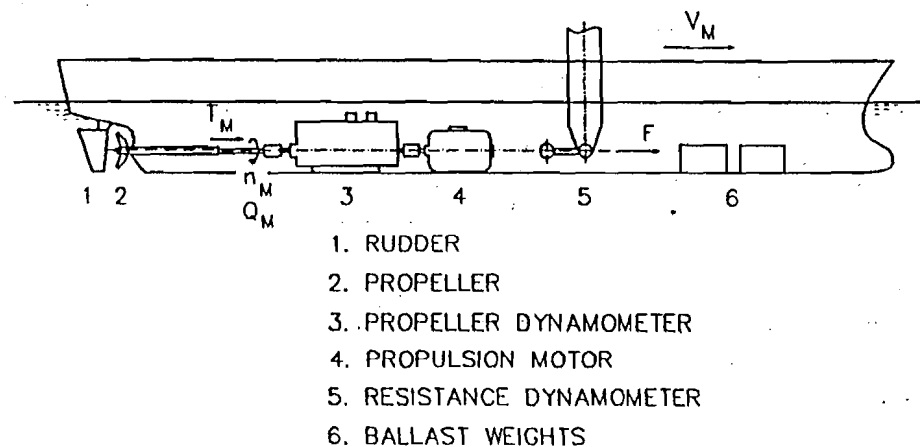


Figure 8.2 : Self-Propulsion Experiment.

The analysis of the data recorded in a self-propulsion experiment is based on the following considerations. When a ship is moving at a steady speed V_S with its propeller producing a thrust T_S , then:

$$R_{TS} = (1 - t) T_S \quad (8.12)$$

where R_{TS} is the resistance of the ship at the speed V_S and t the thrust deduction fraction. If the model scale is λ , and D_M and D_S are the model and ship propeller diameters:

$$D_S = D_M \lambda \quad (8.13)$$

The model must be tested at a speed V_M such that the Froude numbers of the model and the ship are equal, which implies that:

$$V_M = V_S \lambda^{-0.5} \quad (8.14)$$

If during the self-propulsion experiment at the speed V_M the model propeller runs at a revolution rate n_M and has a thrust T_M and torque Q_M while the force applied to the model through the resistance dynamometer is F , then:

$$F = R_{TM} - (1 - t) T_M \quad (8.15)$$

R_{TM} being the resistance of the model at the speed V_M . This may be written as:

$$F = R_{TM} - (1 - t) K_{TBM} \rho_M n_M^2 D_M^4 \quad (8.16)$$

where K_{TBM} is the thrust coefficient of the model propeller in the behind condition, and ρ_M the density of water in which the experiment is carried out. If the model propeller and the ship propeller are to fulfil the conditions of dynamic similarity, then:

$$J_S = J_M \quad (8.17)$$

$$K_{TBS} = K_{TBM}$$

$$w_S = w_M$$

where J_S and J_M are the advance coefficients of the ship propeller and the model propeller, w_S and w_M the corresponding wake fractions, and K_{TBS} the thrust coefficient of the ship propeller in the behind condition. Using Eqns. (8.13) and (8.14) with the first equation of the Eqns. (8.17), one obtains:

$$n_M = n_S \lambda^{0.5} \quad (8.18)$$

and then one may write Eqn. (8.16) with the help of Eqns. (8.12) and (8.13) as follows:

$$\begin{aligned} F &= R_{TM} - (1-t) K_{TBS} \rho_S n_S^2 D_S^4 \frac{\rho_M}{\rho_S} \left(\frac{n_M}{n_S} \right)^2 \left(\frac{D_M}{D_S} \right)^4 \\ &= R_{TM} - (1-t) T_S \frac{\rho_M}{\rho_S} \lambda \lambda^{-4} \\ &= R_{TM} - \frac{\rho_M}{\rho_S} \frac{R_{TS}}{\lambda^3} \end{aligned} \quad (8.19)$$

In terms of the total resistance coefficients of the model and the ship, this becomes:

$$\begin{aligned} F &= C_{TM} \frac{1}{2} \rho_M S_M V_M^2 - \frac{\rho_M}{\rho_S} \frac{1}{\lambda^3} (1+x) C_{TS} \frac{1}{2} \rho_S S_S V_S^2 \\ &= C_{TM} \frac{1}{2} \rho_M S_M V_M^2 - (1+x) C_{TS} \frac{1}{2} \rho_M S_M V_M^2 \frac{S_S}{S_M} \left(\frac{V_S}{V_M} \right)^2 \frac{1}{\lambda^3} \\ &= \frac{1}{2} \rho_M S_M V_M^2 [C_{TM} - (1+x) C_{TS}] \end{aligned} \quad (8.20)$$

Eqns. (8.19) and (8.20) show that for dynamic similarity as indicated by Eqn. (8.17), the ship model is not fully self-propelled, and the thrust of the model propeller must be augmented by the force F applied through the resistance dynamometer. The condition represented by Eqn. (8.19) or (8.20) is termed the "ship self-propulsion point on the model" in contrast to the "model self-propulsion point" at which $F = 0$ and the model is fully self-propelled by its propeller. It may be noted that whereas at the ship self-propulsion point $K_{TBM} = K_{TBS}$, at the model self-propulsion point K_{TBM} is greater than K_{TBS} (at least for $x = 0$) so that the model propeller is overloaded in comparison to the ship propeller and is therefore operating less efficiently. It is possible for F to be negative if the overload fraction x is sufficiently large.

If the self-propulsion experiment is to be carried out for only one value of the load factor $(1 + x)$, then for each speed V_M the value of the force F is calculated in advance using Eqns. (8.19) or (8.20), and with the model moving steadily with the speed V_M the propeller revolution rate n_M is adjusted until the calculated value of F is achieved. The thrust T_M and the torque Q_M are then measured along with V_M , F and n_M . This procedure may be repeated for several speeds to cover a range corresponding to the operating speed range of the ship. This method of conducting a self-propulsion experiment is called the "constant loading" method or the "Continental" method because of its use in European ship model tanks. If self-propulsion test data are required for a different loading, the experiment is repeated for a new value of F at each speed.

In an alternative method of carrying out self-propulsion experiments, called the "constant speed" method or sometimes the "British" method, tests are carried out for several values of n_M at each value of V_M , and F , T_M and Q_M are measured. This allows the data to be analysed for different load factors $(1 + x)$, which may be selected after the experiment is over. In actual practice, the constant loading method for different loadings and the constant speed method for different speeds are equivalent since both lead to values of F , T_M and Q_M as functions of both V_M and n_M .

The analysis of the data of a self-propulsion experiment requires the resistance of the model and the resistance of the ship derived from it, as well as the open water characteristics of the model propeller obtained through the open water experiment. The resistance of the model should be for the same model condition as in the self-propulsion experiment. This may involve correcting the model resistance data for any temperature difference between the resistance experiment and the self-propulsion experiment. The analysis then proceeds as described in the following.

For each model speed V_M and the corresponding ship speed V_S , the required force F is determined from the model resistance R_{TM} and the ship resistance R_{TS} using Eqn. (8.19). The model propeller revolution rate n_M for this value of F , and the corresponding values of T_M and Q_M are then obtained, directly in the Continental method, and by interpolation if necessary in the British method. These are the values of n_M , T_M and Q_M at the ship-propulsion point on the model for the speed V_M . T_M and Q_M are

converted to the thrust and torque coefficients K_{TBM} and K_{QBM} for the behind condition:

$$K_{TBM} = \frac{T_M}{\rho_M n_M^2 D_M^4} \quad K_{QBM} = \frac{Q_M}{\rho_M n_M^2 D_M^5} \quad (8.21)$$

Referring to the open water characteristics of the model propeller (K_{TM} , K_{QM} and η_O as functions of J), one determines:

- (a) the values of J , K_{QM} and η_O for $K_{TM} = K_{TBM}$, i.e. for thrust identity
- (b) the values of J , K_{TM} and η_O for $K_{QM} = K_{QBM}$, i.e. for torque identity.

Then:

$$\begin{aligned} w &= 1 - \frac{J n_M V_M}{D_M} \\ t &= 1 - \left(\frac{\rho_M R_{TS}}{\rho_S \lambda^3} \right) / T_M \\ \eta_H &= \frac{1-t}{1-w} \\ \eta_R &= \frac{K_{QM}}{K_{QBM}} \quad (\text{thrust identity}) \\ \eta_R &= \frac{K_{TBM}}{K_{TM}} \quad (\text{torque identity}) \\ \eta_D &= \eta_O \eta_R \eta_H \end{aligned} \quad (8.22)$$

There are usually small differences between the values of w , η_H and η_R obtained using thrust identity and the values obtained using torque identity, and the two sets of values are identified by the suffixes T and Q , e.g. w_T and w_Q are the wake fractions determined by thrust identity and torque identity

respectively. The values of t and η_D with thrust identity are the same as with torque identity.

One may also determine the revolution rate and delivered power of the ship propeller from the following equations:

$$\begin{aligned}
 V_S &= V_M \lambda^{0.5} \\
 n_S &= n_M \lambda^{-0.5} \\
 P_E &= R_{TS} V_S \\
 P_D &= 2\pi \rho_S n_S^3 D_S^5 K_{QBM} \\
 \eta_D &= \frac{P_E}{P_D}
 \end{aligned} \tag{8.23}$$

The values of η_D obtained by Eqns. (8.22) and (8.23) are identical.

The analysis of self-propulsion experiment data may be carried out using non-dimensional coefficients throughout. If the wake fraction, thrust deduction fraction and relative rotative efficiency are not required, the open water data of the model propeller are not required, and one may directly calculate the delivered power and revolution rate of the ship propeller from the self-propulsion experiment data using the Eqns. (8.23).

The procedure for analysing self-propulsion experiments described in the foregoing ignores the differences that exist between the model and the ship. These differences may cause the values of the delivered power and propeller revolution rate of the ship determined from the self-propulsion experiment to differ from the values obtained during the speed trials of the ship. A simple way to allow for these differences is to introduce correlation factors based on experience with previously built ships into the values predicted from self-propulsion experiments:

$$\begin{aligned}
 n'_S &= n_M \lambda^{-0.5} k_1 \\
 P'_{DS} &= 2\pi \rho_S n_S^3 D_S^5 K_{QBM} k_2
 \end{aligned} \tag{8.24}$$

where k_1 and k_2 are correlation factors for the propeller revolution rate and delivered power respectively.

Example 3

The effective power of a single screw ship of length 100 m at a speed of 15 knots is 2150 kW. The resistance of a 4.0 m long model with appendages is 25.4 N at the corresponding speed. Determine the tow force to be applied to the model in a self-propulsion test at this speed to obtain the ship self-propulsion point. The model propeller of diameter 0.2 m is found to run at 534 rpm for this tow force to be obtained, and the propeller thrust and torque are then 21.75 N and 0.682 N m. The open water data of the model propeller are:

J	:	0.600	0.700	0.800
K_T	:	0.199	0.144	0.088
$10K_Q$:	0.311	0.249	0.186

Analyse these data and determine the rpm of the ship propeller and the delivered power given that the correlation factors for rpm and delivered power are respectively 1.02 and 1.00.

$$L_S = 100 \text{ m} \quad P_E = 2150 \text{ kW} \quad V_S = 15 \text{ k} = 7.716 \text{ ms}^{-1}$$

$$L_M = 4 \text{ m} \quad R_{TM} = 25.4 \text{ N} \quad n_M = 534 \text{ rpm} = 8.9 \text{ s}^{-1}$$

$$D_M = 0.2 \text{ m} \quad T_M = 21.75 \text{ N} \quad Q_M = 0.682 \text{ N m}$$

$$\lambda = \frac{L_S}{L_M} = \frac{100}{4} = 25 \quad V_M = V_S \lambda^{-0.5} = \frac{7.716}{5} = 1.5432 \text{ ms}^{-1}$$

$$D_S = D_M \lambda = 0.2 \times 25 = 5.0 \text{ m} \quad R_{TS} = \frac{P_E}{V_S} = \frac{2150}{7.716} = 278.6418 \text{ kN}$$

$$F = R_{TM} - \frac{\rho_M}{\rho_S} \frac{R_{TS}}{\lambda^3} = 25.4 - \frac{1.000}{1.025} \times \frac{278.6418 \times 1000}{25^3} \text{ N}$$

$$= 25.4 - 17.3981 = 8.0019 \text{ N}$$

$$t = 1 - \frac{\frac{\rho_M}{\rho_S} \frac{R_{TS}}{\lambda^3}}{T_M} = 1 - \frac{17.3981}{21.75} = 1 - 0.7999 = 0.2001$$

$$K_{TBM} = \frac{T_M}{\rho_M n_M^2 D_M^4} = \frac{21.75}{1000 \times 8.9^2 \times 0.2^4} = 0.1716$$

$$K_{QBM} = \frac{Q_M}{\rho_M n_M^2 D_M^5} = \frac{0.682}{1000 \times 8.9^2 \times 0.2^5} = 0.02691$$

Thrust Identity

$$K_T = K_{TBM} = 0.1716$$

$$J = 0.6500 \quad K_{QM} = 0.02801$$

$$\eta_O = \frac{K_{TM} J}{K_{QM} 2\pi} = \frac{0.1716}{0.02801} \times \frac{0.6500}{2\pi} = 0.6338$$

$$w_T = 1 - \frac{J n_M D_M}{V_M} = 1 - \frac{0.6500 \times 8.9 \times 0.2}{1.5432} = 1 - 0.7497 = 0.2503$$

$$\eta_H = \frac{1-t}{1-w} = \frac{0.7999}{0.7497} = 1.0670$$

$$\eta_R = \frac{K_{QM}}{K_{QBM}} = \frac{0.02801}{0.02691} = 1.0409$$

$$\begin{aligned} \eta_D &= \eta_H \eta_O \eta_R \\ &= 1.0670 \times 0.6338 \times 1.0409 \\ &= 0.7039 \end{aligned}$$

Torque Identity

$$K_Q = K_{QBM} = 0.02691$$

$$J = 0.6678 \quad K_T = 0.1618$$

$$\eta_O = \frac{0.1618}{0.02691} \times \frac{0.6678}{2\pi} = 0.6390$$

$$w_Q = 1 - \frac{0.6678 \times 8.9 \times 0.2}{1.5432} = 1 - 0.7703 = 0.2297$$

$$\eta_H = \frac{0.7999}{0.7703} = 1.0384$$

$$\eta_R = \frac{K_{TBM}}{K_{TM}} = \frac{0.1716}{0.1618} = 1.0606$$

$$\begin{aligned} \eta_D &= 1.0384 \times 0.6390 \times 1.0606 \\ &= 0.7037 \end{aligned}$$

$$n_S = n_M \lambda^{-0.5} = 8.9 \times \frac{1}{5} = 1.78 \text{ s}^{-1} = 106.8 \text{ rpm}$$

$$\begin{aligned} P_D &= 2\pi \rho_S n_S^3 D_S^5 K_{QBM} = 2\pi \times 1.025 \times 1.78^3 \times 5.0^5 \times 0.02691 \\ &= 3054.41 \text{ kW} \end{aligned}$$

$$\eta_D = \frac{P_E}{P_D} = \frac{2150}{3054.41} = 0.7039$$

Ship prediction:

$$n'_S = n_S k_1 = 106.8 \times 1.02 = 108.9 \text{ rpm}$$

$$P'_D = P_D k_2 = 3054.41 \times 1.00 = 3054.41 \text{ kW}$$

This neglects the differences between the open water characteristics of the model and ship propellers.

In the ITTC ship performance prediction method, a specific correction for the difference between the wake fractions of the ship and the model is introduced:

$$w_{TS} = (t + 0.04) + (w_{TM} - t - 0.04) \frac{C_{VS}}{C_{VM}} \quad (8.25)$$

where w_{TS} and w_{TM} are the wake fractions of the ship and the model, based on thrust identity, and C_{VS} and C_{VM} are the viscous resistance coefficients given by:

$$\begin{aligned} C_{VS} &= (1 + k) C_{FS} + \Delta C_F \\ C_{VM} &= (1 + k) C_{FM} \end{aligned} \quad (8.26)$$

The quantity 0.04 associated with the thrust deduction fraction t accounts for the thrust deduction contributed by a rudder in the propeller slipstream, and should be omitted if the rudder is not in the propeller slipstream, e.g. when there is a single rudder on the centre line of a twin screw ship. The thrust deduction fractions of the ship and the model are assumed to be equal. Should Eqn. (8.25) yield a value of w_{TS} greater than w_{TM} , w_{TS} should be taken equal to w_{TM} .

The propeller loading at the ship self-propulsion point is then determined as follows:

$$(1 - t) T_S = R_{TS}$$

that is,

$$(1-t) K_{TS} \rho_S n_S^2 D_S^4 = C_{TS} \frac{1}{2} \rho_S S_S V_S^2$$

which reduces to:

$$\frac{K_{TS}}{J_{TS}^2} = \frac{S_S}{2 D_S^2} \frac{C_{TS}}{(1-t)(1-w_{TS})^2} \quad (8.27)$$

where K_{TS} is the thrust coefficient of the ship propeller in open water, and:

$$J_{TS} = \frac{(1-w_{TS}) V_S}{n_S D_S}$$

The value of K_{TS}/J_{TS}^2 is first obtained from Eqn. (8.27). The values of J_{TS} , K_{TS} and K_{QS} corresponding to this value of K_{TS}/J_{TS}^2 are then determined from the open water characteristics of the ship propeller (i.e. after correcting the characteristics of the model propeller for the difference in drag coefficients of the model propeller and the ship propeller.) The revolution rate of the ship propeller and the delivered power are then easily obtained:

$$n_S = \frac{(1-w_{TS}) V_S}{J_{TS} D_S} \quad (8.28)$$

$$P_D = 2\pi \rho_S n_S^3 D_S^5 \frac{K_{QS}}{\eta_R}$$

These are values for the ship in conditions corresponding to the ideal conditions of the model experiments. The propeller revolution rate n'_S and delivered power P'_D for a ship during trials are obtained by applying correlation factors or allowances, for which two alternative methods have been proposed:

Method 1:

$$n'_S = n_S C_N \quad P'_D = P_D C_P \quad (8.29)$$

This is similar to the method described earlier.

Method 2:

In this, correlation allowances are applied to the resistance coefficient and the wake fraction of the ship for calculating the propeller loading:

$$\frac{K_{TS}}{J_{TS}^2} = \frac{S_S}{2D_S^2} \frac{C_{TS} + \Delta C_{FC}}{(1-t)(1-w_{TS} + \Delta w_C)^2} \quad (8.30)$$

This value is used to determine J_{TS} , K_{TS} and K_{QS} from the open water characteristics of the ship propeller, and then:

$$\begin{aligned} n'_S &= \frac{(1-w_{TS} + \Delta w_C) V_S}{J_{TS} D_S} \\ P'_D &= 2\pi \rho_S n_S'^3 D_S^5 \frac{K_{QS}}{\eta_R} \end{aligned} \quad (8.31)$$

The correlation factors C_N and C_P and the correlation allowances ΔC_{FC} and Δw_C are obtained by analysing the data from previous model experiments and ship trials.

The analysis of self-propulsion experiments described in the foregoing is for single screw ships. For twin screw ships, the analysis is identical except that the resistance is shared equally by the two propellers and this must be taken into account. Self-propulsion experiments for ships with more than two propellers are complicated because there is an additional variable involved, viz. the distribution of loading among the different propellers.

8.5 Wake Measurements

Although the wake fraction is determined indirectly through a self-propulsion test, it is desirable to observe the flow past a ship model at the position of the propeller to determine the distribution of wake velocity over the propeller disc directly. Wake measurements are also carried out to determine the radial and circumferential distribution of wake velocity. Such measurements are useful for propeller design and for calculating unsteady propeller forces, and could indicate unacceptable flow conditions at the stern, requiring changes in the hull form of the ship.

Direct methods of wake measurement make use of devices such as wake wheels and pitot tubes, Fig. 8.3, with a ship model in a towing tank or circulating water channel. These devices can only be used when the propeller is not fitted to the ship model, and hence they yield only the nominal wake

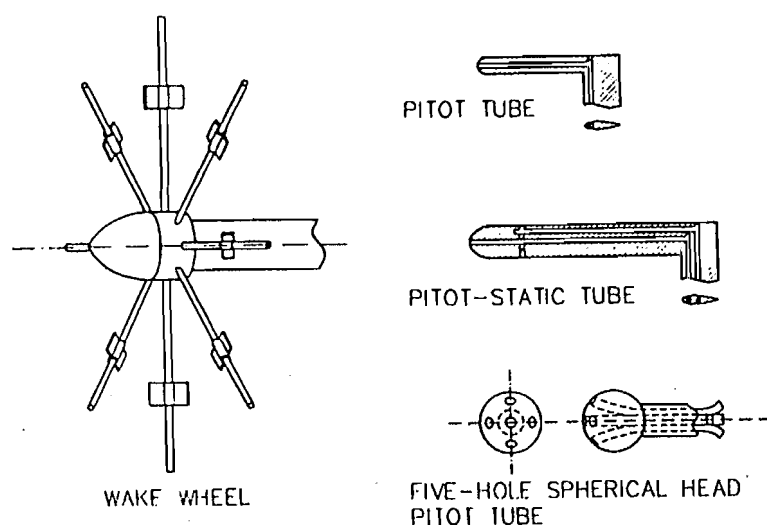


Figure 8.3 : Instruments for Wake Measurement.

(Sec. 5.2). Other disadvantages of these devices are that their presence affects the flow around the ship model and that their response is slow.

The wake wheel consists of a number of small vanes attached to radial spokes from a hub mounted on a shaft supported by very low friction bearings. The flow causes the wake wheel to revolve at a speed proportional to the flow velocity, and hence the average circumferential flow velocity at a given radius can be obtained. Repeated measurements with the vanes set at different radii provide the radial variation of wake. The pitot tube measures the total (hydrostatic plus hydrodynamic) pressure at a point, and by subtracting the hydrostatic pressure the hydrodynamic pressure is obtained which is proportional to the square of the flow velocity. Pitot-static tubes allow the total and the hydrostatic pressures to be measured together. By having a "wake rake" consisting of a series of pitot tubes mounted on a streamlined holder and connected to a manometer bank, wake measurements at several points can be obtained simultaneously. Pitot tubes however can be used only for the measurement of the axial velocity component of the flow. For obtaining all the three components of flow velocity at a point, it is necessary to use a five-hole spherical head pitot tube. Wake wheels, pitot tubes and five-hole pitot tubes are calibrated by running them in undisturbed water

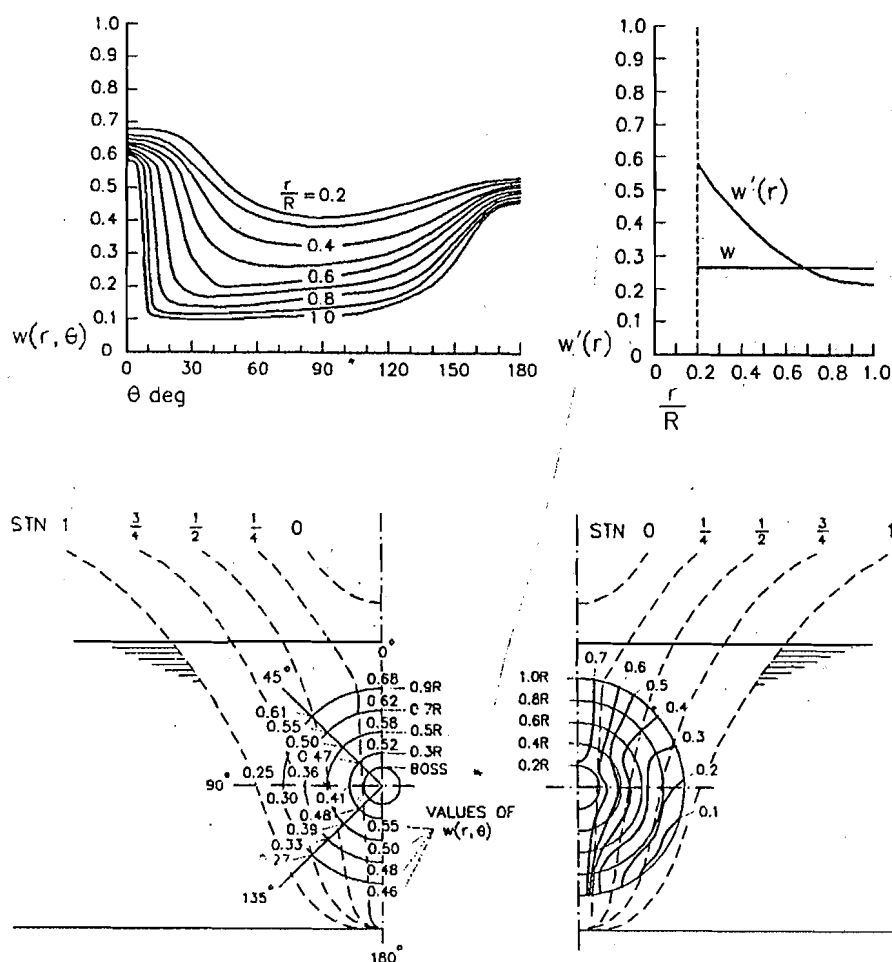


Figure 8.4: Presentation of Wake Data.

at known velocities. The disadvantages of these wake measurement devices are eliminated in laser doppler velocimeters, which allow velocity measurements to be made without disturbing the flow, are very accurate and have a quick response. Advanced laser doppler velocimeters allow all three velocity components to be measured simultaneously.

The results of wake measurements may be presented in various forms, Fig.8.4. Wake wheel measurements may be used to determine the wake fraction at various radii, and the results presented in a form showing the

wake fraction as a function of radius. Pitot tube measurements may be presented in the form of diagrams showing the wake fraction at various points of the propeller disc at equal angular and radial spacing, or contours of constant wake fraction. If all the components of wake velocity are determined, separate diagrams may be prepared for each component.

Wake measurement data may be analysed to obtain the average wake fraction or the mean circumferential wake fraction at each radius. If $v(r, \theta)$ is the axial velocity at any point (r, θ) of the propeller disc, the average nominal wake fraction w is given by:

$$\begin{aligned} (1 - w) V \pi (R^2 - r_b^2) &= \int_{r_b}^R \int_0^{2\pi} v(r, \theta) r d\theta dr \\ &= 2\pi \int_{r_b}^R r v'(r) dr \end{aligned} \quad (8.32)$$

where V is the speed of the model, R the radius of the propeller, r_b the boss radius, and $v'(r)$ the axial velocity at the radius r averaged over the circumference (i.e. the value that would be found by a wake wheel at the radius r). Alternatively, one may write:

$$\begin{aligned} (1 - w) V \pi (R^2 - r_b^2) &= \int_{r_b}^R \int_0^{2\pi} V[1 - w(r, \theta)] r d\theta dr \\ &= \int_{r_b}^R 2\pi V [1 - w'(r)] r dr \end{aligned} \quad (8.33)$$

where $w(r, \theta)$ is the local wake fraction at the point (r, θ) and $w'(r)$ the average circumferential wake fraction at the radius r . The average wake fraction obtained in this way is the "volumetric mean", i.e. both sides of the Eqns. (8.32) and (8.33) represent the volume of water flowing through the propeller disc per unit time.

For studying unsteady propeller forces and propeller excited vibration, the local wake fraction $w(r, \theta)$ may be expressed in the form of a Fourier Series:

$$w(r, \theta) = \sum_{m=0}^n [a_m(r) \cos m\theta + b_m(r) \sin m\theta] \quad (8.34)$$

the coefficients $a_m(r)$ and $b_m(r)$ being found by a least squares fit and the series being truncated after, say, twenty terms.

Example 4

The local wake fractions obtained by measurements at various angular and radial positions at the location of the propeller in a single screw ship model are as follows:

$x = r/R$	θ deg:	0	30	60	90	120	150	180
0.2		0.5832	0.4690	0.3426	0.3013	0.2843	0.3524	0.4082
0.3		0.5622	0.4521	0.3303	0.2905	0.2741	0.3397	0.3935
0.4		0.5328	0.4285	0.3130	0.2753	0.2597	0.3219	0.3730
0.5		0.4950	0.3980	0.2908	0.2558	0.2413	0.2991	0.3465
0.6		0.4489	0.3609	0.2637	0.2319	0.2188	0.2712	0.3142
0.7		0.3942	0.3170	0.2316	0.2037	0.1922	0.2381	0.2759
0.8		0.3312	0.2663	0.1946	0.1711	0.1615	0.2001	0.2318
0.9		0.2598	0.2089	0.1526	0.1342	0.1267	0.1570	0.1819
1.0		0.1800	0.1448	0.1058	0.0930	0.0878	0.1088	0.1260

Determine the average circumferential wake fraction at each radius and the average wake fraction over the propeller disc.

For a single screw ship, the flow normally has port and starboard symmetry. The average circumferential wake at any fractional radius $x = r/R$:

$$w'(x) = \frac{1}{2\pi} \int_0^{2\pi} w(x, \theta) d\theta = 2 \times \frac{1}{2\pi} \int_0^{\pi} w(x, \theta) d\theta$$

For $x = 0.2$, using integration by Simpson's Rule:

θ deg	$w(r, \theta)$	SM	$f(w')$
0	0.5832	1	0.5832
30	0.4690	4	1.8760
60	0.3426	2	0.6852
90	0.3013	4	1.2052
120	0.2843	2	0.5686
150	0.3524	4	1.4096
180	0.4082	1	0.4082
			6.7360

$$w'(0.2) = \frac{1}{\pi} \times \frac{1}{3} \times \frac{\pi}{6} \times 6.7360 = 0.3742$$

where $1/3$ is the common multiplier in Simpson's Rule and $\pi/6 = 30^\circ$ is the spacing.

The average circumferential wakes at the other radii are similarly obtained as:

$$\begin{aligned} w'(0.3) &= 0.3607 & w'(0.4) &= 0.3419 & w'(0.5) &= 0.3176 \\ w'(0.6) &= 0.2880 & w'(0.7) &= 0.2529 & w'(0.8) &= 0.2125 \\ w'(0.9) &= 0.1667 & w'(1.0) &= 0.1155 \end{aligned}$$

The average wake fraction over the whole propeller disc is given by:

$$(1-w) = \frac{2}{1-x_b^2} \int_{x_b}^{1.0} [1-w'(x)] x \, dx = 1 - \frac{2}{1-x_b^2} \int_{x_b}^{1.0} w'(x) x \, dx$$

In the present case $x_b = 0.2$, so that:

$$w = \frac{2}{1-0.2^2} \int_{0.2}^{1.0} w'(x) x \, dx = \frac{1}{0.48} \int_{0.2}^{1.0} w'(x) x \, dx$$

Using integration by Simpson's Rule:

x	$w'(x)$	$xw'(x)$	SM	$f(w)$
0.2	0.3742	0.07484	1	0.07484
0.3	0.3607	0.10821	4	0.43284
0.4	0.3419	0.13676	2	0.27352
0.5	0.3176	0.15880	4	0.63520
0.6	0.2880	0.17280	2	0.34560
0.7	0.2529	0.17703	4	0.70812
0.8	0.2125	0.17000	2	0.34000
0.9	0.1667	0.15003	4	0.60012
1.0	0.1155	0.11550	1	0.11550
				3.52574

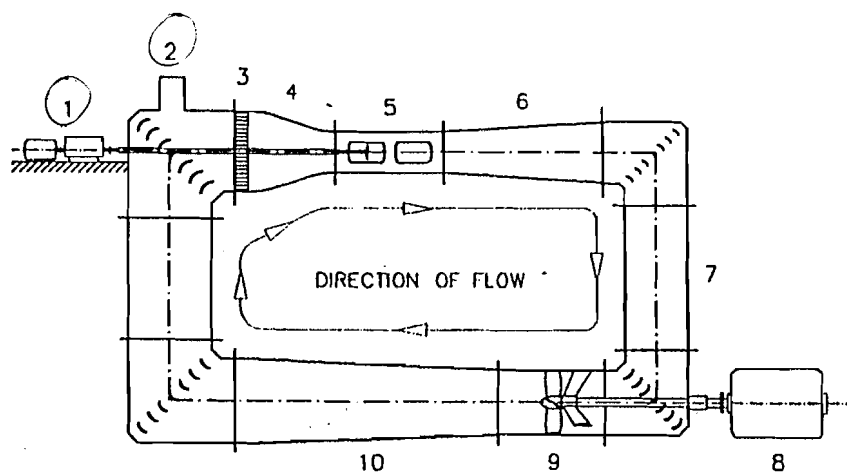
$$w = \frac{1}{0.48} \times \frac{1}{3} \times 0.1 \times 3.52574 = 0.2448$$

8.6 Cavitation Experiments

Cavitation experiments with propellers are carried out to study propeller cavitation and determine its effects on propeller performance. In addition to observing cavitation patterns on propeller blades and the effect of cavitation on the open water characteristics, such experiments allow one to study cavitation erosion and noise due to cavitation. Although it is possible to study cavitation on full size propellers in ships with the aid of underwater television cameras, cavitation experiments are usually conducted with model propellers in cavitation tunnels. There is also a depressurised towing tank at MARIN, the Netherlands, which is a unique facility for studying cavitation.

A variable pressure recirculating water tunnel, usually called a "cavitation tunnel", Fig. 8.5, has a shell made up of a number of pieces bolted together, an impeller to circulate the water in the tunnel, an air pump to control the pressure in the tunnel, and the equipment associated with the model whose cavitation characteristics are to be studied. The tunnel is normally erected in a vertical plane with the impeller at one end of the lower horizontal limb, and the working section in which the model is placed in the upper limb. The flow is guided around the corners at the junctions of the horizontal and vertical limbs by guide vanes, and the rotation of the flow caused by the impeller is reduced to a great extent by a "honeycomb" section. A contraction section just ahead of the working section increases the flow velocity to the desired value. A diffuser after the working section decelerates the flow and increases the pressure at the impeller position to minimise the possibility of impeller cavitation. A pressure coaming at the highest point of the tunnel is connected to an air chamber from which air may be evacuated by a vacuum pump to allow the pressure of air above the water in the tunnel to be reduced. The pressure can also be increased to a high value to simulate the operating conditions of a submarine at great depth.

For cavitation experiments with propellers, a model propeller is placed in the working section and attached to a propeller dynamometer, which can measure the thrust and torque of the propeller while it runs at a steady revolution rate. The working section has large airtight windows to allow cavitation to be observed with the help of stroboscopic lighting. Instruments are provided to measure the speed of water in the working section and the pressure. Non-uniform wake conditions may be simulated by providing flow



1. PROPELLER MOTOR AND DYNAMOMETER
2. PRESSURE COAMING
3. HONEYCOMB ✓
4. CONTRACTION ✓
5. WORKING SECTION ✓
6. DIFFUSER ✓
7. VERTICAL LIMB ✓
8. IMPELLER MOTOR ✓
9. IMPELLER ✓
10. DIFFUSER ✓

Figure 8.5 : Cavitation Tunnel.

regulators, wire mesh screens or partial ship models ahead of the propeller. The non-uniform velocity field is measured by a wake rake and the flow regulating devices adjusted until the desired velocity field is obtained.

It has been seen that cavitation is affected by the amount of air dissolved in water. An instrument to measure air content is therefore provided. However, air liberated from water by cavitation does not easily go back into solution and the air bubbles circulate with the water in the tunnel, interfering with the cavitation phenomena and their observation. This problem is usually overcome by removing the air dissolved in the tunnel water. Alternatively, the tunnel may be provided with a "resorber" in which the tunnel

water is circulated at low velocity and high pressure to force the air back into solution. The reduced air content and the purity of the tunnel water in comparison with sea water cause substantial differences between the cavitation phenomena observed in a cavitation tunnel and those occurring with full scale propellers at sea. Better correlation between the cavitation of a model propeller in a cavitation tunnel and of the ship propeller at sea is obtained by reducing the cavitation number of the model propeller in comparison to the ship propeller by as much as 15–20 percent when air is removed from the tunnel water. Cavitation nuclei may be artificially introduced by electrolysis in the tunnel water to increase its similarity with sea water in which microscopic particles act as nuclei.

In carrying out propeller cavitation experiments in a cavitation tunnel, the thrust and torque of the model propeller are measured for different speeds of advance, revolution rates and pressures so that the complete range of advance coefficient and cavitation number is covered. In addition, the temperature of the tunnel water (on which vapour pressure depends) and its air content are also measured. Cavitation patterns are observed and recorded using powerful stroboscopic lighting and high speed photography. Noise measurements using hydrophones may also be carried out. Cavitation erosion may be studied by covering the propeller blade surfaces with a suitable coating that is easily eroded by the collapsing cavities.

The results of cavitation experiments are usually presented in terms of the thrust and torque coefficients as functions of the advance coefficient for different cavitation numbers, as shown in Fig. 6.4. Sketches showing the type and extent of cavitation for different advance coefficients and cavitation numbers or photographs may also be given. Zones of different types of cavitation may be shown in a diagram similar to Fig. 6.3. Cavitation noise and erosion parameters may be determined for given advance coefficients and cavitation numbers.

In addition to cavitation experiments with model propellers, cavitation tunnels are also used to study cavitation on other bodies such as hydrofoils using appropriate instruments and equipment.

The variable pressure towing tank of MARIN is 240 m long and 18 m wide, and has water up to a depth of 8 m. The towing carriage is driven by a cable towing system. The air pressure in the tank can be brought down to about 4 kN per m². The performance of the model propeller can be seen through a

periscope by observers in a chamber in which normal atmospheric pressure is maintained and which is sealed off when the pressure in the tank is reduced.

Example 5

A ship has a propeller of 4.0 m diameter with its centre line 3.0 m below the surface of water. The propeller in its design condition has a speed of advance of 8.0 m per sec at 150 rpm and 2500 kW delivered power. Experiments are to be carried out with a 1/16 scale model propeller in a cavitation tunnel in which the maximum speed of water in the working section is 10.0 m per sec, the maximum propeller rpm is 3000, the maximum torque is 45 N m and the minimum static pressure at the centre line of the working section is 15 kN per m². Determine the speed of water, the model propeller rpm and the static pressure at the propeller position if the model propeller is to be run (a) at the correct Froude number, and (b) just within the limits of the cavitation tunnel. The tunnel water is deaerated and the tunnel cavitation number must be reduced by 15 percent compared to the ship. What is the minimum cavitation number of the tunnel based on the speed of water in the working section?

$$D_S = 4.0 \text{ m} \quad n_S = 150 \text{ rpm} = 2.5 \text{ s}^{-1} \quad V_{AS} = 8.0 \text{ ms}^{-1} \quad P_{DS} = 2500 \text{ kW}$$

$$h_S = 3.0 \text{ m} \quad \lambda = 16 \quad D_M = D_S/\lambda = 4.0/16 = 0.25 \text{ m} \quad \sigma_M = 0.85 \sigma_S$$

$$V_{AM} \text{ max} = 10.0 \text{ ms}^{-1} \quad n_M \text{ max} = 3000 \text{ rpm} = 50 \text{ s}^{-1} \quad Q_M \text{ max} = 45 \text{ N m}$$

$$p_{\text{Tunnel min}} = 15 \text{ kN m}^{-2}$$

$$J_S = \frac{V_{AS}}{n_S D_S} = \frac{8.0}{2.5 \times 4.0} = 0.800$$

$$K_{QS} = \frac{P_{DS}}{2\pi \rho_S n_S^3 D_S^5} = \frac{2500}{2\pi \times 1.025 \times 2.5^3 \times 4.0^5} = 0.02426$$

$$\sigma_S = \frac{p_A + \rho_S g h_S - p_V}{\frac{1}{2} \rho_S V_{AS}^2} = \frac{101.325 + 1.025 \times 9.81 \times 3.0 - 1.704}{\frac{1}{2} \times 1.025 \times 8.0^2}$$

$$= 3.9569$$

(a) At the correct Froude number

$$V_{AM} = V_{AS} \lambda^{-0.5} = 8.0 \times 16^{-0.5} = 2.0 \text{ ms}^{-1}$$

$$n_M = \frac{V_{AM}}{J_M D_M} = \frac{2.0}{0.800 \times 0.25} = 10.0 \text{ s}^{-1} \quad J_M = J_S$$

$$\sigma_M = \frac{p_{Tunnel} - p_V}{\frac{1}{2} \rho_M V_{AM}^2} = \frac{p_{Tunnel} - 1.704}{\frac{1}{2} \times 1.000 \times 2.0^2} = 0.85 \sigma_S$$

$$= 0.85 \times 3.9569 = 3.3634$$

$$p_{Tunnel} = 1.704 + \frac{1}{2} \times 1.000 \times 2.0^2 \times 3.3634 = 8.4307 \text{ kN m}^{-2}$$

(which is below the minimum limit of pressure)

(b) At the limits of the cavitation tunnel

If $V_{AM} = 10.0 \text{ m s}^{-1}$:

$$n_M = \frac{V_{AM}}{J_M D_M} = \frac{10.0}{0.800 \times 0.25} = 50.0 \text{ s}^{-1}$$

$$Q_M = \rho_M n_M^2 D_M^5 K_{QM}$$

$$= 1.000 \times 50.0^2 \times 0.25^5 \times 0.02426 \quad (K_{QM} = K_{QS})$$

$$= 0.05923 \text{ kN m} = 59.23 \text{ N m, which is above the limit.}$$

Hence, keeping $Q_M = 45 \text{ N m}$, the limiting value,

$$n_M^2 = \frac{Q_M}{\rho_M D_M^5 K_{QM}} = \frac{45.0}{1000 \times 0.25^5 \times 0.02426} = 1899.4229$$

$$n_M = 43.5824 \text{ s}^{-1}$$

$$V_{AM} = J_M n_M D_M = 0.800 \times 43.5824 \times 0.25 = 8.7165 \text{ m s}^{-1}$$

$$p_{Tunnel} = p_V + \frac{1}{2} \rho_M V_{AM}^2 \sigma_M = 1.704 + \frac{1}{2} \times 1.000 \times 8.7165^2 \times 3.3634$$

$$= 129.475 \text{ kN m}^{-2}$$

The minimum cavitation number of the tunnel is:

$$\sigma_T = \frac{p_{Tunnel}^{\min} - p_V}{\frac{1}{2} \rho_M V_{AM}^{\max^2}} = \frac{15.0 - 1.704}{\frac{1}{2} \times 1.000 \times 10.0^2} = 0.2659$$

Problems

1. A resistance experiment is carried out on a 5.0 m long model of a ship of length 120 m and wetted surface 3200 m^2 . The following results are obtained:

Model speed, m per sec	:	1.050	1.260	1.470	1.680	1.890
Model resistance, N	:	12.13	17.78	25.45	36.29	52.02

Determine the effective power of the ship at the corresponding speeds using the ITTC friction line with a form factor of 1.06 and a correlation allowance of 0.0004.

2. A ship of length 150 m has a transverse projected area above water of 403 m^2 , the wetted surface of the hull being 6200 m^2 . The bilge keels have a wetted surface of 260 m^2 . The roughness of the hull surface is 150 microns. The resistance of a model of length 6.0 m as measured during a resistance test is as follows:

Model speed, m per sec	:	1.235	1.440	1.646	1.852	2.058
Model resistance, N	:	26.99	38.45	54.54	77.71	111.56

Determine the effective power of the ship at the corresponding speeds using the ITTC performance prediction method with a form factor of 1.05.

3. An open water experiment covering the complete range of advance coefficient is to be carried out on a model of a propeller of diameter 5.0 m and pitch ratio 1.0. The effective pitch ratio of the propeller is expected to be about 1.08, and the torque coefficient at zero speed of advance to be 0.0625. The maximum speed at which the model propeller can be made to advance is 6.0 m per sec, and the maximum rpm and torque of the propeller dynamometer are 3000 and 3.0 N m respectively. Determine the maximum model propeller diameter if (a) the model propeller is to run at a constant 3000 rpm for the complete range of advance coefficient, and (b) the model propeller is to run at 2400 rpm. If the minimum propeller diameter is to be 150 mm, what is the maximum rpm? Calculate for each case at zero advance and zero slip the Reynolds number of the model propeller using the resultant velocity at $0.75R$, given that the chord diameter ratio is 0.28 for this radius.
4. An open water experiment is carried out with a four-bladed model propeller of 200 mm diameter and 0.8 pitch ratio. The blade section at $0.75R$ has a chord of 50 mm and a thickness of 2.5 mm. The model propeller is run at 2100 rpm over a range of speeds and the following values of thrust and torque (corrected for idle thrust and torque) are obtained:

Speed, m per sec	:	0.000	0.700	1.400	2.100	2.800
Thrust, N	:	666	612	551	484	412
Torque, N m	:	15.29	14.54	13.57	12.38	10.98

Speed, m per sec	:	3.500	4.200	4.900	5.600	6.300
Thrust, N	:	333	247	156	59	-45
Torque, N m	:	9.35	7.50	5.43	3.14	0.62

Determine the open water characteristics of the full size propeller of diameter 4.0 m, assuming that its surface roughness is 30 microns.

5. In a self-propulsion test, the model speed is 2.0 m per sec and at the ship self-propulsion point the 0.2 m diameter model propeller runs at 900 rpm and the thrust, torque and tow force are respectively 55.00 N, 1.33 N m and 2.55 N. The resistance of the model at 2.0 m per sec is 49.03 N. The model propeller has open characteristics as follows:

J	:	0.300	0.400	0.500	0.600	0.700
K_T	:	0.210	0.182	0.152	0.120	0.086
$10K_Q$:	0.253	0.225	0.195	0.164	0.132

Calculate the propulsive efficiency and its components on the basis of (a) thrust identity, and (b) torque identity. If the model scale is 1:25, determine the effective power, the delivered power and the propeller rpm of the ship at the corresponding speed. Neglect the difference between the open water characteristics of the model and ship propellers.

6. In a self-propulsion test with a twin screw ship model, the model is self-propelled at a speed of 2.3 m per sec when the two propellers together have a total thrust of 34 N and a total torque of 1.18 N m at 720 rpm. In the open water test with either propeller running at 720 rpm a thrust of 17 N is obtained at a speed of 2.0 m per sec, the torque being 0.61 N m. The resistance of the model at a speed of 2.3 m per sec is 29 N. Calculate the propulsive efficiency and its components. Are these values applicable to the ship?
7. A ship of length 100 m and a wetted surface of 2250 m² has a propeller of diameter 5.0 m. At its design speed of 20 knots, the ship has an effective power of 5000 kW. A self-propulsion test is carried out on a 1/25-scale model, which has a resistance of 35 N at the corresponding speed. The following readings (after correction) are obtained at this speed:

Propeller rpm	:	500	550	600	650	700
Thrust, N	:	27.15	30.84	35.83	42.22	50.81
Torque, N m	:	0.75	0.93	1.42	2.08	3.10
Tow Force, N	:	6.33	5.47	4.65	3.70	2.63

The open water data of the model propeller are as follows:

J	:	0.700	0.800	0.900	1.000
K_T	:	0.255	0.224	0.191	0.153
$10K_Q$:	0.508	0.468	0.420	0.368

Calculate the delivered power of the ship and its propeller rpm at 20 knots and the propulsion factors using the ITTC ship prediction method with the following values:

$$\begin{aligned}
 1+k &= 1.05 & \Delta C_F &= 0.6 \times 10^{-3} & \Delta K_T &= -0.0002 \\
 \Delta K_Q &= 0.0003 & C_N &= 1.005 & C_P &= 1.010
 \end{aligned}$$

8. In a model of a single-screw ship, the following average velocities over the circumference at various radii at the propeller position are measured with the model moving at a speed of 5.0 m per sec in undisturbed water:

Radius, mm	:	20	30	40	50	60
Velocity, m per sec	:	3.503	3.557	3.632	3.730	3.848
Radius, mm	:	70	80	90	100	
Velocity, m per sec	:	3.988	4.150	4.333	4.538	

Determine the nominal wake fraction, the model propeller having a diameter of 200 mm and a boss diameter ratio of 0.2.

9. In a twin screw ship model, the axial velocities measured at various radii r and angular positions θ at the propeller disc when the model has a speed of 4.0 m per sec are as follows:

θ° :	0	30	60	90	120	150
r mm	Axial velocity, v m per sec					
15.0	3.600	3.680	3.792	3.880	3.960	3.960
22.5	3.552	3.636	3.788	3.880	3.956	3.956
30.0	3.488	3.596	3.764	3.876	3.952	3.948
37.5	3.440	3.552	3.760	3.876	3.952	3.936
45.0	3.368	3.508	3.752	3.872	3.948	3.924
52.5	3.308	3.448	3.728	3.868	3.948	3.916
60.0	3.228	3.400	3.716	3.852	3.940	3.892
67.5	3.136	3.348	3.696	3.840	3.928	3.872
75.0	3.040	3.280	3.680	3.828	3.920	3.840

θ° :	180	210	240	270	300	330
r mm	Axial velocity, v m per sec					
15.0	3.936	3.880	3.844	3.640	3.440	3.200
22.5	3.928	3.872	3.836	3.608	3.408	3.120
30.0	3.920	3.856	3.816	3.568	3.312	3.032
37.5	3.896	3.836	3.792	3.528	3.236	2.936
45.0	3.880	3.808	3.760	3.484	3.160	2.844
52.5	3.864	3.776	3.724	3.440	3.080	2.744
60.0	3.840	3.740	3.680	3.392	2.996	2.640
67.5	3.800	3.700	3.632	3.340	2.896	2.520
75.0	3.756	3.656	3.584	3.280	2.800	2.348

Determine the mean circumferential wake fraction at the various radii and the nominal wake fraction. The model propeller is of 150 mm diameter with a boss diameter of 30 mm.

10. A single-screw ship has a design speed of 22 knots with its propeller running at 150 rpm and the delivered power being 12500 kW. The propeller has a diameter of 6.0 m and its centre line is 5.2 m below the water line. Model experiments are to be carried out in a cavitation tunnel with a free surface working section using a ship model to create a variable wake. The model propeller diameter is 150 mm. Determine the speed of water in the working section ahead of the model, the model propeller rpm and torque, and the pressure in the air above the water surface in the working section for simulating the conditions in the ship propeller. Assume that the cavitation number of the model propeller must be 10 percent less than that of the ship propeller.

CHAPTER 9

Propeller Design

9.1 Propeller Design Approaches

Propellers for ships may be designed to fulfil two purposes: (i) to utilise the available propelling power efficiently to propel the ship alone, or (ii) to use the power to allow the ship to tow other vessels or gear. Propellers designed for propelling the ship alone are called "free running propellers". Propellers fitted to tugs, towboats and trawlers are called "towing duty propellers".

The design of propellers can be approached in two different ways. In the first approach, propeller design is based on methodical series data so that many design features such as the blade outline and blade section shapes are fixed by the methodical series adopted, and the design of a propeller reduces to determining the diameter, the pitch ratio and the blade area ratio. This approach has been widely used for several decades and is even now often adopted for designing propellers which are moderately loaded and in which cavitation is not a major problem. Even when a design method using the other approach is to be adopted, a design obtained from a methodical series often forms the starting point.

The second approach to propeller design is based on the use of propeller theory. A suitable distribution of circulation required to give the specified thrust is determined, and then the detailed design of the blade sections at a number of radii is carried out so that the required circulation is obtained while at the same time the minimum pressures are kept within safe limits to avoid harmful cavitation. A major advantage of this approach is that the

blade sections can be designed to suit the average radial wake variation in the flow incident on the propeller. The calculations in the design approach based on propeller theory are somewhat involved but can now be routinely carried out with the help of computers.

9.2 General Considerations in Propeller Design

Before discussing propeller design procedures in detail, it is useful to examine the considerations involved in selecting the major design features of a propeller. These considerations often form an important part of the propeller design process, and in many cases necessitate a compromise between several conflicting requirements.

The propeller revolution rate (rpm) is usually determined by the propulsion plant that is selected for a given ship. However, in deciding upon the propeller rpm it is necessary to consider several factors related to propeller design. It is important to select the propeller rpm so that resonance with the natural frequencies of vibration of the hull and the propeller shafting system are avoided. An unduly high propeller rpm may increase susceptibility to cavitation. On the other hand, a low propeller rpm results in a large propeller diameter (other things being equal) and an increase in efficiency. This has resulted in recent years in the development of very low speed diesel engines with speeds as low as 50–60 rpm, which in association with large diameter propellers have led to substantial improvements in propeller efficiency.

From the point of view of vibration, propeller rpm must be considered in association with the number of propeller blades. The propeller excited frequency of vibration is the product of the propeller rpm and the number of blades and it is this product which must lie well clear of the natural frequencies of hull vibration (vertical, horizontal and torsional) as well as the natural frequencies of the propulsion shafting system. One may also note that the larger the number of blades the smaller is the exciting force per blade. On the other hand, the smaller the number of blades the greater is the optimum propeller diameter and higher the propeller efficiency, but there is also an increase in the weight of the propeller.

The diameter of the propeller is influenced by the propeller rpm, a lower rpm resulting in a higher optimum diameter and a higher efficiency. The

maximum propeller diameter is limited by the need to maintain adequate clearances between the propeller and the hull and rudder. Typical values of the minimum clearances required by a classification society (Lloyd's Register of Shipping) are given in Fig. 9.1. While a larger propeller diameter reduces the possibility of cavitation by reducing the propeller loading, it could lead to excessive wake variations and to a reduction in propulsive efficiency due to a decrease in the average value of the wake fraction.

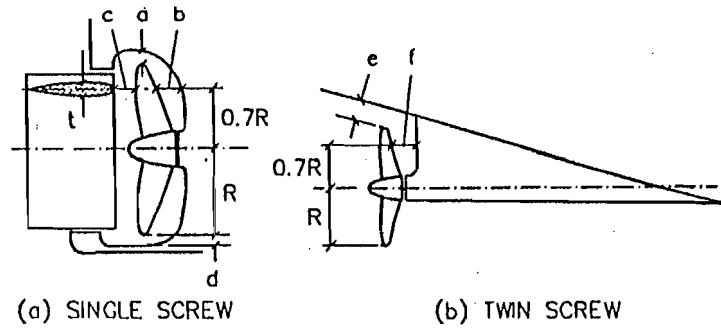
The pitch ratio of a propeller governs the power that it will absorb in given operating conditions, i.e. speed of advance and rpm: the higher the pitch ratio the higher the delivered power at a constant advance coefficient. The effect of pitch ratio on propeller rpm is given approximately by the following empirical relationships due to van Manen (1957):

$$\begin{aligned}\frac{\partial n/n}{\partial (P/D)/(P/D)} &= 1 && \text{at constant torque} \\ \frac{\partial n/n}{\partial (P/D)/(P/D)} &= 1.5 && \text{at constant power} \\ P + D &= \text{constant} && \text{at constant power and rpm}\end{aligned}\tag{9.1}$$

These relations may be used to make small corrections to the pitch and diameter of an existing propeller design in which the relationship between power and rpm is not fully satisfactory.

The blade area ratio is selected basically from considerations of cavitation, a certain minimum blade area being necessary to ensure that even if cavitation occurs it is within acceptable limits. Unduly large blade area ratios cause a reduction in propeller efficiency due to an increase in blade section drag. Very low expanded blade area ratios (below about 0.3) may lead to difficulties in generating adequate astern thrust. A small increase in blade area ratio may be made to keep propeller blade stresses within permissible limits without an increase in the blade thickness fraction.

The boss diameter ratio of fixed pitch propellers usually lies between 0.15 and 0.20, values outside this range resulting in a drop in propeller efficiency. The minimum permissible boss diameter, however, depends upon the diameter of the propeller shaft.



Number of Blades	a	b	c	d	e	f
3	1.20 KD	1.80 KD	0.12 D	0.03 D	1.20 KD	1.20 KD
4	1.00 KD	1.50 KD	0.12 D	0.03 D	1.00 KD	1.20 KD
5	0.85 KD	1.275 KD	0.12 D	0.03 D	0.85 KD	0.85 KD
6	0.75 KD	1.125 KD	0.12 D	0.03 D	0.75 KD	0.75 KD
Minimum Value	0.10 D	0.15 D	t	-	0.20 D ⁽ⁱ⁾ 0.16 D ⁽ⁱⁱ⁾	0.15 D
					(i) for 3 or 4 blades (ii) for 5 or 6 blades	

$$K = \left(0.1 + \frac{L}{3050} \right) \left(\frac{3.48 C_B P_S}{L} + 0.3 \right)$$

L = Length of the ship in m

C_B = Block coefficient at load draught

P_S = Designed power on one shaft in kW

t = Thickness of rudder in m measured at 0.7R above the propeller shaft centre line

R = Propeller radius in m measured at 0.7R

D = Propeller diameter in m

Figure 9.1 : Propeller-Hull Clearances.

Propeller blades are sometimes raked aft to increase the clearances between the hull and the propeller blade tips and leading edges. This allows a propeller of a larger diameter to be used, and results in a higher efficiency provided that the propeller rpm can be suitably selected. Aft rake, however, causes an increase in the bending moment due to the centrifugal force on each blade, thus requiring thicker blades which have a lower efficiency. Slow running propellers may be given a rake aft of up to 15 degrees, but in propellers running at high rpms aft rake is best avoided.

Propellers in which the blades are skewed back (i.e. towards the trailing edge) result in a lower magnitude of unsteady forces generated by the propeller in a circumferentially varying wake. Skewed blades are also believed to be less liable to get entangled with ropes or chains that accidentally come in way of the propeller. However, propellers with heavily skewed blades have low backing efficiencies, are difficult to manufacture and require special strength considerations.

In the foregoing, the factors to be considered in selecting the overall propeller design parameters, viz. number of blades, diameter, pitch ratio, blade area ratio, boss diameter ratio, rake and skew, have been discussed. Some of these parameters can be selected by a designer using the methodical series method of propeller design. When a design method based on propeller theory is used, some additional parameters must be considered.

The radial distribution of loading (i.e. the variation of circulation with radius upon which the radial distribution of thrust depends) is normally made optimum for the given average wake at each radius. In some cases, however, the loading may be decreased towards the blade tips to reduce cavitation, blade stresses and propeller induced hull vibration. Departures from the optimum load distribution are naturally accompanied by a loss in efficiency.

The shape of the expanded blade outline is chosen in accordance with the radial load distribution, the higher the load the greater the blade width required at that radius to ensure that cavitation is kept within limits. Narrow blade tips result in an increase in propeller efficiency but also a greater risk of harmful cavitation. The shape of the blade outline for a given expanded area also depends upon how the skew is distributed along the radius. The radial distribution of skew (i.e. the shape of the line joining the midpoints of the blade widths at the different radii) affects the unsteady forces generated

by the propeller blades in a variable wake field, and it is possible to choose the shape of the blade outline so as to minimise these unsteady forces.

The efficiency of a propeller depends upon the shape of its blade sections. Aerofoil sections with their high lift-drag ratios result in high efficiencies. However, such sections also have a high suction pressure peak and are thus more prone to cavitation. Segmental blade sections have a somewhat lower lift-drag ratio but a more uniform pressure distribution making them less efficient but also less liable to cavitation. Propellers are therefore often designed to have aerofoil sections at the inner radii where cavitation is less likely and segmental sections towards the blade tip where back cavitation usually starts. For propellers in which cavitation is likely to be a problem, special sections such as the Karman-Trefftz section and the NACA-16 and NACA-66 sections with $a = 0.8$ and $a = 1.0$ mean lines are used. Details of these NACA sections are given in Appendix 2.

The blade section thickness is governed mostly by the strength requirements of the propeller. A lower thickness-chord ratio reduces drag and increases propeller efficiency but also reduces the range of angles of attack in which no cavitation occurs. The thickness and chord of the blade sections at different radii must therefore be based on loading, strength, cavitation and efficiency considerations.

The blade section camber depends upon the loading at each radius and must be such that in association with the angle of attack it results in the required lift coefficient. The angle of attack depends upon the direction of the resultant velocity and the pitch angle of the blade section at a particular radius. The pitch angle should be chosen so that the ideal angle of attack is obtained. However, a propeller normally works in a variable wake, and it is necessary to choose the pitch angle so that back cavitation due to high angles of attack and face cavitation due to low (negative) angles of attack are both avoided in the given flow field.

From the foregoing discussion, it is evident that in common with most design processes, propeller design involves a number of mutually conflicting considerations, and compromises must often be made in the pursuit of an optimum design. It may be added that specific decisions regarding each and every design variable discussed in this section are neither necessary nor possible in normal propeller design calculations. These general design

considerations merely serve as a background to the methods used in propeller design.

9.3 Propeller Design using Methodical Series Data

Methodical series data may be used to design both free running and towing duty propellers. The design of towing duty propellers is considered in the next section. The first decision to be made in propeller design based on methodical series data is the choice of the methodical series. This decision may be based on the considerations discussed in the previous section taking into account the particular features of the different methodical series available. The MARIN B-Series is widely used for propeller design because experience has shown that it has excellent performance characteristics, particularly for moderate loadings. For heavily loaded propellers used in high speed twin screw ships, the Gawn series may be preferred because it has segmental blade sections which are less likely to cavitate.

Propeller methodical series data are available in the form of design charts or as regression equations suitable for use with a computer. The most convenient type of propeller design chart is the $B_P - \delta$ diagram, or its modern variant in which B_P is replaced by K_Q/J^5 and δ by J .

Design problems for free running propellers are of two types:

- (i) Given the propeller diameter and the ship speed, design the optimum propeller to minimise the power required, and determine the corresponding propeller rpm.
- (ii) Given the engine power and propeller rpm, design the optimum propeller to maximise the ship speed.

The first type of problem basically provides guidance in selecting the propulsion plant for a ship. The second type of problem yields a propeller design to suit a given propulsion plant, which is selected considering several factors in addition to the requirements of the propeller. Incidentally, if one first starts with a given propeller diameter and ship speed and determines the optimum propeller rpm [type (i) problem], and then takes this rpm as given and determines the optimum diameter [type (ii) problem], one obtains a higher

diameter than the initial value. If this process is repeated, one gets higher and higher values of diameter and correspondingly lower values of propeller rpm, keeping the ship speed constant.

The data required for propeller design include the following:

- (a) Effective power for a range of speeds, [one speed for a type (i) problem].
- (b) The propulsion factors – wake fraction, thrust deduction fraction and relative rotative efficiency.
- (c) The depth of immersion of the propeller axis.
- (d) The shafting efficiency.
- (e) The ship speed and the propeller diameter for a type (i) design problem or the engine power and rpm and the gear ratio (engine rpm: propeller rpm) if gearing is provided between the engine and the propeller, for a type (ii) design problem.

Individual propeller designers have their own procedures for designing propellers. Typical design procedures for propeller design using methodical series design charts (or data extracted from them) and regression equations are illustrated in the following examples. The methodical series data used in these examples are given in Tables 9.1 and 9.2. It is important to note that these data are only for illustrative purposes and are not based on the data of an actual methodical propeller series. The data in these tables should be used only in the following ranges of pitch ratio and advance coefficient:

$$0.7 \leq \frac{P}{D} \leq 1.1 \quad \left(\frac{P}{D} - 0.3 \right) \leq J \leq \frac{P}{D}$$

Example 1

A ship is to have a design speed of 16 knots at which its effective power is 3388 kW. The maximum propeller diameter that can be fitted is 5.5 m. The propulsion factors based on thrust identity are: $w = 0.200$, $t = 0.150$, $\eta_R = 1.050$. The shafting efficiency may be taken as 0.970. The minimum blade area ratio required to keep cavitation within acceptable limits is estimated to be 0.55. Determine the

Table 9.1
Optimum Efficiency Line for 4-Bladed Propellers*

$\left(\frac{K_Q}{J^5}\right)^{\frac{1}{4}}$	$\frac{A_E}{A_O} = 0.40$			$\frac{A_E}{A_O} = 0.55$			$\frac{A_E}{A_O} = 0.70$		
	J	$\frac{P}{D}$	η_O	J	$\frac{P}{D}$	η_O	J	$\frac{P}{D}$	η_O
0.5000	0.8679	1.0999	0.7111	0.8625	1.1000	0.7084	0.8614	1.1002	0.6989
0.5500	0.7802	0.9968	0.6926	0.7838	1.0141	0.6886	0.7894	1.0350	0.6848
0.6000	0.7161	0.9320	0.6763	0.7180	0.9445	0.6720	0.7201	0.9567	0.6678
0.6500	0.6647	0.8840	0.6607	0.6671	0.8979	0.6562	0.6690	0.9091	0.6519
0.7000	0.6220	0.8482	0.6453	0.6249	0.8625	0.6407	0.6276	0.8753	0.6362
0.7500	0.5854	0.8184	0.6303	0.5889	0.8343	0.6254	0.5922	0.8483	0.6208
0.8000	0.5533	0.7930	0.6156	0.5574	0.8104	0.6104	0.5613	0.8260	0.6057
0.8500	0.5249	0.7708	0.6014	0.5297	0.7905	0.5959	0.5339	0.8069	0.5909
0.9000	0.4998	0.7523	0.5876	0.5049	0.7727	0.5818	0.5096	0.7909	0.5766
0.9500	0.4770	0.7348	0.5743	0.4827	0.7578	0.5682	0.4876	0.7766	0.5628
1.0000	0.4565	0.7199	0.5616	0.4624	0.7438	0.5551	0.4677	0.7640	0.5495

* These data may be obtained from diagrams similar to Fig. 4.6.

Table 9.2

Regression Equations for Thrust and Torque Coefficients of
4-Bladed Propellers

$$\begin{aligned}
 K_T = & 0.446 - 0.3130 J + 0.3447 \frac{P}{D} - 0.0315 J \frac{P}{D} + 0.0495 \left(\frac{P}{D} \right)^2 \\
 & - 0.0100 J \left(\frac{P}{D} \right)^2 - 0.3844 \frac{A_E}{A_O} + 0.2823 J \frac{A_E}{A_O} + 0.8590 \frac{P}{D} \frac{A_E}{A_O} \\
 & - 0.9800 J \frac{P}{D} \frac{A_E}{A_O} - 0.3533 \left(\frac{P}{D} \right)^2 \frac{A_E}{A_O} + 0.5000 J \left(\frac{P}{D} \right)^2 \frac{A_E}{A_O} \\
 10K_Q = & 0.0391 + 0.1664 J - 0.0881 \frac{P}{D} - 0.6128 J \frac{P}{D} + 0.6817 \left(\frac{P}{D} \right)^2 \\
 & + 0.0050 J \left(\frac{P}{D} \right)^2 - 0.1092 \frac{A_E}{A_O} + 0.1533 J \frac{A_E}{A_O} + 0.1352 \frac{P}{D} \frac{A_E}{A_O} \\
 & - 0.6667 J \frac{P}{D} \frac{A_E}{A_O} + 0.2183 \left(\frac{P}{D} \right)^2 \frac{A_E}{A_O} + 0.1333 J \left(\frac{P}{D} \right)^2 \frac{A_E}{A_O}
 \end{aligned}$$

optimum propeller rpm, the corresponding brake power and the pitch ratio of the propeller.

(a) Solution using Optimum Efficiency Line data, Table 9.1

$$V = 16 \text{ knots} = 8.2304 \text{ m s}^{-1} \quad P_E = 3388 \text{ kW}$$

$$D = 5.5 \text{ m} \quad w = 0.200 \quad t = 0.150 \quad \eta_R = 1.050 \quad \eta_S = 0.970 \quad \frac{A_E}{A_O} = 0.550$$

$$V_A = (1 - w) V = (1 - 0.200) \times 8.2304 = 6.5843 \text{ m s}^{-1}$$

$$J = \frac{V_A}{n D} = \frac{6.5843}{n \times 5.5} \quad \text{or} \quad n = \frac{1.19715}{J} \text{ s}^{-1}$$

$$\eta_H = \frac{1-t}{1-w} = \frac{1-0.150}{1-0.200} = 1.0625$$

$$P_D = 2\pi \rho n^3 D^5 K_Q / \eta_R = 2\pi \times 1.025 \times n^3 \times 5.5^5 K_Q / 1.050 \text{ kW}$$

$$= 30869 n^3 K_Q \text{ kW}$$

$$P_D \eta_O \eta_H \eta_R = P_D \eta_O \times 1.0625 \times 1.050 = 1.11562 P_D \eta_O$$

From Optimum η_O line for $A_E/A_O = 0.55$							
$\left(\frac{K_Q}{J^5}\right)^{\frac{1}{4}}$	J	$\frac{P}{D}$	η_O	$10 K_Q$	n s^{-1}	P_D kW	$P_D \eta_O \eta_R \eta_H$ kW
0.5000	0.8625	1.1000	0.7084	0.2983	1.3880	2462	1946
0.5500	0.7838	1.0141	0.6886	0.2707	1.5274	2977	2287
0.6000	0.7180	0.9445	0.6720	0.2473	1.6673	3538	2653
0.6500	0.6671	0.8979	0.6562	0.2358	1.7946	4207	3080
0.7000	0.6249	0.8625	0.6407	0.2288	1.9157	4966	3549
0.7500	0.5889	0.8343	0.6254	0.2241	2.0329	5812	4055

[K_Q from $(K_Q/J^5)^{\frac{1}{4}}$ and J]

At $P_D \eta_O \eta_R \eta_H = P_E = 3388 \text{ kW}$, by linear interpolation:

$$n = 1.8741 s^{-1} = 112.4 \text{ rpm}$$

$$P_D = 4705 \text{ kW} \quad P_B = \frac{P_D}{\eta_S} = \frac{4705}{0.970} = 4851 \text{ kW}$$

$$\frac{P}{D} = 0.8747$$

(b) Solution using Regression Equations, Table 9.2

$\frac{A_E}{A_O} = 0.55$ Hence, substituting this value in the equations in Table 9.2:

$$K_T = -0.1668 - 0.1577 J + 0.8172 \frac{P}{D} - 0.5705 J \frac{P}{D} - 0.1448 \left(\frac{P}{D}\right)^2$$

$$+ 0.2650 J \left(\frac{P}{D}\right)^2$$

$$10K_Q = -0.0210 + 0.2507 J - 0.0137 \frac{P}{D} - 0.9795 J \frac{P}{D} + 0.8018 \left(\frac{P}{D} \right)^2$$

$$+ 0.0783 J \left(\frac{P}{D} \right)^2$$

$$\frac{K_T}{J^2} = \frac{T}{\rho n^2 D^4} \frac{n^2 D^2}{V_A^2} = \frac{\frac{R}{1-t}}{\rho D^2 (1-w)^2 V^2} = \frac{1}{\rho D^2 (1-t)(1-w)^2} \frac{P_E}{V^3}$$

$$= \frac{1}{1.025 \times 5.5^2 \times (1-0.150)(1-0.200)^2} \frac{3388}{8.2304^3} = 0.3603$$

The pitch ratio has to be determined that will give the highest efficiency at this value of K_T/J^2 . One may proceed as follows:

$$\frac{P}{D} = 0.8 \quad : \quad K_T = 0.39429 - 0.44450 J$$

$$10K_Q = 0.48119 - 0.48279 J$$

$$\frac{K_T}{J^2} = 0.39429 \left(\frac{1}{J} \right)^2 - 0.44450 \frac{1}{J} = 0.3603$$

$$\frac{1}{J} = 1.67341 \quad J = 0.59758$$

$$K_T = 0.12867 \quad 10K_Q = 0.19268$$

$$\eta_O = \frac{K_T J}{K_Q 2\pi} = \frac{0.12867}{0.019268} \times \frac{0.59758}{2\pi} = 0.63512$$

Proceeding similarly for other pitch ratios until the values of efficiency converge to the optimum, one obtains:

$\frac{P}{D}$	J	K_T	$10K_Q$	η_O
0.8000	0.59758	0.12867	0.19268	0.63512
0.9000	0.65263	0.15346	0.24581	0.64846
1.0000	0.70496	0.17906	0.30852	0.65118
0.9500	0.67906	0.16615	0.27595	0.65073
0.9750	0.69207	0.17257	0.29193	0.65111
0.9875	0.69853	0.17581	0.30015	0.65118
0.9938	0.70177	0.17744	0.30435	0.65118
0.9906	0.70015	0.17662	0.30225	0.65118

$$n = \frac{V_A}{J D} = \frac{6.5843}{0.70015 \times 5.5} = 1.7098 \text{ s}^{-1} = 102.6 \text{ rpm}$$

$$P_D = \frac{P_E}{\eta_O \eta_R \eta_H} = \frac{3388}{0.65118 \times 1.050 \times 1.0625} = 4663 \text{ kW}$$

$$P_B = \frac{P_D}{\eta_S} = \frac{4663}{0.970} = 4808 \text{ kW}$$

$$\frac{P}{D} = 0.9906$$

The differences between the answers obtained by the two methods arise because of the difference between the definitions of the optimum efficiency in the two cases: in the method using the data of Table 9.1, the optimum efficiency is calculated for constant values of K_Q/J^5 , whereas in using the regression equations, the optimum efficiency is calculated for a constant value of K_T/J^2 . The latter is theoretically more correct for this type of problem, but most methodical series design charts give only the optimum efficiency line for K_Q/J^5 (or B_P) constant. The error at least so far as power is concerned is small, and since the object in this problem is to obtain an estimate of the power for selecting the propulsion plant, this error is usually acceptable.

Example 2

The effective powers (naked hull) at different speeds of a single-screw ship are as follows:

V knots:	10.0	11.0	12.0	13.0	14.0	15.0	16.0	17.0
P_{En} kW:	544.5	760.8	1031.2	1364.9	1769.2	2252.2	2823.3	3490.7

A service allowance of 20 percent must be added. The propulsion factors based on thrust identity are:

$$w = 0.200 \quad t = 0.150 \quad \eta_R = 1.050$$

The main engine of the ship has a brake power of 5000 kW at 126 rpm, and is directly connected to the propeller, the shafting efficiency being 0.970. The depth of immersion of the propeller axis is 3.5 m. Based on vibration considerations, the propeller is to have four blades. The Burrill cavitation criterion for merchant ship

propellers is to be used for determining blade area. The propeller is to belong to the methodical series for which the data are given in Tables 9.1 and 9.2. Design the propeller.

(a) Solution based on Optimum Efficiency Line data, Table 9.1

V knots	:	10.0	11.0	12.0	13.0	14.0	15.0	16.0	17.0
$P_E = 1.2 P_{En}$ kW:		653.4	913.0	1237.4	1637.9	2123.0	2702.6	3388.0	4188.8

$$w = 0.200 \quad t = 0.150 \quad \eta_R = 1.050 \quad \text{thrust identity}$$

$$P_B = 5000 \text{ kW} \quad n = 126 \text{ rpm} = 2.1000 \text{ s}^{-1} \quad \eta_S = 0.970$$

$$h = 3.5 \text{ m} \quad Z = 4$$

Optimum diameter and pitch ratio:

$$P_D = P_B \eta_S = 5000 \times 0.970 = 4850 \text{ kW}$$

$$\eta_H = \frac{1-t}{1-w} = \frac{1-0.150}{1-0.200} = 1.0625$$

$$J = \frac{V_A}{nD} = \frac{V_A}{2.1D} \quad \text{or } D = \frac{V_A}{2.1J} \text{ m}$$

$$V = \frac{V_A}{1-w} = \frac{V_A}{1-0.200} = 1.2500 V_A \text{ ms}^{-1} = 2.4300 V_A \text{ knots}$$

$$K_Q = \frac{Q_O}{\rho n^2 D^5} = \frac{\frac{P_D \eta_R}{2\pi n}}{\rho n^2 D^5} = \frac{P_D \eta_R}{2\pi \rho n^3 D^5}$$

$$\frac{K_Q}{J^5} = \frac{P_D \eta_R}{2\pi \rho n^3 D^5} \frac{n^5 D^5}{V_A^5} = \frac{n^2 P_D \eta_R}{2\pi \rho V_A^5}$$

$$V_A^5 = \frac{n^2 P_D \eta_R}{2\pi \rho} \frac{1}{\frac{K_Q}{J^5}} = \frac{n^2 P_D \eta_R}{2\pi \rho} \frac{1}{\left[(K_Q/J^5)^{\frac{1}{4}}\right]^4}$$

$$V_A = \left[\frac{n^2 P_D \eta_R}{2\pi \rho}\right]^{\frac{1}{5}} \left[(K_Q/J^5)^{\frac{1}{4}}\right]^{-\frac{4}{5}} = \left[\frac{2.1^2 \times 4850 \times 1.050}{2\pi \times 1.025}\right]^{\frac{1}{5}} \left[(K_Q/J^5)^{\frac{1}{4}}\right]^{-\frac{4}{5}}$$

$$= 5.11085 \left[(K_Q/J^5)^{\frac{1}{4}}\right]^{-\frac{4}{5}}$$

$$P_D \eta_O \eta_R \eta_H = 4850 \times \eta_O \times 1.050 \times 1.0625 = 5410.78 \eta_O \text{ kW}$$

From Optimum Efficiency Line for $A_E/A_O = 0.40$						
$\left(\frac{K_Q}{J^5}\right)^{\frac{1}{4}}$	J	$\frac{P}{D}$	η_O	V_A ms^{-1}	V k	$P_D \eta_O \eta_R \eta_H$ kW
0.6500	0.6647	0.8840	0.6607	7.2138	17.5296	3574.9
0.7000	0.6220	0.8482	0.6453	6.7985	16.5204	3491.6
0.7500	0.5854	0.8184	0.6303	6.4335	15.6333	3410.4
0.8000	0.5533	0.7930	0.6156	6.1097	14.8466	3330.9
0.7237	0.6041	0.8336	0.6379	6.6195	16.0855	3451.8 = P_E

$$D = \frac{6.6195}{2.1 \times 0.6041} = 5.2179 \text{ m}$$

From Optimum Efficiency Line for $A_E/A_O = 0.55$						
$\left(\frac{K_Q}{J^5}\right)^{\frac{1}{4}}$	J	$\frac{P}{D}$	η_O	V_A ms^{-1}	V k	$P_D \eta_O \eta_R \eta_H$ kW
0.6500	0.6671	0.8979	0.6562	7.2138	17.5296	3550.6
0.7000	0.6249	0.8625	0.6407	6.7985	16.5204	3466.7
0.7500	0.5889	0.8343	0.6254	6.4335	15.6333	3383.9
0.8000	0.5574	0.8104	0.6104	6.1097	14.8466	3302.7
0.7259	0.6057	0.8474	0.6325	6.6034	16.0463	3422.4 = P_E

$$D = \frac{6.6034}{2.1 \times 0.6057} = 5.1915 \text{ m}$$

From Optimum Efficiency Line for $A_E/A_O = 0.70$						
$\left(\frac{K_Q}{J^5}\right)^{\frac{1}{4}}$	J	$\frac{P}{D}$	η_O	V_A ms^{-1}	V k	$P_D \eta_O \eta_R \eta_H$ kW
0.6500	0.6690	0.9091	0.6519	7.2138	17.5296	3527.3
0.7000	0.6276	0.8753	0.6362	6.7985	16.5204	3442.3

$\left(\frac{K_Q}{J^5}\right)^{\frac{1}{4}}$	From Optimum Efficiency Line for $A_E/A_O = 0.70$					
	J	$\frac{P}{D}$	η_O	V_A ms^{-1}	V k	$P_D \eta_O \eta_R \eta_H$ kW
0.7500	0.5922	0.8483	0.6208	6.4335	15.6333	3359.0
0.8000	0.5613	0.8260	0.6057	6.1097	14.8466	3277.3
0.7285	0.6072	0.8597	0.6273	6.5878	16.0084	3394.2 = P_E

$$D = \frac{6.5878}{2.1 \times 0.6072} = 5.1664 \text{ m}$$

Cavitation:

$$V_{0.7R}^2 = V_A^2 + (0.7\pi n D)^2 = V_A^2 + 21.3272 D^2 \text{ m}^2 \text{ s}^{-2}$$

$$\begin{aligned} \sigma_{0.7R} &= \frac{p_A + \rho gh - p_v}{\frac{1}{2} \rho V_{0.7R}^2} = \frac{101.325 + 1.025 \times 9.81 \times 3.5 - 1.704}{\frac{1}{2} \times 1.025 V_{0.7R}^2} \\ &= \frac{263.0505}{V_{0.7R}^2} \end{aligned}$$

$$\tau_c = 0.0321 + 0.3886 \sigma_{0.7R}^2 - 0.1984 \sigma_{0.7R}^3 + 0.0501 \sigma_{0.7R}^3$$

(Burrill cavitation criterion for merchant ship propellers.)

$$R_T = \frac{P_E}{V} \quad T = \frac{R_T}{1-t} = \frac{R_T}{1-0.150}$$

$$\frac{T}{A_P} = \frac{1}{2} \rho V_{0.7R}^2 \tau_c = \frac{1}{2} \times 1.025 V_{0.7R}^2 \tau_c = 0.5125 V_{0.7R}^2 \tau_c$$

$$A'_E = \frac{A_P}{1.067 - 0.229 P/D} \quad (\text{Blade area required})$$

$$A_O = \frac{\pi}{4} D^2$$

The values of the various parameters for the different values of A_E/A_O are put down in the following table and used to find the required value of A'_E/A_O , by interpolation.

$\frac{A_E}{A_O}$:	0.40	0.55	0.70	0.5019
D m	:	5.2179	5.1915	5.1664	5.2000
$\frac{P}{D}$:	0.8336	0.8474	0.8597	0.8430
V_A m s ⁻¹	:	6.6195	6.6034	6.5878	6.6086
V k	:	16.0855	16.0463	16.0084	16.0589
P_E kW	:	3451.2	3422.4	3394.2	3431.6
R_T kN	:	417.09	414.62	412.18	415.41
T kN	:	490.70	487.79	484.92	488.72
$V_{0.7R}^2$ m ² s ⁻²	:	624.48	618.41	612.66	620.36
$\sigma_{0.7R}$:	0.4212	0.4253	0.4294	0.4240
τ_c	:	0.1643	0.1653	0.1663	0.1650
$\frac{T}{A_P}$ kN m ⁻²	:	52.5912	52.4018	52.2310	52.4648
A_P m ²	:	9.3305	9.3087	9.2841	9.3152
A'_E m ²	:	10.6500	10.6636	10.6698	10.6587
A_O m ²	:	21.3836	21.1678	20.9636	21.2372
$\frac{A'_E}{A_O}$:	0.4980	0.5038	0.5090	0.5019 = $\frac{A_E}{A_O}$

The values at which A_E/A_O (first row in this table) and A'_E/A_O (last row) are equal are obtained by interpolation.

The particulars of the design propeller are therefore as follows:

$$D = 5.200 \text{ m} \quad \frac{P}{D} = 0.8430 \quad \frac{A_E}{A_O} = 0.5019 \quad V = 16.059 \text{ k}$$

The blade thickness fraction and the boss diameter ratio, which are fixed for a given methodical series of propellers, must be checked to complete the propeller design, and a propeller drawing prepared. It is also desirable to carry out performance estimates, i.e. to determine the variation of brake power and propeller rpm with speed for various ship operating conditions, as shown in Example 3.

(b) Solution based on Regression Equations, Table 9.2

The design of a propeller using regression equations for K_T and K_Q involves far too much calculation to be carried out by hand, even with the simplified equations of Table 9.2. A computer program for propeller design is more or less essential, and several propeller design programs are available. Different programs may approach the propeller design problem in different ways. A typical approach, summarised in Table 9.3, consists in determining the values of propeller diameter D , blade area ratio A_E/A_O , pitch ratio P/D and advance coefficient J by a process of systematic trial-and-error such that the highest speed V is obtained subject to the conditions: (a) the propeller thrust T is in balance with the total resistance R_T at that speed, (b) the delivered power P_D required by the propeller is equal to that delivered by the engine, and (c) the specified cavitation criterion (e.g. the Burrill criterion) is satisfied.

A computer program based on this approach produces virtually the same result as that obtained by using the optimum efficiency line data:

$$D = 5.194 \text{ m} \quad \frac{P}{D} = 0.8437 \quad \frac{A_E}{A_O} = 0.5030 \quad V = 16.052 \text{ k}$$

the small differences being due to round-off errors.

Table 9.3

Outline of Propeller Design Program

Start with the given input data

Choose a value of D

Choose a value of A_E/A_O

Choose a value of P/D

Choose a value of J

Calculate K_T and K_Q from equations

Determine V for this value of J

Calculate T from K_T and R_T from P_E/V

Adjust the value of J until $T = (1 - t)R_T$

From K_Q determine P_D

Adjust the value of P/D until $P_D = P_B \eta_S$

Adjust the value of A_E/A_O until the cavitation criterion is satisfied

Adjust the value of D until the highest speed is obtained.

The propeller design parameters obtained by procedures similar to that used in the foregoing example are really optimum only for uniform flow. The flow behind a ship, particularly a single screw ship, is far from uniform. Some designers therefore recommend that the optimum propeller diameter determined by such procedures be reduced by a small amount (2-5 per cent) for single screw ships with a consequent change in the other design parameters, viz. pitch ratio and blade area ratio. Since the mean circumferential wake at any radius is greater at the inner radii in a single screw ship, a reduction in the propeller diameter results in an increase in the average wake fraction w and in the hull efficiency η_H so that the propulsive efficiency $\eta_D = \eta_O \eta_R \eta_H$ increases even if there is a small decrease in the open water efficiency η_O . If the variation in the propulsion factors w , t and η_R with propeller diameter can be determined, it is possible to incorporate this variation in a propeller design program to determine the exact optimum design parameters instead of making a somewhat arbitrary reduction in the propeller diameter determined from the methodical series open water data.

Example 3

Estimate the performance characteristics of a ship in a lightly loaded trial condition given the following data:

Effective Power (naked hull):

V knots:	10.0	11.0	12.0	13.0	14.0	15.0	16.0	17.0	18.0
P_{En} kW:	419	574	765	996	1272	1597	1976	2414	2915

Trial allowance: 10 percent

Propulsion Factors (thrust identity):

$$w = 0.180 \quad t = 0.160 \quad \eta_R = 1.060$$

Propeller:

$$Z = 4 \quad D = 5.200 \text{ m} \quad P/D = 0.8430 \quad A_E/A_O = 0.5020$$

Open water characteristics from Table 9.2

Engine:

Brake power = 5000 kW rpm = 126 Shafting efficiency = 0.970

Engine directly connected to the propeller.

From Table 9.2, for $\frac{P}{D} = 0.8430$ $\frac{A_E}{A_O} = 0.5020$

$$K_T = 0.4149 - 0.4413 J$$

$$10K_Q = 0.5296 - 0.5043 J$$

$$\begin{aligned} \frac{K_T}{J^2} &= \frac{T}{\rho n^2 D^4} \frac{n^2 D^2}{V_A^2} = \frac{\frac{R_T}{1-t}}{\rho D^2 (1-w)^2 V^2} = \frac{1}{\rho D^2 (1-t)(1-w)^2 V^3} P_E \\ &= \frac{1}{1.025 \times 5.200^2 \times (1-0.160)(1-0.180)^2 V^3} P_E = \frac{1}{15.6544 V^3} P_E \end{aligned}$$

$$\text{Also, } \frac{K_T}{J^2} = \frac{0.4149}{J^2} - \frac{0.4413}{J}$$

$$\begin{aligned} \text{so that } \frac{1}{J} &= \frac{0.4413 + \sqrt{(0.4413)^2 + 4 \times 0.4149 \times \frac{K_T}{J^2}}}{2 \times 0.4149} \\ &= 0.5318 + \left[0.282827 + \frac{K_T/J^2}{0.4149} \right]^{0.5} \end{aligned}$$

from which J can be determined, and hence K_T , K_Q and η_O using the equations for K_T and K_Q .

Then:

$$n = \frac{V_A}{J D} = \frac{(1-w)V}{J D} = \frac{(1-0.180)V}{J \times 5.200} = 0.157692 \frac{V}{J} \text{ s}^{-1}$$

$$\begin{aligned} P_D &= \frac{2\pi \rho n^3 D^5 K_Q}{\eta_R} = \frac{2\pi \times 1.025 \times n^3 \times 5.200^5 K_Q}{1.060} \\ &= 23100 n^3 K_Q \text{ kW} \end{aligned}$$

$$\eta_H = \frac{1-t}{1-w} = \frac{1-0.160}{1-0.180} = 1.0244$$

Alternatively,

$$P_D = \frac{P_E}{\eta_O \eta_R \eta_H} = \frac{P_E}{\eta_O \times 1.060 \times 1.0244} = \frac{1}{1.0859} \frac{P_E}{\eta_O}$$

$$P_B = \frac{P_D}{\eta_S} = \frac{P_D}{0.970}$$

The calculations of power and rpm at different speeds can then be carried out as shown in the following table (p. 237).

In this condition, at the rated propeller rpm of 126, the ship is estimated to have a speed of 17.49 k with the engine developing a brake power of 4166 kW, i.e. about 80 percent of its normal rating. This type of information is often useful during the acceptance trials of a ship.

9.4 Design of Towing Duty Propellers

The design of propellers for tugs, towboats and trawlers is somewhat more complex than that of free running propellers because towing duty propellers are usually required to perform efficiently in more than one operating condition. A tug propeller, for example, may be required to produce a high static pull when the tug is attached to a bollard as well as to have a high speed when running free. The bollard pull condition and the free running condition represent the two extreme conditions of operation of a propeller in practice. A towing duty propeller may also be designed for maximum efficiency when towing at some intermediate speed between zero speed (static condition) and the free running (maximum) speed.

Most tugs and trawlers today have propellers driven by diesel engines through reduction gearing with reversing arrangements. A diesel engine has the characteristic that the maximum torque that it can produce is nearly constant over a wide range of rpm, so that the maximum power available from the engine varies almost linearly with rpm. A fixed pitch propeller, on the other hand, can absorb a given power at a given rpm only at a fixed speed of advance: the higher the speed the lower the power at a given rpm. A propeller designed to absorb the full power available from the engine at a particular speed of advance will therefore tend to overload the engine at lower speeds unless the rpm is reduced, while at higher speeds the engine will tend to run at higher rpms than its rated value unless the fuel supply is decreased because the power available from the engine is more than that absorbed by the propeller.

Various methods are available to overcome this problem. A multi-speed gearbox can be fitted between the engine and the propeller, so that low propeller rpm : engine rpm ratios can be used at low speeds and higher values at

Calculation of Performance Characteristics (Example 3)

	V	$P_E = 1.1P_{En}$	$\frac{K_T}{J^2}$	J	K_T	$10K_Q$	η_O	n		P_D	P_B
k	ms^{-1}	kW						s^{-1}	rpm	kW	kW
10.0	5.1440	460.9	0.2163	0.7000	0.1060	0.1766	0.6687	1.1588	69.53	634.8	654.4
11.0	5.6584	631.4	0.2226	0.6959	0.1078	0.1787	0.6681	1.2822	76.93	870.2	897.1
12.0	6.1728	841.5	0.2285	0.6921	0.1095	0.1806	0.6679	1.4064	84.39	1160.5	1196.4
13.0	6.6972	1095.6	0.2340	0.6887	0.1110	0.1823	0.6674	1.5312	91.87	1511.8	1558.6
14.0	7.2016	1399.2	0.2393	0.6854	0.1124	0.1840	0.6669	1.6569	99.41	1933.4	1993.2
15.0	7.7160	1756.7	0.2443	0.6824	0.1138	0.1855	0.6663	1.7830	106.98	2428.9	2504.0
16.0	8.2304	2173.6	0.2490	0.6796	0.1150	0.1869	0.6655	1.9097	114.59	3006.9	3099.9
17.0	8.7448	2655.4	0.2537	0.6768	0.1162	0.1883	0.6647	2.0375	122.25	3675.2	3793.0
18.0	9.2592	3206.5	0.2580	0.6743	0.1173	0.1896	0.6639	2.1654	129.92	4447.0	4584.5
17.489	8.9963	2915.8	0.2558	0.6756	0.1167	0.1889	0.6642	2.1000	126.00	4041.1	4166.1

higher speeds. A diesel electric drive can be used instead of a geared diesel drive, the motor rpm being controlled to suit the operating conditions. Instead of using a fixed pitch propeller, a controllable pitch propeller may be used so that the pitch can be changed with changing speed. Controllable pitch propellers are discussed later (Chapter 12). However, these solutions to the problem of matching engine and propeller characteristics have their own disadvantages such as higher cost or lower efficiency, and most tugs and trawlers have diesel engines driving fixed pitch propellers through single speed reduction gearing. Sometimes, propellers in nozzles are used. The design of towing duty propellers therefore usually demands a compromise between the conflicting requirements of the static and the free running conditions.

Towing duty propellers are designed using methodical series data. Three- or four-bladed propellers with aerofoil type blade sections (e.g. B-Series propellers) are normally used, although propellers with segmental sections (Gawn Series) are also used sometimes.

The blade area ratio is determined from considerations of cavitation. The Burrill cavitation criterion for tug and trawler propellers may be used for this purpose. Alternatively, one may use the following empirical formula:

$$\frac{A_E}{A_O} = K \frac{P_D}{n D^3 [p_A + \rho g(h - 0.8R) - p_V]} \quad (9.2)$$

where:

$$\begin{aligned} K &= 4.50 \text{ for open propellers} \\ &= 3.22 \text{ for propellers in nozzles} \end{aligned}$$

Once the number of blades and the blade area ratio have been selected, the thrust and torque coefficients become functions of only the pitch ratio and the advance coefficient for a particular methodical series. In addition to these coefficients, one also requires data on the propulsion factors, which may be obtained from empirical formulas or from the data of similar vessels. The wake fraction, thrust deduction fraction and relative rotative efficiency vary in a somewhat complex manner with speed in a tug or trawler, but for design purposes, it is usual to assume that the wake fraction and relative rotative efficiency are constant while the thrust deduction fraction varies

linearly with speed from its value in the static condition (0.03–0.05 for open propellers and up to 0.12 for propellers in nozzles), to the value in the free running condition.

Design problems of propellers for tugs and trawlers may be divided into three types:

- (i) The determination of the optimum propeller rpm and the corresponding delivered power to achieve both a specified bollard pull and a specified free running speed.
- (ii) The design of a propeller for a given propulsion plant.
- (iii) The estimation of the performance characteristics of a vessel with a given propeller and propulsion plant.

The data required for a type (i) problem are the open water characteristics of the selected propeller series (K_T and K_Q as functions of J and P/D), the propulsion factors (w , t and η_R) in both the static and the free running conditions, the required bollard pull BP , the required free running speed V_1 and the corresponding effective power P_{E1} . The propeller diameter D should be the maximum that can be accommodated in the propeller aperture keeping adequate clearances. The calculations are based on the assumption that in the bollard pull condition the torque is the maximum available from the engine with the propeller rpm being reduced, whereas in the free running condition the torque is less than the maximum available with the propeller running at its full rpm. The procedure for determining the optimum propeller rpm and the corresponding delivered power is illustrated by the following example.

Example 4

The maximum propeller diameter that can be accommodated in the aperture of a single screw tug is 3.10 m. The required blade area ratio (expanded) is estimated to be 0.500. The tug is required to have a bollard pull of 15 tonnes and a free running speed of 12 knots. In the bollard pull condition, the thrust deduction fraction is 0.050, and in the free running condition at 12 knots, the effective power is 285 kW, the wake fraction being 0.200 and the thrust deduction fraction 0.180. The relative rotative efficiency may be taken as 1.000. Determine the optimum propeller rpm and the corresponding delivered power. Use the open water data of Table 4.3.

$$D = 3.10 \text{ m} \quad \text{Bollard pull, } BP = 15 \text{ tonnes} = 15 \times 9.81 = 147.15 \text{ kN}$$

$$\text{Free running speed, } V_1 = 12 \text{ k} = 6.1728 \text{ m s}^{-1} \quad P_{E1} = 285 \text{ kW}$$

$$w_1 = 0.200 \quad t_1 = 0.180 \quad \eta_R = 1.000 \quad t_0 = 0.050$$

At the free running speed (subscript 1):

$$\begin{aligned} \frac{K_{T1}}{J_1^2} &= \frac{1}{\rho D^2 (1 - t_1) (1 - w)^2} \frac{P_{E1}}{V_1^3} \\ &= \frac{1}{1.025 \times 3.10^2 \times (1 - 0.180) (1 - 0.200)^2} \times \frac{285}{6.1728^3} \\ &= 0.23440 \end{aligned}$$

$$J_1 = \frac{V_{A1}}{n_1 D} = \frac{(1 - w) V_1}{n_1 D} = \frac{(1 - 0.200) \times 6.1728}{n_1 \times 3.10} = \frac{1.59298}{n_1}$$

The propeller revolution rate n_1 in the free running condition is obtained for different pitch ratios by finding the values of J at which $K_T/J^2 = 0.23440$. This may be done by finding the intersections of the $K_T - J$ lines for different pitch ratios with the curve $K_T = 0.23440 J^2$.

$\frac{P}{D}$:	0.5	0.6	0.7	0.8	0.9	1.0	1.1	1.2
J	:	0.4618	0.5287	0.5928	0.6554	0.7171	0.7781	0.8390	0.8973
K_T	:	0.0500	0.0655	0.0824	0.1007	0.1205	0.1419	0.1650	0.1887
$n_1 \text{ s}^{-1}$:	3.4492	3.0130	2.6872	2.4305	2.2214	2.0473	1.8987	1.7753

In the bollard pull condition (subscript 0), the bollard pull and the propeller torque are given by:

$$BP = (1 - t_0) \rho n_0^2 D^4 K_{T0}$$

$$Q_0 = \frac{\rho n_0^2 D^5 K_{Q0}}{\eta_R}$$

where K_{T0} and K_{Q0} are the values at $J = 0$. Then:

$$BP = (1 - 0.050) \times 1.025 \times n_0^2 \times 3.10^4 K_{T0} = 147.15 \text{ kN}$$

so that

$$n_0^2 = \frac{1.63631}{K_{T0}}$$

$$Q_0 = 1.025 \times n_0^2 \times 3.10^5 \frac{K_{Q0}}{1.000} = 293.4488 K_{Q0} \text{ kN m}$$

This is the maximum torque required by the propeller. The maximum revolutions are given by n_1 . Therefore, the engine must be capable of producing a delivered power $P_{D\max}$ at n_1 revolutions per sec where:

$$P_{D\max} = 2\pi n_1 Q_0$$

The calculations for different pitch ratios are set out in the following table:

$\frac{P}{D}$	K_{T0}	$10K_{Q0}$	n_0^2	n_0 s^{-1}	Q_0 kN m	n_1 s^{-1}	$P_{D\max}$ kW
0.5	0.2044	0.1826	8.0054	2.8294	42.896	3.4492	929.6
0.6	0.2517	0.2455	6.5010	2.5497	46.834	3.0130	886.6
0.7	0.2974	0.3187	5.5021	2.3456	51.457	2.6872	868.8
0.8	0.3415	0.4021	4.7915	2.1890	56.538	2.4305	863.4
0.9	0.3840	0.4956	4.2612	2.0643	61.972	2.2214	865.0
1.0	0.4250	0.5994	3.8501	1.9622	67.721	2.0473	871.1
1.1	0.4644	0.7133	3.5235	1.8771	73.753	1.8987	879.9
1.2	0.5022	0.8374	3.2583	1.8051	80.068	1.7753*	893.1*

* Note that at $P/D = 1.2$ and above, n_1 is less than n_0 . This violates the assumption that the torque is maximum in the bollard pull condition while the propeller revolution rate is maximum in the free running condition.

The optimum value of pitch ratio is that at which $P_{D\max}$ has the lowest value:

$$\frac{P}{D} = 0.827 \quad n_0 = 2.1524 s^{-1} \quad Q_0 = 57.969 \text{ kN m}$$

$$P_{D\max} = 863.1 \text{ kW} \quad n_1 = 2.3696 s^{-1} = 142.2 \text{ rpm}$$

A tug or trawler propeller may be designed to absorb the full power available from the propulsion plant in the bollard pull condition, or in the free

running condition, or at a given speed for towing. The propeller can also be designed to produce a combination of high bollard pull and a high free running speed.

If the propeller is to be designed for absorbing the full power in the bollard pull condition, and it is possible to select the optimum propeller revolution rate through a proper choice of the gear ratio between engine and propeller, the propeller diameter can be made the largest practicable. Then, the bollard pull is given by:

$$BP = (1 - t_0) \left(\frac{\rho}{4\pi^2} \right)^{\frac{1}{3}} \frac{K_{T0}}{K_{Q0}^{2/3}} (\eta_R P_{D0} D) \quad (9.3)$$

in which all the quantities except K_{T0} and K_{Q0} are known and thrust identity is assumed. The maximum bollard pull is obtained by choosing the pitch ratio for which $K_{T0}/K_{Q0}^{2/3}$ is maximum, and the propeller revolution rate is then given by:

$$n_0^3 = \frac{P_{D0} \eta_R}{2\pi \rho D^5 K_{Q0}} \quad (9.4)$$

Usually however, the power and revolutions must be regarded as fixed, i.e. a given engine and gearbox. In that case:

$$BP = (1 - t_0) \left(\frac{\rho}{16\pi^4} \right)^{\frac{1}{5}} \frac{K_{T0}}{K_{Q0}^{4/5}} \left(\frac{\eta_R P_{D0}}{\sqrt{n_0}} \right)^{\frac{4}{5}} \quad (9.5)$$

and the pitch ratio must be selected to make $K_{T0}/K_{Q0}^{4/5}$ maximum, the propeller diameter being given by:

$$D^5 = \frac{P_{D0} \eta_R}{2\pi \rho n_0^3 K_{Q0}} \quad (9.6)$$

If the propeller revolution rate n_0 is too low, the diameter obtained may be greater than the maximum that can be fitted to the vessel with adequate clearances.

An advantage of designing propellers for the bollard pull condition is that there is little risk of overloading the engine. However, at all forward speeds

the torque will be less than the maximum available from the engine, and the penalty in free running speed may be considerable. Another disadvantage is that propellers designed for the bollard pull condition, i.e. for $K_{T0}/K_{Q0}^{2/3}$ or $K_{T0}/K_{Q0}^{4/5}$ maximum, usually have low pitch ratios so that when the vessel is running free, the blade sections at the outer radii may have negative angles of attack over a part of the revolution, and this may give rise to face cavitation and blade vibration.

If a tug or trawler propeller is to be designed for the free running condition, the propeller must be designed for the maximum efficiency at K_Q/J^5 constant at the speed for which:

$$P_{D1} \eta_O \eta_R \eta_H = P_{E1} \quad (9.7)$$

The procedure has been described in Section 9.3 (Example 2). Designing a tug or trawler propeller for the free running condition has the disadvantage of very low bollard pull since the propeller revolution rate has to be greatly reduced to keep the torque within permissible limits. There is, thus, also a danger of overloading the engine (exceeding the permissible torque) if the propeller revolutions are not reduced suitably during towing or trawling.

If the propeller is to be designed for a specific towing speed, the diameter and pitch ratio must be chosen for the maximum efficiency for K_Q/J^5 constant at that speed. The available towrope power is then given by:

$$P_{Tow} = P_D \eta_O \eta_R \eta_H - P_E \quad (9.8)$$

A tug or trawler propeller may also be designed to give the optimum compromise between high bollard pull and high free running speed, since an increase in the one is associated with a decrease in the other. The design data required include the engine power, rpm, gear ratio and shafting efficiency so that the maximum delivered power P_{Dmax} and the maximum propeller revolution rate n_1 are known. The propeller diameter D is taken to be the highest practicable when n_1 is equal to or less than the optimum determined as illustrated in Example 4; otherwise, the design calculations must be carried out for several diameters and the optimum diameter determined. The bollard pull and the free running speed are determined for different pitch ratios for a given diameter, and the pitch ratio selected to

give the optimum combination of bollard pull and free running speed. The design procedure is illustrated by the following example.

Example 5

A single screw tug is to have an engine of 900 kW brake power at 600 rpm driving the propeller through 4:1 reduction gearing, the shafting efficiency being 0.950. The wake fraction in the free running condition is 0.200, and the thrust deduction fraction may be assumed to vary linearly with speed with a value of 0.050 at zero speed and 0.180 at 12 knots. The relative rotative efficiency is 1.000. The effective power of the tug is as follows:

V knots:	0	2.0	4.0	6.0	8.0	9.0	10.0	11.0	12.0	13.0	14.0
P_E kW :	0	0.5	6.1	25.2	68.9	104.1	150.6	210.2	285.0	377.1	488.8

Design the propeller for both high bollard pull and high free running speed. Assume that the propeller diameter is 3.0 m, and its depth of immersion is 2.75 m.

$$P_B = 900 \text{ kW at } 600 \text{ rpm} \quad \text{Gear ratio} = 4:1 \quad \eta_S = 0.950$$

$$w = 0.200 \quad t_0 = 0.050 \quad t_1 = 0.180 \text{ at } V_1 = 12.0 \text{ k} \quad \eta_R = 1.000$$

$$D = 3.0 \text{ m} \quad h = 2.75 \text{ m}$$

$$P_{D\max} = P_B \eta_S = 900 \times 0.950 = 855 \text{ kW} \quad n_{\max} = \frac{600}{4} = 150 \text{ rpm} \\ = 2.5 \text{ s}^{-1}$$

$$Q_{\max} = \frac{P_{D\max}}{2\pi n_{\max}} = \frac{855}{2\pi \times 2.5} = 54.431 \text{ kN m}$$

Q_{\max} and n_{\max} are the limiting values of propeller torque and revolution rate respectively.

Preliminary estimation of blade area ratio:

$$\frac{A_E}{A_O} = 4.5 \frac{P_{D\max} \eta_R}{n_{\max} D^3 [p_A + \rho g (h - 0.8R) - p_V]} \\ = 4.5 \frac{855 \times 1.000}{2.5 \times 3.0^3 [101.325 + 1.025 \times 9.81 (2.75 - 0.8 \times 1.5) - 1.704]} \\ = 0.4948$$

One may therefore use the data of Table 4.3 since it is for a blade area ratio of 0.500. It is necessary to plot the data to obtain $K_T - J$ and $K_Q - J$ curves for different pitch ratios.

In the bollard pull condition:

$$K_{Q0} = \frac{Q_{\max} \eta_R}{\rho n_0^2 D^5} \quad (n_0 \leq n_{\max})$$

so that

$$\begin{aligned} n_0^2 &= \frac{Q_{\max} \eta_R}{K_{Q0} \rho D^5} = \frac{54.431 \times 1.000}{K_{Q0} \times 1.025 \times 3.0^5} \\ &= \frac{0.2185}{K_{Q0}} \text{ s}^{-2} \quad (n_0 \neq n_{\max}) \end{aligned}$$

$$\begin{aligned} BP &= (1 - t_0) K_{T0} \rho n_0^2 D^4 = (1 - 0.050) K_{T0} \times 1.025 \times n_0^2 \times 3.0^4 \\ &= 78.8738 K_{T0} n_0^2 \text{ kN} \end{aligned}$$

$$\begin{aligned} P_{D0} &= \frac{2\pi \rho n_0^3 D^5 K_{Q0}}{\eta_R} = \frac{2\pi \times 1.025 \times n_0^3 \times 3.0^5 K_{Q0}}{1.000} \\ &= 1564.9844 n_0^3 K_{Q0} \text{ kW} \end{aligned}$$

The calculation of the bollard pull and the corresponding revolution rate and delivered power for different pitch ratios is carried out in the following table:

$\frac{P}{D}$:	0.5	0.6	0.7	0.8	0.9	1.0
K_{T0}	:	0.2044	0.2517	0.2974	0.3415	0.3840	0.4250
$10K_{Q0}$:	0.1826	0.2455	0.3187	0.4025	0.4956	0.5994
$n_0 \text{ s}^{-1}$:	2.5000	2.5000	2.5000	2.3313	2.0999	1.9094
$BP \text{ kN}$:	100.76	124.08	146.61	146.39	133.55	122.21
$P_{D0} \text{ kW}$:	446.51	600.32	779.31	797.33	718.19	653.01

($n_0 = n_{\max}$ and $Q_0 < Q_{\max}$ for $\frac{P}{D} < 0.7386$; $n_0 < n_{\max}$ and $Q_0 = Q_{\max}$ for $\frac{P}{D} > 0.7386$.)

In the free running condition:

$$J_1 = \frac{V_{A1}}{n_1 D} = \frac{(1 - w_1) V_1}{n_1 D} = \frac{(1 - 0.200) V_1}{2.500 \times 3.000} = 0.1067 V_1$$

$$K_{T1} = \frac{T_1}{\rho n_1^2 D^4} = \frac{\frac{R_{T1}}{1 - t_1}}{\rho n_1^2 D^4} = \frac{1}{\rho n_1^2 D^4} \frac{P_{E1}}{(1 - t_1) V_1}$$

$$= \frac{1}{1.025 \times 2.500^2 \times 3.0^4} \frac{P_{E1}}{(1 - t_1) V_1} = 0.001927 \frac{P_{E1}}{(1 - t_1) V_1}$$

$$P_{D1} = \frac{2\pi \rho n_1^3 D^5 K_{Q1}}{\eta_R} = \frac{2\pi \times 1.025 \times 2.500^3 \times 3.0^5 K_{Q1}}{1.000}$$

$$= 24452.88 K_{Q1} \quad (P_{D1} \neq P_{Dmax})$$

The values of J_1 and K_{T1} are calculated for the different given speeds:

V_1 { knots	:	8.0	9.0	10.0	11.0	12.0	13.0	14.0
ms^{-1}	:	4.1152	4.6296	5.1440	5.6584	6.1728	6.6872	7.2016
P_{E1} kW	:	68.9	104.1	150.6	210.2	285.0	377.1	488.8
t_1	:	0.1367	0.1475	0.1583	0.1692	0.1800	0.1908	0.2017
J_1	:	0.4390	0.4938	0.5487	0.6036	0.6584	0.7133	0.7682
K_{T1}	:	0.0374	0.0508	0.0670	0.0862	0.1085	0.1343	0.1638

Plotting this $K_{T1} - J_1$ curve on the $K_T - J$ diagram derived from Table 4.3, one may determine the values of J , K_T and K_Q at which the $K_{T1} - J_1$ curve intersects the $K_T - J$ curves for the different pitch ratios. The calculations are carried out as follows:

$\frac{P}{D}$:	0.5	0.6	0.7	0.8	0.9	1.0
J_1	:	0.4725	0.5349	0.5931	0.6482	0.7010	0.7515
K_{T1}	:	0.0452	0.0627	0.0823	0.1041	0.1282	0.1545
$10K_{Q1}$:	0.0647	0.0901	0.1228	0.1629	0.2106	0.2667
V_1 { ms^{-1}	:	4.4297	5.0147	5.5603	6.0769	6.5718	7.0453
k	:	8.6114	9.7486	10.8093	11.8135	12.7758	13.6961
P_{D1} kW	:	158.09	220.39	300.33	398.24	514.90	652.21

Finally, one may plot the bollard pull and the free running speed as a function of the pitch ratio, and select that pitch ratio which best meets the design requirements. One could, for example, choose to maximise a function such as:

$$F = aBP + bV_1$$

where a and b represent the relative weights of the bollard pull and the free running speed. More simply, one could merely select a pitch ratio that gives an acceptable combination of bollard pull and free running speed. Thus, if one chooses a pitch ratio of 0.850, the following values are obtained:

$$\frac{P}{D} = 0.850 : \quad BP = 139.77 \text{ kN} \quad V_1 = 12.300 \text{ k}$$

$$n_0 = 2.2094 \text{ s}^{-1} = 132.6 \text{ rpm} \quad n_1 = 2.5000 \text{ s}^{-1} = 150 \text{ rpm}$$

$$P_{D0} = 755.48 \text{ kW} \quad P_{D1} = 454.19 \text{ kW}$$

To complete the design of the propeller, it is necessary to check that its strength, is adequate.

The determination of the performance characteristics of a tug or trawler propeller involves calculating the delivered power, propeller revolution rate, and the maximum towrope pull or towrope power as a function of the speed of the vessel. There is a particular speed V_m at which the propeller absorbs the maximum torque available from the engine at the maximum revolution rate, i.e. at the speed V_m , the delivered power is equal to $P_{D\max}$. Below this speed, the propeller revolution rate must be reduced to limit the torque to its maximum value. At speeds above V_m , even at the maximum propeller revolution rate, the torque and hence the delivered power remain below their maximum values. The calculations required to determine the performance characteristics of a towing duty propeller are illustrated by the following example.

Example 6

Determine the performance characteristics of the tug propeller of Example 5.

$$D = 3.0 \text{ m} \quad \frac{P}{D} = 0.850 \quad \frac{A_E}{A_O} = 0.500 \quad Z = 4$$

$$w = 0.200 \quad \eta_R = 1.000 \quad t_0 = 0.050 \quad t_1 = 0.180 \text{ at 12 knots}$$

$$P_B = 900 \text{ kW at 600 rpm} \quad \text{Gear ratio} = 4 : 1 \quad \eta_S = 0.950$$

$$P_{D\max} = P_B \eta_S = 900 \times 0.950 = 855 \text{ kW}$$

$$n_{\max} = \frac{600}{4} = 150 \text{ rpm} = 2.5 \text{ s}^{-1}$$

The open water characteristics of the propeller, interpolated from Table 4.3, are:

J	: 0	0.100	0.200	0.300	0.400	0.500	0.600	0.700	0.800	0.900
K_T	: 0.3630	0.3355	0.3048	0.2710	0.2340	0.1938	0.1504	0.1039	0.0542	0.0014
$10K_Q$: 0.4476	0.4211	0.3904	0.3553	0.3160	0.2724	0.2244	0.1722	0.1157	0.0550

At the speed V_m : $P_D = P_{D\max} = 855 \text{ kW}$

$$n = n_{\max} = 2.5 \text{ s}^{-1}$$

$$K_Q = \frac{P_D \eta_R}{2\pi \rho n^3 D^5} = \frac{855 \times 1.000}{2\pi \times 1.025 \times 2.5^3 \times 3.0^5} = 0.0350$$

For this value of K_Q , $J = 0.3151$

$$V_m = \frac{J n D}{(1-w)} = \frac{0.3151 \times 2.5 \times 3}{1-0.200} = 2.9540 \text{ m s}^{-1} = 5.7426 \text{ k}$$

At speeds below V_m , $Q = Q_{\max} = \frac{P_{D\max}}{2\pi n_{\max}}$

$$= \frac{855}{2\pi \times 2.5} = 54.4310 \text{ kN m}$$

$$K_Q = \frac{Q \eta_R}{\rho n^2 D^5} = \frac{54.4310 \times 1.000}{1.025 \times n^2 \times 3.0^5} = \frac{0.2185}{n^2}$$

$$J = \frac{V_A}{n D} = \frac{(1-w)V}{n D} = \frac{(1-0.200)V}{n \times 3.0} = 0.2667 \frac{V}{n}$$

from which n for a particular V can be determined.

$$T = K_T \rho n^2 D^4 = K_T \times 1.025 \times n^2 \times 3.0^4 = 83.025 n^2 K_T \text{ kN}$$

$$P_D = \frac{2\pi \rho n^3 D^5 K_Q}{\eta_R} = \frac{2\pi \times 1.025 \times n^3 \times 3.0^5 K_Q}{1.000} = 1564.98 n^3 K_Q \text{ kW}$$

The towrope pull TP and the towrope power P_{Tow} are then given by:

$$TP = (1 - t)T - R_T \text{ where } R_T = \frac{P_E}{V}$$

$$P_{Tow} = TP \times V$$

At speeds above V_m , $n = n_{\max} = 2.5 \text{ s}^{-1}$

$$\text{and } J = \frac{(1 - w)V}{nD} = \frac{(1 - 0.200)V}{2.5 \times 3.0} = 0.1067 V$$

from which K_T and K_Q may be determined and the various quantities calculated as before.

The calculations may be carried out as shown in the following table.

$V \left\{ \begin{array}{l} \text{k :} \\ \text{ms}^{-1} : \end{array} \right.$	0	2.0	4.0	5.7426	6.0	8.0
$P_E \text{ kW :}$	0	0.5	6.1	21.6	25.2	68.9
t	0.0500	0.0717	0.0933	0.1122	0.1150	0.1367
$R_T \text{ kN :}$	-	0.4860	2.9646	7.3121	8.1648	16.7428
J	0	0.1196	0.2290	0.3151	0.3292	0.4390
K_T	0.3630	0.3297	0.2953	0.2656	0.2605	0.2187
$10K_Q$	0.4476	0.4154	0.3806	0.3496	0.3443	0.2995
$n \left\{ \begin{array}{l} \text{s}^{-1} : \\ \text{rpm :} \end{array} \right.$	2.2094	2.2934	2.3959	2.5000	2.5000	2.5000
$T \text{ kN :}$	147.12	143.98	140.74	137.82	135.16	113.47
$Q \text{ kNm :}$	54.431	54.431	54.431	54.431	53.598	46.624
$TP \text{ kN :}$	139.77	133.17	124.64	115.04	111.45	81.22
$P_{Tow} \text{ kW :}$	-	137.00	256.47	339.84	343.98	334.22

P_D	kW :	755.48	784.34	819.19	855.00	841.91	732.63	
P_B	kW :	795.24	825.62	862.31	900.00	886.22	771.19	
V	k:	9.0	10.0	11.0	12.0	12.300	13.0	14.0
	ms^{-1} :	4.6296	5.1440	5.6584	6.1728	6.3271	6.6872	7.2016
P_E	kW:	104.1	150.6	210.2	285.0	310.7	377.1	488.8
t	:	0.1475	0.1583	0.1692	0.1800	0.1832	0.1908	0.2017
R_T	kN:	22.4857	29.2768	37.1483	46.1703	49.1062	56.3913	67.8738
J	:	0.4938	0.5487	0.6036	0.6584	0.6749	0.7133	0.7682
K_T	:	0.1963	0.1731	0.1488	0.1236	0.1159	0.0975	0.0704
$10K_Q$:	0.2752	0.2496	0.2226	0.1945	0.1857	0.1821	0.1673
n	s^{-1} :	2.5000	2.5000	2.5000	2.5000	2.5000	2.5000	2.5000
	rpm:	150.00	150.00	150.00	150.00	150.00	150.00	150.00
T	kN:	101.89	89.80	77.23	64.16	60.14	50.59	36.53
Q	kNm:	42.841	38.856	34.653	30.278	28.908	28.348	26.044
TP	kN:	64.38	46.31	27.01	6.44	0	-	-
P_{Tbw}	kW:	298.03	238.21	152.86	39.76	0	-	-
P_D	kW:	672.94	610.34	544.32	475.61	454.19	454.09	409.10
P_B	kW:	708.36	642.46	572.97	500.64	478.09	477.99	430.63

The values of towrope pull and delivered power at zero speed tally with the values of bollard pull and delivered power obtained in the previous example. Similarly, the towrope pull is zero at the free running speed whose value and the corresponding delivered power tally with the values in the previous example.

9.5 Propeller Design using Circulation Theory

The circulation theory of propellers, discussed in Section 3.5, may be used to design a propeller in detail to obtain a prescribed distribution of loading

along the radius, a pitch distribution matching the mean circumferential wake at each radius and blade section shapes that fulfil desired cavitation and strength requirements. Circulation theory methods are used for the design of propellers that are likely to have cavitation problems and work in very non-uniform velocity fields. In such cases, these theoretical design methods offer significant advantages with respect to efficiency and cavitation over methods based on experimental propeller methodical series data. Although there have been considerable advances in propeller theory and the design methods based on it, particularly since the advent of computers so that many empirical corrections required in the earlier versions of the theory have been eliminated, it is still necessary to apply some corrections and to carry out experiments in a cavitation tunnel to confirm the correctness of a propeller design based on theory. As with design methods using methodical series data, several methods exist for designing propellers using the circulation theory. All these methods are fundamentally the same, but have differences only in detail. One such method is considered here.

It is assumed that the following quantities are known, possibly through a preliminary design calculation using methodical series data: the ship speed V and the corresponding propeller thrust T , the propeller diameter D , the number of blades Z , an estimated expanded blade area ratio A_E/A_O , the depth of immersion h of the shaft axis and the propeller revolution rate n . For a "wake adapted" propeller, the mean effective circumferential wake fraction $w(x)$ as a function of the non-dimensional radius $x = r/R$ must also be known. This may be determined by a wake survey as described in Section 8.5, but must then be corrected for the difference between effective and nominal wake as follows:

$$1 - w(x) = \frac{1 - \bar{w}}{1 - \bar{w}_{nom}} [1 - w_{nom}(x)] \quad (9.9)$$

where \bar{w} is the effective wake fraction determined through a self-propulsion test using thrust identity, $w_{nom}(x)$ is the mean nominal circumferential wake fraction at radius x determined through a wake survey, and \bar{w}_{nom} is the volumetric mean nominal wake fraction given by:

$$1 - \bar{w}_{nom} = \frac{2}{1 - x_b^2} \int_{x_b}^1 [1 - w_{nom}(x)] x dx \quad (9.10)$$

x_b being the non-dimensional boss radius. The mean velocity of advance of the propeller is therefore:

$$\bar{V}_A = (1 - \bar{w})V \quad (9.11)$$

The next step is to determine the thrust loading coefficient:

$$C_{TL} = \frac{T}{\frac{1}{2}\rho A_O \bar{V}_A^2} \quad (9.12)$$

where $A_O = \pi D^2/4$ is the disc area of the propeller, and the advance ratio:

$$\lambda = \frac{\bar{V}_A}{\pi n D} \quad (9.13)$$

One may then estimate the ideal thrust loading coefficient (i.e. for an inviscid fluid):

$$C_{TLi} = (1.02 \text{ to } 1.06) C_{TL} \quad (9.14)$$

Alternatively, one may make an initial estimate of the average drag-lift ratio, $\tan \gamma$, for the whole propeller, using the following relation:

$$\tan \gamma = \frac{0.4}{Z} \frac{A_E}{A_O} - 0.02 \quad (9.15)$$

and then obtain:

$$C_{TLi} = \frac{C_{TL}}{1 - 2\lambda \tan \gamma} \quad (9.16)$$

Next, it is necessary to estimate the ideal efficiency η_i of the propeller. This is usually done with the help of the Kramer diagram, Fig. 9.2, which gives η_i as a function of C_{TLi} , λ and Z . However, one may also select any suitable value and arrive at the correct η_i by the iterative process described in the following. This allows the hydrodynamic pitch angles (see Fig. 3.11) to be determined at the various radii x :

$$\tan \beta = \frac{[1 - w(x)]V}{2\pi n r} = \frac{[1 - w(x)]V}{\pi n D x} \quad (9.17)$$

$$\tan \beta_I = \frac{1}{\eta_i} \tan \beta \left[\frac{1 - \bar{w}}{1 - w(x)} \right]^{\frac{1}{2}} \quad (9.18)$$

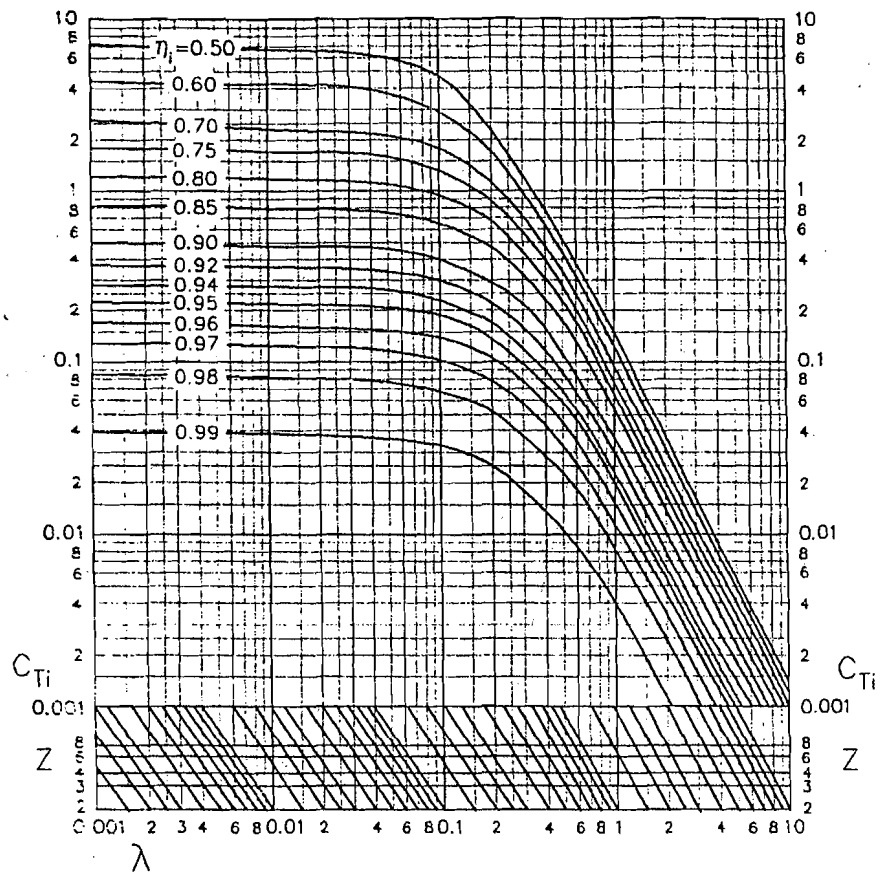


Figure 9.2 : Kramer Diagram.

or

$$\tan \beta_I = \frac{1}{\eta_i} \tan \beta \left[\frac{1 - \bar{w}}{1 - w(x)} \right]^{\frac{3}{4}} \quad (9.19)$$

Equations (9.18) and (9.19) are the optimum criteria for wake adapted propellers proposed by Lerbs (1952) and by van Manen (1955) respectively, and are based on making the product of the ideal efficiency and the hull efficiency constant over the radius.

Sometimes, it is necessary to decrease the loading on the blades near the tip to reduce the risk of cavitation. In such a case, the values of $\tan \beta_I$ may be reduced at the outer radii and increased at the inner radii by multiplying the values of $\tan \beta_I$ obtained from Eqns (9.18) or (9.19) by an appropriate pitch distribution factor for each radius. A typical radial distribution of hydrodynamic pitch to give reduced loading over the outer radii has been suggested by O'Brien (1962) and is given in Table 9.4, which shows the ratio of the tangent of the hydrodynamic pitch angle at a non-dimensional radius x to that at $0.7R$. The loading on the blades may also be reduced at the inner radii to minimise hub vortex cavitation.

Table 9.4

**Radial Distribution of Hydrodynamic Pitch Angle
for Reduced Thrust Loading at Outer Radii**

$0.2 \leq x \leq 0.4:$	$\frac{\tan \beta_I(x)}{\tan \beta_I(0.7)} = 1.11 - 0.1x$
$0.4 \leq x \leq 0.6:$	$\frac{\tan \beta_I(x)}{\tan \beta_I(0.7)} = 1.03 + 0.3x - 0.5x^2$
$0.6 \leq x \leq 1.0:$	$\frac{\tan \beta_I(x)}{\tan \beta_I(0.7)} = 1.21 - 0.3x$

After determining the hydrodynamic pitch angles at the different radii, one may calculate the local advance ratios including the induced velocity components:

$$\lambda_I = x \tan \beta_I \quad (9.20)$$

This enables one to obtain at each radius the Goldstein factors κ which are given as functions of $1/\lambda_I$, the non-dimensional radius x and the number of blades Z , Appendix 6.

One may now calculate the radial distribution of the ideal thrust loading coefficient from Eqn. (3.39) after including the Goldstein factor:

$$\frac{dC_{TLi}}{dx} = 8x\kappa \frac{\frac{1}{2}u_t}{V_A} \frac{V_R}{V_A} \cos \beta_I \quad (9.21)$$

where, from Eqns. (3.28):

$$\begin{aligned}\frac{\frac{1}{2}u_t}{V_A} &= \frac{\tan \beta_I (\tan \beta_I - \tan \beta)}{\tan \beta (1 + \tan^2 \beta_I)} = \frac{\sin \beta_I \sin(\beta_I - \beta)}{\sin \beta} \\ \frac{V_R}{V_A} &= \frac{\cos(\beta_I - \beta)}{\sin \beta}\end{aligned}\quad (9.22)$$

Eqn. (9.21) is sometimes written in terms of a non-dimensional circulation defined by:

$$G = \frac{\Gamma}{\pi D V_A} = \frac{2x\kappa}{Z} \frac{\frac{1}{2}u_t}{V_A} \quad (9.23)$$

so that:

$$\frac{dC_{TLi}}{dx} = 4ZG \left[\frac{1}{\tan \beta} - \frac{\frac{1}{2}u_t}{V_A} \right] \quad (9.24)$$

Integration then yields a value of the ideal thrust loading coefficient:

$$C_{TLi} = \int_{x_b}^1 \frac{dC_{TLi}}{dx} dx \quad (9.25)$$

This value of C_{TLi} must be equal to the initial value of C_{TLi} calculated from Eqn. (9.14) or Eqn. (9.16). If the two values of C_{TLi} are not in agreement, the value of η_i must be altered and the calculation repeated until the initial value of C_{TLi} from Eqns. (9.14) or (9.16) and the final value obtained from Eqn. (9.25) are in sufficiently close agreement. Eckhardt and Morgan (1955) suggest that the number of iterations to bring this about can be reduced by using the following empirical relation:

$$\eta_{i(k+1)} = \frac{\eta_{ik}}{1 + \frac{C_{TLi0} - C_{TLik}}{5 C_{TLi0}}} \quad (9.26)$$

where η_{ik} and $\eta_{i(k+1)}$ are the values of η_i for the k^{th} and $(k+1)^{\text{th}}$ iterations, C_{TLi0} is the desired value of C_{TLi} , and C_{TLik} the value obtained in the k^{th} iteration. However, see the procedure adopted in Example 7.

Once the radial distribution of hydrodynamic pitch angle for a specified ideal thrust loading coefficient has been determined, the values of the product $C_L c/D$ at various radii can be obtained, since as shown in Section 3.5:

$$C_L \frac{c}{D} = \frac{4\pi}{Z} x \kappa \sin \beta_I \tan(\beta_I - \beta) \quad (9.27)$$

The remaining design process consists in determining the shape of the blade sections at the different radii and their pitch angles. The lift coefficient C_L depends upon the type of aerofoil section, and its camber ratio, thickness-chord ratio and the angle of attack. It is necessary to choose these geometrical parameters such that the desired values of $C_L c/D$ are obtained at the different radii subject to the requirements of minimum risk of cavitation, adequate blade strength and minimum drag. Various alternative procedures are available for designing the blade sections.

The types of aerofoil section generally used in propellers designed using the circulation theory are the Karman-Trefftz section and the NACA sections with $\alpha = 0.8$ and $\alpha = 1.0$ mean lines and NACA-16 and NACA-66 thickness distributions. (NACA stands for the National Advisory Committee for Aeronautics, USA, now the National Aeronautics and Space Administration, NASA). The basic Karman-Trefftz section is built up of two circular arcs, but it is usual to use the circular arc mean line of this section with other thickness distributions such as the NACA-16 and NACA-66 distributions. The NACA $\alpha = 0.8$ and $\alpha = 1.0$ mean lines indicate the fraction of the chord over which the suction pressure on the back of the section is constant at the "ideal" angle of attack. The $\alpha = 0.8$ mean line has been found to give excellent results in practice and is widely used along with the NACA-66 (modified) thickness distribution in propeller design. The geometrical details of the various types of sections used in propellers designed by the circulation theory are given in Appendix 2.

The hydrodynamic characteristics of such sections are generally available in the form of diagrams giving $C_L/(t/c)$ for cavitation inception as a function of the minimum pressure coefficient $-C_{p_{\min}}$ for various values of the thickness chord ratio t/c and the camber ratio f/c for "shock free entry" (or ideal angle of attack at which the suction pressure variation does not have a sharp peak). The hydrodynamic characteristics of section shapes used in propellers are also given in the form of "bucket diagrams" which indicate the range of

angles of attack for which the section will not cavitate for a given $-C_{p_{\min}}$ (see Fig. 6.7). Data for some sections used in propeller design are given in Appendix 7.

Although the NACA sections have been widely used in propeller design, better methods for designing aerofoils for a prescribed pressure distribution have now been developed. In blade sections designed by this new procedure (Eppler-Shen sections), the leading edge is unloaded and the loading shifted as far towards the trailing edge as possible without causing flow separation. This causes an increase in the cavitation free zone of the angle of attack and increases the cavitation inception speed by as much as 2-3 knots.

After having selected the type of section to be used, one may use its hydrodynamic characteristics to determine the blade section geometry, i.e. the chord c , the thickness t and the camber f at the various radii r . The value of the minimum pressure coefficient is calculated at each radius from:

$$-C_{p_{\min}} = \frac{p_A + \rho g(h - xR) - p_V}{\frac{1}{2}\rho V_R^2} \quad (9.28)$$

and a suitable variation of blade thickness t with radius assumed. The values of t/c and f/c are then determined so that the required value of $C_L c/D$ is obtained at each radius without exceeding the limiting value of $C_L/(t/c)$ for cavitation inception at the calculated $-C_{p_{\min}}$. The value of $-C_{p_{\min}}$ is sometimes reduced by up to 20 percent to allow for the non-uniform flow field. This procedure for selecting t/c and f/c often leads to an "unfair" variation of f and c with radius r , and it is necessary to fair these values to obtain a smooth variation. It is recommended that t/c should not exceed 0.22. After having determined the fair values of c and t at each radius, the value of C_L can be calculated from Eqn. (9.27).

Alternatively, one may first select a suitable blade thickness distribution satisfying a given strength criterion and a suitable blade width distribution, i.e. the variation of c with r . A linear variation of blade thickness is often adopted:

$$\frac{t(x)}{D} = (1 - x) \frac{t_0}{D} + x \frac{t_1}{D} \quad (9.29)$$

where $t(x)$ is the blade thickness at the non-dimensional radius x , t_0/D the blade thickness fraction and t_1 the tip thickness; a common value for t_1/D is 0.003. Two standard blade width distributions used in propeller design are

one used in the Troost B Series (described in Section 4.6) and one proposed by Morgan, Silovic and Denny (1968). These chord distributions are given by:

$$\frac{c(x)}{D} = \frac{c_1(x)}{Z} \frac{A_E}{A_O} \quad (9.30)$$

where the values of $c_1(x)$ are given in Table 9.5.

Table 9.5

Blade Chord Distribution

$\frac{c(x)}{D} = \frac{c_1(x)}{Z} \frac{A_E}{A_O}$		
Values of $c_1(x)$		
x	B Series	Morgan
0.20	1.662	1.6338
0.30	1.882	1.8082
0.40	2.050	1.9648
0.50	2.152	2.0967
0.60	2.187	2.1926
0.70	2.144	2.2320
0.80	1.970	2.1719
0.90	1.582	1.8931
0.95	1.274	1.5362
1.00	0.000	0.0000

A suitable distribution of skew to define the shape of the expanded blade outline may also be selected at this stage. The distribution of skew must be selected to minimise unsteady propeller forces due to a non-uniform wake. Unsteady propeller forces are considered in Chapter 11. A typical distribution of skew given by Morgan, Silovic and Denny is as follows:

$$\frac{skew(x)}{R} = R_S - [R_S^2 - (x - 0.2)^2]^{0.5} \quad (9.31)$$

where:

$$R_S = \frac{0.32}{skew(1)} + \frac{skew(1)}{2}$$

and

$$\text{skew}(1) = \frac{\theta_S}{57.3 \cos \beta_I(1)}$$

θ_S being the skew angle in degrees and $\beta_I(1)$ the hydrodynamic pitch angle at the blade tip.

Once the blade chord distribution has been selected, the value of C_L can be calculated at each radius from Eqn. (9.27). It is usual to assume that at the ideal angle of attack the drag coefficient $C_D = 0.008$ and this allows the lift-drag ratio at each radius to be calculated:

$$\tan \gamma = \frac{C_D}{C_L} = \frac{0.008}{C_L} \quad (9.32)$$

One may then determine the thrust-loading coefficient for viscous flow:

$$C_{TL} = \int_{x_b}^{1.0} \frac{dC_{TLi}}{dx} (1 - \tan \beta_I \tan \gamma) dx \quad (9.33)$$

and this should agree sufficiently well with the initial value at the start of the design calculation obtained from Eqn. (9.12). If the value of C_{TL} obtained from Eqn. (9.33) differs widely from the value obtained from Eqn. (9.12), the value of C_{TL} must be altered and the entire calculation starting with an initial estimate of η_i repeated until a satisfactory agreement is obtained between the initial and final values of C_{TL} .

After this, one may determine the power coefficient:

$$C_P = \frac{P_D}{\frac{1}{2} \rho A_O \bar{V}_A^3} = \int_{x_b}^1 \frac{dC_{TLi}}{dx} \frac{\tan \beta_I + \tan \gamma}{\tan \beta} dx \quad (9.34)$$

The delivered power P_D obtained from this value of C_P must match the design delivered power of the ship propulsion plant; otherwise, the ship speed and the corresponding propeller thrust must be changed and the calculations repeated until the calculated C_P matches the delivered power available.

The efficiency of the design propeller in the behind condition is obtained as:

$$\eta_B = \frac{C_{TL}}{C_P} \quad (9.35)$$

After these iterative processes have converged to satisfactory values of C_{TL} and C_P , one may proceed with the design of the blade sections. The camber ratio f/c and the ideal angle of attack α_i are determined at each radius from the corresponding values of C_L :

$$\frac{f}{c} = k_1 C_L \quad \alpha_i^\circ = k_2 C_L \quad (9.36)$$

where k_1 and k_2 depend upon the type of mean line and are given in Table 9.6.

Table 9.6

Camber Ratio, Ideal Angle of Attack
and Viscosity Correction Factor (μ)

	$\frac{f}{c} = k_1 C_L$		$\alpha_i^\circ = k_2 C_L$
Mean Line	k_1	k_2	μ
NACA $a = 0.8$	0.06790	1.54	1.05
NACA $a = 0.8$ (modified)	0.06651	1.40	1.00
NACA $a = 1.0$	0.06515	0	0.74
Circular Arc	0.07958	0	0.80

The value of α_i should lie within the cavitation free zone as indicated in the "bucket diagram" illustrated in Fig. 6.7. The maximum and minimum values of the angle of attack for cavitation free operation with a given $-C_{p_{min}}$, t/c and f/c for blade sections with different types of mean line and thickness distributions may be determined from the data in Appendix 7.

The values of f/c and α_i obtained from Table 9.6 are correct if the lift coefficient is due to a lifting line in inviscid flow. Since the propeller blades are like lifting surfaces, have a finite thickness and operate in a viscous flow, it is necessary to correct the values of camber ratio and angle of attack to account for lifting surface, thickness and viscosity effects.

Experience has shown that for the NACA $a = 0.8$ mean line, the correction for viscosity is very small. Blade sections with the NACA $a = 0.8$ mean line and NACA-66 (modified) thickness distribution are therefore often preferred for the design of propellers. For other types of sections, a small increase in

the camber ratio or the angle of attack or both is necessary to obtain the required lift coefficient. A method for making this correction suggested by van Manen (1957) is as follows:

$$\begin{aligned} \text{Increase in angle of attack, } \Delta\alpha^\circ &= 0.7 \frac{1-\mu}{\mu} k \frac{f}{c} \times 57.3 \\ \text{Increase in camber ratio, } \Delta\frac{f}{c} &= 0.35 \frac{1-\mu}{\mu} k \frac{f}{c} \end{aligned} \quad (9.37)$$

where μ is the viscous correction factor given in Table 9.6 and k is the Ludwig-Ginzler curvature correction factor which is a function of the number of blades, the blade area ratio, the non-dimensional radius and the hydrodynamic pitch angle.

Lifting surface corrections may be made using the factors due to Morgan, Silovic and Denny (1968):

$$\begin{aligned} \frac{f}{c} \text{ corrected} &= k_c \frac{f}{c} \\ \alpha_i^\circ \text{ corrected} &= k_\alpha \alpha_i^\circ \\ \alpha_t^\circ &= 57.3 k_t \frac{t_0}{D} \end{aligned} \quad (9.38)$$

where k_c and k_α are lifting surface correction factors for camber ratio and angle of attack respectively, and α_t is a correction to the angle of attack to account for the finite thickness of the blade, k_t being the corresponding factor and t_0/D the blade thickness fraction. These correction factors, which are given in Appendix 8, have been derived under certain restricted conditions (such as constant hydrodynamic pitch over the radius, and NACA $a = 0.8$ mean line and NACA-66 thickness distribution), and it is not strictly correct to regard these factors as applicable in all cases.

The pitch angle at each radius is then obtained:

$$\varphi = \beta_I + \alpha_i + \alpha_t \quad (9.39)$$

and the pitch ratio at each radius becomes:

$$\frac{P(x)}{D} = \pi x \tan \varphi \quad (9.40)$$

This concludes the design of the propeller using lifting line theory with lifting surface corrections. The following example illustrates the procedure for such a design.

Example 7

Design a propeller for a single screw ship using the circulation theory. The ship is to have a speed of 24.5 knots at which its effective power is 16500 kW. The propeller is to have six blades, a diameter of 7.0 m, an expanded blade area ratio of 0.775 and a blade thickness fraction of 0.060. The skew angle is to be 15 degrees. The propeller shaft is 6.50 m below the load water line of the ship. The propeller is to run at 108 rpm. The effective wake fraction is 0.220 and the thrust deduction fraction 0.160. The radial variation of nominal wake is as follows:

$x = r/R :$	0.2	0.3	0.4	0.5	0.6	0.7	0.8	0.9	1.0
$w_{nom}(x) :$	0.418	0.350	0.302	0.269	0.246	0.227	0.215	0.204	0.192

The propeller blades are to be unloaded at the tip in accordance with Table 9.4. The blade chord distribution is to be in accordance with Table 9.5 (Morgan) and the blade sections are to have the NACA $a = 0.8$ mean line and the NACA-66 (modified) thickness distribution.

$$V = 24.5 \text{ k} = 24.5 \times 0.5144 = 12.6028 \text{ ms}^{-1}$$

$$n = 108 \text{ rpm} = 1.8 \text{ s}^{-1} \quad P_E = 16500 \text{ kW} \quad w = 0.220 \quad t = 0.160$$

$$D = 7.0 \text{ m} \quad Z = 6 \quad \frac{A_E}{A_O} = 0.775 \quad \frac{t_0}{D} = 0.060 \quad h = 6.5 \text{ m}$$

Blade chord distribution according to Morgan

Radial load distribution according to Table 9.4

Blade sections: NACA $a = 0.8$ mean line

NACA-66 (modified) thickness distribution

Distribution of Effective Wake

This is calculated using Simpson's Rule as follows:

x	w_{nom}	$1 - w_{nom}$	$x(1 - w_{nom})$	SM	$f(1 - \bar{w}_{nom})$	$1 - w(x)$
0.2	0.418	0.582	0.1164	1	0.1164	0.5989
0.3	0.350	0.650	0.1950	4	0.7800	0.6689
0.4	0.302	0.698	0.2792	2	0.5584	0.7183
0.5	0.269	0.731	0.3655	4	1.4620	0.7522
0.6	0.246	0.754	0.4524	2	0.9048	0.7759
0.7	0.227	0.773	0.5411	4	2.1644	0.7954
0.8	0.215	0.785	0.6280	2	1.2560	0.8078
0.9	0.204	0.796	0.7164	4	2.8656	0.8191
1.0	0.192	0.808	0.8080	1	0.8080	0.8315
					<u>10.9156</u>	

$$1 - \bar{w}_{nom} = \frac{2}{1 - x_b^2} \int_{x_b}^{1.0} (1 - w_{nom}) x \, dx = \frac{2}{1 - 0.2^2} \times \frac{1}{3} \times 0.1 \times 10.9156$$

$$= 0.7580$$

$$1 - w(x) = \frac{1 - \bar{w}}{1 - \bar{w}_{nom}} (1 - w_{nom}) = \frac{1 - 0.220}{0.7580} (1 - w_{nom})$$

$$= 1.0290 (1 - w_{nom})$$

Thrust loading coefficient and ideal efficiency:

$$\bar{V}_A = (1 - \bar{w}) V = (1 - 0.220) \times 12.6028 = 9.8302 \, \text{m s}^{-1}$$

$$R_T = \frac{P_E}{V} = \frac{16500}{12.6028} = 1309.23 \, \text{kN}$$

$$T = \frac{R_T}{1 - t} = \frac{1309.23}{1 - 0.160} = 1558.61 \, \text{m}^2$$

$$A_O = \frac{\pi}{4} D^2 = \frac{\pi}{4} \times 7.0^2 = 38.4845 \, \text{m}^2$$

$$C_{TL} = \frac{T}{\frac{1}{2} \rho A_O \bar{V}_A^2} = \frac{1558.61}{\frac{1}{2} \times 1.025 \times 38.4845 \times 9.8302^2} = 0.8178$$

$$\lambda = \frac{\bar{V}_A}{\pi n D} = \frac{9.8302}{\pi \times 1.8 \times 7.0} = 0.2483$$

$$\tan \gamma = \frac{0.4}{Z} \frac{A_E}{A_O} - 0.02 = \frac{0.4}{6} \times 0.775 - 0.02 = 0.03167$$

$$C_{TLi} = \frac{C_{TL}}{1 - 2\lambda \tan \gamma} = \frac{0.8178}{1 - 2 \times 0.2483 \times 0.03167} = 0.8309$$

From the Kramer diagram for $Z = 6$, $\lambda = 0.2483$ and $C_{TLi} = 0.8309$, the ideal efficiency:

$$\eta_i = 0.800$$

Hydrodynamic pitch angles—first iteration with $\eta_i = 0.800$

$$\tan \beta = \frac{[1 - w(x)] V}{\pi n D x} = \frac{[1 - w(x)] \times 12.6028}{\pi \times 1.8 \times 7.0 \times x} = 0.31838 \frac{1 - w(x)}{x}$$

$$\text{Optimum } \tan \beta_I = \frac{\tan \beta}{\eta_i} \left[\frac{1 - \bar{w}}{1 - w(x)} \right]^{\frac{1}{2}} \quad (\text{Lerbs})$$

$$\tan \beta_I = \text{Optimum } \tan \beta_I \times \text{tip unloading factor (tuf)}$$

$$= \frac{\tan \beta}{\eta_i} \left[\frac{1 - \bar{w}}{1 - w(x)} \right]^{\frac{1}{2}} \times \text{tuf}$$

The calculations are carried out in the following table:

x	$1 - w(x)$	$\tan \beta$	β°	$\left[\frac{1 - \bar{w}}{1 - w(x)} \right]^{\frac{1}{2}}$	tuf	$\tan \beta_I$	β_I°	$\beta_I^\circ - \beta^\circ$
0.2	0.5989	0.9534	43.6331	1.1412	1.090	1.4824	55.9979	12.3648
0.3	0.6689	0.7099	35.3703	1.0799	1.080	1.0349	45.9818	10.6115
0.4	0.7183	0.5717	29.7580	1.0421	1.070	0.7968	38.5478	8.7919
0.5	0.7522	0.4790	25.5931	1.0183	1.055	0.6432	32.7491	7.1564
0.6	0.7759	0.4117	22.3779	1.0026	1.030	0.5315	27.9901	5.6122
0.7	0.7954	0.3618	19.8887	0.9903	1.000	0.4478	24.1235	4.2348
0.8	0.8078	0.3215	17.8218	0.9826	0.970	0.3830	20.9586	3.1368
0.9	0.8191	0.2898	16.1596	0.9758	0.940	0.3322	18.3788	2.2192
1.0	0.8315	0.2647	14.8280	0.9685	0.910	0.2917	16.2598	1.4318

(The values in this table and other tables have been rounded off to four decimals, and this may result in minor discrepancies.)

$$\lambda_I = x \tan \beta_I$$

κ from Appendix 6

$$\frac{\frac{1}{2}u_t}{V_A} = \frac{\sin \beta_I \sin(\beta_I - \beta)}{\sin \beta} \quad \frac{V_R}{V_A} = \frac{\cos(\beta_I - \beta)}{\sin \beta}$$

$$\frac{dC_{TLi}}{dx} = 8x\kappa \frac{\frac{1}{2}u_t}{V_A} \frac{V_R}{V_A} \cos \beta_I$$

C_{TLi} is calculated using Simpson's Rule as follows:

x	λ_I	κ	$\frac{\frac{1}{2}u_t}{V_A}$	$\frac{V_R}{V_A}$	$\frac{dC_{TLi}}{dx}$	SM	$f(C_{TLi})$
0.2	0.2965	1.0529	0.2573	1.4156	0.3431	1	0.3431
0.3	0.3105	1.0078	0.2288	1.6980	0.6530	4	2.6119
0.4	0.3187	0.9913	0.1919	1.9911	0.9479	2	1.8958
0.5	0.3216	0.9855	0.1560	2.2969	1.1880	4	4.7518
0.6	0.3189	0.9783	0.1206	2.6141	1.3072	2	2.6145
0.7	0.3135	0.9565	0.0887	2.9315	1.2712	4	5.0846
0.8	0.3064	0.9035	0.0640	3.2625	1.1275	2	2.2550
0.9	0.2990	0.7563	0.0439	3.5904	0.8145	4	3.2580
1.0	0.2917	0	0.0273	3.9063	0	1	0
							22.8148

$$C_{TLi} = \frac{1}{3} \times 0.1 \times 22.8148 = 0.7605$$

The required value is $C_{TLi} = 0.8309$

The value of η_i for the next iteration is given by:

$$\eta'_i = \frac{\eta_i}{1 + \frac{C_{TLi0} - C_{TLi}}{5 C_{TLi0}}} = \frac{0.800}{1 + \frac{0.8309 - 0.7605}{5 \times 0.8309}} = 0.7867$$

Hydrodynamic pitch angles—second iteration (with $\eta_i = 0.7867$)

x	$\tan \beta$	β°	$\left[\frac{1 - \bar{w}}{1 - w(x)} \right]^{\frac{1}{2}}$	tuf	$\tan \beta_I$	β_I°	$\beta_I^\circ - \beta^\circ$
0.2	0.9534	43.6331	1.1412	1.090	1.5075	56.4418	12.8087
0.3	0.7099	35.3703	1.0799	1.080	1.0524	46.4617	11.0914

x	$\tan \beta$	β°	$\left[\frac{1 - \bar{w}}{1 - w(x)} \right]^{\frac{1}{2}}$	tuf	$\tan \beta_I$	β_I°	$\beta_I^\circ - \beta^\circ$
0.4	0.5717	29.7580	1.0421	1.070	0.8103	39.0189	9.2609
0.5	0.4790	25.5931	1.0183	1.055	0.6541	33.1881	7.5950
0.6	0.4117	22.3779	1.0026	1.030	0.5405	28.3900	6.0121
0.7	0.3618	19.8887	0.9903	1.000	0.4554	24.4838	4.5951
0.8	0.3215	17.8218	0.9826	0.970	0.3895	21.2814	3.4596
0.9	0.2898	16.1596	0.9758	0.940	0.3379	18.6681	2.5085
1.0	0.2647	14.8280	0.9685	0.910	0.2966	16.5198	1.6918

x	λ_I	κ	$\frac{\frac{1}{2}u_t}{V_A}$	$\frac{V_R}{V_A}$	$\frac{dC_{TLi}}{dx}$	SM	$f(C_{TLi})$
0.2	0.3015	1.0558	0.2677	1.4131	0.3533	1	0.3533
0.3	0.3157	1.0082	0.2409	1.6953	0.6808	4	2.7232
0.4	0.3241	0.9917	0.2041	1.9883	1.0006	2	2.0011
0.5	0.3270	0.9851	0.1675	2.2946	1.2674	4	5.0697
0.6	0.3243	0.9771	0.1308	2.6122	1.4098	2	2.8195
0.7	0.3188	0.9543	0.0976	2.9301	1.3908	4	5.5634
0.8	0.3116	0.9001	0.0716	3.2614	1.2535	2	2.5069
0.9	0.3041	0.7519	0.0503	3.5896	0.9261	4	3.7042
1.0	0.2966	0	0.0328	3.9058	0	1	0
							24.7414

$$C_{TLi} = \frac{1}{3} \times 0.1 \times 24.7414 = 0.8247$$

For $\eta_i = 0.8000$, $C_{TLi} = 0.7605$

For $\eta_i = 0.7867$, $C_{TLi} = 0.8247$

By linear extrapolation, for the required $C_{TLi} = 0.8309$

$$\eta_i = 0.8000 + \frac{0.7867 - 0.8000}{0.8247 - 0.7605} \times (0.8309 - 0.7605) = 0.7854$$

Hydrodynamic pitch angles—third iteration (with $\eta_i = 0.7854$)

x	$\tan \beta$	β°	$\left[\frac{1 - \bar{w}}{1 - w(x)} \right]^{\frac{1}{2}}$	tuf	$\tan \beta_I$	β_I°	$\beta_I^\circ - \beta^\circ$
0.2	0.9534	43.6331	1.1412	1.090	1.5100	56.4854	12.8523

x	$\tan \beta$	β°	$\left[\frac{1-\bar{w}}{1-w(x)} \right]^{\frac{1}{2}}$	tuf	$\tan \beta_I$	β_I°	$\beta_I^\circ - \beta^\circ$
0.3	0.7099	35.3703	1.0799	1.080	1.0541	46.5090	11.1387
0.4	0.5717	29.7580	1.0421	1.070	0.8116	39.0652	9.3072
0.5	0.4790	25.5931	1.0183	1.055	0.6552	33.2315	7.6384
0.6	0.4117	22.3779	1.0026	1.030	0.5414	28.4297	6.0518
0.7	0.3618	19.8887	0.9903	1.000	0.4561	24.5196	4.6309
0.8	0.3215	17.8218	0.9826	0.970	0.3901	21.3135	3.4917
0.9	0.2898	16.1596	0.9758	0.940	0.3385	18.6969	2.5373
1.0	0.2647	14.8280	0.9685	0.910	0.2971	16.5457	1.7177

x	λ_I	κ	$\frac{\frac{1}{2}u_t}{V_A}$	$\frac{V_R}{V_A}$	$\frac{dC_{TLi}}{dx}$	SM	$f(C_{TLi})$
0.2	0.3020	1.0561	0.2688	1.4129	0.3543	1	0.3543
0.3	0.3162	1.0084	0.2421	1.6950	0.6835	4	2.7340
0.4	0.3245	0.9916	0.2053	1.9882	1.0056	2	2.0113
0.5	0.3276	0.9850	0.1686	2.2944	1.2749	4	5.0995
0.6	0.3248	0.9770	0.1318	2.6120	1.4197	2	2.8395
0.7	0.3193	0.9541	0.0985	2.9299	1.4029	4	5.6116
0.8	0.3121	0.8998	0.0723	3.2613	1.2650	2	2.5300
0.9	0.3046	0.7515	0.0510	3.5895	0.9383	4	3.7530
1.0	0.2971	0	0.0334	3.9057	0	1	0
							24.9332

$$C_{TLi} = \frac{1}{3} \times 0.1 \times 24.9332 = 0.8311$$

This is almost exactly what is required, and no further iterations are necessary

Design of blade sections and cavitation checks

$$C_L \frac{c}{D} = \frac{4\pi}{Z} x \kappa \sin \beta_I \tan(\beta_I - \beta)$$

$\frac{c}{D}$ from Table 9.5 (Morgan)

$$\frac{t}{D} = (1-x) \frac{t_0}{D} + x \frac{t_1}{D} = (1-x) \times 0.060 + x \times 0.003 = 0.060 - 0.057x$$

x	β_I°	$\beta_I^\circ - \beta^\circ$	κ	$C_L \frac{c}{D}$	$\frac{c}{D}$	$\frac{t}{D}$	$\frac{t}{c}$	C_L
0.2	56.4854	12.8523	1.0561	0.08415	0.2110	0.0486	0.2303	0.3988
0.3	46.5090	11.1387	1.0084	0.09050	0.2336	0.0429	0.1836	0.3874
0.4	39.0652	9.3072	0.9917	0.08580	0.2538	0.0372	0.1466	0.3381
0.5	33.2315	7.6384	0.9850	0.07581	0.2708	0.0315	0.1163	0.2799
0.6	28.4297	6.0518	0.9770	0.06197	0.2832	0.0258	0.0911	0.2188
0.7	24.5196	4.6309	0.9541	0.04702	0.2883	0.0201	0.0697	0.1631
0.8	21.3135	3.4917	0.8998	0.03344	0.2805	0.0144	0.0513	0.1192
0.9	18.6969	2.5373	0.7515	0.02012	0.2445	0.0087	0.0356	0.0823
1.0	16.5457	1.7177	0	0	0	0.0030	-	-

$$\frac{f}{c} = 0.06790 C_L \quad (a = 0.8 \text{ mean line})$$

$$\alpha_i^\circ = 1.54 C_L$$

$$V_A = [1 - w(x)] V = [1 - w(x)] \times 12.6028 \text{ m s}^{-1}$$

$$V_R = V_A \frac{\cos(\beta_I - \beta)}{\sin \beta}$$

$$\begin{aligned} -C_{p_{\min}} &= \frac{p_A + \rho g(h - xR) - p_V}{\frac{1}{2} \rho V_R^2} \\ &= \frac{101.325 + 1.025 \times 9.81(6.50 - 3.5x) - 1.704}{\frac{1}{2} \times 1.025 \times V_R^2} \\ &= \frac{164.9801 - 35.1934x}{0.5125 V_R^2} \end{aligned}$$

α_{\max} and α_{\min} , the limits of the cavitation free "bucket" are obtained from Appendix 7.

x	$\frac{f}{c}$	α_i°	$1 - w(x)$	V_A	V_R	$-C_{p_{\min}}$	α_{\max}°	α_{\min}°
0.2	0.0271	0.6142	0.5989	7.5478	10.6643	2.7098	10.2370	-8.6027
0.3	0.0263	0.5966	0.6689	8.4300	14.2889	1.4758	6.1553	-3.9016
0.4	0.0230	0.5206	0.7183	9.0526	17.9984	0.9089	3.9466	-1.8831
0.5	0.0190	0.4311	0.7522	9.4798	21.7505	0.6079	2.6202	-0.8732
0.6	0.0149	0.3370	0.7759	9.7785	25.5415	0.4303	1.8030	-0.4736

x	$\frac{f}{c}$	α_i°	$1 - w(x)$	V_A	V_R	$-C_{p_{min}}$	α_{max}°	α_{min}°
0.7	0.0111	0.2512	0.7954	10.0243	29.3701	0.3175	1.1770	-0.2034
0.8	0.0081	0.1836	0.8078	10.1805	33.2018	0.2422	0.7809	-0.1328
0.9	0.0056	0.1267	0.8191	10.3230	37.0542	0.1894	0.4997	-0.1043
1.0	-	-	0.8315	10.4792	40.9287	0.1512	-	-

The values of α_i lie between α_{max} and α_{min} , leaving a reasonable margin for variations in angle of attack due to circumferential variations in wake at each radius.

Thrust loading and power coefficients

$$\tan \gamma = \frac{0.008}{C_L}$$

$$\frac{dC_{TL}}{dx} = \frac{dC_{TLi}}{dx} (1 - \tan \beta_I \tan \gamma)$$

$$\frac{dC_P}{dx} = \frac{dC_{TLi}}{dx} \frac{\tan \beta_I + \tan \gamma}{\tan \beta}$$

x	β°	β_I°	$\tan \gamma$	γ°	$\frac{dC_{TLi}}{dx}$	$\frac{dC_{TL}}{dx}$	$\frac{dC_P}{dx}$	SM	$f(C_{TL})$	$f(C_P)$
0.2	43.6331	56.4854	0.02006	1.1492	0.3543	0.3436	0.5686	1	0.3436	0.5686
0.3	35.3703	46.5090	0.02063	1.1818	0.6835	0.6686	1.0348	4	2.6745	4.1392
0.4	29.7580	39.0652	0.02367	1.3556	1.0056	0.9863	1.4693	2	1.9726	2.9385
0.5	25.5931	33.2315	0.02858	1.6369	1.2749	1.2510	1.8200	4	5.0041	7.2798
0.6	22.3779	28.4297	0.03656	2.0938	1.4197	1.3916	1.9928	2	2.7832	3.9857
0.7	19.8887	24.5196	0.04905	2.8081	1.4029	1.3715	1.9591	4	5.4860	7.8362
0.8	17.8218	21.3135	0.06711	3.8396	1.2650	1.2319	1.7993	2	2.4638	3.5986
0.9	16.1596	18.6969	0.09721	5.5521	0.9383	0.9074	1.4106	4	3.6297	5.6426
1.0	14.8280	16.5457	-	-	0	0	0	1	0	0
Totals									24.3575	35.9891

$$C_{TL} = \frac{1}{3} \times 0.1 \times 24.3575 = 0.8119$$

$$C_P = \frac{1}{3} \times 0.1 \times 35.9891 = 1.1996$$

The value of C_{TL} finally obtained is different from the initial value of 0.8178 by less than one percent. Hence, no iteration for C_{TL} is necessary.

The delivered power:

$$P_D = C_P \frac{1}{2} \rho A_O \bar{V}_A^3 = 1.1996 \times 0.5 \times 1.025 \times 38.4845 \times 9.8302^3$$

$$= 22476 \text{ kW}$$

The propeller efficiency in the behind condition:

$$\eta_B = \frac{C_{TL}}{C_P} = \frac{0.8119}{1.1996} = 0.6768$$

Lifting surface corrections

$$Z = 6 \quad \frac{A_E}{A_O} = 0.775 \quad \theta_S = 15^\circ \quad \frac{t_0}{D} = 0.060$$

$$\text{Corrected } \frac{f}{c} = k_c \times \frac{f}{c}$$

$$\text{Corrected } \alpha_i^\circ = k_\alpha \times \alpha_i^\circ$$

$$\alpha_t^\circ = k_t \frac{t_0}{D} \times 57.3 = k_t \times 0.060 \times 57.3 = 3.438 k_t$$

k_c , k_α and k_t from Appendix 8.

$$\varphi = \beta_I + \alpha_i + \alpha_t \quad \frac{P}{D} = \pi x \tan \varphi$$

x	β_I°	λ_I	Uncorrected			Corrected			
			α_i°	f/c	k_α	k_c	k_t	α_i°	α_t°
0.2	56.4854	0.3020	0.6142	0.0271	2.0390	2.2262	1.2936	1.2524	4.4474
0.3	46.5090	0.3162	0.5966	0.0263	2.6057	1.5432	0.9155	1.5546	3.1475
0.4	39.0652	0.3245	0.5206	0.0230	2.7543	1.1944	0.6492	1.4339	2.2319
0.5	33.2315	0.3276	0.4311	0.0190	2.4742	1.1500	0.4499	1.0666	1.5468
0.6	28.4297	0.3248	0.3370	0.0149	2.2124	1.1759	0.2982	0.7456	1.0252
0.7	24.5196	0.3193	0.2512	0.0111	1.8584	1.2720	0.1871	0.4668	0.6432
0.8	21.3135	0.3121	0.1836	0.0081	1.3108	1.4475	0.1167	0.2407	0.4012
0.9	18.6969	0.3046	0.1267	0.0056	0.2995	1.9178	0.0823	0.0379	0.2829
1.0	16.5457	0.2971	-	-	-	-	-	-	-

x	φ°	P/D	Corrected
			f/c
0.2	62.1852	1.1910	0.0603
0.3	51.2111	1.1727	0.0406
0.4	42.7310	1.1609	0.0275
0.5	35.8449	1.1348	0.0218
0.6	30.2005	1.0971	0.0175
0.7	25.6296	1.0550	0.0141
0.8	21.9554	1.0132	0.0117
0.9	19.0177	0.9745	0.0107
1.0	16.5457	0.9333	-

Final blade geometry

x	$\frac{P}{D}$	$\frac{c}{D}$	$\frac{t}{D}$	$\frac{f}{c}$
0.2	1.1910	0.2110	0.0486	0.0603
0.3	1.1727	0.2336	0.0429	0.0406
0.4	1.1609	0.2538	0.0372	0.0275
0.5	1.1348	0.2708	0.0315	0.0218
0.6	1.0971	0.2832	0.0258	0.0175
0.7	1.0550	0.2883	0.0201	0.0141
0.8	1.0132	0.2805	0.0144	0.0117
0.9	0.9745	0.2445	0.0087	0.0107
1.0	0.9333	0	0.0030	-

(It is necessary to "fair" the values of P/D and f/c)

The blade sections are to have the NACA $\alpha = 0.8$ mean line and the NACA 66 (modified) thickness distribution.

As Example 7 illustrates, the design of a propeller using the circulation theory involves considerable computation. It is therefore customary nowadays to use computers for propeller design based on circulation theory. When computers are used, it is possible to adopt further refinements in the design procedure such as the use of the Lerbs induction factors instead of the Goldstein factors. It is also possible to modify the initial design obtained

by using the lifting line theory to take the lifting surface effects into account more accurately than is possible using the correction factors described here. Modern computer aided propeller design procedures use Computational Fluid Dynamics techniques such as surface panel methods.

As mentioned earlier, there are several different approaches to the design of propellers using the circulation theory. Any one of these approaches may be adopted, including the various corrections that it involves, but it is necessary to verify these propeller designs by model experiments in a cavitation tunnel at least until confidence in the design procedure has been developed.

Problems

1. A twin screw ship with a geared steam turbine propulsion plant has a design speed of 35 knots at which the effective power is 16000 kW. The wake fraction, thrust deduction fraction and relative rotative efficiency based on thrust identity are 0.000, 0.050 and 0.990 respectively. The shafting efficiency is 0.940 and the estimated blade area ratio required is 0.800. The propellers are to have three blades and a diameter of 3.5 m. Determine the total shaft power of the propulsion plant, the propeller rpm and the pitch ratio of the two propellers using the Gawn Series data given below. Do you think that the results are correct? Explain your answer.

$\left[\frac{K_Q}{J^5}\right]^{\frac{1}{4}}$	$\frac{A_D}{A_O} = 0.650$			$\frac{A_D}{A_O} = 0.800$			$\frac{A_D}{A_O} = 0.950$		
	J	P/D	η_O	J	P/D	η_O	J	P/D	η_O
0.3000	1.4364	1.7026	0.8390	1.4560	1.7290	0.8354	1.4858	1.7747	0.8325
0.3500	1.2313	1.4875	0.8092	1.2433	1.5024	0.8044	1.2556	1.5176	0.8000
0.4000	1.0892	1.3490	0.7801	1.0998	1.3620	0.7750	1.1090	1.3721	0.7704
0.4500	0.9817	1.2485	0.7520	0.9924	1.2625	0.7469	1.0025	1.2748	0.7422
0.5000	0.8961	1.1707	0.7253	0.9061	1.1832	0.7201	0.9157	1.1946	0.7155

2. A twin-screw ship has two steam turbines each producing a shaft power of 11500 kW at 3000 rpm. The turbines are connected to the two three-bladed propellers through reduction gearing of ratio 12:1. The shafting efficiency is 0.940. The effective power of the ship is as follows:

Speed, knots	:	30.0	32.0	34.0	36.0	38.0	40.0
Effective Power, kW	:	9329	11693	14457	17658	21337	25533

The wake fraction, thrust deduction fraction and relative rotative efficiency based on thrust identity are 0.000, 0.050 and 0.990 respectively. The depth of immersion of the propeller axes is 3.2 m. Design the propellers using the Gawn Series data given in Problem 1 and the Burrill cavitation criterion for warship propellers.

3. A coaster is to have an engine of 600 kW brake power at 900 rpm connected to the propeller through 5:1 reduction gearing. The shafting efficiency is 0.950. The effective power of the vessel is as follows:

Speed, knots	:	6.0	8.0	10.0	12.0	14.0
Effective power, kW	:	26.8	75.5	168.6	325.0	566.1

The wake fraction, thrust deduction fraction and relative rotative efficiency based on torque identity are respectively 0.270, 0.250 and 1.010. The propeller shaft axis is 1.8 m below the waterline. Design the propeller using the data of Table 9.1 and determine the maximum speed of the vessel.

4. A twin screw ship with geared steam turbine machinery has three-bladed propellers of diameter 3.5 m, pitch ratio 1.5 and blade area ratio 0.85. The open water characteristics of the propellers are as follows:

J	:	1.2000	1.2500	1.3000	1.3500	1.4000
K_T	:	0.2040	0.1780	0.1523	0.1270	0.1022
$10K_Q$:	0.4956	0.4399	0.3854	0.3322	0.2803

At various speeds V , the effective power P_E , the wake fraction w , the thrust deduction fraction t and the relative rotative efficiency η_R (based on thrust identity) are as follows:

V , knots	:	15.0	20.0	25.0	30.0	35.0	40.0
P_E , kW	:	825	2257	4928	9329	16000	25533
w	:	0.040	0.030	0.020	0.010	-0.010	0.010
t	:	0.070	0.065	0.060	0.055	0.050	0.055
η_R	:	0.995	0.995	0.994	0.992	0.990	0.992

The shafting efficiency is 0.940. Determine the shaft power and rpm of the turbines as a function of ship speed, the gear ratio between the turbines and

the propellers being 12:1. Determine also the ship speed at which the turbines run at their rated speed of 3000 rpm and the corresponding shaft power.

5. A single-screw ship has an engine of brake power 5000 kW at 126 rpm directly connected to the propeller of diameter 5.200 m, pitch ratio 0.8430 and blade area ratio 0.502. The shafting efficiency is 0.970. The effective power of the ship in the clean naked hull condition is as follows:

Speed, knots	:	10.0	12.0	14.0	16.0
Effective power, kW:		544.5	1031.2	1769.2	2823.3

The open water characteristics of the propeller may be obtained from Table 9.2. After the ship has been in service for a year, its effective power is found to have increased by 30 percent over the clean naked hull condition, and the wake fraction, thrust deduction fraction and relative rotative efficiency based on thrust identity are 0.250, 0.200 and 1.020 respectively. The roughening of the propeller blade surfaces causes a decrease in K_T of 0.0012 and an increase in K_Q of 0.00013. Determine the maximum speed of the ship in this condition and the corresponding brake power and engine rpm if the maximum torque of the engine is not to be exceeded.

6. A single screw tug has an engine of 900 kW brake power at 600 rpm connected to the propeller through a 4:1 reduction gearbox. The shafting efficiency is 0.950. The wake fraction is 0.200, while the thrust deduction fraction varies linearly with speed with values of 0.050 and 0.180 at zero speed and 12 knots respectively. The relative rotative efficiency is 1.000. The effective power P_E of the tug at different speeds V is as follows:

V , knots:	8.0	9.0	10.0	11.0	12.0	13.0	14.0	15.0
P_E , kW :	68.9	104.1	150.6	210.2	285.0	377.1	488.8	622.3

Design the propeller for maximum bollard pull. Calculate the free running speed of the tug and the corresponding brake power and rpm of the engine. Compare the results obtained with this design and the results of Example 4. Use the data of Table 4.3.

7. Design the propeller for the tug in Problem 6 for maximum free running speed, and determine the bollard pull and the corresponding brake power and engine rpm. Compare these results with those of Problem 6. The optimum propeller diameter is 3.0 m.

8. A single screw fishing trawler has an engine of 1150 kW brake power at 240 rpm directly connected to the propeller. The shafting efficiency is 0.970. The effective power of the trawler is as follows:

Speed, knots	:	2.0	4.0	6.0	8.0	10.0	12.0	14.0
Effective power, kW:		0.44	5.99	27.24	82.30	191.31	381.11	682.51

The wake fraction is 0.180 and the relative rotative efficiency 1.030 based on thrust identity. The thrust deduction fraction varies linearly with speed being 0.075 at 4.0 knots and 0.150 at 14.0 knots. The depth of immersion of the propeller shaft axis is 2.5 m. Design the propeller for full power absorption at the design trawling speed of 4.0 knots, and determine the maximum pull that can be exerted on the trawl gear at this speed. Determine also the free running speed of the trawler and the corresponding brake power. If the resistance of the trawl gear when full of fish is as given in the following table, calculate the maximum speed of the trawler with a full catch and the corresponding brake power and engine rpm.

Speed, knots	:	2.0	4.0	6.0	8.0	10.0
Trawl resistance, kN:		18.66	69.64	150.47	259.92	397.16

Use the data of Table 4.3 and check that the expanded blade area ratio of 0.500 is adequate with the help of Eqn. 9.2.

9. A twin-screw tug has two engines each of brake power 500 kW at 1200 rpm connected to the propellers through a 4:1 reduction gearbox. The propellers are of diameter 2.0 m, pitch ratio 0.700 and blade area ratio 0.500, their open water characteristics being as given in Table 4.3. The effective power of the tug at various speeds is as follows:

Speed, knots	:	2.0	4.0	6.0	8.0	10.0	12.0	14.0
Effective power, kW:		0.04	5.32	23.57	67.74	153.65	300.00	528.23

The wake fraction is 0.100 and the relative rotative efficiency is 0.980 based on torque identity. The thrust deduction fraction varies linearly with speed, being 0.040 at zero speed and 0.100 at 12.0 knots. Determine the maximum towrope pull and the corresponding brake power and engine rpm as a function of speed. Also calculate the speed at which the engines develop the maximum brake power and the free running speed of the tug. The maximum rated torque and rpm of the engines are not to be exceeded.

10. Design the propellers for a twin-screw liner using the lifting line theory with lifting surface corrections. The ship has a design speed of 35.0 knots at which the effective power is 16000 kW. The three-bladed propellers are to have a diameter of 3.5 m and to run at 300 rpm. The propeller shaft centre lines are 3.2 m below the waterline. The wake fraction is 0.000, the thrust deduction fraction 0.050 and the relative rotative efficiency 0.990 based on thrust identity. The wake may be assumed to be uniform. The expanded blade area ratio is estimated to be 0.850 and the blade outline is to be according to Morgan, Silovic and Denny, Table 9.4, with no skew. The blade thickness fraction is to be 0.050 and the tip thickness 0.003 times the propeller diameter with a linear thickness variation. The blade sections are to have NACA $a = 0.8$ mean lines and NACA-16 (modified) thickness distribution. Calculate the required shaft power of the propulsion turbines if the shafting efficiency is 0.940.

CHAPTER 10

Ship Trials and Service Performance

10.1 Introduction

As the construction of a ship nears completion and just after it is complete, a wide range of tests and trials are carried out on the ship. These tests and trials are carried out for quality assurance purposes, to check that the various systems in the ship function properly and to see that the ship meets the requirements of the contract between the ship owner and the shipbuilder. Tests and trials may be divided into (a) shop tests for testing system components, (b) installation tests to see that the systems installed in the ship function as required and meet their specifications, (c) dock trials to observe the operation of the various ship systems in typical operating conditions, and finally (d) sea trials to observe the performance of a ship at sea. Dock trials, which are carried out after the ship has been launched and is nearly complete and after the installation tests are over, establish that the propulsion plant and its auxiliaries are ready for sea trials. Sea trials are often carried out twice: (i) the builder's trials to observe the performance of the ship at sea, to identify any deficiencies and determine how they are to be overcome, and (ii) acceptance trials to demonstrate that the ship meets the contractual requirements. Sea trials include a number of tests that can only be carried out at sea: speed trials, economy power tests, manoeuvring trials, anchor windlass tests, distillation plant tests and calibration of navigation equipment. Dock

trials and speed trials are basically tests of the ship propulsion system. For certain types of ships such as tugs, it is necessary to determine the maximum static pull that the ship can exert; bollard pull trials are carried out for this purpose.

The service performance of a ship is routinely monitored to ensure that it continues to perform efficiently and to decide what remedial actions are to be taken and when. The analysis of service performance data on speed and power can result in several benefits:

- The effect on speed and power of the worsening hull and propeller surfaces can be determined and used to decide upon the most advantageous drydocking, cleaning and painting schedules as well as the time when the propeller must be replaced by one of lower pitch.
- The effect of weather (wind and waves) on ship speed and power can be determined, and this information may be used to decide the optimum route for a ship in given weather conditions.

The analysis of ship trials and service performance data is also useful in the design of future ships.

10.2 Dock Trials

In dock trials, the ship is secured to the pier by mooring lines and the propulsion plant run. Since the ship is stationary, the propeller runs at 100 percent slip, so that the thrust and torque coefficients are much higher than they would be in normal operating conditions. The maximum speed (rpm) at which the engine may be allowed to run is limited by the maximum torque or thrust that is permissible, the allowable loads in the mooring system and the disturbance created by the propeller in the dock or basin in which the dock trials are carried out.

Example 1

A ship has an engine of rating 5000 kW brake power at 120 rpm directly connected to a propeller of 5.0 m diameter and 1.0 pitch ratio. Determine the maximum rpm at which the engine may be run in the dock trials if the maximum rated torque of

the engine is not to be exceeded. The propeller has a K_Q of 0.0600 at $J = 0$. The shafting efficiency is 0.970 and the relative rotative efficiency 1.030 (thrust identity).

$$P_B = 5000 \text{ kW} \quad n = 120 \text{ rpm} = 2.0 \text{ s}^{-1}$$

$$D = 5.000 \text{ m} \quad \frac{P}{D} = 1.000 \quad K_Q = 0.0600 \text{ at } J = 0$$

$$\eta_S = 0.970 \quad \eta_R = 1.030$$

$$P_D = P_B \eta_S = 5000 \times 0.970 = 4850 \text{ kW}$$

Propeller torque at engine rated power:

$$Q = \frac{P_D}{2\pi n} = \frac{4850}{2\pi \times 2.000} = 385.951 \text{ kN m}$$

$$n^2 = \frac{Q \eta_R}{\rho D^5 K_Q} = \frac{385.951 \times 1.030}{1.025 \times 5.0^5 \times 0.0600} = 2.0684$$

$$n = 1.4328 \text{ s}^{-1} = 86.29 \text{ rpm}$$

10.3 Speed Trials

The speed trials of a ship may have many objectives:

- to determine the relationship between ship speed, engine power and propeller rpm at a specified displacement and trim with the ship hull clean and newly painted and the propeller surfaces clean;
- to see that the ship meets its contract requirements of speed, power, rpm and fuel consumption;
- to determine the correlation between the speed-power-rpm relationship predicted from model tests and that obtained in the speed trials.

The speed trials may also be used to calibrate speed logs (instruments to determine the speed of the ship by measuring the relative velocity of water close to the hull) and to determine the relation between ship speed and propeller rpm for use in navigation. Both the speed log calibration and the speed-rpm relationship depend upon the condition of the hull surface and therefore change with time.

The basic procedure for carrying out speed trials is to run the ship several times in opposite directions over a known distance (usually one nautical mile) and measure the time taken to traverse this distance along with measurements of propeller rpm, power and, if possible, thrust. Runs in opposite directions are necessary to eliminate the effect of currents in the water and obtain the true speed of the ship through the water. It is important to carry out the speed trials in good weather with low winds and a calm sea.

The "measured mile" over which the speed trials are carried out must fulfil certain requirements:

- The depth of water on the trials course should be sufficient to ensure that there are no shallow water effects. A depth of water exceeding twenty times the draught of the ship is normally recommended. For high speed ships even this may be insufficient and a criterion involving ship speed must be used, e.g. $h \geq 30F_n T$, where h is the depth of water, F_n the Froude number and T the draught.
- The measured mile should be close enough to the shore to allow the range beacons that define the measured mile to be clearly observed in good weather.
- There should be sufficient space for the ship to turn at the end of a run in either direction and attain a steady speed during the approach to the measured mile in the opposite direction. The length of approach required depends upon the size and speed of the ship and must be sufficient to allow 99.8 percent of the required speed to be attained before the ship reaches the start of the measured mile.
- The trials area should be sheltered, and be close to a good anchorage and near shipbuilding centres.

- It should be possible to ensure that there is no other traffic in the area during the trials.
- The current in the water should be small and not subject to sudden and large changes in magnitude and direction.

A measured mile meeting all these requirements is difficult to find, particularly for very large ships. Since the measured mile is required basically for determining the speed of the ship accurately, alternative methods of speed measurement are necessary if one is to dispense with the measured mile. Two methods which are increasingly being adopted today are the use of shore based radio positioning systems and satellite navigation systems which allow the position of a ship at any instant to be determined with sufficient accuracy. The use of such systems allows speed trials to be carried out in water of adequate depth, with the direction of the runs chosen to minimise the effect of the wind and waves, and at locations close to the shipyard.

Speed trials may be carried out only at the highest speed to demonstrate that the ship meets its contractual obligations. However, it is more useful to carry out "progressive speed trials" in which groups of runs are made at engine power settings between half full power and full power. At least four engine settings should be used, more if the speed of the ship is very high. There should be a minimum of two runs, one in each direction at each engine setting, preferably three and even four or five at the highest power. However, the trials should be completed without interruption, and there should be no break in the sequence of runs at any one engine setting so that the runs in each group occur at approximately equal intervals of time.

Just before the speed trials, the ship is surveyed to see that the propeller is clean and polished and the hull is in the standard clean, newly painted condition. The hull roughness is measured. The weather for the trials should be good with a minimum of wind and waves in the sea.

When the ship is ready for the trials to commence and the engine has warmed up, the ship proceeds on the prescribed course. As the approach buoy is reached (2-3 miles from the start of the measured mile), the ship is steadied on the course, the engine rpm is fixed and the rudder is used as little as possible so that a constant speed is attained by the beginning of the measured mile. At the end of the measured mile, the ship turns slightly

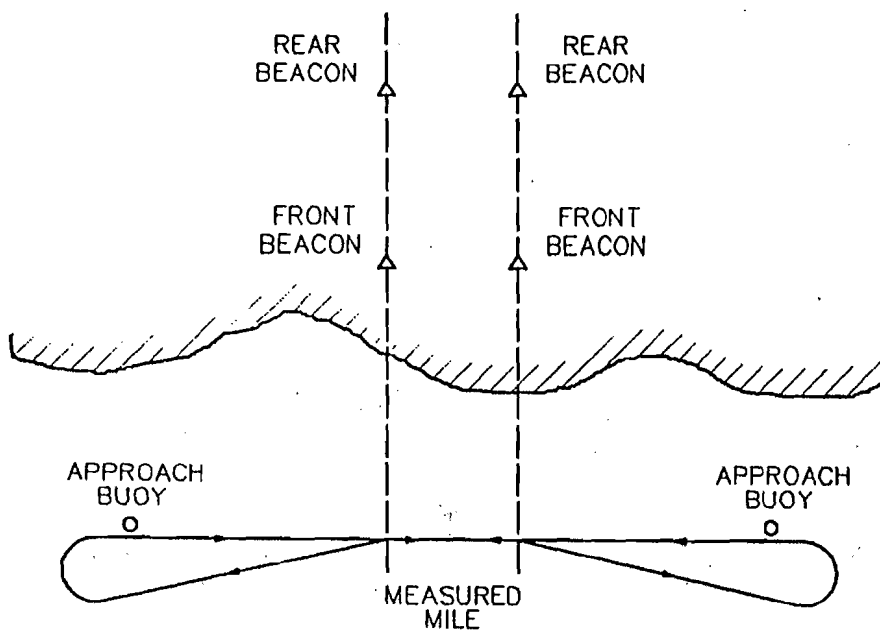


Figure 10.1 : Measured Mile.

and proceeds some two or three miles further before turning to traverse the measured mile in the opposite direction, as shown in Fig. 10.1.

The following are the observations made in the speed trials:

- the draughts of the ship forward and aft just before and just after the trials;
- the temperature and density of the water on the trials course;
- the condition of the sea;
- in each run:
 - the direction of the run;
 - the time of day at the start of the measured mile;
 - elapsed time over the measured mile, or the speed of the ship;

- the average propeller rpm, or the total number of revolutions over the measured mile;
 - the corresponding engine power;
 - the relative wind velocity and direction;
 - the propeller thrust, if possible;
 - large rudder angles, if any;
- the consumption of consumables and the addition of water ballast and its redistribution.

If the trials are carried out on a measured mile, the time over the mile is measured independently by three or four observers who start their stop watches when the rear and forward beacons at the start come in line and stop them when the beacons at the end of the measured mile come in line. The readings of the independent observers should agree. Radio positioning and satellite navigation systems allow the time taken to traverse a given distance to be automatically recorded.

The engine power may be measured by indicators fitted to each cylinder of the main (diesel) engine. Indicators give the indicated power, and to obtain the brake power the mechanical efficiency determined in the engine test-bed trials must be used. It is preferable to measure the power by a torsionmeter fitted on the propeller shaft. It is necessary to correct the torsionmeter readings for the residual torque in the propeller shaft. The "torsionmeter zero" is determined in turbine ships by allowing the shaft to coast to a stop after running at a moderate speed ahead and then astern and taking the average of the minimum ahead torque and the minimum astern torque as the zero reading. In diesel ships, the propeller shaft is turned first ahead and then astern by the engine turning gear, and the zero reading taken as the average of the readings after the ahead and the astern revolutions. In a ship fitted with an electrical drive, the power may be determined from the power consumption of the drive motor. Finally, the measured power must be multiplied by an estimated shafting efficiency to obtain the delivered power.

Ships are not usually fitted with thrust meters, but thrust measurements are necessary for a complete analysis of the trial results. Appropriate instruments such as a revolution counter, a wind vane and an anemometer are provided to measure the other parameters.

Running plots of P_S/n^3 versus V/n and of V/n versus the time of day at mid-run are made during the trials to check for errors in measurement or in recording the data. P_S is the shaft power, n the propeller revolution rate and V the ship speed.

The ship speed obtained from the measurement of the elapsed time over the measured mile is the speed over the ground. What is needed, however, is the speed of the ship through the water, i.e. the speed over the ground corrected for the speed of the current in the water. When three or more runs in opposite directions are made at a constant power setting, the correct speed through the water is usually obtained by determining the "mean of means" of the individual values of speed, as illustrated in the following example.

Example 2

Four runs in opposite directions are made by a ship over a measured mile at constant power and the following times are recorded. Determine the speed of the ship through the water at this power and the speed of the current to the North in each run.

Run No.	1	2	3	4
Direction	N	S	N	S
Time over mile, secs	208.0	158.8	203.1	167.2

Run No.	Direction	Time s	V_G knots	Mean of Means		Speed through water, V_W knots	Speed of Current, V_C knots
				1	2		
1	N	208.0	17.308	19.9890			-2.695 N
2	S	158.8	22.670		20.0932		-2.667 N
				20.1975		20.003	
3	N	203.1	17.725		19.9128		-2.278 N
				19.6280			
4	S	167.2	21.531				-1.528 N

$$\text{Speed over ground, } V_G = \frac{3600}{\text{Time in secs}} \text{ knots}$$

$$\text{Speed of current to the North, } V_C = \pm(V_G - V_W) \text{ +for N runs, -for S runs.}$$

The use of the "mean of means" method to determine the speed through the water is based on the assumption that the speed of the current V_C can be expressed as a polynomial:

$$V_C = a_0 + a_1\hat{t} + a_2\hat{t}^2 + \dots \quad (10.1)$$

where \hat{t} is the time measured from some fixed instant, the degree of the polynomial being one less than the number of speed readings. Thus, if there are three values of the speed over the ground, it is assumed that $V_C = a_0 + a_1\hat{t} + a_2\hat{t}^2$. It can be shown that if the intervals between the runs are equal the mean of means gives the correct speed through the water. This is the reason for the requirement that all the runs for a particular engine setting be completed in an unbroken sequence without interruption.

In trials in which only two runs, one in each direction, are made at each engine setting, and in cases where the time interval between consecutive runs is far from being constant, a different method of correcting for the effect of the current in the water may be used. In this method two curves of V/n , one for each direction, are drawn separately as a function of the time of day at mid-run, and a mean between the two curves is taken to give the corrected speed through the water. The procedure is used in the next example, which illustrates a method of analysing speed trials data.

Example 3

The following are the observations made in the speed trials of a tanker in which two runs in opposite directions were taken at each engine setting:

Run No.	:	1	2	3	4	5	6
Direction	:	E	W	E	W	E	W
Time at start, hr-min:		07-46	09-19	10-01	10-48	11-47	12-22
Time on mile, secs	:	277.2	252.6	247.2	223.8	223.8	213.0
Total revolutions	:	397	363	413	369	407	380
Shaft power, kW	:	4556	4592	7908	7996	10626	10552

Run No.	:	7	8	9	10	11	12
Direction	:	E	W	W	E	W	E
Time at start, hr-min:		13-28	14-03	16-02	16-45	17-56	18-32
Time on mile, secs	:	213.6	212.4	210.0	198.0	201.0	197.4
Total revolutions	:	399	398	421	396	422	412
Shaft power, kW	:	11484	11498	13952	14154	16890	16742

The ship has a propeller of 6.5 m diameter and 0.8 pitch ratio, whose open water characteristics are as given in Table 4.3. The effective power of the ship estimated from model tests is as follows:

Speed, knots	:	12.0	14.0	16.0	18.0	20.0
Effective power, kW:		1530	3062	5584	9486	15241

Analyse these trial trip data.

The calculations are carried out in the following table:

Run No.	:	1	2	3	4	5	6
Direction	:	E	W	E	W	E	W
Start time,	hr-min:	07-46	09-19	10-01	10-48	11-47	12-22
Time on mile,	s:	277.2	252.6	247.2	223.8	223.8	213.0
Total revolutions	:	397	363	413	369	407	380
Shaft power, P_S	kW:	4556	4592	7908	7996	10626	10552
Speed over ground, V_G	knots:	12.987	14.252	14.563	16.086	16.086	16.901
	ms^{-1} :	6.6805	7.3311	7.4913	8.2745	8.2745	8.6914
Revolution rate, n	s^{-1} :	1.4322	1.4371	1.6707	1.6488	1.8186	1.7840
	rpm:	85.93	86.22	100.24	98.93	109.12	107.04
V_G/n	m:	4.6645	5.1013	4.4839	5.0185	4.5499	4.8734
Time at mid-run,	hr:	7.8052	9.3518	10.0510	10.8311	11.8144	12.3962
Mean V/n	m:	4.9147	4.7967	4.7756	4.7607	4.7425	4.7279
Speed through water, V_W	ms^{-1} :	7.0388	6.8933	7.9786	7.8494	8.6247	8.4346
	knots:	13.684	13.401	15.510	15.259	16.767	16.397
Speed of current, V_C (East),	ms^{-1} :	-0.3583	-0.4378	-0.4873	-0.4251	-0.3502	-0.2595
	knots:	-0.697	-0.851	-0.947	-0.826	-0.681	-0.504

Run No.	:	7	8	9	10	11	12
Direction	:	E	W	W	E	W	E
Start time,	hr-min:	13-28	14-03	16-02	16-45	17-56	18-32
Time on mile,	s:	213.6	212.4	210.0	198.0	201.0	197.4
Total revolutions	:	399	398	421	396	422	412
Shaft power, P_S	kW:	11484	11498	13952	14154	16890	16742
Speed over ground, V_G	knots:	16.854	16.949	17.143	18.182	17.910	18.237
	ms^{-1} :	8.6697	8.7186	8.8183	9.3527	9.2131	9.3812
Revolution rate, n	s^{-1} :	1.8680	1.8738	2.0048	2.0000	2.0995	2.0871
	rpm:	112.08	112.43	120.29	120.00	125.97	125.23
V_G/n	m:	4.6412	4.6529	4.3986	4.6764	4.3882	4.4948
Time at mid-run,	hr:	13.4963	14.0795	16.0625	16.7775	17.9612	18.5608

Mean V/n	m:	4.6878	4.6599	4.5482	4.5133	4.4848	4.4930
Speed through water, ms^{-1} :		8.7568	8.7317	9.1182	9.0266	9.4158	9.3773
V_W	knots:	17.023	16.975	17.726	17.548	18.305	18.230
Speed of current, ms^{-1} :		-0.0871	0.0131	0.2999	0.3261	0.2027	0.0039
V_C (East),	knots:	-0.169	0.025	0.583	0.634	0.394	0.008

In this table, the speed over the ground V_G is obtained by dividing the distance 1 nautical mile by the time over the measured mile, the propeller revolution rate n by dividing the total revolutions over the measured mile by the time over the measured mile, and the time at mid-run by adding half the time on the measured mile to the time of day at the start of the measured mile, taking care of the appropriate units in each case. The values of V_G/n are plotted as a function of the time at mid-run separately for the East runs and the West runs, and the mean curve between these two obtained. This mean curve is taken to give the value of V/n corrected for the influence of the current. The speed through water V_W for each run is then obtained from the mean V/n curve, and the speed of the current is given by:

$$V_C = \pm(V_G - V_W)$$

the positive sign being for runs in one direction and the negative sign for the runs in the opposite direction. The subsequent analysis is carried out as given in the following table.

Run No.	:	1 & 2	3 & 4	5 & 6	7 & 8	9 & 10	11 & 12
Mean V , ms^{-1} :		6.9661	7.9140	8.5296	8.7442	9.0724	9.3966
	knots:	13.542	15.385	16.582	16.999	17.637	18.267
Mean n , s^{-1} :		1.4346	1.6598	1.8013	1.8709	2.0024	2.0933
	rpm:	86.08	99.58	108.08	112.25	120.14	125.60
Mean P_S , kW:		4574	7952	10589	11491	14053	16816
P_D , kW:		4437	7713	10271	11146	13631	16312
P_E , kW:		2636	4681	6558	7333	8655	10136
η_D (qpc)	:	0.5941	0.6069	0.6385	0.6579	0.6349	0.6214
$10K_{QB}$:	0.2011	0.2257	0.2352	0.2278	0.2272	0.2380
J	:	0.5699	0.5166	0.4952	0.5119	0.5132	0.4889
K_T	:	0.1402	0.1636	0.1727	0.1656	0.1651	0.1754
η_O	:	0.6323	0.5960	0.5787	0.5923	0.5935	0.5734
V_A ms^{-1} :		5.3143	5.5734	5.7980	6.2251	6.6796	6.6522
w_Q	:	0.2371	0.2957	0.3202	0.2881	0.2637	0.2921
$\eta_H \eta_R$:	0.9396	1.0183	1.1033	1.1464	1.0698	1.0837

The mean values of V , n and P_S for each pair of runs have been obtained from the previous table, and:

$$P_D = P_S \eta_S \quad P_E \text{ from the } P_E - V \text{ curve} \quad \eta_D = \frac{P_E}{P_D}$$

$$K_{QB} = \frac{P_D}{2\pi \rho n^3 D^5} \quad J \text{ and } K_T \text{ from torque identity}$$

$$\eta_O = \frac{K_T}{K_Q} \frac{J}{2\pi} \quad V_A = J n D \quad w_Q = 1 - \frac{V_A}{V} \quad \eta_H \eta_R = \frac{\eta_D}{\eta_O}$$

When the thrust is not measured during the trials, the wake fraction may be determined only by torque identity. Also, it is not possible to determine individually the hull efficiency and the relative rotative efficiency. However, if one adopts an assumed value of the relative rotative efficiency (or the thrust deduction fraction), for example on the basis of model test data, the trial results can be analysed using thrust identity also, and the individual components of the propulsive efficiency determined.

In the method used in Example 3 for determining the correct speed through the water by obtaining a mean curve between the curves of V/n for the two opposite directions as a function of the time-of-day, it is assumed that the effects of the wind on the performance of the ship for the two directions cancel each other. The power-rpm-speed relation that is thus obtained refers to the performance of the ship in still air. However, the assumption that the effect of the wind on performance can be eliminated simultaneously with the effect of the current in the water by taking a mean between two runs in opposite directions is not strictly correct. The current in the water only affects the speed of the ship over the ground whereas the wind affects the resistance of the ship and hence the speed, power and propeller rpm. Moreover, particularly for ship-model correlation purposes, it is necessary to determine the performance of the ship for the "no air" condition which corresponds closely to the conditions of the model test. Therefore, a different and slightly more complex method may be used to correct for the effect of the wind.

The method that is generally used is to estimate the air and wind resistance R_{AA} from the measured relative wind velocity and direction, calculate the increase in effective power ΔP_E , and to make a corresponding increase ΔV in the speed of the ship over the ground. The air and wind resistance may be determined from model tests in a wind tunnel, or estimated by empirical methods based on such tests, e.g.:

$$R_{AA} = C_D k_w \frac{1}{2} \rho_a A_T V_{rw}^2 \quad (10.2)$$

where:

C_D = drag coefficient;

k_w = wind direction coefficient;

ρ_a = density of air;

A_T = equivalent transverse projected area of the ship above water equal to 0.3 times the transverse projected area of the main hull above water plus the transverse projected area of the superstructure above the main hull;

V_{rw} = relative wind velocity.

The density of air is 1.226 kg per m³ (at 15° C). The values of C_D and k_w depend upon the shape of the ship above water, typical values being:

$$\begin{aligned} C_D &= 1.2 \\ k_w &= a_0 + a_1 \theta + a_2 \theta^2 + a_3 \theta^3 \end{aligned} \quad (10.3)$$

where:

$$a_0 = 1.000 \quad a_1 = 2.769 \times 10^{-2} \quad a_2 = -6.248 \times 10^{-4} \quad a_3 = 2.309 \times 10^{-6}$$

θ = angle in degrees of the relative wind off the bow of the ship.

The method of analysing speed trials data to obtain the "no air" condition is illustrated in the following example.

Example 4

The following data are obtained from the speed trials of a ship for four runs at the highest power setting:

Run No.	:	16	17	18	19
Direction	:	N	S	N	S
Time at start of the measured mile, hr-min:	:	15-49	16-21	16-55	17-30
Time on the measured mile, s	:	146.8	155.3	147.5	152.6
Average propeller rpm	:	113.7	112.8	113.3	112.5
Average shaft power, kW	:	21385	21272	21304	21268
Average thrust, kN	:	1512	1495	1507	1492
Relative wind velocity, ms ⁻¹	:	17.128	8.281	18.025	9.576
Relative wind direction off the bow, deg	:	10.63	34.05	16.99	31.95

The ship has a propeller of 7.0 m diameter and 1.0 pitch ratio whose open water characteristics may be taken from Table 4.3. The transverse projected area of the ship above water consists of 120 m² of the main hull and 176.5 m² of the superstructure. The effective power of the ship in the condition of the trials is as follows:

Speed, knots	:	20	22	24	26
Effective power, kW	:	6788	10325	15140	21532

Analyse these data.

Run No.	Direction	Time at Start hr-min	Time on Mile s	Observed Speed, V_O knots	ms^{-1}
16	N	15-49	146.8	24.523	12.6147
17	S	16-21	155.3	23.181	11.9243
18	N	16-55	147.5	24.407	12.5548
19	S	17-30	152.6	23.591	12.1353
Mean of means				23.860	12.2734

Run No.	Relative Wind Speed V_{rw} ms^{-1}	Relative Wind Direction, θ deg	Wind Direction Coefficient, k_w	Wind Resistance R_{AA} kN
16	17.128	10.63	1.2265	56.245
17	8.281	34.05	1.3096	14.038
18	18.025	16.99	1.3014	66.094
19	9.576	31.95	1.3222	18.952

Run No.	Increase in Effective Power due to Wind ΔP_E kW	Slope of Effective Power Curve $\Delta P_E/\Delta V$ kW/knot	Wind Correction to Speed ΔV knots	Corrected Speed over Ground V_G knots ms^{-1}	
16	709.51	2721	0.261	24.784	12.7489
17	167.39		0.062	23.243	11.9562
18	829.80		0.305	24.712	12.7119
19	229.99		0.085	23.676	12.1789
Mean of means				24.041	12.3665

Run No.	Propeller Revolutions		Average	Speed through Water		Speed of Current	Time at Mid-run
	n		$\frac{n}{V}$	V_W		V_C	
	rpm	s ⁻¹	m ⁻¹	m s ⁻¹	knots	m s ⁻¹	hr
16	113.7	1.8950		12.4326	24.176	0.3127 N	15.837
17	112.8	1.8800		12.3378	23.985	0.3816 N	16.372
18	113.3	1.8883	0.152377	12.3925	24.091	0.3194 N	16.937
19	112.5	1.8750		12.3050	23.921	0.1261 N	17.521
Mean of means	113.06	1.8844		12.3665	24.041		

Run No.	Shaft Power	Propeller Thrust
	P_S	T
	kW	kN
16	21385	1512
17	21272	1495
18	21304	1507
19	21268	1492
Mean of means	21298	1501

Notes

$$V_O = \frac{3600}{\text{Time on mile, s}} \text{ knots}$$

k_w from Eqn. (10.3)

Equivalent transverse projected area above water

$$A_T = 0.3 \times 120 + 176.5 = 212.5 \text{ m}^2$$

$$R_{AA} = C_D k_w \frac{1}{2} \rho_a A_T V_{rw}^2 = 1.2 k_w \times \frac{1}{2} \times \frac{1.226}{1000} \times 212.5 \times V_{rw}^2 \text{ kN}$$

$$\Delta P_E = R_{AA} V_O$$

$\frac{\Delta P_E}{\Delta V}$ from Effective Power-Speed curve at the mean speed

$$\Delta V = \frac{\Delta P_E}{\Delta P_E / \Delta V}$$

$$V_G = V_O + \Delta V$$

$$\text{Average } \frac{n}{V} = \frac{1.8844}{12.3665} = 0.152377 \text{ m}^{-1}$$

$$V_W = \frac{n}{\text{Average } \frac{n}{V}}$$

$$\begin{aligned} V_C &= V_G - V_W \text{ for N runs} \\ &= V_W - V_G \text{ for S runs} \end{aligned}$$

Time at mid-run = Time at start + $\frac{1}{2} \times$ Time on mile

Average values for this group of runs:

$$V = 12.3665 \text{ m s}^{-1} = 24.041 \text{ k}$$

$$n = 1.8844 \text{ s}^{-1} = 113.1 \text{ rpm}$$

$$P_S = 21298 \text{ kW} \quad P_D = P_S \eta_S = 21298 \times 0.970 = 20659 \text{ kW}$$

$$T = 1501 \text{ kN}$$

$$P_E = 15254 \text{ kW (from } P_E - V \text{ curve)}$$

$$R_T = \frac{P_E}{V} = \frac{15254}{12.3665} = 1233 \text{ kN}$$

$$K_{QB} = \frac{P_D}{2\pi \rho n^3 D^5} = \frac{20659}{2\pi \times 1.025 \times 1.8844^3 \times 7.0^5} = 0.02852$$

$$K_{TB} = \frac{T}{\rho n^2 D^4} = \frac{1501}{1.025 \times 1.8844^2 \times 7.0^4} = 0.1718$$

Torque identity:

$$K_Q = K_{QB} = 0.02852 \quad J = 0.7209 \quad K_T = 0.1686$$

$$\eta_O = \frac{K_T}{K_Q} \frac{J}{2\pi} = \frac{0.1686}{0.02852} \times \frac{0.7209}{2\pi} = 0.6783$$

$$V_A = J n D = 0.7209 \times 1.8844 \times 7.0 = 9.5092 \text{ m s}^{-1}$$

$$w_Q = 1 - \frac{V_A}{V} = 1 - \frac{9.5092}{12.3665} = 0.2311$$

$$t = 1 - \frac{R_T}{T} = 1 - \frac{1233}{1501} = 0.1785$$

$$\eta_H = \frac{1-t}{1-w} = \frac{0.8215}{0.7689} = 1.0684$$

$$\eta_R = \frac{K_{TB}}{K_T} = \frac{0.1718}{0.1686} = 1.0190$$

$$\eta_D = \eta_O \eta_R \eta_H = 0.6783 \times 1.0190 \times 1.0684 = 0.7385$$

$$= \frac{P_E}{P_D} = \frac{15254}{20659} = 0.7384$$

Thrust identity:

$$K_T = K_{TB} = 0.1718 \quad J = 0.7140 \quad K_Q = 0.02893$$

$$\eta_O = \frac{K_T}{K_Q} \frac{J}{2\pi} = 0.6748$$

$$V_A = J n D = 0.7140 \times 1.8844 \times 7.0 = 9.4182 \text{ ms}^{-1}$$

$$w_T = 1 - \frac{V_A}{V} = 1 - \frac{9.4182}{12.3665} = 0.2384$$

$$t = 0.1785$$

$$\eta_H = \frac{1-t}{1-w} = \frac{0.8215}{0.7616} = 1.0787$$

$$\eta_R = \frac{K_Q}{K_{QB}} = \frac{0.02893}{0.02852} = 1.0144$$

$$\eta_D = \eta_O \eta_R \eta_H = 0.6748 \times 1.0144 \times 1.0787 = 0.7384$$

As this example shows, if the propeller thrust is measured during the trials, it is possible to analyse the results by both thrust identity and torque identity, and to obtain the individual components of the propulsive efficiency. It is, however, necessary to have an estimated value of the effective power based on model tests and a suitable correlation allowance. Alternatively, one may assume that the propulsion factors based on model tests after suitable corrections for scale effects apply to the ship on trials, and determine the correlation allowance on effective power determined from model tests.

10.4 Bollard Pull Trials

Bollard pull trials are carried out to determine the maximum static pull that can be exerted by a vessel used for towing duties, e.g. a tug. The tug is attached by a long towline to a bollard on the quayside. A load cell or other device to measure the tension in the towline is inserted at the bollard end of the towline. The propeller is run slowly at first until the towline becomes taut and then quickly brought up to the maximum rpm that can be achieved without exceeding the specified or the maximum permissible torque or rpm of the engine. The bollard pull (i.e. the tension in the towline indicated by the load cell), the propeller rpm and the engine power are measured. If necessary, special instruments may be fitted to the propeller shafting to measure rpm and power. The bollard pull rises sharply as the propeller rpm is increased initially and becomes steady when the rpm becomes constant, although there is usually a small cyclic variation caused by oscillations in the towline and by rudder movements needed to keep the vessel in a fixed position. After some time however, the disturbance imparted to the water by the propeller is reflected back to the vessel by the quay walls, and this usually causes the bollard pull to fall. It is therefore important to have a sufficiently long towline (at least two ship lengths) and to position the vessel with respect to the quay walls in such a way as to delay and minimise the reflection of the disturbance as much as possible. The vessel should also be well clear of the shore and the depth of water should be sufficient (at least twice the draught aft). As far as possible, bollard pull trials should be carried out in a location such that the effects of currents, tides, waves and wind are minimal. It is also desirable to have sufficient space to allow for the slight sideways oscillation of the vessel that often occurs during the bollard pull trial, and to allow the vessel to stop safely in case the towline parts.

10.5 Service Performance Analysis

The propulsive performance of a ship at sea is determined by the relation between the ship speed, the engine power and the propeller revolution rate. The relationship depends basically upon three parameters: (i) the displacement and trim of the ship, (ii) the environmental conditions, and (iii) the condition of the hull surface and the propeller. It is therefore necessary to

measure and record the speed, power and propeller rpm together with values of displacement and trim, measures representing the environmental conditions (wind and waves) and the condition of the hull and propeller of the ship in service. The data so collected can be analysed to find the effect of displacement and trim, wind and waves, and hull and propeller condition on the speed-power-rpm relationship. The results of such service performance analyses can then be used to devise methods to operate ships in an optimum manner.

Unfortunately, there are many difficulties in obtaining reliable service performance data unless special instrumentation and specially trained personnel are provided on board the ship. The development of automatic data logging equipment has greatly improved the reliability of the data on engine power and propeller rpm, but the measurement of ship speed is still problematic. The speed is usually determined by observation of the ship's position at regular intervals, e.g. once every watch. This speed must then be corrected for the currents in the water on the basis of ocean current data. Alternatively, one may determine ship speed by using a speed log but this depends upon the calibration of the log, which changes with time. A third method is to use what is known as the Dutchman's log in which objects are dropped into the sea sufficiently far from the ship and the time taken for them to float a known distance past the ship determined. In modern times, one may use satellite global positioning systems to determine ship speed.

The displacement and trim of the ship can be determined accurately at the start and the end of a voyage, and a record of the consumption of fuel, water, provisions etc. provides reasonably accurate estimates of displacement and trim during the voyage. The condition of the hull surface and the propeller can only be determined when the ship is dry-docked, and the average hull roughness and the roughness of the propeller surface measured. It is, however, more convenient to represent the condition of the hull and propeller in terms of the "number of days out of dry-dock" for the purpose of service performance analysis. This simple criterion ignores the effect of such factors as the number of days in port and at sea, and the number of days in tropical waters and in temperate waters, which affect the rate of fouling and hence the condition of the hull surface. However, for a ship following a more or less fixed route and voyage schedule, days out of dry-dock is a sufficiently accurate measure of hull and propeller condition.

Numerical measures of the environmental conditions in which a ship operates are also necessary for the analysis of service performance. The wind speed and direction relative to the ship are measured by an anemometer and wind vane on board, and the true wind velocity then determined. The average wave height and the wave direction relative to the ship are usually estimated by the ship staff. The effect of wind on speed and power can be determined with the help of model tests in a wind tunnel. Similarly, model tests in waves can be used to estimate the effect of waves on speed and power. Such model test data are not always available, and normally much simpler methods are used for service performance analysis. The true wind speed is related to the Beaufort number, which is widely used as a measure of the environmental conditions, and this together with a wave direction factor may be used to obtain a "weather number" for the purpose of analysis.

Service performance data consisting of observations of power, speed and rpm and values of displacement and trim together with days out of dry-dock and estimated wind and wave conditions must then be analysed. The object of the analysis is to separate out the effects of the three major factors: displacement, weather and days out of dry-dock. There are two approaches to the problem, the first involving heuristic methods and the other using statistical methods.

In the heuristic methods, the data are first corrected to a standard displacement and speed. This may be done using model test data for different displacements and trims, but more usually it is assumed that the power is related to displacement and speed as follows:

$$P_S \propto \Delta^{\frac{2}{3}} V^3 \quad (10.4)$$

Other formulas for correcting power to a standard displacement are:

$$\frac{P_{S1}}{P_{S0}} = 0.65 \frac{\Delta_1}{\Delta_0} + 0.35 \quad (10.5)$$

and:

$$\frac{P_{S1}}{P_{S0}} = \frac{\nabla_1/S_1}{\nabla_0/S_0} \quad (10.6)$$

where P_S is the shaft power, Δ the displacement, ∇ the displacement volume and S the wetted surface, the subscripts 0 and 1 referring to the standard and any other displacement respectively. The effect of displacement on the power may also be obtained directly from the service performance data by plotting a power coefficient such as $\Delta^{2/3} V^3 / P_S$ as a function of displacement and drawing a trend line. It is preferable to consider the loaded and the ballast voyages separately since these simple methods may not be able to cater to large changes in displacement and trim.

The effect of weather must then be determined. For this purpose, it is necessary to devise a numerical measure of the weather conditions for the period during which power, speed and rpm are measured. A simple method is to use the Beaufort number (based on the true wind speed) together with a wind direction factor. Alternatively, the power corrected to a standard displacement and speed can be plotted as a function of the Beaufort number for different wind directions, viz. ahead, bow quarter, stern quarter and astern. Another method is to classify the weather encountered into groups, assign a numerical value to each group, and obtain a weighted average of the weather number for each voyage. Burrill (1960), for example, divides the weather into four groups—good (0–25), moderate (25–50), heavy (50–75) and very heavy (75–100), and derives a “weather intensity factor”:

$$W = \frac{\sum d_i w_i}{\sum d_i} \quad (10.7)$$

where W is the weather intensity factor and d_i the number of days in which the weather had a numerical value w_i (12.5 for good, 37.5 for moderate, 62.5 for heavy and 87.5 for very heavy weather) in a particular voyage. The average value of the Admiralty Coefficient $\Delta^{2/3} V^3 / P_S$ for each voyage is then plotted as a function of W , and the mean curve through the points then gives the effect of weather on the ship's performance. Once the effect of weather on the power at a given displacement and speed has been determined by one of the methods described in the foregoing, the power can be corrected to a specific weather condition, e.g. to still air and calm sea conditions, or perhaps “moderate” weather.

Finally, the power corrected to a standard displacement and speed and to a specific weather condition can be plotted as a function of days out of dry-dock to determine the effect of hull and propeller condition on power.

When this is done over several dry-docking cycles, it is observed that the cleaning and painting of the hull does not bring the performance of the ship back to the level at the end of the previous dry-docking. Thus, the effect of time in service on the performance of a ship can be divided into two components, the effect of fouling of the hull surface which is removed when the ship is dry-docked, and the effect of permanent hull deterioration which cannot be eliminated by cleaning and painting of the hull surface and which grows slowly but steadily as the ship ages.

One may also calculate the values of P_S/n^3 and V/n for each set of measurements and then determine the wake fraction based on torque identity with the help of the open water characteristics of the propeller. If the values of power are corrected to standard displacement, speed and weather conditions, the effect of hull surface conditions on the wake fraction may be determined.

Example 5

A ship of design displacement 19000 tonnes and speed 16.5 k has an engine of 9500 kW at 130 rpm directly connected to a propeller of diameter 5.5 m and pitch ratio 0.75. The open water characteristics of the propeller are as follows:

J	:	0	0.100	0.200	0.300	0.400	0.500	0.600	0.700	0.800
K_T	:	0.328	0.301	0.270	0.237	0.200	0.160	0.116	0.070	0.020
$10K_Q$:	0.366	0.346	0.320	0.290	0.255	0.215	0.170	0.120	0.065

The following data are collected for the first two years of service during which the ship made 25 voyages and was dry-docked at the end of 383 days for a period of 15 days for cleaning and painting of the hull and routine maintenance.

Voyage No.	Days in Service d_0	Displacement Δ tonnes	Voyage Averages			Weather
			Speed V knots	Shaft Power P_S kW	Propeller Rpm n	
1	15	18100	16.7	6680	130.1	Good
2	45	18400	16.4	7090	130.9	Moderate
3	73	17500	16.3	6750	129.1	Moderate
4	101	18200	16.0	7360	131.2	Heavy
5	133	18100	15.8	8050	133.3	Very Heavy

Voyage No.	Days in Service d_0	Displacement Δ tonnes	Voyage Averages			Weather
			Speed V knots	Shaft Power P_s kW	Propeller Rpm n	
6	164	18800	16.4	6750	128.5	Good
7	194	17900	15.9	7360	129.8	Heavy
8	223	17600	16.1	6810	127.8	Moderate
9	253	18200	16.0	6850	127.8	Moderate
10	284	18300	15.7	7310	129.2	Heavy
11	313	18600	15.7	7460	129.6	Heavy
12	342	17900	16.1	6340	125.1	Good
13	369	18100	16.0	6290	124.7	Good
14	416	18400	16.6	6790	129.8	Good
15	448	17400	16.1	7410	130.9	Heavy
16	478	18600	16.0	7720	131.6	Heavy
17	508	18000	15.8	8250	133.7	Very Heavy
18	537	17800	16.2	7010	128.5	Moderate
19	567	18200	16.1	7060	128.6	Moderate
20	595	18800	15.8	7660	130.3	Heavy
21	628	17700	15.6	8160	132.2	Very Heavy
22	656	17600	15.9	6780	126.6	Moderate
23	685	18200	15.9	7020	127.2	Moderate
24	713	18300	16.0	6480	125.1	Good
25	744	17900	15.4	8110	131.2	Heavy

Analyse these data.

A method of analysing these data is given in the following table:

Voyage No.	Days out of Dry-dock d_1	Weather Number W	$\frac{\Delta^{\frac{2}{3}} V^3}{P_s}$	$\frac{\Delta^{\frac{2}{3}} V^3}{P_s^*}$	P_s^* kW	$\frac{V}{nD}$	$10K_{QB}$	J	w_Q
1	15	12.5	481	436	6476	0.7203	0.1961	0.5405	0.2496
2	45	37.5	434	434	6512	0.7031	0.2043	0.5198	0.2607
3	73	37.5	432	432	6529	0.7085	0.2028	0.5237	0.2608
4	101	62.5	385	428	6591	0.6843	0.2107	0.5036	0.2641
5	133	87.5	338	424	6652	0.6651	0.2197	0.4800	0.2783
6	164	12.5	462	419	6744	0.7162	0.2056	0.5165	0.2789
7	194	62.5	374	417	6770	0.6874	0.2176	0.4857	0.2935
8	223	37.5	415	415	6810	0.7069	0.2109	0.5030	0.2885
9	253	37.5	414	414	6825	0.7026	0.2121	0.4998	0.2886

Voyage No.	Days out of Dry-dock d_1	Weather Number W	$\frac{\Delta^{2/3} V^3}{P_S}$	$\frac{\Delta^{2/3} V^3}{P_S^*}$	P_S^* kW	$\frac{V}{nD}$	$10K_{QB}$	J	w_Q
10	284	62.5	368	411	6870	0.6819	0.2121	0.4816	0.2937
11	313	62.5	364	408	6929	0.6798	0.2215	0.4752	0.3010
12	342	12.5	450	407	6937	0.7222	0.2093	0.5070	0.2980
13	369	12.5	449	406	6962	0.7200	0.2097	0.5061	0.2971
14	18	12.5	470	426	6626	0.7177	0.2007	0.5290	0.2629
15	50	62.5	378	422	6699	0.6902	0.2136	0.4961	0.2812
16	80	62.5	372	416	6791	0.6823	0.2190	0.4820	0.2936
17	110	87.5	328	415	6803	0.6632	0.2231	0.4709	0.2898
18	139	37.5	413	413	6829	0.7075	0.2136	0.4961	0.2988
19	169	37.5	409	409	6904	0.7025	0.2146	0.4934	0.2977
20	197	62.5	364	407	6931	0.6805	0.2238	0.4691	0.3106
21	230	87.5	316	403	7012	0.6622	0.2283	0.4572	0.3096
22	258	37.5	401	401	7039	0.7048	0.2160	0.4898	0.3051
23	287	37.5	396	396	7127	0.7015	0.2205	0.4779	0.3186
24	315	12.5	439	396	7138	0.7177	0.2139	0.4951	0.3102
25	346	87.5	308	395	7151	0.6587	0.2321	0.4468	0.3216

Notes:

Days out of dry-dock $d_1 = d_0$ for the first 13 voyages
 $= d_0 - 398$ for the remaining 12 voyages

Weather Number $W = 12.5$ for good, 37.5 for moderate, 62.5 for heavy
and 87.5 for very heavy weather.

Correction for weather according to:

$$\frac{\Delta^{2/3} V^3}{P_S^*} = \frac{\Delta^{2/3} V^3}{P_S} + 1.7862 (W - 37.5)$$

obtained from a plot of $\frac{\Delta^{2/3} V^3}{P_S}$ as a function of W .

Shaft power corrected to moderate weather and to 18100 tonnes displacement
and 16.0 knots speed (approximate average values for the 25 voyages) given by:

$$P_S^* = \frac{18100^{2/3} \times 16.0^3}{(\Delta^{2/3} V^3 / P_S)}$$

$$\frac{V}{nD} : V \text{ in m per sec}$$

$$10 K_{QB} = 10 \frac{P_S \eta_S}{2\pi \rho n^3 D^5}, \quad \eta_S = 0.970 \text{ assumed.}$$

J : from propeller open water characteristics

$$w_Q = 1 - \frac{J}{(V/nD)}$$

These data can be plotted in various ways. A graph of $\Delta^{2/3} V^3 / P_S$ as a function of the weather number W shows the effect of weather on power, and can be used to obtain $\Delta^{2/3} V^3 / P_S^*$ where P_S^* is the power for a specific weather condition, "moderate" in the example. The power for a specific displacement, speed and weather condition is then determined, and plotted as a function of days in service to show the effect of hull surface conditions. Finally, the torque coefficient K_Q is calculated and used to find the torque identity wake fraction w_Q , which is plotted as function of days in service. One must expect such diagrams to show a fair amount of scatter.

In statistical methods of analysing service performance data, linear multiple regression analysis is used to fit an equation of the form:

$$y_{est} = a_0 + a_1 x_1 + a_2 x_2 \cdots + a_n x_n \quad (10.8)$$

to the data such that $\sum (y_{est} - y)^2$ is minimised. The dependent variable y may be the shaft power P_S or a power coefficient such as $P_S / \Delta^{2/3} V^3$ and the independent variables x_1, x_2, \dots may be displacement, trim, speed, a weather number, days out of dry dock, or combinations of these quantities and other parameters. The variables included in a regression analysis must be carefully chosen, and the significance of each variable must be examined by determining the magnitude of the reduction in $\sum (y_{est} - y)^2$ caused by the inclusion of that variable. For further details, one may refer to a book on Statistics.

Problems

1. A ship with a propeller of 4.0 m diameter and 0.8 pitch ratio is moored along the quayside by two mooring ropes. During dock trials, the propeller is run at 90 rpm and the mooring ropes become inclined at 15 degrees to the ship

centre line. Calculate the power delivered to the propeller, the tension in the mooring ropes and the reaction between the ship and the quayside. Assume that the thrust deduction fraction is 0.050, the relative rotative efficiency is 1.000 and the open water characteristics of the propeller are as given in Table 4.3.

2. A ship on speed trials makes six groups of runs, each group consisting of two runs in opposite directions at the same power setting over the measured mile. The following data are recorded:

Run No.	Direction	Time at start hr-min	Time over mile s	Shaft power kW	Propeller revolution rate rpm	Propeller thrust kN
1	N	8-51	321.8	1481	87.8	241
2	S	9-38	455.1	1501	88.4	247
3	N	10-25	299.4	1992	97.5	291
4	S	11-08	369.9	2020	98.3	295
5	N	11-52	293.1	2525	106.6	334
6	S	12-32	315.6	2585	106.2	352
7	N	13-12	287.5	3320	116.2	402
8	S	13-49	267.3	3360	117.2	410
9	N	14-24	273.1	4182	125.7	459
10	S	14-59	238.1	4242	126.1	465
11	N	15-32	249.0	5095	136.5	522
12	S	16-04	214.6	5155	137.1	528

Determine the speed of the ship through the water for each run and plot the speed of the current to the North as a function of the time of day. Calculate also the average speed, shaft power, propeller rpm and thrust for each of the six groups of runs.

3. The effective power of the ship in Problem 2 is as follows:

Speed, knots :	9.0	10.0	11.0	12.0	13.0	14.0	15.0	16.0
Effective power :	856	1084	1404	1792	2225	2679	3130	3554

The propeller of the ship has a diameter of 5.0 m and a pitch ratio of 0.8, and its open water characteristics are as given in Table 4.3. Analyse the data of the trials by both thrust identity and torque identity. The shafting efficiency is 0.970.

4. A ship is taken out on trials and the following observations recorded:

Run No.	Direction	Time at start	Time on mile	Average relative wind Velocity	Direction	Shaft power	Propeller revolution rate
		hr-min	secs	m per sec	deg	kW	rpm
1	N	8-04	229.1	11.3	23.5	2350	73.6
2	S	8-46	265.7	20.0	167.4	2300	72.8
3	N	9-28	228.1	10.3	23.2	2360	73.1
4	S	10-16	236.9	22.3	179.8	3600	83.4
5	N	10-52	210.2	10.9	15.2	3640	83.8
6	S	11-40	219.9	22.6	175.3	3610	83.5
7	N	12-16	182.2	12.0	4.1	7360	104.6
8	S	12-58	218.8	24.7	0.5	7370	104.2
9	N	13-39	180.1	12.1	170.5	7380	104.5
10	S	142-2	194.6	26.3	7.7	9760	113.7
11	N	15-05	171.6	14.6	161.4	9860	114.1
12	S	15-40	189.3	26.3	11.6	9830	114.9
13	N	16-17	176.5	15.2	157.1	9790	114.0

The ship has an equivalent above-water transverse projected area of 250 m^2 , and its effective power based on model tests with a correlation allowance of 0.4×10^3 is as follows:

Speed, knots	:	13.0	15.0	17.0	19.0	21.0
Effective power, kW:		1477	2220	3439	5135	7306

Determine the speed of the ship corrected for wind and current, the shaft power and the propeller rpm for each of the four groups of runs. Determine also how the speed of the current varies with the time of day. Use Eqns. (10.2) and (10.3) to estimate the wind resistance.

5. The ship in Problem 4 has a wetted surface of 3750 m^2 . Its propeller is of 6.0 m diameter and 1.0 pitch ratio, its open water characteristics being as given in Table 4.3. The shafting efficiency is 0.970, and the propulsion factors determined from a self-propulsion test on the basis of torque identity are as follows:

V knots:	13.0	15.0	17.0	19.0	21.0
w_Q	: 0.2255	0.2349	0.2392	0.2384	0.2327

t	:	0.1757	0.1784	0.1797	0.1796	0.1781
η_R	:	1.0183	1.0245	1.0274	1.0271	1.0236

Determine the correlation allowance and the wake scale effect.

6. A ship has an engine of maximum continuous rating 20000 kW at 114 rpm. The equivalent above water transverse projected area of the ship is 300 m². The contract for the ship requires it to have a minimum speed of 18 knots in calm water at 85 percent maximum continuous rated power and 100 percent rated rpm. During the acceptance trials, the following data are recorded:

Run No.	:	1	2	3	4	5
Direction	:	W	E	W	E	W
Time at start, hr-min	:	10-30	10-57	11-25	11-53	12-19
Time on mile	:	207.4	190.5	202.6	201.8	187.9
Relative wind velocity, m per sec	:	9.908	7.495	11.164	7.765	10.468
Wind direction off the bow, deg	:	7.5	17.0	13.9	14.3	9.1
Shaft power	:	16920	16930	16980	16960	16950
Propeller rpm	:	113.5	113.6	114.2	114.1	114.0

The slope of the effective power-speed curve of the ship at 18 knots is 2300 kW per knot. The wind resistance of the ship may be estimated using Eqns. (10.2) and (10.3). Determine the speed that the ship would attain in calm water, still air conditions. Does the ship fulfil the contract requirements?

7. A single screw ship has an engine with a maximum continuous rating, when new, of 10500 kW at 126 rpm directly connected to the propeller of diameter 6.2 m and pitch ratio 0.7. The effective power of the ship in average service conditions when new is as follows:

Speed, knots	:	15.0	15.5	16.0	16.5	17.0	17.5
Effective power, kW	:	3699	4149	4637	5164	5733	6345

The wake fraction is 0.250, the thrust deduction fraction 0.200 and the relative rotative efficiency 1.030 based on thrust identity. The shafting efficiency is 0.970. As the ship ages, its effective power in average service conditions increases uniformly at the rate of 5 percent per year, so that at the end of 10 years the effective power is 1.50 times the effective power when the ship was new. The wake fraction similarly increases at the rate of 0.5 percent per year and the thrust deduction fraction at the rate of 0.7 percent per year. The changes in the relative rotative efficiency and the shafting efficiency are negligible. The maximum continuous power rating of the engine decreases by

1.0 percent every year. Determine the changes in the speed and power of the ship in average service conditions at the end of every year for ten years. If the propeller is to be changed when the power required exceeds the maximum available power at 126 rpm, in which year should the propeller be changed? What should be the pitch ratio of the new propeller if it is to have the same diameter as the original propeller and run at 126 rpm with 90 percent of the available power? What will be the resulting ship speed? Use Table 4.3 for the propeller open water characteristics.

8. The service performance data of a ship are collected for a two year period during which the ship made twenty voyages. The average displacement of the ship during these voyages was 15000 tonnes and the average speed 16.0 knots. In the following data, the brake power has been corrected to correspond to the average displacement and speed, and the clean hull condition.

Voyage No.	Brake power kW	Wind speed knots	Wind direction deg
1	7370	2	100
2	7570	2	50
3	11520	23	35
4	9290	14	15
5	7120	9	140
6	8140	24	165
7	10310	19	10
8	8160	9	85
9	9570	30	125
10	10190	26	75
11	7640	20	150
12	7770	15	130
13	8480	9	40
14	8690	12	70
15	9365	18	60
16	6990	2	175
17	7480	10	115
18	8360	28	180
19	8850	25	95
20	7930	5	25

(True wind speed and direction off the bow)

The brake power in calm water for 15000 tonnes displacement and 16.0 knots speed is 7500 kW. Analyse these data to obtain curves showing the percentage

increase in power over that in calm water as a function of the Beaufort number for (a) head seas (0–45 degrees off the bow), (b) bow quartering seas (45–90 degrees off the bow), (c) stern quartering seas (90–135 degrees off the bow), and (d) following seas (135–180 degrees off the bow). The relation between wind speed and Beaufort number is as follows:

Beaufort No.	Wind speed knots	Beaufort No.	Wind speed knots
1	2	5	18–20
2	5	6	22–26
3	8.5–10	7	28–32
4	12–16	8	34–40

Hence, find the percentage increase in power for a wind speed of 5 knots for the four direction ranges.

9. A ship has a design displacement of 13000 tonnes and a speed of 17.0 knots. In its first four years of service, it makes eleven voyages each year, and is then dry-docked when its hull is cleaned and repainted. Average values of speed and power observed during voyages when fair weather prevailed are given in the following table:

Voyage No.	Mean days out of drydock	Displacement tonnes	Average speed knots	Average power kW
1	10	11000	17.0	8586
5	120	12000	16.8	9029
11	310	9000	17.2	8218
Ship dry-docked				
12	25	13000	16.8	9450
18	170	9500	17.1	8333
21	300	10500	17.1	9069
Ship dry-docked				
23	20	12500	16.7	9166
28	160	11500	16.8	9099
33	320	9750	17.2	8941
Ship dry-docked				

Voyage No.	Mean days out of drydock	Displacement tonnes	Average speed knots	Average power kW
34	15	12750	16.7	9417
39	140	10250	17.1	8997
43	290	9250	17.3	8886

Correct these data to the design speed and displacement and plot the corrected power to a base of days in service. Attempt to separate the effect of fouling which is removed at each dry-docking from the effect of irreversible hull deterioration. Hence, predict the power required at the end of the fifth year in service just before the ship is dry-docked.

10. A ship has a propulsion plant consisting of a two-stroke turbo-charged diesel engine of maximum continuous rating 10500 kW at 144 rpm directly connected to a propeller of 5.0 m diameter and 1.0 pitch ratio. The propulsion factors based on thrust identity are: wake fraction 0.240, thrust deduction fraction 0.200, relative rotative efficiency 1.030. The shafting efficiency is 0.980. The effective power of the ship in calm water is as follows:

Speed, knots	:	15.5	16.0	16.5	17.0	17.5	18.0
Effective power, kW:		3926	4402	4918	5475	6078	6726

It is desired to estimate the effect of weather on the service performance of the ship. For this purpose, draw two sets of curves showing (a) brake power as a function of engine rpm, and (b) ship speed as a function of engine rpm for increases in effective power of 0, 10, 20, 30, 40 and 50 percent over that in calm water. Hence deduce the resulting drop in ship speed and engine rpm as bad weather causes the given increases in effective power. Assume that the engine torque and rpm at the maximum continuous rating cannot be exceeded.

CHAPTER 11

Some Miscellaneous Topics

11.1 Unsteady Propeller Loading

The thrust and torque of a propeller operating behind a ship are not constant even when the ship is moving at a constant speed in calm water with the propeller running at a fixed rpm. Fluctuations in the thrust and torque arise because the flow into the propeller varies along the circumference at each radius. This results in a periodic variation of the relative velocity of the flow with respect to a point on the propeller, and produces an unsteady loading on the propeller blades. The fundamental frequency of these unsteady propeller forces is the propeller revolution rate or "shaft frequency" but higher harmonics also exist.

Unsteady propeller loading causes several adverse effects. The periodic forces and moments created by the propeller operating in a non-uniform flow are transmitted through the propeller shaft bearings and through the water to the hull of the ship, leading to vibration of the propulsion shafting system and the hull. The periodic stresses in the propeller, the shafting and the hull due to unsteady propeller loading may eventually result in fatigue failure. Non-uniform flow into the propeller may also result in periodic cavitation causing enhanced vibration, noise and erosion. The severity and importance of these adverse effects vary with the type of vessel. Some hull vibration due to periodic cavitation is fairly common in merchant ships with single propellers operating with the minimum permissible clearances between hull and propeller and is usually acceptable. In warships, on the other hand,

noise due to periodic cavitation may be unacceptable. Fortunately, high speed warships have twin screws with comparatively large clearances from the hull, so that the flow into the propellers is much more uniform than in a single screw merchant ship, and the effects of unsteady propeller loading are small.

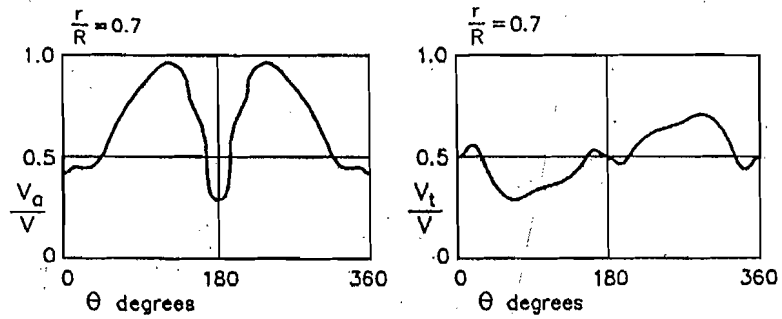


Figure 11.1 : Circumferential Variation of Velocities in the Propeller Disc.

The axial and tangential components of the flow velocity into the propeller disc of a single screw ship typically vary around the circumference at a given radius as shown in Fig. 11.1. V_a and V_t are the axial and tangential velocities, θ is the angle measured from the vertical upward, and V the ship speed. Owing to the port and starboard symmetry of the ship hull, the axial velocity should be an even function of θ , i.e. $V_a(\theta) = V_a(-\theta)$, and the tangential velocity an odd function, i.e. $V_t(\theta) = -V_t(-\theta)$. This is not always found to be so because of experimental errors in the measurement of these velocities and also because of vortex shedding by the hull in full form ships. For a propeller not on the ship centre line, there is naturally no flow symmetry. In general, therefore, the axial and tangential velocities in the propeller disc can be represented in terms of Fourier Series:

$$\begin{aligned}
 V_a(r, \theta) &= \sum_{m=0}^{\infty} \{a_m(r) \cos m\theta + b_m(r) \sin m\theta\} \\
 V_t(r, \theta) &= \sum_{m=0}^{\infty} \{a'_m(r) \cos m\theta + b'_m(r) \sin m\theta\}
 \end{aligned}
 \tag{11.1}$$

Truncating these series at $m = 15$ or 20 usually gives a reasonably accurate representation.

The Fourier series representation of the axial and tangential velocities may be used to determine the unsteady propeller forces. Various methods for doing so exist, of which the simplest is based on a quasi-static approach. The thrust and torque of the i^{th} blade at an angle θ to the upward vertical are given by:

$$\begin{aligned} T_i &= \int_{x_b}^{1.0} \frac{dT(x, \theta)}{dx} dx \\ Q_i &= \int_{x_b}^{1.0} \frac{dQ(x, \theta)}{dx} dx \end{aligned} \quad (11.2)$$

where $dT(x, \theta)$ and $dQ(x, \theta)$ are the thrust and torque of a blade element dx at $x = r/R$ calculated for the known velocities $V_a(x, \theta)$ and $V_t(x, \theta)$. x_b is the non-dimensional boss radius. The thrust and torque for all the Z blades will then be:

$$\begin{aligned} T(\theta) &= \sum_{i=1}^Z T_i \left[\theta + \frac{2\pi(i-1)}{Z} \right] \\ Q(\theta) &= \sum_{i=1}^Z Q_i \left[\theta + \frac{2\pi(i-1)}{Z} \right] \end{aligned} \quad (11.3)$$

and the mean thrust and torque of the propeller will be:

$$\begin{aligned} T &= \frac{1}{2\pi} \int_0^{2\pi} T(\theta) d\theta \\ Q &= \frac{1}{2\pi} \int_0^{2\pi} Q(\theta) d\theta \end{aligned} \quad (11.4)$$

The tangential force on the i^{th} blade of the propeller at the angle θ is given by:

$$F_i = \int_{x_b}^{1.0} \frac{1}{x R} \frac{dQ(x, \theta)}{dx} dx \quad (11.5)$$

so that for all the Z blades, the tangential force and its horizontal and vertical components are given by:

$$\begin{aligned} F(\theta) &= \sum_{i=1}^Z F_i \left[\theta + \frac{2\pi(i-1)}{Z} \right] \\ F_H(\theta) &= \sum_{i=1}^Z F_i \left[\theta + \frac{2\pi(i-1)}{Z} \right] \cos \left[\theta + \frac{2\pi(i-1)}{Z} \right] \\ F_V(\theta) &= \sum_{i=1}^Z F_i \left[\theta + \frac{2\pi(i-1)}{Z} \right] \sin \left[\theta + \frac{2\pi(i-1)}{Z} \right] \end{aligned} \quad (11.6)$$

It is assumed that unsteady propeller loading is a linear phenomenon, i.e. a pure harmonic velocity variation of a given frequency will produce a pure harmonic force variation of the same frequency with possibly a phase difference. Also, the resultant of several harmonics is the linear superposition of those harmonics. If the velocity components are represented by Eqn. (11.1), the resulting thrust and torque of the i^{th} blade are represented by:

$$\begin{aligned} T_i(\theta) &= \sum_{m=0}^{\infty} \{A_{mT} \cos m\theta + B_{mT} \sin m\theta\} \\ Q_i(\theta) &= \sum_{m=0}^{\infty} \{A_{mQ} \cos m\theta + B_{mQ} \sin m\theta\} \end{aligned} \quad (11.7)$$

The thrust and torque for all the Z blades will be:

$$\begin{aligned}
T(\theta) &= \sum_{i=1}^Z \sum_{m=0}^{\infty} \left\{ A_{mT} \cos \left[m\theta + \frac{2\pi(i-1)m}{Z} \right] \right. \\
&\quad \left. + B_{mT} \sin \left[m\theta + \frac{2\pi(i-1)m}{Z} \right] \right\} \\
Q(\theta) &= \sum_{i=1}^Z \sum_{m=0}^{\infty} \left\{ A_{mQ} \cos \left[m\theta + \frac{2\pi(i-1)m}{Z} \right] \right. \\
&\quad \left. + B_{mQ} \sin \left[m\theta + \frac{2\pi(i-1)m}{Z} \right] \right\}
\end{aligned} \tag{11.8}$$

It can be shown that:

$$\begin{aligned}
\sum_{i=1}^Z \cos \left[m\theta + \frac{2\pi(i-1)m}{Z} \right] &= Z \cos m\theta \quad \text{for } m = kZ, \quad k = 0, 1, 2, 3, \dots \\
&= 0 \quad \text{otherwise} \\
\sum_{i=1}^Z \sin \left[m\theta + \frac{2\pi(i-1)m}{Z} \right] &= 0 \quad \text{for all } m
\end{aligned} \tag{11.9}$$

Therefore, owing to the angular symmetry of the propeller (Z identical blades spaced $2\pi/Z$ radians apart), the only harmonics in the velocity field that result in a net thrust and torque are those corresponding to $m = 0, Z, 2Z, 3Z, \dots$. The propeller thus filters out many of the frequencies present in the velocity field.

The direction of the tangential force $F_i(\theta)$ on the i^{th} blade changes with θ , and it is therefore necessary to consider its horizontal and vertical components, whose directions are fixed. The horizontal component for all the Z blades in the velocity field given by Eqn. (11.1) may be represented as:

$$\begin{aligned}
F_H(\theta) &= \sum_{i=1}^Z \sum_{m=0}^{\infty} \left[\left\{ A_{mH} \cos \left(m\theta + \frac{2\pi(i-1)m}{Z} \right) \right. \right. \\
&\quad \left. \left. + B_{mH} \sin \left(m\theta + \frac{2\pi(i-1)m}{Z} \right) \right\} \cos \left(\theta + \frac{2\pi(i-1)}{Z} \right) \right] \\
&= \sum_{i=1}^Z \sum_{m=0}^{\infty} \left[\frac{1}{2} A_{mH} \left\{ \cos \left[(m+1)\theta + \frac{2\pi(i-1)}{Z}(m+1) \right] \right. \right. \\
&\quad \left. \left. + \cos \left[(m-1)\theta + \frac{2\pi(i-1)}{Z}(m-1) \right] \right\} \right. \\
&\quad \left. + \sum_{m=0}^{\infty} \left[\frac{1}{2} B_{mH} \left\{ \sin \left[(m+1)\theta + \frac{2\pi(i-1)}{Z}(m+1) \right] \right. \right. \right. \\
&\quad \left. \left. + \sin \left[(m-1)\theta + \frac{2\pi(i-1)}{Z}(m-1) \right] \right\} \right] \right] \quad (11.10)
\end{aligned}$$

The various terms in Eqn. (11.10) all add up to zero when summed up over the Z blades except when $m+1 = kZ$ or $m-1 = kZ$, $k = 0, 1, 2, \dots$. A similar result can be obtained for the vertical component $F_V(\theta)$ of the tangential force. Thus, the tangential force $F(\theta)$ is excited only by those harmonic components in the velocity field for which $(m+1)/Z$ or $(m-1)/Z$ are integers. For other values of m , the individual contributions of the Z blades cancel each other.

The calculation of the periodic forces on the propeller as a function of the angular position θ from the experimentally determined propeller characteristics using a quasi-static approach is simple. However, this method has been found to give variations in thrust and torque which are nearly twice the values observed in model experiments. More sophisticated methods are therefore necessary. An improvement on the quasi-static approach consists in determining the thrust and torque on the blade elements at various radii, $dT(x, \theta)$ and $dQ(x, \theta)$, using two-dimensional unsteady aerofoil theory. An even more accurate method for determining unsteady propeller loading is based on using unsteady lifting surface theory.

Theoretical and experimental studies of unsteady propeller loading confirm that the fluctuations in the thrust and torque of all the blades arise only from those harmonics in the velocity field that are an integer times the number of blades, ($m = kZ$, $k = 0, 1, 2, 3, \dots$). The tangential force and the resulting moments at the propeller shaft bearings arise only for those harmonics for which $m + 1 = kZ$ or $m - 1 = kZ$. The harmonics in the velocity field at the propeller depend mainly on the shape of the afterbody of the ship. The amplitudes a_m and b_m in Eqn. (11.1) decrease with increasing m , this decrease being monotonic for open sterns in single screw ship while for conventional sterns the amplitudes are greater for $m = 0, 2, 4, \dots$ than for $m = 1, 3, 5, \dots$. The tangential velocity variation is usually large and has a strong first harmonic.

In the design of propellers to minimise unsteady propeller loading for a given non-uniform velocity field, calculations are carried out for different values of number of blades and different skew magnitudes and radial distributions. That combination of blade number, skew magnitude and its radial distribution is selected which gives the minimum fluctuations in thrust and torque and the smallest values of the tangential force components and the resulting moments. Excessive magnitudes and extreme distributions of skew may not be acceptable because they would cause difficulties in propeller manufacture. In some cases, it may be necessary to consider modifications to the afterbody of the ship to restrict unsteady propeller loadings to acceptable levels.

Example 1

A single screw ship has a four-bladed propeller of 5.0 m diameter and 0.8 pitch ratio running at 150 rpm with the ship moving ahead at a speed of 10.85 m per sec. The axial and tangential components of the relative velocity of water with respect to the ship in the plane of the propeller at $0.7R$ are given in m per sec by:

$$V_a(\theta) = 8.0000 - 0.4 \cos \theta - 0.3 \cos 2\theta + 0.2 \cos 3\theta - 0.1 \cos 4\theta + 0.05 \cos 5\theta$$

$$V_t(\theta) = -1.2 \sin \theta + 0.6 \sin 2\theta - 0.3 \sin 3\theta + 0.15 \sin 4\theta - 0.075 \sin 5\theta$$

Determine the values of the thrust, the torque and the horizontal and vertical components of the tangential force for different values of the blade angle θ . Assume that the blade section at $0.7R$ represents the whole propeller, and that the centroid of the tangential force on each blade is at a radius of 1.5 m. The propeller open water characteristics are given by:

$$K_T = 0.3415 - 0.2588 J - 0.1657 J^2$$

$$10K_Q = 0.4021 - 0.2330 J - 0.2100 J^2$$

$$Z = 4 \quad D = 5.0 \text{ m} \quad \frac{P}{D} = 0.8 \quad n = 150 \text{ rpm} = 2.5 \text{ s}^{-1} \quad V = 10.85 \text{ m s}^{-1}$$

Centroid of tangential force on each blade at a radius $r_Q = 1.500 \text{ m}$

For a blade at an angle θ to the upward vertical, the tangential velocity relative to the water is given at $0.7R$ by:

$$V_{rt}(\theta) = 0.7\pi R n - V_t(\theta)$$

The instantaneous revolution rate at the angle θ is then:

$$n(\theta) = \frac{V_{rt}(\theta)}{0.7\pi R} = \frac{0.7\pi R n - V_t(\theta)}{0.7\pi R} = n - \frac{V_t(\theta)}{0.7\pi R}$$

The advance coefficient for a blade at the angle θ is:

$$J(\theta) = \frac{V_a(\theta)}{n(\theta) D}$$

for which the thrust and torque coefficients can be obtained from the open water characteristics. The thrust and torque of the blade at the angle θ are then:

$$T_1(\theta) = \frac{1}{Z} K_T(\theta) \rho n^2(\theta) D^4$$

$$Q_1(\theta) = \frac{1}{Z} K_Q(\theta) \rho n^2(\theta) D^5$$

The tangential force and its horizontal and vertical components are:

$$F_1(\theta) = Q_1(\theta)/r_Q$$

$$F_{1H}(\theta) = F_1(\theta) \cos \theta$$

$$F_{1V}(\theta) = F_1(\theta) \sin \theta$$

The calculations are given in Tables 11.1 (a), (b), (c) and (d).

Table 11.1(a)

Unsteady Propeller Loading Calculations (Example 1)

θ deg	V_a ms^{-1}	V_t ms^{-1}	$n(\theta)$ s^{-1}	$J(\theta)$	$K_T(\theta)$	$10K_Q(\theta)$
0	7.4500	0.0000	2.5000	0.5960	0.1284	0.1886
15	7.4582	-0.1653	2.5301	0.5896	0.1313	0.1917
30	7.5103	-0.2880	2.5524	0.5885	0.1318	0.1923
45	7.6404	-0.4076	2.5741	0.5936	0.1295	0.1898
60	7.8250	-0.5846	2.6063	0.6005	0.1264	0.1865
75	8.0132	-0.7963	2.6448	0.6059	0.1238	0.1838
90	8.2000	-0.9750	2.6773	0.6125	0.1208	0.1806
105	8.4065	-1.1365	2.7067	0.6212	0.1168	0.1763
120	8.5750	-1.3640	2.7481	0.6241	0.1155	0.1749
135	8.5596	-1.6076	2.7924	0.6131	0.1206	0.1803
150	8.2897	-1.5870	2.7887	0.5945	0.1291	0.1893
165	7.9222	-1.0251	2.6865	0.5898	0.1312	0.1916
180	7.7500	0.0000	2.5000	0.6200	0.1173	0.1769
195	7.9222	1.2051	2.3135	0.6849	0.0865	0.1440
210	8.2897	1.5870	2.2113	0.7497	0.0543	0.1094
225	8.5596	1.6076	2.2076	0.7755	0.0412	0.0951
240	8.5750	1.3640	2.2519	0.7616	0.0483	0.1029
255	8.4065	1.1365	2.2933	0.7331	0.0627	0.1184
270	8.2000	0.9750	2.3277	0.7061	0.0762	0.1329
285	8.0132	0.7963	2.3552	0.6805	0.0887	0.1463
300	7.8250	0.5846	2.3937	0.6538	0.1015	0.1600
315	7.6404	0.4076	2.4259	0.6299	0.1127	0.1720
330	7.5103	0.2880	2.4476	0.6137	0.1203	0.1800
345	7.4582	0.1653	2.4699	0.6039	0.1248	0.1848
360	7.4500	0.0000	2.5000	0.5960	0.1284	0.1886

Table 11.1(b)

Unsteady Propeller Loading Calculations (Example 1)

θ deg	$T_1(\theta)$ kN	$Q_1(\theta)$ kNm	$F_1(\theta)$ kN	$F_{1H}(\theta)$ kN	$F_{1V}(\theta)$ kN
0	128.52	94.41	62.94	62.94	0.00
15	134.63	98.28	65.52	63.29	16.96
30	137.53	100.29	66.86	57.91	33.43
45	137.41	100.70	67.13	47.47	47.47

Table 11.1 (b) (Contd.)

θ	$T_1(\theta)$	$Q_1(\theta)$	$F_1(\theta)$	$F_{1H}(\theta)$	$F_{1V}(\theta)$
deg	kN	kNm	kN	kN	kN
60	137.47	101.44	67.62	33.81	58.56
75	138.74	102.96	68.64	17.77	66.30
90	138.68	103.66	69.10	0.00	69.10
105	137.06	103.46	68.97	-17.85	66.62
120	139.65	105.77	70.52	-35.26	61.07
135	150.56	112.60	75.07	-53.08	53.08
150	160.75	117.91	78.61	-68.08	39.30
165	151.67	110.75	73.83	-71.32	19.11
180	117.46	88.54	59.03	-59.03	0.00
195	74.19	61.74	41.16	-39.75	-10.65
210	42.54	42.82	28.55	-24.72	-14.27
225	32.13	37.12	24.75	-17.50	-17.50
240	39.23	41.77	27.84	-13.92	-24.11
255	52.81	49.87	33.24	-8.60	-32.11
270	65.80	57.41	38.27	0.00	-38.27
285	78.77	64.99	43.32	11.21	-41.85
300	93.11	73.41	48.94	24.47	-42.38
315	106.25	81.06	54.04	38.21	-38.21
330	115.40	86.36	57.58	49.86	-28.79
345	121.91	90.28	60.19	58.13	-15.58
360	128.52	94.41	62.94	62.94	0.00

Table 11.1 (c)

Unsteady Propeller Loading Calculations (Example 1)

$$T_i(\theta) = T_1 \left[\theta + \frac{2\pi(i-1)}{Z} \right] \quad T(\theta) = \sum_{i=1}^Z T_i(\theta)$$

θ	$T_1(\theta)$	$T_2(\theta)$	$T_3(\theta)$	$T_4(\theta)$	$T(\theta)$
deg	kN	kN	kN	kN	kN
0	128.52	138.68	117.46	65.80	450.46
15	134.63	137.06	74.19	78.77	424.65
30	137.53	139.65	42.54	93.11	412.83
45	137.41	150.56	32.13	106.25	426.34
60	137.47	160.75	39.23	115.40	452.84

Table 11.1 (c) (Contd.)

θ deg	$T_1(\theta)$ kN	$T_2(\theta)$ kN	$T_3(\theta)$ kN	$T_4(\theta)$ kN	$T(\theta)$ kN
75	138.74	151.67	52.81	121.91	465.14
90	138.68	117.46	65.80	128.52	450.46
105	137.06	74.19	78.77	134.63	424.65
120	139.65	42.54	93.11	137.53	412.83
135	150.56	32.13	106.25	137.41	426.34
150	160.75	39.23	115.40	137.47	452.84
165	151.67	52.81	121.91	138.74	465.14
180	117.46	65.80	128.52	138.68	450.46
195	74.19	78.77	134.63	137.06	424.65
210	42.54	93.11	137.53	139.65	412.83
225	32.13	106.25	137.41	150.56	426.34
240	39.23	115.40	137.47	160.75	452.84
255	52.81	121.91	138.74	151.67	465.14
270	65.80	128.52	138.68	117.46	450.46
285	78.77	134.63	137.06	74.19	424.65
300	93.11	137.53	139.65	42.54	412.83
315	106.25	137.41	150.56	32.13	426.34
330	115.40	137.47	160.75	39.23	452.84
345	121.91	138.74	151.67	52.81	465.14
360	128.52	138.68	117.46	65.80	450.46

$Q(\theta)$, $F_H(\theta)$ and $F_V(\theta)$ calculated in a similar manner are obtained as follows:

Table 11.1 (d)

Unsteady Propeller Loading Calculations (Example 1)

θ deg	$Q(\theta)$ kN m	$F_H(\theta)$ kN	$F_V(\theta)$ kN
0	344.02	3.91	30.83
15	328.46	16.90	31.08
30	322.30	22.39	37.84
45	331.48	15.10	44.84
60	347.48	1.68	44.97
75	353.85	-4.02	37.72
90	344.02	3.91	30.83

Table 11.1 (d) (Contd.)

θ	$Q(\theta)$	$F_H(\theta)$	$F_V(\theta)$
deg	kN m	kN	kN
105	328.46	16.90	31.08
120	322.30	22.39	37.84
135	331.48	15.10	44.84
150	347.48	1.68	44.97
165	353.85	-4.02	37.72
180	344.02	3.91	30.83
195	328.46	16.90	31.08
210	322.30	22.39	37.84
225	331.48	15.10	44.84
240	347.48	1.68	44.97
255	353.85	-4.02	37.72
270	344.02	3.91	30.83
285	328.46	16.90	31.08
300	322.30	22.39	37.84
315	331.48	15.10	44.84
330	347.48	1.68	44.97
345	353.85	-4.02	37.72
360	344.02	3.91	30.83

As expected, all the four quantities, $T(\theta)$, $Q(\theta)$, $F_H(\theta)$ and $F_V(\theta)$, can be represented by $A + B \cos(4\theta + \varepsilon)$ where ε is a phase angle, the other harmonics giving a zero net contribution when summed over all the four blades, Fig. 11.2.

11.2 Vibration and Noise

The propeller in a ship is a source of vibration and noise. The unsteady forces due to the operation of the propeller in a non-uniform wake field give rise to the vibrations of the hull and the propeller shafting system. The propeller blades themselves may also vibrate. These vibrations may produce noise that is undesirable, particularly in warships.

Propeller excited vibration occurs due to the pressure pulses of the propeller being transmitted through the water to the hull. The propeller and the hull also interact through the shafting system. The forces and moments

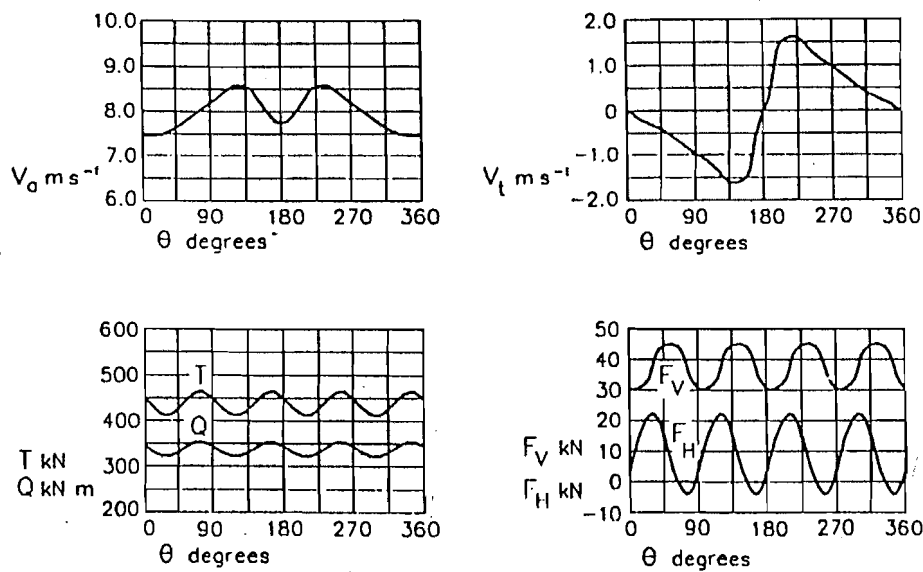


Figure 11.2 : Unsteady Propeller Loading (Example 1).

that act through the propeller shaft bearings are termed bearing forces, and include the effects of the weight of the propeller in water and the propeller inertia, the added mass, added inertia and damping due to the water around the propeller, and the propeller forces and moments. The propeller forces and moments, which can be divided into steady and cyclic components, are transmitted through the shaft bearings to the hull. The pressure pulses that are transmitted to the hull through the water are caused by the pressure field accompanying the propeller blades as they pass close to the hull and by cavitation.

The pressure at a point due to the pressure field of a propeller in the absence of cavitation varies in a continuous manner with time. The variations in pressure are comparatively small, and depend on the thickness of the blades and their pressure distribution. The pressure pulse p_0 due to the propeller when there is no cavitation decreases sharply as the distance s from the propeller increases, p_0 being proportional to $s^{-2.5}$. The pressure pulses due to cavitation depend upon the type of cavitation, the pressure fluctuations being the greatest for bubble cavitation, somewhat less for sheet cavitation and still less for tip vortex cavitation. The pressure fluctuations

depend upon $\partial^2 v / \partial \hat{t}^2$ where v is the cavity volume and \hat{t} the time, so that the pressure fluctuation produced by the sudden collapse (implosion) of a cavity is much larger than that produced by a growing cavity volume. The pressure change p_c due to cavitation varies inversely as the distance from the cavity, i.e. p_c is proportional to s^{-1} , so that the pressure pulse at a point due to a cavitating propeller is much stronger than that due to a non-cavitating propeller. The pressure at a point in the water is also influenced by the presence of a solid boundary: the pressure pulse at a point on a flat plate placed close to the propeller is nearly twice the pressure pulse at that point in the absence of the plate. This effect is represented by the "solid boundary factor" defined as the ratio of the pressure pulse at a point in the presence of the solid boundary to the pressure pulse without the solid boundary. The solid boundary factor depends upon the shape of the surface and for a ship hull is typically equal to about 1.8. In addition to the pressure fluctuations caused by the propeller, it is also necessary to take into account the pressure fluctuations caused by the vibration of the hull surface in water.

The determination of hull pressure fluctuations due to a propeller may be carried out by theoretical means using unsteady lifting surface theory. However, to obtain accurate results it is necessary to take into account wake scale effects, the solid boundary factor and the effect of hull vibration on the pressure. Hull pressures may also be determined by model experiments in a cavitation tunnel. It can be shown by dimensional analysis that the pressure at a point in the water near the propeller is given by:

$$\frac{p}{\rho n^2 D^2} = f \left(J, K_T, \sigma, R_n, F_n, \frac{s}{D} \right) \quad (11.11)$$

where s is the distance of the point from the propeller, and the other symbols have their usual meanings. In the experiment, all the parameters for the geometrically similar model are made equal to those for the ship except for the Reynolds number, and then:

$$\frac{p_S}{p_M} = \frac{\rho_S}{\rho_M} \lambda \quad (11.12)$$

the suffixes S and M referring to the ship and the model, λ being the model scale.

Hull surface pressures caused by the propeller may also be predicted by empirical methods based on an analysis of a number of ships. In one such method, due to Holden, Fagerjord and Frostad (1980), the hull surface pressures at a point are given by:

$$\begin{aligned}
 p_0 &= 12.45 \rho n^2 D^2 Z^{-1.53} \left(\frac{t_{0.7}}{D} \right)^{1.33} \left(\frac{2s}{D} \right)^{-a} \\
 p_c &= 0.098 \rho n^2 D^2 V (w_{\max} - w) b \sigma^{-0.5} \left(\frac{2s}{D} \right)^{-a_1} \\
 p &= (p_0^2 + p_c^2)^{0.5}
 \end{aligned} \tag{11.13}$$

where:

- p = pressure at a point due to the propeller;
- p_0 = pressure due to the propeller without cavitation;
- p_c = pressure due to cavitation;
- ρ = density of water;
- n = propeller revolution rate;
- D = propeller diameter;
- Z = number of blades;
- $t_{0.7}$ = blade thickness at $0.7R$;
- s = distance of the point from $0.9R$ when the blade is upright;
- V = ship speed;
- w_{\max} = maximum value of the wake fraction in the propeller disc;
- w = mean effective wake fraction for the ship;
- σ = cavitation number based on the tangential velocity at $0.7R$.

$$\begin{aligned}
 a &= 1.8 + 0.8 \frac{s}{D} \text{ for } \frac{s}{D} \leq 1.0 & a_1 &= 1.7 - 1.4 \frac{s}{D} \text{ for } \frac{s}{D} \leq 0.5 \\
 &= 2.6 \text{ for } \frac{s}{D} \geq 1.0 & &= 1.0 \text{ for } \frac{s}{D} \geq 0.5 \\
 b &= \frac{(\text{pitch} \times \text{camber}) \text{ at } 0.95R}{(\text{pitch} \times \text{camber}) \text{ at } 0.80R}
 \end{aligned}$$

These formulas have been criticised for not having a proper theoretical basis. In any case, such empirical formulas give only approximate values and large differences can occur between the values predicted by such formulas and those obtained in practice.

In addition to exciting hull vibration, the propeller blades may themselves undergo flexural and torsional vibration. The higher modes of propeller blade vibration after the fundamental mode and the first flexural and torsional modes are extremely complex due to the shape of the blades: non-symmetrical blade outline, variable blade thickness along the radius and along the chord at each radius, and the twist of the blades due to the varying pitch angles along the radius. The surrounding water also influences propeller blade vibration significantly: the mode shapes and frequencies of a propeller blade vibrating in air are quite different from those of a blade vibrating in water.

Simple empirical formulas proposed by Baker (1940-41) are often used for estimating the frequencies of the fundamental flexural and torsional blade vibration:

$$\begin{aligned}
 f_f &= \frac{0.305 t_0}{(R - r_0)^2} \left[\frac{c_0 t_m g E}{c_m t_0 \rho_m} \right]^{0.5} \\
 f_t &= \frac{0.92 t_{0.5} c_0}{R - r_0 c_{0.5} c_m} \left[\frac{g G}{\rho_m} \right]^{0.5}
 \end{aligned} \tag{11.14}$$

where:

$$\begin{aligned}
 f_f &= \text{fundamental frequency of flexural vibration in air;} \\
 f_t &= \text{fundamental frequency of torsional vibration in air;}
 \end{aligned}$$

- R = propeller radius;
- r_0 = radius of root section;
- t_0 = thickness of root section;
- t_m = mean of the blade section thicknesses;
- $t_{0.5}$ = blade thickness at a radius of $0.5(R + r_0)$;
- c_0 = chord length of the root section;
- c_m = mean chord length of the blade;
- $c_{0.5}$ = chord length at a radius of $0.5(R + r_0)$;
- g = acceleration due to gravity;
- ρ_m = density of the propeller material;
- E = modulus of elasticity of the propeller material;
- G = modulus of rigidity of the propeller material.

The blade frequencies in water are about 65 percent of the corresponding frequencies in air. The material of the propeller affects blade vibration through its damping properties. Commonly used propeller materials have low damping, but special materials having high damping characteristics are available. Propeller blade vibration may be studied using the finite element technique, but it is necessary to model the conditions at the blade root properly and to take into account the effects of added mass and inertia. In propellers running at high rpm it is also necessary to consider the effects of centrifugal force.

The noise generated by the hull, the machinery and the propeller is of great importance in a warship. The noise not only betrays the position of the ship and helps in its identification but also interferes with the ship's own sensors. Noise is also important in oceanographic research vessels where it may interfere with the operation of sensitive instruments. The importance of minimising noise is growing in merchant ships also since noise is a health hazard. An important source of noise in a ship is the propeller.

The speed of sound in water is more than four times the speed of sound in air, and therefore the wavelength of a sound wave of a given frequency is greater in water than in air. The transmission of sound in water depends upon the frequency: high frequency sounds are attenuated more rapidly than low frequency sounds, i.e. low frequency sounds travel farther. The noise level is measured in decibels (dB) by the ratio of the power P of the sound source to the power P_0 of a reference source, or in terms of the ratio of the sound pressure p to a reference pressure p_0 :

$$L_P = 10 \log_{10} \left(\frac{P}{P_0} \right) \quad L_p = 20 \log_{10} \left(\frac{p}{p_0} \right) \quad (11.15)$$

The reference pressure in water is taken as $1 \mu\text{Pa}$ ($10^{-6} \text{ N per m}^2$). Acoustic measurements are usually given for octave or one-third octave bands, i.e. the ratio of the highest frequency to the lowest frequency considered is 2 or $2^{1/3}$ respectively.

Propeller noise arises basically from four causes: _____

- The acceleration imparted to the water by the propeller,
- The rotating pressure field of the propeller,
- The periodic fluctuation in the size and shape of cavities caused by the propeller operating in a non-uniform flow, and
- The collapse of cavities.

The noise due to the first two causes is generally small and of the same level as the noise due to the machinery or that due to the passage of the hull through the water (boundary layer noise). However, once cavitation starts, propeller noise becomes predominant; hence the importance of delaying cavitation as much as possible. The noise due to the action of a propeller without cavitation consists of sound at the blade passing frequency (number of blades \times propeller revolution rate) and its multiples, i.e. there are several distinct frequencies, usually below the audible range (20 Hz). There is also a broad band noise (comprising sounds with a wide frequency range) at higher frequencies due to turbulence and vortex shedding. When cavitation occurs, the collapse of bubble cavities produces noise covering a wide

range of frequencies, up to 1 MHz. The greatest contributions to noise are made by sheet cavitation, cloud cavitation and tip vortex cavitation. The distribution of noise levels for different frequencies is given in the form of a noise spectrum $L_p(f)$, which gives the sound pressure level as a function of frequency. Sounds of distinct frequencies appear as vertical spikes in a plot of the noise spectrum whereas broad band noise appears as a continuous line, Fig. 11.3. The noise spectrum of a ship helps to identify it and is therefore sometimes called its signature.

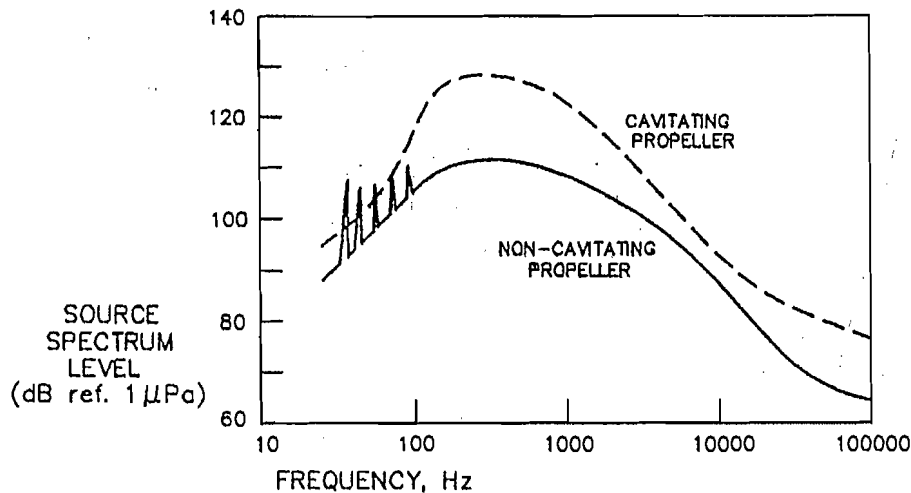


Figure 11.3 : Propeller Noise Spectra.

The prediction of propeller noise may be done with the help of empirical formulas, such as one due to Ross (1976):

$$L_p(f) = 135 + 10 \log_{10} (Z n^6 D^6 f^{-2}) \text{ dB} \quad (11.16)$$

where the reference pressure is $1 \mu\text{Pa}$, the band width is 1 Hz, and the sound pressure is measured at a distance of 1 m from the source of sound. Theoretical methods are as yet incapable of predicting cavitation noise, and predictions of propeller noise are usually made with the help of experiments in a cavitation tunnel. The reverberation of noise in a cavitation tunnel is a major problem. There are also problems of scaling up the noise measured on the model scale to full scale.

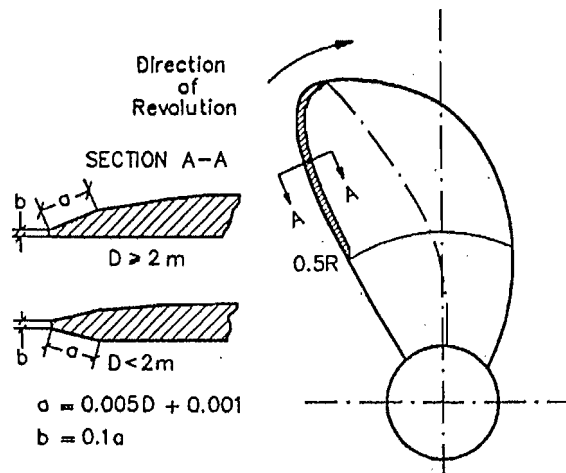


Figure 11.4 : Anti-singing Edge in a Propeller Blade.

A particular type of noise occurs when the propeller blades vibrate in the audible frequency range. This is known as the singing of propellers. Singing is probably due to the blades being set into vibration by boundary layer separation near the trailing edges, resulting in the shedding of vortices alternately from the face and the back of the blades. The phenomenon of singing is unpredictable since it is often found that of two propellers of the same design one sings while the other is silent. The singing of propellers takes many forms, and may occur at different frequencies from low to high in a particular range of propeller rpm. Propeller singing is usually unimportant except when it occurs in the normal range of operation of the ship. If necessary, the propeller blades can be given a special "anti-singing" edge in which the trailing edge in the outer part of the blade has a sharp wedge shape, Fig. 11.4. This eliminates the alternate shedding of vortices and the resulting blade vibration because the boundary layer separation occurs at fixed points near the trailing edge.

11.3 Propulsion in a Seaway

The power required to propel a ship at a given speed increases with the severity of the conditions in the sea. At a given power, the speed attained

decreases as the sea state increases. This decrease in speed at constant power due to the sea conditions is termed "involuntary speed loss". If the severity of the sea conditions become excessive, it is necessary to reduce the power to limit the motions of the ship and prevent damage. The decrease in speed due to a deliberate reduction in power is termed "voluntary speed loss".

There are two approaches to estimating the effect of sea conditions on ship propulsion: (i) self-propulsion tests with models in waves, and (ii) calculations based on measurement or calculation of the added resistance of the ship in waves and estimated values of the propulsion factors. In carrying out self-propulsion tests in waves, it is necessary to take into account the response of the propulsion plant to the fluctuations in the loading of the propeller in waves. Diesel engines have constant torque characteristics, so that an increase in the loading causes a decrease in the propeller rpm and delivered power at constant torque. Turbines, on the other hand, have constant power characteristics so that increased propeller loading causes an increase in the torque and a decrease in the propeller rpm at constant delivered power. These characteristics must be incorporated into the control system of the drive motor used in the model self-propulsion tests in waves.

In calculating the effect of the seaway on the propulsion of a ship, the added resistance in waves and the wind resistance are calculated and added to the calm water resistance. It is usually assumed that the propulsion factors (wake fraction, thrust deduction fraction, and relative rotative efficiency) are independent of the wave frequency and have the same values as in calm water at a propeller loading equal to the average loading in waves. It is also assumed that the propeller characteristics (K_T, K_Q, J) in waves are the same as in calm water. However, these assumptions are obviously untenable if the propeller emerges out of water due to ship motions and if there is air drawing.

Self-propulsion experiments and the calculation of power in waves are carried out for regular waves for a range of wave frequencies. An "added power operator" $\delta P/\bar{\zeta}^2$ is determined as a function of the wave encounter frequency ω_E , δP being the increase in average power in waves over that in calm water and $\bar{\zeta}$ the wave amplitude. The mean added power in irregular long crested seas is then given by:

$$\delta \bar{P} = 2 \int \frac{\delta P(\omega_E)}{\bar{\zeta}^2} S_{\zeta}(\omega_E) d\omega_E \quad (11.17)$$

where $S_{\zeta}(\omega_E)$ is the encounter spectrum of the seaway and represents the distribution of wave energy as a function of the frequency of wave encounter. In this way, self-propulsion tests or added power calculations for different ship speeds and headings (relative to the waves) can be used to predict power as a function of speed for various sea conditions represented by their energy spectra.

Example 2

The effective power of a ship in calm water is as follows:

Speed, knots	:	14.0	14.5	15.0	15.5	16.0	16.5
Effective power, kW	:	2100	2375	2674	2999	3352	3733

The ship has a propulsion plant giving a delivered power of 4900 kW at 120 rpm to the propeller, which has a diameter of 5.5 m and a pitch ratio of 0.8. Determine the speed of the ship in calm water. What will be the involuntary speed loss in waves if the average increase in effective power over that in calm water is 40 percent and (a) if the propulsion plant of the ship consists of a diesel engine directly connected to the propeller, and (b) if the propulsion plant consists of a geared steam turbine? Calculate the propeller rpm, torque and delivered power in the two cases. Assume that the propeller open water characteristics and the propulsion factors are not affected by the waves, and are as follows:

$$K_T = 0.3415 - 0.2588 J - 0.1657 J^2 \quad 10K_Q = 0.4021 - 0.2330 J - 0.2100 J^2$$

Wake fraction = 0.220, thrust deduction fraction = 0.190, relative rotative efficiency = 1.030, thrust identity.

$$P_D = 4900 \text{ kW} \quad n_1 = 120 \text{ rpm} = 2.000 \text{ s}^{-1} \text{ (rated rpm)} \quad D = 5.5 \text{ m}$$

$$\begin{aligned} \frac{K_T}{J^2} &= \frac{T}{\rho n^2 D^4} \frac{n^2 D^2}{V_A^2} = \frac{R/(1-t)}{\rho D^2 (1-w) V^2} = \frac{1}{\rho D^2 (1-t) (1-w)^2} \frac{P_E}{V^3} \\ &= \frac{1}{1.025 \times 5.5^2 \times (1-0.190) \times (1-0.220)^2} \frac{P_E}{V^3} = \frac{1}{15.2800} \frac{P_E}{V^3} \end{aligned}$$

From this, the values of J can be determined for different speeds V using the open water characteristics:

$$0.3415 \left(\frac{1}{J} \right)^2 - 0.2588 \frac{1}{J} - \left(0.1657 + \frac{K_T}{J^2} \right) = 0$$

and the values of $10K_Q$ calculated. The speed of the ship will be given by that value of V at which the K_Q from the open water characteristics is equal to the K_Q calculated from the delivered power:

(a) For the diesel plant:

$$Q = \frac{P_D}{2\pi n_1} = \frac{4900}{2\pi \times 2.00} = 389.930 \text{ kNm}$$

and this is constant, so that:

$$K'_Q = \frac{Q \eta_R}{\rho n^2 D^5} = \frac{389.930 \times 1.030}{1.025 \times n^2 \times 5.5^5} = \frac{0.077855}{n^2}$$

$$n = \frac{V_A}{JD} = \frac{(1-w)V}{JD} = \frac{(1-0.220)V}{J \times 5.5} = 0.141818 \frac{V}{J}$$

$$P_D = 2\pi n Q$$

(b) For the geared turbine plant:

P_D is constant and:

$$K'_Q = \frac{P_D \eta_R}{2\pi \rho n^3 D^5} = \frac{4900 \times 1.030}{2\pi \times 1.025 \times n^3 \times 5.5^5} = \frac{0.155710}{n^3}$$

Table 11.2 (a)

Calm Water Propulsion Characteristics (Example 2)

$V \text{ k}$	14.0	14.5	15.0	15.5	16.0	16.5
ms^{-1}	7.2016	7.4588	7.7160	7.9732	8.2304	8.4876
$P_E \text{ kW}$	2100	2375	2674	2999	3352	3733
K_T/J^2	0.3680	0.3746	0.3809	0.3872	0.3935	0.3996
J	0.5934	0.5908	0.5884	0.5860	0.5836	0.5814
K_T	0.1296	0.1308	0.1319	0.1330	0.1340	0.1350
$10K_Q$	0.1899	0.1911	0.1923	0.1935	0.1946	0.1957
$n \text{ s}^{-1}$	1.7211	1.7904	1.8599	1.9297	2.0000	2.0705
rpm	103.3	107.4	111.6	115.8	120.0	124.2
(a) $10K'_Q$	0.2628	0.2429	0.2251	0.2091	0.1946	0.1816
(b) $10K'_Q$	0.3054	0.2713	0.2420	0.2167	0.1946	0.1794

Table 11.2 (b)
Propulsion Characteristics in Waves (Example 2)

40 percent increase in Effective Power					
V k	:	14.0	14.5	15.0	14.176 14.365
ms^{-1}	:	7.2016	7.4588	7.7160	7.2923 7.3894
P_E kW	:	2940	3325	3744	3073 3218
K_T/J^2	:	0.5152	0.5244	0.5333	0.5185 0.5220
J	:	0.5432	0.5405	0.5379	0.5422 0.5412
K_T	:	0.1520	0.1532	0.1543	0.1525 0.1529
$10K_Q$:	0.2136	0.2148	0.2160	0.2140 0.2145
n s ⁻¹	:	1.8801	1.9570	2.0342	1.9073 1.9363
rpm	:	112.8	117.4	122.1	114.4 116.2
(a) $10K'_Q$:	0.2203	0.2033	0.1882	0.2140 -
(b) $10K'_Q$:	0.2343	0.2077	0.1850	- 0.2145
Q kNm	:				389.93 402.75
P_D kW	:				4673 4900
					Diesel Turbine
					<u>Diesel</u> <u>Turbine</u>
Involuntary speed loss, k					1.824 1.635
Propeller rpm					114.4 116.2
Torque, kNm					389.93 402.75
Delivered Power, kW					4673 4900

11.4 Propeller Roughness

When a ship goes into service, its hull and propeller surfaces get progressively rougher. The increase in hull surface roughness causes an increase in the effective power of the ship. The roughness of the blade surfaces of a propeller affects its performance characteristics. There is an increase in the torque

coefficient K_Q and a decrease in the thrust coefficient K_T , which together cause a significant decrease in propeller efficiency.

The effect of propeller roughness depends on both the amplitude of the roughness and its texture. A measure of propeller surface roughness is Musker's h' parameter which is expressed in many ways, one of which is:

$$h' = 0.0147 R_{a2.5}^2 p_c \quad (11.18)$$

where $R_{a2.5}$ is the root mean square roughness height in microns over a 2.5 mm length and p_c is the peak count per mm as determined by a portable roughness gauge. A simpler approach to determine propeller blade surface roughness is to compare the propeller surface with the Rubert comparator gauge, which has six representative surfaces of different roughnesses as follows:

Surface :	A	B	C	D	E	F
h' microns:	1.1	5.4	17.3	61	133	311

If the roughness varies over the propeller surface, an average propeller roughness may be calculated by dividing the surface into a number of parts, determining the roughness parameter for each part and finding a weighted average taking into account the area of each part and the radius at which it is located. Thus, if the propeller blade surface is divided into radial strips, the average propeller roughness is given by:

$$k_p = \frac{\int c r^3 h' dr}{\int c r^3 dr} \quad (11.19)$$

where c and r are the mean chord and mean radius of each strip and h' the roughness parameter for that strip.

The drag coefficients of a propeller blade section with smooth and rough surface are given according to Mishkevich (1995) by:

$$C_{Ds} = 0.05808 \left(1 + 2.3 \frac{t}{c} \right) R_{nc}^{-0.1458} \quad (11.20)$$

$$C_{Dr} = \left(1 + 2.3 \frac{t}{c}\right) \left(2.34 + 1.121 \log \frac{c}{k_p}\right)^{-2.5} \quad (11.21)$$

where t and c are the thickness and chord of the representative blade section of the propeller, i.e. at $0.7R$ or $0.75R$, and R_{nc} is the Reynolds number based on the resultant velocity and chord of the section. The change in the drag coefficient ΔC_D for differing degrees of roughness can then be determined. One may alternatively use the formulas in Eqn. (8.11), Chapter 8, to determine ΔC_D .

The roughness of the propeller blade surface also causes a change in the lift coefficient of the blade section. According to Mishkevich, this change ΔC_L is given by:

$$\Delta C_L = -1.2882 \Delta C_D^{0.94} \quad (11.22)$$

or more simply according to Townsin, Spencer, Mosaad and Patience (1985) by:

$$\Delta C_L = -1.1 \Delta C_D \quad (11.23)$$

These changes in the lift and drag coefficients of the propeller blade sections cause changes in the thrust and torque coefficients which, it can be shown, are given by:

$$\begin{aligned} \Delta K_T &= \frac{\pi^2}{4} Z \int_{x_b}^{1.0} \frac{c}{D} x^2 \frac{\cos^2(\beta_I - \beta)}{\cos^2 \beta} [\Delta C_L \cos \beta_I - \Delta C_D \sin \beta_I] dx \\ \Delta K_Q &= \frac{\pi^2}{8} Z \int_{x_b}^{1.0} \frac{c}{D} x^3 \frac{\cos^2(\beta_I - \beta)}{\cos^2 \beta} [\Delta C_L \sin \beta_I + \Delta C_D \cos \beta_I] dx \end{aligned} \quad (11.24)$$

where:

- Z = number of blades;
- x_b = non-dimensional boss radius;
- c = chord at radius r ;
- D = propeller diameter;
- x = non-dimensional radius r/R ;

β_I = hydrodynamic pitch angle including induced velocities;

β = hydrodynamic pitch angle excluding induced velocities.

(See Fig. 3.4)

The effects of propeller roughness on the performance characteristics can thus be calculated.

These expressions can be greatly simplified by making various assumptions and approximations. If it is assumed that the blade section at $x = x_1$ is representative of the whole propeller and that:

$$\begin{aligned}\frac{dK_T}{dx} &= k_1 x^2 (1-x)^{0.5} \\ \frac{dK_Q}{dx} &= k_2 x^2 (1-x)^{0.5}\end{aligned}\quad (11.25)$$

then:

$$K_T = \int_{x_b}^{1.0} k_1 x^2 (1-x)^{0.5} dx = m(x_1) k_1 x_1^2 (1-x_1)^{0.5}$$

where $m(x_1)$ is a coefficient that depends on the value of x_1 chosen, and which is then given by:

$$m(x_1) = \frac{(1-x_b)^{0.5} (8 + 12x_b + 15x_b^2)}{x_1^2 (1-x_1)^{0.5}} \quad (11.26)$$

One may write:

$$\begin{aligned}\Delta K_T &= m(x_1) \frac{\pi^2}{4} Z \frac{c}{D} x_1^2 \frac{\cos^2(\beta_I - \beta)}{\cos^2 \beta} \cos \beta_I (\Delta C_L - \Delta C_D \tan \beta_I) \\ \Delta K_Q &= m(x_1) \frac{\pi^2}{8} Z \frac{c}{D} x_1^3 \frac{\cos^2(\beta_I - \beta)}{\cos^2 \beta} \cos \beta_I (\Delta C_L \tan \beta_I + \Delta C_D)\end{aligned}\quad (11.27)$$

where $c, \beta, \beta_I, \Delta C_L$ and ΔC_D all refer to the section at x_1 .

Still further simplifications are possible if one makes the following assumptions:

$$J = 0.8 \frac{P(x_1)}{D} \quad (11.28)$$

$$\tan \beta_I = \frac{P(x_1)/D}{\pi x_1} \quad (11.29)$$

which imply that the propeller works at a 20 percent nominal slip ratio and zero angle of attack. Since:

$$\tan \beta = \frac{J}{\pi x_1} \quad (11.30)$$

the values of β_I and β can be calculated for a given propeller, and numerical values of ΔK_T and ΔK_Q determined for a given average propeller roughness k_p . However, it is found that $\cos^2(\beta_I - \beta) \cos \beta_I / \cos^2 \beta$ varies only slightly with pitch ratio, having values of 1.003 at $P/D = 0.4$ and 1.061 at $P/D = 1.6$ based on Eqns. (11.28), (11.29) and (11.30), and an average value of 1.026 over this range of pitch ratio. Then:

$$\begin{aligned} \Delta K_T &= 1.026 m(x_1) \frac{\pi^2}{4} Z \frac{c}{D} x_1^2 \left(\Delta C_L - \Delta C_D \frac{P/D}{\pi x_1} \right) \\ \Delta K_Q &= 1.026 m(x_1) \frac{\pi^2}{8} Z \frac{c}{D} x_1^3 \left(\Delta C_L \frac{P/D}{\pi x_1} + \Delta C_D \right) \end{aligned} \quad (11.31)$$

If one takes the representative section of the propeller to be at $x_1 = 0.75$ and the root section at $x_b = 0.20$, $m(x_1) = 0.6663$ and:

$$\begin{aligned} \Delta K_T &= \left(0.9488 \Delta C_L - 0.4027 \Delta C_D \frac{P}{D} \right) \frac{c}{D} Z \\ \Delta K_Q &= \left(0.1510 \Delta C_L \frac{P}{D} + 0.3558 \Delta C_D \right) \frac{c}{D} Z \end{aligned} \quad (11.32)$$

Example 3

A four-bladed propeller of 5.0 m diameter and 0.8 pitch ratio has a chord of 1.375 m and a thickness of 0.0675 m at $0.75R$. The propeller runs at 150 rpm. The thrust and torque coefficients of the propeller when new are:

$$J = 0.640 \quad K_T = 0.1080 \quad 10K_Q = 0.1670$$

Assuming that the new propeller has a smooth surface, determine the thrust and torque coefficients when the propeller roughness is 300 microns.

$$Z = 4 \quad D = 5.0 \text{ m} \quad \frac{P}{D} = 0.8 \quad c = 1.375 \text{ m} \quad t = 0.0675 \text{ m}$$

$$\frac{c}{D} = \frac{1.375}{5.00} = 0.275 \quad \frac{t}{c} = \frac{0.0675}{1.375} = 0.0491 \quad n = 150 \text{ rpm} = 2.5 \text{ s}^{-1}$$

$$K_{Ts} = 0.1080 \quad 10K_{Qs} = 0.1670$$

(Subscripts *s* and *r* for smooth and rough respectively)

$$\eta_{Os} = \frac{K_{Ts} J}{K_{Qs} 2\pi} = \frac{0.1080}{0.01670} \times \frac{0.640}{2\pi} = 0.6857$$

$$V_A = J n D = 0.640 \times 2.5 \times 5.0 = 8.000 \text{ m s}^{-1}$$

$$V_R^2 = V_A^2 + (0.75 \pi n D)^2 = 8.000^2 + (0.75 \pi \times 2.5 \times 5.0)^2$$

$$= 931.446 \text{ m}^2 \text{ s}^{-2}$$

$$V_R = 30.520 \text{ m s}^{-1}$$

$$R_{nc} = \frac{V_R c}{\nu} = \frac{30.520 \times 1.375}{1.188 \times 10^{-6}} = 35.323 \times 10^6$$

$$C_{Ds} = 0.05808 \left(1 + 2.3 \frac{t}{c} \right) R_{nc}^{-0.1458}$$

$$= 0.05808 (1 + 2.3 \times 0.0491) \times (3.5323 \times 10^7)^{-0.1458}$$

$$= 0.005128$$

$$C_{Dr} = \left(1 + 2.3 \frac{t}{c} \right) \left(2.34 + 1.121 \log \frac{c}{k_p} \right)^{-2.5}$$

$$= (1 + 2.3 \times 0.0491) \times \left(2.34 + 1.121 \log \frac{1.375}{300 \times 10^{-6}} \right)^{-2.5}$$

$$= 0.010557$$

$$\Delta C_D = C_{Dr} - C_{Ds} = 0.005429$$

$$\Delta C_L = -1.2882 \Delta C_D^{0.94} = -0.009564$$

$$\Delta K_T = \left(0.9488 \Delta C_L - 0.4027 \Delta C_D \frac{P}{D} \right) \frac{c}{D} Z$$

$$= [0.9488 \times (-0.009564) - 0.4027 \times 0.005429 \times 0.8] \times 0.275 \times 4$$

$$= -0.0119$$

$$\Delta K_Q = \left(0.1510 \Delta C_L \frac{P}{D} + 0.3558 \Delta C_D \right) \frac{c}{D} Z$$

$$= [0.1510 \times (-0.009564) \times 0.8 + 0.3558 \times 0.005429] \times 0.275 \times 4$$

$$= 0.00085$$

$$K_{Tr} = K_{Ts} + \Delta K_T = 0.1080 - 0.0119 = 0.0961$$

$$K_{Qr} = K_{Qs} + \Delta K_Q = 0.01670 + 0.00085 = 0.01755$$

$$\eta_{Or} = \frac{K_{Tr}}{K_{Qr}} \frac{J}{2\pi} = \frac{0.0961}{0.01755} \times \frac{0.640}{2\pi} = 0.5578$$

As this example shows, propeller roughness can have a significant effect on propeller efficiency, and it is necessary to service the propeller properly every time the ship is dry-docked. Proper servicing of the propeller includes:

- rectification of any damage
- correction of edge deformation
- light grinding and polishing of the blade surfaces to produce a finish as good as new, i.e. less than 3 microns roughness.

Great care should be taken near the leading edges and near the blade tips to ensure that the blade shape is not altered during grinding.

11.5 Propeller Manufacture

The manufacture of marine propellers is a specialised activity requiring the use of facilities for making large castings and then machining them to the specified degree of accuracy. It is necessary to ensure that the castings are free of defects and the finished propeller is in accordance with the shape and dimensions specified by the propeller designer. An inaccurately manufactured propeller may have a low efficiency and suffer from cavitation, vibration, erosion and noise.

The mould for casting a small propeller (less than 2.5 m diameter) may be made using a wooden pattern of one blade, with the mould being in two parts. For large propellers, the mould for the face of the propeller blades is made by "sweep moulding". A sweeping board or "knife" is used to form a helicoidal surface by rotating the knife about an axis while guiding it along a template in the form of a helix of the appropriate pitch. This produces a helicoidal surface of constant pitch. If the inner and outer ends of the knife are constrained to follow different pitch templates when the knife is rotated about the axis, a helicoidal surface with a linearly varying pitch is obtained. By displacing the knife axis from the propeller axis, it is possible to obtain a hyperbolic pitch variation along the radius. The mould itself is made of sand and cement with appropriate internal steel reinforcements.

Once the mould for the faces of the propeller blades is made, templates for the radial sections are set up at a number of radii. The helicoidal surface for each blade face is also filled with a sand-cement mixture to incorporate the required pitch variation and the washaway on face. The radial section templates are then used to make a sand blade shape on each helicoidal surface of the face mould. The back mould is cast in sand and cement on the face mould with its sand blades. After the cement moulds have cured, the two parts are separated and faired (i.e. the surfaces are made smooth and blemishes removed). Runners and risers for the casting are provided. Trailing edge recesses are also made if necessary to ensure that the liquid metal flows upward during the casting process and no air is trapped inside. The two parts of the mould are then put back together and firmly held by girders and rings.

The metal of which the propeller is to be made is melted in a furnace and the molten metal is then poured into the mould through the runners provided

at the sides. It is usually necessary in large propeller castings to pour the molten metal in two or three stages to counteract the effect of contraction while cooling. The molten metal is at a sufficiently high temperature to ensure that there is complete fusion (950–1100° C for Manganese Bronze and 1050–1200° C for Aluminium Bronze).

After the propeller casting has cooled, the mould is broken and the casting taken out. The casting is checked for its soundness by dye penetrant or ultrasonic tests, and the mechanical properties and chemical composition of the material are determined from specimens taken from the runners and risers.

The next step is to determine the position of the propeller axis and a reference plane normal to the axis such that the finished blades lie within the casting. Once this has been done, the propeller bore is machined in a horizontal boring machine using plug gauges supplied by the shafting manufacturer. After the propeller bore has been machined, the blades are machined to their specified shape. At one time, this was done by special planing machines for finishing the propeller blade face. This has been superseded by a manual method which is found to be more economical. A large number of points on the face and the back are marked, and at each point the amount of material to be removed is determined. The unwanted material is then removed by pneumatic chisels, and the blade surfaces finished by grinding using various grades of grinding wheels.

In recent years, propeller manufacturers have been switching over to the use of numerically controlled milling machines for finishing propellers. CNC (computer numerical control) five-axis machines with as-machined animation and adaptive control are being increasingly used. Animation and solid modellers provide a computer simulation of the cutter paths and display the material to be removed and the final finished product. With adaptive control, the machining parameters are sensed and automatic adjustments made to cutter speeds and feeds. The use of computer aided design and manufacture (CAD/CAM) in manufacturing propellers has many advantages: greater accuracy and savings in time, labour, space and cost.

After the propeller has been machined, it is checked for dimensional accuracy: diameter, pitch and blade thicknesses at various radii, shapes of the root fillets and the leading and trailing edges, the axial alignment of the blades and their angular spacing, and the surface roughness. Finally, the

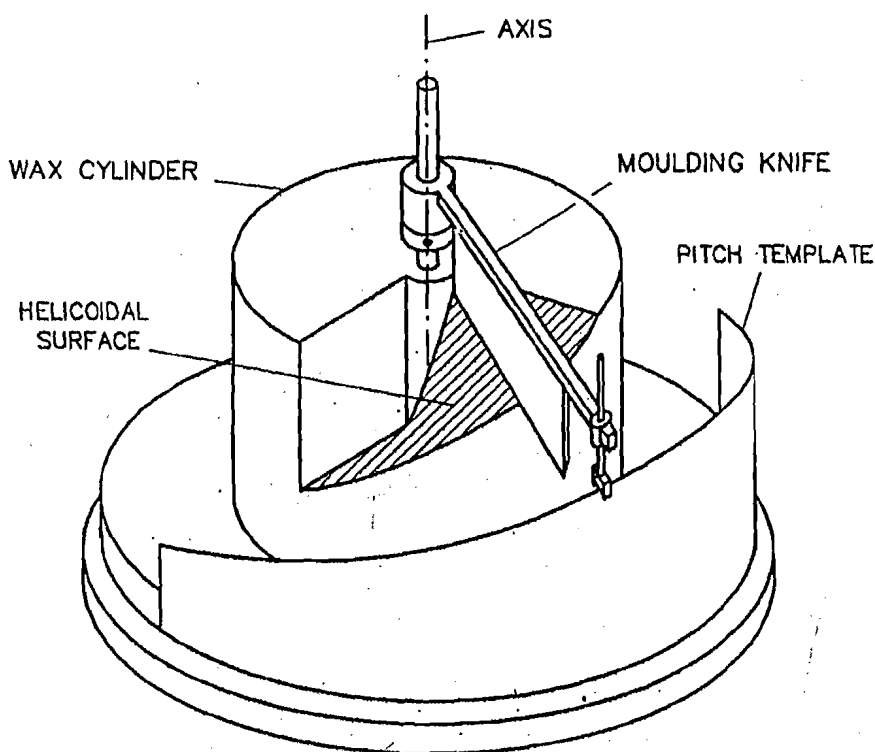


Figure 11.5 : Moulding a Helicoidal Surface.

propeller is statically balanced. The manufacturing tolerances for marine propellers specified by the International Standards Organisation (ISO) are given in Table 11.3.

Model propellers for use in model experiments are made in a manner similar to ship propellers. A wax cylinder is shaped into helicoidal surfaces, one for each blade, using a knife revolving about an axis while moving along a helical template of the appropriate pitch, Fig. 11.5. A plaster of paris mould is made from this wax surface for the faces of the propeller blades. Templates representing the radial sections of the model propeller are set up at a number of radii, and clay blades made on each helicoidal surface. Another plaster of paris mould is cast over the clay blades to form the mould for the

Table 11.3

Summary of Manufacturing Tolerances for Ship Propellers according to ISO

No	ITEM	CLASS			
		S	I	II	III
1.	<i>Manufacturing Accuracy</i>	Very High	High	Medium	Wide Tolerances
2.	<i>Radius</i>				
	Tolerance as percentage of propeller radius	± 0.2	± 0.3	± 0.4	± 0.5
	with a minimum of (mm)	1.5	1.5	2.0	2.5
3.	<i>Pitch</i>				
	a) Local Pitch				
	Tolerance as percentage of design pitch				
	at each radius	± 1.5	± 2.0	± 3.0	—
	Minimum (mm)	10	15	20	—
	b) Mean pitch at each radius of each blade				
	Tolerance as percentage of design pitch	± 1.0	± 1.5	± 2.0	± 5.0
	at each radius				
	Minimum (mm)	7.5	10	15	25
	c) Mean pitch of each blade				
	Tolerance as percentage of	± 0.75	± 1.0	± 1.5	± 4
	design mean pitch				
	Minimum (mm)	5.0	7.5	10.0	20.0
	d) Mean pitch for all the blades				
	Tolerance as percentage of design mean	± 0.5	± 0.75	± 1.0	± 3.0
	pitch				
	Minimum (mm)	4.0	5.0	7.5	15.0

Table 11.3 (Contd.)
Summary of Manufacturing Tolerances for Ship Propellers according to ISO

No	ITEM	CLASS			
		S	I	II	III
4.	<i>Blade thickness</i>				
	a) Plus tolerance as percentage of the local thickness	+2.0	+2.5	+4.0	+6.0
	Minimum (mm)	0.5	1.0	2.0	3.0
	b) Minus tolerance as percentage of the local thickness	-1.0	-1.5	-2.0	-4.0
	Minimum (mm)	-0.5	-1.0	-1.5	-2.0
5	<i>Blade width</i>				
	Tolerance as percentage of D/Z	± 1.5	± 2.0	± 3.0	± 5.0
	Minimum (mm)	4	7	10	12
6.	<i>Angular spacing of blades</i>				
	Tolerance in degrees	± 1	± 1	± 2	± 2
7.	<i>Axial position of blades</i>				
	Tolerance as percentage of diameter D	± 0.5	± 1.0	± 1.5	± 1.5
8.	<i>Surface finish</i>				
	Maximum roughness in microns	3	6	12	25

Measurements should be made at:

- a section near the boss and at $r/R = 0.4, 0.5, 0.6, 0.7, 0.8, 0.9$ and 0.95 for Class S and Class I propellers
- a section near the boss and at $r/R = 0.5, 0.7$ and 0.9 for Class II and Class III propellers.

back surfaces of the propeller blades. After this has set, the two parts of the plaster mould are separated and faired. Runners and risers for casting the metal are made, and the two parts of the mould fitted firmly together. The molten metal, usually white metal or aluminium alloy, is then poured into the mould and the model propeller casting obtained.

The finishing of the model propeller casting is carried out in several ways. The commonest method is to use a special propeller point drilling machine in which a large number of points are drilled on the face and the back of each blade to their specified cylindrical polar coordinates (r, θ, z) . The blades are then finished by hand grinding and filing. Another method is to use a copy milling machine with an accurately made blade pattern. However, today the trend is to use CNC five-axis milling machines even for model propellers, but this usually requires the blades to be suitably supported to prevent their deflection under the load imposed by the milling cutter. Instead of machining a casting of the model propeller, one may start with a solid block of metal and machine it to the final model propeller shape. Typical manufacturing tolerances for model propellers are given in Table 11.4.

Table 11.4

Manufacturing Tolerances for Model Propellers

Dimeter	: ± 0.75 mm
Mean pitch at each radius:	± 0.5 % of design value
Blade thickness	: ± 0.125 mm
Blade width	: ± 0.2 mm

11.6 Acceleration and Deceleration

The acceleration and deceleration of a ship using its propulsion system involve rather complex phenomena and are difficult to calculate. The principles involved are, however, quite simple. Consider a ship undergoing acceleration. The net force causing the acceleration is:

$$F = (1 - t)T - R_T = (1 + c)\Delta \frac{dV}{dt} \quad (11.33)$$

where:

- t = thrust deduction fraction;
- T = propeller thrust (positive forward);
- R_T = total resistance of the ship;
- c = added mass coefficient;
- Δ = displacement (mass) of the ship;
- V = ship speed;
- \hat{t} = time.

The resistance of the ship is a function of the ship speed while the thrust depends upon the speed of the ship, the propeller revolution rate, the propulsion factors and the open water characteristics of the propeller. The added mass coefficient depends upon the hull form of the ship. The time required for the speed of the ship to change from V_1 to V_2 is:

$$\hat{t} = (1 + c) \Delta \int_{V_1}^{V_2} \frac{1}{F} dV \quad (11.34)$$

and the distance travelled by the ship in this period is:

$$s = (1 + c) \Delta \int_{V_1}^{V_2} \frac{V}{F} dV \quad (11.35)$$

These equations may be used to calculate the acceleration, stopping and reversing characteristics of a ship. However, the determination of the various quantities involved in these equations requires propulsion and open water tests covering the four quadrant operation of the propeller, i.e. both directions of revolution and speeds of advance, over the required speed range, as well as resistance tests for both directions, forward and aft. It is also necessary to know the machinery characteristics involved in limiting the propeller revolution rate at different ship speeds and in stopping the revolution of the propeller in one direction and starting it in the opposite direction. Finally, it must be noted that when a ship is being stopped by reversing its propeller

it tends to follow a curved path, and this is not taken into account in the foregoing equations.

Example 4

A ship of 10000 tonnes displacement has an effective power as follows:

Speed, knots	:	4.0	8.0	12.0	16.0	20.0
Effective Power, kW:		27.2	329.9	1420.0	4000.0	8931.7

The propeller has a diameter of 6.0 m and a pitch ratio of 0.7, and its open water characteristics are given by:

$$K_T = 0.2974 - 0.2536 J - 0.1840 J^2 \quad 10K_Q = 0.3187 - 0.2114 J - 0.2004 J^2$$

The propulsion factors, which may be assumed not to vary with speed, are as follows: wake fraction = 0.250, thrust deduction fraction = 0.200, relative rotative efficiency = 1.050, based on thrust identity. The ship is propelled by a diesel engine of maximum rating 6000 kW at 120 rpm directly coupled to the propeller, the shafting efficiency being 0.980. Calculate the accelerating force on the ship at different speeds assuming that the maximum rated torque of the engine is not to be exceeded. If the added mass coefficient of the ship is 0.050, determine approximately the time taken for the ship starting from rest to reach a speed of 16 knots, and the distance travelled before this speed is attained.

$$\Delta = 10000 \text{ tonnes} \quad c = 0.050 \quad D = 6.0 \text{ m} \quad \frac{P}{D} = 0.7$$

$$K_T = 0.2974 - 0.2536 J - 0.1840 J^2 \quad 10K_Q = 0.3187 - 0.2114 J - 0.2004 J^2$$

$$w = 0.250 \quad t = 0.200 \quad \eta_R = 1.050 \quad \text{Thrust Identity}$$

$$P_B = 6000 \text{ kW} \quad n = 120 \text{ rpm} = 2.0 \text{ s}^{-1} \quad \eta_S = 0.980$$

$$P_D = P_B \eta_S = 6000 \times 0.980 = 5880 \text{ kW}$$

$$Q = \frac{P_D}{2\pi n} = \frac{5880}{2\pi \times 2.0} = 467.916 \text{ kNm}$$

$$10K_Q = \frac{10Q\eta_R}{\rho n^2 D^5} = \frac{10 \times 467.916 \times 1.050}{1.050 n^2 \times 6.0^5} = \frac{0.61642}{n^2}$$

$$(i) \quad V = 0 \quad V_A = 0 \quad P_E = 0 \quad R_T = 0 \quad J = 0$$

$$10 K_Q = \frac{0.61642}{n^2} = 0.3187 \quad n = 1.3907 \text{ s}^{-1} = 83.44 \text{ rpm}$$

$$T = K_T \rho n^2 D^4 = 0.2974 \times 1.025 \times 1.3907^2 \times 6.0^4 = 764.1 \text{ kN}$$

$$F = (1 - t)T - R_T = (1 - 0.200)764.1 - 0 = 611.3 \text{ kN}$$

$$(ii) \quad V = 4.0 \text{ k} = 2.0576 \text{ ms}^{-1} \quad P_E = 27.2 \text{ kW}$$

$$V = (1 - w)V = (1 - 0.025) \times 2.0576 = 1.5432 \text{ ms}^{-1}$$

$$R_T = \frac{P_E}{V} = \frac{27.2}{2.0576} = 13.219 \text{ kN}$$

$$J = \frac{V_A}{nD} = \frac{1.5432}{n \times 6.0} = \frac{0.2572}{n}$$

$$\frac{10 K_Q}{J^2} = 0.3187 \left(\frac{1}{J} \right)^2 - 0.2114 \frac{1}{J} - 0.2004$$

$$= \frac{0.61642}{n^2} \frac{n^2}{0.2572^2} = 9.3183$$

$$\frac{1}{J} = 5.8068 \quad J = 0.1722 \quad K_T = 0.2483 \quad 10 K_Q = 0.2764$$

$$n = \frac{0.2572}{J} = \frac{0.2572}{0.1722} = 1.4935 \text{ s}^{-1} = 89.61 \text{ rpm}$$

$$T = K_T \rho n^2 D^4 = 0.2483 \times 1.025 \times 1.4935^2 \times 6.0^4 = 735.6 \text{ kN}$$

$$F = (1 - t)T - R_T = (1 - 0.200)735.6 - 13.2 = 575.3 \text{ kN}$$

Similarly, for the remaining speeds one obtains:

V knots:	8.0	12.0	16.0	20.0
n rpm :	97.80	107.80	119.36	132.18
F kN :	481.8	300.2	6.2	-638.2

The integrations are performed as follows:

V		F	$\frac{1000}{F}$	$\frac{1000 V}{F}$	SM	$f(\hat{t})$	$f(s)$
k	ms^{-1}	kN					
0	0.0000	611.3	1.6359	0	1	1.6359	0
4.0	2.0576	575.3	1.7382	3.5766	4	6.9528	14.3064
8.0	4.1152	481.8	2.0756	8.5413	2	4.1512	17.0826
12.0	6.1728	300.2	3.3311	20.5623	4	13.3244	82.2492
16.0	8.2304	6.2	162.1271	1334.3709	1	162.1271	1334.3709
						188.1914	1448.0091

$$\hat{t} = \Delta(1+c) \int_{V_1}^{V_2} \frac{1}{F} dV$$

$$= 10000(1+0.050) \times \frac{1}{3} \times 2.0576 \times \frac{188.1914}{1000} \text{ tonnes ms}^{-1} \text{ kN}^{-1}$$

$$= 1355.3 \text{ s}$$

$$s = \Delta(1+c) \int_{V_1}^{V_2} \frac{V}{F} dV$$

$$= 10000(1+0.050) \times \frac{1}{3} \times 2.0576 \times \frac{1448.0091}{1000} \text{ tonnes m}^2 \text{ s}^{-2} \text{ kN}^{-1}$$

$$= 10428 \text{ m}$$

The integrations using Simpson's Rule are not very accurate because as the steady speed is approached the acceleration reduces asymptotically to zero and the integrands tend to infinity.

11.7 Engine-Propeller Matching

In the design of the propulsion system of a ship, it is important to match the ship, the propeller and the propulsion machinery so that the propulsion system as a whole operates in the optimum manner. The task of optimising

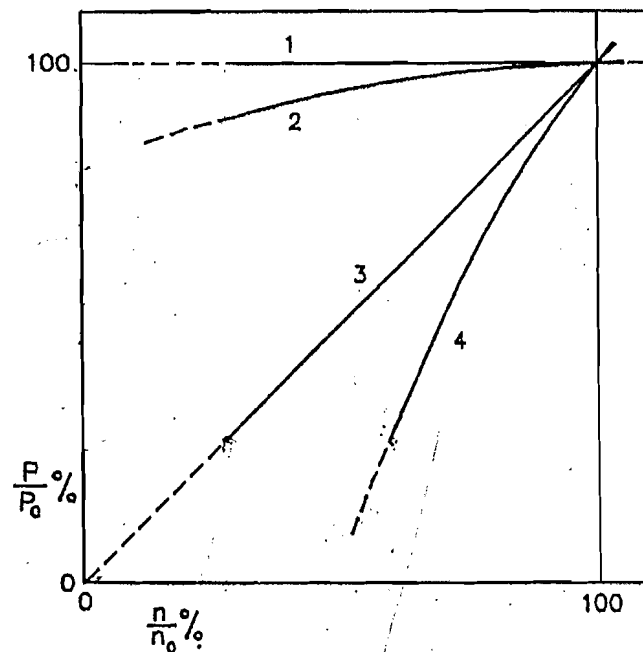
the propulsion system is difficult because the power-speed characteristics of the ship and propeller taken together are very different from those of the engine. The power-speed characteristics of the ship and propeller moreover change with the loading of the ship and the sea conditions, and with time as the hull and the propeller get progressively rougher due to fouling, corrosion and possibly cavitation erosion. In selecting the propulsion plant for a ship and designing its propeller or propellers, it is necessary to ensure that the desired ship speed is achieved without overloading the engine or exceeding its rated rpm in the varying operating conditions of the ship. If the engine and the propeller are not properly matched, the life of the engine may be reduced, maintenance costs may be higher and the fuel consumption may be greater.

The relation between the power and the speed (rpm) for different types of engines is illustrated in Fig. 11.6. While the maximum power output of a steam turbine remains more or less constant as its speed is changed, the maximum power of a d.c. motor decreases slightly as speed is reduced. The maximum power available from a diesel engine is approximately proportional to its rpm, the diesel engine being a constant torque engine. As the rpm of a gas turbine reduces, the maximum power that it can produce drops quite sharply. It is, of course, possible to run an engine at less than its full power by regulating the supply of steam, fuel or electric power, depending upon the type of engine.

The power-speed characteristics of the propeller are quite different. In a given operating condition, the speed of the ship varies almost linearly with propeller rpm if the wake fraction is nearly constant. This implies that the advance coefficient J and hence the torque coefficient K_Q are constant, so that:

$$\begin{aligned} P_B &= \frac{P_D}{\eta_S} = \frac{2\pi \rho n^3 D^5 K_Q / \eta_R}{\eta_S} \\ &= k n^3 \end{aligned} \quad (11.36)$$

i.e. the power required by the propeller is proportional to the cube of its revolution rate. A curve of P_B as a function of n in which P_B is proportional to n^3 is called the "propeller curve" in contrast to the curves in Fig. 11.6



P_0, n_0 : Maximum Engine Power and Speed Rating

- 1. Steam Turbine
- 2. Electric Motor (D.C.)
- 3. Diesel Engine
- 4. Gas Turbine

Figure 11.6 : Power-Speed Characteristics of Different Types of Propulsion Engines.

which are “engine curves”. Since engines can be run at less than full power, it would appear that the problem of engine-propeller matching has a simple solution: design the propeller so that the propeller curve intersects the engine curve at the maximum rating of the engine (P_{B0}, n_0). Unfortunately, the problem is more complex as discussed in the following with respect to a diesel engine.

Fig. 11.7 illustrates the normal working limits of a diesel engine along with its curves of specific fuel consumption. P_B is the brake power at the revolu-

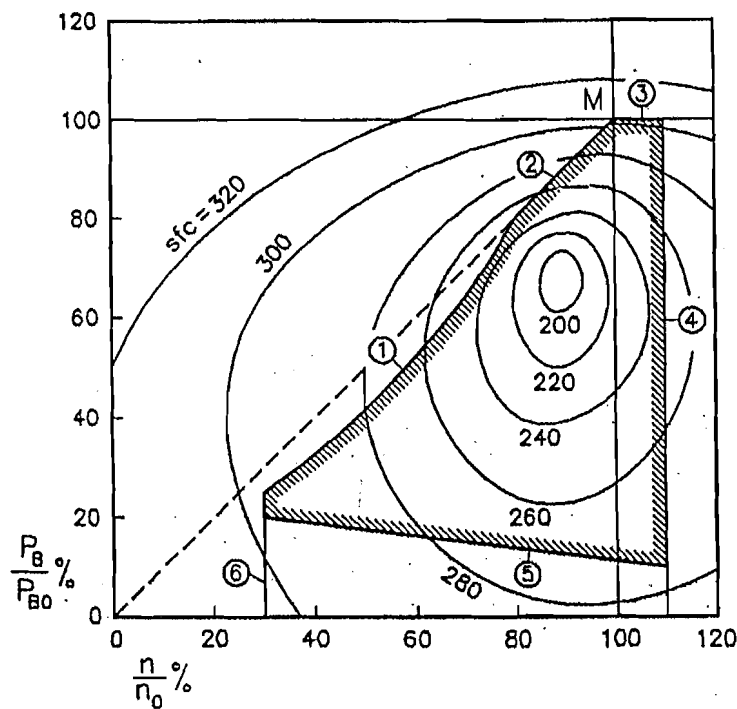
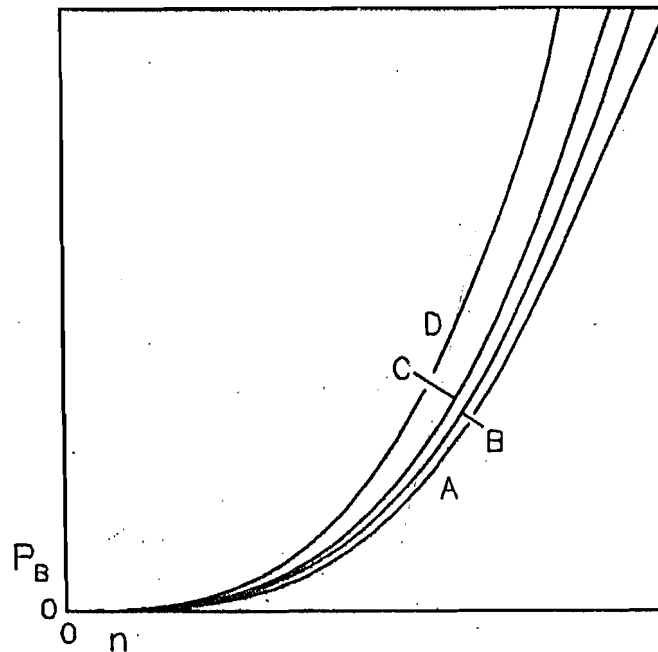


Figure 11.7: Working Limits of a Diesel Engine.

tion rate n , P_{B0} and n_0 being the maximum continuous rating of the engine denoted by the point M, while sfc is the specific fuel consumption in grams per kW hr. There is an upper limit to the power at a given engine speed, exceeding which will cause incomplete combustion of the fuel because of insufficient air, Line 1, or excessive cylinder pressures, Line 2. Line 3 gives the maximum power for continuous operation. Line 4 gives the upper speed limit of the engine up to which the dynamic effects on the engine parts are within acceptable limits. There is also a lower limit on the power at varying engine speeds below which the fuel supply cannot be properly regulated leading to incomplete combustion and contamination of the lubricating oil, Line 5. Finally, the engine should not be run at very low speeds (25–40 percent of n_0 , Line 6) because the temperatures attained in the engine cylinders may be insufficient for ignition and the fuel combustion may be erratic. The curves of specific fuel consumption show that its minimum value occurs at about

90 percent of the rated engine speed and 75–85 per cent of the rated power, the specific fuel consumption at the maximum continuous rating being some 5 percent higher than the minimum.



OPERATING CONDITIONS

- A. BALLAST
- B. FULLY LOADED TRIAL
- C. FULLY LOADED AVERAGE SERVICE
- D. FULLY LOADED, FOULED HULL, BAD WEATHER

Figure 11.8: Propeller Curves for Different Operating Conditions of a Ship.

The power-speed characteristics of the propeller (the propeller curve) depend upon the operating conditions of the ship, as shown in Fig. 11.8. The engine-propeller matching problem lies in positioning these curves in relation to the operating envelope of the engine. A typical solution is shown in Fig. 11.9. The propeller curve for the average service condition is made

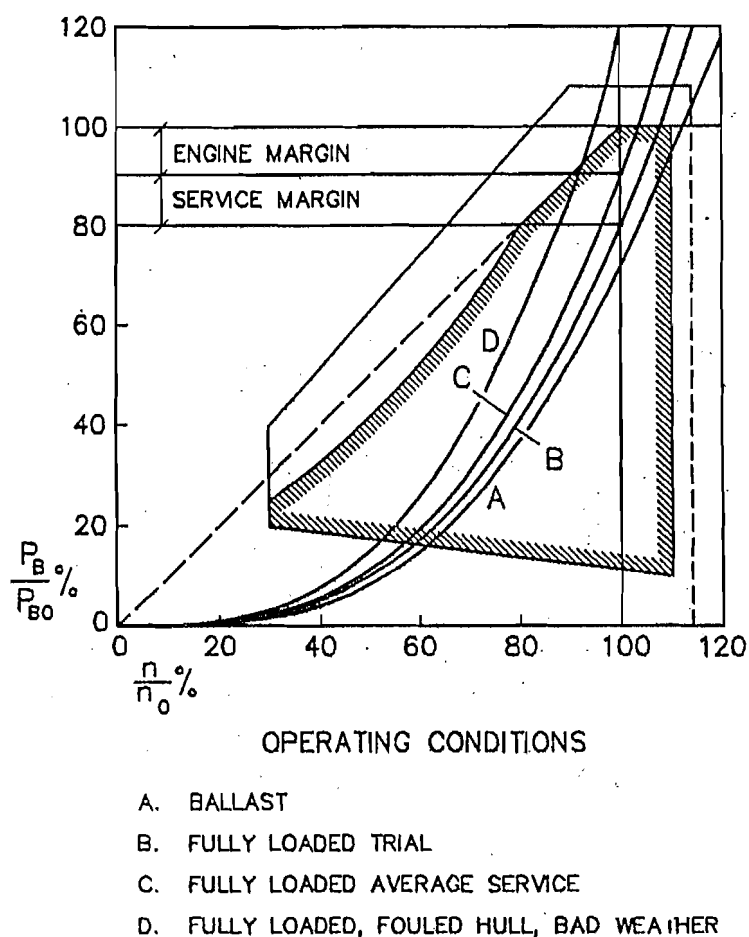


Figure 11.9: Propeller Curves in Relation to the Engine Operating Envelope.

to pass through a point corresponding to what is termed the "continuous service rating", 80–90 percent of the maximum rated power at slightly less than 100 percent of the maximum rated rpm. The difference between the maximum continuous rating and the continuous service rating is termed the "engine margin". The difference between the power in the average service condition and the fully loaded trial condition (clean hull and propeller, good weather) is the "service margin". A propeller operating on a curve to the

right of the Curve B in Fig. 11.9 is said to be running "light", and a propeller operating on the left of Curve B is said to be running "heavy". With most marine diesel engines, it is permissible to overload the engine for short periods, e.g. 1 hour in every 12, or 2000 hours cumulative per year. The limits of permitted overloading are shown by dotted lines in Fig. 11.9. Some overspeeding during speed trials is also sometimes permitted.

The maximum continuous rating of a diesel engine, i.e. the maximum power and rpm at which it can be safely run continuously for long periods, is given by the engine manufacturer for certain specified ambient conditions, e.g. air temperature 20° C, pressure 1 atmosphere (1.013 bar), relative humidity 60 percent, and water temperature for cooling the turbocharged air 30° C. These conditions do not necessarily obtain on board a ship, and it is necessary to "derate" the engine for the differences between the ambient conditions for which the maximum continuous rating is given by the engine manufacturer and the actual conditions in the ship. Another factor to be considered, particularly in connection with fuel consumption, is the heating value or energy content of the fuel. The specific fuel consumption figures given by the engine manufacturer are based on a particular value, e.g. 42500 kJ per kg, which may be different from the value for the fuel used in the ship. Finally, if there are engine driven auxiliaries, such as a main engine shaft driven generator, the power consumed by these auxiliaries must be deducted from the maximum continuous rating of the engine to obtain the maximum power available for driving the propeller.

The service margin, i.e. the difference between the power required in the average service condition and that required in the fully loaded trial condition, depends upon the mission profile of the ship. Typical values of the service margin vary between 15 and 35 percent depending upon the average weather conditions of the ship's route, the higher values being for the North Atlantic in winter. Larger margins are adopted when:

- the ship is required to maintain a rigid time schedule, e.g. a passenger / ferry;
- the long term effects of increased hull and propeller roughness are / expected to be large;
- the ship is expected to be dry docked at long intervals;

- a large allowance is necessary for adverse weather conditions;
- the ship is expected to spend long periods in warm water ports.

A large service margin ensures that the engine can be run at high rpms without being overloaded even when the hull and propeller become rough or the weather is bad. However, a larger service margin also means that a larger engine has to be selected, leading to increased machinery weight and higher initial cost. Moreover, it may not be possible to achieve the full engine power without exceeding the rated rpm. On the other hand, with a large service margin, the operating costs of the ship are reduced because of lower fuel consumption and reduced maintenance and replacement costs. There is thus an optimum service margin for each ship that will minimise its life cycle cost.

Example 5

A ship has a diesel engine of maximum continuous rating 6000 kW at 120 rpm directly connected to the propeller, which is designed to operate in the average service condition at the continuous service rating of 85 percent maximum rated power and 95 percent rated rpm. (a) If the service margin is 20 percent, determine the propeller rpm in the fully loaded trial condition at which the maximum rated power of the engine will be absorbed. (b) If due to exceptionally bad weather the power demand of the propeller increases by 40 percent over that in the trial condition, what is the maximum rpm at which the propeller can be run if 10 percent overloading of the engine over the maximum rated torque is permitted?

Maximum continuous rating (mcr):

$$P_{B0} = 6000 \text{ kW} \quad n_0 = 120 \text{ rpm} = 2.0 \text{ s}^{-1}$$

$$Q_0 = \frac{P_{B0}}{2\pi n} = \frac{6000}{2\pi \times 2.0} = 477.465 \text{ kN m (maximum rated torque)}$$

Continuous service rating (csr):

$$P_{B1} = 0.85 P_{B0} = 0.85 \times 6000 = 5100 \text{ kW}$$

$$n_1 = 0.95 n_0 = 0.95 \times 2.0 = 1.9 \text{ s}^{-1}$$

(a) Trial Condition:

$$P_{BTrial} = kn^3 = \frac{P_{B1}}{1.2} = \frac{5100}{1.2} = 4250 \text{ kW} \quad n_{Trial} = n_1 = 1.9 \text{ s}^{-1}$$

$$k = \frac{P_{BTrial}}{n_{Trial}^3} = \frac{4250}{1.9^3} = 619.624 \text{ kW s}^3$$

The value of n at which the maximum rated power of the engine will be absorbed is given by:

$$n^3 = \frac{P_{B0}}{k} = \frac{6000}{619.624}$$

$$n = 2.1314 \text{ s}^{-1} = 127.9 \text{ rpm, i.e. } 106.6\% \text{ of } n_0, \text{ the rated rpm.}$$

(b) Bad Weather:

$$P_B = 1.4 \times P_{BTrial} = 1.4 \times 619.624 n^3 = 867.473 n^3 \text{ kW}$$

$$Q = 1.10 Q_0 = 1.10 \times 477.465 = 525.212 \text{ kNm}$$

so that:

$$Q = \frac{P_B}{2\pi n} = \frac{867.473 n^3}{2\pi n} = 525.212 \text{ kNm}$$

$$n^2 = 3.8042 \text{ s}^{-2}$$

$$n = 1.9504 \text{ s}^{-1} = 117.0 \text{ rpm}$$

Problems

1. A single-screw ship has a design speed of 16.0 knots with its propeller of 4.5 m diameter running at 120 rpm. The axial and tangential components of the relative velocity of water with respect to the ship in the propeller disc at $0.7R$ are as follows:

θ deg	:	0	30	60	90	120	150	180
V_a m per sec	:	4.5267	5.8436	7.0781	6.5843	6.2551	5.8436	5.3498
V_t m per sec	:	0.0000	-1.5520	-0.5702	0.4115	0.5702	0.7289	0.0000

where θ is measured from the vertically up position. The ship may be fitted with either a four-bladed propeller or a six-bladed propeller. The four-bladed propeller of 0.9 pitch ratio has the following open water characteristics:

$$K_T = 0.3840 - 0.2582 J - 0.1523 J^2 \quad 10K_Q = 0.4956 - 0.2535 J - 0.2184 J^2$$

The six-bladed propeller has a pitch ratio of 0.925 and open water characteristics as follows:

$$K_T = 0.3950 - 0.2707 J - 0.1575 J^2 \quad 10K_Q = 0.5031 - 0.2630 J - 0.2205 J^2$$

The point of action of the tangential force on each blade is at a radius of 1.41 m. From the point of view of minimising unsteady propeller forces, which of the two propellers should be selected? What can you say about the harmonics present in the wake velocities?

2. A single-screw ship has a diesel engine of maximum continuous rating 10000 kW at 150 rpm directly connected to the propeller. The effective power of the ship in calm water is as follows:

Speed, knots	:	15.0	16.0	17.0	18.0	19.0
Effective power, kW:		3427	4324	5378	6607	8027

The propeller is of 5.0 m diameter and 0.7 pitch ratio. Its open water characteristics are as follows:

$$K_T = 0.5214 - 0.3953 J - 0.2528 J^2 \quad 10K_Q = 0.5745 - 0.3327 J - 0.3002 J^2$$

Determine the ship speed, propeller rpm and engine power in calm water, and in waves which cause increases in effective power of 15, 30, 45 and 60 percent over that in calm water, given that the maximum rated torque and rpm are not to be exceeded. The wake fraction is 0.280, the thrust deduction fraction 0.250, the relative rotative efficiency 1.000 and the shafting efficiency 0.980.

3. A ship when new has an effective power in calm water as follows:

Speed, knots	:	15.0	16.0	17.0	18.0	19.0	20.0
Effective power, kW:		2503	3178	3977	4914	6002	7256

The ship has a propeller with four blades, a diameter of 6.0 m and a pitch ratio of 0.75. When new, the propeller has a surface roughness of 30 microns and its open water characteristics are as follows:

$$K_T = 0.3360 - 0.2547 J - 0.1629 J^2 \quad 10K_Q = 0.3911 - 0.2266 J - 0.2044 J^2$$

The width and thickness of the propeller blades at $0.75R$ are 1.650 m and 0.085 m respectively. The main engine of the ship, directly connected to the propeller, has a maximum continuous rating of 9000 kW at 126 rpm. The ship has a wake fraction of 0.250, a thrust deduction fraction of 0.210, a relative rotative efficiency of 1.000 and a shafting efficiency of 0.980. Determine the maximum speed of the ship and the corresponding propeller rpm and brake power when the ship is new.

After a year in service, the effective power of the ship increases by 20 percent, the wake fraction by 10 percent and the thrust deduction fraction by 5 percent, the relative rotative efficiency and the shafting efficiency remaining unchanged. The maximum power available from the engine at the rated rpm drops by 3 percent. The propeller surface roughness increases to 150 microns. Determine the maximum speed of the ship in calm water after a year in service and the corresponding propeller rpm and brake power if the maximum torque of the engine is not to be exceeded.

4. A ship is moving ahead at a speed of 16.0 knots when orders are given for the ship to stop and go astern. The engine is stopped immediately and started in the opposite direction after two minutes, attaining a revolution rate of 90 rpm almost at once. The ship has a displacement of 10000 tonnes and its added mass coefficient may be taken as 0.05. The ship's propeller is of 5.5 m diameter and 0.85 pitch ratio, and is directly connected to the engine of 8000 kW brake power at 132 rpm. The effective power of the ship is as follows:

Speed, knots	:	0	5	10	15	20
Effective power, kW	:	0	85	965	4500	10919

With the ship moving ahead and the propeller reversed, the wake fraction is 0.240, the thrust deduction fraction -0.100 , the relative rotative efficiency 1.000 and the shafting efficiency 0.980. The open water characteristics of the propeller for a positive speed of advance and a negative revolution rate are as follows:

$$K_T = -0.300 - 0.750 J - 1.500 J^2 - 0.400 J^3$$

$$10K_Q = -0.550 - 1.058 J - 1.675 J^2 - 0.317 J^3$$

Estimate the time it takes to stop the ship and the distance that the ship travels forward before stopping and reversing. Carry out the calculation at 15-second intervals.

5. The effective power of a single-screw ship in the fully loaded trial condition (clean, newly painted hull, polished propeller, calm water) is as follows:

Speed, knots	:	10.0	12.0	14.0	16.0	18.0	20.0
Effective power, kW:		893	1721	2998	4848	7408	10825

The ship has a propeller of diameter 6.0m and pitch ratio 1.0 whose open water characteristics are as follows:

$$K_T = 0.4250 - 0.2517 J - 0.1441 J^2 \quad 10K_Q = 0.5994 - 0.2733 J - 0.2254 J^2$$

The wake fraction is 0.280, the thrust deduction fraction 0.240, the relative rotative efficiency 1.040 (thrust identity) and the shafting efficiency 0.980. The propulsion plant of the ship consists of a diesel engine of 15000 kW at 118rpm maximum continuous rating. Calculate the maximum speed of the ship in the trial condition and the corresponding brake power.

In the average service condition, the effective power of the ship is 15 percent higher than in the trial condition, the wake fraction is 0.300, the thrust deduction fraction 0.250, the relative rotative efficiency 1.050 and the shafting efficiency 0.980. Calculate the maximum speed of the ship in the average service condition and the corresponding propeller rpm and brake power, and determine the "service margin" and the "engine margin".

Determine for the service condition, the maximum permissible percentage increase in effective power over that in the trial condition for the engine to run at its rated rpm without exceeding the rated torque, and the corresponding ship speed.

CHAPTER 12

Unconventional Propulsion Devices

12.1 Introduction

Propeller design aims at achieving high propulsive efficiency at low levels of vibration and noise, usually with minimum cavitation. Achieving this aim has become progressively more difficult with conventional propellers, i.e. the type of propellers discussed in the preceding chapters, as ships have become larger and faster and propeller diameters have remained limited by draught and other factors. Therefore, unconventional propulsion devices have been proposed for ships in which the performance of conventional propellers is not fully satisfactory.

Modern unconventional propulsion devices or propulsors attempt to increase propulsive efficiency by decreasing kinetic energy losses, and to reduce vibration, noise and cavitation by improved inflow to the propulsor. The energy losses that occur in the propulsor are associated with the axial and tangential induced velocities in the propulsor slipstream. The axial loss for a given thrust may be reduced by increasing the mass of water flowing through the propulsor per unit time and reducing the axial induced velocity. The rotational loss may be reduced by recovering the energy carried away in the slipstream by the tangential velocity. There are also drag losses and it is essential that the energy recovered from the slipstream by the various devices be greater than the energy lost due to the additional drag of these devices.

In addition to the hydrodynamic factors of increased propulsive efficiency and reduced vibration, noise and cavitation, in any proposal to use an unconventional propulsion device it is also necessary to consider the initial cost, weight and volume of the device and its associated machinery, and the reliability and maintainability of the device. The economy effected by the adoption of an unconventional propulsion device of greater efficiency compared to a conventional propeller must be sufficient to recover the additional cost in a reasonable period, say five years.

A number of unconventional propulsion devices have been proposed in recent times. Many are still in an experimental stage. On the other hand, some devices antedate the conventional propeller: the paddle wheel has a history nearly 200 years old, the contra-rotating propeller was first tried out more than 150 years ago, and a patent for waterjet propulsion was granted in 1661.

12.2 Paddle Wheels

A paddle wheel is a wheel that carries paddles or "floats" at its periphery and rotates about a transverse axis of the ship well above the waterline. The paddles accelerate the water and experience a reactive thrust that is transmitted to the ship. Steamers with paddle wheels appeared at the beginning of the 19th century but paddle wheels were gradually superseded after 1850 by screw propellers for oceangoing ships. Paddle wheels are still occasionally used for shallow draught vessels operating on inland waterways.

Paddle wheels are of two types: those with fixed paddles and those with "feathering" paddles, Fig. 12.1. In the fixed paddle wheel, the paddles are rigidly attached to the wheel along radial lines. Such paddle wheels are of simple and solid construction. However, it is necessary to have a very large diameter wheel with only a small segment of the wheel immersed in water. This ensures that the paddles enter and leave the water at a large angle to the waterline, thereby minimising the shock and the loss of energy in depressing the water at entry and elevating the water at exit. The large wheel diameter requires that the wheel run at a very low rpm, and this increases the size and weight of the propulsion machinery. In the feathering paddle wheel, the paddles are pivoted at the periphery of the wheel and attached by a

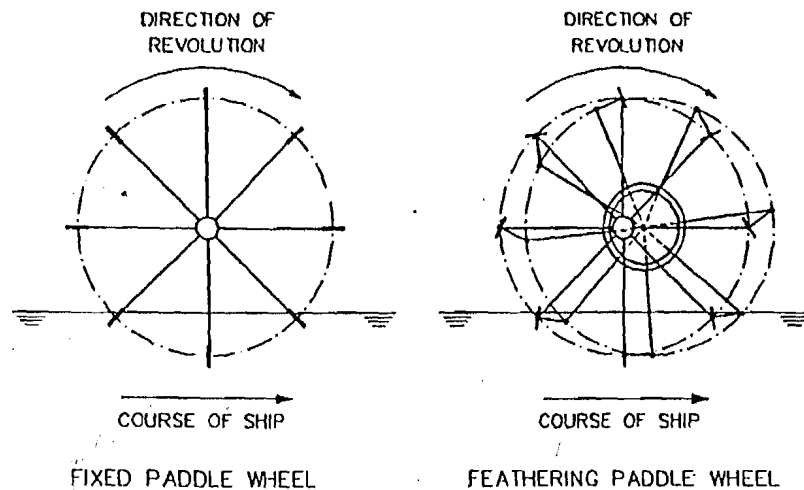


Figure 12.1 : Paddle Wheels.

mechanical linkage to an eccentric point of the wheel such that the paddles entering and leaving the water are at a much larger angle to the waterline than the corresponding radial lines. This allows the wheel diameter to be substantially reduced (to as little as half that of a wheel with fixed paddles) and to be run at a much higher speed by a smaller propulsion plant. The efficiency of a feathering wheel is also higher than that of a fixed paddle wheel by about 10 percent and is comparable to the efficiency of a screw propeller. However, a feathering paddle wheel is heavier and costlier than a fixed paddle wheel. Moreover, the mechanical linkage system requires a high degree of maintenance.

There are two paddle wheel arrangements. In "side wheelers", the paddle wheels are fitted on both sides of the ship near mid-length, so that changes in trim and the pitching of the ship have little effect on the immersion of the paddle wheels. There should preferably be a crest of the transverse wave system generated by the ship at the location of the paddle wheel. The wave wake is positive at a wave crest and the higher wake fraction increases the propulsive efficiency. Side wheelers, however, have a greater overall breadth and suffer from erratic steering while rolling in a seaway. In "stern wheelers", the paddle wheel is fitted at the stern. Stern wheels are used in vessels such

as river towboats with wide flat sterns in which draught and trim variations are small and which operate in narrow waterways.

The immersion of the paddles in their lowest position varies from 0.1 to 0.8 times the height of the paddle, the larger values being used for the thinner paddles. The thrust and torque of the paddle wheel are proportional to the width of the paddle for a given height at constant wheel diameter and rpm, and for a constant ship speed. Other things being equal, the thrust and torque are also proportional to the immersed area of the wheel projected on a longitudinal plane.

Design diagrams for paddle wheels have been developed by Krappinger (1954) and by Volpich and Bridge (1956, 1957, 1958). In one form of these diagrams, curves representing the following functional relationships are plotted:

$$\begin{aligned}\frac{T}{\rho g D^3} &= f\left(\frac{V_A}{\sqrt{gD}}, \frac{nD}{\sqrt{gD}}\right) \\ \frac{Q}{\rho g D^4} &= f\left(\frac{V_A}{\sqrt{gD}}, \frac{nD}{\sqrt{gD}}\right)\end{aligned}\quad (12.1)$$

D is the diameter of the paddle wheel.

Example 1

A feathering paddle wheel consists of paddles pivoted about points on a circle of radius 2.00 m. The arm attached at right angles to each paddle is of length 0.30 m and the link attached to this arm is on a straight line which passes through a point 0.25 m forward of the centre of the paddle wheel. The waterline is 1.8 m below the centre. Determine the angles of the paddle to the vertical when its pivot enters and leaves the surface of water. What would be the angle of the paddles entering and leaving water if the paddles were fixed instead of feathering?

In the Fig. 12.2:

$$\overline{OA} = \overline{CB} = R, \text{ radius of paddle wheel}$$

$$\overline{OC} = eR = \text{eccentricity}$$

$$\overline{AB} = a = \text{length of paddle arm}$$

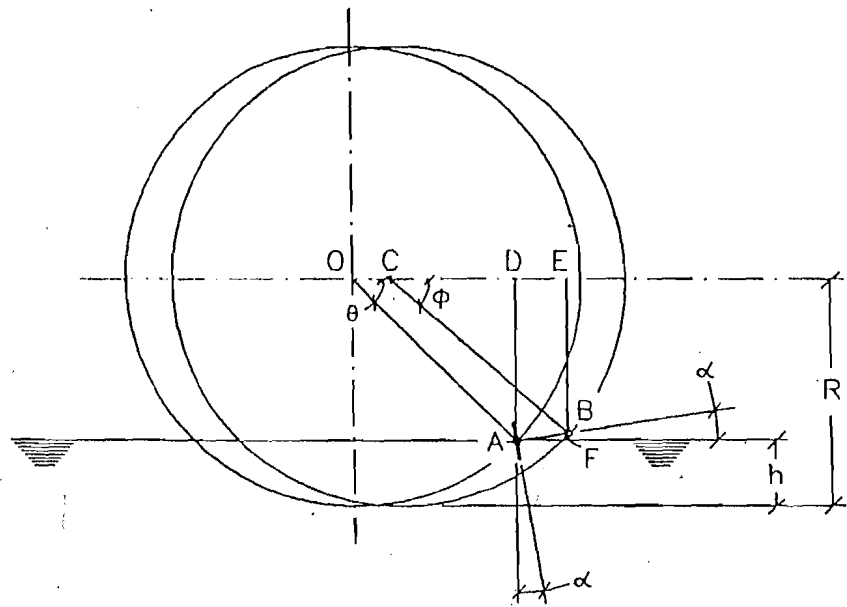


Figure 12.2 : Action of a Feathering Paddle Wheel (Example 1).

Let the angles made with the horizontal by \overline{OA} , \overline{CB} and \overline{AB} be θ , φ and α respectively.

Then:

$$\overline{AF} = \overline{DE} = \overline{OC} + \overline{CE} - \overline{OD}$$

i.e. $a \cos \alpha = eR + R \cos \varphi - R \sin \theta$

$$\overline{BF} = \overline{DA} - \overline{EB}$$

i.e. $a \sin \alpha = R \sin \theta - R \sin \varphi$

$$\overline{DA} = R - h$$

i.e. $R \sin \theta = R - h$

Therefore,

$$\frac{a^2}{R^2} = (e + \cos \varphi - \cos \theta)^2 + (\sin \theta - \sin \varphi)^2 \quad (a)$$

$$\tan \alpha = \frac{\sin \theta - \sin \varphi}{e + \cos \varphi - \cos \theta} \quad (b)$$

In the present example:

$$R = 2.00 \text{ m} \quad eR = 0.25 \text{ m} \quad a = 0.30 \text{ m} \quad R - h = 1.80 \text{ m}$$

$$\sin \theta = \frac{R - h}{R} = \frac{1.80}{2.00} = 0.9$$

$$\theta = 64.16^\circ \text{ (at entry) and } 115.84^\circ \text{ (at exit)}$$

At entry: $\sin \theta = 0.9 \quad \cos \theta = 0.4359$

Substituting in (a) above:

$$\left(\frac{0.30}{2.00}\right)^2 = \left(\frac{0.25}{2.00} + \cos \varphi - 0.4359\right)^2 + (0.9 - \sin \varphi)^2$$

so that: $\varphi = 62.59^\circ$

From (b):

$$\tan \alpha = \frac{0.9 - \sin \varphi}{\frac{0.25}{2.00} + \cos \varphi - 0.4359} = \frac{-0.01228}{0.1495} = -0.0821$$

$$\alpha = -4.70^\circ$$

At exit: $\theta = 115.84^\circ \quad \sin \theta = 0.9 \quad \cos \theta = -0.4359$

$$\left(\frac{0.30}{2.00}\right)^2 = \left(\frac{0.25}{2.00} + \cos \varphi + 0.4359\right)^2 + (0.9 - \sin \varphi)^2$$

so that: $\varphi = 114.29^\circ$

$$\tan \alpha = \frac{0.01149}{0.1496} = 0.0768$$

$$\alpha = 4.39^\circ$$

i.e. the angles of the paddle to the vertical when entering and leaving the water surface are 4.70 and 4.39 degrees respectively.

If the paddles were fixed, the angle of the paddles to the horizontal would be $\theta = 64.16^\circ$ (i.e. 25.84° to the vertical), since the paddle would be aligned along \overline{OA} .

12.3 Controllable Pitch Propellers

In a controllable pitch propeller, the blades are not made integral with the boss but are mounted on separate spindles perpendicular to the propeller shaft axis. These spindles can be made to turn about their individual axes through a mechanism inside the boss, thereby changing the pitch of the propeller blades. Many types of pitch control mechanisms have been tried out over the years, but reliable mechanisms date back to about 1935. A typical pitch control mechanism consists of a spring loaded piston which can move a small distance forward and aft inside the propeller boss in response to hydraulic pressure transmitted to it through an oil channel in the propeller shaft. The reciprocating motion of the piston is converted into an angular motion of the spindles by crossheads. A typical arrangement of a controllable pitch propeller is shown in Fig. 12.3. A stepless change in the pitch of the blades and hence the propeller thrust from full ahead to full astern can be made without changing the revolution rate or reversing the direction of revolution of the propeller. The pitch of the propeller may be changed from a remote location, e.g. from the navigation bridge of the ship.

Controllable pitch propellers have several advantages over conventional fixed pitch propellers:

- The full power of the machinery can be utilised in all loading conditions: static, towing and free running conditions, during ice breaking, and when the resistance of the ship increases due to weather, hull roughness, greater displacement, shallow water or other causes.
- Controllable pitch propellers provide better acceleration, stopping and manoeuvring characteristics.
- The propulsion plant may be operated at optimum efficiency over a range of ship speeds and displacements, even at very low speeds.
- Non-reversing propulsion machinery may be used, thereby reducing its cost, weight and the space it occupies.
- The speed of the ship may be varied without altering the speed of the main engine. This is useful when the main engine has a shaft driven alternator for generating electricity.

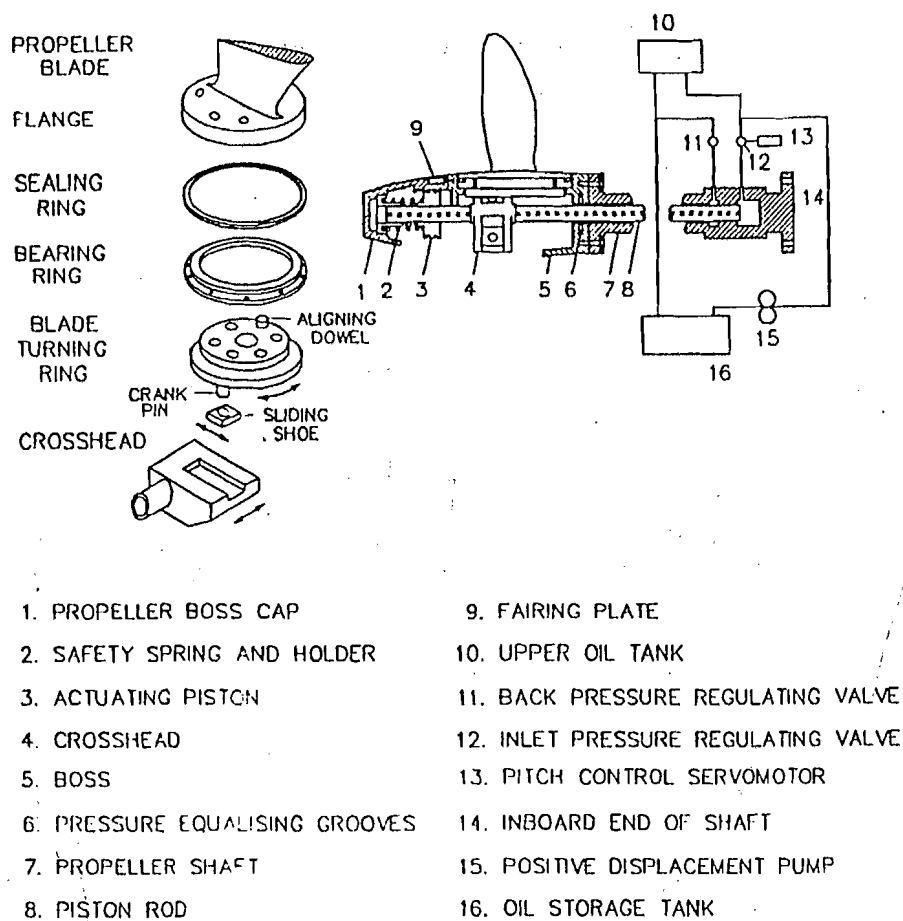


Figure 12.3 : Controllable Pitch Propeller.

- The speed of the ship may be directly controlled from the navigation bridge.
- A controllable pitch propeller is capable of producing a higher astern thrust and at a higher efficiency.

Controllable pitch propellers also have some serious disadvantages:

- The pitch control mechanism is very complicated.

- Controllable pitch propellers have a high initial cost, which rises sharply with diameter.
- Maintenance costs are also high.
- Controllable pitch propellers are highly vulnerable to damage.
- The length and diameter of the propeller boss are large.
- The pitch variation of the blades along the radius, optimum at the design pitch, does not remain optimum when the pitch is changed since all the blade sections rotate through the same angle.
- The blade area has to be limited to enable the pitch to be reversed, and this requires thicker blade sections to be used.
- The efficiency of a controllable pitch propeller at its design point is lower than that of an equivalent fixed pitch propeller because of the larger boss diameter, the limited blade area and the thicker blade sections. When the pitch is changed from its basic design value, the efficiency falls still further because of the non-optimum pitch distribution.
- The limited blade area and thicker blade sections result in greater cavitation and more noise.

Controllable pitch propellers are used only in those ships in which the positive features of such propellers are very important, i.e. in ships which require full power operation in widely different speed or resistance ranges, which require exceptional acceleration, stopping and manoeuvring characteristics, or which are fitted with non-reversing propulsion machinery. The types of ships in which controllable pitch propellers are often fitted include tugs, trawlers, coasters, fire floats, ferries, ice-breakers and small warships with gas turbine engines.

The design of a controllable pitch propeller is carried out in a manner similar to that for conventional propellers. The design condition is selected according to the proportion of the different conditions in the operating profile of the ship. In addition to the factors considered in the design of conventional propellers, controllable pitch propeller design must also take into account the

maximum permissible spindle torque during the pitch changing operation, the limit imposed on the blade area to allow the blades to be reversed, and the higher boss diameter ratio to house the pitch changing mechanism. The boss diameter ratio of a controllable pitch propeller is usually in the range $d/D = 0.30-0.32$.

Example 2

A controllable pitch propeller of 4.0 m diameter has a constant pitch ratio of 0.800 at a particular setting. If the pitch is increased by turning the blades through an angle of 10 degrees, determine the resulting radial distribution of pitch and the mean pitch. The root section is at $0.3R$.

At any radius $r = xR$, the blade angle is given by $\tan \varphi = \frac{P}{2\pi r} = \frac{P/D}{\pi x}$.

Initially, $P_0/D = 0.800$, and the corresponding pitch angles are φ_0 . With the pitch increased, the pitch angles are $\varphi_1 = \varphi_0 + 10$ degrees.

x	$\tan \varphi_0$	φ_0°	φ_1°	$\tan \varphi_1$	P_1/D
0.30	0.8488	40.3255	50.3255	1.2056	1.1362
0.40	0.6366	32.4816	42.4816	0.9157	1.1508
0.50	0.5093	26.9896	36.9896	0.7533	1.1832
0.60	0.4244	22.9970	32.9970	0.6493	1.2240
0.70	0.3638	19.9905	29.9905	0.5771	1.2692
0.80	0.3183	17.6568	27.6568	0.5241	1.3171
0.90	0.2829	15.7984	25.7984	0.4834	1.3667
0.95	0.2681	15.0054	25.0054	0.4664	1.3920
1.00	0.2546	14.2866	24.2866	0.4512	1.4176

The mean pitch is calculated using Simpson's Rule as follows:

x	P_1/D	$x P_1/D$	SM	$f(x P_1/D)$	$f(x)$
0.30	1.1362	0.3409	1	0.3409	0.30
0.40	1.1508	0.4603	4	1.8413	1.60
0.50	1.1832	0.5916	2	1.1832	1.00
0.60	1.2240	0.7344	4	2.9376	2.40

x	P_1/D	$x P_1/D$	SM	$f(x P_1/D)$	$f(x)$
0.70	1.2692	0.8844	2	1.7769	1.40
0.80	1.3171	1.0537	4	4.2147	3.20
0.90	1.3667	1.2300	$1\frac{1}{2}$	1.8450	1.35
0.95	1.3920	1.3224	2	2.6448	1.90
1.00	1.4176	1.4176	$\frac{1}{2}$	0.7088	0.50
				17.4932	13.65

$$\text{Mean pitch ratio} = \frac{\sum f(x P_1/D)}{\sum f(x)} = \frac{17.4932}{13.65} = 1.2816$$

12.4 Ducted Propellers

A ducted propeller consists of a screw propeller surrounded by a non-rotating duct (shroud or nozzle) usually in the form of an axisymmetric (annular) aerofoil with a very small gap between the propeller blade tips and the internal surface of the duct, Fig. 12.4. The concept of ducted propellers is due to Stipa (1931) and to Kort (1934). The ducts in ducted propellers are of two kinds: accelerating ducts which increase the inflow to the propeller, and decelerating ducts which reduce the velocity of the flow through the propeller. Accelerating ducts are often called Kort nozzles following the extensive experimentation carried out by Kort in developing such ducts. Decelerating ducts are sometimes termed pump jets, especially when combined with fixed blades or "stators".

Accelerating ducts, Fig. 12.5(a), are used in heavily loaded propellers. The small clearance between the propeller blade tips and the duct suppresses the trailing free vortices shed by the blades, the bound vortices on the blades joining the bound vortex ring on the duct. The shape of the accelerating duct at the forward end (leading edge) increases the mass flow to the propeller. At the after end, the duct is so shaped that the cross-section increases going aft and the normal slipstream contraction is suppressed. The increased inflow velocity causes a decrease in the thrust and torque of the propeller. At

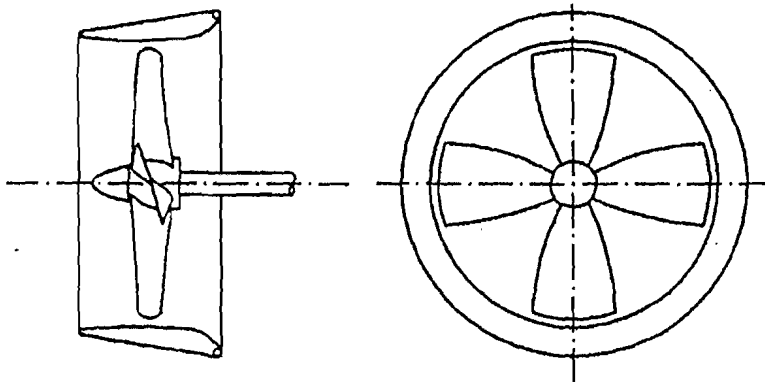


Figure 12.4 : Ducted Propeller.

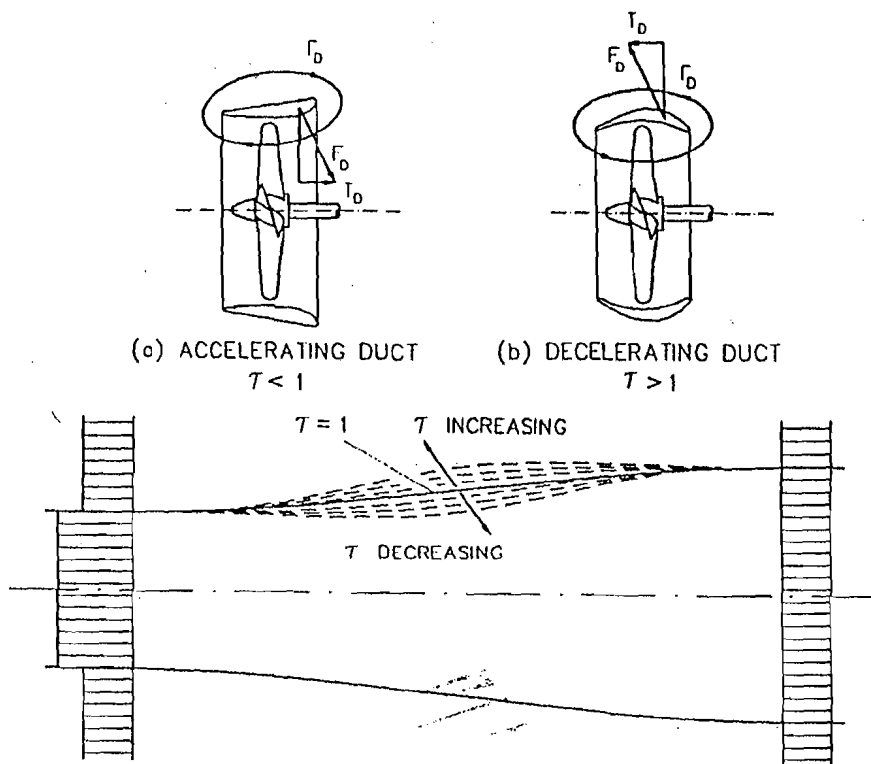


Figure 12.5 : Accelerating and Decelerating Ducts.

the same time, a circulation develops around the duct section resulting in an inward directed force which has a forward component, the duct thrust. The duct also has a drag directed aft, and this should be substantially less than the duct thrust. The total thrust of the propeller and duct taken together is then usually greater than that of an equivalent open propeller (i.e. one without a duct) whereas the torque is smaller. The efficiency of the ducted propeller is therefore greater than that of the open propeller. The improved efficiency of the ducted propeller may also be explained by the reduced kinetic energy losses in the slipstream due to the suppression of the trailing vortices and the reduction of the slipstream contraction.

A decelerating duct, Fig. 12.5(b), decreases the inflow velocity into the propeller thereby increasing the pressure at the propeller location. This delays cavitation. The duct has a circulation around it which produces an outward directed lift with a component directed aft, i.e. the duct thrust is negative. The efficiency of a ducted propeller with a decelerating duct is lower than that of an equivalent open propeller, but its cavitation properties are superior. Decelerating ducts are therefore used for high speed hydrodynamic bodies in which it is necessary to minimise cavitation and underwater noise.

An insight into the performance of ducted propellers is provided by applying the axial momentum theory. Consider the fluid column flowing through a ducted propeller of cross-sectional area A_O , Fig. 12.6. The pressures far ahead, just ahead, just behind and far behind the propeller are p_0, p_1, p'_1 and p_2 respectively, the propeller being regarded as an actuator disc causing an abrupt increase in pressure from p_1 to p'_1 . The velocities of the fluid with respect to the propeller far ahead, at the propeller and far behind are V_A , $V_A + v_1$ and $V_A + v_2$. The mass of fluid flowing through the propeller per unit time is:

$$m = \rho A_O (V_A + v_1) \quad (12.2)$$

The total thrust of the propeller is equal to the rate of change of momentum of the fluid in the slipstream, and is given by:

$$\begin{aligned} T &= m [(V_A + v_2) - V_A] \\ &= \rho A_O (V_A + v_1) v_2 \end{aligned} \quad (12.3)$$

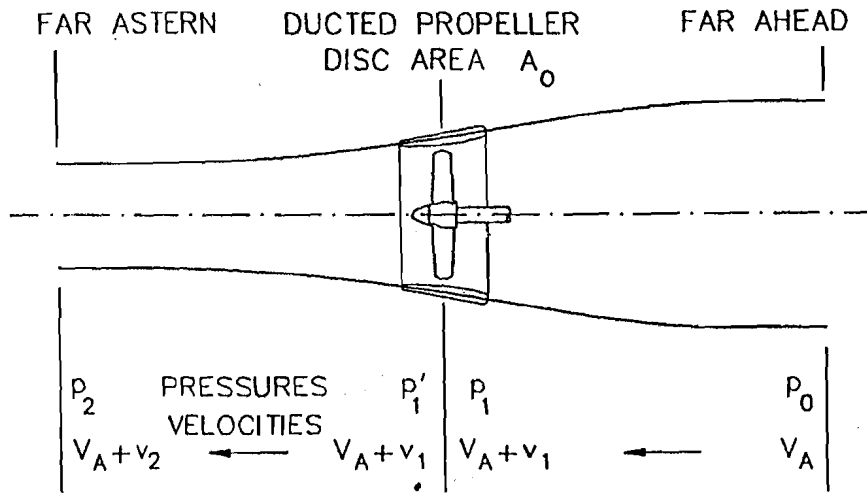


Figure 12.6: Flow through a Ducted Propeller.

Applying the Bernoulli theorem to the sections far ahead and just ahead of the propeller, one obtains:

$$p_0 + \frac{1}{2}\rho V_A^2 = p_1 + \frac{1}{2}\rho (V_A + v_1)^2 \quad (12.4)$$

Similarly, for the sections far behind and just behind the propeller:

$$p_2 + \frac{1}{2}\rho (V_A + v_2)^2 = p'_1 + \frac{1}{2}\rho (V_A + v_1)^2 \quad (12.5)$$

Far astern of the propeller the flow is parallel to the axis and hence there is no radial pressure gradient, so that $p_2 = p_0$ and:

$$p'_1 - p_1 = \frac{1}{2}\rho (V_A + v_2)^2 - \frac{1}{2}\rho V_A^2 = \rho (V_A + \frac{1}{2}v_2)v_2 \quad (12.6)$$

The thrust of the propeller alone is then:

$$T_P = (p'_1 - p_1) A_0 = \rho A_0 (V_A + \frac{1}{2}v_2)v_2 \quad (12.7)$$

A thrust ratio τ is now defined as the ratio of the propeller thrust T_P to the total thrust $T = T_P + T_D$, where T_D is the thrust of the duct:

$$\tau = \frac{T_P}{T_P + T_D} = \frac{T_P}{T}$$

$$= \frac{1 + \frac{\frac{1}{2}v_2}{V_A}}{1 + \frac{v_1}{V_A}} \quad (12.8)$$

The thrust loading coefficient is given by:

$$\begin{aligned} C_{TL} &= \frac{T}{\frac{1}{2}\rho A_O V_A^2} = \frac{\rho A (V_A + v_1) v_2}{\frac{1}{2}\rho A_O V_A^2} \\ &= \frac{2}{\tau} \left(1 + \frac{\frac{1}{2}v_2}{V_A} \right) \frac{v_2}{V_A} \end{aligned} \quad (12.9)$$

This gives the following results:

$$\begin{aligned} 1 + \frac{\frac{1}{2}v_2}{V_A} &= \frac{1}{2} [1 + (1 + \tau C_{TL})^{0.5}] \\ 1 + \frac{v_1}{V_A} &= \frac{1}{2\tau} [1 + (1 + \tau C_{TL})^{0.5}] \\ \frac{v_D}{V_A} &= \frac{v_1}{V_A} - \frac{\frac{1}{2}v_2}{V_A} = \frac{1 - \tau}{\tau} [1 + (1 + \tau C_{TL})^{0.5}] \end{aligned} \quad (12.10)$$

where v_D is the induced velocity due to the duct.

The delivered power of the propeller is equal to the increase in the kinetic energy of the fluid per unit time:

$$\begin{aligned} P_D &= \frac{1}{2}m (V_A + v_2)^2 - \frac{1}{2}m V_A^2 \\ &= \frac{1}{2}\rho A_O (V_A + v_1)(V_A + \frac{1}{2}v_2) v_2 \end{aligned} \quad (12.11)$$

The ideal efficiency of the ducted propeller is then:

$$\eta_i = \frac{T V_A}{P_D} = \frac{\rho A_O (V_A + v_1) v_2 V_A}{\frac{1}{2}\rho A_O (V_A + v_1)(V_A + \frac{1}{2}v_2) v_2}$$

$$\begin{aligned}
 &= \frac{1}{1 + \frac{\frac{1}{2}v_2}{V_A}} \\
 &= \frac{2}{1 + (1 + \tau C_{TL})^{0.5}} \quad (12.12)
 \end{aligned}$$

Putting $\bar{p} = \frac{1}{2}(p_1 + p'_1)$, the pressure coefficient at the propeller is given by:

$$\begin{aligned}
 C_{\bar{p}} &= \frac{\bar{p} - p_0}{\frac{1}{2}\rho V_A^2} \\
 &= 1 + \frac{\tau C_{TL}}{2} + \left[\frac{1 + (1 + \tau C_{TL})^{0.5}}{2\tau} \right]^2 \quad (12.13)
 \end{aligned}$$

The effect of the drag of the duct on the efficiency of the ducted propeller can be taken into account approximately as follows:

$$\begin{aligned}
 D_D &= \frac{1}{2}\rho \pi D l V_A^2 C_D \\
 k_D &= \frac{T - D_D}{T} = 1 - \frac{\frac{1}{2}\rho \pi D l V_A^2 C_D}{\frac{1}{2}\rho A_O V_A^2 C_{TL}} \\
 &= 1 - \frac{4l C_D}{D C_{TL}}
 \end{aligned}$$

noting that $A_O = \pi D^2/4$. Then:

$$\eta = k_D \eta_i = \left(1 - \frac{4l C_D}{D C_{TL}} \right) \frac{2}{1 + (1 + \tau C_{TL})^{0.5}} \quad (12.14)$$

where:

D_D = duct drag;

D = propeller diameter;

- l = duct length;
- C_D = duct drag coefficient;
- k_D = drag correction factor;
- η = ducted propeller efficiency including duct drag.

Eqns. (12.12), (12.13) and (12.14) yield some interesting conclusions:

- The ideal efficiency of the ducted propeller increases as τ decreases. In practice, reducing τ below a certain limit would cause the flow past the inner surface of the duct to break down due to boundary layer separation, resulting in a sharp drop in the efficiency of the ducted propeller.
- The static pressure at the propeller increases as τ increases, thereby delaying cavitation. By definition, if τ is greater than 1 the duct has a negative thrust.
- The effect of duct drag reduces as the thrust loading of the ducted propeller increases. For values of C_{TL} exceeding about 1.5 the drag of the duct is insignificant compared to the kinetic energy losses.
- The effect of duct drag on efficiency can be reduced by minimising the length of the duct. In practice, however, there is a lower limit to the duct length for a given duct loading below which the flow through the duct breaks down resulting in a severe degradation of performance.

The axial momentum theory only illustrates some principles and overall trends of the performance of ducted propellers. It gives no indication regarding the actual shapes of the propeller and the duct required for generating the specified thrust; nor does it consider the effect of slipstream rotation and tip clearance losses. A more complete treatment requires the development of a mathematical model employing singularity distributions on the propeller blades and the duct.

Increasingly sophisticated theoretical analyses and design methods have been developed by, among others, Morgan and Caster (1968), Dyne (1973),

Oosterweld (1970), Ryan and Glover (1972), and Kerwin, Kinnas, Lee and Wei-Zen (1987).

The design of ducted propellers is often based on the extensive model experiment data that are available. Model experiments and practical experience with ducted propellers offer useful design guidelines, which have been summarised by Schneekluth (1987). It has been observed that the optimum diameter of a propeller in a duct is smaller than that of an equivalent open propeller, although the external diameter of the duct and the diameter of the open propeller are usually comparable. The optimum duct section profile is of an aerofoil shape, e.g. the NACA 4415 profile. However, it is possible to use a simplified profile shape, e.g. the Shushkin profile, to make the construction of the duct easier. It is necessary to adopt a well-rounded trailing edge to obtain good astern performance, though at the cost of a small decrease in ahead performance. Typical duct section profiles are illustrated in Figs. 12.7 (a) and 12.7 (b). The optimum length-diameter ratio of the duct increases with increasing thrust loading coefficient and varies from $l/D = 0.4$ to $l/D = 0.8$. A smaller duct length may permit a larger propeller diameter depending upon the stern shape. The duct dihedral angle (the angle between the nose-tail line of the section profile and the centre line of the duct) should be such that the flow cross-section at the trailing edge is not narrowed. At the same time, the profile camber should not be so large as to give rise to boundary layer separation inside the duct. Duct dihedral angles $\alpha = 10\text{--}15^\circ$ are often used with camber ratios f/c as high as 0.05. The duct exit angle β should not be greater than about 2 degrees for a simplified profile and 4 degrees for an aerofoil shape.

The duct cross-section is normally circular. However, in ships with very blunt waterlines aft, the forward part of the duct may be widened laterally, giving the forward part of the duct an elliptical cross-section, Fig. 12.7 (c). The middle and aft parts of the duct remain of circular cross-section to keep the clearance between the inner surface of the duct and the propeller blade tips small. The clearance between the duct and the propeller blades sometimes results in the jamming of the propeller in the duct due to small objects getting into the clearance space. Various measures can be taken to prevent this from happening. Fins may be fitted ahead of the duct to guide solids in the flow outside the nozzle. Several annular grooves may be provided on the inner surface of the nozzle to thicken the boundary layer and

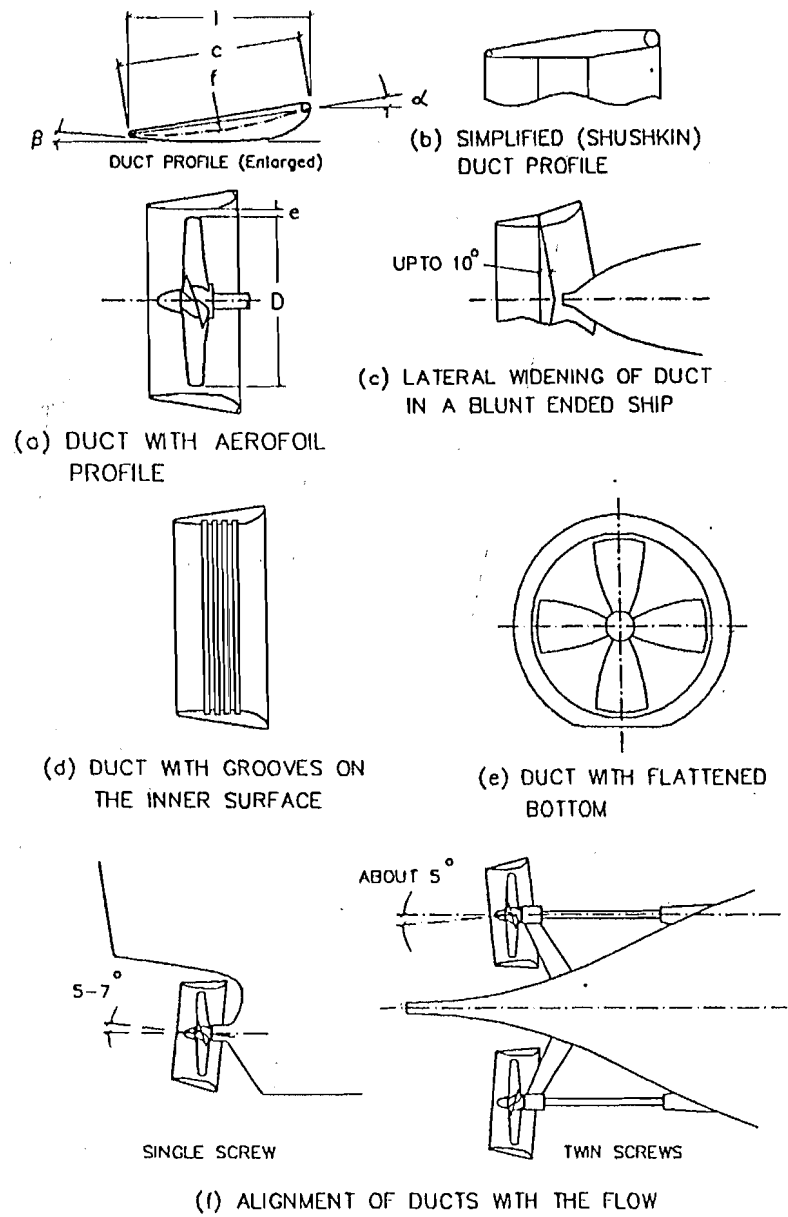


Figure 12.7: Ducted Propeller Features.

draw the solid objects towards the centre of the propeller rather than into the clearance gap, Fig. 12.7 (d). Since many of these solid objects are stones picked up from the bottom when the ship is operating in shallow water, the duct may be flattened at the bottom so that the velocity induced by the duct is reduced locally and the stones are not lifted into the flow, Fig. 12.7 (e). The slight loss in efficiency that this entails may be compensated for by an increase in the diameter of the duct and propeller.

Another problem that sometimes occurs is the drawing of air from the atmosphere into the duct leading to a loss of thrust. This is likely to occur when the leading edge of the duct is close to the surface of water and is not covered by the ship hull. The fitting of barrier plates between the atmosphere and the duct usually clears up this problem, although a better course would be to fit the duct as low down below the waterline as possible, tucked well below the stern of the ship.

Cavitation may occur near the propeller blade tips and the collapse of the cavities on the adjacent duct surface may cause erosion. To deal with this, the inner surface of the duct in way of the blade tips is sometimes made of stainless steel or coated with an erosion resistant material.

The duct is usually attached to the ship hull by streamlined struts. The shape of the stern is modified to facilitate the fitting of the duct and to guide the flow into it. In another arrangement the top of the duct penetrates into the hull. This allows a larger propeller diameter to be used. The wake fraction is higher resulting in an increased hull efficiency, but the flow is more inhomogeneous and propeller induced vibration may be a problem. The duct centre line normally coincides with the propeller shaft axis, but it may be advantageous to align the duct with the flow. In ships with twin ducted propellers, the ducts may be inclined 5 degrees inward towards the aft, while in single ducted propeller ships the duct may be inclined 5–7 degrees upwards, Fig. 12.7 (f).

The radial distribution of circulation in a ducted propeller is quite different from that in an open propeller, as shown in Fig. 12.8. The sharp drop in circulation towards the blade tips in an open propeller is not present in the ducted propeller because the trailing vortices at the tips are suppressed by the duct. Therefore, it is necessary in a ducted propeller to use a blade outline matching its different loading distribution. Propellers operating in ducts usually have wide-tipped outlines, and are known as Kaplan type

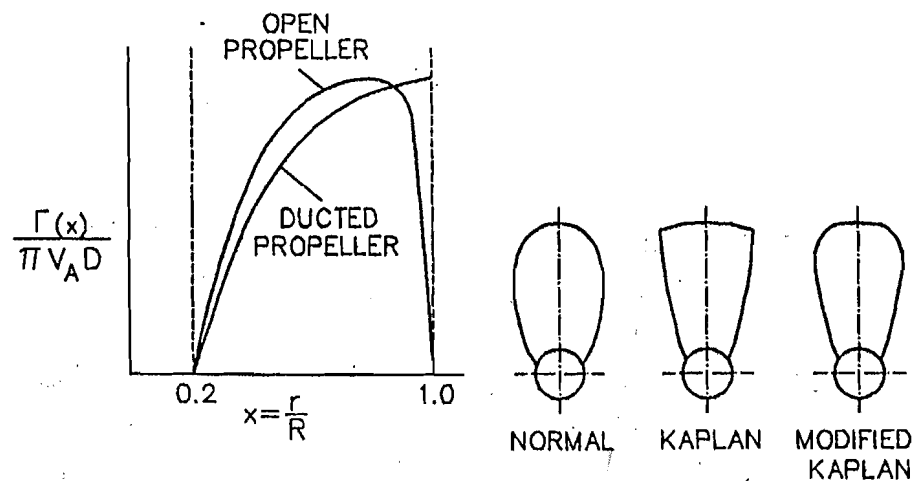


Figure 12.8 : Circulation Distribution and Blade Outlines for Ducted Propellers.

propellers. A Kaplan type propeller has a higher efficiency than a propeller with a normal blade outline when operating in a duct. In shallow water, a Kaplan propeller has a greater likelihood of getting jammed in the duct due to stones entrained in the flow, and hence a modified Kaplan outline is sometimes adopted.

Extensive methodical series data for ducted propellers have been generated at MARIN. The Ka propeller series in Nozzle 19A is widely used for the design of ducted propellers. Where very good astern performance is required, Nozzle 37 with its thicker trailing edge may be adopted. Data are also available for propellers in ducts with l/D ratios of 0.8 and 1.0, designated as Nozzle 22 and Nozzle 24 respectively. Some of these data are given in Appendix 3.

Ducted propellers have the following advantages over open propellers:

- improved efficiency at high loading;
- more homogeneous flow into the propeller and hence reduced vibration;
- smaller effect of loading and speed variations on efficiency;

- improved course stability;
- lower vulnerability to damage due to large floating debris.

The disadvantages of ducted propellers are:

- poor astern propulsive performance;
- reduced astern manoeuvrability and directional stability;
- increased susceptibility to cavitation;
- greater vulnerability to damage in shallow water due to stones being drawn into the gap between duct and propeller.

Ducted propellers with accelerating ducts (Kort nozzles) may be used with advantage in low speed vessels having high thrust loads such as tugs and trawlers. Large tankers and bulk carriers may also benefit by adopting ducted propellers. For a thrust loading coefficient C_{TL} below 0.7, a ducted propeller is less efficient than an equivalent open propeller, but for C_{TL} greater than 1.5 the efficiency of a ducted propeller increases sharply above that of an open propeller. Tugs normally have a C_{TL} greater than 3.0 while towing, and substantial improvements of as much as 30 percent in the bollard pull can be attained by using ducted propellers. For large tankers and bulk carriers of limited draught C_{TL} is often between 2.5 and 5.0, and ducted propellers should improve efficiency. In the few cases in which such ships have been fitted with ducted propellers replacing conventional propellers, savings in power between 5 and 12 percent have been found. However, blade tip cavitation when the blades are in the vertically up position and the implosion of the resulting cavities is a problem.

Ducted propellers are sometimes used for steering ships. The duct is pivoted about a vertical axis, attached by a shaft (rudderstock) to the steering gear on top and supported on the solepiece at the bottom, Fig. 12.9. By turning the duct about the vertical axis, a lateral force is produced to steer the ship. The clearance between the duct and the propeller blade tips has to be increased slightly, at the sides to allow for the turning of the duct and at the top and bottom for bearing play. The steering duct by itself is "over-balanced", i.e. it has a tendency to turn away from its position on the centre

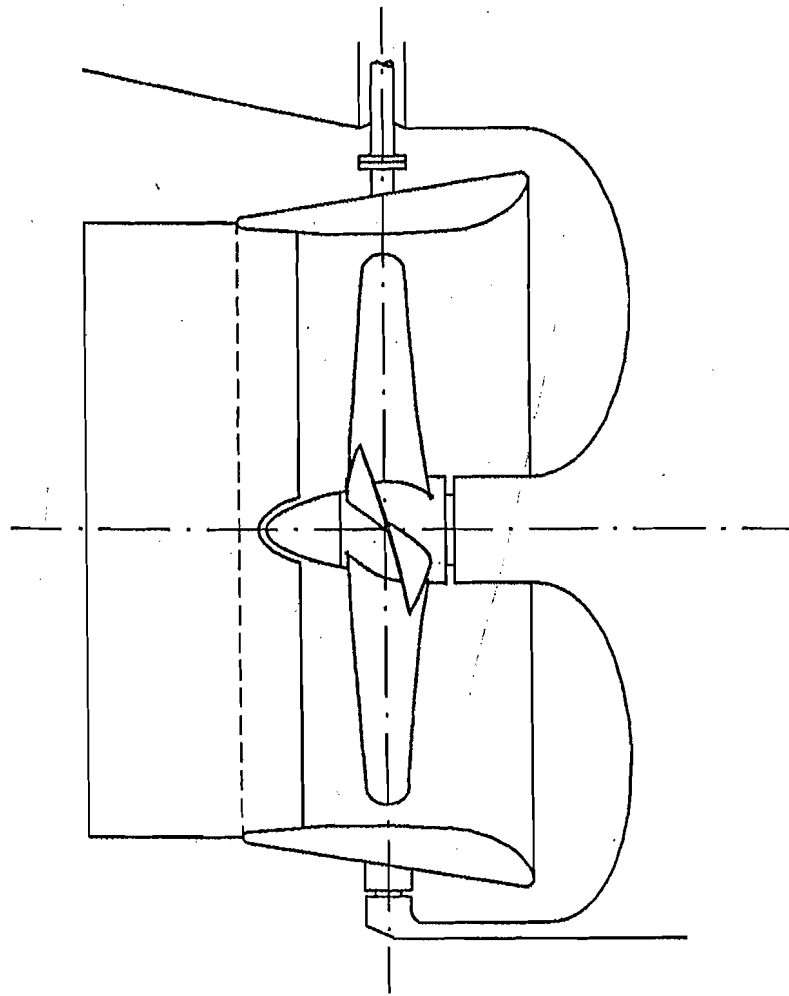


Figure 12.9 : Steering Duct.

line of the ship. This occurs because the centre of pressure of the duct is at about a quarter length behind the leading edge whereas the pivoting axis is at mid-length. Therefore, a vertical plate is usually fitted to the duct at its centre line just aft of the propeller. Such a plate balances the duct, improves steering and by reducing slipstream rotation improves efficiency. A steering ducted propeller has to be made smaller than a fixed one to allow for the

rudderstock coupling on the top and the support bearing at the bottom. However, since the rudder is eliminated, the ducted propeller can be moved further aft. This allows the waterline slopes aft to be reduced and a greater distance provided between the hull and the propeller, resulting in a lower resistance and a lower thrust deduction.

Decelerating ducts, as mentioned earlier, are used in high speed bodies moving in water to minimise cavitation and noise. Such ducts are usually combined with a row of fixed fins or stator blades, the combination of duct, fins and propeller being known as a pump-jet, Fig. 12.10. The fins are used to minimise the rotation or swirl imparted to the water by the propeller. The fins are also used to support the duct. If the fins are placed ahead of the

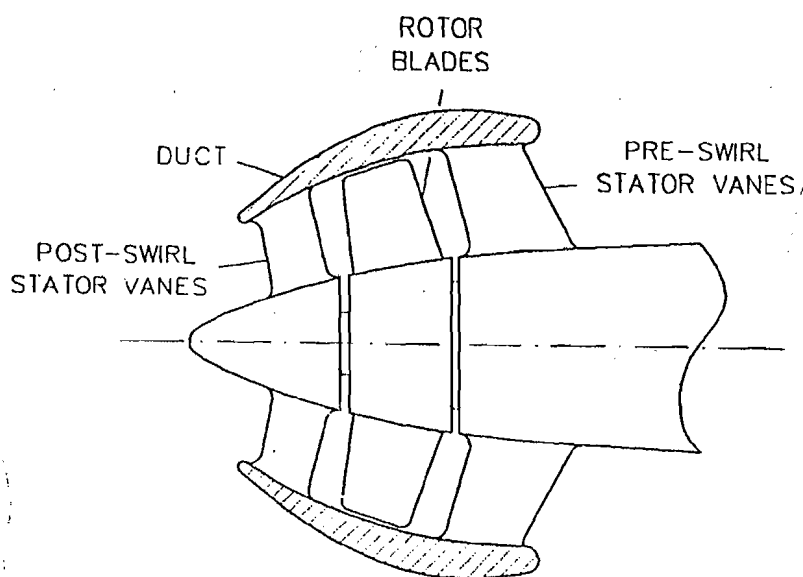


Figure 12.10 : Pumpjet.

propeller, they are designed to impart a rotation to the flow in a direction opposite to that of the propeller. Such "pre-swirl" stators can be designed to minimise the rotation of the slipstream only at one speed. Fins fitted behind the propeller are designed to eliminate rotation in the flow leaving them. Such "post-swirl" stators provide a low swirl in all operating conditions and are more effective than fins placed ahead of the propeller because the

velocity behind the propeller is higher. Minimisation of slipstream rotation is necessary to reduce the reaction torque on the body and prevent it spinning about its own axis. The close fitting duct suppresses tip vortices and allows increased tip loading in a manner similar to an accelerating duct. It also suppresses noise.

The design of pump-jets may be carried out using a simplified lifting line theory, but CFD (Computational Fluid Dynamics) techniques are being increasingly used for complex stator-rotor configurations. Decelerating duct methodical propeller series data have been produced by MARIN: Kd 5-100 propeller series in Nozzle 33. Decelerating duct propellers are widely used for torpedoes and have also been used in small, high speed warships.

Example 3

A tug has a propeller of 3.0 m diameter and 0.8 pitch ratio, the open water characteristics of which are as given in Table 4.3. The tug has a wake fraction of 0.200, a thrust deduction fraction of 0.180 in the free running condition and 0.050 in the bollard pull condition, a relative rotative efficiency of 1.000 and a shafting efficiency of 0.950. The effective power of the tug is as follows:

Speed, knots	:	10.0	11.0	12.0	13.0
Effective power, kW	:	137.7	192.2	260.7	344.9

If the propeller is run at 150 rpm in both the free running condition and the bollard pull condition, determine the free running speed and the bollard pull, and the corresponding brake powers.

The propeller is replaced by a ducted propeller of the same diameter and 0.912 pitch ratio, whose open water characteristics are as follows:

J	:	0	0.100	0.200	0.300	0.400	0.500	0.600	0.700
K_T	:	0.4427	0.3957	0.3493	0.3019	0.2518	0.1976	0.1376	0.0702
$10K_Q$:	0.3497	0.3467	0.3382	0.3237	0.3026	0.2739	0.2365	0.1887

Determine the free running speed and the bollard pull and the corresponding brake powers.

$$D = 3.0 \text{ m} \quad w = 0.200 \quad t_0 = 0.050 \quad t_1 = 0.180$$

$$\eta_R = 1.000 \quad \eta_S = 0.950 \quad n = 150 \text{ rpm} = 2.5 \text{ s}^{-1}$$

Free running condition:

$$R_T = \frac{P_E}{V} \quad T = \frac{R_T}{1-t}$$

$$J = \frac{(1-w)V}{nD} = \frac{(1-0.200)V}{2.5 \times 3.0} = \frac{1}{9.375} V$$

$$K_T = \frac{T}{\rho n^2 D^4} = \frac{T}{1.05 \times 2.5^2 \times 3.0^4} = \frac{T}{518.906}$$

$V \left\{ \begin{array}{l} \text{k} \\ \text{ms}^{-1} \end{array} \right.$:	10.0	11.0	12.0	13.0
	:	5.1440	5.6584	6.1728	6.6872
P_E kW	:	137.7	192.2	260.7	344.9
R_T kN	:	26.679	33.967	42.234	51.576
T kN	:	32.645	41.423	51.504	62.898
J	:	0.5487	0.6036	0.6584	0.7133
K_T	:	0.0629	0.0795	0.0993	0.1212

Open Propeller

The K_T - J curves from the above table and from Table 4.3 for $P/D = 0.800$ intersect at:

$$J = 0.6584 \quad K_T = 0.0993$$

for which $10K_Q = 0.1577$

$$\begin{aligned} \text{Free running speed} \quad V &= 9.375 J = 9.375 \times 0.6584 \\ &= 6.1728 \text{ ms}^{-1} = 12.0 \text{ knots} \end{aligned}$$

$$\begin{aligned} \text{Delivered power,} \quad P_D &= 2\pi \rho n^3 D^5 \frac{K_Q}{\eta_R} \\ &= 2\pi \times 1.025 \times 2.5^3 \times 3.0^5 \times \frac{0.01577}{1.000} \text{ kW} \\ &= 385.54 \text{ kW} \end{aligned}$$

$$\text{Brake power, } P_B = \frac{P_D}{\eta_S} = \frac{385.54}{0.950} = 405.8 \text{ kW}$$

Bollard pull condition:

From Table 4.3 for $P/D = 0.800$:

$$K_{T0} = 0.3415 \quad K_{Q0} = 0.04021 \text{ at } J = 0$$

$$\begin{aligned} \text{Bollard pull, } BP &= (1 - t_0) T_0 = (1 - t_0) K_{T0} \rho n_0^2 D^4 \\ &= (1 - 0.050) \times 0.3415 \times 1.025 \times 2.5^2 \times 3.0^4 \text{ kN} \\ &= 168.346 \text{ kN} \end{aligned}$$

$$\begin{aligned} \text{Delivered power, } P_D &= 2\pi \rho n_0^3 D^5 \frac{K_{Q0}}{\eta_R} \\ &= 2\pi \times 1.025 \times 2.5^3 \times 3.0^5 \times \frac{0.04021}{1.000} \text{ kW} \\ &= 983.25 \text{ kW} \end{aligned}$$

$$\text{Brake power, } P_B = 1035 \text{ kW}$$

Ducted Propeller

Free running condition:

The K_T - J curve for the ducted propeller intersects the K_T - J curve from the foregoing table at the same values of J and K_T as the open propeller; i.e. at the free running speed:

$$J = 0.6584 \quad K_T = 0.0993 \quad 10K_Q = 0.2098$$

$$\begin{aligned} \text{Delivered power, } P_D &= 2\pi \rho n^3 D^5 \frac{K_Q}{\eta_R} \\ &= 2\pi \times 1.025 \times 2.5^3 \times 3.0^5 \times \frac{0.02098}{1.000} \text{ kW} \\ &= 513.14 \text{ kW} \end{aligned}$$

$$\text{Brake power, } P_B = 540.15 \text{ kW}$$

Bollard pull condition:

$$\begin{aligned}
 \text{Bollard pull,} \quad BP &= (1 - t_0) K_{T0} \rho n^2 D^4 \\
 &= (1 - 0.050) \times 0.4427 \times 1.025 \times 2.5^2 \times 3.0^4 \text{ kN} \\
 &= 218.233 \text{ kN}
 \end{aligned}$$

$$\begin{aligned}
 \text{Delivered power,} \quad P_D &= 2\pi \rho n^3 D^5 \frac{K_{Q0}}{\eta_R} \\
 &= 2\pi \times 1.025 \times 2.5^3 \times 3.0^5 \times \frac{0.03497}{1.000} \text{ kW} \\
 &= 855.12 \text{ kW}
 \end{aligned}$$

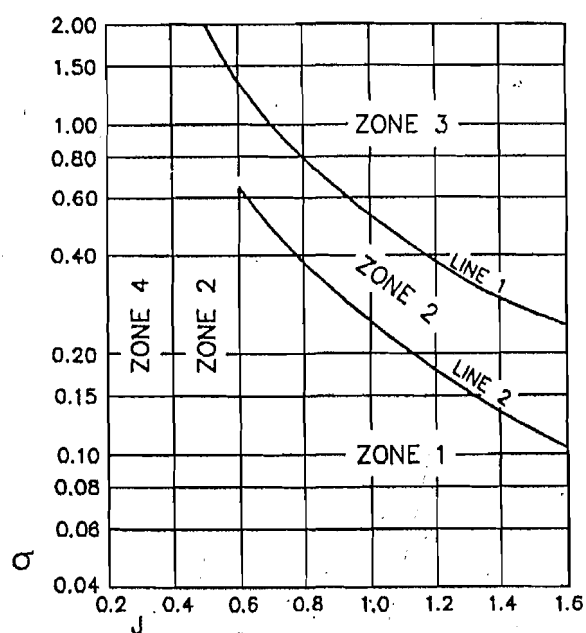
$$\text{Brake power,} \quad P_B = \frac{P_D}{\eta_S} = \frac{855.12}{0.950} = 900.1 \text{ kW}$$

Both the open propeller and the ducted propeller thus give the same free running speed in this example, but the ducted propeller provides a higher bollard pull at a lower power.

12.5 Supercavitating Propellers

When the design conditions of a propeller are such that unacceptable levels of cavitation cannot be avoided, it is necessary to consider the use of a supercavitating propeller. In a supercavitating propeller, a vapour filled cavity covers the whole of the back of the propeller blade. Under proper conditions, a supercavitating propeller can provide high thrust at nearly the same efficiency as a conventional subcavitating propeller without cavitation erosion and excessive noise and vibration. Supercavitating propellers are used in ships in which high engine powers, ship speeds and propeller rpms are combined with small propeller diameters and low depths of immersion.

For a supercavitating propeller to work efficiently a proper combination of the advance coefficient J and the cavitation number σ are essential. The recommended field of application for supercavitating propellers given by Tachmindji and Morgan (1958) is shown in Fig. 12.11, and is based on achieving a propeller efficiency of at least 0.64 and ensuring that the propellers are fully cavitating. Line 1 in the figure is based on the occurrence of incipient



ZONE 1 : Best region for super-cavitating propellers

ZONE 2 : Marginal region with some cavitation on all propellers

ZONE 3 : Best region for conventional propellers

ZONE 4 : Region of low efficiency for all propellers

Figure 12.11 : Application of Supercavitating Propellers.

cavitation and gives the lower limit of σ for conventional (non-cavitating) propellers. Line 2 represents the upper limit of σ for full cavitation to occur and is based on obtaining a local cavitation number at $0.7R$, $\sigma_{0.7R}$, of 0.045. If partial cavitation cannot be avoided (Zone 2) it is preferable to use propellers specially designed for such conditions, e.g. those belonging to the Gawn-Burrill Series, Gawn and Burrill (1957).

Supercavitating propellers were first used in racing motor boats, the design of such propellers being based on trial and error. Pioneering research on supercavitating propellers was carried out by Posdunine (1944), who developed a theoretical model of the flow, derived expressions for the thrust and efficiency of such propellers and suggested the use of wedge shaped sections. Tulin (1964) formulated a theory of cavity flows and this led to the development of the modern theory of supercavitating propellers.

The blade section shape in supercavitating propellers differs considerably from that in conventional propellers. Since the back of the blade section is not supposed to be in contact with water in a supercavitating propeller, its design is based on ensuring a complete separation of flow on the back at the leading edge and at the trailing edge while at the same time providing a high lift-drag ratio. Tulin developed a method for determining the shape of the camber centre line and the thickness distribution of a supercavitating foil to obtain a given lift coefficient and the optimum lift-drag ratio in two-dimensional flow. This was then used in designing propellers following a method similar to that used in designing conventional propellers with the circulation theory. A propeller design based on this approach requires various empirical corrections and testing in a cavitation tunnel to ensure that it satisfies the design requirements.

Design charts based on this theoretical design method have been produced by Caster (1963) which cover the following ranges of design parameters:

Number of blades Z	:	2, 3 and 4
Blade area ratio, A_E/A_O	:	0.3–0.5 (2 blades) 0.4–0.6 (3 blades) 0.4–0.7 (4 blades)
Advance coefficient, J	:	0–1.6
Thrust loading coefficient, C_{TL}	:	0.3–2.25
Cavitation number, σ	:	0

Correction factors have been provided for cavitation numbers greater than zero.

The lifting line theory in association with Tulin's linearised cavity flow theory has been used by Venning and Haberman (1962) to develop a design procedure for supercavitating propellers. Unfortunately, experiments in a cavitation tunnel have shown that this design procedure often results in propellers that have a thrust deficiency of as much as 15 percent and in which the cavity does not cover the whole of the back of the propeller blade.

Improved design methods have been developed in which the blade sections are designed using a non-linear cavity flow theory and the effect of the cavity volume on the flow is taken into account. Supercavitating propeller design procedures now use vortex lattice and surface panel techniques.

Initially in supercavitating propellers, aerofoil and crescent shaped (Karman-Trefftz) blade sections were tried out, but with disappointing results. Later, after the work of Tulin, wedge shaped sections began to be used. The Tulin section based on the linearised cavity flow theory has a very sharp and thin leading edge, and has to be modified for practical use by a slight increase in thickness near the leading edge. New types of blade sections for supercavitating propellers have been developed which have thicker flat leading edges and cupped trailing edges. Such sections have been found to give better results than the Tulin sections. Blade section shapes used in supercavitating propellers are illustrated in Fig. 12.12.

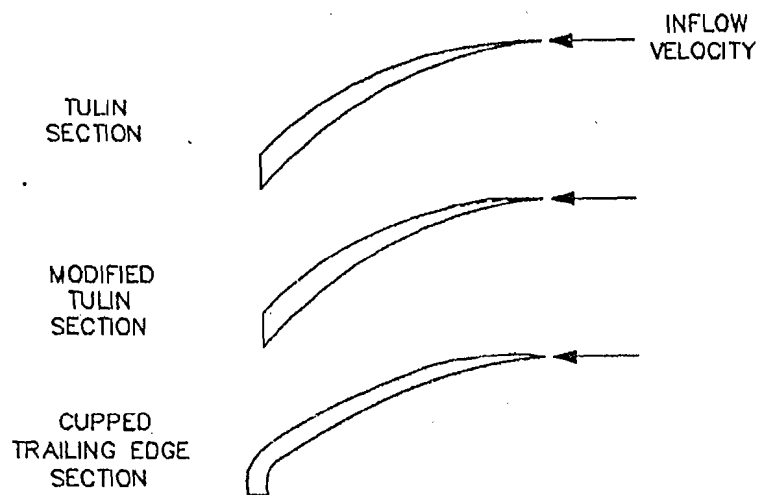


Figure 12.12 : Supercavitating Propeller Blade Sections.

Design charts for supercavitating propellers based on experiments in a cavitation tunnel have been given by Rutgersson (1979). Propellers designed on the basis of these charts perform as expected, but their efficiency is low.

The open water characteristics of a series of propellers for high performance craft derived from cavitation tunnel experiments have been given by Newton and Rader (1961). This Newton-Rader Series covers the following parameters:

Number of blades, Z	:	3		
Blade area ratio, A_D/A_O	:	0.48	0.71	0.95
Pitch ratios, P/D	:	1.05	1.05	1.04
for the different values		1.26	1.25	1.24
of A_D/A_O		1.67	1.66	1.65
		2.08	2.06	2.04
Cavitation number, σ	:	0.25 to a value corresponding to atmospheric pressure		

The blade section shapes used in the Newton-Rader Series are, however, not the typical wedge shapes used in supercavitating propellers, and these propellers are therefore sometimes characterised as transcavitating rather than supercavitating. However, the term transcavitating propeller is more usually applied to a propeller in which the sections at the inner radii, which have a lower resultant velocity V_R , are designed to work in the subcavitating zone while the sections at the outer radii with a higher resultant velocity are designed for supercavitating operation.

Propeller blade strength is a major problem in supercavitating propellers, particularly because of the thin leading edge of the blade. It is usually necessary to use special materials such as titanium alloys, copper-beryllium alloys and special stainless steels of high strength and hardness instead of the nickel-copper-aluminium alloys commonly used in conventional propellers.

Supercavitating propellers have another major problem: their performance in off-design conditions. A supercavitating propeller works efficiently only when it is cavitating fully, i.e. at or near the design speed. However, to reach this condition from rest, the propeller has to pass through a low speed

range in which it will not cavitate fully and hence work at low efficiency. As a result, unless there is a very large power margin, the vessel may never get past its low speed range. Some solutions have been proposed for dealing with this problem, Fig. 12.13. One is to promote the development of a

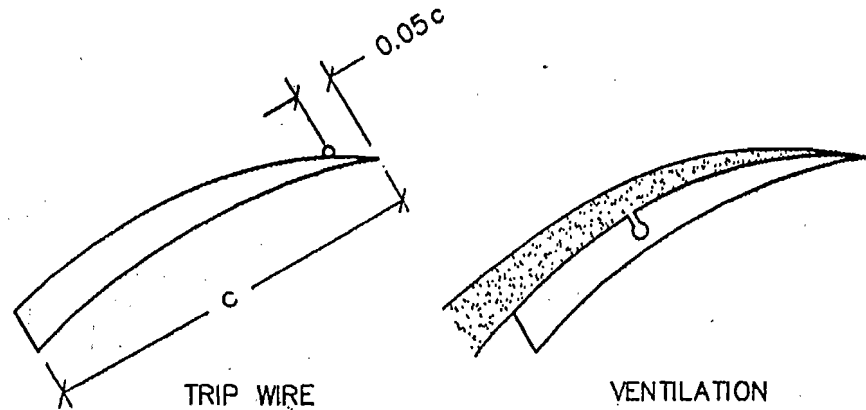


Figure 12.13 : Cavity Generation at Low Speeds.

cavity on the back of the blade at low speeds by causing flow separation through a trip wire fitted just behind the leading edge. A second method is to create a cavity artificially on the back of the propeller blade by introducing air through an opening in the blade, i.e. produce a cavity by ventilation. A third method which has been adopted in some cases is to have two sets of propellers—conventional subcavitating propellers for low speed operation and supercavitating propellers for high speed operation. Controllable pitch supercavitating propellers and variable camber propellers, in which the blades are made in two parts one of which can be moved to alter the blade section camber, have also been used to deal with the problem of operation in off-design conditions.

12.6 Surface Propellers

A surface propeller or surface piercing propeller is a screw propeller which operates partly submerged in water so that the propeller blades enter and leave the surface of water once every revolution. Surface propellers are fitted

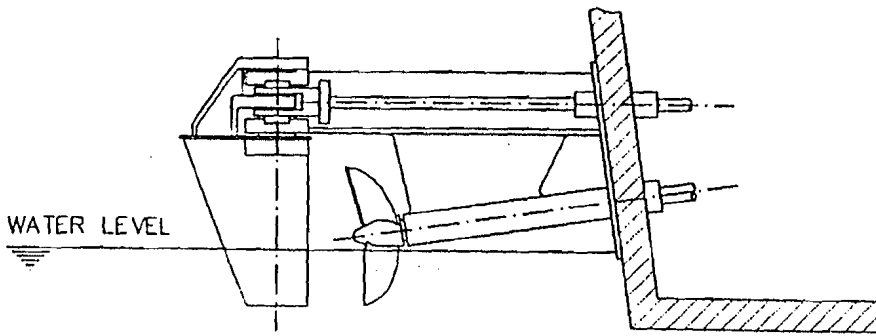


Figure 12.14 : Surface Piercing Propeller.

just behind the hull of the ship instead of under it, Fig. 12.14. As a result, the underwater appendages required for supporting the propeller are eliminated leading to a sharp drop in appendage resistance, which can be considerable in a small high speed vessel, as much as 30 percent of the total in some cases. At the same time, the decrease in efficiency due to the propeller not being fully submerged is not very large. Therefore, the total power required to attain a given speed with a surface propeller may be substantially less than the power required with a conventional fully submerged propeller. Surface propellers have other advantages. They are not susceptible to cavitation since the low pressure areas on the blades are covered with air filled cavities which do not implode violently on reaching high pressure areas as water vapour filled cavities do. Since cavitation is not a problem, surface propellers may have low blade areas and hence a low drag. Also, because the surface propeller is located behind the hull and is not fully submerged, it can have a large diameter even when the vessel is designed to operate in shallow water. Thus, surface propellers have a good potential for use in small high speed craft of limited draught.

Surface propellers also have serious disadvantages. Since the propeller blades enter and leave the water once in every revolution, the hydrodynamic forces on the blades are unsteady and, compared to a fully submerged propeller producing the same thrust, are also much greater in magnitude. The strength of the propeller is therefore of major concern. The periodic loading on the propeller blades also creates problems due to fatigue and vibration. The submergence of only the lower part of the propeller gives rise to a sig-

nificant component of the hydrodynamic forces normal to the propeller axis, which must be withstood by the propeller shaft bearings. The unsteady propeller torque affects the engine and the propeller shafting adversely. Surface propellers also have very poor astern performance. Finally, the submergence of a surface propeller fitted to a high speed craft may vary with speed as the craft rises in the water and trims, and this may cause the propeller to overload the engine at low speeds when the submergence is high.

Ferrando (1997) suggests that the action of a surface propeller may be divided into six phases, Fig. 12.15. At high values of the advance coefficient J , a negligible amount of air enters the water with the propeller blade and

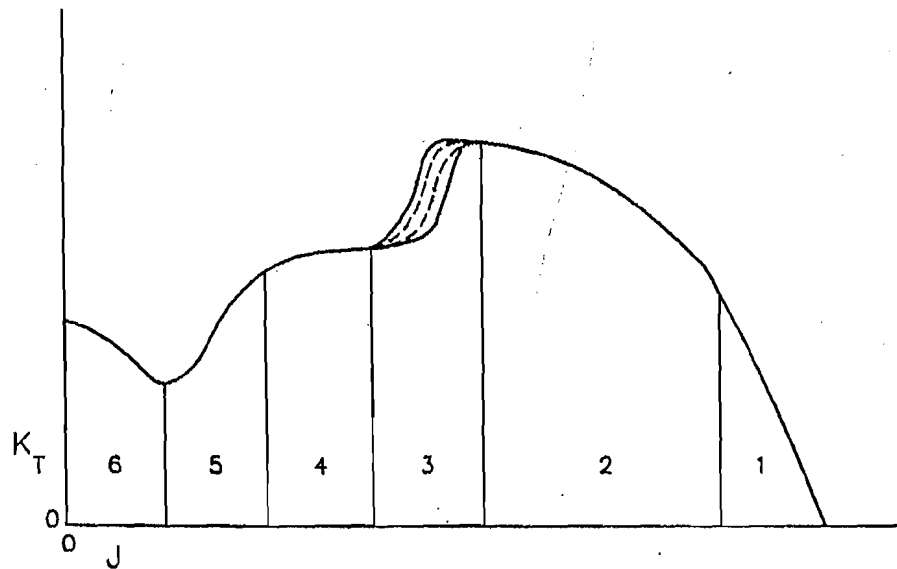


Figure 12.15 : Phases of Action of a Surface Propeller.

is confined to the region behind the trailing edge, there being a balance between the volume of the cavity and the suction of the blade. The tip vortex of the blade is also ventilated with air. This phase is known as the "base vented" phase, 1. As the loading increases and J decreases, the suction on the back of the blade draws increasing amounts of air, and the cavity increases in size. The cavity remains confined to the region behind the trailing edge of the blade, but there may be streaks of air over the back

of the blade. This is the "partially vented" phase, 2. A further reduction in J results in an unstable "transition" phase, 3. The air cavity is unstable and the back of the propeller blade fluctuates between the fully wetted, partially wetted (i.e. with streaks of air covering parts of the back), and the fully dry conditions. The thrust and torque coefficients, K_T and K_Q , also fluctuate over a significant range of values. With a still further reduction in J , the air filled cavity covers the whole of the back of the blade in the "fully vented" phase, 4. The volume of the cavity increases as J decreases. The shapes of the K_T and K_Q curves depart from those of a conventional propeller because only the face of the propeller blade contributes to the thrust and torque while the back is covered with air and contributes almost nothing. The air cavities attached to the blades have a large thickness and there is considerable mutual interference between the blades. As J is reduced even further, the size of the air cavities increases to such an extent that the flow between the propeller blades becomes restricted. In this "cavity blockage" phase, 5, K_T and K_Q decrease as J decreases. At very low values of J , the air supply to the cavities accompanying the propeller blades may be blocked by excessive spray. In this "cavity choking" phase, 6, the pressure in the cavities may be lower than atmospheric, resulting in an increase in thrust and torque.

For a surface propeller of a given geometry, the thrust and torque coefficients are functions not only of the advance coefficient, the Reynolds number, the Froude number and the cavitation number, but also of the Weber number, $W_n = V^2 L / \kappa$ where κ is the kinematic capillarity (surface tension per unit length/density) of water:

$$\frac{K_T}{K_Q} = f(J, R_n, F_n, \sigma, W_n) \quad (12.15)$$

In addition, the immersion of the propeller as a ratio of its diameter and the angle between the propeller shaft axis and the line of flow also affect surface propeller performance significantly.

Since the propeller blades pierce the surface of water twice in every revolution, surface tension is obviously an important factor in the behaviour of surface propellers. Experience has shown that the critical value of J at which transition to full ventilation occurs and there is a sharp drop in K_T and K_Q depends on the value of the Weber number W_n .

The Froude number also influences surface propeller behaviour because such propellers operate at the surface of water and give rise to surface waves. However, model experiments seem to indicate that at sufficiently high values the effect of the Froude number vanishes, i.e. for a Froude number defined as $F_n = nD/\sqrt{gD}$ greater than 4, there is no effect.

Surface propellers rarely suffer from cavitation. Only if high values of J , at which the air-filled cavities are small and confined to the trailing edge, are combined with very low values of the cavitation number σ is there a possibility of cavitation. Otherwise, the air filled cavities prevent the formation of cavities filled with water vapour which characterise cavitation.

The immersion of a surface propeller has a considerable effect upon its performance, and the immersion ratio h/D , where h is the maximum tip immersion in calm water and D the propeller diameter, greatly affects the values of K_T and K_Q . However, if the thrust and torque coefficients are defined in a modified form as:

$$K'_T = \frac{T}{\rho n^2 D^2 A'_O} \quad K'_Q = \frac{Q}{\rho n^2 D^3 A'_O} \quad (12.16)$$

where A'_O is the area of the immersed segment of the propeller disc, the effect of h/D (as separate from the effect of A'_O) appears to be negligible, particularly in the base vented and partially vented phases, 1 and 2.

The angle of the propeller shaft axis to the direction of flow has a greater effect upon performance in a surface propeller than in a fully submerged propeller. The inclination of the propeller shaft axis to the relative velocity of water gives rise to an unbalanced force in a transverse plane. Such an unbalanced force is also produced by the partial submergence of the propeller. By suitably choosing the angle of the propeller shaft in the vertical and horizontal planes, it is possible to neutralise the transverse force due to partial submergence by the transverse force due to shaft inclination. Apart from reducing the loading on the propeller shaft bearing, the elimination of the resultant transverse force also enhances propeller efficiency. There is thus an optimum shaft angle, which gives maximum propeller efficiency and zero average transverse force at the design speed of the ship.

The design of surface propellers is largely based on model experiments. In carrying out model experiments, however, it must be remembered that the Froude number, the Weber number and the cavitation number cannot

be ignored as is usually the case in model experiments with non-cavitating fully submerged propellers. Blade section shapes used in surface propellers include wedge shaped sections, wedge shaped sections with cupped trailing edges and a patented "diamond back" shape, Fig. 12.16. The blade outline may be suitably skewed to minimise the amplitude of the unsteady forces and reduce vibration.

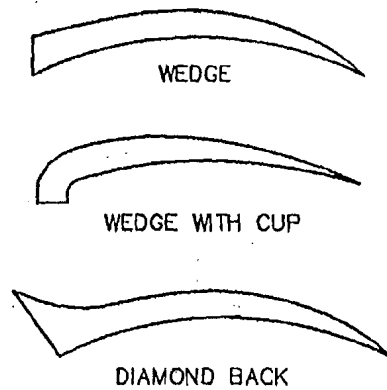


Figure 12.16 : Surface Propeller Blade Section Shapes.

Like supercavitating propellers, surface propellers also have problems with operation at low speeds. Surface propellers have high pitch ratios and may have a greater immersion at speeds lower than the design speed. This may result in the engine being overloaded at low speeds. A solution to this problem is to artificially ventilate the backs of the blades by introducing air through a pipe or to direct the engine exhaust into the wake just ahead of the propeller. Alternatively, the surface propeller may be fitted to an articulated shaft by which the immersion of the propeller may be reduced if necessary to prevent overloading the engine. If the propeller shaft can be angled sideways, the surface propeller can also be used for steering and the rudder eliminated. In addition, the shaft angle can be adjusted so as to minimise the side force at each speed.

Example 4

A four-bladed surface piercing propeller of 1.5 m diameter has a speed of advance of 10.0 m per sec at 600 rpm. The flow is along the propeller axis which is 0.1941 m

above the surface of water. The thrust and torque per unit length for each blade are constant over the immersed part of the blade, and are equal to 45.00 kN per m and 14.25 kN m per m respectively. Determine the variation of the thrust, the torque and the horizontal and vertical components of the transverse force on the propeller in each revolution, and their average values. Assume that the blades are narrow.

$$Z = 4 \quad D = 1.5 \text{ m} \quad n = 600 \text{ rpm} = 10.0 \text{ s}^{-1} \quad V_A = 10.0 \text{ m s}^{-1}$$

Propeller axis above water, $a = 0.1941 \text{ m}$

$$\frac{dT}{dr} = 45.00 \text{ kN m}^{-1} \quad \frac{dQ}{dr} = 14.25 \text{ kN m m}^{-1} \quad \text{for each blade.}$$

If the angles with the upward vertical at which each blade enters and leaves the surface of water are θ_1 and θ_2 :

$$\theta_1 = 90^\circ + \sin^{-1} \frac{a}{R} = 90^\circ + \sin^{-1} \frac{0.1941}{0.75} = 90^\circ + 15^\circ = 105^\circ$$

$$\theta_2 = 270^\circ - \sin^{-1} \frac{a}{R} = 270^\circ - 15^\circ = 255^\circ$$

At any angle θ , $\theta_1 \leq \theta \leq \theta_2$:

$$\text{radius at inner edge of immersed blade, } r_0 = \frac{a}{\cos(180^\circ - \theta)} = -\frac{a}{\cos \theta}$$

$$\text{length of immersed blade} = R - r_0$$

$$\text{thrust of the blade, } T_1 = \frac{dT}{dr} (R - r_0)$$

$$\text{blade torque, } Q_1 = \frac{dQ}{dr} (R - r_0)$$

$$\text{tangential force, } F_1 = \int_{r_0}^R \frac{1}{r} \frac{dQ}{dr} dr = \frac{dQ}{dr} \ln \frac{R}{r_0}$$

$$\text{horizontal component, } F_{1H} = F_1 \cos(180^\circ - \theta) = -F_1 \cos \theta$$

$$\text{vertical component, } F_{1V} = F_1 \sin(180^\circ - \theta) = F_1 \sin \theta$$

θ°	r_0 m	T_1 kN	Q_1 kNm	F_1 kN	F_{1H} kN	F_{1V} kN
105	0.7500	0	0	0	0	0
120	0.3882	16.281	5.156	9.878	4.939	8.555
135	0.2745	21.398	6.776	15.077	10.661	10.661
150	0.2241	23.664	7.494	18.118	15.690	9.059
165	0.2009	24.707	7.824	19.756	19.082	5.113
180	0.1941	25.016	7.992	20.276	20.276	0
195	0.2009	24.707	7.824	19.756	19.082	-5.113
210	0.2241	23.664	7.494	18.118	15.690	-9.059
225	0.2745	21.398	6.776	15.077	10.661	-10.661
240	0.3882	16.281	5.156	9.878	4.939	-8.555
255	0.7500	0	0	0	0	0

The thrust of all the blades is calculated as follows:

$$T_{i+1}(\theta) = T_i(\theta + 90^\circ)$$

$$T(\theta) = \sum_{i=1}^4 T_i(\theta)$$

$$\text{Average } T = \frac{\int_0^{2\pi} T(\theta) d\theta}{\int_0^{2\pi} d\theta}$$

θ deg	T_1 kN	T_2 kN	T_3 kN	T_4 kN	T kN	SM	$f(T)$
0	0.000	0.000	25.016	0.000	25.016	1	25.016
15	0.000	0.000	24.707	0.000	24.707	4	98.830
30	0.000	16.281	23.664	0.000	39.945	2	79.891
45	0.000	21.398	21.398	0.000	42.795	4	171.180
60	0.000	23.664	16.281	0.000	39.945	2	79.891
75	0.000	24.707	0.000	0.000	24.707	4	98.830
90	0.000	25.016	0.000	0.000	25.016	2	50.031
105	0.000	24.707	0.000	0.000	24.707	4	98.830
120	16.281	23.664	0.000	0.000	39.945	2	79.891
135	21.398	21.398	0.000	0.000	42.795	4	171.180
150	23.664	16.281	0.000	0.000	39.945	2	79.891

θ deg	T_1 kN	T_2 kN	T_3 kN	T_4 kN	T kN	SM	$f(T)$
165	24.707	0.000	0.000	0.000	24.707	4	98.830
180	25.016	0.000	0.000	0.000	25.016	2	50.031
195	24.707	0.000	0.000	0.000	24.707	4	98.830
210	23.664	0.000	0.000	16.281	39.945	2	79.891
225	23.398	0.000	0.000	21.398	42.795	4	171.180
240	16.281	0.000	0.000	23.664	39.945	2	79.891
255	0.000	0.000	0.000	24.707	24.707	4	98.830
270	0.000	0.000	0.000	25.016	25.016	2	50.031
285	0.000	0.000	0.000	24.707	24.707	4	98.830
300	0.000	0.000	16.281	23.664	39.945	2	79.891
315	0.000	0.000	21.398	21.398	42.795	4	171.180
330	0.000	0.000	23.664	16.281	39.945	2	79.891
345	0.000	0.000	24.707	0.000	24.707	4	98.830
360	0.000	0.000	25.016	0.000	25.016	1	25.016
							2314.606

$$\text{Average thrust, } T = \frac{\frac{1}{3} \times 15^\circ \times 2314.606}{360^\circ} = 32.147 \text{ kN (by Simpson's Rule)}$$

Similarly, the variation of torque and the horizontal and vertical components of the tangential force can be obtained, and their average values calculated. The results are given in the following table, and in Fig. 12.17.

θ deg	Q kNm	F_H kN	F_V kN
0	7.922	20.275	0.000
15	7.824	19.082	-5.113
30	12.649	20.630	-0.504
45	13.552	21.322	0.000
60	12.649	20.630	0.504
75	7.824	19.082	5.113
90	7.922	20.275	0.000
105	7.824	19.082	-5.113
120	12.649	20.630	-0.504
135	13.552	21.322	0.000
150	12.649	20.630	0.504
165	7.824	19.082	5.113
180	7.922	20.275	0.000

θ deg	Q kNm	F_H kN	F_V kN
195	7.824	19.082	-5.113
210	12.649	20.630	-0.504
225	13.552	21.322	0.000
240	12.649	20.630	0.504
255	7.824	19.082	5.113
270	7.922	20.275	0.000
285	7.824	19.082	-5.113
300	12.649	20.630	-0.504
315	13.552	21.322	0.000
330	12.649	20.630	0.504
345	7.824	19.082	5.113
360	7.922	20.275	0

The average values calculated by using Simpson's Rule to integrate the various quantities over a revolution are:

$$Q = 10.180 \text{ kNm} \quad F_H = 20.056 \text{ kN} \quad F_V = 0$$

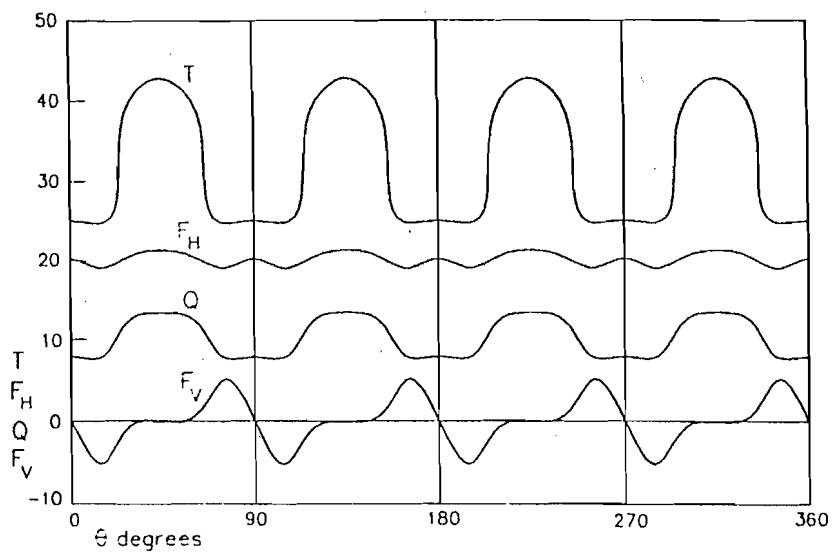


Figure 12.17: Loading of a Surface Propeller (Example 4).

12.7 Contra-rotating Propellers

A contra-rotating propeller (set) consists of two propellers rotating in opposite directions on coaxial shafts, one propeller being placed close behind the other, Fig. 12.18. The aim is to reduce the rotational energy losses in the slipstream. The first recorded use of a contra-rotating propeller is that

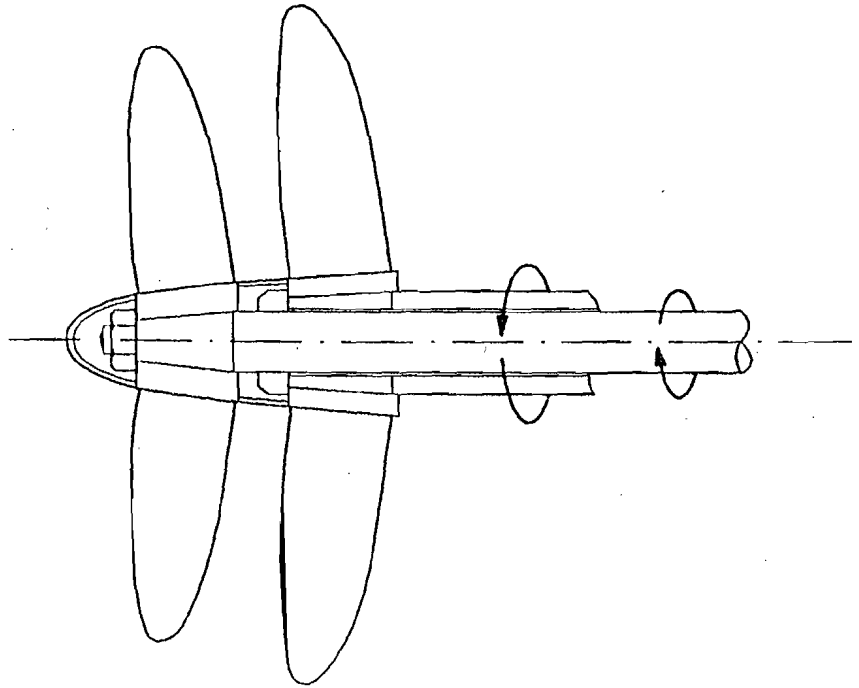


Figure 12.18 : Contra-rotating Propeller.

by Ericsson in 1837. Contra-rotating propellers have long been used in torpedoes in which the mutual cancellation of the torque reactions of the two propellers prevents the torpedo from rotating about its axis and thereby imparts it directional stability.

For ship propulsion, a contra-rotating propeller has the advantage that the required thrust load is distributed between two propellers so that the efficiency is higher than with an equivalent single propeller, and the propeller diameter and blade area ratio can be reduced. However, the efficiency of a

contra-rotating propeller is less than two single propellers producing the same total thrust. Contra-rotating propellers also have the disadvantages of greater weight and the complexity of the gearing and coaxial shafts. The sealing of the shafting against the ingress of water from outside is also a major problem.

In the design of contra-rotating propellers, the aft propeller is made of a slightly smaller diameter than the forward propeller taking the slipstream contraction into account. The pitch is selected to suit the required power absorption and to ensure that the slipstream rotation induced by the forward propeller is cancelled by that induced by the aft propeller. The circulation theory is used in the design of contra-rotating propellers, and a practical design method has been developed by Morgan (1960) based on the theory of Lerbs. This method gives good torque balance between the two propellers, a high efficiency and accurate values of the inflow velocities so that cavitation is better controlled. More recent design procedures are based on vortex lattice methods.

Apart from their long-standing use in torpedoes, contra-rotating propellers have been tried out in a submarine, and more recently in a Japanese bulk carrier and a car carrier. It appears that improvements in efficiency of up to 15 percent can be obtained compared to single screws, provided favourable hull-propeller interaction can be ensured. In general, however, the mechanical complications of fitting contra-rotating propellers are not justified by the increases in efficiency that can be achieved.

12.8 Tandem Propellers

Tandem propellers consist of two propellers mounted on the same shaft and turning in the same direction, Fig. 12.19. When a high thrust requirement is combined with a restricted propeller diameter, there is a problem with reduced efficiency and increased cavitation. Tandem propellers are a solution to this problem since the total thrust is divided between the two propellers. The propellers are usually of the same diameter and have the same number of blades. The two propellers must be designed taking into account the induced velocities due to each propeller. A set of tandem propellers

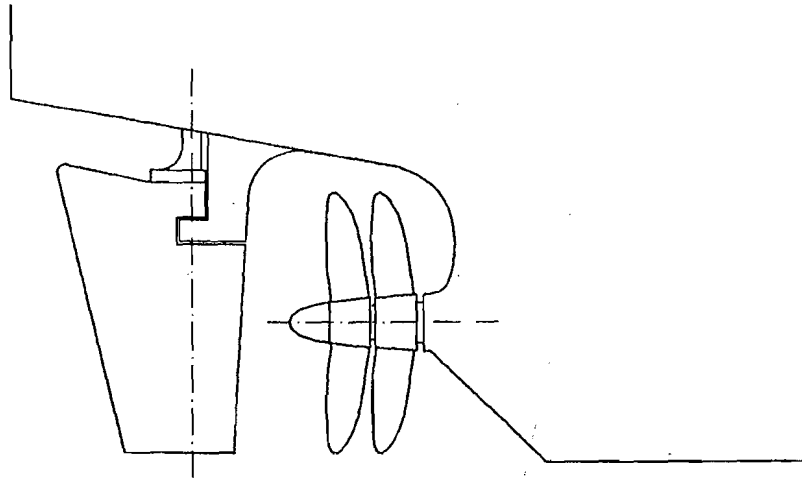


Figure 12.19: Tandem Propellers.

fitted to a British destroyer in 1900 showed that the aft propeller should have greater pitch than the forward propeller. Experiments indicate that at normal thrust loadings, tandem propellers have no significant advantage over equivalent single propellers. At high loadings, tandem propellers have higher efficiencies than single propellers and lower propeller induced vibration. However, tandem propellers have higher rotational energy losses, and a greater weight and cost.

Semi-tandem propellers are two propellers placed one behind the other on the same shaft in which the blades of the two propellers are skewed in opposite directions at the inner radii while at the outer radii the blades are in the same line. This arrangement is designed to reduce the effects of non-uniform inflow to the propellers.

Propeller boss cap fins, Fig. 12.20, are small blades or fins fitted to the propeller boss cap, the number of fins being equal to the number of blades in the propeller. These fins weaken the hub vortex, thereby eliminating hub vortex cavitation and the noise due to the collapse of the hub vortex cavities on the rudder. Propeller boss cap fin propellers have efficiencies 3–7 percent higher than normal propellers.



Figure 12.20 : Propeller Boss Cap Fin Propeller.

12.9 Overlapping Propellers

Overlapping propellers, Fig. 12.21, consist of two propellers located at the longitudinal position of a conventional single propeller but with their shafts at a transverse separation less than the diameter of either propeller. If the two propellers are in the same transverse plane, the two shafts must be interlocked. If the propellers are a small distance apart along the length of the ship, their shafts may be independent. Although overlapping propellers have been investigated in detail both theoretically and experimentally they have rarely been used in practice.

Overlapping propellers have the advantage of distributing the load between two propellers and therefore having a higher efficiency than an equivalent single propeller. Compared to twin screws, overlapping propellers work in a region of high wake and therefore the hull efficiency is higher. The appendages required to support the twin screws are also eliminated and the resistance of the ship reduced.

The mutual interaction between the overlapping propellers may result in increased vibration and cavitation. It may be necessary to have the two propellers with different numbers of blades. There are also difficulties in

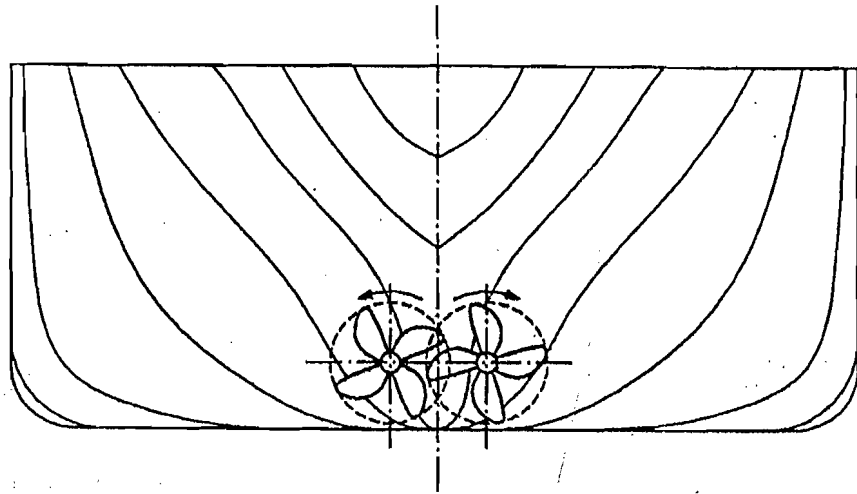


Figure 12.21 : Overlapping Propellers.

supporting two propeller shafts close to each other. If the two shafts run at different speeds there may be vertical and torsional vibration. Unsteady propeller forces with overlapping propellers are greater than with a single propeller. However, the lateral forces tend to cancel each other.

Overlapping propellers are usually designed to be outward turning, i.e. for ahead thrust the starboard propeller turns clockwise and the port propeller anti-clockwise when viewed from behind. The longitudinal separation between the propellers has only a small effect on efficiency though it may influence ship hull vibration. There is an optimum transverse separation between the propellers. At low separations the wake is higher. On the other hand, the aft propeller is affected by the slipstream of the forward propeller to a greater extent. The optimum transverse separation between the centre lines of overlapping propellers has been found to lie between 0.6 and 0.8 times the propeller diameter. Model experiments also show that overlapping propellers offer the greatest improvements in efficiency for full form ships with U-shaped afterbody sections. Substantial improvements in propulsive efficiency of as much 20-25 percent can be obtained with overlapping propellers compared to conventional twin screws. Compared to a single screw, the gain in efficiency is small: 5-8 percent.

12.10 Other Multiple Propeller Arrangements

In addition to contra-rotating propellers, tandem propellers and overlapping propellers, two other multiple propeller arrangements have been proposed. In the "fore propeller", Fig. 12.22, a small propeller is fitted just ahead of the main propeller and above its shaft on the ship centre line. This additional propeller, which is driven through a right angle drive by a vertical shaft extending from the hull above, can be made to turn about a vertical axis.

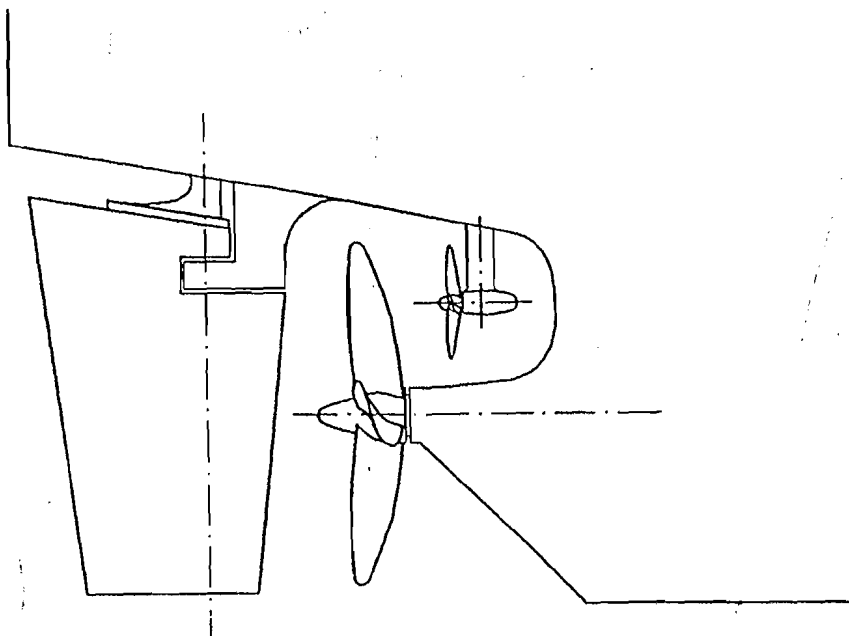


Figure 12.22 : Fore-Propeller.

This arrangement has the advantages that the additional propeller can be used for steering and for propulsion when very low ship speeds are required which are below the operating range of the main engine. The additional propeller also increases the velocity of flow in the upper part of the main propeller disc thereby producing a more uniform flow and reducing vibration and intermittent cavitation. The disadvantages of this arrangement include the higher cost and the complex mechanism of the additional propeller, and

the necessity of "feathering" the blades of the main propeller when it is idle and the ship is being propelled by the fore propeller alone.

The second unconventional two-propeller arrangement consists in fitting two conventional propellers one above the other at the location of the normal single propeller, Fig. 12.23. Since the load is shared between two propellers the propeller efficiency is higher than that of a single propeller, while the higher wake at the ship centre line results in a higher hull efficiency as

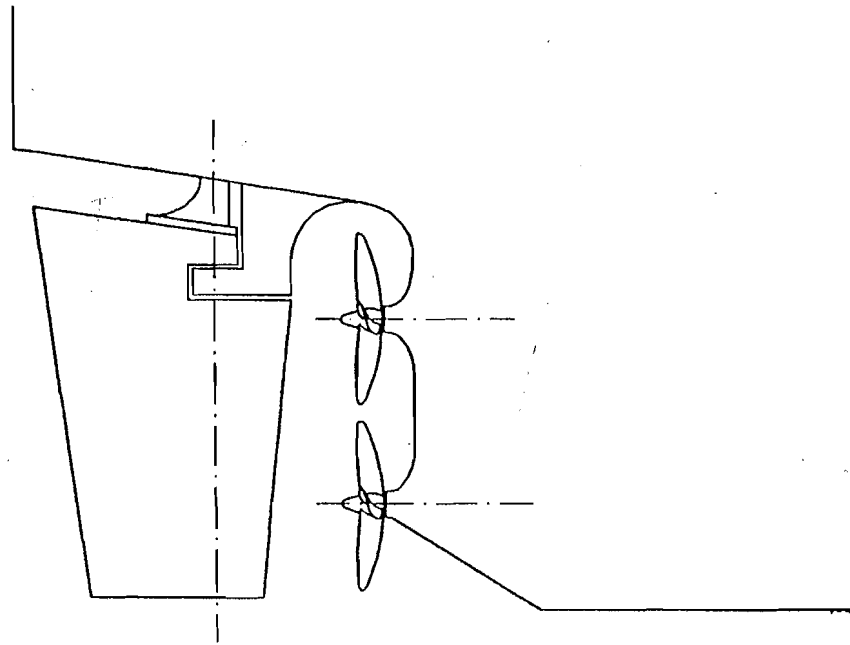


Figure 12.23 : Two Propellers, One above the Other.

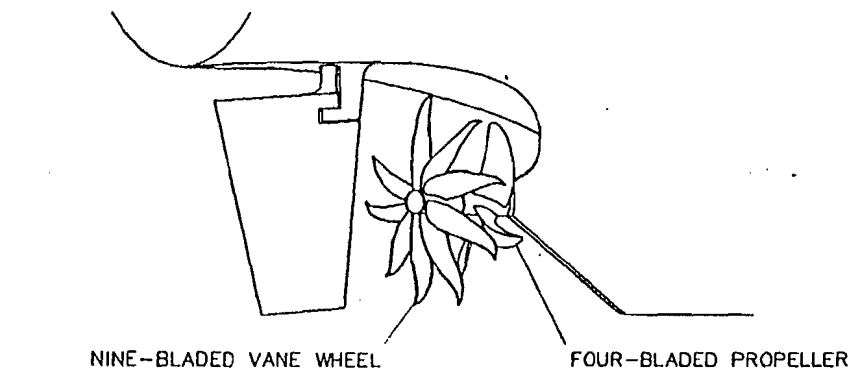
compared to twin screws. On the other hand, the diameters of the two propellers one above the other are limited and high blade areas are required to avoid cavitation. The small propeller diameters allow higher engine speeds to be used and hence lighter engines to be fitted. This arrangement of two propellers also gives better stopping ability to the ship. There may be difficulties in arranging engines and shafts one above the other, and the shafts may need to be inclined to the ship centre line. This then gives the propellers a steering capability also.

12.11 Vane Wheel Propellers

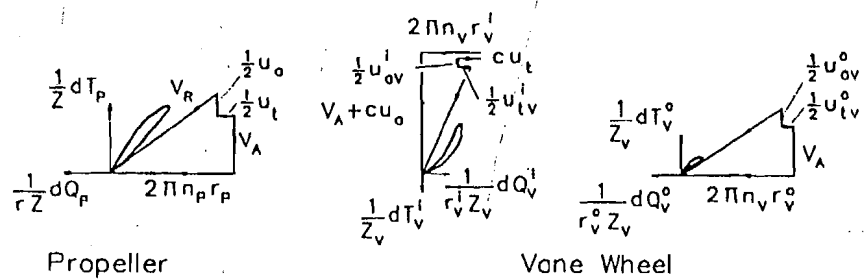
The vane wheel propeller, due to Otto Grim, consists of a number of narrow blades or vanes mounted on a hub just behind the propeller. The vane wheel rotates freely around the propeller shaft, which extends abaft the propeller, Fig. 12.24(a). The vane wheel has a larger diameter than the propeller, and the vanes are designed to act as turbine blades at the inner radii absorbing energy from the propeller slipstream and as propeller blades at the outer radii imparting energy to the fluid outside the slipstream. The vane wheel thus recovers some of the energy, which would otherwise be lost in the slipstream, and imparts momentum to a greater mass of fluid thereby improving the ideal efficiency of the propulsor for a given thrust.

Since a part of the thrust required is produced by the vane wheel, the loading of the propeller is reduced and its diameter may be decreased. The reduced loading also improves propeller efficiency, lowers hull pressures fluctuations and decreases intermittent propeller cavitation. The vane wheel diameter is some 25 percent greater than the propeller diameter, but the clearance between the vanes and the hull and rudder need not be large because the vanes are lightly loaded. The number of vanes is larger than the number of propeller blades: a four bladed propeller will typically have a vane wheel with nine blades. The vane wheel revolves in the same direction as the propeller and at an rpm which is 30–50 percent of the propeller rpm. The pitch distribution of the vanes is such that energy is absorbed from the flow at the inner radii while at the outer radii energy is imparted to the flow. This is shown by the velocity diagrams in Fig. 12.24(b). The radial distributions of circulation for the propeller and for the vane wheel are shown in Fig. 12.24(c).

The vane wheel propeller has a higher efficiency than an equivalent single propeller because (a) the vane wheel provides additional thrust without absorbing additional power, (b) the propeller loading is reduced, (c) the propeller diameter may be reduced resulting in a higher wake and hence a higher hull efficiency. and (d) the removal of energy from the slipstream by the vane wheel reduces the flow velocities past the rudder, reducing its resistance and thereby increasing the relative rotative efficiency. The smaller propeller diameter also implies a higher propeller rpm and hence a decrease in engine weight and cost. Vane wheel propellers are also less likely to suffer

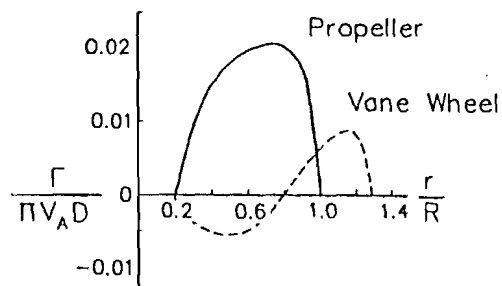


(a) ARRANGEMENT



Subscripts : P : Propeller Superscripts : i : Inner radius
 V : Vane Wheel o : Outer Radius

(b) VELOCITY DIAGRAMS



(c) CIRCULATION

Figure 12.24 : Vane Wheel Propeller.

from cavitation and vibration, although the strength of the vanes may be critical in a seaway. The propeller thrust loading must be sufficiently high, i.e. C_{TL} greater than 1.0, for a significant improvement in efficiency to take place. Increases in propulsive efficiency of 7–10 percent can be achieved provided the designs of the propeller and the vane wheel are optimised together and the thrust loading coefficient is high enough.

12.12 Other Unconventional Screw Propellers

The use of *propellers with end plates*, Fig. 12.25 (a), has been proposed to improve propeller efficiency by suppressing the trailing vortices shed from the propeller blade tips. Such propellers are sometimes known as TVF (tip vortex free) propellers or CLT (contracted and loaded tip) propellers. The end plates at the blade tips modify the distribution of circulation along the

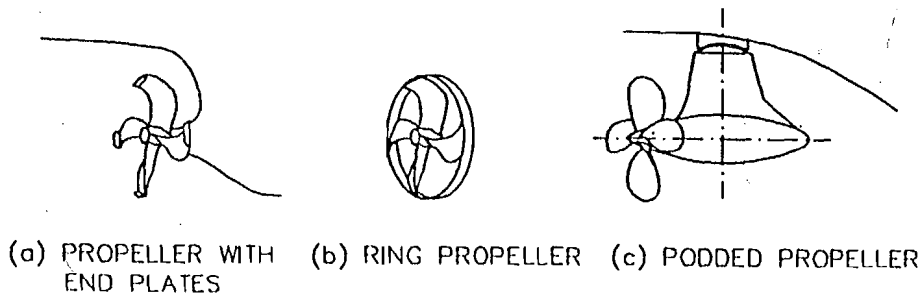


Figure 12.25 : Some Unconventional Propellers.

radius and give a better spread of the trailing vortices. This decreases the induced drag of the blades and reduces tip vortex cavitation. Several different types of end plates have been tried: end plates at a constant radius or aligned with the streamline at the blade tip, end plates on the suction side (back of the blade) near the leading edge and on the pressure side (face) towards the trailing edge, and end plates of different shapes – bulbous blade tips, porous tips and winglets. An improvement in efficiency up to 4 percent can be obtained provided the blades and the end plates are optimised together to obtain the optimum distribution of circulation. Sophisticated

lifting surface procedures may be used for designing propellers with end plates, but it is difficult to account for the mutual interference of the blades and end plates. There have been very few practical applications of such propellers, which may therefore be regarded as being in a developmental stage.

In a *ring propeller*, a ring or a small duct is attached to the propeller blade tips so that the ring revolves with the propeller, Fig. 12.25(b). The action of the ring is similar to that of the end plates: spreading the trailing vortices at the tip, altering the radial distribution of circulation, reducing tip vortex cavitation, and thus improving efficiency. A ring propeller has been found to produce a greater bollard pull than a conventional propeller. The ring also increases the strength of the propeller and reduces blade vibration.

In a *podded propeller*, the propeller is supported in a streamlined body of revolution (pod) by a vertical strut extending downward from the hull of the ship, Fig. 12.25(c). The propeller is driven through a shaft from inside the hull through bevel gears contained within the pod. The propeller with its pod and supporting strut can be rotated about a vertical axis through 360 degrees by a separate mechanism so that the propeller thrust can be directed at any angle in a horizontal plane. To allow for the rotation of the inflow to the propeller, the strut is usually not symmetrical on the two sides about its centre plane. It is possible to design the strut so that it augments the propeller thrust and compensates for the drag of the pod. The interaction between the strut and the pod is important. Podded propellers, which are also known by several other names such as "azimuthing thrusters" and "steering rudder propellers", offer several advantages for small vessels: excellent manoeuvrability, very good backing performance, good speed control over the complete range and the use of non-reversing machinery. However, podded propeller units are available only upto a limited power, and the complicated Z-drive and azimuthing mechanism are serious disadvantages. There is also the possibility of interference between the podded propeller strut and the hull, or between the different podded propeller units, which are often used in pairs. In recent years, the Z-drive has been replaced by an electric motor housed within the pod, and the power range has been continuously extended.

12.13 Cycloidal Propellers

A cycloidal propeller consists of a number of spade like blades fitted to a disc usually set flush with the ship hull, Fig. 12.26. The disc is made to revolve about a vertical or nearly vertical axis while the blades are made to rotate

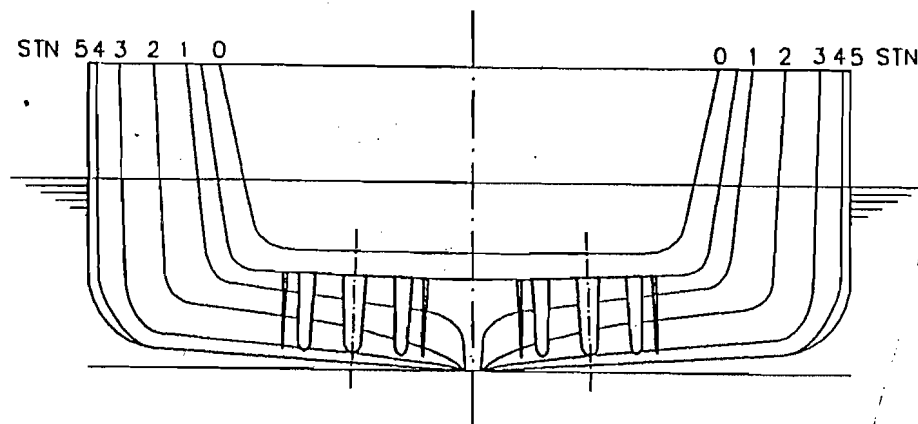


Figure 12.26 : Afterbody of a Ship with Twin Cycloidal Propellers.

about their own individual axes through a mechanical linkage system. The concept of cycloidal propellers was proposed as early as 1870, and of the two main types of such propellers that have been used in practice, the Kirsten-Boeing propeller was introduced in 1928 and the Voith-Schneider propeller in 1931. In the Kirsten-Boeing propeller, the individual blades make half a rotation about their own axes for every revolution of the disc about the propeller axis. In the Voith-Schneider propeller the blades make one rotation about their own axes for every revolution of the disc. With the ship moving with a speed V and the propeller revolving at an angular velocity ω the path described by each blade is some form of cycloid—an epicycloid if V is less than ωR , a cycloid if V is equal to ωR , and a trochoid if V is greater than ωR , where R is the radius of the circle described by the blades around the propeller (disc) axis.

The action of the Kirsten-Boeing propeller is illustrated in Fig. 12.27. Each blade revolves about the centre O of the propeller while rotating about its own axis A in a manner such that the blade is aligned along the line joining

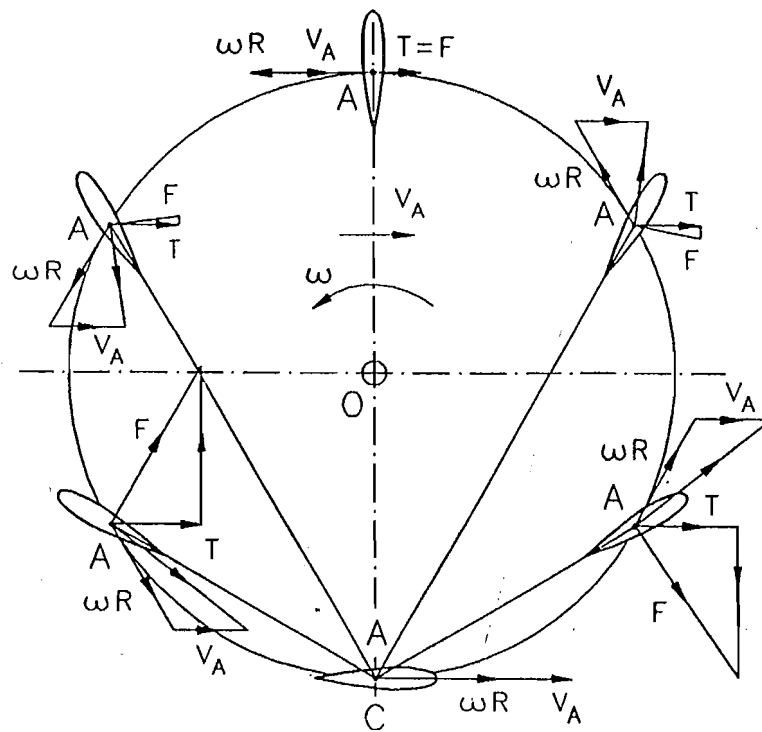


Figure 12.27 : Action of a Kirsten-Boeing Propeller.

A and a point C. The resultant of the velocity of advance V_A of the propeller and the tangential velocity ωR of the blade produces a hydrodynamic force F which has components parallel and perpendicular to \overline{OC} . By varying the position of the point C the thrust can be directed at any angle to the velocity of advance of the propeller. It may be seen from the figure that each blade undergoes half a rotation about its own axis A for each complete revolution about the centre O. In a Kirsten-Boeing propeller, the distance \overline{OC} (eccentricity) is fixed and the magnitude of the thrust can only be varied for a given speed of advance by varying the angular velocity $\omega = 2\pi n$ of the propeller. The eccentricity of a vertical axis propeller is analogous to the pitch of a screw propeller. The Kirsten-Boeing propeller thus behaves like a fixed pitch screw propeller.

The action of the Voith-Schneider propeller is shown in Fig. 12.28 and is similar to that of the Kirsten-Boeing propeller except that each blade makes a complete rotation about its own axis A for each revolution about the propeller axis O . The eccentricity \overline{OC} can also be adjusted between zero and a value less than R , so that the magnitude of the resultant thrust of the propeller can be controlled by varying the distance \overline{OC} while the

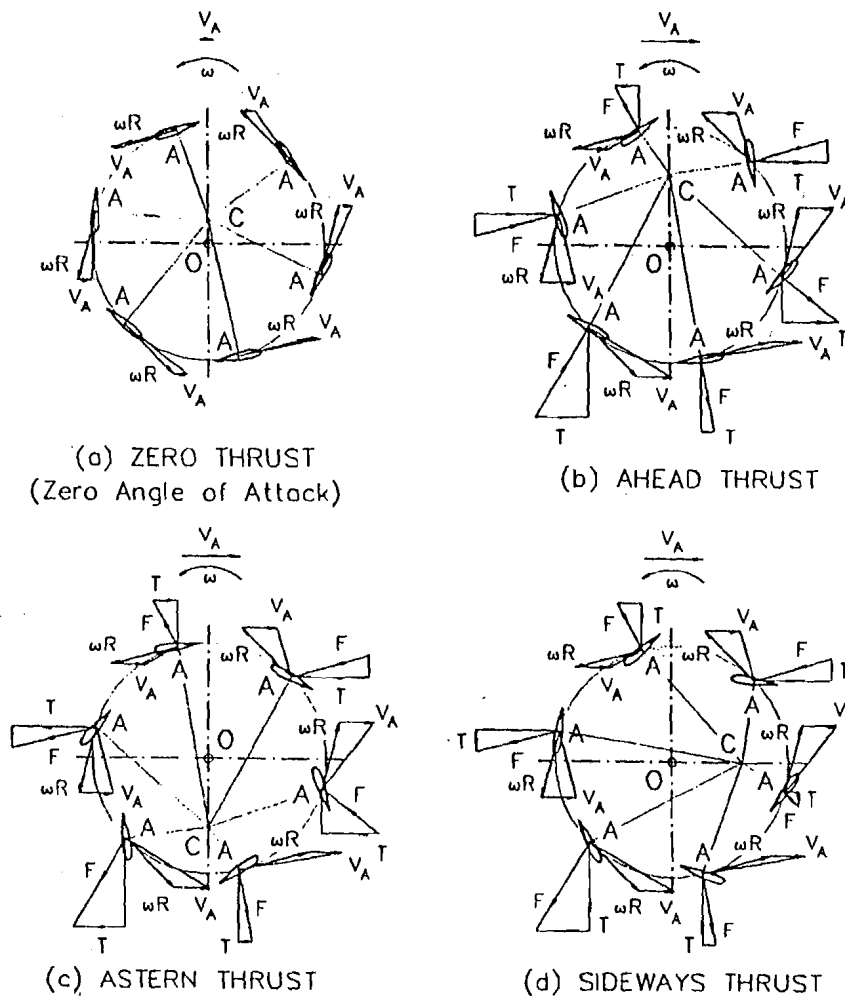


Figure 12.28 : Action of a Voith-Schneider Propeller.

direction of the thrust can be controlled by varying the angle between \overline{OC} and the velocity of advance V_A . For a given propeller thrust there is an optimum combination of eccentricity \overline{OC} and angular velocity ω which gives the minimum delivered power. However, it is usual to run the propeller at a constant rpm and control the magnitude of thrust by controlling only the eccentricity. The Voith-Schneider propeller with its controllable eccentricity is thus analogous to a controllable pitch screw propeller.

The Voith-Schneider propeller may be driven by an electric motor mounted above the disc on the vertical axis of the propeller, or through a horizontal shaft and a right-angled bevel gear drive by a diesel engine or electric motor, Fig. 12.29. The control point C is controlled by two hydraulic rams at right angles to each other so that a stepless variation in the magnitude and direction of the propeller thrust can be obtained. The tangential velocity

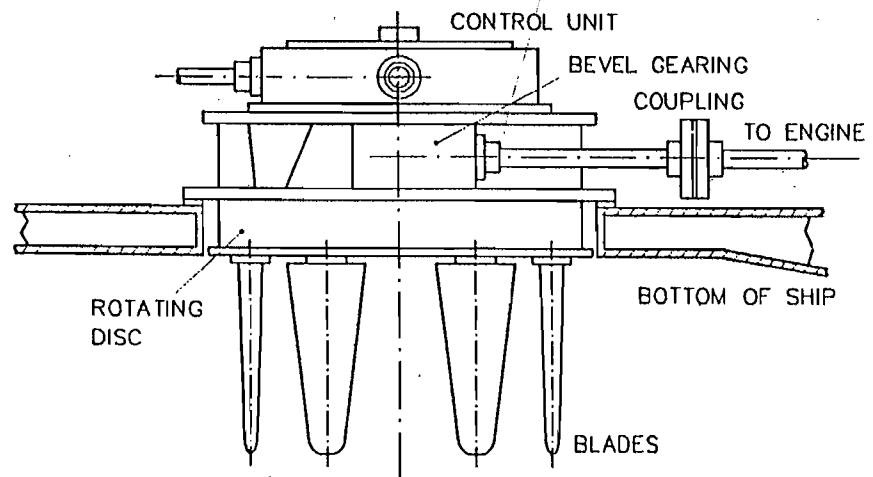


Figure 12.29 : Voith-Schneider Propeller Arrangement.

of the blades is usually in the range of 10-20 m per sec, and it may be necessary to provide reduction gearing between the engine and the propeller. For moderate speed reductions, the right angle bevel gearing may be used for both speed reduction and turning the direction of power transmission through 90 degrees. The power transmission also includes elements such as flexible couplings to deal with misalignments, vibration and torque fluctua-

tions. The blades of a Voith-Schneider propeller may be made of stainless steel to withstand cavitation erosion and corrosion.

Voith-Schneider propellers are usually fitted in pairs, the location of the two propellers depending upon the type of ship. In ferries, the propellers may be fitted one forward and one aft which would allow the vessel to move sideways or to turn within a circle of its own length. In a pusher tug, they may be fitted side by side at the stern, whereas in a tractor tug, the Voith-Schneider propellers may be fitted side by side at the bow.

The efficiency of a Voith-Schneider propeller is significantly lower than that of a conventional screw propeller. Voith-Schneider propellers are therefore fitted only in those ships in which exceptional manoeuvrability is required. The other advantages of Voith-Schneider propellers include the ability to vary the direction and magnitude of thrust without changing the speed or direction of revolution of the engine, the elimination of the rudder and steering gear and some simplification to the hull form of the ship. The complex mechanism requiring high maintenance is a disadvantage.

A recent innovation is a cycloidal propeller rotating about a transverse horizontal axis fitted at the stern of the ship. Such a propeller is known as a "Whale Tail" propeller.

Example 5

A Voith-Schneider propeller has six blades each of area 0.05 m^2 set on a circle of 1.0 m radius. The blades have lift and drag coefficients given by:

$$C_L = 0.1 \alpha \quad C_D = 0.03 + 0.1 C_L^2$$

where α is the angle of attack in degrees. The propeller runs at 180 rpm and the blades are set at an eccentricity ratio of 0.50 to provide a forward thrust. The speed of advance is 5.0 m per sec . Determine the thrust and torque of the propeller.

$$Z = 6 \quad A = 0.05 \text{ m}^2 \text{ per blade} \quad R = 1.0 \text{ m}$$

$$n = 180 \text{ rpm} = 3.0 \text{ s}^{-1} \quad e = 0.50 \quad V_A = 5.0 \text{ ms}^{-1}$$

In Fig. 12.30, O is the centre of the propeller disc, A the centre of a blade which is oriented such that it is normal to \overline{CA} . \overline{OC}/R is the eccentricity ratio e . The inclinations of \overline{OA} and \overline{CA} with the ship centre line are θ and φ respectively, where:

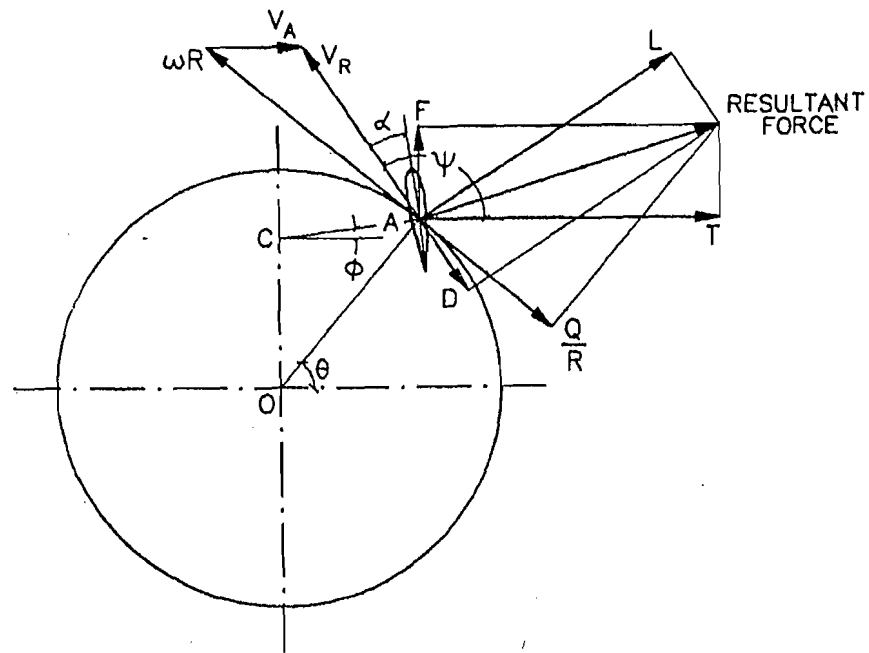


Figure 12.30 : Forces on a Voith-Schneider Propeller Blade (Example 5).

$$\tan \varphi = \frac{R \sin \theta - e R}{R \cos \theta} = \frac{\sin \theta - e}{\cos \theta}$$

The tangential velocity of the blade:

$$\omega R = 2\pi n R = 2\pi \times 3.0 \times 1.0 = 18.8496 \text{ ms}^{-1}$$

The resultant velocity of the blade V_R makes an angle ψ with the forward direction of motion. where:

$$V_R \cos \psi = -\omega R \sin \theta + V_A$$

$$V_R \sin \psi = \omega R \cos \theta$$

The angle of attack is:

$$\alpha = \psi - (90 + \varphi)$$

from which C_L and C_D can be determined. The lift and drag of the blade are then given by:

$$L = C_L \frac{1}{2} \rho A V_R^2 \quad D = C_D \frac{1}{2} \rho A V_R^2$$

and the thrust, torque and transverse force by:

$$T = L \sin \psi - D \cos \psi$$

$$\frac{Q}{R} = L \cos(\psi - \theta) + D \sin(\psi - \theta)$$

$$F = L \cos \psi - D \sin \psi$$

The calculation is carried out in the following tables:

Angles

θ deg	$\tan \varphi$	φ deg	$V_R \cos \psi$ ms^{-1}	$V_R \sin \psi$ ms^{-1}	V_R ms^{-1}	ψ deg	α deg
0	-0.5000	333.43	7.500	18.850	20.287	68.303	4.468
30	0	0	-1.925	16.324	16.437	96.725	6.725
60	0.7320	36.206	-8.824	9.437	12.911	133.115	6.909
90	∞	90.000	-11.350	0	11.35	180.000	0
120	-0.7320	143.794	-8.824	-9.425	12.911	226.885	-6.909
150	0	180.000	-1.925	-16.324	16.437	263.275	-6.725
180	0.5000	206.565	7.500	-18.850	20.287	291.697	-4.868
210	1.1547	229.107	16.925	-16.324	23.514	316.035	-3.072
240	2.7320	249.896	23.824	-9.425	25.621	338.416	-1.480
270	∞	270.000	26.350	0	26.350	360.000	0
300	-2.7320	290.104	23.824	9.425	25.621	21.584	1.480
330	-1.1547	310.893	16.925	16.324	23.514	43.965	3.072
360	-0.5000	333.43	7.500	18.850	20.287	68.303	4.868

Forces on each blade

θ deg	C_L	C_D	L kN	D kN	T kN	Q/R kN	F kN
0	0.4868	0.0537	5.134	0.566	4.561	2.424	1.372
30	0.6725	0.0752	4.656	0.521	4.685	2.318	-1.062
60	0.6909	0.0777	2.951	0.332	2.381	1.175	-2.2594
90	0	0.0300	0	0.099	0.099	0.099	0
120	-0.6909	0.0777	-2.951	0.332	2.381	1.175	2.2594
150	-0.6725	0.0752	-4.656	0.521	4.685	2.318	1.0624
180	-0.4868	0.0537	-5.134	0.566	4.561	2.424	-1.372

θ deg	C_L	C_D	L kN	D kN	T kN	Q/R kN	F kN
210	-0.3072	0.0394	-4.352	0.559	2.619	1.739	-2.745
240	-0.1480	0.0322	-2.489	0.541	0.412	0.900	-2.115
270	0	0.0300	0	0.534	-0.534	0.534	0
300	0.1480	0.322	2.489	0.541	0.412	0.900	2.115
330	0.3072	0.0394	4.352	0.559	2.619	1.739	2.745
360	0.4868	0.0537	5.134	0.566	4.561	2.424	1.372

Total thrust

$$T_{i+1}(\theta) = T_i(\theta + 60^\circ)$$

$$T(\theta) = \sum_{i=1}^6 T_i(\theta)$$

$$\text{Average thrust } T = \frac{\int_0^{2\pi} T(\theta) d\theta}{\int_0^{2\pi} d\theta}$$

θ deg	T_1 kN	T_2 kN	T_3 kN	T_4 kN	T_5 kN	T_6 kN	T kN
0	4.561	2.381	2.381	4.561	0.412	0.412	14.708
30	4.685	0.099	4.685	2.619	-0.534	2.619	14.173
60	2.381	2.381	4.561	0.412	0.412	4.561	14.708
90	0.099	4.685	2.619	-0.534	2.619	4.685	14.173
120	2.381	4.561	0.412	0.412	4.561	2.381	14.708
150	4.685	2.619	-0.534	2.619	4.685	0.099	14.173
180	4.561	0.412	0.412	4.561	2.381	2.381	14.708
210	2.619	-0.534	2.619	4.685	0.099	4.685	14.173
240	0.412	0.412	4.561	2.381	2.381	4.561	14.708
270	-0.534	2.619	4.685	0.099	4.685	2.619	14.173
300	0.412	4.561	2.381	2.381	4.561	0.412	14.708
330	2.619	4.685	0.099	4.685	2.619	-0.534	14.173
360	4.561	2.381	2.381	4.561	0.412	0.412	14.708

The average thrust over each revolution:

$$T = \frac{\int_0^{2\pi} T d\theta}{\int_0^{2\pi} d\theta} = 14.352 \text{ kN}$$

evaluating the integrals by Simpson's rule.

The average torque is similarly obtained as:

$$Q = 8.831 \text{ kNm}$$

The transverse force F is equal to zero when summed up over all the blades at all angles.

12.14 Waterjet Propulsion

Waterjet propulsion is said to be the oldest mechanical propulsion device considered for use in ships. Attempts to use waterjet propulsion were first made in the 17th century. Later, in 1775 Benjamin Franklin again proposed the use of waterjets and such a device was actually used in 1782 by James Rumsey to propel an 81-foot vessel on the River Potomac. In its present form, a waterjet propulsion unit consists of a pump inside the ship which draws water from outside, imparts an acceleration to it and discharges it in a jet above the waterline at the stern, the jet reaction providing the thrust to propel the ship. By directing the jet sideways the ship can be manoeuvred, and by deflecting the jet forward an astern thrust can be obtained.

Waterjets have many advantages over conventional screw propellers:

- There are no appendages and hence there is a reduction in resistance.
- Waterjet propulsion can be used in shallow water without any limitation on the size of the pump.
- Improved manoeuvrability, stopping and backing ability are obtained.
- There is no need to reverse the main engine, i.e. no reversing gear is required in the propulsion plant.

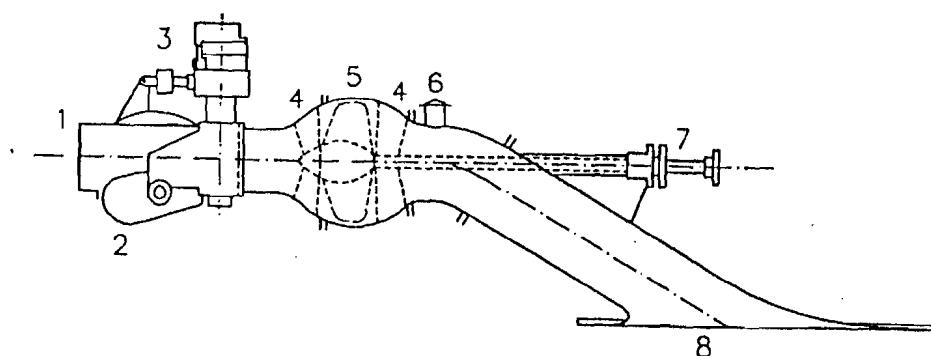
- The torque of the waterjet unit is constant over the complete speed range, i.e. full power can be maintained at low speeds without overloading the engine.
- The speed of the ship from full ahead to full astern can be controlled without altering the rpm of the engine.
- A higher static thrust can be obtained permitting high acceleration to full speed.
- There is less noise and vibration.

There are two important disadvantages:

- The waterjet propulsion unit occupies considerable space inside the ship, and the water passing through causes a significant decrease in buoyancy.
- It is necessary to provide a grating at the water inlet to prevent debris from getting in and damaging the pump. This grating decreases the efficiency of the system, particularly as it gets clogged.

Waterjet propulsion is less efficient than conventional screw propulsion at moderate speeds, but for high speed craft, waterjets may have a higher efficiency. Waterjet propulsion should be considered for ships of moderate size having speeds exceeding 25 knots.

Waterjet propulsion units come in a variety of designs depending upon the manufacturer. A typical unit is illustrated in Fig. 12.31. The pump is usually a mixed flow pump with an impeller comprising of a large number of wide blades with very small clearances from the casing, and stator blades before and after the impeller to minimise rotational energy losses. The pump thus has a high efficiency. The waterjet is discharged through a nozzle which can be rotated about a vertical axis to approximately 45 degrees on either side to turn the vessel. There is also a scoop or bucket which can be rotated about a horizontal axis and which can be used to deflect the waterjet downward and forward, thereby producing an astern thrust. By adjusting the position of the scoop the thrust of the waterjet can be varied from full ahead through zero to full astern without altering the discharge of the pump.



1. SWIVELLING NOZZLE
2. REVERSING SCOOP
3. STEERING AND REVERSING MECHANISM
4. STATOR VANES
5. IMPELLER
6. INSPECTION HATCH
7. IMPELLER SHAFT
8. WATER INLET

Figure 12.31 : Waterjet Propulsion Unit.

The waterjet propulsion unit thus provides excellent manoeuvring, stopping and reversing qualities to the vessel. There are variations in the design of waterjet propulsion units. Instead of a mixed flow pump, an axial flow pump may be used, or a radial flow pump with an axial discharge. In one design of a waterjet propulsion unit, there is a centrifugal pump with a vertical axis. The pump suction is flush with the bottom of the vessel and the discharge is through a volute casing which can be rotated through 360 degrees about the vertical pump axis. Exceptionally good manoeuvrability is obtained, particularly if twin units are fitted.

Waterjet propulsion may be analysed by the axial momentum theory. If m is the mass of water flowing through the waterjet system per unit time, and V_J is the exit velocity of the jet, the gross thrust is given by:

$$T_G = m V_J \quad (12.17)$$

If the relative velocity of water with respect to the ship at the waterjet inlet is V_A (velocity of advance), the force required to give the ingested water

the speed of the ship is the momentum drag:

$$D_M = m V_A \quad (12.18)$$

The net thrust on the ship is therefore:

$$T = T_G - D_M = m (V_J - V_A) \quad (12.19)$$

and the thrust power:

$$P_T = T V_A = m (V_J - V_A) V_A \quad (12.20)$$

The delivered power under ideal conditions is the increase in energy of water passing through the system per unit time:

$$P_D = \frac{1}{2} m V_J^2 - \frac{1}{2} m V_A^2 \quad (12.21)$$

and the "ideal jet efficiency" is then given by:

$$\eta_{iJ} = \frac{P_T}{P_D} = \frac{m (V_J - V_A) V_A}{\frac{1}{2} m (V_J^2 - V_A^2)} = \frac{2 V_A}{V_J + V_A} \quad (12.22)$$

A thrust loading coefficient is defined as:

$$C_{TL} = \frac{T}{\frac{1}{2} \rho A_J V_A^2} \quad (12.23)$$

where A_J is the area of the jet cross-section. Substituting the value of T and noting that $m = \rho A_J V_J$, one obtains:

$$C_{TL} = \frac{\rho A_J V_J (V_J - V_A)}{\frac{1}{2} \rho A_J V_A^2} = 2 \left[\left(\frac{V_J}{V_A} \right)^2 - \frac{V_J}{V_A} \right] \quad (12.24)$$

From Eqn. (12.22):

$$\frac{V_J}{V_A} = \frac{2}{\eta_{iJ}} - 1 \quad (12.25)$$

so that:

$$C_{TL} = 2 \left[\left(\frac{2}{\eta_{iJ}} - 1 \right)^2 - \left(\frac{2}{\eta_{iJ}} - 1 \right) \right] = 4 \left[\frac{2}{\eta_{iJ}^2} - \frac{3}{\eta_{iJ}} + 1 \right] \quad (12.26)$$

and:

$$\eta_{iJ} = \frac{4}{3 + (1 + 2 C_{TL})^{0.5}} \quad (12.27)$$

The losses that take place in the system can be incorporated into this analysis. Some energy loss takes place at the inlet, so that the energy in the water entering the system is $\frac{1}{2}mV_A^2\eta_I$, where η_I is the inlet efficiency. The water has to be raised through a height h above the undisturbed waterline, and the energy required for this purpose is mgh . Also, there are some losses in the nozzle so that the energy in the jet before these losses occur is $\frac{1}{2}mV_J^2/\eta_N$, where η_N is the nozzle efficiency. Therefore, the actual energy imparted to the waterjet is given by:

$$P_J = \frac{1}{2}mV_J^2/\eta_N - \frac{1}{2}mV_A^2\eta_I + mgh \quad (12.28)$$

The jet efficiency taking these losses into account is then given by:

$$\eta_J = \frac{TV_A}{\frac{1}{2}mV_J^2/\eta_N - \frac{1}{2}mV_A^2\eta_I + mgh}$$

$$= \frac{2(V_J - V_A)V_A}{V_J^2/\eta_N - V_A^2\eta_I + 2gh}$$

The propulsive efficiency is given by:

$$\eta_D = \frac{P_E}{P_D} = \frac{P_E}{P_T} \frac{P_T}{P_J} \frac{P_J}{P_D} = \eta_H \eta_J \eta_{PO} \eta_R \quad (12.33)$$

and the overall efficiency by:

$$\eta_{overall} = \frac{P_E}{P_B} = \eta_H \eta_J \eta_{PO} \eta_R \eta_S \quad (12.34)$$

where $\eta_S = P_D/P_B$ is the shafting efficiency and P_B the brake power of the engine. If the main engine is a gas turbine, P_B should be replaced by the shaft power P_S . In the foregoing analysis, it has been assumed that the ship is propelled by a single waterjet propulsion unit.

The analysis, which is based on that given by Allison (1993), follows closely the analysis of conventional screw propellers. However, this may be misleading, and it is necessary to define concepts such as wake fraction and thrust deduction carefully in the context of waterjet propulsion and to use appropriate values. The model testing of waterjet propulsion systems is still in a stage of evolution and the ITTC has set up a special group to consider its various aspects.

The design of waterjet systems is a highly specialised activity closely guarded by the manufacturers of such systems. One may, however, consider a few general design features of such systems, particularly those that have an impact on the overall design of the ship.

The ingestion of water from outside the hull into the waterjet system has the effect of suction on the boundary layer around the hull and reduces its resistance. The waterjet inlet is therefore made wide laterally so that the boundary layer thickness may be reduced over a greater width. On the other hand, water ingestion also causes an increase in the relative velocity of water around the hull and a decrease in pressure (or "thrust deduction"). It is therefore desirable not to locate the inlet too close to the stern where the decreased pressure would cause a large increase in resistance. Placing the inlet too far forward would increase the length of the inlet duct resulting in larger inlet losses and greater susceptibility to pump cavitation. An increased inlet duct length would also cause a larger loss in buoyancy to the ship and occupy more internal space. The inlet duct must provide good pressure recovery and low flow distortion. This requires that the change

in direction of the flow in the duct be as small and as gradual as possible. Another important requirement is that the inlet should be located so that there is no possibility of ingestion of air. Inlets flush with the hull surface are normally used. In hydrofoil craft propelled by waterjets, the water is taken in through inlets in pods attached to the foils and led through ducts in the struts supporting the foils to the pump inside the hull. Variable area inlets may be used to match the inflow with the speed of the vessel, but fixed area inlets are more common. The design of waterjet inlets is a critical area, and sophisticated techniques of Computational Fluid Dynamics are often used for the purpose.

The choice between the different types of pumps, axial flow, radial flow or mixed flow, depends upon the "specific speed":

$$N_S = \frac{n Q^{0.5}}{(gH)^{0.75}} \quad (12.35)$$

where n is the revolution rate, Q the discharge and H the head of the pump. Axial flow pumps have higher efficiencies at high specific speeds (0.52 and higher), whereas radial flow (centrifugal) pumps have higher efficiencies at low specific speeds (less than about 0.25), with mixed flow pumps being most efficient in the intermediate range. For most waterjet propulsion applications, mixed flow pumps have the highest efficiency among the different types of pumps, although axial flow pumps have a smaller diameter. For small high speed craft, axial flow pumps may be more suitable. Where the inlet and duct losses are of such magnitude as to result in cavitation of the main pump impeller, an "inducer" may be provided to increase the pressure and reduce the possibility of cavitation.

The design of a waterjet propulsion system is normally entrusted to a waterjet system manufacturer when the machinery is to be selected and the design of the system finalised. The preliminary design of a waterjet propulsion unit may, however, be carried out using design charts provided by waterjet system manufacturers. A design chart of the type shown in Fig. 12.32 enables the power required to be estimated. It is necessary to apply suitable margins on the required thrust and the estimated power when selecting the machinery at the preliminary design stage, and to consider overload design conditions, i.e. displacements greater than normal, and operation in high sea states. The preliminary design of a waterjet propulsion unit can be carried

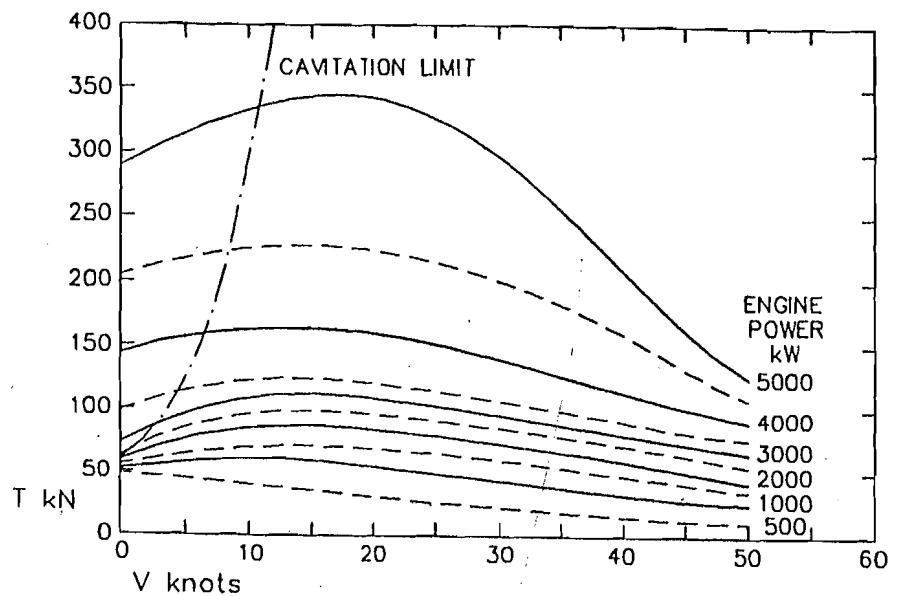


Figure 12.32 : Waterjet Propulsion Preliminary Design Chart.

out and its performance estimated using performance characteristics given in charts as shown in Figs. 12.33 and 12.34. (It is important to note that Figs. 12.32, 12.33 and 12.34 are only illustrative, and are not to be used for an actual design.)

Example 6

A vessel to be propelled by twin waterjets has an effective power of 2400 kW at its design speed of 30 knots. Carry out a preliminary design of the waterjets assuming the following values: wake fraction 0.05, thrust deduction fraction 0.03, pump efficiency in uniform inflow 0.89, relative rotative efficiency 0.96, inlet efficiency 0.82, nozzle efficiency 0.99, shafting efficiency 0.95, and height of nozzles above water level at 30 k 0.75 m.

$$V = 30 \text{ k} = 15.432 \text{ ms}^{-1} \quad P_E = 2400 \text{ kW}$$

$$w = 0.05 \quad t = 0.03 \quad \eta_P = 0.89 \quad \eta_R = 0.96$$

$$\eta_I = 0.82 \quad \eta_N = 0.99 \quad \eta_S = 0.95 \quad h = 0.75 \text{ m}$$

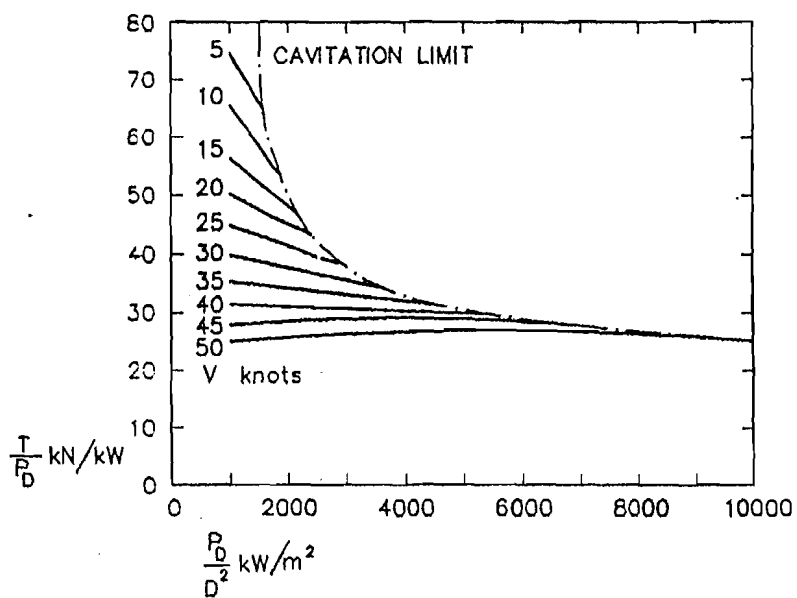


Figure 12.33 : Waterjet Performance Characteristics I.

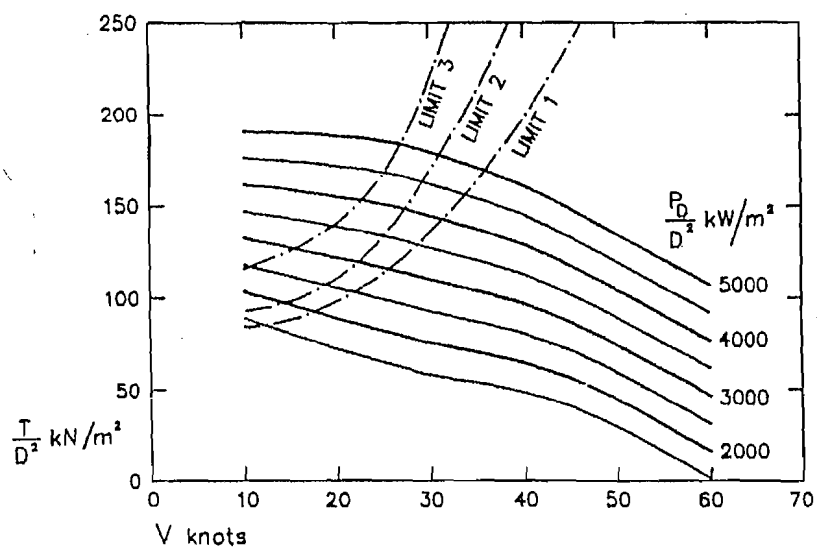


Figure 12.34 : Waterjet Performance Characteristics II.

Assume an overall propulsive efficiency, $\eta_{\text{overall}} = 0.530$. Then, the shaft power for each unit is:

$$P_S = \frac{P_E}{2\eta_{\text{overall}}} = \frac{2400}{2 \times 0.530} = 2264.15 \text{ kW}$$

Delivered power, $P_D = P_S \eta_S = 2264.15 \times 0.950 = 2150.94 \text{ kW}$

Resistance, $R_T = \frac{P_E}{V} = \frac{2400}{15.432} = 155.521 \text{ kN}$

Thrust of each unit, $T = \frac{R_T}{2(1-t)} = \frac{155.521}{2(1-0.03)} = 80.165 \text{ kN}$

Hence, $\frac{T}{P_D} = \frac{80.165}{2150.94} = 0.03727 \text{ kN kW}^{-1} = 37.27 \text{ N kW}^{-1}$

From Fig. 12.32, for $V = 30 \text{ k}$, $\frac{T}{P_D} = 37.27 \text{ N kW}^{-1}$:

$$\frac{P_D}{D^2} = 2481.4 \text{ kW m}^{-2}$$

Since $P_D = 2150.94 \text{ kW}$, $D^2 = \frac{2150.94}{2481.4} = 0.8668 \text{ m}^2$ $D = 0.9310 \text{ m}$

The thrust at full power as a function of ship speed is obtained from Fig. 12.33 as given in the following.

For $\frac{P_D}{D^2} = 2481.4 \text{ kW m}^{-2}$:

V knots	:	15	20	25	30	35
$T/D^2 \text{ kN m}^{-2}$:		111.92	105.18	99.108	92.484	86.827
$T \text{ kN}$:	97.012	91.172	85.907	80.165	75.261
$2(1-t)T \text{ kN}$:		188.203	176.874	166.660	155.520	146.006

Fig. 12.33 also indicates that full power should not be continuously maintained below about 22 knots (Limit 1).

Assuming that $\frac{\text{Nozzle Area}}{\text{Inlet Area}} = 0.40$

$$\begin{aligned}
 \text{Nozzle area (jet area)} \quad A_J &= 0.40 \times \frac{\pi}{4} D^2 \\
 &= 0.40 \times \frac{\pi}{4} \times 0.9310^2 \\
 &= 0.2723 \text{ m}^2
 \end{aligned}$$

If the velocity of the jet is V_J :

$$\text{Mass flux,} \quad m = \rho A_J V_J$$

$$\begin{aligned}
 \text{Speed of advance,} \quad V_A &= (1 - w) V = (1 - 0.05) \times 15.432 \\
 &= 14.6604 \text{ ms}^{-1}
 \end{aligned}$$

$$\text{Thrust,} \quad T = m(V_J - V_A) = \rho A_J V_J (V_J - V_A)$$

$$\text{i.e.} \quad 80.165 = 1.025 \times 0.2723 V_J (V_J - 14.6604)$$

$$\text{so that} \quad V_J = 25.7956 \text{ ms}^{-1}$$

$$\text{and} \quad m = 1.025 \times 0.2723 \times 25.7956 = 7.1997 \text{ tonnes s}^{-1}$$

$$\text{The hull efficiency,} \quad \eta_H = \frac{1 - t}{1 - w} = \frac{1 - 0.03}{1 - 0.05} = 1.0211$$

The jet efficiency is given by:

$$\begin{aligned}
 \eta_J &= \frac{T V_A}{\frac{1}{2} m [V_J^2 / \eta_N - V_A^2 \eta_I + 2 g h]} \\
 &= \frac{80.165 \times 14.6604}{\frac{1}{2} \times 7.1997 [25.7956^2 / 0.99 - 14.6604^2 \times 0.82 + 2 \times 9.81 \times 0.75]} \\
 &= 0.6394
 \end{aligned}$$

The overall propulsive efficiency is then:

$$\begin{aligned}
 \eta_{\text{overall}} &= \eta_H \eta_P \eta_R \eta_J \eta_S \\
 &= 1.0211 \times 0.89 \times 0.96 \times 0.6394 \times 0.95 \\
 &= 0.5299
 \end{aligned}$$

This is very close to the initially assumed value. If there had been a significant difference between the initial and final values, the calculations would have to be iterated until a satisfactory agreement was obtained.

12.15 Flow Improvement Devices

The propeller in a single screw ship works in an extremely complex flow. There is the boundary layer on the hull which grows in thickness from forward to aft and within which the velocity rises sharply from zero to approximately the free stream velocity (the velocity determined on the basis of inviscid flow). In many ships, there may be boundary layer separation resulting in eddies being carried to the propeller. The flow at the propeller is not usually parallel to its axis and there may be significant crossflow velocities normal to the axis. The ship may shed bilge vortices. The non-uniform flow resulting from all these factors causes a reduction in the efficiency of the propeller and tends to increase intermittent cavitation and propeller induced vibration. The undesirable effects of the complex flow at the stern of a ship can be mitigated to some extent by fitting devices to improve the nature of the flow into the propeller. In addition to improving the flow, some of these devices also directly improve the efficiency of the propeller.

The asymmetric stern, in which the transverse sections at the after end of the ship are not symmetrical port and starboard, is designed to impart a swirl to the flow just ahead of the propeller to counter the rotation of the flow induced by the propeller, Fig. 12.35. The rotational energy lost in the propeller slipstream is thereby reduced. The asymmetric stern produces a smaller mean wake fraction and a lower turbulence level but a somewhat greater non-uniformity in the flow. The obvious disadvantage of an asymmetric stern is the increased difficulty in its construction and the higher cost. An improvement in propulsive efficiency of 6-7 percent may be obtained by using this type of stern instead of a conventional stern.

The object of imparting a rotation to the flow opposite to that caused by the propeller can also be achieved by fitting an array of fixed blades radiating outwards just ahead of the propeller. Such a "pre-swirl" stator increases the relative tangential velocity of the blades. The propeller can be provided a more uniform radial distribution of circulation, the circulation

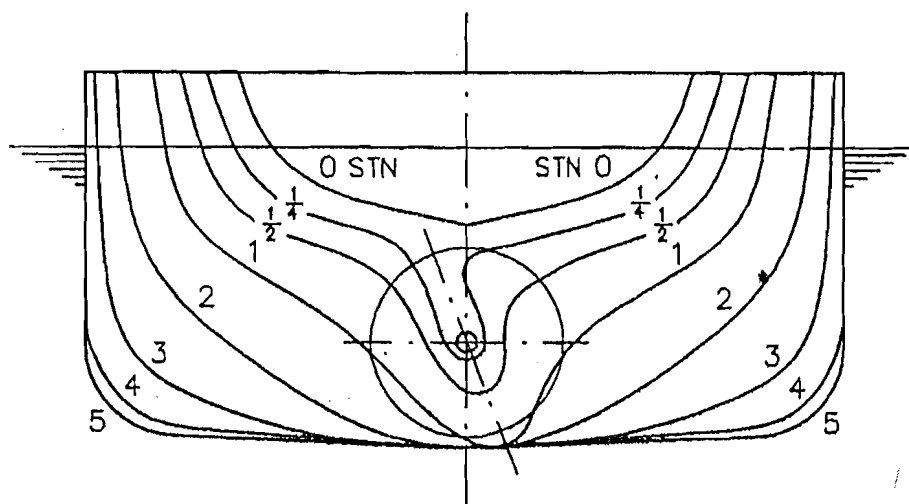


Figure 12.35 : Asymmetric Stern.

on the stator blades being opposite to that on the propeller blades. The tips of the stator blades should be at a radius some 15 percent greater than the radius of the propeller to ensure that the tip vortices shed by the stator blades pass clear of the propeller. The number of fixed blades and the number of propeller blades should be such that their least common multiple is large, e.g. 5 propeller blades and 9 stator blades. It may also be necessary to arrange the stator blades non-uniformly for reducing vibration. Fixed blades may also be fitted behind the propeller. Such a "post-swirl" stator is designed to recover the rotational energy in the propeller slipstream and convert it into a forward thrust.

A typical pre-swirl stator is the Mitsubishi reaction fin system, Fig. 12.36. In addition to providing a pre-swirl to cancel the slipstream rotation of the propeller, the fins are supposed to reduce the turbulence in the flow and decrease noise and vibration. In some cases, a ring at the fin tips is fitted to provide support. The fins improve the flow at the inner radii of the propeller and eliminate blade root erosion. The improved flow to the propeller also produces better hull-propeller interaction. The fins have a radially varying pitch such that a forward thrust is produced. A 4-8 percent

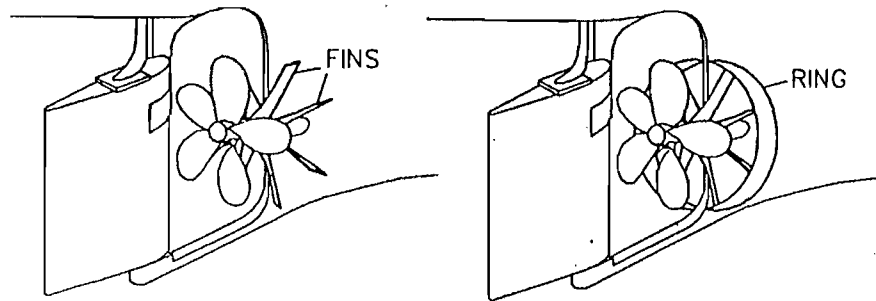


Figure 12.36 : Mitsubishi Reaction Fin System.

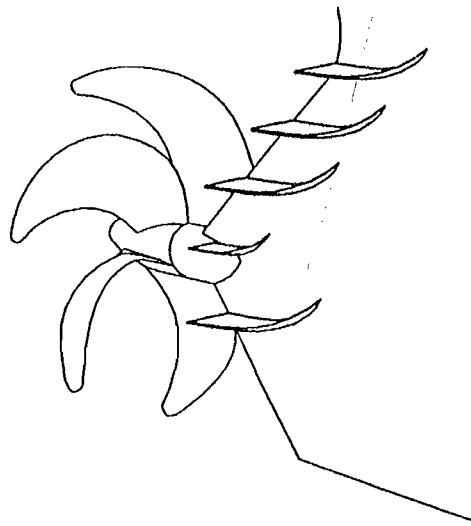


Figure 12.37 : Grothues Spoilers.

saving in power may be obtained by fitting the Mitsubishi reaction fin, the effect being greater in the ballast condition.

Grothues spoilers, named after their inventor Grothues-Spork, consist of a set of triangular fins attached to the hull just ahead of the propeller, Fig.12.37. The fins are designed to improve the flow into the propeller by converting the vertical component of the flow due to bilge vortices into a horizontal flow, and thus recover energy. The fins produce a small forward thrust, increase the mass flow through the propeller disc and reduce angular velocity variations in the flow. Grothues spoilers thereby reduce resistance,

improve propeller efficiency and reduce vibration. The shape, position and number of fins must be determined by model tests. Power savings ranging from about 3 percent for fine vessels with low breadth-draught ratios to about 9 percent for full tankers are possible using Grothues spoilers, greater improvements being achieved in the ballast condition.

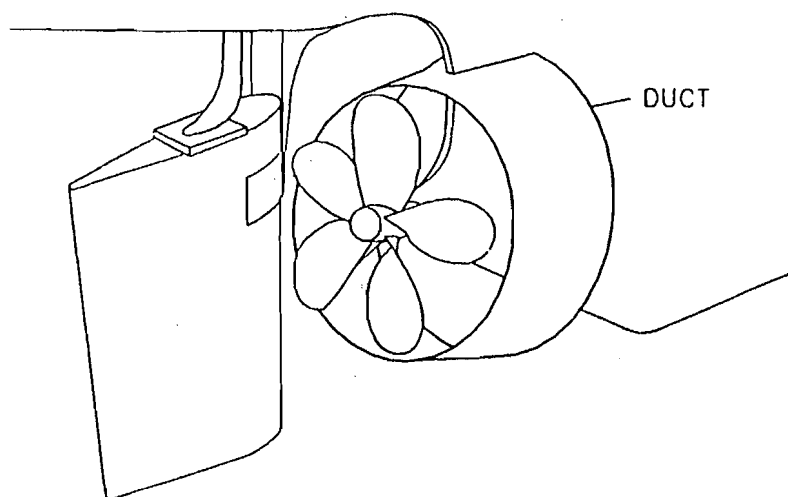


Figure 12.38 : Mitsui Integrated Duct.

The Mitsui integrated duct is a duct located just forward of the propeller and integrated into the ship hull, Fig. 12.38. The duct is asymmetric port and starboard and the profile chord is larger at the top than at the bottom. The trailing edge of the duct is aligned with the propeller blade tips. The integrated duct stabilises and homogenises the flow into the propeller. There is also a small decrease in the resistance of the ship. The duct increases the mass of water flowing through the propeller per unit time, and therefore increases the propeller efficiency. The thrust deduction is also reduced. The improvement in the flow to the propeller causes a slight reduction in cavitation and hull pressure fluctuation. There is also said to be some improvement in manoeuvrability due to the integrated duct. Owing to the inward direction of the flow at the stern the duct produces a forward thrust. The power saving that can be obtained by fitting a Mitsui integrated duct is about 5–10 percent, the greater values being obtained for full form ships.

The wake equalising duct, due to Schneekluth, is a duct attached to the hull ahead of the propeller in the upper part, the diameter of the duct being about half the propeller diameter, Fig. 12.39. The duct may be in the form of a complete ring or as two halves on either side of the hull. In ships with

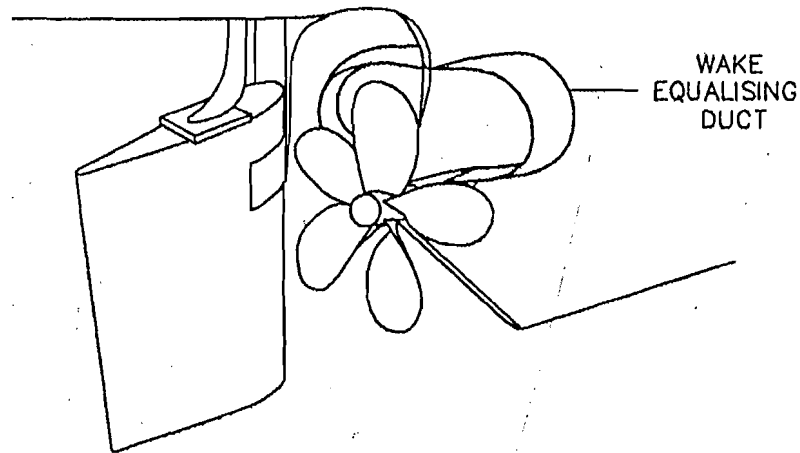


Figure 12.39 : Schneekluth Wake Equalising Duct.

an asymmetric stern or in high speed ships the duct may be fitted only on one side. The wake equalising duct is sometimes used in combination with Grothues spoilers. The main function of the duct is to accelerate the flow in the upper half of the propeller disc where it is normally slower than in the lower half. This increases the amount of water flowing through the propeller disc. The advantages that a wake equalising duct can give include:

- Increase in propeller efficiency due to a greater mass flow through the propeller disc.
- Reduction in flow separation at the stern resulting in reduced ship resistance.
- Generation of forward thrust by the duct.
- Reduction in unsteady propeller forces due to a more uniform inflow.
- Reduced cavitation due to lower propeller loading resulting from the increased mass flow and also because of more uniform flow.

- Improved manoeuvrability through better flow to the rudder, and better course-keeping due to the lateral area of the duct.

The design parameters of the wake equalising duct, viz. diameter, profile shape and length, duct dihedral angle (cone angle), and the angle of the duct axis with respect to horizontal and vertical planes, may be determined by comparison with existing installations or by model tests. Model experiments indicate that a saving in power of as much as 15 percent may be obtained by fitting a Schneekluth duct, although the gains realised in full size ships are somewhat smaller. The main advantages of the duct are a reduction in resistance and an improvement in propulsive efficiency. The greatest benefits are obtained in ships with block coefficients of 0.60 and more, propeller diameters exceeding 2.20 m, angles of run at $0.75R$ above the propeller axis greater than 10 degrees, and speeds in the range 12–18 knots. The benefits of the wake equalising duct are greater in the fully loaded condition than in the ballast condition with the vessel trimmed aft. In high speed ships, the advantages of the duct lie mostly in its producing more uniform flow, thereby reducing propeller induced vibration and cavitation.

12.16 Design Approach

The detailed design of unconventional propulsion devices must take into account the nature of the flow at the stern of a ship and the interaction between the propeller and its inflow. Various computational methods ranging from potential flow-based lifting line methods to viscous flow RANS solvers are being tried out for the design of such devices. The agreement between the results of CFD codes and model experiments is not satisfactory in many cases. Nevertheless, CFD codes are being used for the practical design of complex hull-propulsor configurations. On the other hand, lifting line and lifting surface techniques are often adequate for the design of unconventional propellers and flow improvement devices. Generally, however, model testing is the most reliable method for the design optimisation of unconventional propulsion devices at present. Scale effects are a major problem, and the improvements in efficiency predicted on the basis of model tests for a particular device are often found to be somewhat optimistic in actual practice.

Problems

1. A feathering paddle wheel consists of paddles pivoted about points on a circle of radius 2.5 m. The arm attached at right angles to each paddle is 0.35 m long. The waterline is 2.0 m below the centre of the paddle wheel. Determine the distance from the wheel centre of the point through which the link attached to the paddle arm must pass if the paddle is to have an angle of 10 degrees to the vertical when its pivot enters water. What would be the diameter of a paddle wheel with fixed paddles to have the same angle?
2. The open water characteristics of a controllable pitch propeller of 3.0 m diameter are given by:

$$K_T = \left(-0.077 \frac{P^2}{D^2} + 0.546 \frac{P}{D} - 0.054 \right) + \left(0.289 \frac{P^2}{D^2} - 0.485 \frac{P}{D} - 0.050 \right) J$$

$$+ \left(-0.252 \frac{P^2}{D^2} + 0.558 \frac{P}{D} - 0.447 \right) J^2$$

$$10K_Q = \left(0.522 \frac{P^2}{D^2} + 0.072 \frac{P}{D} + 0.021 \right) + \left(0.044 \frac{P^2}{D^2} - 0.287 \frac{P}{D} - 0.038 \right) J$$

$$+ \left(0.067 \frac{P^2}{D^2} - 0.199 \frac{P}{D} - 0.099 \right) J^2$$

This propeller is fitted in a tug which has an engine of 1035 kW brake power at 600 rpm connected to the propeller through 4:1 reduction gearing. The effective power P_E of the tug at different speeds V_K in knots is as follows:

V_K , knots:	2.0	4.0	6.0	8.0	10.0	12.0	14.0	16.0
P_E , kW :	0.49	5.57	23.04	63.07	137.72	260.69	447.13	713.52

The wake fraction is 0.200, the relative rotative efficiency is 1.000, the thrust deduction fraction is given by $t = 0.05 + 0.01083 V_K$, and the shafting efficiency is 0.950. Determine how the pitch ratio must be varied with speed to ensure full power absorption. Calculate the towrope pull at the different speeds. What is the free running speed of the tug?

3. A tug is fitted with a ducted propeller of 3.0 m diameter and 0.973 pitch ratio, the open water characteristics of which are as follows:

J	:	0	0.200	0.400	0.600	0.800	1.000
K_T	:	0.4862	0.3897	0.2902	0.1752	0.0320	-0.1522
$10K_Q$:	0.4021	0.3891	0.3539	0.2866	0.2196	0.0152
K_{TD}	:	0.2469	0.1587	0.0885	0.0223	-0.0724	-0.2232

K_{TD} is the duct thrust coefficient, $K_{TD} = T_D / \rho n^2 D^4$.

The tug has a diesel engine of 1035 kW brake power at 600 rpm connected to the propeller through 4:1 reduction gearing. The wake fraction is 0.200, the thrust deduction fraction is given by $t = 0.050 + 0.01083 V_K$ where V_K is the speed of the vessel in knots, the relative rotative efficiency is 1.000 and the shafting efficiency 0.950. The effective power of the tug is as follows:

Speed, knots	:	10.0	11.0	12.0	13.0
Effective power, kW	:	137.72	192.25	260.69	344.98

Assuming that the maximum torque and rpm of the engine are not to be exceeded, determine the bollard pull and the free running speed of the tug, and the corresponding engine powers and rpms. Calculate also the duct thrust in the two conditions.

4. In a shallow draught vessel with two surface piercing propellers, each propeller has four blades, a diameter of 1.5 m and a pitch ratio of 1.0. At the design speed, the propellers run at 600 rpm and the relative velocity of water with respect to each propeller is 5.0 m per sec in a horizontal direction parallel to the centre line of the vessel. The propeller axes are horizontal but inclined at 10 degrees outward towards aft to the vessel centre line, and are 0.1941 m above the waterline. For the section at $0.7R$ of each propeller, the lift and drag coefficients per degree angle of attack are 0.015 and 0.001 respectively, and the section chord is 0.3 m. Assuming that the axial and tangential forces per unit immersed blade length are constant and equal to the values at $0.7R$, determine the thrust, the torque and the horizontal and vertical components of the force normal to the axis of each propeller. If the wake fraction is 0.05 and the thrust deduction fraction 0.02, what is the effective power of the vessel? Assume that the propeller blades are narrow and that the induced velocities can be neglected.
5. A tug is fitted with two Voith-Schneider propellers, each consisting of six blades each of area 0.05 m^2 set on a circle of 1.0 m radius. The blades have lift and drag coefficients given by:

$$C_L = 0.1\alpha \quad C_D = 0.03 + 0.1C_L^2$$

where α is the angle of attack in degrees. Each propeller runs at 180 rpm and the blades are set at an eccentricity ratio of 0.20. Determine the bollard pull and the delivered power, assuming that there is no thrust deduction.

6. A planing craft is propelled by a single waterjet unit of 3000 kW shaft power. The inlet diameter is 1.0 m and the nozzle diameter is 0.6325 m. The effective power of the planing craft is as follows:

Speed	Effective power	Speed	Effective power
knots	kW	knots	kW
15.0	47.9	35.0	1548.3
20.0	148.5	40.0	1897.5
25.0	439.1	45.0	2280.6
30.0	1232.4	50.0	2697.3

The wake fraction and the thrust deduction fraction relevant to the waterjet unit are 0.060 and 0.020 respectively. The waterjet nozzle is 0.6 m above the waterline at full power. The shafting efficiency is 0.970, the nozzle efficiency 0.985 and the waterjet inlet efficiency 0.850. Using Fig. 12.33, determine the speed of the craft at full power, and the waterjet pump efficiency as installed.

APPENDIX 1

Some Properties of Air and Water

Density:

Density ρ in kg per m³; temperature t in degrees Celsius.

1. Air (at normal atmospheric pressure)

$$\rho_{air} = \frac{353.172}{273.16 + t} \quad (A1.1)$$

2. Fresh water

$$\begin{aligned} \rho_{FW} = 999.9227 + 0.4671409 \frac{t}{10} - 0.6834635 \left(\frac{t}{10} \right)^2 \\ + 0.01943808 \left(\frac{t}{10} \right)^3 \end{aligned} \quad (A1.2)$$

3. Sea water (3.5 percent salinity)

$$\begin{aligned} \rho_{SW} = 1028.1474 - 0.5547975 \frac{t}{10} - 0.6344066 \left(\frac{t}{10} \right)^2 \\ + 0.03629289 \left(\frac{t}{10} \right)^3 \end{aligned} \quad (A1.3)$$

Kinematic Viscosity:

Kinematic viscosity ν in m^2 per sec.

(The following formulas are simplifications of those given in the ITTC 1978 performance prediction method.)

1. Fresh water

$$10^6 \nu_{FW} = 0.000585 t^2 - 0.04765 t + 1.72256 \quad (\text{A1.4})$$

2. Sea water (3.5 percent salinity)

$$10^6 \nu_{SW} = 0.000695 t^2 - 0.052078 t + 1.820219 \quad (\text{A1.5})$$

Vapour Pressure:

Vapour pressure p_V in kN per m^2 .

1. Fresh water

$$p_V = 0.6108 + 0.4442 \left(\frac{t}{10} \right) + 0.001414 \left(\frac{t}{10} \right)^2 + 0.02788 \left(\frac{t}{10} \right)^3 \\ + 0.002474 \left(\frac{t}{10} \right)^4 + 0.03007 \left(\frac{t}{10} \right)^5 \quad (\text{A1.6})$$

The vapour pressure of sea water is about 3.3 percent less than the vapour pressure of fresh water at the same temperature.

APPENDIX 2

Aerofoil Sections used in Marine Propellers

Source: Abbott and Doenhoff (1959)

Table A2.1

Geometry

	Mean Lines		Thickness Distributions	
	NACA $\alpha = 0.8$ (modified)	NACA $\alpha = 1.0$	NACA-16	NACA-66 (modified)
x/c	$y_c(x)/f$	$y_c(x)/f$	$y_t(x)/t$	$y_t(x)/t$
0	0	0	0	0
0.0125	0.0907	0.097	0.1077	0.1044
0.0250	0.1586	0.169	0.1504	0.1466
0.0500	0.2711	0.287	0.2091	0.2066
0.0750	0.3657	0.384	0.2527	0.2525
0.1000	0.4482	0.469	0.2881	0.2907
0.2000	0.6993	0.722	0.3887	0.4000
0.3000	0.8633	0.881	0.4514	0.4637
0.4000	0.9614	0.971	0.4879	0.4952
0.5000	1.0000	1.000	0.5000	0.4962
0.6000	0.9785	0.971	0.4862	0.4653
0.7000	0.8890	0.881	0.4391	0.4035
0.8000	0.7026	0.722	0.3499	0.3110

Table A2.1 (Contd.)

Mean Lines		Thickness Distributions		
NACA	NACA	NACA-16	NACA-66	
$a = 0.8$	$a = 1.0$			
(modified)			(modified)	
x/c	$y_c(x)/f$	$y_c(x)/f$	$y_t(x)/t$	$y_t(x)/t$
0.9000	0.3687	0.469	0.2098	0.1877
1.0000	0	0	0.0100	0.0333

x = distance from leading edge along nose-tail line;

c = section chord;

t = section thickness;

f = section camber;

y_c = ordinate of mean line from nose-tail line;

y_t = ordinate of section face (and back) from the mean line.

For the NACA-66 (modified) thickness distribution, $y_t(x)/t = 0.5000$ at $x/c = 0.4500$.

The leading edge radii of the two sections are as follows:

NACA-16: radius = $0.4885 t^2/c$ NACA-66: radius = $0.448 t^2/c$
(modified)

APPENDIX 3

Propeller Methodical Series Data

(a) B-Series (Troost, Wageningen, MARIN)

Geometry

Nomenclature

- c : Blade section chord
- D : Propeller diameter
- r : Blade section radius
- R : Propeller radius
- t : Maximum thickness of blade section
- t_0 : Blade thickness extrapolated to zero radius
- t_1 : Blade thickness at blade tip
- t_{LE} : Thickness at leading edge (before rounding)
- t_{TE} : Thickness at trailing edge (before rounding)
- x : Distance from leading edge of blade section
- x_0 : Distance of leading edge from propeller reference line

x_m : Distance of position of maximum thickness from leading edge

y_f : Ordinate of face of blade section at x

y_b : Ordinate of back of blade section at x

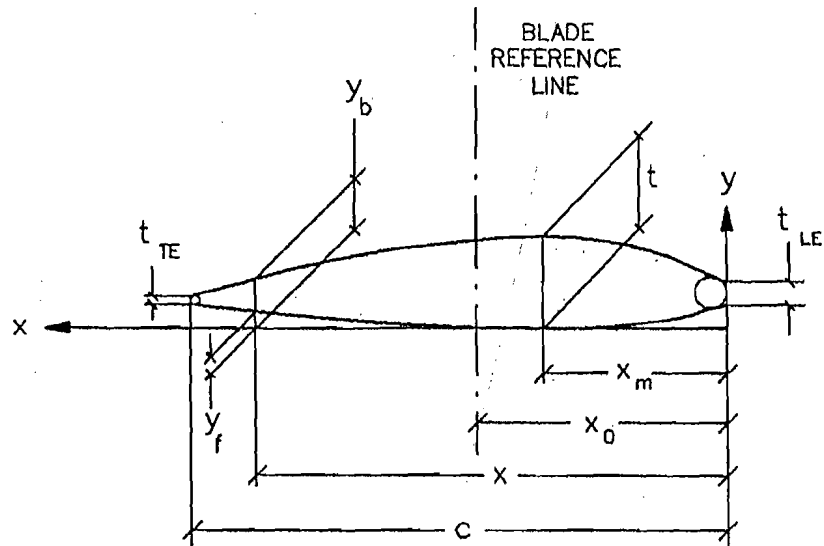


Figure A3.1 : Blade Section Geometry of B Series Propellers.

Table A3.1

Blade Thickness

Z	:	2	3	4	5	6	7
t_0/D	:	0.055	0.050	0.045	0.040	0.035	0.030
t_1/D	:	0.003	0.003	0.003	0.003	0.003	0.003

$$\frac{t}{D} = \frac{t_0}{D} - \frac{r}{R} \left(\frac{t_0}{D} - \frac{t_1}{D} \right) \quad (\text{A3.1})$$

Table A3.2
Blade Outline for B-Series

$$\frac{c}{D} = c_1 \frac{A_E/A_O}{Z} \quad (\text{A3.2})$$

r/R	$Z = 2, 3$			$Z = 4, 5, 6, 7$		
	c_1	x_0/c	x_m/c	c_1	x_0/c	x_m/c
0.2	1.633	0.616	0.350	1.662	0.617	0.350
0.3	1.832	0.611	0.350	1.882	0.613	0.350
0.4	2.000	0.599	0.350	2.050	0.601	0.350
0.4	2.120	0.583	0.355	2.152	0.586	0.350
0.6	2.186	0.558	0.389	2.187	0.561	0.389
0.7	2.168	0.526	0.442	2.144	0.524	0.443
0.8	2.127	0.481	0.478	1.970	0.463	0.479
0.9	1.657	0.400	0.500	1.582	0.351	0.500
1.0	0	-	-	0	-	-

At MARIN, a modified B-Series has been developed that has a blade outline which is wider towards the tip and narrower towards the root, and thus has better cavitation properties. The open water characteristics of this modified series, known as the BB-Series, are said to be identical to those of the B-Series. The particulars of the blade outline of the BB-Series are given in Table A3.3.

Table A3.3
Blade Outline for BB-Series

r/R	Blade Outline of BB-Series		
	c_1	x_0/c	x_m/c
0.200	1.600	0.581	0.350
0.300	1.832	0.584	0.350
0.400	2.023	0.580	0.351
0.500	2.163	0.570	0.355

Table A3.3 (Contd.)

r/R	Blade Outline of BB-Series		
	c_1	x_0/c	x_m/c
0.600	2.243	0.552	0.389
0.700	2.247	0.524	0.443
0.800	2.132	0.480	0.486
0.850	2.005	0.448	0.498
0.900	1.798	0.402	0.500
0.950	1.434	0.318	0.500
0.975	1.122	0.227	0.500
1.000	0	-	-

Blade Section Face and Back Ordinates

$$\text{For } x \leq x_m \quad : \quad y_f = u(t - t_{LE}) \quad y_b = v(t - t_{LE}) \quad (\text{A3.3})$$

$$\text{For } x_m \leq x \leq c \quad : \quad y_f = u(t - t_{TE}) \quad y_b = v(t - t_{TE})$$

where u and v are given in Table A3.4(a-d)

 K_T, K_Q Polynomials

$$K_T = \sum_{i,j,k,l} C_T(i,j,k,l) J^i \left(\frac{P}{D} \right)^j \left(\frac{A_E}{A_O} \right)^k Z^l$$

$$K_Q = \sum_{i,j,k,l} C_Q(i,j,k,l) J^i \left(\frac{P}{D} \right)^j \left(\frac{A_E}{A_O} \right)^k Z^l \quad (\text{A3.4})$$

These polynomials are given for a Reynolds number of 2×10^6 . The coefficients C_T and C_Q are given in Tables A3.5 and A3.6 respectively.

Table A3.4
Blade Section Ordinates

(a)

r/R	x/x_m										
	0	0.05	0.10	0.15	0.20	0.30	0.40	0.50	0.60	0.80	1.00
	Values of u										
0.2	0.3560	0.2821	0.2353	0.2000	0.1685	0.1180	0.0804	0.0520	0.0304	0.0049	0
0.3	0.2923	0.2186	0.1760	0.1445	0.1191	0.0790	0.0503	0.0300	0.0148	0.0027	0
0.4	0.2131	0.1467	0.1088	0.0833	0.0637	0.0357	0.0189	0.0090	0.0033	0	0
0.5	0.1278	0.0778	0.0500	0.0328	0.0211	0.0085	0.0034	0.0008	0	0	0
0.6	0.0382	0.0169	0.0067	0.0022	0.0006	0	0	0	0	0	0
0.7-1.0	0	0	0	0	0	0	0	0	0	0	0

Table A3.4
Blade Section Ordinates
(h)

r/R	$(x - x_m)/(c - x_m)$									
	0	0.20	0.40	0.50	0.60	0.70	0.80	0.90	0.95	1.00
Values of u										
0.2	0	0.0172	0.0592	0.0880	0.1207	0.1570	0.1967	0.2400	0.2630	0.2826
0.3	0	0.0033	0.0202	0.0376	0.0623	0.0943	0.1333	0.1790	0.2040	0.2306
0.4	0	0	0.0044	0.0116	0.0214	0.0395	0.0630	0.0972	0.1200	0.1467
0.5	0	0	0	0.0012	0.0040	0.0100	0.0190	0.0330	0.0420	0.0522
0.6-1.0	0	0	0	0	0	0	0	0	0	0

Table A3.4
Blade Section Ordinates

(c)											
r/R	x/x_m										
	0	0.05	0.10	0.15	0.20	0.30	0.40	0.50	0.60	0.80	1.00
Values of v											
0.2	0.3560	0.4381	0.5193	0.5905	0.6462	0.7370	0.8081	0.8690	0.9179	0.9799	1.0000
0.3	0.2293	0.4076	0.4957	0.5710	0.6321	0.7295	0.8023	0.8615	0.9068	0.9777	1.0000
0.4	0.2181	0.3402	0.4323	0.5168	0.5857	0.6947	0.7782	0.8435	0.8966	0.9725	1.0000
0.5	0.1278	0.2528	0.3556	0.4463	0.5250	0.6515	0.7512	0.8283	0.8880	0.9710	1.0000
0.6	0.0382	0.1654	0.2787	0.3797	0.4626	0.6060	0.7200	0.8090	0.8790	0.9690	1.0000
0.7	0	0.1240	0.2337	0.3300	0.4140	0.5615	0.6840	0.7850	0.8660	0.9675	1.0000
0.8	0	0.1050	0.2028	0.2925	0.3765	0.5265	0.6545	0.7635	0.8520	0.9635	1.0000
0.9	0	0.0975	0.1900	0.2775	0.3600	0.5100	0.6400	0.7500	0.8400	0.9600	1.0000

Table A3.4
Blade Section Ordinates
(d)

r/R	$(x - x_m)/(c - x_m)$									
	0	0.20	0.40	0.50	0.60	0.70	0.80	0.90	0.95	1.00
	Values of v									
0.2	1.0000	0.9618	0.8576	0.7875	0.7049	0.6105	0.5027	0.3855	0.3270	0.2826
0.3	1.0000	0.9616	0.8467	0.7711	0.6818	0.5828	0.4693	0.3460	0.2840	0.2306
0.4	1.0000	0.9645	0.8459	0.7641	0.6567	0.5435	0.4130	0.2782	0.2105	0.1467
0.5	1.0000	0.9639	0.8456	0.7580	0.6451	0.5240	0.3759	0.2195	0.1370	0.0522
0.6	1.0000	0.9613	0.8426	0.7530	0.6415	0.5110	0.3585	0.1885	0.0965	0
0.7-0.9	1.0000	0.9600	0.8400	0.7500	0.6400	0.5100	0.3600	0.1900	0.0975	0

Table A3.5
Coefficients C_T for K_T Polynomial

No.	i	j	k	l	$C_T(i, j, k, l)$
1	0	0	0	0	+0.00880496
2	1	0	0	0	-0.204554
3	0	1	0	0	+0.166351
4	0	2	0	0	+0.158114
5	2	0	1	0	-0.147581
6	1	1	1	0	-0.481497
7	0	2	1	0	+0.415437
8	0	0	0	1	+0.0144043
9	2	0	0	1	-0.0530054
10	0	1	0	1	+0.0143481
11	1	1	0	1	+0.0606826
12	0	0	1	1	-0.0125894
13	1	0	1	1	+0.0109689
14	0	3	0	0	-0.133698
15	0	6	0	0	+0.00638407
16	2	6	0	0	-0.00132718
17	3	0	1	0	+0.168496
18	0	0	2	0	-0.0507214
19	2	0	2	0	+0.0854559
20	3	0	2	0	-0.0504475
21	1	6	2	0	+0.010465
22	2	6	2	0	-0.00648272
23	1	6	2	0	+0.010465
24	1	3	0	1	+0.168424
25	3	3	0	1	-0.00102296
26	0	3	1	1	-0.0317791
27	1	0	2	1	+0.018604
28	0	2	2	1	-0.00410798
29	0	0	0	2	-0.000606848
30	1	0	0	2	-0.0049819
31	2	0	0	2	+0.0025983
32	3	0	0	2	-0.000560528

Table A3.5 (Contd.)

33	1	2	0	2	-0.00163652
34	1	6	0	2	-0.000328787
35	2	6	0	2	+0.000116502
36	0	0	1	2	+0.000690904
37	0	3	1	2	+0.00421749
38	3	6	1	2	+0.0000565229
39	0	3	2	2	-0.00146564

Table A3.6

Coefficients C_Q for K_Q Polynomial

No.	i	j	k	l	$C_Q(i, j, k, l)$
1	0	0	0	0	+0.00379368
2	2	0	0	0	+0.00886523
3	1	1	0	0	-0.032241
4	0	2	0	0	+0.00344778
5	0	1	1	0	-0.0408811
6	1	1	1	0	-0.108009
7	2	1	1	0	-0.0885381
8	0	2	1	0	+0.188561
9	1	0	0	1	-0.00370871
10	0	1	0	1	+0.00513696
11	1	1	0	1	+0.0209449
12	2	1	0	1	+0.00474319
13	2	0	1	1	-0.00723408
14	1	1	1	1	+0.00438388
15	0	2	1	1	-0.0269403
16	3	0	1	0	+0.0558082
17	0	3	1	0	+0.0161886
18	1	3	1	0	+0.00318086
19	0	0	2	0	+0.015896
20	1	0	2	0	+0.0471729
21	3	0	2	0	+0.0196283
22	0	1	2	0	-0.0502782
23	3	1	2	0	-0.030055

Table A3.6 (Contd.)

24	2	2	2	0	+0.0417122
25	0	3	2	0	-0.0397722
26	0	6	2	0	-0.00350024
27	3	0	0	1	-0.0106854
28	3	3	0	1	+0.00110903
29	0	6	0	1	-0.000313912
30	3	0	1	1	+0.0035985
31	0	6	1	1	-0.00142121
32	1	0	2	1	-0.00383637
33	0	2	2	1	+0.0126803
34	2	3	2	1	-0.00318278
35	0	6	2	1	+0.00334268
36	1	1	0	2	-0.00183491
37	3	2	0	2	+0.000112451
38	3	6	0	2	-0.0000297228
39	1	0	1	2	+0.000269551
40	2	0	1	2	+0.00083265
41	0	2	1	2	+0.00155334
42	0	6	1	2	+0.000302683
43	0	0	2	2	-0.0001843
44	0	3	2	2	-0.000425399
45	3	3	2	2	+0.0000869243
46	0	6	2	2	-0.0004659
47	1	6	2	2	+0.0000554194

(b) Gawn Series (Admiralty Experimental Works 20 inch Series)

Geometry

The geometrical particulars of the Gawn Series are given in Table 4.1 and Fig. 4.4. The developed blade outline is an ellipse. The centre of the ellipse is at a distance of $0.275D$ from the centre of the propeller and the semi-axes of the ellipse, a and b , are given by:

$$a = 0.225D \quad \frac{b}{D} = \sum_{i,j} c(i,j) \left(\frac{A_D}{A_O}\right)^i \left(\frac{P}{D}\right)^j \quad (\text{A3.5})$$

where the coefficients $c(i,j)$ are given in Table A3.7.

Table A3.7
Blade Outline

i	j	$c(i,j)$
0	0	0.53836624e-02
1	0	0.37401561e+00
2	0	-0.34196916e-02
0	1	-0.58167525e-02
1	1	0.25190058e-01
2	1	-0.90211731e-02
0	2	0.14566425e-02
1	2	-0.67853528e-02
2	2	0.35134575e-02

K_T, K_Q Polynomials

$$K_T = \sum_{i,j,k} C_T(i,j,k,l) J^i \left(\frac{P}{D}\right)^j \left(\frac{A_D}{A_O}\right)^k$$

$$K_Q = \sum_{i,j,k} C_Q(i,j,k,l) J^i \left(\frac{P}{D}\right)^j \left(\frac{A_D}{A_O}\right)^k \quad (\text{A3.6})$$

The coefficients C_T and C_Q are given in Table A3.8.

Table A3.8

 C_T and C_Q in the Polynomials for K_T and $10K_Q$

i	j	k	$C_T(i, j, k)$	$C_Q(i, j, k)$
0	0	0	0.97408086e-01	0.63692808e-01
1	0	0	-0.21572784e+00	-0.80089413e-01
2	0	0	-0.20117083e+00	-0.16184720e+00
3	0	0	0.68857059e-01	-0.21572175e-01
0	1	0	0.16099279e+00	0.77811621e-01
1	1	0	0.29145467e+00	0.24702819e+00
2	1	0	0.19188970e-01	0.62403660e-01
3	1	0	-0.55956569e-01	-0.53570643e-01
0	2	0	-0.13744167e-01	0.14384213e+00
1	2	0	-0.10454782e+00	-0.13415100e+00
2	2	0	0.38724232e-01	0.35848316e-01
3	2	0	0.61652786e-02	0.12422566e-01
0	0	1	-0.40506446e+00	-0.48559698e+00
1	0	1	0.19004023e+00	0.74163526e+00
2	0	1	-0.13912685e+00	-0.72897837e-01
3	0	1	0.66181317e-01	0.10767796e+00
0	1	1	0.10065955e+01	0.84972864e+00
1	1	1	-0.11633307e+01	-0.21723540e+01
2	1	1	0.32121539e+00	-0.87905906e-01
3	1	1	-0.12919416e-01	0.21879166e+00
0	2	1	-0.23608254e+00	0.30810708e+00
1	2	1	0.50920802e+00	0.75812680e+00
2	2	1	-0.20886181e+00	-0.19750497e+00
3	2	1	0.16416967e-01	-0.49353302e-01

More elaborate regression coefficients have been given by Blount and Hubble (1981).

(c) Ka Series in Nozzle 19A (MARIN)

Geometry

The nomenclature used is the same as that used for the B Series.

Table A3.9

Blade Outline and Blade Thickness

r/R	c_1	x_0/c	x_m/c	t/D
0.2	1.3222	0.5501	0.3498	0.0400
0.3	1.5081	0.5277	0.3976	0.0352
0.4	1.6774	0.5134	0.4602	0.0300
0.5	1.8314	0.5055	0.4913	0.0245
0.6	1.9690	0.5013	0.4998	0.0190
0.7	2.0844	0.5000	0.5000	0.0138
0.8	2.1675	0.5000	0.5000	0.0092
0.9	2.2183	0.5000	0.5000	0.0061
1.0	2.4195	0.5000	0.5000	0.0050

Table A3.10

Blade Section Face and Back Ordinates

(a)								
r/R	x/x_m							
	0	0.05	0.10	0.20	0.40	0.60	0.80	1.00
Values of u								
0.2	0.3333	0.2062	0.1604	0.1052	0.0437	0.0146	0.0021	0
0.3	0.2118	0.1030	0.0828	0.0615	0.0272	0.0083	0.0012	0
0.4	0.1347	0.0444	0.0389	0.0292	0.0139	0.0042	0	0
0.5	0.0781	0.0153	0.0136	0.0102	0.0051	0.0017	0	0
0.6-1.0	0	0	0	0	0	0	0	0

Table A3.10

(b)						
r/R	$(x - x_m)/(c - x_m)$					
	0	0.20	0.40	0.60	0.80	1.00
Values of u						
0.2	0	0	0.0010	0.0177	0.0729	0.2021
0.3	0	0	0	0.0107	0.0462	0.1385
0.4	0	0	0	0.0056	0.0236	0.0917
0.5	0	0	0	0.0017	0.0068	0.0662
0.6-1.0	0	0	0	0	0	0

Table A3.10

(c)								
r/R	x/x_m							
	0	0.05	0.10	0.20	0.40	0.60	0.80	1.00
Values of v								
0.2	0.3333	0.4802	0.5479	0.6552	0.8156	0.9229	0.9813	1.0000
0.3	0.2118	0.3787	0.4615	0.5917	0.7834	0.9089	0.9775	1.0000
0.4	0.1347	0.3027	0.3861	0.5292	0.7500	0.8931	0.9722	1.0000
0.5	0.0781	0.2377	0.3158	0.4686	0.7097	0.8727	0.9677	1.0000
0.6	0	0.2044	0.2859	0.4358	0.6826	0.8589	0.9647	1.0000
0.7	0	0.2288	0.3079	0.4531	0.6924	0.8633	0.9658	1.0000
0.8	0	0.2690	0.3439	0.4816	0.7084	0.8704	0.9676	1.0000
0.9	0	0.3187	0.3887	0.5175	0.7294	0.8809	0.9717	1.0000
1.0	0	0.3231	0.3925	0.5200	0.7300	0.8800	0.9700	1.0000

Table A3.10

(d)						
r/R	$(x - x_m)/(c - x_m)$					
	0	0.20	0.40	0.60	0.80	1.00
Values of v						
0.2	1.0000	0.9500	0.8250	0.6542	0.4552	0.2021
0.3	1.0000	0.9586	0.8414	0.6770	0.4367	0.1385
0.4	1.0000	0.9625	0.8569	0.6750	0.4292	0.0917
0.5	1.0000	0.9660	0.8642	0.6876	0.4245	0.0662
0.6	1.0000	0.9647	0.8589	0.6826	0.4358	0
0.7	1.0000	0.9658	0.8633	0.6924	0.4531	0
0.8	1.0000	0.9676	0.8704	0.7084	0.4816	0
0.9	1.0000	0.9717	0.8803	0.7294	0.5175	0
1.0	1.0000	0.9700	0.8800	0.7300	0.5200	0

Geometry of Nozzle 19A:

Nomenclature

 D : Propeller diameter e : Clearance between propeller and nozzle l : Length of nozzle r_i : Radius of inner surface of nozzle r_o : Radius of outer surface of nozzle x : Distance along axis from leading edge of nozzle y_i : Offset of inner surface of nozzle y_o : Offset of outer surface of nozzle

$$\frac{l}{D} = 0.5 \quad r_i = 0.5D + e + y_i \quad r_o = 0.5D + e + y_o \quad (\text{A3.7})$$

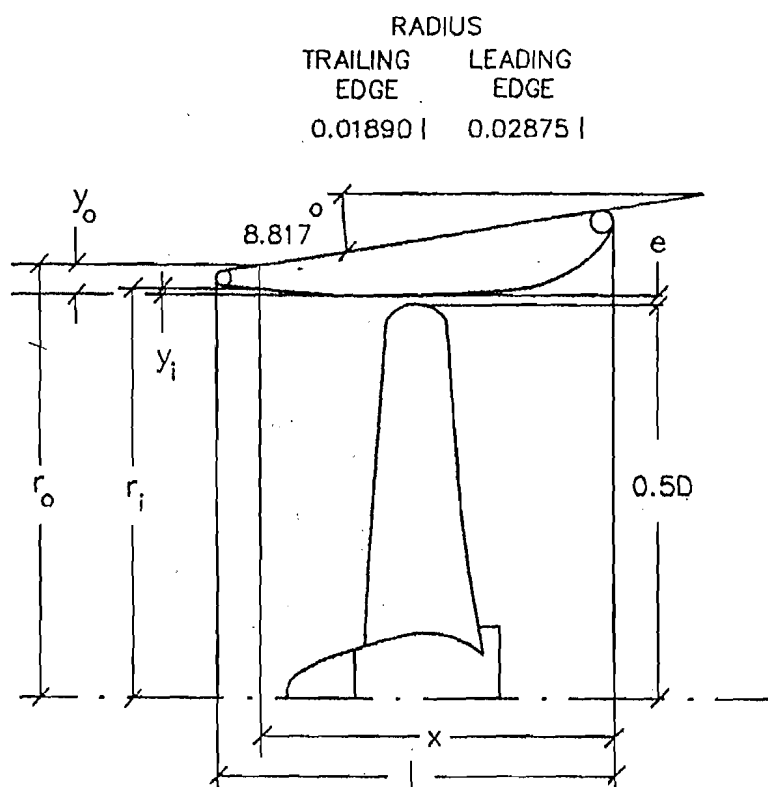


Figure A3.2 : Geometry of Nozzle 19A.

Table A3.11
Nozzle 19A Profile

x/l	y_i/l	y_o/l
0	0.1825	0.1825
0.0125	0.1466	0.2072
0.0250	0.1280	0.2107
0.0500	0.1007	0.2080
0.0750	0.0800	0.1969
0.1000	0.0634	0.1858
0.1500	0.0387	0.1747
0.2000	0.0217	0.1636

Table A3.11 (Contd.)

0.2500	0.0110	0.1525
0.3000	0.0048	0.1414
0.4000	0	0.1302
0.5000	0	0.1191
0.6000	0	0.1080
0.7000	0.0029	0.0969
0.8000	0.0082	0.0858
0.9000	0.0145	0.0747
0.9500	0.0186	0.0692
1.0000	0.0236	0.0636

 K_T, K_Q Polynomials

$$\text{Total thrust coefficient : } K_T = \sum_{i,j} C_T(i,j) \left(\frac{P}{D}\right)^i J^j \quad (\text{A3.8})$$

$$\text{Torque coefficient : } K_Q = \sum_{i,j} C_Q(i,j) \left(\frac{P}{D}\right)^i J^j \quad (\text{A3.9})$$

$$\text{Duct thrust coefficient : } K_{TD} = \sum_{i,j} C_{TD}(i,j) \left(\frac{P}{D}\right)^i J^j \quad (\text{A3.10})$$

Table A3.12

Coefficients C_T , C_Q and C_{TD} in
Polynomials for K_T , K_Q and K_{TD}

(a)

Propeller: Ka 3.65 in Nozzle 19A				
i	j	$C_T(i,j)$	$C_Q(i,j)$	$C_{TD}(i,j)$
0	0	0.028100	0.006260	0.154000
0	1	-0.143910	0.0	0.115560
0	2	0.0	-0.017942	-0.123761
0	3	-0.383783	0.0	0.0

Table A3.12(a) (Contd.)

0	4	0.0	-0.008089	0.0
0	5	0.0	0.0	-0.741240
0	6	0.0	0.0	0.646894
1	0	0.0	0.0	-0.542674
1	1	-0.429709	0.0	0.749643
1	2	0.0	-0.016644	0.0
1	6	0.0	0.0	-0.162202
2	0	0.671268	0.0	0.972388
2	2	0.286926	0.0	1.468570
3	0	-0.182294	0.040041	-0.317664
3	2	0.0	0.0	-1.084980
3	6	0.0	0.0	-0.032298
4	3	0.0	0.0	0.199637
5	1	0.0	0.0	0.060168
6	0	0.0	-0.003460	0.0
6	1	-0.017378	-0.000674	0.0
6	2	0.0	0.001721	0.0

Table A3.12

(b)

Propeller: Ka 4.55 in Nozzle 19A

i	j	$C_T(i, j)$	$C_Q(i, j)$	$C_{TD}(i, j)$
0	0	-0.375000	-0.034700	-0.045100
0	1	-0.203050	0.018568	0.0
0	2	0.830306	0.0	0.0
0	3	-2.746930	0.0	-0.663741
0	4	0.0	-0.195582	-0.244626
0	5	0.0	0.317452	0.0
0	6	0.067548	-0.093739	0.0
0	7	0.0	0.022850	0.0
1	0	2.030070	0.158951	0.244461
1	1	-0.392301	-0.048433	-0.578464
1	2	-0.611743	0.0	1.116820
1	3	4.319840	0.024157	0.751953

Table A3.12(b) (Contd.)

1	4	-0.341290	0.0	0.0
1	5	0.0	-0.123376	0.0
1	6	0.0	0.0	-0.089165
2	0	-3.031670	-0.212253	0.0
2	1	0.0	0.0	-0.146178
2	2	0.0	0.0	-0.917516
2	3	-2.007860	0.0	0.0
3	0	2.836970	0.156133	0.068186
3	1	0.0	0.0	0.174041
3	2	0.0	0.0	0.102331
3	3	0.391304	0.0	0.0
4	0	-0.994962	0.0	0.0
4	1	0.0	0.030740	0.0
4	2	0.0	0.073587	0.0
5	0	0.0	-0.031826	0.0
5	1	0.015742	-0.014568	0.0
5	2	0.0	-0.109363	0.0
5	4	0.0	0.043862	0.0
6	0	0.043782	0.007947	-0.008581
6	2	0.0	0.038275	0.0
6	4	0.0	-0.021971	0.0
6	6	0.0	0.000700	0.0

Table A3.12

(c)

Propeller: Ka 4.70 in Nozzle 19A				
i	j	$C_T(i, j)$	$C_Q(i, j)$	$C_{TD}(i, j)$
0	0	0.030550	0.006735	0.076594
0	1	-0.148687	0.0	0.075223
0	2	0.0	-0.016306	-0.061881
0	3	-0.391137	0.0	-0.138094
0	4	0.0	-0.007244	0.0
0	5	0.0	0.0	-0.370620
0	6	0.0	0.0	0.323447

Table A3.12(c) (Contd.)

1	0	0.0	0.0	-0.271337
1	1	-0.432612	0.0	-0.687921
1	2	0.0	-0.024012	0.225189
1	6	0.0	0.0	-0.081101
2	0	0.667657	0.0	0.666028
2	2	0.285076	0.005193	0.734285
3	0	-0.172529	0.046605	-0.202467
3	2	0.0	0.0	-0.542490
3	6	0.0	0.0	-0.016149
4	0	0.0	-0.007366	0.0
4	3	0.0	0.0	0.099819
5	1	0.0	0.0	0.030084
6	0	0.0	-0.001730	0.0
6	1	-0.017293	-0.000337	0.0
6	2	0.0	0.000861	-0.001876

Table A3.12

(d)

Propeller: Ka 5.75 in Nozzle 19A				
i	j	$C_T(i, j)$	$C_Q(i, j)$	$C_{TD}(i, j)$
0	0	0.033000	0.007210	-0.000813
0	1	-0.153463	0.0	0.034885
0	2	0.0	-0.014670	0.0
0	3	-0.398491	0.0	-0.276187
0	4	0.0	-0.006398	0.0
1	1	-0.435515	0.0	-0.626198
1	2	0.0	-0.031380	0.450379
2	0	0.664045	0.0	0.359718
2	2	0.283225	0.010386	0.0
3	0	-0.162764	0.053169	-0.087289
4	0	0.0	-0.014731	0.0
6	1	-0.017208	0.0	0.0
6	2	0.0	0.0	-0.003751

APPENDIX 4

Propulsion Factors

Nomenclature

A_E	Expanded blade area ratio of the propeller
A_O	Disc area of the propeller
B	Breadth of the ship
C_A	Correlation allowance
C_B	Block coefficient
C_F	Frictional resistance coefficient
C_M	Midship section coefficient
C_P	Prismatic coefficient
C_{PV}	Vertical prismatic coefficient
C_V	Viscous resistance coefficient
C_W	Waterplane coefficient
D	Propeller diameter
F_n	Froude number
h	Depth of immersion of the propeller axis

L	Length of the ship
LCB	Longitudinal coordinate of the centre of buoyancy of the ship forward of amidships as a percentage of the length of the ship
P	Pitch of the propeller
S	Wetted surface of the ship
t	Thrust deduction fraction
T	Draught of the ship
T_A	Draught at after perpendicular
TC	Propeller tip clearance from hull
V	Ship speed
w	Wake fraction
w_F	Froude wake fraction
ε	Rake angle
η_R	Relative rotative efficiency
ψ	Angle of bossing to the horizontal
∇	Displacement volume of the ship

Wake Fraction

Taylor (1933)

Single screw ships

$$w = 1.7489 C_B^2 - 1.8612 C_B + 0.7272 \quad (\text{A4.1})$$

Twin screw ships

$$w = 1.7643 C_B^2 - 1.4745 C_B + 0.2574 \quad (\text{A4.2})$$

Schoenherr (Rossell and Chapman, 1939)

Single screw ships

$$w = 0.10 + 4.5 \frac{C_{PV} C_P B/L}{(7 - 6 C_{PV})(2.8 - 1.8 C_P)} + 0.5 \left(\frac{T-h}{T} - \frac{D}{B} - k' \varepsilon \right) \quad (\text{A4.3})$$

 $k' = 0.3$ for normal sterns $= 0.5-0.6$ sterns with cutaway deadwood ε in radians.

Twin screw ships

With bossings and outward turning propellers

$$w = 2 C_B^5 (1 - C_B) + 0.2 \cos^2 \frac{3}{2} \psi - 0.02 \quad (\text{A4.4})$$

With bossings and inward turning propellers

$$w = 2 C_B^5 (1 - C_B) + 0.2 \cos^2 \frac{3}{2} (90 - \psi) - 0.02 \quad (\text{A4.5})$$

With propellers supported by struts

$$w = 2 C_B^5 (1 - C_B) + 0.04 \quad (\text{A4.6})$$

Burrill (1943)

Single screw ships

$$w_F = \frac{w}{1-w} = 0.285 - 0.417 C_B + 0.796 C_B^2 \quad (\text{A4.7})$$

Twin screw ships

With bossings at 10 degrees to the horizontal

$$w_F = \frac{w}{1-w} = 0.171 - 0.847 C_B + 1.341 C_B^2 \quad (\text{A4.8})$$

With bossings at 30 degrees to the horizontal

$$w_F = \frac{w}{1-w} = 0.052 - 0.648 C_B + 1.138 C_B^2 \quad (\text{A4.9})$$

Harvald (1983)

Harvald's data are given in the form of diagrams, which have been converted to the following formulas:

Single screw ships

$$w = \sum_{i,j} a(i,j) C_B^i \left(\frac{B}{L}\right)^j \pm \sum_i b(i) C_B^i + \sum_i c(i) \left(\frac{D}{L}\right)^i \quad (\text{A4.10})$$

where the + sign in the second term applies to U-form hulls and the - sign to V-form hulls and the constants $a(i,j)$, $b(i)$ and $c(i)$ are given in Table A4.1.

Table A4.1

Wake Coefficients for Single Screw Ships

i	j	$a(i,j)$	i	$b(i)$	$c(i)$
0	0	-0.25561270e+01	0	-0.13033033e+02	0.59075583e+00
1	0	0.15080732e+02	1	0.11350812e+03	-0.33099666e+02
2	0	-0.27680372e+02	2	-0.38820110e+03	0.70200373e+03
3	0	0.16433867e+02	3	0.65072329e+03	-0.72595229e+04
0	1	0.17220405e+02	4	-0.53369306e+03	0.29089242e+05
1	1	-0.93048350e+02	5	0.17128503e+03	-
2	1	0.16557534e+03			
3	1	-0.92065689e+02			

Twin screw ships

$$w = \sum_{i,j} a(i,j) C_B^i \left(\frac{B}{L}\right)^j + \delta w \quad (\text{A4.11})$$

where δw is 0.04 for ships with pronounced U-sections and -0.03 for ships with shaft brackets instead of bossings. The coefficients $a(i,j)$ are as given in Table A4.2:

Table A4.2

Wake Coefficients for Twin Screw Ships

i	j	$a(i,j)$
0	0	-0.20940003e+01
1	0	0.10263335e+02
2	0	-0.16825002e+02
3	0	0.94166677e+01
0	1	0.18200002e+02
1	1	-0.87500009e+02
2	1	0.14250001e+03
3	1	-0.75000007e+02

B.S.R.A. (Parker, 1966)

Single screw ships

$$w = a_0 + a_1 C_B + a_2 C_B^2 + a_3 \frac{V}{\sqrt{L}} C_B + a_4 \left(\frac{V}{\sqrt{L}} C_B\right)^2 + a_5 D_w C_B + a_6 \delta LCB \quad (\text{A4.12})$$

where

$$a_0 = -0.8715 \quad a_1 = 2.490 \quad a_2 = -1.475 \quad a_3 = -0.3722$$

$$a_4 = 0.2525 \quad a_5 = 0.226 \quad a_6 = -7.176 \times 10^{-3}$$

$$D_w = B / \sqrt{\nabla^{1/3} D}$$

$$\delta LCB = LCB - 20(C_B - 0.675)$$

V in knots, L in feet.

Holtrop (1984)

Single screw ships

$$w = c_9 c_{20} C_V \frac{L}{T_A} \left(0.050776 + 0.93405 c_{11} \frac{C_V}{1 - C_{P1}} \right) + 0.27915 c_{20} \left(\frac{B}{L(1 - C_{P1})} \right) + c_{19} c_{20} \quad (\text{A4.13})$$

$$c_8 = BS/(LDT_A) \text{ when } B/T_A \leq 5$$

$$c_8 = S(7B/T_A - 25)/(LD(B/T_A - 3)) \text{ when } B/T_A \geq 5$$

$$c_9 = c_8 \text{ when } c_8 \leq 28 \text{ and } c_9 = 32 - 16/(c_8 - 24) \text{ when } c_8 \geq 28$$

$$c_{11} = T_A/D \text{ when } T_A/D \leq 2$$

$$c_{11} = 0.833333 (T_A/D)^3 + 1.33333 \text{ when } T_A/D \geq 2$$

$$c_{19} = 0.12997/(0.95 - C_B) - 0.11056/(0.95 - C_P) \text{ when } C_P \leq 0.7$$

$$c_{19} = 0.18567/(1.3571 - C_M) - 0.71276 + 0.38648 C_P \text{ when } C_P \geq 0.7$$

$$c_{20} = 1 + 0.015 C_{stern} \text{ where } C_{stern} \text{ depends upon the type of stern as given in Table A4.3.}$$

Table A4.3

Wake Coefficients for Different Stern Types

Stern Type	C_{stern}
Pram with gondola	-25.0
V shape sections	-10.0
Normal stern	0.0
U shape sections with Hogner stern	10.0

$$C_{P1} = 1.45 C_P - 0.315 - 0.0225 LCB$$

$$C_V = (1 + k) C_F + C_A$$

Single screw ships with open stern

$$w = 0.3 C_B + 10 C_V C_B - 0.1 \quad (A4.14)$$

Twin screw ships

$$w = 0.3095 C_B + 10 C_V C_B - 0.23 D/\sqrt{BT} \quad (A4.15)$$

Papmel (Reference not known)

$$w = 0.165 C_B^k \left(\frac{\nabla^{1/3}}{D} \right)^{\frac{1}{2}} + F_n - 0.2 \quad (A4.16)$$

where $k = 1.0$ for single screw ships and $k = 2.0$ for twin screw ships.

Thrust Deduction Fraction

Schoenherr (Rossell and Chapman, 1939)

Single screw ships

$$t = kw \quad (A4.17)$$

where

$k = 0.50-0.70$ with streamlined or contra rudders;

$k = 0.70-0.90$ with double plate rudders attached to square rudder posts;

$k = 0.90-1.05$ with single plate rudders.

Twin screw ships

$$t = 0.25 w + 0.14 \text{ with bossings} \quad (\text{A4.18})$$

$$t = 0.70 w + 0.06 \text{ with struts} \quad (\text{A4.19})$$

Edstrand (Reference not known)

Single screw ships

$$\frac{t}{w} = 1.57 - 2.3 \frac{C_B}{C_W} + 1.5 C_B \quad (\text{A4.20})$$

Twin screw ships

$$\frac{t}{w} = 1.67 - 2.3 \frac{C_B}{C_W} + 1.5 C_B \quad (\text{A4.21})$$

Harvald (1983)

Single screw ships

$$t = \sum_{i,j} a(i,j) C_B^i \left(\frac{B}{L} \right)^j \pm 0.02 + \left(1.98 \frac{D}{L} - 0.08 \right) \quad (\text{A4.22})$$

where the + sign is for U forms, the - sign is for V forms and the coefficients $a(i,j)$ are given in Table A4.4.

Table A4.4
Coefficients for Thrust Deduction
(Single Screw Ships)

<i>i</i>	<i>j</i>	<i>a</i> (<i>i, j</i>)
0	0	0.44197757e+00
1	0	-0.13492692e+01
2	0	0.11528267e+01
0	1	-0.11373258e+01
1	1	0.60955480e+01
2	1	-0.41455395e+01

Twin screw ships

$$t = \sum_i a(i) C_B^i + 4 \left(\frac{D}{L} - 0.03 \right) - 6 \left(\frac{TC}{L} - 0.005 \right) + \Delta t \quad (\text{A4.23})$$

where $\Delta t = 0$ with bossings, $\Delta t = -0.02$ with struts and the coefficients $a(i)$ are as given in Table A4.5.

Table A4.5
Coefficients for Thrust Deduction
(Twin Screw Ships)

<i>i</i>	<i>a</i> (<i>i</i>)
0	0.17300000e+00
1	-0.40928571e+00
2	0.64285714e+00

B.S.R.A. (Parker, 1966)

Single screw ships

$$\begin{aligned}
 t = & b_0 + b_1 C_B + b_2 C_B^2 + b_3 \frac{V}{C_B \sqrt{L}} + b_4 \left(\frac{V}{C_B \sqrt{L}} \right)^2 \\
 & + b_5 \left(\frac{V}{C_B \sqrt{L}} \right)^3 + b_6 \frac{V}{\sqrt{L}} + b_7 D_t \\
 & + b_8 \delta LCB + b_9 C_B \delta LCB
 \end{aligned} \tag{A4.24}$$

$$b_0 = -0.1158 \quad b_1 = 0.08859 \quad b_2 = 0.3133 \quad b_3 = 0.2758$$

$$b_4 = 0.05432 \quad b_5 = -0.02419 \quad b_6 = -0.4542 \quad b_7 = 0.6044$$

$$b_8 = 0.05171 \quad b_9 = -0.08622$$

$$D_t = \frac{DB}{\nabla^{\frac{2}{3}}} \quad \delta LCB = LCB - 20(C_B - 0.675)$$

V in knots, L in feet.

Holtrop (1984)

Single screw ships

$$t = \frac{0.25014 (B/L)^{0.28956} (\sqrt{BT}/D)^{0.2624}}{(1 - C_P + 0.0225 LCB)^{0.01762}} + 0.0015 C_{stern} \tag{A4.25}$$

Single screw ships with open sterns

$$t = 0.10 \tag{A4.26}$$

Twin screw ships

$$t = 0.325 C_B - 0.1885 D/\sqrt{BT} \tag{A4.27}$$

Relative Rotative Efficiency

Schoenherr (Rossell and Chapman, 1939)

Single screw ships

$$\eta_R = 1.02 \quad \text{average} \quad (\text{A4.28})$$

Twin screw ships

$$\eta_R = 0.985 \quad \text{average} \quad (\text{A4.29})$$

van Manen (Reference not known)

Single screw ships

$$\eta_R = 1.02-1.07 \quad \text{average} = 1.05 \quad (\text{A4.30})$$

Twin screw ships

$$\eta_R = 0.95-1.00 \quad \text{average} = 0.97 \quad (\text{A4.31})$$

B.S.R.A. (Parker, 1966)

Single screw ships

$$\eta_R = c_0 + c_1 C_B + c_2 C_B^2 + c_3 C_B \frac{V}{\sqrt{L}} + c_4 \frac{D}{\nabla^{1/3}} \quad (\text{A4.32})$$

$$c_0 = 1.716 \quad c_1 = -2.378 \quad c_2 = 1.742$$

$$c_3 = -0.0308 \quad c_4 = 0.6931$$

 V in knots, L in feet.

Holtrop (1984)

Single screw ships

$$\eta_R = 0.9922 - 0.05908 \frac{A_E}{A_O} + 0.07424 (C_P - 0.0225 LCB) \quad (A4.33)$$

Single screw ships with open sterns

$$\eta_R = 0.98 \quad (A4.34)$$

Twin screw ships

$$\eta_R = 0.9737 + 0.111 (C_P - 0.0225 LCB) - 0.06325 P/D \quad (A4.35)$$

APPENDIX 5

Propeller Blade Section Pressure Distribution

Table A5.1
Effect of Camber

$a = 0.8$		NACA Mean Lines $a = 0.8$ (modified)		$a = 1.0$	
$C_{Li} = 1.0$	$\alpha_i = 1.54^\circ$	$C_{Li} = 1.0$	$\alpha_i = 1.40^\circ$	$C_{Li} = 1.0$	$\alpha_i = 0^\circ$
x/c	$\Delta V_f/V_0$	x/c	$\Delta V_f/V_0$	x/c	$\Delta V_f/V_0$
0.0125	0.278	0.0125	0.273	0.0125	0.250
0.0250	0.278	0.0250	0.273	0.0250	0.250
0.0500	0.278	0.0500	0.273	0.0500	0.250
0.0750	0.278	0.0750	0.273	0.0750	0.250
0.1000	0.278	0.1000	0.273	0.1000	0.250
0.1500	0.278	0.1500	0.274	0.1500	0.250
0.2000	0.278	0.2000	0.274	0.2000	0.250
0.3000	0.278	0.3000	0.274	0.3000	0.250
0.4000	0.278	0.4000	0.275	0.4000	0.250
0.5000	0.278	0.5000	0.276	0.5000	0.250
0.6000	0.278	0.6000	0.276	0.6000	0.250
0.7000	0.278	0.7000	0.277	0.7000	0.250
0.8000	0.278	0.8000	0.278	0.8000	0.250

Table A5.1 (Contd.)

0.9000	0.139	0.9000	0.147	0.9000	0.250
0.9500	0.069	0.9500	0.092	0.9500	0.250
1.0000	0	1.0000	0	1.0000	0.250

Table A5.2

Effect of Thickness Distribution

(a)

Thickness Distribution: NACA 16

x/c	Values of $\Delta V_t/V_0$					
	$t/c = 0.06$	$t/c = 0.09$	$t/c = 0.12$	$t/c = 0.15$	$t/c = 0.18$	$t/c = 0.21$
0	0	0	0	0	0	0
0.0125	0.029	0.021	0.001	-0.022	-0.050	-0.091
0.0250	0.042	0.053	0.053	0.051	0.045	0.031
0.0500	0.047	0.067	0.083	0.095	0.103	0.105
0.0750	0.051	0.073	0.094	0.113	0.128	0.138
0.1000	0.053	0.076	0.099	0.121	0.141	0.159
0.1500	0.055	0.081	0.106	0.130	0.154	0.179
0.2000	0.057	0.085	0.112	0.139	0.165	0.191
0.3000	0.060	0.091	0.121	0.152	0.183	0.214
0.4000	0.064	0.096	0.128	0.161	0.194	0.227
0.5000	0.066	0.100	0.134	0.168	0.203	0.239
0.6000	0.068	0.106	0.137	0.172	0.205	0.237
0.7000	0.064	0.099	0.129	0.161	0.192	0.223
0.8000	0.057	0.075	0.097	0.120	0.143	0.166
0.9000	0.017	0.022	0.025	0.026	0.025	0.019
0.9500	-0.019	-0.031	-0.047	-0.065	-0.085	-0.105
1.0000	0	0	0	0	0	0

Table A5.2
Effect of Thickness Distribution
(b)
Thickness Distribution: NACA 66

x/c	Values of $\Delta V_t/V_0$					
	$t/c = 0.06$	$t/c = 0.09$	$t/c = 0.12$	$t/c = 0.15$	$t/c = 0.18$	$t/c = 0.21$
0	0	0	0	0	0	0
0.0125	0.031	0.018	-0.010	-0.036	-0.103	-0.131
0.0250	0.035	0.039	0.036	0.027	0.002	-0.024
0.0500	0.042	0.058	0.067	0.078	0.074	0.069
0.0750	0.048	0.069	0.085	0.099	0.111	0.116
0.1000	0.052	0.077	0.097	0.114	0.134	0.148
0.1500	0.058	0.085	0.112	0.134	0.162	0.185
0.2000	0.062	0.091	0.122	0.148	0.180	0.208
0.3000	0.067	0.100	0.134	0.164	0.202	0.236
0.4000	0.070	0.105	0.142	0.175	0.217	0.255
0.5000	0.073	0.110	0.148	0.184	0.228	0.269
0.6000	0.075	0.114	0.154	0.192	0.238	0.284
0.7000	0.057	0.083	0.105	0.122	0.141	0.155
0.8000	0.020	0.025	0.026	0.026	0.022	0.015
0.9000	-0.026	-0.043	-0.062	-0.080	-0.104	-0.127
0.9500	-0.057	-0.084	-0.112	-0.137	-0.168	-0.195
1.0000	-0.093	-0.136	-0.171	-0.201	-0.234	-0.266

Table A5.3
Effect of Angle of Attack
(a)
Thickness Distribution: NACA 16

x/c	Values of $\Delta V_{\alpha i}/V_0$					
	$t/c = 0.06$	$t/c = 0.09$	$t/c = 0.12$	$t/c = 0.15$	$t/c = 0.18$	$t/c = 0.21$
0	5.471	3.644	2.624	2.041	1.744	1.574
0.0125	1.376	1.330	1.268	1.209	1.140	1.069

Table A5.3(a) (Contd.)

0.0250	0.980	0.964	0.942	0.916	0.883	0.828
0.0500	0.689	0.684	0.677	0.668	0.657	0.640
0.0750	0.557	0.554	0.551	0.547	0.541	0.534
0.1000	0.476	0.475	0.473	0.471	0.468	0.463
0.1500	0.379	0.378	0.378	0.377	0.376	0.374
0.2000	0.319	0.319	0.319	0.318	0.318	0.317
0.3000	0.244	0.245	0.245	0.245	0.245	0.245
0.4000	0.196	0.197	0.197	0.197	0.198	0.198
0.5000	0.160	0.160	0.161	0.161	0.162	0.162
0.6000	0.130	0.131	0.131	0.131	0.131	0.131
0.7000	0.104	0.103	0.102	0.102	0.102	0.102
0.8000	0.077	0.076	0.075	0.074	0.073	0.072
0.9000	0.049	0.047	0.045	0.043	0.042	0.041
0.9500	0.032	0.030	0.027	0.025	0.024	0.023
1.0000	0	0	0	0	0	0

Table A5.3

Effect of Angle of Attack

(b)

Thickness Distribution: NACA 66

x/c	Values of $\Delta V_{\alpha i}/V_0$					
	$t/c = 0.06$	$t/c = 0.09$	$t/c = 0.12$	$t/c = 0.15$	$t/c = 0.18$	$t/c = 0.21$
0	4.941	3.352	2.569	2.139	1.773	1.547
0.0125	1.500	1.340	1.237	1.172	1.121	1.054
0.0250	0.967	0.940	0.913	0.895	0.858	0.828
0.0500	0.695	0.686	0.674	0.663	0.649	0.635
0.0750	0.554	0.552	0.549	0.547	0.545	0.542
0.1000	0.474	0.473	0.473	0.473	0.472	0.472
0.1500	0.379	0.379	0.380	0.381	0.381	0.381
0.2000	0.320	0.322	0.323	0.323	0.323	0.324
0.3000	0.245	0.246	0.246	0.248	0.250	0.251
0.4000	0.197	0.197	0.197	0.200	0.201	0.202
0.5000	0.161	0.161	0.162	0.163	0.163	0.165

Table A5.3(b) (Contd.)

0.6000	0.130	0.130	0.132	0.131	0.131	0.132
0.7000	0.102	0.100	0.098	0.096	0.095	0.093
0.8000	0.075	0.071	0.069	0.065	0.061	0.058
0.9000	0.047	0.043	0.040	0.039	0.037	0.034
0.9500	0.030	0.028	0.031	0.025	0.022	0.020
1.0000	0	0	0	0	0	0

APPENDIX 6

Goldstein Factors

$$\kappa = a + b \left(\frac{1}{\lambda_I} \right) + c \left(\frac{1}{\lambda_I} \right)^2 + d \left(\frac{1}{\lambda_I} \right)^3 \quad (\text{A6.1})$$

Table A6.1
Number of Blades, $Z = 3$

r/R	a	b	c	d
0.200	0.17886909e+01	-0.31486830e+00	0.40256411e-01	-0.16456876e-02
0.300	0.12344242e+01	-0.13838772e+00	0.24405595e-01	-0.14421134e-02
0.400	0.85886669e+00	0.22855088e-01	0.12983683e-02	-0.32012432e-03
0.500	0.62018788e+00	0.12671252e+00	-0.13955711e-01	0.45532247e-03
0.600	0.41573334e+00	0.21640132e+00	-0.28552448e-01	0.13177933e-02
0.700	0.27236363e+00	0.25907344e+00	-0.34629371e-01	0.16923076e-02
0.800	0.14103636e+00	0.28452680e+00	-0.40822845e-01	0.23263404e-02
0.850	0.10892727e+00	0.25856760e+00	-0.35081584e-01	0.19533799e-02
0.900	0.26095757e+00	0.11420357e-01	0.41284382e-01	-0.54623154e-02
0.950	0.34436364e-01	0.17165734e+00	-0.21487178e-01	0.11934732e-02
0.975	0.14018182e-01	0.12805361e+00	-0.16160838e-01	0.95571094e-03

Table A6.2
Number of Blades, $Z = 4$

r/R	a	b	c	d
0.200	0.17496364e+01	-0.33573776e+00	0.50925408e-01	-0.26573427e-02
0.300	0.13368727e+01	-0.19570281e+00	0.36153845e-01	-0.22237762e-02
0.400	0.10046545e+01	-0.29904429e-01	0.76526809e-02	-0.53613057e-03

Table A6.2 (Contd.)

0.500	0.74438787e+00	0.10496193e+00	-0.15128205e-01	0.71173272e-03
0.600	0.50827879e+00	0.23900738e+00	-0.41976690e-01	0.25905205e-02
0.700	0.36886668e+00	0.27456838e+00	-0.43508161e-01	0.24397825e-02
0.800	0.21533333e+00	0.30709362e+00	-0.48083916e-01	0.28236208e-02
0.850	0.16254544e+00	0.28706294e+00	-0.41976690e-01	0.23682984e-02
0.900	0.94375759e-01	0.26828283e+00	-0.38787879e-01	0.22626263e-02
0.950	0.26442423e-01	0.22522765e+00	-0.33561774e-01	0.20916860e-02
0.975	0.30242424e-02	0.16694678e+00	-0.23643358e-01	0.14390054e-02

Table A6.3

Number of Blades, $Z = 5$

r/R	a	b	c	d
0.200	0.16373152e+01	-0.30654624e+00	0.50608393e-01	-0.29106450e-02
0.300	0.12795818e+01	-0.15718766e+00	0.27790209e-01	-0.16177156e-02
0.400	0.10774000e+01	-0.63247085e-01	0.13892774e-01	-0.97902096e-03
0.500	0.85581213e+00	0.63054390e-01	-0.97389277e-02	0.47241646e-03
0.600	0.65652120e+00	0.17247047e+00	-0.29790210e-01	0.16985236e-02
0.700	0.46110910e+00	0.26796621e+00	-0.47247086e-01	0.28717949e-02
0.800	0.32359999e+00	0.28312004e+00	-0.44466201e-01	0.25128205e-02
0.850	0.22852121e+00	0.29787374e+00	-0.46969697e-01	0.28080808e-02
0.900	0.16675758e+00	0.26352641e+00	-0.37958041e-01	0.21740482e-02
0.950	0.57478789e-01	0.24161461e+00	-0.37601400e-01	0.24413364e-02
0.975	0.15157576e-01	0.18922222e+00	-0.28424243e-01	0.17777778e-02

Table A6.4

Number of Blades, $Z = 6$

r/R	a	b	c	d
0.200	0.14782788e+01	-0.21982946e+00	0.33473194e-01	-0.16891997e-02
0.300	0.13151879e+01	-0.18757537e+00	0.35438228e-01	-0.21507381e-02
0.400	0.11262424e+01	-0.94499610e-01	0.21074591e-01	-0.14840715e-02
0.500	0.92697579e+00	0.32015931e-01	-0.50023310e-02	0.24397824e-03
0.600	0.73245454e+00	0.15420629e+00	-0.30512821e-01	0.20186480e-02
0.700	0.57758790e+00	0.22007382e+00	-0.39191142e-01	0.23294482e-02
0.800	0.38398787e+00	0.28972650e+00	-0.49876455e-01	0.30287490e-02
0.850	0.31183636e+00	0.27915269e+00	-0.43412589e-01	0.24568764e-02
0.900	0.20169698e+00	0.28262860e+00	-0.43582752e-01	0.25905205e-02
0.950	0.19169698e-01	0.32737219e+00	-0.64843826e-01	0.51686093e-02
0.975	0.40769696e-01	0.19129409e+00	-0.28200466e-01	0.17700078e-02

APPENDIX 7

Cavitation Buckets

The following formulas are based on material given in Breslin and Andersen (1994).

The maximum and minimum values of angle of attack within which there is no cavitation are given by:

$$\begin{aligned}\alpha_{\max} &= a_1 \frac{f}{c} + a_2 \frac{t}{c} \sqrt{\left[-C_{p\min} + a_3 \frac{t}{c} + a_4 \frac{f}{c} \right]} \\ \alpha_{\min} &= a_1 \frac{f}{c} - a_2 \frac{t}{c} \sqrt{\left[-C_{p\min} + a_3 \frac{t}{c} - a_4 \frac{f}{c} \right]}\end{aligned}\quad (\text{A7.1})$$

where the constants a_1, a_2, a_3, a_4 depend on the mean line and the thickness distribution of the blade section and are given in Table A7.1.

Table A7.1
Coefficients of Minimum and Maximum Angles of Attack

Mean Line	Thickness Distribution	a_1	a_2	a_3	a_4
$a = 0.8$	NACA-16	22.6804	28.3183	-2.28	8.1820
$a = 0.8$ (modified)	NACA-66 (modified)	21.0495	27.1163	-2.42	8.3530
$a = 0.8$ (modified)	NACA-16	22.6804	28.3183	-2.28	8.3530
$a = 1.0$	NACA-16	0	28.3183	-2.28	9.0662
$a = 1.0$	NACA-66 (modified)	0	27.11631	-2.42	9.0662

APPENDIX 8

Lifting Surface Correction Factors

A complete set of tables of the lifting surface correction factors (which are functions of the number of blades, the expanded blade area ratio and the skew angle as well as the non-dimensional radius and the advance ratio) would occupy too much space. Only three tables are given here for use with the problems given in the book.

Table A8.1

Number of blades = 3

Expanded blade area ratio = 0.8500

Skew angle = 0 degrees

$\lambda_I:$		0.1000	0.2000	0.3000	0.4000	0.5000	0.6000	0.7000
x								
0.2000	$k_a:$	4.0881	2.4545	1.1668	0.2252	-0.3704	-0.6200	-0.5237
	$k_c:$	1.9633	1.2688	1.0742	1.3794	2.1846	3.4896	5.2945
	$k_t:$	2.4393	2.1302	1.8698	1.6583	1.4956	1.3818	1.3167
0.3000	$k_a:$	2.7960	2.3315	1.9668	1.7018	1.5366	1.4712	1.5055
	$k_c:$	1.4609	1.2802	1.2666	1.4202	1.7409	2.2288	2.8838
	$k_t:$	0.9068	0.5941	0.3594	0.2027	0.1240	0.1233	0.2006
0.4000	$k_a:$	2.1372	2.1309	2.0856	2.0013	1.8780	1.7157	1.5144
	$k_c:$	1.2192	1.3359	1.4265	1.4913	1.5300	1.5428	1.5297
	$k_t:$	0.5065	0.3627	0.2541	0.1808	0.1428	0.1400	0.1724
0.5000	$k_a:$	1.6594	1.9082	2.0099	1.9645	1.7721	1.4326	0.9461
	$k_c:$	1.2382	1.4358	1.5539	1.5926	1.5519	1.4317	1.2321
	$k_t:$	0.2625	0.2136	0.1767	0.1520	0.1394	0.1388	0.1504

Table A8.1 (Contd.)

0.6000	k_a :	1.6879	1.8825	2.0145	2.0837	2.0902	2.0341	1.9152
	k_c :	1.2147	1.5719	1.7117	1.6341	1.3391	0.8266	0.0967
	k_t :	0.1295	0.1261	0.1237	0.1223	0.1219	0.1225	0.1241
0.7000	k_a :	1.7113	2.0131	2.1133	2.0119	1.7089	1.2042	0.4980
	k_c :	1.6042	1.7956	1.9230	1.9865	1.9861	1.9218	1.7936
	k_t :	0.0733	0.0830	0.0901	0.0947	0.0967	0.0961	0.0930
0.8000	k_a :	1.8759	2.2440	2.3479	2.1878	1.7635	1.0751	0.1225
	k_c :	2.0898	2.1562	2.1864	2.1803	2.1379	2.0593	1.9444
	k_t :	0.0455	0.0575	0.0658	0.0704	0.0712	0.0684	0.0618
0.9000	k_a :	3.5358	2.9384	2.8928	3.3990	4.4571	6.0669	8.2285
	k_c :	2.9693	2.8880	2.7861	2.6637	2.5207	2.3571	2.1730
	k_t :	0.0061	0.0262	0.0415	0.0519	0.0574	0.0581	0.0539

Table A8.2

Number of blades = 4

Expanded blade area ratio = 0.5000

Skew angle = 10 degrees

	λ_f :	0.1000	0.2000	0.3000	0.4000	0.5000	0.6000	0.7000
x								
0.2000	k_a :	2.5026	2.3229	2.1816	2.0786	2.0139	1.9875	1.9993
	k_c :	1.9198	1.8014	1.7290	1.7028	1.7226	1.7886	1.9006
	k_t :	0.7149	0.5356	0.3903	0.2790	0.2016	0.1582	0.1488
0.3000	k_a :	2.2003	2.1983	2.2008	2.2076	2.2189	2.2347	2.2548
	k_c :	1.2921	1.2883	1.2975	1.3197	1.3550	1.4033	1.4647
	k_t :	0.4565	0.3733	0.3033	0.2464	0.2028	0.1723	0.1549
0.4000	k_a :	1.9155	2.0267	2.1209	2.1981	2.2582	2.3013	2.3275
	k_c :	0.9709	1.0347	1.0910	1.1399	1.1815	1.2156	1.2423
	k_t :	0.2539	0.2409	0.2260	0.2093	0.1907	0.1704	0.1482
0.5000	k_a :	1.6481	1.8081	1.9421	2.0499	2.1317	2.1875	2.2172
	k_c :	0.9562	1.0405	1.1095	1.1633	1.2019	1.2253	1.2335
	k_t :	0.1074	0.1385	0.1586	0.1676	0.1656	0.1525	0.1284
0.6000	k_a :	1.5556	1.6800	1.7882	1.8801	1.9558	2.0152	2.0584
	k_c :	1.0260	1.1075	1.1727	1.2217	1.2545	1.2710	1.2713
	k_t :	0.0497	0.0850	0.1101	0.1252	0.1301	0.1249	0.1096

Table A8.2 (Contd.)

0.7000	k_a :	1.4797	1.5251	1.5721	1.6207	1.6710	1.7230	1.7766
	k_c :	1.1490	1.2248	1.2835	1.3249	1.3491	1.3561	1.3460
	k_t :	0.0307	0.0559	0.0748	0.0877	0.0944	0.0949	0.0893
0.8000	k_a :	1.3785	1.3087	1.2565	1.2217	1.2045	1.2047	1.2223
	k_c :	1.3493	1.4030	1.4437	1.4712	1.4857	1.4871	1.4754
	k_t :	0.0228	0.0379	0.0502	0.0596	0.0662	0.0699	0.0708
0.9000	k_a :	1.1158	0.8078	0.5715	0.4070	0.3142	0.2931	0.3437
	k_c :	1.8914	1.8661	1.8463	1.8318	1.8227	1.8189	1.8206
	k_t :	-0.0050	0.0169	0.0342	0.0468	0.0548	0.0581	0.0568

Table A8.3

Number of blades = 6

Expanded blade area ratio = 0.7750

Skew angle = 15 degrees

	λ_I :	0.1000	0.2000	0.3000	0.4000	0.5000	0.6000	0.7000
x								
0.2000	k_a :	2.1223	2.0849	2.0400	1.9876	1.9277	1.8603	1.7854
	k_c :	2.6302	2.3942	2.2288	2.1339	2.1097	2.1559	2.2728
	k_t :	2.5350	1.8469	1.3030	0.9033	0.6477	0.5362	0.5689
0.3000	k_a :	2.5408	2.5774	2.6027	2.6167	2.6195	2.6109	2.5911
	k_c :	1.5118	1.5221	1.5397	1.5645	1.5966	1.6359	1.6824
	k_t :	1.5705	1.2302	0.9542	0.7424	0.5950	0.5117	0.4928
0.4000	k_a :	2.5051	2.6288	2.7321	2.8149	2.8773	2.9193	2.9409
	k_c :	0.9198	1.0581	1.1707	1.2577	1.3190	1.3547	1.3647
	k_t :	0.8741	0.7662	0.6707	0.5877	0.5173	0.4593	0.4139
0.5000	k_a :	2.0151	2.2391	2.4282	2.5823	2.7014	2.7856	2.8348
	k_c :	0.8543	1.0022	1.1219	1.2136	1.2770	1.3123	1.3195
	k_t :	0.4459	0.4548	0.4525	0.4391	0.4146	0.3790	0.3322
0.6000	k_a :	1.7607	1.9792	2.1695	2.3318	2.4660	2.5721	2.6502
	k_c :	0.9034	1.0410	1.1523	1.2373	1.2960	1.3284	1.3344
	k_t :	0.2160	0.2627	0.2931	0.3074	0.3056	0.2875	0.2534
0.7000	k_a :	1.5517	1.7010	1.8345	1.9521	2.0539	2.1399	2.2100
	k_c :	1.0287	1.1547	1.2555	1.3311	1.3815	1.4067	1.4067
	k_t :	0.1118	0.1531	0.1827	0.2007	0.2071	0.2018	0.1848

Table A8.1 (Contd.)

0.8000	k_a :	1.2863	1.2938	1.3085	1.3305	1.3597	1.3962	1.4399
	k_c :	1.2231	1.3441	1.4379	1.5047	1.5443	1.5568	1.5422
	k_t :	0.0644	0.0930	0.1146	0.1291	0.1365	0.1369	0.1303
0.9000	k_a :	0.8551	0.5528	0.3093	0.1246	-0.0013	-0.0684	-0.0767
	k_c :	1.9001	1.9105	1.9176	1.9212	1.9215	1.9184	1.9118
	k_t :	-0.0008	0.0463	0.0810	0.1033	0.1132	0.1107	0.0957

Review Questions

1. Describe the development of ocean transportation from prehistoric times to the present day.
2. On a sketch of a screw propeller, indicate the following: boss, blade, root, tip, face, back, leading edge and trailing edge.
3. The momentum theory of propellers is said to be based on correct fundamental principles while the blade element theory is said to rest on observed facts. Explain.
4. What are the conditions that must be fulfilled in carrying out model tests with propellers?
5. Explain how the hull and the propeller of a ship interact with each other.
6. What is cavitation? How is cavitation affected by the temperature and the air content of water?
7. What are the forces that are normally taken into account in calculating the stresses in a propeller blade? What are the factors that are not taken into account?
8. What are the objectives of carrying out (a) resistance experiments, (b) open water experiments and (c) self-propulsion experiments with ship models and model propellers?
9. What is the main difference between the design of propellers for merchant ships and the design of propellers for tugs and trawlers?

10. What are the tests and trials that are carried out on a ship before it is delivered to its owners?
11. What are the steps that can be taken to minimise propeller excited vibration in a ship?
12. What are the reasons for adopting unconventional propulsion devices in some ships?
13. Enumerate the different types of ships commonly used today.
14. Explain the concept of the pitch of a screw propeller. What is variable pitch?
15. Why is the propeller efficiency derived from the axial momentum theory called an "ideal efficiency"? In which condition will this efficiency be 100 percent?
16. Why is it not possible to make the Reynolds numbers of a ship propeller and its model equal and simultaneously make the two Froude numbers equal too? Why are the Froude numbers made equal rather than the Reynolds numbers?
17. The wake of a ship has three component causes. Which of these components would be absent if: (a) the ship was moving in an inviscid fluid, (b) the ship had an infinitesimal breadth, and (c) the ship was moving deeply submerged? Can you think of a situation in which the wake fraction would be zero at all speeds?
18. How does cavitation affect the performance of a marine propeller?
19. How are the stresses in a propeller blade affected by (a) the mass of the blade, (b) the propeller rpm, (c) the rake of the blade and (d) its skew, the thrust and torque being fixed?
20. How are the differences between the conditions of the model experiment and the operating conditions of a ship taken into account in determining the effective power of the ship?
21. What are the two approaches to propeller design? Discuss their comparative advantages.

22. Why are the speed trials of a ship carried out?
23. How does the number of blades in a propeller affect the occurrence of unsteady forces at certain frequencies?
24. What are the advantages and disadvantages of using feathering paddle wheels instead of wheels with fixed paddles?
25. Discuss the development of ship propulsion machinery during the last two hundred years.
26. Explain the terms rake and skew with reference to a propeller blade. What is skew induced rake? What is warp?
27. In the axial momentum theory, the pressure in the slipstream far astern of the propeller is equal to the pressure far ahead. Will this be true if the rotation of the slipstream is taken into account?
28. In an open water test with a model propeller, the thrust and torque coefficients are taken to be functions only of the advance coefficient, while the Froude number, the Reynolds number and the Euler number are neglected. How is this justified?
29. What is the difference between the nominal wake and the effective wake?
30. Describe the different types of cavitation and the conditions under which they occur.
31. What are the desirable properties in a material used for making propellers?
32. Why is it important to obtain turbulent flow in model experiments with ship models and model propellers? What steps are taken to ensure turbulent flow?
33. What are the considerations in selecting (a) the number of propellers in a ship, (b) the number of blades in a propeller, (c) the propeller diameter, (d) the rake of the propeller blades, and (d) the propeller blade skew?

34. If you were charged with carrying out the speed trials of a ship, how would you go about it?
35. Explain how an anti-singing edge eliminates the singing of a propeller.
36. In what types of ships would you consider the use of a controllable pitch propeller, and why?
37. What are the contributions made to ship propulsion by its pioneers: Colonel Stevens, Josef Ressel, Ericsson and Petit-Smith?
38. How would you obtain the expanded and developed blade outlines of a propeller from the projected outline?
39. Sketch the velocity and force diagrams of a propeller blade section (a) neglecting induced velocities and section drag, (b) including induced velocities but neglecting drag, and (c) including both induced velocities and drag.
40. Why can propeller cavitation not be studied by model experiments in a conventional ship model tank?
41. Why does thrust deduction occur?
42. What are the steps that a propeller designer can take to prevent propeller cavitation?
43. What are the additional forces and moments that occur in a propeller blade due to large skew?
44. What are the quantities that are measured in a self-propulsion test?
45. What are the factors to be considered in determining the shape of propeller blade sections and their thicknesses?
46. In analysing the data of speed trials, how does one account for the effects of (a) currents in the water, and (b) wind?
47. How are self-propulsion experiments carried out in waves?
48. Ducted propellers may have either accelerating ducts or decelerating ducts. What are the reasons for choosing one type or the other?

49. What are the different types of propulsion devices used in ships?
50. A propeller blade section is of a segmental shape with a chord c and a thickness t . What is its camber ratio? If the blade section were lenticular, what would be its camber?
51. Explain the concept of circulation and describe how it gives rise to lift in an aerofoil section.
52. What is a methodical propeller series? What are the parameters that are varied in a typical methodical series?
53. Why is the relative rotative efficiency not equal to 1 in general?
54. How is the cavitation of a propeller blade section affected by the shape of its mean line, the camber ratio, the thickness ratio and the angle of attack?
55. How do the blade sections of a supercavitating propeller differ from those of a conventional propeller?
56. Explain the concept of "ship self-propulsion point on the model". Why is a ship model not generally fully self-propelled in a self-propulsion experiment?
57. In propeller design why is the optimum propeller diameter determined from methodical series data sometimes reduced by a small amount?
58. What are the major factors that affect the propulsive performance of a ship in service?
59. What is the effect of surface roughness on the performance of a propeller?
60. How do the open water characteristics of a surface piercing propeller differ from those of a conventional propeller?
61. Distinguish between nominal slip, apparent slip and effective slip. How is effective slip related to the effective pitch of a propeller?
62. Describe the vortex system of a wing of finite span. How is this vortex system related to the vortex system of a propeller blade?

63. Why are B_P - δ diagrams more convenient to use in propeller design than K_T - K_Q diagrams?
64. What are the components of the propulsive efficiency of a ship? How would these components be affected if the propeller were placed in front of the ship rather than behind it?
65. What are the dimensional parameters whose values must be carefully controlled in manufacturing a propeller?
66. Why are contra-rotating propellers more efficient than single propellers for the same thrust?
67. Why is it desirable to carry out direct wake measurements instead of merely determining the wake fraction through open water and self-propulsion experiments?
68. What are the advantages and disadvantages of designing a tug propeller for (a) the bollard pull condition and (b) the free running condition?
69. What are the benefits of analysing the service performance of a ship?
70. Describe how you would determine theoretically the time taken to stop a ship moving full speed ahead if its propeller is used for stopping the ship.
71. In a vane wheel propeller, the vanes act as turbine blades at the inner radii and as propeller blades at the outer radii. Explain.
72. What are the major non-dimensional parameters used to describe a screw propeller?
73. Discuss the condition in which a propeller has the highest efficiency for a given speed of advance and revolution rate.
74. Why can B_P - δ diagrams not be used for designing tug propellers? What type of diagrams are specially meant for designing tug propellers?

75. What do you understand by the effective power of a ship? Describe the stages by which the power produced by the main engine of the ship is transformed into the effective power.
76. Discuss the relation between the maximum rated output of the propulsion plant and the power for which the propeller is designed.
77. Outline the principal steps in designing a propeller using the lifting line theory.
78. Explain the concepts of "service margin" and "engine margin" on the power of a ship propulsion plant. On what factors do these margins depend?
79. Explain the action of a Voith-Schneider propeller, and show with the help of a sketch how it may be used to stop a ship moving ahead.
80. What are the geometrical parameters upon which the mass and polar moment of inertia of a screw propeller depend? If in two geometrically similar propellers one has a diameter twice that of the other, what will be the ratios of their masses and polar moments of inertia?
81. Describe the recent developments in propeller theory.
82. Discuss the components of the overall efficiency of a waterjet propulsion system.

Miscellaneous Problems

1. A ship with a resistance of 500 kN at a speed of 15 knots has a propeller whose thrust is 585 kN and torque 425 kN m. The shaft losses are 3 percent, the propeller rpm being 120. The propeller is estimated to produce a thrust of 585 kN in open water when running at 120 rpm at a speed of 12 knots, the corresponding torque being 450 kN m. Determine the effective power, the thrust power, the delivered power, the brake power, the wake fraction, the thrust deduction fraction, the hull efficiency, the propeller open water efficiency and the relative rotative efficiency. What is the propulsive efficiency?
2. A ship is to have a speed of 20 knots with its propeller of 5.0 m diameter running at 180 rpm, the depth of immersion of the propeller axis being 4.0 m. At what speed of advance and at what pressure must a 0.125 m diameter model of the propeller be tested in a cavitation tunnel if the model propeller is to be run at 900 rpm? Wake fraction = 0.250.
3. A four-bladed propeller of 4.0 m diameter and 0.6 constant pitch ratio develops a thrust of 300 kN and a torque of 150 kN m at 180 rpm. The propeller has a blade thickness fraction of 0.045, the thickness varying linearly along the radius to 12 mm at the blade tip. The root section is at $0.2R$ and has an area given by $0.75ct$ and a section modulus equal to $0.12ct^2$, where c is the chord and t the thickness. The chord at $0.2R$ has a length of 900 mm. Each blade of the propeller has a mass of 400 kg, its centroid being at a radius of 0.950 m and 0.100 m aft of the centroid of the root section. The thrust and torque per unit length increase linearly from a value of $0.4k$ at $0.2R$ to $1.0k$ at $0.5R$, remain constant up to $0.9R$, and decrease linearly to zero at $1.0R$, k being a constant. Determine the tensile stress in the root section.

4. A resistance experiment is carried out on a model of length 4.0 m and wetted surface 4.50 m^2 without appendages, and the following results obtained:

Model speed, ms^{-1} :	0.514	0.772	1.029	1.286	1.543	1.800
Model resistance, N :	2.594	5.486	9.663	15.397	26.029	42.069

Determine for the corresponding speeds the resistance of a geometrically similar ship of length 100 m using the ITTC friction line with a correlation allowance of 0.0004 and adding 10 percent to allow for appendages and air resistance. Neglect form factor.

5. A single-screw ship is required to have a speed of 20 knots at which its effective power is 9500 kW. The wake fraction is 0.180, the thrust deduction fraction 0.145 and the relative rotative efficiency 1.030, based on thrust identity. The maximum propeller diameter that can be fitted in the ship is 6.0 m, while the minimum expanded blade area required is estimated to be 0.700. The propeller is to have four blades and to be directly connected to the engine placed aft in the ship. Using the data of Table 9.2, determine the brake power and rpm of the engine, and the corresponding pitch ratio of the propeller.
6. A ship has an engine of maximum continuous rating 9500 kW at 132 rpm directly connected to a propeller of 5.5 m diameter and 0.8 pitch ratio. Determine the maximum rpm at which the engine can be run during dock trials if (a) the torque is not to exceed 80 percent of the maximum rated torque, (b) the maximum allowable longitudinal force on the ship is 800 kN, and (c) the propeller slipstream velocity is to be limited to 8.0 ms^{-1} . The thrust and torque coefficients of the propeller are $K_T = 0.3415$, $10K_Q = 0.4021$ at $J = 0$. The thrust deduction fraction in the static condition is 0.050 and the relative rotative efficiency (thrust identity) is 1.030. The shafting efficiency is 0.970. The slipstream velocity may be calculated from the axial momentum theory.
7. A ship of displacement 8750 tonnes has a propeller of 6.5 m diameter and 0.8 pitch ratio whose open water characteristics are given by:

$$K_T = 0.3415 - 0.2589J - 0.1656J^2$$

$$10K_Q = 0.4021 - 0.2329J - 0.2101J^2$$

The wake fraction of the ship is 0.250, independent of speed, the thrust deduction fraction is given by $t = 0.100 + 0.007 V_K$, where V_K is the ship speed in knots, and the relative rotative efficiency is 1.000. The effective power of the ship is given by $0.1665 V_K^{3.6}$ kW. The propeller is directly connected to a diesel engine of 9000 kW brake power at 108 rpm, the shafting efficiency being 0.980. The ship has a design speed of 18.00 knots. If the ship starts from rest, determine the time taken by it to reach a speed of 17.99 knots and the distance travelled, given that neither the maximum engine torque nor the maximum rpm may be exceeded. The added mass is 5 percent of the ship's displacement. Carry out the calculations at 15 second intervals.

8. The expanded blade widths of a four-bladed propeller of 5.0 m diameter are as follows:

r/R	:	0.2	0.3	0.4	0.5	0.6	0.7	0.8	0.9	1.0
Blade width, mm:		989	1483	1760	1879	1978	1928	1701	1315	0

Determine the expanded blade area ratio.

9. A propeller of diameter 4.0 m operating 4.5 m below the surface of water has a speed of advance of 5.0 m per sec. The axial velocity of water in the slipstream is 2.5 m per sec far behind the propeller. Using the axial momentum theory, determine the propeller thrust and the pressures and velocities in the slipstream relative to the propeller far ahead, just ahead, just behind and far behind the propeller.
10. A ship propeller of diameter 5.0 m running at 120 rpm and a speed of advance of 6.0 m per sec has a thrust of 500 kN and a torque of 375 kN m. If a model propeller of 0.25 m diameter is to be tested at the same Reynolds number and the same advance coefficient, determine its speed of advance, rpm, thrust and torque. If the depth of immersion of the ship propeller is 6.0 m, what should be the depth of immersion of the model propeller? What will be the ratio of the Froude number

of the ship propeller to that of the model propeller and the ratio of the corresponding cavitation numbers?

11. A ship has a propeller of 5.0 m diameter. When the propeller runs at 120 rpm, it has a delivered power of 6000 kW and the ship has a speed of 16 knots at which its effective power is 4000 kW. The wake fraction is 0.280, the thrust deduction fraction 0.190 and the relative rotative efficiency 1.050, based on thrust identity. Calculate the hull efficiency, the propeller efficiency in open water, the propeller thrust and torque, the thrust power, and the advance, thrust and torque coefficients.
12. A ship has a propeller of 5.0 m diameter whose axis is 4.5 m below the load waterline. The ship has a speed of 20 knots at a propeller rpm of 180. The effective power of the ship at 20 knots is 7500 kW, and the propeller efficiency in open water is 0.600. The wake fraction is 0.200, the thrust deduction fraction 0.150 and the relative rotative efficiency 1.020. A model of the propeller made to a scale 1:10 is to be tested in a cavitation tunnel at an rpm of 1200. What should be the speed of water and the pressure in the cavitation tunnel? Determine the thrust and torque of the model propeller.
13. A four-bladed propeller of 5.0 m diameter has the following distribution of pitch ratio and blade widths:

$r/R :$	0.2	0.3	0.4	0.5	0.6	0.7	0.8	0.9	1.0
$P/D :$	0.7000	0.7217	0.7425	0.7625	0.7817	0.8000	0.8175	0.8342	0.8500
$c/D :$	0.225	0.249	0.270	0.288	0.301	0.307	0.299	0.260	0

The section modulus of the blade sections is given by $0.108ct^2$, where t is the thickness distributed linearly from root to tip, the tip thickness being 15 mm and the blade thickness fraction being 0.050. The propeller has a speed of advance of 7.5 m per sec at 150 rpm, the delivered power being 6000 kW and the thrust power 4000 kW. The thrust and torque distributions are given by:

$$\frac{dK_T}{dx} = k_1 x^2 (1-x)^{0.5} \quad \frac{dK_Q}{dx} = k_2 x^2 (1-x)^{0.5}$$

Determine the stress due to thrust and torque at the different radii, taking the root section to be at $0.2R$.

14. An open water experiment is carried out with a model propeller of 0.175 m diameter and 1.000 pitch ratio. The propeller has four blades, and at the section at $0.75R$ the chord-diameter ratio is 0.260 and the thickness-chord ratio 0.050. At the advance coefficient corresponding to the normal operating condition of the propeller, the following values are obtained:

$$\text{Speed of advance} = 6.3 \text{ m s}^{-1}$$

$$\text{Thrust} = 237.4 \text{ N}$$

$$\text{Model propeller rpm} = 2700$$

$$\text{Torque} = 7.810 \text{ N m}$$

Determine the advance coefficient, thrust coefficient, torque coefficient and open water efficiency of the model propeller. If the ship propeller of diameter 4.9 m has the same thrust, torque and advance coefficients as the model propeller, estimate the surface roughness of the ship propeller.

15. A single screw ship has an engine of 15000 kW at 150 rpm directly connected to the propeller. The wake fraction, thrust deduction fraction and relative rotative efficiency based on thrust identity are 0.180, 0.145 and 1.030 respectively, and the shafting efficiency is 0.980. The propeller axis is 5.5 m below the waterline. The effective power of the ship at different speeds is as follows:

Ship speed, knots	:	18.0	19.0	20.0	21.0
Effective power, kW:		6570	7939	9500	11269

Design the propeller using the data of Table 9.1.

16. A single-screw ship of length 90 m, wetted surface 1800 m^2 and above water transverse projected area 150 m^2 is taken out on trials and the following readings obtained during successive runs at constant power setting:

Run No.	1	2	3	4
Direction	N	S	N	S
Time at start, hr-min	15-15	15-41	16-06	16-33
Time on mile, min-sec	4-2.8	4-4.6	4-0.8	4-7.1
Propeller rpm	143.3	144.3	143.2	144.8
Shaft torque, kNm	198.2	201.8	199.2	202.4
Relative wind speed, knots	3.3	32.8	3.4	32.9

The wind during the trials has no significant component transverse to the ship. The slope of the effective power-speed curve for the ship speed under consideration is 512.4 kW per knot. The total resistance coefficient of the ship derived from model tests without any correlation allowance is as follows:

F_n	:	0.150	0.200	0.250	0.300
$10^3 C_T$:	3.0659	3.8799	4.5900	5.1960

If the overall propulsive coefficient of the ship is taken as 0.710, determine the correlation allowance C_A for the ship in the trial condition.

17. A single-screw tug has a propeller of 3.08 m diameter and 0.8 pitch ratio whose open water characteristics are given by:

$$K_T = 0.3415 - 0.2589 J - 0.1656 J^2$$

$$10K_Q = 0.4021 - 0.2329 J - 0.2101 J^2$$

The wake fraction is 0.250, the thrust deduction fraction in the free running condition is 0.210 and the relative rotative efficiency is 1.020, based on thrust identity. The effective power of the tug is given by $P_E = 0.01791 V_K^{3.7}$ kW, where V_K is the speed in knots. The propeller is connected through a double input single output gearbox to two identical diesel engines each of which can be uncoupled from the propeller. The shafting efficiency is 0.950. If the propeller is to run at a constant 180 rpm over the complete speed range of the tug, determine the minimum brake power of each engine. Determine also the speed of the

tug at which one of the engines can be uncoupled from the propeller without the maximum rated torque being exceeded. What is the free running speed of the tug and the brake power of the engine in this condition?

18. A propeller of diameter 5.0 m has a pitch ratio of 0.8. The expanded blade section of the propeller at $0.6R$ has a chord length of 1.750 m with the leading edge being 0.600 m forward of the reference line. The propeller has a rake of 10 degrees aft. Calculate the coordinates of the leading and trailing edges at $0.6R$ in the projected outline.
19. A propeller of diameter 3.0 m has a delivered power of 263 kW at zero speed. What is its thrust on the basis of the axial momentum theory?
20. It is estimated that a model propeller of 200 mm diameter has open water characteristics as follows:

$$K_T = 0.206 - 0.165 J - 0.106 J^2$$

$$10K_Q = 0.239 - 0.139 J - 0.125 J^2$$

Determine the maximum rpm and maximum speed of advance of the model propeller if the delivered power available from the drive motor is 1.0 kW and the open water test is to be carried out at the maximum rpm to cover the range of slip from zero to 100 percent. What is the maximum thrust to be measured?

21. A ship has a main engine of 10000 kW rated brake power at 120 rpm directly connected to a propeller of 5.0 m diameter. The ship has a wake fraction of 0.240, a thrust deduction fraction of 0.164 and a relative rotative efficiency of 1.050, based on thrust identity. The shaft losses are 2.0 percent. The ship attains a speed of 15.55 knots with the rated brake power and rpm. Its effective power at this speed is 6000 kW. Find the open water efficiency and the thrust and torque of the propeller.
22. A ship is to have a propeller of 4.5 m diameter and 0.75 pitch ratio with its axis 4.0 m below the load waterline. The ship speed is estimated to

be 16 knots at which the effective power is 4000 kW and the propeller rpm 120. The wake fraction is 0.280 and the thrust deduction fraction 0.190. Determine the blade area ratio of the propeller using the Burrill criterion for merchant ship propellers.

23. A four-bladed propeller of 6.0 m diameter has the following distribution of pitch ratio and blade width:

$$\frac{P(x)}{D} = 0.655 + 0.240x - 0.045x^2 \quad \frac{c(x)}{D} = 1.7x^{1.5}(1-x)$$

The blade thickness fraction of the propeller is 0.050, the blade thickness varies linearly with radius, and at the tip the thickness is 20 mm. The blade sections have an area given by $0.7ct$ and a section modulus given by $0.100ct^2$, where c and t are the chord length and thickness of the section. The propeller is made of Manganese Bronze of density 8300 kg per m^3 . The propeller has a speed of advance of 8.5 m per sec at 120 rpm, the delivered power being 7500 kW and the thrust power 5250 kW. The thrust and torque distributions are given by:

$$\frac{dK_T}{dx} = k_1 x^2 (1-x)^{0.5} \quad \frac{dK_Q}{dx} = k_2 x^2 (1-x)^{0.5}$$

The root section is at $0.2R$. Determine the stresses at the different radii, neglecting the bending moment due to centrifugal force.

24. A ship has a propeller of 5.0 m diameter and 0.8 pitch ratio. At the service speed of 20 knots, the propeller rpm is 180 and the brake power 14700 kW, while the effective power is 9500 kW. The shafting efficiency is 0.970. A self-propulsion test carried out with a 1/25-scale model gives a wake fraction of 0.200, a thrust deduction fraction of 0.120 and a relative rotative efficiency of 1.050 based on thrust identity. Calculate the thrust, torque and rpm of the model propeller and the speed of the ship model for conditions corresponding to the ship self-propulsion point. If the tow force applied to the model is 1.0 N, what is the resistance of the model at this speed? If in the open water test the model propeller is run at 1800 rpm, what should be its speed of advance, and what will be the corresponding thrust and torque?

25. A single-screw tug is required to have a bollard pull of 20 tonnes and a free running speed of 15 knots at which its effective power is 625 kW. The wake fraction at 15 knots is 0.250, the thrust deduction fraction being 0.190. In the static condition, the thrust deduction fraction is 0.050. The relative rotative efficiency may be taken as 1.000 and the shafting efficiency as 0.950. The propeller diameter is 3.5 m. Determine the minimum brake power required and the corresponding propeller rpm and pitch ratio. Use the data of Table 4.3.
26. A twin-screw ship with propellers of 4.80 m diameter and 0.9 pitch ratio is taken out on speed trials and the following data recorded:

Run No.	Direction	Time at start hr-min	Time on measured mile sec	Propeller rpm	Propeller thrust kN	Shaft power kW	Relative wind speed knots	Wind direction off bow deg
1	SW	9-15	416.2	95.9	225.4	1785	13.58	10.6
2	NE	10-06	326.9	96.4	226.6	1805	5.15	38.0
3	SW	11-10	402.4	95.7	224.9	1780	18.66	10.0
4	NE	11-51	266.6	124.7	381.6	3935	3.87	47.3
5	SW	12-34	289.1	125.0	382.5	3940	25.15	4.8
6	NE	13-15	289.7	124.5	381.0	3925	1.09	95.4
7	SW	13-48	219.2	153.4	576.8	7310	29.40	0.0
8	NE	14-24	238.8	153.9	578.7	7330	3.22	19.0
9	SW	14-57	215.7	153.2	576.1	7275	28.35	4.0
10	NE	15-27	198.0	191.7	948.5	14965	8.09	20.6
11	SW	15-55	186.5	192.6	953.0	15035	28.66	6.5
12	NE	16-24	192.5	191.5	947.5	14960	12.37	14.9
13	SW	16-53	192.9	192.0	950.1	14990	23.77	6.6

Determine the speed of the ship through the water for each of the four groups of runs and the speed of the current as a function of the time of day. Use Eqn. (10.3) for calculating the wind resistance. If the open water characteristics of the propellers are as given in Table 4.3, the shafting efficiency is 0.960 and the effective power of the ship is as given in the following, analyse the trials data to obtain the propulsion

factors as a function of ship speed by both thrust identity and torque identity.

Speed, knots	:	10	12	14	16	18	20
Effective power, kW:		2044	3641	5458	8277	12881	20051

27. A propeller has a constant pitch ratio of 1.0 and a diameter of 3.0 m. Determine the pitch angles from $0.2R$ to the blade tip at intervals of $0.1R$.
28. A propeller of diameter 5.0 m has a speed of advance of 6.0 m per sec at 120 rpm. Its axial inflow factors from root to tip are as follows:

r/R :	0.2	0.3	0.4	0.5	0.6	0.7	0.8	0.9	1.0
a	: 0.127	0.194	0.237	0.265	0.282	0.294	0.303	0.309	0.313

Using the impulse theory and neglecting drag, determine the thrust and torque of the propeller. Is the propeller working close to its optimum efficiency?

29. A propeller of 5.0 m diameter and 1.0 pitch ratio has the following open water characteristics:

$$K_T = 0.4250 - 0.2517 J - 0.1441 J^2$$

$$10K_Q = 0.5994 - 0.2733 J - 0.2254 J^2$$

The propeller absorbs a delivered power of 7500 kW at 150 rpm. Determine the speed of advance, the thrust and the open water efficiency of the propeller. The relative rotative efficiency is 1.000.

30. A ship has a total resistance of 500 kN at its design speed of 15 knots. The engine, directly connected to the propeller, has a brake power of 5500 kW at 150 rpm. The shafting efficiency is 0.970 and the propulsion factors are: wake fraction 0.200, thrust deduction fraction 0.150 and relative rotative efficiency 1.040. Calculate the effective power, the

thrust power, the delivered power, the propeller thrust and torque, the open water efficiency, the hull efficiency and the propulsive efficiency.

31. A ship has a draught of 6.0 m. Its propeller of 4.0 m diameter and 0.9 pitch ratio has its axis 3.5 m above the base line of the ship. The propeller develops a thrust of 300 kN at 180 rpm and a speed of advance of 6.0 m per sec. Determine the blade area ratio using the Burrill criterion for merchant ship propellers.
32. A four-bladed propeller of 6.0 m diameter and 0.8 pitch ratio has a delivered power of 7500 kW at 120 rpm. The propeller is made of Manganese Bronze of density 8300 kg per m³. The root section of the propeller at $0.2R$ has a chord of 1350 mm, the maximum chord length of the propeller being 1900 mm. The propeller blades have a 15 deg rake aft. The blade thickness fraction is 0.050, the blade thickness at the tip being 20 mm. Determine the tensile and compressive stresses using Taylor's method.
33. A 4.0 m long ship model with a wetted surface of 3.60 m² has a resistance of 35 N at a speed corresponding to 20 knots for the ship, whose length is 100 m. A self-propulsion test is carried out on the model and the following results obtained at this speed:

Propeller rpm:	500	550	600	650	700
Thrust, N :	27.15	30.84	35.83	42.22	50.81
Torque, N m :	0.61	0.93	1.42	2.08	2.91
Tow Force, N :	6.33	5.47	4.65	3.70	2.63

The open water characteristics of the model propeller, which has a diameter of 0.200 m, are as follows:

J :	0.700	0.800	0.900	1.000
K_T :	0.2551	0.2242	0.1913	0.1534
$10K_Q$:	0.508	0.468	0.420	0.368

Calculate the effective power, the delivered power and the propeller rpm of the ship at 20 knots in the trial condition using the ITTC ship performance prediction method, given the following values:

$$\begin{aligned} 1+k &= 1.065 & \Delta C_F &= 0.4 \times 10^{-3} & C_{AA} &= 0.7 \times 10^{-3} \\ \Delta K_T &= -0.0002 & \Delta K_Q &= 0.0003 & \Delta C_{FC} &= 0.3 \times 10^{-3} \\ \Delta w_c &= 0.005 \end{aligned}$$

What are the predicted values of wake fraction, thrust deduction fraction and relative rotative efficiency of the ship in the trial condition?

34. A single screw tug has an engine of 1500 kW at 480 rpm connected to a propeller of diameter 3.5 m through 3 : 1 reduction gearing, the shafting efficiency being 0.950. The depth of immersion of the propeller shaft centre line is 3.3 m. The wake fraction is 0.250, the thrust deduction fraction varies linearly with speed being 0.050 at zero speed and 0.190 at 15 knots, and the relative rotative efficiency is 1.000. The effective power of the tug at different speeds is as follows:

Speed, knots	:	8	10	12	14	16	18
Effective power, kW	:	69.2	151.2	286.2	490.9	783.4	1183.1

Show that the required expanded blade area ratio is less than 0.500. Using the data of Table 4.3, determine the limits within which the pitch ratio must lie so that the bollard pull is not less than 20 tonnes and the free running speed not less than 15 knots.

35. The fine weather data extracted from a record of the service performance of a ship are given in the following table. Analyse these data to determine the effect of days out of dry dock on the power of the ship at a displacement of 15000 tonnes and a speed of 17.0 knots. Estimate the brake power at 15000 tonnes displacement and 17.0 knots speed at zero and 400 days out of dry dock.

No.	Displacement tonnes	Speed knots	Days out of dry dock	Brake power kW
1.	14100	17.5	25	6860

2.	15300	16.9	80	6650
3.	15800	16.6	100	6470
4.	14700	17.2	150	6935
5.	14900	17.1	175	6910
6.	15300	16.8	210	6710
7.	14500	17.5	250	7360
8.	15900	16.3	290	6360
9.	14700	17.3	320	7250
10.	15200	16.3	360	6820

36. A propeller of diameter 5.0 m has a constant geometric face pitch ratio of 1.0. The blade section at $0.7R$, which may be regarded as representing the whole propeller, is of aerofoil shape such that the line joining the leading and trailing edges ("nose-tail line") makes an angle of 1.5 degrees with the face chord. The no-lift angle with respect to the nose tail line is 2.0 degrees. Determine the effective pitch ratio of the propeller.
37. A four-bladed propeller of diameter 5.0 m and constant face pitch ratio 0.8 is advancing into undisturbed water at a speed of 6.0 m per sec at 120 rpm. The blades are composed of NACA-66 (modified) sections for which:

$$C_L = 0.1097(1 - 0.83t/c)(\alpha + 2.35) \quad \alpha \text{ in degrees}$$

$$C_D = 0.0100 + 0.0125 C_L^2$$

The blade widths and thicknesses at the various radii are as follows:

r/R :	0.2	0.3	0.4	0.5	0.6	0.7	0.8	0.9	1.0
c/D :	0.208	0.235	0.256	0.269	0.273	0.268	0.246	0.198	0
t/c :	0.176	0.138	0.110	0.089	0.072	0.058	0.046	0.036	-

Calculate the thrust, torque and efficiency of the propeller, neglecting induced velocities.

38. A propeller is required to produce a thrust of 350 kN at 120 rpm at a speed of advance of 12.0 knots. Using the B_P - δ diagram, Fig. 4.6, determine the optimum diameter and pitch ratio of the propeller, and the corresponding delivered power in open water.
39. A ship has a design speed of 15 knots, its resistance at this speed being 500 kN. The ship has a propeller of 5.0 m diameter directly connected to an engine of brake power 5500 kW at 120 rpm. The propeller is designed to operate at $J = 0.620$, $K_T = 0.230$, $10K_Q = 0.350$. If the shaft losses are 3 percent, determine the propulsive efficiency and its components based on thrust identity. Determine also the effective power, the thrust power and the delivered power.
40. A four-bladed propeller of diameter 6.0 m and pitch ratio 0.8 has a brake power of 7500 kW and a thrust power of 5250 kW at an rpm of 120 and a speed of advance of 8.5 m per sec. The propeller has a blade thickness fraction of 0.050, the tip thickness being 20 mm. The blades are raked aft at 15 deg and have a normal blade outline. The expanded blade area ratio of the propeller is 0.550. The propeller is made of Manganese Bronze of density 8300 kg per m³. The root section is at $0.2R$, and has an area of 23000 mm² and a section modulus of 8.05×10^6 mm³. Determine the stress in the root section using Burrill's method.
41. In a self propulsion test at the ship self propulsion point on a 1/25 scale model at a speed of 2.0 m per sec, the propeller thrust and torque are 23.04 N and 0.728 N m respectively with the model propeller of 200 mm diameter running at 800 rpm. The resistance of the model is 25.00 N and the resistance of the ship at the corresponding speed is 315 kN. The model propeller has a thrust of 23.04 N and a torque of 0.760 N m when running at 13.333 revolutions per sec at a speed of advance of 1.60 m per sec in open water. Calculate the tow force applied to the model, and determine the wake fraction, the thrust deduction fraction and the relative rotative efficiency. Calculate the effective power and the delivered power of the ship.
42. A twin-screw tug has two engines each of brake power 500 kW at 1200 rpm connected to the propellers of 2.00 m diameter through 4 : 1 reduction gearing. The effective power of the tug is as follows:

Speed, knots	:	10	12	14	16
Effective power, kW:		153.7	300.0	528.2	862.3

The wake fraction is 0.100, the thrust deduction fraction varies linearly from 0.040 at zero speed to 0.120 at 16 knots, and the relative rotative efficiency is 0.980 based on thrust identity. The shafting efficiency is 0.950. The depth of immersion of the propeller shaft centre line is 1.8 m. Determine the expanded blade area ratio required for the propellers, and calculate the pitch ratio that will give the maximum bollard pull with a minimum free running speed of 12.50 knots. Calculate the engine rpm and brake power in the bollard pull and free running conditions. Use the data of Table 4.3.

43. A method of determining the effect of weather on the service performance of a ship is to plot P_B/n^3 and V/n as functions of a "weather intensity number" W , where P_B is the brake power, n the propeller rpm and V the ship speed. W may be taken to be the product of the wind speed squared and a "wind direction factor", equal to 1.0 for bow winds (0–45 degrees off the bow), 0.5 for beam winds (45 to 135 off the bow) and 0.2 for stern winds (135–180 degrees off the bow). Analyse by this method the following data for a ship (which have been corrected to the fully loaded, clean hull condition) and determine the brake power and ship speed at the rated propeller rpm of 119 in fine weather ($W = 0$).

No.	Ship Speed knots	Propeller rpm	Brake Power kW	True Speed knots	Wind Direction deg
1.	11.28	114.3	6770	33	40
2.	11.82	105.2	5090	39	150
3.	10.35	105.2	5380	40	95
4.	7.75	100.3	5150	40	40
5.	11.50	100.0	4030	27	145
6.	8.38	108.7	6410	42	10
7.	14.24	111.8	5610	22	165
8.	13.01	115.1	6250	22	5

Contd.

9.	14.61	115.1	6410	15	160
10.	12.04	114.6	6330	38	60
11.	13.15	113.3	6020	28	70
12.	7.25	96.9	4910	42	5
13.	9.96	92.2	3390	44	170
14.	6.67	79.3	2650	40	20
15.	6.55	76.3	2280	41	110
16.	5.12	68.5	1690	45	140
17.	11.42	97.9	4070	23	145
18.	7.83	76.3	1830	23	35
19.	9.27	100.4	4770	45	85
20.	8.00	91.9	3920	38	35
21.	7.75	98.6	4840	38	35
22.	11.55	94.6	3650	28	175
23.	12.07	108.3	5600	33	65
24.	12.10	107.7	5530	32	60
25.	11.05	109.8	5670	26	30

44. A propeller of constant pitch ratio 0.8038 has blades that are raked aft at an angle of 15 deg. Determine the skew angles at $r/R = 0.2, 0.3, 0.4, \dots, 0.9, 1.0$ for the blade reference line to lie in the blade reference plane normal to the propeller axis.
45. A four-bladed propeller of diameter 4.0 m has a speed of advance of 7.5 m per sec at 150 rpm. The ideal thrust of the propeller is 400 kN. Determine the ideal thrust loading coefficient. If for this value, the ideal efficiency is 0.800 and the blade width distribution is as given in the following table, determine the lift coefficients at the different radii.

r/R	0.2	0.3	0.4	0.5	0.6	0.7	0.8	0.9	1.0
c/D	0.225	0.249	0.270	0.288	0.301	0.307	0.299	0.260	0

The Goldstein factors may be determined from Appendix 6.

46. A propeller of 4.0 m diameter and 0.8 pitch ratio has a delivered power of 2000 kW at 180 rpm. Using the μ - σ diagram, Fig. 4.7, determine the speed of advance and the thrust of the propeller. If the torque is

constant, calculate the rpm, thrust and delivered power at 0, 5, 10 and 15 knots speed of advance.

47. A ship has a speed of 15 knots when the engine produces 5000 kW brake power at 180 rpm. The effective power of the ship is 3600 kW. The propeller is directly connected to the engine. The wake fraction is 0.250, the thrust deduction fraction 0.150, the relative rotative efficiency 1.030 and the shafting efficiency 0.980. Determine the delivered power, the thrust power, the overall propulsive efficiency, the propulsive efficiency (quasi-propulsive coefficient), the hull efficiency, the open water efficiency, the speed of advance, the resistance of the ship, and the propeller thrust and torque.
48. The axial velocities measured at various angular and radial positions in the plane of the propeller of a single-screw ship model moving at a speed of 3.0 m per sec are as follows:

Angular position, deg	0	30	60	90	120	150	180
Radius, mm	Axial velocity, m per sec						
20	1.250	1.593	1.972	2.096	2.147	1.943	1.775
30	1.313	1.644	2.009	2.128	2.178	1.981	1.820
40	1.402	1.714	2.061	2.174	2.221	2.034	1.881
50	1.515	1.806	2.128	2.233	2.276	2.103	1.960
60	1.653	1.917	2.209	2.304	2.344	2.186	2.057
70	1.817	2.049	2.305	2.389	2.423	2.286	2.172
80	2.006	2.201	2.416	2.487	2.516	2.400	2.305
90	2.221	2.373	2.542	2.597	2.620	2.529	2.454
100	2.460	2.566	2.683	2.721	2.737	2.674	2.622

Determine the average circumferential wake fraction at each radius and the average wake fraction over the propeller disc. The model propeller has a diameter of 200 mm and a boss diameter ratio of 0.200.

49. Design a propeller for a single screw ship using the circulation theory (lifting line theory with lifting surface corrections). The design speed of the ship is 16.0 knots at which the effective power is 3460 kW. The

wake fraction is 0.200 and the thrust deduction fraction 0.150. Preliminary design calculations indicate a propeller with four blades, 5.200 m diameter, 0.500 expanded blade area ratio, 0.045 blade thickness fraction and a skew angle at the blade tip of 10 degrees. The propeller rpm is 126 and the immersion of the shaft axis is 3.5 m. The effective wake fractions at the different radii are as follows:

$x = r/R$:	0.2	0.3	0.4	0.5	0.6	0.7	0.8	0.9	1.0
w	: 0.305	0.295	0.279	0.259	0.235	0.206	0.174	0.136	0.095

The expanded blade outline is to conform to the B-series, and the Lerbs criterion for wake-adapted propellers is to be used. Determine the delivered power and the propeller efficiency in the behind condition.

50. A ship is fitted with an engine of 5500 kW brake power at 120 rpm directly connected to a propeller of 5.0 m diameter. The ship has a speed of 15 knots and a resistance of 500 kN. The propeller operates at $J = 0.625$, $K_T = 0.220$, $10K_Q = 0.330$. The relative rotative efficiency is 1.060. Determine the propulsive efficiency and its components based on torque identity, and the effective power, the delivered power and the shafting efficiency.

Answers to Problems

Chapter 1

—

Chapter 2

1. Arc length of projected outline = 404.9 mm
Arc length of developed outline = 480.0 mm
2. Face pitch = 3.996 m. Pitch ratio = 0.7992
3. Width of expanded outline = 720.0 mm
Distance of reference line from leading edge = 288.0 mm
Pitch ratio = 0.864
4. Expanded blade area ratio = 0.6499
Developed blade area ratio = 0.6455
Projected blade area ratio = 0.5667
5. Thickness chord ratio = 0.1488
Camber ratio = 0.0250
6. Mean pitch ratio = 0.9716
Pitch at $0.7R$ = 5.892 m

7. Speed of advance for zero slip = 11 m s^{-1}
Speed of advance for 100 percent slip = 0
8. Pitch ratio = 0.9000
Blade area ratio (expanded) = 0.4400
Blade thickness fraction = 0.0510
Boss diameter ratio = 0.1670
9. Diameter = 1.624 m
Expanded blade area ratio = 0.2838
Projected blade area ratio = 0.2006
Mean pitch ratio = 2.1227
10. Mass = 4961.1 kg Polar moment of inertia = 4235.55 kg m^2

Chapter 3

1.

Location	Pressure, kN m^{-2}	Velocity, m s^{-1}
Far ahead	45.249	5.000
Just ahead	38.083	6.244
Just astern	53.999	6.244
Far astern	45.249	7.487

2. Thrust = 130.4 kN Efficiency = 0.750
3. Diameter = 2.056 m
4. Delivered power = 262.4 kW
5. Thrust = 222.58 kN Torque = 132.44 kN m Efficiency = 0.8559

6. Thrust = 503.10 kN Torque = 320.28 kNm

7. Thrust = 1263.94 kN Torque = 665.08 kNm Efficiency = 0.9074

8.

x	α°	f/c	P/D
0.2	1.5725	0.0095	0.8514
0.4	1.3309	0.0080	0.8454
0.6	1.0210	0.0062	0.8440
0.8	0.8341	0.0050	0.8426
1.0	0.7521	0.0045	0.8457

9.

x	dT_i/dx	dQ_i/dx
0.2	96.623	100.335
0.3	231.254	240.852
0.4	404.473	421.260
0.5	589.995	614.481
0.6	783.274	815.785
0.7	919.680	957.849
0.8	986.480	1027.422
0.9	897.800	935.061

Delivered power = 4908 kW

10.

x	$C_L \frac{c}{D}$
0.2	0.08452
0.3	0.09558
0.4	0.09428
0.5	0.08726
0.6	0.07818
0.7	0.06702
0.8	0.05430
0.9	0.03833
1.0	0

Chapter 4

1. Speed of advance = 1.342 m s^{-1} Rpm = 536.66
 Thrust = 60.976 N Torque = 2.287 N m
 Ratio of cavitation numbers = 0.0761
 Ratio of Reynolds numbers = 85.756

2. Diameter = 0.2000 m Speed of advance = 1.789 m s^{-1}
 Rpm = 670.71 Thrust = 15.610 N Torque = 0.5854 N m

3.

J	K_T	$10K_Q$	η_o
0	0.4250	0.6100	0
0.1111	0.3948	0.5711	0.1222
0.2222	0.3611	0.5280	0.2419
0.3333	0.3240	0.4806	0.3577
0.4444	0.2834	0.4289	0.4674
0.5556	0.2393	0.3730	0.5673
0.6667	0.1917	0.3129	0.6500
0.7778	0.1406	0.2485	0.7004
0.8889	0.0860	0.1799	0.6763
1.0000	0.0280	0.1070	0.4165

 Effective pitch ratio = 1.0514

4. Diameter = 4.854 m Pitch ratio = 1.150 Thrust = 704.6 kN

5. Rpm = 122.3 Efficiency = 0.630 Pitch ratio = 1.241
 Delivered power = 2852.8 kW

6.

V_A , knots:	0	2.5	5.0	7.5	10.0	13.5
n , rpm :	88.54	98.37	112.23	129.39	149.34	180.00
T , kN :	61.74	58.36	54.38	49.46	43.20	31.39
P_D , kW :	202.23	224.71	256.35	295.52	341.13	411.14

7. Diameter = 4.608 m Pitch ratio = 0.972
Delivered power = 6040 kW
8. Rpm = 144.3 Pitch ratio = 0.920 Thrust = 622.08 kN
9. Pitch ratio = 0.800
- | | | | | | |
|-----------------|------|------|------|------|------|
| V_A , knots : | 0 | 3.0 | 6.0 | 9.0 | 12.0 |
| n , rpm : | 150 | 158 | 173 | 190 | 210 |
| P_D , kW : | 1000 | 1056 | 1155 | 1264 | 1400 |
| T , kN : | 176 | 171 | 161 | 152 | 141 |
10. Diameter = 4.052 m Pitch ratio = 0.5 Thrust = 221.5 kN
(Lower limit of pitch ratio)
For diameter = 3.50 m: Pitch ratio = 0.751 Thrust = 197.4 kN

Chapter 5

1. Effective power = 4526.72 kW Thrust = 687.50 kN
Torque = 467.92 kN m Thrust power = 4243.80 kW
Open water efficiency = 0.7007 Delivered power = 5880.00 kW
Overall propulsive efficiency = 0.7545
2. Effective power = 4115.20 kW
Thrust power = 3703.68 kW
Delivered power = 5820.00 kW
Hull efficiency = 1.1111
Relative rotative efficiency = 1.0796
Open water efficiency = 0.5895
Propulsive efficiency = 0.7071

5. x : 0.2 0.3 0.4 0.5 0.6 0.7 0.8 0.9 1.0
 t , mm: 161.4 140.0 117.6 96.3 75.8 56.0 36.7 18.0 -
6. Blade thickness fraction = 0.04638
 Stress in root section = 40.208 N mm^{-2}
7. Blade thickness fraction = 0.06495
8. Blade thickness at $0.25R$ = 189.806 mm
 Blade thickness at $0.60R$ = 83.176 mm
 Blade thickness fraction = 0.0496
9. Blade thickness fraction = 0.0488
10. Bending moment about x -axis = -543.083 kN m
 Bending moment about y -axis = 433.330 kN m
 Torsion about radial axis = -289.613 kN m
 Tensile force on the root section = 913.562 kN

Chapter 8

1. Speed, knots 10.0 12.0 14.0 16.0 18.0
 Effective power, kW 551 1010 1771 3048 5198
2. Speed, knots 12.0 14.0 16.0 18.0 20.0
 Effective power, kW 1787 3106 5291 8926 14953
3. (a) Diameter = 0.1111 m
 Reynolds number = 3.932×10^5 at zero slip
 Reynolds number = 3.574×10^5 at 100 percent slip
- (b) Diameter = 0.1246 m
 Reynolds number = 3.958×10^5 at zero slip
 Reynolds number = 3.598×10^5 at 100 percent slip

(c) Maximum rpm = 1508.5

Reynolds number = 3.604×10^5 at zero slip

Reynolds number = 3.277×10^5 at 100 percent slip.

4.	J	0.0000	0.1000	0.2000	0.3000	0.4000
	K_{TS}	0.3399	0.3123	0.2812	0.2470	0.2103
	$10K_{QS}$	0.3893	0.3701	0.3454	0.3150	0.2793
	η_{OS}	0.0000	0.1343	0.2591	0.3744	0.4793

	J	0.5000	0.6000	0.7000	0.8000	0.9000
	K_{TS}	0.1700	0.1261	0.0797	0.0302	-0.0228
	$10K_{QS}$	0.2377	0.1906	0.1378	0.0794	0.0151
	η_{OS}	0.5691	0.6318	0.6444	0.4843	-

5.		<u>Thrust Identity</u>	<u>Torque Identity</u>
	Wake Fraction	0.2538	0.1998
	Thrust deduction fraction	0.1549	0.1549
	Hull efficiency	1.1325	1.0561
	Open water efficiency	0.6179	0.6505
	Relative rotative efficiency	1.0601	1.0799
	Propulsive efficiency	0.7418	0.7418

Ship speed = 19.44 knots

Effective power = 7444 kW

Propeller rpm = 180

Delivered power = 10035 kW

6. Wake fraction = 0.1304 Thrust deduction fraction = 0.1471
 Hull efficiency = 0.9808 Open water efficiency = 0.7392
 Relative rotative efficiency = 1.0339
 Propulsive efficiency = 0.7496

These results in general are not applicable to the ship since they have been obtained at the model self propulsion point and not at the ship self propulsion point on the model.

5. x : 0.2 0.3 0.4 0.5 0.6 0.7 0.8 0.9 1.0
 t , mm: 161.4 140.0 117.6 96.3 75.8 56.0 36.7 18.0 -
6. Blade thickness fraction = 0.04638
 Stress in root section = 40.208 N mm^{-2}
7. Blade thickness fraction = 0.06495
8. Blade thickness at $0.25R$ = 189.806 mm
 Blade thickness at $0.60R$ = 83.176 mm
 Blade thickness fraction = 0.0496
9. Blade thickness fraction = 0.0488
10. Bending moment about x -axis = -543.083 kN m
 Bending moment about y -axis = 433.330 kN m
 Torsion about radial axis = -289.613 kN m
 Tensile force on the root section = 913.562 kN

Chapter 8

1. Speed, knots 10.0 12.0 14.0 16.0 18.0
 Effective power, kW 551 1010 1771 3048 5198
2. Speed, knots 12.0 14.0 16.0 18.0 20.0
 Effective power, kW 1787 3106 5291 8926 14953
3. (a) Diameter = 0.1111 m
 Reynolds number = 3.932×10^5 at zero slip
 Reynolds number = 3.574×10^5 at 100 percent slip
- (b) Diameter = 0.1246 m
 Reynolds number = 3.958×10^5 at zero slip
 Reynolds number = 3.598×10^5 at 100 percent slip

(c) Maximum rpm = 1508.5

Reynolds number = 3.604×10^5 at zero slip

Reynolds number = 3.277×10^5 at 100 percent slip.

4.	J	0.0000	0.1000	0.2000	0.3000	0.4000
	K_{TS}	0.3399	0.3123	0.2812	0.2470	0.2103
	$10K_{QS}$	0.3893	0.3701	0.3454	0.3150	0.2793
	η_{OS}	0.0000	0.1343	0.2591	0.3744	0.4793

J	0.5000	0.6000	0.7000	0.8000	0.9000
K_{TS}	0.1700	0.1261	0.0797	0.0302	-0.0228
$10K_{QS}$	0.2377	0.1906	0.1378	0.0794	0.0151
η_{OS}	0.5691	0.6318	0.6444	0.4843	-

5.		<u>Thrust Identity</u>	<u>Torque Identity</u>
	Wake Fraction	0.2538	0.1998
	Thrust deduction fraction	0.1549	0.1549
	Hull efficiency	1.1325	1.0561
	Open water efficiency	0.6179	0.6505
	Relative rotative efficiency	1.0601	1.0799
	Propulsive efficiency	0.7418	0.7418

Ship speed = 19.44 knots

Effective power = 7444 kW

Propeller rpm = 180

Delivered power = 10035 kW

6.	Wake fraction = 0.1304	Thrust deduction fraction = 0.1471
	Hull efficiency = 0.9808	Open water efficiency = 0.7392
	Relative rotative efficiency = 1.0339	
	Propulsive efficiency = 0.7496	

These results in general are not applicable to the ship since they have been obtained at the model self propulsion point and not at the ship self propulsion point on the model.

7. Wake fraction = 0.2127 Thrust deduction fraction = 0.1531
 Hull efficiency = 1.0757 Open water efficiency = 0.6170
 Relative rotative efficiency = 1.0545
 Propulsive efficiency = 0.6999
 Delivered power = 7215 kW Propeller rpm = 126.5
8. Nominal wake fraction = 0.1959
9. r , mm: 15.0 22.5 30.0 37.5 45.0 52.5 60.0 67.5 75.0
 $\bar{w}(r)$: 0.069 0.075 0.083 0.092 0.098 0.110 0.122 0.134 0.150
 Nominal wake fraction = 0.1118
10. Speed of water = 1.7893 ms^{-1} Model propeller rpm = 948.6
 Model propeller torque = 0.3032 Nm Pressure = 3.7631 kN m^{-2}

Chapter 9

1. Total shaft power = 22407 kW Propeller rpm = 243.98
 Pitch ratio = 1.5255
2. Diameter = 3.470 m Pitch ratio = 1.5133
 Blade area ratio = 0.8506 Speed = 35.212 knots
3. Diameter = 2.733 m Pitch ratio = 0.8044
 Blade area ratio = 0.3851 Speed = 12.429 knots
4. Speed, knots : 15.0 20.0 25.0 30.0 35.0 40.0 35.157
 Turbine rpm : 1158 1589 2035 2495 2987 3414 3000
 Shaft power, kW: 1111 3068 6774 12974 22685 35993 23037
- Ship speed at 3000 rpm of turbines = 35.157 knots
 Shaft power = 23037 kW

5. Speed = 15.091 knots Brake power = 4712.4 kW
Rpm = 118.75
6. Diameter = 3.416 m Pitch ratio = 0.5 (minimum in Table 4.3)
Bollard pull = 169.43 kN
Free running speed = 10.036 knots Brake power = 300.3 kW
Rpm = 600
7. Pitch ratio = 1.1257 Bollard pull = 109.83 kN
Brake power = 616.9 kW Engine rpm = 411.28
8. Diameter = 2.829 m Pitch ratio = 0.5 (minimum of Table 4.3)
Maximum tow rope pull = 140.6 kN
Free running speed = 11.640 knots Brake power = 594.8 kW

Trawling with full catch:
Speed = 5.628 knots Brake power = 1046.6 kW
Engine rpm = 240
9. Speed, knots : 0.0 2.0 4.0 6.0 8.0 9.643
Tow rope pull, kN: 132.74 128.18 120.85 110.71 96.41 80.97⁴²
Engine rpm : 912.8 954.6 1006.2 1067.2 1136.9 1200.0
Brake power, kW : 380.3 397.8 419.2 444.6 473.6 500.0

Speed, knots : 10.0 12.0 14.0 12.859
Tow rope pull, kN: 72.95 23.51 -33.51 0.00
Engine rpm : 1200 1200 1200 1200
Brake power, kW : 482.4 378.0 264.4 330.3

Speed at which engines develop maximum brake power = 9.643 knots
Free running speed = 12.859 knots

10.	x	P/D	c/D	t/D	f/c
	0.2	1.2109	0.4629	0.0406	0.0106
	0.3	1.2396	0.5123	0.0359	0.0154
	0.4	1.2332	0.5567	0.0312	0.0141
	0.5	1.2280	0.5941	0.0265	0.0137
	0.6	1.2244	0.6212	0.0218	0.0127
	0.7	1.2201	0.6324	0.0171	0.0131
	0.8	1.2174	0.6154	0.0124	0.0122
	0.9	1.2189	0.5364	0.0077	0.0113
	1.0	1.1915	-	0.0030	-

Brake power = 12863 kW

Chapter 10

1. Delivered power = 895.0 kW Tension in mooring rope = 99.15 kN
Reaction = 51.32 kN

2.	Run No.	Direction	Time at Mid-run hours	Speed through water knots	Speed of current to North knots
	1.	N	8.895	9.317	1.870
	2.	S	9.696	9.525	1.615
	3.	N	10.459	10.593	1.431
	4.	S	11.184	10.725	0.993
	5.	N	11.908	11.657	0.625
	6.	S	12.577	11.634	0.227
	7.	N	13.240	12.765	-0.242
	8.	S	13.854	12.933	-0.535
	9.	N	14.438	13.967	-0.785
	10.	S	15.016	14.153	-0.967
	11.	N	15.568	15.526	-1.068
	12.	S	16.097	15.855	-0.920

Runs No.	Average Speed knots	Average Power kW	Average Rpm	Average Thrust kN
1 and 2	9.421	1491	88.1	244
3 and 4	10.659	2006	97.9	293
5 and 6	11.646	2555	106.4	343
7 and 8	12.849	3340	116.7	406
9 and 10	14.060	4212	125.9	462
11 and 12	15.690	5125	136.8	525

3. Thrust Identity

V , knots	w	t	η_H	η_O	η_R	η_D
9.421	0.2641	0.2048	1.0792	0.5707	1.0544	0.6494
10.659	0.2600	0.1998	1.0814	0.5803	1.0527	0.6607
11.646	0.2586	0.1979	1.0818	0.5833	1.0538	0.6650
12.849	0.2533	0.1959	1.0769	0.5889	1.0502	0.6661
14.060	0.2513	0.1900	1.0819	0.5955	1.0282	0.6625
15.690	0.2508	0.1913	1.0795	0.6065	1.0529	0.6893

Torque Identity

V , knots	w	t	η_H	η_O	η_R	η_D
9.421	0.2218	0.2048	1.0206	0.5937	1.0718	0.6494
10.659	0.2212	0.1998	1.0275	0.6013	1.0693	0.6607
11.646	0.2194	0.1979	1.0274	0.6041	1.0714	0.6650
12.849	0.2175	0.1959	1.0277	0.6074	1.0670	0.6661
14.060	0.2314	0.1900	1.0539	0.6059	1.0375	0.6625
15.690	0.2169	0.1913	1.0327	0.6228	1.0718	0.6893

4.	Run No.	Speed knots	Shaft Power kW	Propeller rpm
	1 to 3	13.995	2327.5	73.075
	4 to 7	15.874	3622.5	83.625
	8 to 10	19.254	7370.0	104.375
	11 to 13	20.807	9827.5	114.338

Run No.	Time of day hours	Speed of current knots
1	8.099	2.716
2	8.804	2.707
3	9.499	2.698
4	10.300	2.307
5	10.896	1.944
6	11.698	1.581
7	12.292	1.129
8	12.997	0.611
9	13.675	0.093
10	14.394	-0.399
11	15.107	-0.630
12	15.693	-0.915
13	16.308	-1.255

5.	Speed knots	$10^3 C_A$	$w_{\text{Trial}} - w_{\text{Model}}$
	13.995	0.260	-0.0218
	15.874	0.349	-0.0195
	19.254	0.354	-0.0223
	20.807	0.365	-0.0215

6. Ship speed = 18.324 knots Brake power = 16957 kW

Rpm = 113.969

The ship fulfils the contract.

7.	End of Year No.	Speed knots	Propeller Rpm	Brake Power kW	Maximum Brake Power Available kW
	0	17.008	126.0	8815	10500
	1	16.819	126.0	8960	10395
	2	16.638	126.0	9099	10290
	3	16.464	126.0	9232	10185
	4	16.296	126.0	9362	10080
	5	16.135	126.0	9484	9975
	6	15.979	126.0	9602	9870
	7	15.829	126.0	9715	9765
	8	15.579	124.9	9573	9573
	9	15.303	123.8	9384	9384
	10	15.036	122.5	9189	9189

The propeller must be changed at the end of the eighth year.

Pitch ratio of new propeller = 0.6584

Ship speed = 15.135 knots

8.	Wave direction	Increase in power, %
	Head seas	5.4
	Bow quartering seas	3.9
	Stern quartering seas	-2.4
	Following seas	-7.6

9.	Days in service	Corrected power, kW
	10	9597
	120	9868
	310	10139
	Ship Drydocked	
	390	9792
	535	10092

665	10274
Ship Drydocked	
750	9925
890	10231
1050	10458
Ship Drydocked	
1110	10063
1235	10358
1385	10579

Days in service	Power just after drydocking kW	Days after drydocking	Increase in power kW
		0	0
0	9573	60	154
365	9723	120	286
730	9873	180	399
1095	10023	240	491
1460	10173	300	564
1825	10323	360	616
		365	619

10.	Increase in Effective Power %	Propeller rpm	Brake power kW	Ship speed knots
	0	144.0	10123	17.677
	10	144.0	10386	17.122
	20	143.5	10461	16.647
	30	142.3	10379	16.164
	40	141.4	10309	15.737
	50	140.5	10246	15.356

Chapter 11

1. The 6-bladed propeller should be selected.

The 5th, 6th and 7th harmonics in the wake velocities are small.

2.	Increase in effective power over that in calm water	Ship speed	Propeller rpm	Brake power
	%	knots		kW
	0	18.019	150.00	9989
	15	17.158	147.50	9834
	30	16.425	145.38	9692
	45	15.795	143.59	9572
	60	15.246	142.05	9469

3. New : Ship speed = 19.0 knots Brake power = 9000 kW
Rpm = 126.0

After one year: Ship speed = 17.5 knots Brake power = 8272 kW
Rpm = 119.4

4. Time to stop = 207 s Distance travelled = 912.9 m

5. Trial condition : Speed = 18.730 knots
Rpm = 118
Brake power = 13486 kW

Average service condition : Speed = 17.989 knots
Rpm = 118
Brake power = 14236 kW

Service margin = 5.56 percent

Engine margin = 5.37 percent

Maximum permissible increase in effective power over that in the trial condition = 49.83 percent

Corresponding ship speed = 16.668 knots

Chapter 12

1. Distance of feathering point forward of centre = 0.230 m
Diameter of fixed paddle wheel of same entry angle = 65.824 m

2. Speed of Tug knots	Pitch Ratio	Tow rope Pull kN
0	0.7883	161.962
2	0.8205	150.024
4	0.8590	136.176
6	0.9038	119.939
8	0.9545	101.023
10	1.0109	79.177
12	1.0724	54.110
14	1.1383	25.430
15.573	1.1928	0

Free running speed = 15.573 knots

3. Bollard pull = 239.678 kN Free running speed = 12.617 knots
Brake power = 1035 kW Brake power = 623.95 kW
Engine rpm = 600 Engine rpm = 600
Nozzle thrust = 128.118 kN Nozzle thrust = 8.402 kN.
4. Thrust = 27.106 kN Torque = 2.9943 kN m
Horizontal force = 4.937 kN Vertical force = 0
Effective power = 275.4 kW
5. Bollard pull (with both propellers) = 63.312 kN
Delivered power per propeller = 99.16 kW
6. Speed = 40.0 knots Pump efficiency = 0.918

Miscellaneous Problems:

1. Effective power = 3858.00 kW Thrust power = 3611.09 kW
 Delivered power = 5340.71 kW Brake power = 5505.88 kW
 Wake fraction = 0.2000 Thrust deduction fraction = 0.1453
 Hull efficiency = 1.0684 Open water efficiency = 0.6386
 Relative rotative efficiency = 1.0588
 Overall propulsive efficiency = 0.7007
2. Speed = 0.9645 m s^{-1} Pressure = 3.836 kN m^{-2}
3. Stress = 31.921 N mm^{-2}
4. Ship speed, knots: 5.0 7.5 10.0 12.5 15.0 17.5
 Resistance, kN : 26.11 57.74 106.98 179.03 332.95 595.78
5. Brake power = 14287 kW rpm = 127.2 Pitch ratio = 0.970
6. Maximum permissible engine rpm: (a) 96.2, (b) 97.3, (c) 93.6
7. Time taken to reach a speed of 17.99 knots = 240 s
 Distance travelled = 1807 m
8. Expanded blade area ratio = 0.650
9. Thrust = 201.258 kN

Location	Pressure kN m^{-2}	Velocity m s^{-1}
Far ahead	45.249	5.000
Just ahead	38.042	6.250
Just behind	54.057	6.250
Far behind	45.249	7.500

10. Speed of advance = 115.0505 ms^{-1} Rpm = 46020
 Thrust = 448.395 kN Torque = 16.8148 kN m
 Depth of immersion of model propeller = 0.30 m
 Ratio of Froude numbers = 0.01166
 Ratio of cavitation numbers = 559.4305
11. Hull efficiency = 1.1250 Open water efficiency = 0.5644
 Thrust = 600.00 kN Torque = 477.46 kN m
 Thrust power = 3555.6 kW $J = 0.5926$
 $K_T = 0.2341$ $10K_Q = 0.3913$
12. Speed of water = 5.487 ms^{-1} Pressure = $64.521 \text{ kN mm}^{-2}$
 Thrust = 3.719 N Torque = 0.2653 N m
13. r/R : 0.2 0.3 0.4 0.5 0.6 0.7 0.8 0.9 1.0
 Stress: 30.627 29.856 27.966 25.562 22.777 19.379 15.004 8.621 -
 N mm^{-2}
14. Model propeller: $J = 0.8000$ $K_T = 0.1250$
 $10K_Q = 0.2350$ $\eta_O = 0.6773$
 Ship propeller roughness = $46 \mu\text{m}$
15. Diameter = 5.798 m Pitch ratio = 0.8429
 Expanded blade area ratio = 0.6807 Speed = 20.162 knots
16. Correlation allowance = 0.3×10^{-3}
17. Rated brake power of each engine = 1000 kW
 Speed at which one engine may be uncoupled = 13.653 knots
 Free running condition: Speed = 16.00 knots
 Brake power = 759.7 kW.

18. Cartesian coordinates in mm:
 Leading edge: 1399.41, 540.00, -30.08
 Trailing edge: 1141.63, -972.98, 713.78.
19. Thrust = 100.077 kN
20. Maximum rpm = 1650.35
 Maximum speed of advance = 4.5016 m s^{-1}
 Maximum thrust = 0.2494 kN
21. Open water efficiency = 0.5831 Thrust = 986.975 kN
 Torque = 779.859 kN m
22. Blade area ratio = 0.9065
23. r/R : 0.2 0.3 0.4 0.5 0.6 0.7 0.8 0.9 1.0
 Stress: 51.496 34.141 26.047 21.617 18.744 17.194 15.618 12.604 -
 N mm⁻²
24. Self propulsion test:
 Model propeller: Thrust = 65.519 N Torque = 1.889 N m
 Rpm = 900
 Speed of ship model = 2.0576 m s^{-1} Model resistance = 58.657 N
 Open water test:
 Speed of advance = 3.292 m s^{-1} Thrust = 262.080 N
 Torque = 7.557 N m
25. Pitch ratio = 0.830 Brake power = 1423 kW
 Propeller rpm = 147.9
26. Run No. Speed through water
 _____ _____
 knots
 1 to 3 9.956

Run No.	Speed through water knots
4 to 6	12.887
7 to 9	15.935
10 to 13	18.947

Run No.	Time at mid-run hours	Speed of current knots
1	9.3078	-1.2289
2	10.1454	-1.0929
3	11.2226	-0.8524
4	11.8870	-0.6345
5	12.6068	-0.1027
6	13.5415	0.4292
7	13.8304	0.7454
8	14.4332	0.8857
9	14.9800	1.0259
10	15.4775	0.7186
11	15.9426	0.4550
12	16.4267	0.1608
13	16.9101	-0.1641

Thrust Identity

V , knots	w	t	η_H	η_R	η_O	η_D
9.956	0.0589	0.1333	0.9209	0.9823	0.6436	0.5822
12.887	0.0572	0.1363	0.9161	0.9826	0.6431	0.5788
15.935	0.0607	0.1380	0.9176	0.9847	0.6434	0.5814
18.947	0.0426	0.1409	0.8973	0.9752	0.6315	0.5527

Torque Identity

V , knots	w	t	η_H	η_R	η_O	η_D
9.956	0.0718	0.1333	0.9338	0.9738	0.6403	0.5822
12.887	0.0700	0.1363	0.9287	0.9742	0.6398	0.5788
15.935	0.0718	0.1380	0.9286	0.9770	0.6408	0.5814
18.947	0.0629	0.1409	0.9167	0.9652	0.6246	0.5527

27	r/R	φ°
	0.2	57.86
	0.3	46.70
	0.4	38.51
	0.5	32.48
	0.6	27.95
	0.7	24.45
	0.8	21.70
	0.9	19.48
	1.0	17.66

28. Thrust = 503.251 kN Torque = 320.399 kN m
 The propeller is working close to its optimum efficiency (0.7500).
29. Speed of advance = 9.961 m s^{-1} Thrust = 532.258 kN
 Open water efficiency = 0.7067
30. Effective power = 3858 kW Thrust power = 3631 kW
 Delivered power = 5335 kW Propeller thrust = 588.325 kN
 Torque = 339.637 kN m Open water efficiency = 0.6544
 Hull efficiency = 1.0625 Propulsive efficiency = 0.7231
31. Blade area ratio = 0.5232

32. Tensile stress = 55.908 N mm^{-2}
Compressive stress = 60.334 N mm^{-2}
33. Effective power = 5360.5 kW Delivered power = 7445.3 kW
rpm = 122.98 Wake fraction = 0.2054
Thrust deduction fraction = 0.1400
Relative rotative efficiency = 1.0846
34. Pitch ratio limits: 0.7465 to 0.7993
35. For 15000 tonnes displacement and 17.0 knots speed:
- | <u>Days out of dry dock</u> | <u>Brake Power, kW</u> |
|-----------------------------|------------------------|
| 0 | 6940 |
| 400 | 7041 |
36. Effective pitch ratio = 1.167
37. Thrust = 1379.764 kN Torque = 724.391 kN m
Efficiency = 0.9094
38. Diameter = 4.779 m Pitch ratio = 0.925
Delivered power = 3453 kW
39. Propulsive efficiency = 0.7232 Effective power = 3858 kW
Hull efficiency = 1.0559 Thrust power = 3654 kW
Relative rotative efficiency = 1.0563 Delivered power = 5335 kW
Open water efficiency = 0.6484
40. Stress = 45.524 N mm^{-2}
41. Tow force = 5.332 N Relative rotative efficiency = 1.044
Wake fraction = 0.2000 Effective power = 3150 kW
Thrust deduction fraction = 0.1463 Delivered power = 4883.7 kW

42. Required expanded blade area ratio = 0.4872

Pitch ratio = 0.6673

Bollard pull = 136.31 kN

Brake power = 2×391.48 kW

Engine rpm = 939.6

Free running condition:

Brake power = 2×306.39 kW

Engine rpm = 1200

43. Brake power = 6770 kW

Speed = 14.61 knots

- 44.
- r/R
- : 0.2 0.3 0.4 0.5 0.6 0.7 0.8 0.9 1.0
-
- θ
- , deg: -12.0 -18.0 -24.0 -30.0 -36.0 -42.0 -48.0 -54.0 -60.0

45. Ideal thrust loading coefficient = 1.1042

r/R :	0.2	0.3	0.4	0.5	0.6
C_L :	0.2729	0.2974	0.2787	0.2475	0.2166

r/R :	0.7	0.8	0.9	1.0
C_L :	0.1866	0.1599	0.1341	-

46. Speed of advance =
- 9.1365 m s^{-1}
- = 17.761 knots

Thrust = 123.4 kN

Speed of advance, knots:	0	5	10	15
Rpm	: 93.74	108.47	131.65	161.87
Thrust, kN	: 214.17	201.33	176.83	145.00
Delivered power, kW	: 1041.3	1205.3	1462.7	1798.6

47. Delivered power = 4900 kW

Thrust power = 3176.5 kN

Overall propulsive efficiency = 0.7200

Propulsive efficiency = 0.7347

Hull efficiency = 1.1333

Open water efficiency = 0.6294

Speed of advance = 5.787 m s^{-1}

Resistance = 466.563 kN

Thrust = 548.898 kN

Torque = 259.953 kN m

48.	r mm	$w(r)$
	20	0.3742
	30	0.3608
	40	0.3419
	50	0.3176
	60	0.2881
	70	0.2529
	80	0.2125
	90	0.1668
	100	0.1154

Average wake fraction = 0.2449

49. Final blade geometry:

x	P/D	f/c	c/D	t/D
0.2	0.8093	0.0487	0.2078	0.0366
0.3	0.8011	0.0329	0.2353	0.0324
0.4	0.7993	0.0228	0.2562	0.0282
0.5	0.8004	0.0196	0.2690	0.0240
0.6	0.8071	0.0179	0.2734	0.0198
0.7	0.8163	0.0170	0.2680	0.0156
0.8	0.8265	0.0170	0.2462	0.0114
0.9	0.8353	0.0191	0.1978	0.0072
1.0	0.8430	-	0	0.0030

Delivered power = 4864 kW

Propeller efficiency (behind) = 0.6741

50. Propulsive efficiency = 0.7261 Hull efficiency = 1.0330
 Open water efficiency = 0.6631 Wake fraction = 0.1900
 Thrust deduction fraction = 0.1633 Shafting efficiency = 0.9660
 Effective power = 3858 kW Delivered power = 5313 kW

Bibliography and References

Books

1. Abbott, L.H. and Doenhoff, A.E. von (1959), "Theory of Wing Sections", Dover, New York, U.S.A.
2. American Bureau of Shipping (1999), "Rules and Regulations for the Classification of Ships", New York, U.S.A.
3. Breslin, J.P. and Andersen, P. (1994), "Hydrodynamics of Ship Propellers", Cambridge University Press, Cambridge, U.K.
4. Carlton, J.S. (1994), "Marine Propellers and Propulsion", Butterworth Heinemann, Oxford, U.K.
5. Comstock, J.P., Editor, (1967), "Principles of Naval Architecture", Chapter VII, *Resistance and Propulsion* by Todd, F.H., Society of Naval Architects and Marine Engineers, New York, U.S.A.
6. Durand, W.F. (1963), "Aerodynamic Theory", Dover, New York, U.S.A.
7. Harrington, R.L., Editor (1991), "Marine Engineering", Society of Naval Architects and Marine Engineers, Jersey City, New Jersey, U.S.A.
8. Harvald, S.A. (1950), "The Wake of Merchant Ships", Danish Technical Press, Copenhagen, Denmark.
9. Harvald, S.A. (1983), "Resistance and Propulsion of Ships", John Wiley, New York, U.S.A.
10. Isay, W.H. (1981), "Kavitation", Schiffahrts-Verlag "Hansa", C. Schroeder GmbH, Hamburg, Germany.
11. ITTC, "Proceedings of the International Towing Tank Conference". (This conference is held every three years, the last one being held at Rome in 2002).

12. Lammeren, W.P.A. van, Troost, L. and Koning, J.G., (1948), "Resistance, Propulsion and Steering of Ships", The Technical Publishing Company H. Stam, Haarlem, The Netherlands.
13. Lewis, E.V., Editor (1988), "Principles of Naval Architecture", Chapter VI, *Propulsion*, by Manen, J.D. van and Oossanen, P., Society of Naval Architects and Marine Engineers, Jersey City, New Jersey, U.S.A.
14. Lloyd's Register of Shipping (2000), "Rules and Regulations for the Classification of Ships", London, U.K.
15. Manen, J.D. van, (1957), "Fundamentals of Resistance and Propulsion, Part B: Propulsion", Publication 132a of the Netherlands Ship Model Basin, Wageningen, The Netherlands.
16. O'Brien, T.P. (1962), "Design of Marine Propellers", Hutchinson, London, U.K.
17. Prandtl, L. and Tietjens, O.G. (1957), "Fundamentals of Hydro- and Aerodynamics", Dover, New York.
18. Ross, D. (1976), "Mechanics of Underwater Noise", Pergamon Press, New York, U.S.A.
19. Rossell, H.E. and Chapman, L.B., Editors (1939), "Principles of Naval Architecture", Vol. II, Chapter III, *Propulsion and Propellers* by Schoenherr, K.E., Society of Naval Architects and Marine Engineers, New York, U.S.A.
20. Saunders, H.E. (1957), "Hydrodynamics in Ship Design", Society of Naval Architects and Marine Engineers, New York, U.S.A.
21. Schneekluth, H. (1987), "Ship Design for Efficiency and Economy", Butterworth, London, U.K.
22. Taylor, D.W. (1933), "Speed and Power of Ships", U.S. Government Printing Press, Washington, U.S.A.

Papers and Reports

Abbreviations

DTMB	:	David Taylor Model Basin, Carderock, U.S.A.
IESS	:	Transactions of the Institution of Engineers and Shipbuilders of Scotland, Glasgow.
IMarE	:	Transactions of the Institute of Marine Engineers, London.

INA	:	Institution of Naval Architects, London.
ISP	:	International Shipbuilding Progress, Delft, The Netherlands.
JSR	:	Journal of Ship Research (published by the Society of Naval Architects and Marine Engineers, New York).
MT	:	Marine Technology (published by the Society of Naval Architects and Marine Engineers, New York).
NACA	:	National Advisory Committee on Aeronautics, U.S.A.
NECIES	:	Transactions of the North East Coast Institution of Engineers and Shipbuilders, Newcastle upon Tyne, U.K.
RINA	:	Transactions of the Royal Institution of Naval Architects, London.
SNAJ	:	Proceedings of the Society of Naval Architects of Japan, Tokyo.
SNAME	:	Transactions of the Society of Naval Architects and Marine Engineers, Jersey City.
SSPA	:	Statens Skepps Provings Anstalt ([Swedish] State Ship Testing Establishment), Goteborg, Sweden.

1. Aertssen, G. (1966), "Service Performance and Seakeeping Trials on M.V. Jordaens", RINA, Vol. 108.
2. Aertssen, G. and Sluijs, M.F. Van (1972), "Service Performance and Seakeeping Trials on a Large Container Ship", RINA, Vol. 114.
3. Allen, H.J. (1939), "A Simplified Method for the Calculation of Airfoil Pressure Distribution", NACA Technical Note 708.
4. Allison, J.L. (1993), "Marine Waterjet Propulsion", SNAME, Vol. 101.
5. Allison, J.L. (1978), "Propellers for High Performance Craft", MT, Vol. 15, No. 4.
6. Andersen, P. (1976), "Lifting Line Theory Calculations for Supercavitating Propellers", ISP, Vol. 23, No. 266.
7. Andersen, P. and Schwanecke, H. (1992), "Design and Model Tests of Tip Fin Propellers", RINA, Vol. 134.
8. Andersen, S.V. and Andersen, P. (1987), "Hydrodynamic Design of Propellers with Unconventional Geometry", RINA, Vol. 129.

9. Atkinson, P. (1968), "On the Choice of Method for the Calculation of Stresses in Marine Propellers", RINA, Vol. 110.
10. Baker, G.S. (1940-41), "Vibration Patterns of Propeller Blades", NECIES, Vol. 57.
11. Belibasakis, K.A. and Polito, G.K. (1998), "A Non-linear Velocity Based Boundary Element Method for the Analysis of Marine Propellers in Unsteady Flow", ISP, Vol. 45, No. 442.
12. Berkelom, W.P. van, Tragardh, P. and Dellhag, A. (1975), "Large Tankers - Wind Coefficients and Speed Loss due to Wind and Sea", RINA, Vol. 117.
13. Betz, A. (1919), "Schraubenpropeller mit geringstem Energieverlust", reprinted in Prandtl, L. and Betz, A. (1927), "Vier Abhandlungen zur Hydrodynamik und Aerodynamik", Gottingen.
14. Bilen, B., Nikolic, Z., Bilen-Katic, B. and Zerjal, M. (1994), "A Pilot Study of the Efficiency of an Open MHD Propulsion System (One-Dimensional Considerations)", ISP, Vol. 41, No. 428.
15. Blaurock, J. (1983), "Propeller plus Vane Wheel, an Unconventional Propulsion System", International Symposium on Ship Hydrodynamics and Energy Saving, El Pardo, Madrid, Spain.
16. Blount, D.L. and Baree, R.J. (1997), "Design of Propulsion Systems for High Speed Craft", MT, Vol. 34, No. 4.
17. Blount, D.L. and Hubble, E.N. (1981), "Sizing for Segmental Section Commercially Available Propellers for Small Craft", Propellers '81 Conference, Society of Naval Architects and Marine Engineers, New York.
18. Bonebakker, J.W. (1950-51), "The Application of Statistical Methods to the Analysis of Service Performance Data", NECIES, Vol. 67.
19. Boswell, R.J. and Cox, G.G. (1974), "Design and Model Evaluation of a Highly Skewed Propeller for a Cargo Ship", MT, Vol. 11, No. 1.
20. Breslin, J.P. (1970), "Theoretical and Experimental Techniques for Practical Estimation of Propeller Induced Vibratory Forces", SNAME, Vol. 78.
21. Brockett, T. (1966), "Minimum Pressure Envelopes for Modified NACA Sections with NACA $a = 0.8$ Camber and BuShips Type I and Type II Sections", DTMB Report No. 1790.
22. BSRA (1977), "Code of Procedure for Measured Mile Trials", British Ship Research Association, Wallsend.
23. Burrill, L.C. (1943), "Developments in Propeller Design and Manufacture for Merchant Ships", IMarE, Vol. 55.

24. Burrill, L.C. (1943-44), "Calculation of Marine Propeller Performance Characteristics", NECIES, Vol. 60.
25. Burrill, L.C. (1951), "Sir Charles Parsons and Cavitation", IMarE, Vol. 43.
26. Burrill, L.C. (1954), "On Propeller Manufacture", RINA, Vol. 96.
27. Burrill, L.C. (1955-56), "The Optimum Diameter of Marine Propellers : A New Design Approach", NECIES, Vol. 72.
28. Burrill, L.C. (1959), "A Short Note on the Stressing of Marine Propellers", Shipbuilder and Marine Engine Builder, Vol. 66.
29. Burrill, L.C. (1959-60), "Propellers in Action Behind a Ship", NECIES, Vol. 76.
30. Burrill, L.C. and Emerson, A. (1962-63), "Propeller Cavitation : Further Tests on 16 inch propellers in the King's College Cavitation Tunnel", NECIES, Vol. 79.
31. Canham, H.J.S. and Clements, R.E. (1965), "An Analysis of a Sample of Ship Model Correlation Data for Tankers", RINA, Vol. 107.
32. Canham, H.J.S. and Lynn, W.M. (1962), "The Propulsive Performance of a Group of Intermediate Tankers", RINA, Vol. 104.
33. Caster, E.B. (1959), "TMB 3-bladed Supercavitating Propeller Series", DTMB Report No. 1245.
34. Cheng, H.M. (1964, 1965), "Hydrodynamic Aspect of Propeller Design Based on Lifting Surface Theory", Parts 1 and 2, DTMB Reports 1802 and 1803.
35. Clements, R.E. (1956-57), "A Method of Analysing Voyage Data", NECIES, Vol. 73.
36. Comstock, J.P. and Hastings, C.E. (1952), "Raydist Speed Measuring Equipment on the S.S. United States Sea Trials", SNAME, Vol. 60.
37. Conolly, J.E. (1961), "Strength of Propellers", RINA, Vol. 103.
38. Cox, B.D. and Reed, A.M. (1988), "Contra-rotating Propellers - Design Theory and Application", Propellers '88 Symposium, Society of Naval Architects and Marine Engineers, New Jersey.
39. Cox, G.G. and Morgan, W.B. (1972), "The Use of Theory in Propeller Design", MT, Vol. 9, No. 4.
40. Cummings, D.E. (1973), "Numerical Prediction of Propeller Characteristics", JSR, Vol. 17, No. 1.

41. Cummings, R.A., Morgan, W.B. and Boswell, R.J. (1972), "Highly Skewed Propellers", SNAME, Vol. 80.
 42. Denny, S.B., Puckette, L.T., Hubble, F.N., Smith, S.K. and Najarian, R.F. (1989), "A New Usable Propeller Series", MT, Vol. 26, No. 3.
 43. Dyne, G. (1967), "A Method for the Design of Ducted Propellers in Uniform Flow", SSPA Report No. 62, Goteborg.
 44. Eckhardt, M.K. and Morgan, W.B. (1955), "A Propeller Design Method", SNAME, Vol. 63.
 45. Eppler, R. and Shen, Y.T. (1979), "Wing Sections for Hydrofoils - Part 1 Symmetrical Profiles", JSR, Vol. 23, No. 3.
 46. Ferrando, M. (1997), "Surface Piercing Propellers : State of the Art", Ocean Engineering International, Vol. 1, No. 2.
 47. Fornells, R.R. and Gomez, G.P. (1983), "Full Scale Results of the First TVF Propellers", International Symposium on Ship Hydrodynamics and Energy Saving, El Pardo, Madrid.
 48. Friesch, J. (1995), "Correlation Investigation for Wake, Cavitation and Pressure Fluctuations Behind Whole Ship Models", Practical Design of Ships Symposium (PRADS 95), Seoul.
 49. Friesch, J., Johanssen, C. and Payer, H.G. (1992), "Correlation Studies on Propeller Cavitation Making Use of a Large Cavitation Tunnel", SNAME, Vol. 100.
 50. Gawn, R.W.L. and Burrill, L.C. (1957), "Effect of Cavitation on the Performance of a Series of 16-inch Model Propellers", RINA, Vol. 99.
 51. Gawn, R.W.L. (1953), "Effect of Pitch and Blade Width on Propeller Performance", RINA, Vol. 95.
 52. Gent, W. van (1975), "Unsteady Lifting Surface Theory for Ship Screws: Derivation and Numerical Treatment of Integral Equation", JSR, Vol. 19, No. 4.
 53. Gent, W. van (1990), "Some Experiments Related to Ship Hull Vibration and Pressure Fluctuations above the Propeller", RINA, Vol. 132.
 54. Gent, W. van and Oosterveld, M.W.C. (1983), "Ducted Propeller Systems and Energy Saving", International Symposium on Ship Hydrodynamics and Energy Saving, El Pardo, Madrid, Spain.
 55. Gibbon, R.P. (1975), "Service Margins and Power Plant Selection", First Ship Technology and Research (STAR) Symposium, Society of Naval Architects and Marine Engineers, New York.
-

56. Gibson, I.S. (1975), "Performance of Azimuthing Thrusters", ISP, Vol. 22, No. 255.
57. Glover, E.J. (1987), "Propulsion Devices for Improved Propulsive Efficiency", IMarE, Vol. 99.
58. Goldstein, S. (1929), "On the Vortex Theory of Screw Propellers", Proceedings of the Royal Society, London, Vol. 123, Series A.
59. Greeley, D.S. and Kerwin, J.E. (1982), "Numerical Methods for Propeller Design and Analysis in Steady Flow", SNAME, Vol. 90.
60. Grigson, C.W.B. (1981), "Propeller Roughness, its Nature and its Effects upon the Drag Coefficients of Blades and Ship Power", RINA, Vol. 123.
61. Grim, O. (1980), "Propeller and Vane Wheel", JSR, Vol. 24, No. 4.
62. Grothues-Spork, K. (1988), "Bilge Vortex Control Devices and their Benefits for Propulsion", ISP, Vol. 35, No. 402.
63. Gunsteren, L.A. van (1971), "Ring Propellers", IMarE, Vol. 83.
64. Gunsteren, L.A. van and Pronk, C. (1973), "Propeller Design Concepts", ISP, Vol. 20, No. 227.
65. Gutsche, F. (1934), "Verstellepropeller", Zeitschrift der V.D.I., 1934.
66. Hadler, J.B. and Hecker, R. (1968), "Performance of Partially Submerged Propellers", Seventh Symposium on Naval Hydrodynamics, Office of Naval Research, Washington, U.S.A.
67. Hagen, G.R., Comstock, E.N., and Slager, J. (1986), "Investigation of Design Power Margins and Correlation Allowances for Surface Ships", MT, Vol. 23, No. 1.
68. Hanaoka, T. (1969), "Numerical Lifting Surface Theory of Screw Propeller in Non-uniform Flow", Report No. 6, Ship Research Institute, Tokyo.
69. Harvald, S.A. (1978), "Estimation of Power of Ships", ISP, Vol. 25, No. 283.
70. Harvald, S.A. (1980), "Wake Distribution and Wake Measurements", RINA, Vol. 123.
71. Harvald, S.A. and Hee, J.M. (1988), "The Components of the Propulsive Efficiency of Ships in Relation to the Design Procedure", Third International Marine Systems Design Conference (IMSDC), Society of Naval Architects and Marine Engineers, New Jersey.
72. Henderson, R.E., McMahon, J.F. and Wislicenus, G.F. (1964), "A Method for Design of Pump Jets", Ordnance Research Laboratory, Pennsylvania State University.

73. Hill, J.G. (1949), "The Design of Propellers", SNAME, Vol. 57.
74. Holtrop, J. (1984), "A Statistical Reanalysis of Resistance and Propulsion Data", ISP, Vol. 31, No. 363.
75. Holtrop, J. and Mennen, G.G.J. (1982), "An Approximate Power Prediction Method", ISP, Vol. 29, No. 335.
76. Hoshino, T. (1989 a, b), "Hydrodynamic Analysis of Propellers in Steady Flow Using a Surface Panel Method", SNAJ, Vols. 165, 166.
77. Hughes, G. (1945), "On Singing Propellers", INA, Vol. 87.
78. Iawata, A. (1990), "Superconducting Electromagnetic Propulsion System", Bulletin of the Marine Engineering Society, Japan, Vol. 18, No. 1.
79. Isherwood, R.M. (1973), "Wind Resistance of Merchant Ships", RINA, Vol. 115.
80. ISO (1981), "Shipbuilding - Ship Screw Propellers - Manufacturing Tolerances, Parts 1 and 2", ISO Standards 484/1 and 484/2.
81. ITTC (1969), "Guide for Measured Mile Trials", Report of the Performance Committee, Proceedings of the 12th ITTC, Rome.
82. Johnsson, C.-A. (1968), "On Theoretical Prediction of Characteristics and Cavitation Properties of Propellers", SSPA Report No. 64, Goteborg.
83. Jong, K. de (1992), "On the Design of Optimum Ship Screw Propellers including Propellers with End Plates", STG/HSVA International Symposium on Propulsors and Cavitation, Hamburg.
84. Keller, J. Auf'm (1966), "Enige Aspecten bij het Ontwerpen van Scheepsschroeven", Schip en Werf, No. 24.
85. Kerwin, J.E. (1959), "Machine Computation of Marine Propeller Characteristics", ISP, Vol. 6, No. 60.
86. Kerwin, J.E. (1975), "Computer Techniques for Propeller Blade Section Design", ISP, Vol. 20, No. 227.
87. Kerwin, J.E. (1989), "Marine Propellers", Annual Review of Fluid Mechanics, Vol. 18.
88. Kerwin, J.E. and Lee, C.-S. (1978), "Prediction of Steady and Unsteady Propeller Performance by Numerical Lifting Surface Theory", SNAME, Vol. 86.
89. Kerwin, J.E. and Leopold R. (1964), "A Design Theory of Subcavitating Propellers", SNAME, Vol. 72.

90. Kerwin, J.E., Kinnas, S.A., Lee, J.-T. and Shih, W.Z. (1987), "A Surface Panel Method for the Hydrodynamic Analysis of Ducted Propellers", SNAME, Vol. 95.
91. Klassen, H. and Arnoldus, W. (1964), "Actuating Forces in Controllable Pitch Propellers", IMarE, Vol. 76.
92. Kort, L. (1934), "Der neue Duschrauben-Antrieb", Werft Reederei Hafen, Vol. 15. No. 4.
93. Kramer, K.N. (1939), "The Induced Efficiency of Optimum Propellers Having a Finite Number of Blades", NACA TM 884.
94. Krappinger, O. (1954), "Schaufelradberechnung", Schiffstechnik, Vol. 6.
95. Kresic, M. and Haskell, B. (1983), "Effects of Propeller Design Point Definition on the Performance of a Propeller/Diesel Engine System with Regard to In-service Roughness and Weather Conditions", SNAME, Vol. 91.
96. Kudo, T. and Ukon, Y. (1994), "Calculation of Supercavitating Propeller Performance Using a Vortex Lattice Method", Second International Symposium on Cavitation, Tokyo.
97. Kuiper, G. (1992), "The Wageningen Propeller Series", MARIN Report 92-001.
98. Kuiper, G. and Jessup, S.D. (1993), "A Propeller Design Method for Unsteady Conditions", SNAME, Vol. 101.
99. Lackenby, H. (1952-53), "On the Acceleration of Ships", IEES, Vol. 96.
100. Lammeren, W.P.A. van (1955), "Testing of Screw Propellers in a Cavitation Tunnel with Controllable Velocity Distribution over the Screw Disc", SNAME, Vol. 63.
101. Lammeren, W.P.A. van, Manen, J.D. van, Oosterveld, M.W.C. (1969), "The Wageningen Screw Series", SNAME, Vol. 77.
102. Lerbs, H.W. (1952), "Moderately Loaded Propellers with a Finite Number of Blades and an Arbitrary Distribution of Circulation", SNAME, Vol. 60.
103. Lewis, R.I. (1972-73), "Fluid Dynamic Design and Performance Analysis of Ducted Propellers", NECIES, Vol. 88.
104. Lindgren, H. (1961), "Model Tests with a Family of Three- and Five-Bladed Propellers", SSPA Report No. 47.
105. Lindgren, H. and Bjarne, E. (1967), "The SSPA Standard Family of Propellers", SSPA Report No. 60.